



REGULATORY POTENTIAL OF POST-TRANSLATIONAL MODIFICATIONS IN BACTERIA

EDITED BY: Ivan Mijakovic, Christophe Grangeasse and Jörg Stülke
PUBLISHED IN: Frontiers in Microbiology



frontiers

Frontiers Copyright Statement

© Copyright 2007-2015 Frontiers Media SA. All rights reserved.

All content included on this site, such as text, graphics, logos, button icons, images, video/audio clips, downloads, data compilations and software, is the property of or is licensed to Frontiers Media SA ("Frontiers") or its licensees and/or subcontractors. The copyright in the text of individual articles is the property of their respective authors, subject to a license granted to Frontiers.

The compilation of articles constituting this e-book, wherever published, as well as the compilation of all other content on this site, is the exclusive property of Frontiers. For the conditions for downloading and copying of e-books from Frontiers' website, please see the Terms for Website Use. If purchasing Frontiers e-books from other websites or sources, the conditions of the website concerned apply.

Images and graphics not forming part of user-contributed materials may not be downloaded or copied without permission.

Individual articles may be downloaded and reproduced in accordance with the principles of the CC-BY licence subject to any copyright or other notices. They may not be re-sold as an e-book.

As author or other contributor you grant a CC-BY licence to others to reproduce your articles, including any graphics and third-party materials supplied by you, in accordance with the Conditions for Website Use and subject to any copyright notices which you include in connection with your articles and materials.

All copyright, and all rights therein, are protected by national and international copyright laws.

The above represents a summary only. For the full conditions see the Conditions for Authors and the Conditions for Website Use.

ISSN 1664-8714

ISBN 978-2-88919-610-4

DOI 10.3389/978-2-88919-610-4

About Frontiers

Frontiers is more than just an open-access publisher of scholarly articles: it is a pioneering approach to the world of academia, radically improving the way scholarly research is managed. The grand vision of Frontiers is a world where all people have an equal opportunity to seek, share and generate knowledge. Frontiers provides immediate and permanent online open access to all its publications, but this alone is not enough to realize our grand goals.

Frontiers Journal Series

The Frontiers Journal Series is a multi-tier and interdisciplinary set of open-access, online journals, promising a paradigm shift from the current review, selection and dissemination processes in academic publishing. All Frontiers journals are driven by researchers for researchers; therefore, they constitute a service to the scholarly community. At the same time, the Frontiers Journal Series operates on a revolutionary invention, the tiered publishing system, initially addressing specific communities of scholars, and gradually climbing up to broader public understanding, thus serving the interests of the lay society, too.

Dedication to Quality

Each Frontiers article is a landmark of the highest quality, thanks to genuinely collaborative interactions between authors and review editors, who include some of the world's best academicians. Research must be certified by peers before entering a stream of knowledge that may eventually reach the public - and shape society; therefore, Frontiers only applies the most rigorous and unbiased reviews.

Frontiers revolutionizes research publishing by freely delivering the most outstanding research, evaluated with no bias from both the academic and social point of view.

By applying the most advanced information technologies, Frontiers is catapulting scholarly publishing into a new generation.

What are Frontiers Research Topics?

Frontiers Research Topics are very popular trademarks of the Frontiers Journals Series: they are collections of at least ten articles, all centered on a particular subject. With their unique mix of varied contributions from Original Research to Review Articles, Frontiers Research Topics unify the most influential researchers, the latest key findings and historical advances in a hot research area! Find out more on how to host your own Frontiers Research Topic or contribute to one as an author by contacting the Frontiers Editorial Office: researchtopics@frontiersin.org

REGULATORY POTENTIAL OF POST-TRANSLATIONAL MODIFICATIONS IN BACTERIA

Topic Editors:

Ivan Mijakovic, Chalmers University of Technology, Sweden

Christophe Grangeasse, Bases Moléculaires et Structurales des Systèmes Infectieux, UMR5086, CNRS, University of Lyon, Lyon, France

Jörg Stülke, University of Göttingen, Germany

Post-translational modifications (PTMs) are widely employed by all living organisms to control the enzymatic activity, localization or stability of proteins on a much shorter time scale than the transcriptional control. In eukarya, global analyses consistently reveal that proteins are very extensively phosphorylated, acetylated and ubiquitylated. Glycosylation and methylation are also very common, and myriad other PTMs, most with a proven regulatory potential, are being discovered continuously. The emergent picture is that PTM sites on a single protein are not independent; modification of one residue often affects (positively or negatively) modification of other sites on the same protein. The best example of this complex behavior is the histone “bar-code” with very extensive cross-talk between phosphorylation, acetylation and methylation sites.

Traditionally it was believed that large networks of PTMs exist only in complex eukaryal cells, which exploit them for coordination and fine-tuning of various cellular functions. PTMs have also been detected in bacteria, but the early examples focused on a few important regulatory events, based mainly on protein phosphorylation. The global importance (and abundance) of PTMs in bacterial physiology was systematically underestimated. In recent years, global studies have reported large datasets of phosphorylated, acetylated and glycosylated proteins in bacteria. Other modifications of bacterial proteins have been recently described: pupylation, methylation, sirtuin acetylation, lipidation, carboxylation and bacillithiolation. As the landscape of PTMs in bacterial cells is rapidly expanding, primarily due to advances of detection methods in mass spectrometry, our research field is adapting to comprehend the potential impact of these modifications on the cellular physiology. The field of protein phosphorylation, especially of the Ser/Thr/Tyr type, has been profoundly transformed. We have become aware that bacterial kinases phosphorylate many protein substrates and thus constitute regulatory nodes with potential for signal integration. They also engage in cross-talk and eukaryal-like mutual activation cascades. The regulatory potential of protein acetylation and glycosylation in bacteria is also rapidly emerging, and the cross-talk between acetylation and phosphorylation has been documented.

This topic deals with the complexity of the PTM landscape in bacteria, and focus in particular on the physiological roles that PTMs play and methods to study them. The topic is associated to the 1st International Conference on Post-Translational Modifications in Bacteria (September 9-10, 2014, Göttingen, Germany).

Citation: Mijakovic, I., Grangeasse, C., Stülke, J., eds. (2015). Regulatory Potential of Post-Translational Modifications in Bacteria. Lausanne: Frontiers Media.
doi: 10.3389/978-2-88919-610-4

Table of Contents

- 06** *Regulatory potential of post-translational modifications in bacteria*
Christophe Grangeasse, Jörg Stülke and Ivan Mijakovic
- 08** *Comparative Ser/Thr/Tyr phosphoproteomics between two mycobacterial species: the fast growing Mycobacterium smegmatis and the slow growing Mycobacterium bovis BCG*
Kehilwe C. Nakedi, Andrew J. M. Nel, Shaun Garnett, Jonathan M. Blackburn and Nelson C. Soares
- 20** *Phosphoproteome of the cyanobacterium Synechocystis sp. PCC 6803 and its dynamics during nitrogen starvation*
Philipp Spät, Boris Maček and Karl Forchhammer
- 35** *Redox regulation by reversible protein S-thiolation in bacteria*
Vu Van Loi, Martina Rossius and Haike Antelmann
- 57** *Identification of essential amino acid residues in the nisin dehydratase NisB*
Rustem Khusainov, Auke J. van Heel, Jacek Lubelski, Gert N. Moll and Oscar P. Kuipers
- 65** *Characterization of the E.coli proteome and its modifications during growth and ethanol stress*
Boumediene Soufi, Karsten Krug, Andreas Harst and Boris Macek
- 76** *Post-translational modifications are key players of the Legionella pneumophila infection strategy*
Céline Michard and Patricia Doublet
- 88** *Phosphoproteomics analysis of a clinical Mycobacterium tuberculosis Beijing isolate: expanding the mycobacterial phosphoproteome catalog*
Suereta Fortuin, Gisele G. Tomazella, Nagarjuna Nagaraj, Samantha L. Sampson, Nicolaas C. Gey van Pittius, Nelson C. Soares, Harald G. Wiker, Gustavo A. de Souza and Robin M. Warren
- 100** *The length of a lantibiotic hinge region has profound influence on antimicrobial activity and host specificity*
Liang Zhou, Auke J. van Heel and Oscar P. Kuipers
- 108** *Protein-tyrosine phosphorylation in Bacillus subtilis: a 10-year retrospective*
Ivan Mijakovic and Josef Deutscher
- 115** *Activity of the response regulator CiaR in mutants of Streptococcus pneumoniae R6 altered in acetyl phosphate production*
Patrick Marx, Marina Meiers and Reinhold Brückner
- 126** *Post-translational hydroxylation by 2OG/Fe(II)-dependent oxygenases as a novel regulatory mechanism in bacteria*
Laura M. van Staalduinen and Zongchao Jia

- 133** *Interaction between extracellular matrix molecules and microbial pathogens: evidence for the missing link in autoimmunity with rheumatoid arthritis as a disease model*
Nidhi Sofat, Robin Wait, Saralili D. Robertson, Deborah L. Baines and Emma H. Baker
- 139** *Factors that mediate and prevent degradation of the inactive and unstable GudB protein in Bacillus subtilis*
Lorena Stannek, Katrin Gunka, Rachel A. Care, Ulf Gerth and Fabian M. Commichau
- 150** *Post-translational modification of P_{II} signal transduction proteins*
Mike Merrick
- 156** *Association and dissociation of the GlnK–AmtB complex in response to cellular nitrogen status can occur in the absence of GlnK post-translational modification*
Martha V. Radchenko, Jeremy Thornton and Mike Merrick
- 161** *Complexity of bacterial phosphorylation interaction network*
Imrich Barák
- 163** *Far from being well understood: multiple protein phosphorylation events control cell differentiation in Bacillus subtilis at different levels*
Jan Gerwig and Jörg Stülke
- 167** *Protein-tyrosine phosphorylation interaction network in Bacillus subtilis reveals new substrates, kinase activators and kinase cross-talk*
Lei Shi, Nathalie Pigeonneau, Magali Ventrux, Abderahmane Derouiche, Vladimir Bidnenko, Ivan Mijakovic and Marie-Françoise Noirot-Gros
- 182** *Cross-phosphorylation of bacterial serine/threonine and tyrosine protein kinases on key regulatory residues*
Lei Shi, Nathalie Pigeonneau, Vaishnavi Ravikumar, Paula Dobrinic, Boris Macek, Damjan Franjevic, Marie-Francoise Noirot-Gros and Ivan Mijakovic
- 195** *Production of a recombinant vaccine candidate against Burkholderia pseudomallei exploiting the bacterial N-glycosylation machinery*
Fatima Garcia-Quintanilla, Jeremy A. Iwashkiw, Nancy L. Price, Chad Stratilo and Mario F. Feldman

Regulatory potential of post-translational modifications in bacteria

Christophe Grangeasse¹, Jörg Stülke² and Ivan Mijakovic^{3*}

¹ Bases Moléculaires et Structurales des Systèmes Infectieux, UMR 5086, Centre National de la Recherche Scientifique, University of Lyon, Lyon, France, ² Department of General Microbiology, Institute for Microbiology and Genetics, University of Göttingen, Göttingen, Germany, ³ Systems and Synthetic Biology Division, Department of Biology and Biological Engineering, Chalmers University of Technology, Göteborg, Sweden

Keywords: phosphorylation, S-thiolation, dehydration, hydroxylation, N-glycosylation, protein kinases, antimicrobial peptides, proteomics

OPEN ACCESS

Edited by:

Thomas E. Hanson,
University of Delaware, USA

Reviewed by:

Jerry Eichler,
Ben Gurion University
of the Negev, Israel

*Correspondence:

Ivan Mijakovic,
ivan.mijakovic@chalmers.se

Specialty section:

This article was submitted to
Microbial Physiology and Metabolism,
a section of the journal
Frontiers in Microbiology

Received: 25 April 2015

Accepted: 06 May 2015

Published: 28 May 2015

Citation:

Grangeasse C, Stülke J and
Mijakovic I (2015) Regulatory potential
of post-translational modifications in
bacteria. *Front. Microbiol.* 6:500.
doi: 10.3389/fmicb.2015.00500

Bacteria are often viewed as simple organisms, with very basic and robust cellular regulation, optimized for rapid growth. While they certainly fit that description, bacteria also possess an amazing capacity for adaptation, and diversity of survival strategies, including variations of cell morphology, size, mode of growth and developmental behavior. Post-translational modifications (PTMs) of proteins contribute significantly to bacterial adaptability and cell cycle control. Research on PTMs in bacteria started with the assumption that they lack many features regularly found in more complex organisms. However, ongoing investigation keeps revealing new types of PTMs of bacterial proteins. This research topic gathers a number of articles discussing the advanced methods for systematic study of bacterial PTMs, approaches to utilize PTMs for biotechnological purposes, and revealing new cellular functions controlled by PTMs.

Most bacterial PTMs are dynamic and reversible. This allows the cell to exploit them as regulatory devices. It also means that the full understanding of the cellular roles of different PTMs necessitates global, quantitative and time-resolved studies. One seminal paper in this topic reports a novel proteomics approach for such quantitative studies: the Intensity Based Absolute Quantitation (iBAQ). Using this approach, the authors have quantified the expression and the occupancy of various PTM sites in the proteome of *Escherichia coli* (Soufi et al., 2015). The authors report remarkable differences in expression and occupancy of PTMs sites under different growth conditions. The dataset comprised 2300 proteins, which is close to 90% of the expressed proteome. This is an important landmark, since proteomics in general has not yet attained the same level of coverage that global transcriptome studies can achieve.

Among different bacterial PTMs, protein phosphorylation is the most extensively studied one, and in this topic it features prominently. Several papers present global studies of protein phosphorylation in bacteria (Spät et al., 2015), including important bacterial pathogens (Fortuin et al., 2015; Nakedi et al., 2015). The focus on pathogens is understandable, since protein phosphorylation, and several other PTMs, are heavily involved in different infection strategies displayed by bacterial pathogens (Michard and Doublet, 2015). In addition to phosphoproteome studies, interactomics is also featured as a useful approach to chart the phosphorylation-based regulatory networks. It enables researchers to trace the connections among protein kinases, phosphatases, and their substrates (Shi et al., 2014a). This approach for reconstructing phosphorylation networks highlights the capacity of bacterial proteins kinases from different families to interact with, and phosphorylate, each other (Shi et al., 2014b). Protein-tyrosine kinases, and their various roles in bacterial physiology were in the focus of several review and opinion articles in this topic (Barák, 2014; Gerwig and Stülke, 2014; Mijakovic and Deutscher, 2015).

Other topic contributions highlight the broad spectrum of PTMs involved in key cellular processes. In particular, novel modifications are discussed: redox regulation via reversible S-thiolation (Loi et al., 2015), post-translational hydroxylation (van Staalduinen and Jia, 2015) and the role of citrullination for the interaction between bacteria and human mucosal surfaces (Sofat et al., 2015). Several experimental papers report studies on post-translationally modified antimicrobial peptides known as lantibiotics. These are ribosomally synthesized peptides which can efficiently inhibit the growth of Gram-positive bacteria. A study by Zhou et al. (2015) described an engineering strategy to make the lantibiotics more effective in inhibiting several important bacterial pathogens. In another study, Khusainov et al. (2015) describe the active site of the nisin dehydratase. This enzyme, essential for the production of the lantibiotic nisin, converts serines, and threonines, to dehydroalanine and dehydrobutyrine residues, respectively. Interestingly, bacterial PTM systems, such as the N-glycosylation machinery, are also being exploited and engineered to facilitate the production of recombinant vaccines (Garcia-Quintanilla et al., 2014). Another focal point of the topic are the PTMs targeting the PII proteins,

which are the key signal transduction proteins involved in the control of nitrogen metabolism in bacteria and archaea (Radchenko et al., 2014; Merrick, 2015). Finally, Stannek et al. (2015) contributed a study on a regulatory mechanism involving arginine phosphorylation and regulated proteolysis.

In conclusion, the contributions in this topic reflect the diversity of bacterial PTMs. Several studies highlight one important emergent feature of PTM systems: their capacity to interact with each other, creating an additional level of complexity in the cellular regulation. This is one of the key features of bacterial PTM systems and a challenge which future studies will have to address.

Acknowledgments

This topic was organized to accompany the First International Conference on Post-translational Modifications in Bacteria, held in Göttingen (Germany), 9–10 September 2014. We would like to take this opportunity to thank all the conference participants, and especially those who contributed their work to this topic.

References

- Barák, I. (2014). Complexity of bacterial phosphorylation interaction network. *Front. Microbiol.* 5:725. doi: 10.3389/fmicb.2014.00725
- Fortuin, S., Tomazella, G. G., Nagaraj, N., Sampson, S. L., Gey van Pittius, N. C., Soares, N. C., et al. (2015). Phosphoproteomics analysis of a clinical *Mycobacterium tuberculosis* Beijing isolate: expanding the mycobacterial phosphoproteome catalog. *Front. Microbiol.* 6:6. doi: 10.3389/fmicb.2015.00006
- Garcia-Quintanilla, F., Iwashkiw, J. A., Price, N. L., Stratilo, C., and Feldman, M. F. (2014). Production of a recombinant vaccine candidate against *Burkholderia pseudomallei* exploiting the bacterial N-glycosylation machinery. *Front. Microbiol.* 5:381. doi: 10.3389/fmicb.2014.00381
- Gerwig, J., and Stülke, J. (2014). Far from being well understood: multiple protein phosphorylation events control cell differentiation in *Bacillus subtilis* at different levels. *Front. Microbiol.* 5:704. doi: 10.3389/fmicb.2014.00704
- Khusainov, R., van Heel, A. J., Lubelski, J., Moll, G. N., and Kuipers, O. P. (2015). Identification of essential amino acid residues in the nisin dehydratase NisB. *Front. Microbiol.* 6:102. doi: 10.3389/fmicb.2015.00102
- Loi, V. V., Rossius, M., and Antelmann, H. (2015). Redox regulation by reversible protein S-thiolation in bacteria. *Front. Microbiol.* 6:187. doi: 10.3389/fmicb.2015.00187
- Merrick, M. (2015). Post-translational modification of P II signal transduction proteins. *Front. Microbiol.* 5:763. doi: 10.3389/fmicb.2014.00763
- Michard, C., and Doublet, P. (2015). Post-translational modifications are key players of the *Legionella pneumophila* infection strategy. *Front. Microbiol.* 6:87. doi: 10.3389/fmicb.2015.00087
- Mijakovic, I., and Deutscher, J. (2015). Protein-tyrosine phosphorylation in *Bacillus subtilis*: a 10-year retrospective. *Front. Microbiol.* 6:18. doi: 10.3389/fmicb.2015.00018
- Nakedi, K. C., Nel, A. J. M., Garnett, S., Blackburn, J. M., and Soares, N. C. (2015). Comparative Ser/Thr/Tyr phosphoproteomics between two mycobacterial species: the fast growing *Mycobacterium smegmatis* and the slow growing *Mycobacterium bovis* BCG. *Front. Microbiol.* 6:237. doi: 10.3389/fmicb.2015.00237
- Radchenko, M. V., Thornton, J., and Merrick, M. (2014). Association and dissociation of the GlnK-AmtB complex in response to cellular nitrogen status can occur in the absence of GlnK post-translational modification. *Front. Microbiol.* 5:731. doi: 10.3389/fmicb.2014.00731
- Shi, L., Pigeonneau, N., Ravikumar, V., Dobrinic, P., Macek, B., Franjevic, D., et al. (2014b). Cross-phosphorylation of bacterial serine/threonine and tyrosine protein kinases on key regulatory residues. *Front. Microbiol.* 5:495. doi: 10.3389/fmicb.2014.00495
- Shi, L., Pigeonneau, N., Ventroux, M., Derouiche, A., Bidnenko, V., Mijakovic, I., et al. (2014a). Protein-tyrosine phosphorylation interaction network in *Bacillus subtilis* reveals new substrates, kinase activators and kinase cross-talk. *Front. Microbiol.* 5:538. doi: 10.3389/fmicb.2014.00538
- Sofat, N., Wait, R., Robertson, S. D., Baines, D. L., and Baker, E. H. (2015). Interaction between extracellular matrix molecules and microbial pathogens: evidence for the missing link in autoimmunity with rheumatoid arthritis as a disease model. *Front. Microbiol.* 5:783. doi: 10.3389/fmicb.2014.00783
- Soufi, B., Krug, K., Harst, A., and Macek, B. (2015). Characterization of the *E. coli* proteome and its modifications during growth and ethanol stress. *Front. Microbiol.* 6:103. doi: 10.3389/fmicb.2015.00103
- Spät, P., Macek, B., and Forchhammer, K. (2015). Phosphoproteome of the cyanobacterium *Synechocystis* sp. PCC 6803 and its dynamics during nitrogen starvation. *Front. Microbiol.* 6:248. doi: 10.3389/fmicb.2015.00248
- Stannek, L., Gunka, K., Care, R. A., Gerth, U., and Commichau, F. M. (2015). Factors that mediate and prevent degradation of the inactive and unstable GudB protein in *Bacillus subtilis*. *Front. Microbiol.* 5:758. doi: 10.3389/fmicb.2014.00758
- Zhou, L., van Heel, A. J., and Kuipers, O. P. (2015). The length of a lantibiotic hinge region has profound influence on antimicrobial activity and host specificity. *Front. Microbiol.* 6:11. doi: 10.3389/fmicb.2015.00011
- van Staalduinen, L. M., and Jia, Z. (2015). Post-translational hydroxylation by 2OG/Fe(II)-dependent oxygenases as a novel regulatory mechanism in bacteria. *Front. Microbiol.* 5:798. doi: 10.3389/fmicb.2014.00798

Conflict of Interest Statement: The authors declare that the research was conducted in the absence of any commercial or financial relationships that could be construed as a potential conflict of interest.

Copyright © 2015 Grangeasse, Stülke and Mijakovic. This is an open-access article distributed under the terms of the Creative Commons Attribution License (CC BY). The use, distribution or reproduction in other forums is permitted, provided the original author(s) or licensor are credited and that the original publication in this journal is cited, in accordance with accepted academic practice. No use, distribution or reproduction is permitted which does not comply with these terms.

Comparative Ser/Thr/Tyr phosphoproteomics between two mycobacterial species: the fast growing *Mycobacterium smegmatis* and the slow growing *Mycobacterium bovis* BCG

OPEN ACCESS

Edited by:

Ivan Mijakovic,
Chalmers University of Technology,
Sweden

Reviewed by:

Chung-Dar Lu,
Georgia State University, USA
Gustavo Antonio De Souza,
University of Oslo, Norway

*Correspondence:

Jonathan M. Blackburn and
Nelson C. Soares,
Applied and Chemical Proteomics
Group, Division of Medical
Biochemistry and Institute of Infectious
Disease and Molecular Medicine,
Faculty of Health Sciences, University
of Cape Town, Anzio, Observatory,
Cape Town 7925, South Africa
jonathan.blackburn@uct.ac.za;
nelson.dacruzsoares@uct.ac.za

Specialty section:

This article was submitted to Microbial
Physiology and Metabolism, a section
of the journal Frontiers in Microbiology

Received: 30 November 2014

Accepted: 10 March 2015

Published: 08 April 2015

Citation:

Nakedi KC, Nel AJM, Garnett S,
Blackburn JM and Soares NC (2015)
Comparative Ser/Thr/Tyr
phosphoproteomics between two
mycobacterial species: the fast
growing *Mycobacterium smegmatis*
and the slow growing *Mycobacterium*
bovis BCG. *Front. Microbiol.* 6:237.
doi: 10.3389/fmicb.2015.00237

Kehilwe C. Nakedi, Andrew J. M. Nel, Shaun Garnett, Jonathan M. Blackburn* and Nelson C. Soares*

Blackburn Lab, Applied Proteomics and Chemical Biology Group, Division of Medical Biochemistry, Institute of Infectious Disease and Molecular Medicine, University of Cape Town, Cape Town, South Africa

Ser/Thr/Tyr protein phosphorylation plays a critical role in regulating mycobacterial growth and development. Understanding the mechanistic link between protein phosphorylation signaling network and mycobacterial growth rate requires a global view of the phosphorylation events taking place at a given time under defined conditions. In the present study we employed a phosphopeptide enrichment and high throughput mass spectrometry-based strategy to investigate and qualitatively compare the phosphoproteome of two mycobacterial model organisms: the fast growing *Mycobacterium smegmatis* and the slow growing *Mycobacterium bovis* BCG. Cells were harvested during exponential phase and our analysis detected a total of 185 phospho-sites in *M. smegmatis*, of which 106 were confidently localized [localization probability (LP) = 0.75; PEP = 0.01]. By contrast, in *M. bovis* BCG the phosphoproteome comprised 442 phospho-sites, of which 289 were confidently localized. The percentage distribution of Ser/Thr/Tyr phosphorylation was 39.47, 57.02, and 3.51% for *M. smegmatis* and 35, 61.6, and 3.1% for *M. bovis* BCG. Moreover, our study identified a number of conserved Ser/Thr phosphorylated sites and conserved Tyr phosphorylated sites across different mycobacterial species. Overall a qualitative comparison of the fast and slow growing mycobacteria suggests that the phosphoproteome of *M. smegmatis* is a simpler version of that of *M. bovis* BCG. In particular, *M. bovis* BCG exponential cells exhibited a much more complex and sophisticated protein phosphorylation network regulating important cellular cycle events such as cell wall biosynthesis, elongation, cell division including immediately response to stress. The differences in the two phosphoproteomes are discussed in light of different mycobacterial growth rates.

Keywords: mycobacteria, phosphoproteome, protein phosphorylation, cell division, growth rate

Introduction

Mycobacterium tuberculosis is the causative agent of tuberculosis (TB), a major health concern worldwide. The current incidence of tuberculosis disease in South Africa is more than 900 cases per 100,000 people per year. Moreover, the World Health Organisation have estimated that roughly one third of the world's population is latently infected with *M. tuberculosis*. The majority of latently infected individuals will remain asymptomatic throughout their lives, with the risk of developing active TB disease from a latent infection being ~10% per lifetime; in HIV positive individuals though, this risk increases to 10% per year (WHO, 2014). This latent infected population is thus a substantial reservoir of potential new TB cases and is therefore a significant public health concern. The ability of mycobacteria to adapt to, and overcome, hostile environmental conditions in order to survive within host cells depends on a fine-tuned and orchestrated series of events (e.g., response to stress; metabolic remodeling; changes in growth rate) that will ultimately define the success of establishing and maintaining long term infection (McKinney et al., 2000; Marrero et al., 2010). *M. tuberculosis* infection is often described by two distinct phases: an active phase, in which the microorganism is thought to be growing at or close to its maximum rate; and latent infection, in which the bacilli are thought to persist in a viable but perhaps more dormant-like state with lower or non-existent growth rate. Current thinking suggests that there is most likely a continuum of states between latent TB infection (LTBI), sub-clinical TB and active TB disease, but to date no *M. tuberculosis* bacilli have been observed in LTBI individuals, so the exact physiological state of *M. tuberculosis* during a latent infection remains unknown.

Alongside the increasing number of new TB infections there is another matter of great concern, which is the emergence and spread of multi- and extensively drug resistant *M. tuberculosis* strains. Here unique growth related mechanisms of *mycobacteria* which facilitate adaptation to different adverse micro-environments are thought to play an important role in the mechanisms of drug tolerance and acquired resistance that are observed during infection (Corper and Cohn, 1933; Wayne and Hayes, 1996). For instance, a recent study showed that diverse growth-limiting stresses trigger a common signal transduction pathway in *M. tuberculosis* that induces triglyceride synthesis, which is associated with slowing down of growth and reduced antibiotic efficacy (Baek et al., 2011). Therefore, further investigation of the signaling pathways which regulate mycobacterial growth rate might reveal important information regarding the capacity of *M. tuberculosis* to adapt to its environment and in particular how this relates to drug tolerance and to the ability to establish infection.

In *M. tuberculosis*, Ser/Thr phosphorylation is essential for growth and environmental adaptation (as reviewed by Kieser and Rubin, 2014). For instance, the Ser/Thr protein kinases (STPKs) PknA and PknB are essential for growth of *M. tuberculosis* in culture, indicating that phosphorylation plays a pivotal role in the survival of this bacterium (Sasseti et al., 2003; Kang et al., 2005; Fernandez et al., 2006; Molle and Kremer, 2010; Kusebauch et al., 2014). These STPKs are encoded by an operon which

regulates genes involved in cell shape determination, cell wall synthesis, and cell division (Deol et al., 2005; Kang et al., 2005; Kusebauch et al., 2014). In addition to PknA and PknB, another group of STPKs comprised of PknG, PknL, and PknF appear to be involved in different aspects of *M. tuberculosis* growth regulation (Cowley et al., 2004; Deol et al., 2005; Canova et al., 2008). In support of the likely important role played by STPKs in *M. tuberculosis*, a mass spectrometry-based phosphoproteomic study identified more than 500 Ser/Thr phosphorylation sites on 300 proteins in *M. tuberculosis* (Prisic et al., 2010) and, more recently, a complementary study detected a number of Tyr phosphorylated proteins in *M. tuberculosis* (Kusebauch et al., 2014). Notably though, the physiological significance of these findings remains largely unexplored.

In the past years, the use of mycobacterial models such as *M. smegmatis* and *M. bovis* BCG have significantly contributed to our current understanding of *M. tuberculosis* biology and environmental adaptation (as reviewed by Shiloh and Champion, 2010). *M. bovis* BCG is an attenuated bovine tuberculosis bacillus by a serial passage in the laboratory (Calmette et al., 1921). This mycobacterium is a particular convenient model in part due to it is slow growth rate similar to that observed in *M. tuberculosis*. On other hand *M. smegmatis* is a fast growing mycobacterial species (with a doubling time of approximately 4 h) that has been widely used to investigate different aspects of mycobacterial physiology (Barry, 2001; Reyrat and Kahn, 2001; Danilchanka et al., 2008). As part of a concerted program to associate protein phosphorylation in mycobacteria with subsequent macromolecular events which determine growth rate and eventual environmental adaption, we have carried out a phosphopeptide enrichment and high throughput mass spectrometry-based study to investigate and compare the phosphoproteome of two model mycobacterial organisms—the fast growing *M. smegmatis* and the slow growing *M. bovis* BCG—our goal being to begin to elucidate the phosphorylation events and subsequent signal transduction pathways coordinating differential mycobacterial growth rates, which may in due course lead to important insights into *M. tuberculosis* physiology during active and latent infection—including aspects of slow growth associated drug resistance.

Materials and Methods

Bacterial Strains

Wild type strains of *M. smegmatis* mc²155 and *M. bovis* BCG Pasteur strain 1173P2 were grown in 7H9 Middlebrook (BD, Maryland, USA) broth supplemented with 0.05% Tween 80, OADC (Becton Dickinson) and 0.2% glycerol (v/v). Cells were grown at 37°C with continuous agitation (120 rpm).

Protein Extraction

Cells were harvested during the exponential phase (OD₆₀₀ ~1.2 and 0.6 for *M. smegmatis* and *M. bovis* BCG, respectively) by centrifugation at 4000 g for 15 min at 4°C, washed twice with Phosphate Buffered Saline pH (7.5) (PBS). Cells were snap frozen in liquid nitrogen and stored at -80°C until needed. Frozen pellets were suspended in 800 µl lysis buffer [500 mM Tris-HCl, 0.1% (w/v) SDS, 0.15% sodium deoxycolate, 1× protease

inhibitor cocktail, 1× phosphatase inhibitor cocktail (Roche, Mannheim Germany) and 50 µg/ml lysozyme (Repaske, 1956)]. Cells were disrupted by sonication at maximum power for six cycles of 30 s, with 1 min cooling on ice between cycles. Cellular debris was removed by centrifugation at 4000 g for 5 min and the lysate filtered through 20 µm pore size low-protein binding filters (Merck, NJ, USA). Proteins were precipitated using the chloroform-methanol precipitation method as previously described (Wessel and Flügge, 1984). The pellet was re-suspended in urea buffer (6 M urea, 2 M thiourea and 10 mM Tris-HCl, pH 8). Protein concentration was determined using a modified Bradford assay as described by Ramagli (1999).

In-Solution Trypsin Digestion

Five milligram of total protein was reduced with 1 mM DTT for 1 h with agitation and then alkylated with 5.5 mM IAA for 1 h in the dark. Proteins were pre-digested with Lysyl Endopeptidase LysC (Waco, Neuss, Germany) at room temperature for 3 h and diluted 4× with HPLC grade water before adding sequencing grade modified trypsin (Promega, Madison, USA) (1:100 w/w). Proteolysis was carried out at room temperature for 14 h with agitation at 30 rpm. Proteolysis was quenched by addition of trifluoroacetic acid (TFA) (Sigma Aldrich, St Louis, USA).

Phosphopeptide Enrichment with TiO₂ Chromatography

Acetonitrile (ACN) (Sigma Aldrich, St Louis, USA) at a final concentration of 30% was added to the tryptic peptides and the pH was adjusted to 2. Ten milligram of Titasphere TiO₂ beads (MZ Analysentechnik, Mainz, Germany) in loading buffer [30 mg/ml 2,5 dihydrobenzoic acid (Sigma Aldrich, St Louis, USA), 80% ACN] were added to the sample and incubated at room temperature with rotation for 1 h. The beads were pelleted and the decanted supernatant was further incubated with a fresh batch of 5 mg of beads for 30 min. This step was repeated one further time, giving three fractions of enriched phosphoproteins bound to beads in total. Phosphopeptides bound to the beads were washed vigorously with shaking for 10 min in 1 ml of wash buffer 1 (30% acetonitrile, 3% trifluoroacetic acid) followed by an additional 10 min of vigorous wash with wash buffer 2 (80% acetonitrile, 0.1% trifluoroacetic acid). Phosphopeptides were loaded onto C8 stage tip, washed with wash buffer 2 and then eluted with 3 × 50 µl Elution buffer [40% Mass-spec grade NH₄OH (aq, 25% NH₃; Sigma-Aldrich, St Louis, USA), 60% acetonitrile (pH 10.5 or higher)]. Solvent was removed in a speed drying vacuum at room temperature and peptides were resuspended in 20 µl Solvent A (2% ACN, 0.1% formic acid).

LC/MS/MS Analysis

Liquid chromatography separation was carried out using a pre-column (100 µm ID × 20 mm) connected to an analytical column (75 µm × 500 mm) packed with C18 Luna 5 µ 100 Å beads (phenomenex 04A-5452). The columns were connected to an Easy n-LC II system (Proxeon). 5 µl of resuspended phosphopeptides were loaded onto the column with starting mobile phase of 2% ACN, 0.1% formic acid. Peptides were eluted with the following gradient 5% ACN to 35% ACN for 120 min then up to 80% ACN

over 5 min staying at 80% ACN for 10 min, this was followed by a column wash of 7 to 80% gradient for 30 min, and a column equilibration at 2% ACN for 2 min. The flow rate was held at 300 nL/min.

Mass spectra were acquired on an Orbitrap Q Exactive mass spectrometer in a data-dependent manner, with automatic switching between MS and MS/MS scans using a “Top-10” method. MS spectra were acquired at a resolution of 70,000 with a target value of 3×10^6 ions or a maximum injection time of 250 ms. Peptide fragmentation was performed via higher-energy collision dissociation (HCD) with the energy set at 25 NCE. Intensity threshold for ions selection was set at 1.7e4 with charge exclusion of $z = 1$ and $z > 5$. The MS/MS spectra were acquired at a resolution of 17,500, with a target value of 2×10^5 ions or a maximum injection time of 120 ms. The scan range was limited to 300 to 1750 m/z and the isolation window at 4.0 m/z.

Data Processing

Maxquant software package version 1.5.0.3 with integrated Andromeda search engine was used to analyse the raw MS spectra acquired. *M. smegmatis* (taxonomy 246196) and *M. bovis* BCG Pasteur (taxonomy 410289) databases obtained from Uniprot were used as the target-decoy databases for the Andromeda search. LysC and Trypsin were defined as proteases and two missed cleavages were allowed. Phosphorylation on serine, threonine, and tyrosine residues, oxidation of methionines and N-terminal acetylation were specified as variable modifications. Carbamidomethylation on cysteines was defined as a fixed modification. We allowed a FTMS MS/MS match tolerance of 20 ppm. False discovery rate was set at 1% for identification of peptides and proteins without re-quantifying. Stringent filtering criteria were employed to validate phospho sites. Phosphopeptides were considered as high confidence phosphorylation events and taken for further analysis only if they had a localization probability of >0.75, had a posterior error probability (PEP) score of <0.001. We further manually validated the phospho sites on the Maxquant viewer for good b- and y- ion series coverage.

Bioinformatics

Predicted Gene Ontology (GO) cellular functions of identified phosphoproteins with high confidence from two mycobacterium strains were obtained from The Database for Annotation, Visualization and Integrated Discovery (DAVID, v6.7) and were grouped into functional categories. To compare the identified phosphoproteomes of these two mycobacterial species, we identified homologs of the *M. smegmatis* phosphorylated proteins in *M. bovis* BCG using the University of Cape Town's Computational Biology online bioinformatics tool found at <http://galaxy-fen.uct.ac.za/root>. For identification of tyrosine-phosphorylation site motifs, we used the Motif-X algorithm (Schwartz, 2005). We defined a sequence window of +/- 10 amino acids on each side of the tyrosine site and generated the sequence logo by Phosphosite logo generator using the algorithm PSP production (Cell signaling Technology). We aligned genomic sequences of both strains using the online tool, obtained from <http://www.ebi.ac.uk/Tools/msa/clustalw2/> and respective fasta files were obtained from Uniprot.

Results and Discussion

There is increasing evidence indicating that protein phosphorylation plays an essential role during mycobacterial cell division and environmental adaptation. Understanding the mechanistic connection between such regulatory signaling networks and mycobacterial growth rate requires a global view of the phosphorylation events taking place at a given time under defined conditions. Here, we have carried out a comparative phosphoproteomic analysis of two mycobacterial strains—one fast growing (*M. smegmatis*), the other slow growing (*M. bovis* BCG). Our analysis included three rounds of TiO₂ chromatography to enrich phosphorylated peptides (see **Supplementary Figure S1**), followed by subsequent analysis of phosphorylation-events using liquid chromatography coupled with state-of-the-art high resolution tandem mass spectrometry (LC/MS/MS) (**Supplementary Figure S2a and S2b**), in order to compare the phosphoproteomes of these two model mycobacterium species during exponential growth.

In this study we considered all phosphorylation-events that were detected in any of the biological replicates, and only confidently localized phospho-sites (*p*-sites) (**Figure 1**), were considered for qualitative comparative analysis and further discussion. In the two *M. bovis* BCG replicates, we detected a

total of 442 *p*-sites of which 289 were confidently localized (Localization probability (LP) = 0.75; PEP = 0.01) and 169/289 had a LP = 0.99 (**Supplementary Table S1A** and **Figure S2c**). We identified 88,822 MS/MS spectra corresponding to 7784 non-redundant peptide sequences (**Supplementary Figure S2d**) and 1765 protein groups (402 were identified by a single peptide) (**Supplementary Table S1A**). The estimated false discovery rate (FDR) was 0.32 at the peptide level, 0.30 at the modification level, and 1.03 at the protein level. Our initial analysis of two biological replicates of *M. smegmatis* revealed considerable differences in the number of identified *p*-sites between the two Mycobacterial species, 77 *p*-sites for *M. smegmatis* (**Supplementary Figure S2e**) compared to 289 for *M. bovis* BCG. To verify that these differences observed were biological, we further analyzed three additional biological replicates for *M. smegmatis* (**Supplementary Table S1B**). Phosphoproteomic analysis of five biological replicates of *M. smegmatis* protein extracts resulted in identification of 180, 396 MS/MS spectra, corresponding to 16, 185 non-redundant peptide sequences (**Supplementary Figure S2f**) and 2, 462 protein groups (464 were identified by a single peptide) (**Supplementary Table S1B**). The estimated false discovery rate (FDR) was 0.22 at the peptide level, 0.21 at the modification level, and 0.98 at the protein group level. We detected a total of 185 phospho-sites in *M. smegmatis*, of

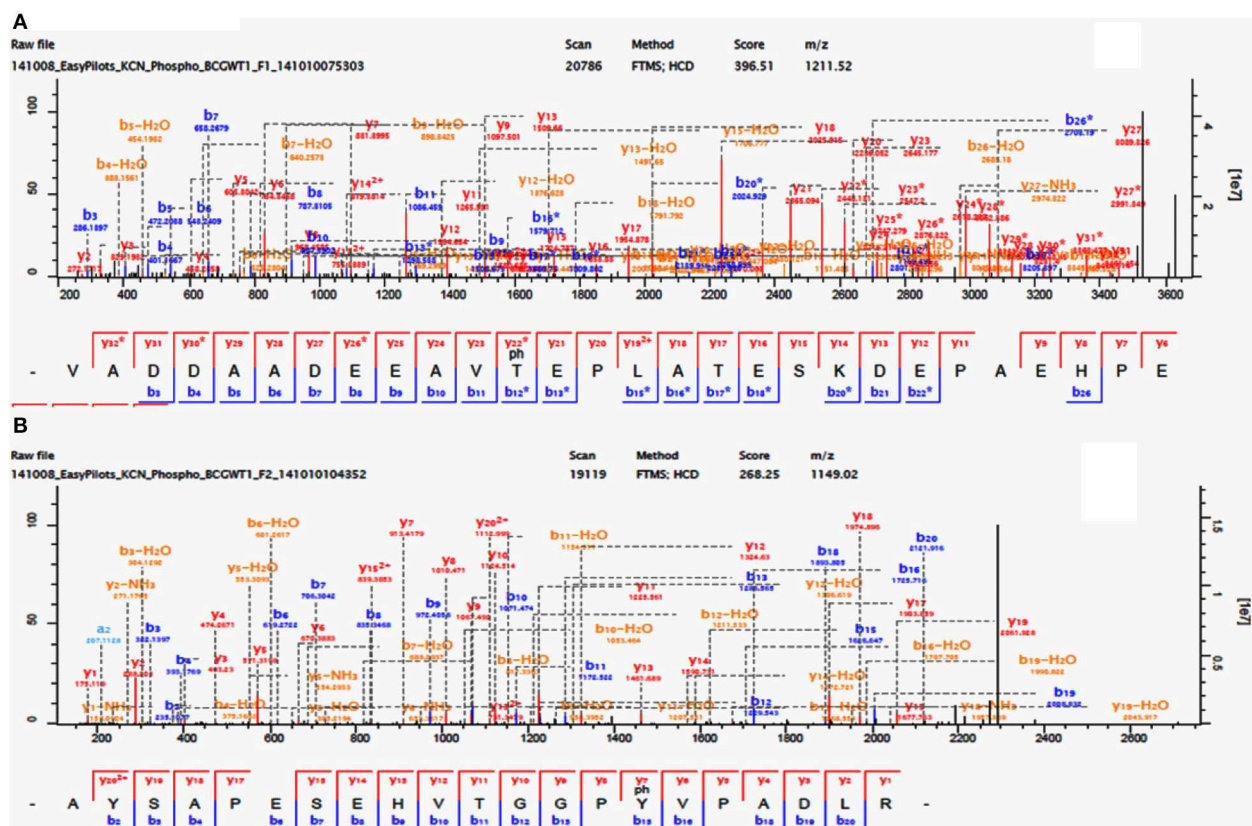


FIGURE 1 | Phosphorylation of *M. bovis* BCG Cell division FtsQ (Thr₂₄) and probable conserved protein membrane mmpS3 (Tyr₇₀).
(A) Identification of phosphorylated residue by mass spectrometry.

Fragmentation spectra for modified peptide bearing the phosphorylated Thr₂₄. (B) Fragmentation spectra for modified peptide bearing the phosphorylated Tyr₇₀.

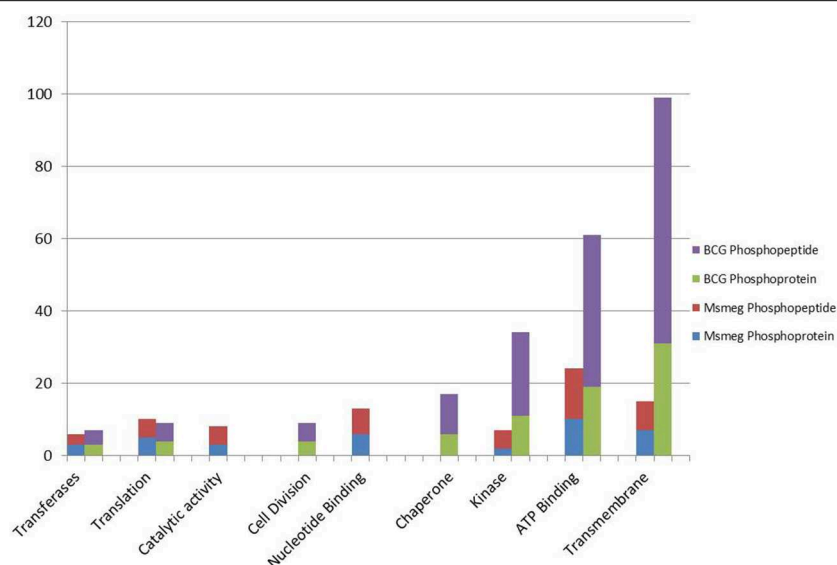


FIGURE 2 | A histogram showing the GO molecular functions of identified phosphoproteins and respective number of phosphopeptides as predicted from their genome annotations.

which 106 were confidently localized ($LP = 0.75$; $PEP = 0.01$) and 64/106 had a $LP = 0.99$ (**Supplementary Table S1B**). In detail, for *M. bovis* BCG, we detected 289 *p*-sites on 203 phosphoproteins: 35.3% on serine (pSer), 61.6% on threonine (pThr) and 3.1% tyrosine (pTyr). For *M. smegmatis* we detected 106 *p*-sites on 76 phosphoproteins: 39.47% on serine (pSer), 57.02% on threonine (pThr) and 3.51% on tyrosine (pTyr). Both phosphoproteomes were biased toward Thr compared with Ser (57–61%; 41–35%), which agrees with previous reports on *M. tuberculosis* H37Rv (Prisic et al., 2010). Importantly, the percentage of Tyr phosphorylation in *M. bovis* BCG was closer to that reported in *M. tuberculosis* (Kusebauch et al., 2014). Although it had previously been suggested that Tyr phosphorylation was non-existent within mycobacterial species, it was recently confirmed that Tyr phosphorylation does in fact occur on a number of diverse *M. tuberculosis* proteins (Kusebauch et al., 2014). Here, we have confidently identified nine Tyr *p*-sites in eight proteins in *M. bovis* BCG (**Table 1**, **Figure 1B** and **Supplementary Table S1A**) and four in *M. smegmatis*, supporting earlier suggestions that phosphorylation on Tyr residues occur in different mycobacterial species (Kusebauch et al., 2014).

The differences between the compared phosphoproteomes compelled us to investigate whether some of these dissimilarities could be explained by genomic events rather than post-translational control. The multiple sequence alignment of 130 selected *M. bovis* BCG phosphoproteins with their respective *M. smegmatis* orthologs (**Supplementary S3A**) revealed that from 197 *M. bovis* BCG Ser/Thr/Tyr phosphorylated sites: 12 are conserved across the two mycobacterial species and were found to be phosphorylated in both species, while 94 conserved Ser/Thr/Tyr residues were found to be phosphorylated in *M. bovis* BCG only. Furthermore, whereas 91 *M. bovis* BCG phosphorylated residues were aligned with

a different non-phosphorylated *M. smegmatis* residue, 72 of these were aligned with a non-phosphorylated amino acid (**Supplementary S3A**) and 19 were aligned with different non-phosphorylated Ser/Thr/Tyr residue. Conversely, the multiple sequence alignment of 64 *M. smegmatis* phosphoproteins with their respective *M. bovis* BCG orthologs showed that besides the 12 conserved Ser/Thr/Tyr residues phosphorylated in both species, 31 conserved residues were found to be phosphorylated in *M. smegmatis* only. In this case, while 43 *M. smegmatis* phosphorylated residues were aligned with a different non-phosphorylated *M. bovis* BCG amino-acid, 36 of these were aligned with a non-phosphorylated amino acid residue (**Supplementary S3B**) and seven were aligned with different non-phosphorylated Ser/Thr/Tyr residue (**Supplementary S3B**). These results point out that some of differences observed between the two phosphoproteomes can be explained by the absence of the corresponding amino acid residue, indicating that during exponential growth phase these two mycobacterial species present an inherently different sub-set of Ser/Thr/Tyr kinase substrates. Additionally, there are some interesting examples in which orthologous proteins were phosphorylated at different *p*-sites. This suggests that kinase specificities for a substrate could be intimately related with the actual site of phosphorylation. Finally, it is notable that occasions the Ser/Thr/Tyr residue was aligned with different Ser/Thr/Tyr residue (in most cases S for T and vice versa) in some punctual situation the respective residue was phosphorylated (e.g., PknB) but for the majority of the cases these were aligned with non-phosphorylated Ser/Thr/Tyr residue. This intriguing observation leaves open the possibility that Ser/Thr exchange could be a result of an evolutionary processes/environmental adaptation, in which the replacement for the respective residue would probably favor site phosphorylation and therefore the gain of an additional mechanism of protein

TABLE 1 | List of Tyr phosphorylated proteins/sites identified in *M. bovis* BCG and *M. smegmatis*.

Acc. number ^a	Protein description	Phosphorylated peptide sequence and phosphorylated site	Position of the phosphorylated Tyr
A1KEI8	Uncharacterized protein FHA domain-containing protein	HPGQGDYPEQIGY(1) ^b PDQGGYPEQR	215*
		GGYPPEGGYPPQPGY(1)PRPR	232*
A1KFR2	60kDa chaperonin 1	VAQIRQEIENSDDSY(0.919)DREK	358*
A1KFP3	Uncharacterized proteinHydrolase domain-containing protein	GLAEGPLIAGGHSY(1)GGR	99
A1KI63	Uncharacterized protein	SAY(0.913)PDGIADHDRPLAPR	8
A1KKP0	Probable isocitrate lyase aceA	MGIEAIY(0.998)LGGWATSAK	104
A1KKP0	Probable conserved membrane protein mmpS3	AYSAPSEHVTGGPY(1)VPADLR	70*
A1KKR9	Uncharacterized protein CYTH-like domain containing protein	Y(0.847)TAATGADNVSQEA	428
A1KPH7	Conserved hypothetical mce associated protein	RDCASVMVY(0.973)LNRTVTDK	122
^A0QWX0	Carbohydrate kinase FGGY	Y(1)NYDTLAGR	1
^A0QQ14	Carbohydrate kinase FGG	ISAWY(0.968)VER	5
^A0QSS3	10 kDa chaperonin	Y(1)GGTEIK	1
^A0QQU5	60 kDa chaperonin 1	AEIENSDDSY(0.915)DREK	10

*Tyr phosphorylated sites that were previously identified in *M. tuberculosis* H37Rv (Kusebauch et al., 2014).

^ Tyr phosphorylated sites in *M. smegmatis*.

^aUniprot protein accession number.

^bPhosphorylated Tyr (Y) and respective Localization probability.

functional regulation. Although speculative, it would be interesting to explore further in which conditions these sub set of Ser/Thr/Tyr sites are phosphorylated.

Finally, the number of phosphoproteins/sites identified in *M. smegmatis* is comparable to those reported in other soil bacteria, e.g., *E. coli* (Macek et al., 2008; Soares et al., 2013), *Bacillus subtilis* (Shi et al., 2014) and *Pseudomonas putida* (Ravichandran et al., 2009), as well as in some pathogenic bacteria such as *Pseudomonas aeruginosa* (Ravichandran et al., 2009), *Streptococcus pneumonia* (Sun et al., 2009), *Helicobacter pylori* (Ge and Shan, 2011), and *Klebsiella pneumonia* (Lin et al., 2009). Whereas, the number of phosphorylated Ser/Thr/Tyr detected in *M. bovis* BCG phosphoproteome is comparable to that described in *M. tuberculosis* H37Rv (Prisic et al., 2010). It is of particular interest that the *M. bovis* BCG phosphoproteome shows a number of phosphoproteins/sites that are orthologous to those reported in *M. tuberculosis* H37Rv (Prisic et al., 2010) but also a number that are not conserved. Recently a comparison between the Ser/Thr/Tyr phosphoproteomes of *Acinetobacter baumannii* reference strain (ATCC17978) and a highly invasive, multidrug resistant clone (AbH12O-A2) demonstrated that, during stationary phase, the multidrug isolate showed twice as many phosphorylation-events as the reference strain (Soares et al., 2014). In contrast to reports on *Pseudomonas* species (Ravichandran et al., 2009), our current study supports the notion that bacteria within the same genus/species may utilize differing numbers of phosphoproteins.

Phosphoproteomic Analysis Reveals Conserved Ser/Thr/Tyr Phosphorylated Sites Across Mycobacterial Species

Conserved Ser/Thr Phosphorylated Sites

Macek et al. (2008) reported evidence of a possible high degree of conservation within potential bacterial phospho-sites although,

as noted by those authors, the conservation of residues does not mean that they are phosphorylated in all species. In fact, as the number of bacterial phosphoproteomic studies increases, it is becoming clearer that the degree of conserved phospho-sites among bacterial species is rather limited and certainly lower than reported within eukaryotic phosphoproteomes (e.g., Freschi et al., 2014). Here, a comparison between the *M. smegmatis*, *M. bovis* BCG, and *M. tuberculosis* H37Rv (Prisic et al., 2010; Kusebauch et al., 2014) phosphoproteomes revealed that these three mycobacterial species share a number of conserved phosphorylated sites (Table 2). Interestingly, we found that *M. bovis* BCG and *M. tuberculosis* H37Rv phosphoproteomes share at least 32 Ser/Thr conserved phospho-sites on 27 proteins, of which three were conserved in all three species (Table 2). As pointed out by Freschi et al. (2014), phosphorylation sites that are phosphorylated in different species are more likely to be functional and this conservation criterion could be used to prioritize phosphorylation events for additional characterization.

In the present study we have focused in particular on the STPKs PknB and PknA that have known or predicted functions in cell wall generation and growth in *M. smegmatis*, *M. bovis* BCG, and *M. tuberculosis* (Gee et al., 2012; Kusebauch et al., 2014). We found PknB to be phosphorylated in Thr₁₇₃ in all three species and in Thr₁₇₁ in *M. smegmatis* and *M. bovis* BCG (Table 2). Previous *in vitro* assays demonstrated that both Thr₁₇₃ and Thr₁₇₁ are conserved auto-phosphorylated residues that lie in the activation loop of PknB (Boitel et al., 2003). Additionally, a *M. tuberculosis* double mutant Thr₁₇₁/Thr₁₇₃ was 300-fold less active than respective wild-type PknB, suggesting a combined effect of both Thr₁₇₁ and Thr₁₇₃ residues on kinase activity. Subsequent studies confirmed that the mutation of these residues had a strong effect not only on PknB kinase activity but also in the process of activation loop-mediated recruitment of its substrates (Villarino et al., 2005). Here we have provided evidence that Thr₁₇₃ and Thr₁₇₁

TABLE 2 | Summary of the phosphorylated sites found in more than one Mycobacterial species.

Acc. number ^a	Protein description	<i>M. bovis</i> BCG	<i>M. smegmatis</i>	Mtb H37Rv [*]
P65727	Ser/Thr-protein kinase PknA	Ser ^b ₃₀₉	Ser ₃₁₀	Ser ₃₀₉
		Ser ₃₁₆	Thr ₃₁₆	-
		Ser ₂₉₉ ; Thr ₃₀₁ ; Thr ₃₀₂	-	Ambiguous Residues 299–302
		Thr ₂₂₄		Thr ₂₂₄
P0A5S5	Ser/Thr-protein kinase PknB	Thr ₁₇₃	Thr ₁₇₃	Thr ₁₇₃
		Thr ₁₇₁	Thr ₁₇₁	-
Q02251	Mycocerosic acid synthase	Ser ₂₁₁₁	-	Ser ₂₁₁₁
Q7TVL9	Possible acyltransferase	Ser ₂₃₀	-	Ser ₂₃₀
P64169	Cell division protein FtsQ	Thr ₂₄	-	Thr ₂₄
Q7TY31	Conserved alanine and glycine and valine rich	Thr ₂₃₂	-	Thr ₂₃₂
Q7U2K5	Possible conserved transmembrane transport protein MMPL3	Thr ₉₁₀	-	Thr ₉₁₀
		Thr ₈₉₃	-	Thr ₈₉₃
Q7U2N3	Probable conserved MCE associated membrane protein	Thr ₁₆	-	Thr ₁₆
Q7VEQ4	L-asparagine permease 1	Thr ₄₇₄	-	Thr ₄₇₄
Q7U280	Isoniazid inducible gene protein	Ser ₆₂	-	Ser ₆₂
P65379	Putative membrane protein mmpS3	Ser ₅₈	-	Ambiguous residues 58–66
		Thr ₆₆	-	Thr ₆₆
		Thr ₄₇	-	Thr ₄₇
		Thr ₅₀	-	Thr ₅₀
P0A515	Guanylate Kinase	Thr ₉	-	Thr ₉
Q7TXB8	Phosphoglucosyltransferase PGMA	Ser ₁₄₇	Ser ₁₄₇	Ser ₁₄₇
		-	Ser ₁₄₂	Ambiguous residues 135–152
P0A521	60 kDa chaperonin 2	Thr ₁₄₆	-	Thr ₁₄₆
P45811	30S ribosomal protein S4	Thr ₁₄₇	-	Thr ₁₄₇
Q7U046	Probable lipase LIPH	Ser ₁₆₅	-	Ser ₁₆₅
Q7TXZ1	Cell division transmembrane protein FTSK	Thr ₆₄₂	-	Thr ₆₄₂
P66947	Probable acetolactate synthase	Thr ₅	-	Thr ₅
P66843	Signal recognition particle receptor FtsY	Thr ₇₂	-	Thr ₇₂
P66890	Sec-independent protein translocase TatA	Thr ₆₀	-	Thr ₆₀
		Thr ₇₈	-	Thr ₇₈
P0A549	Chaperone protein DnaJ1	Thr ₁₂₀	-	Thr ₁₂₀
Q7TVL6	Possible phosphotransferase	Ser ₂₅₀	-	Ser ₂₅₀
P6387	Chaperone protein ClpB	Thr ₇₉	-	Thr ₇₉
P63857	Cytochrome c oxidase subunit 3	Thr ₇	-	Ambiguous residues 2–14
		Thr ₁₃	Thr ₁₃	Ambiguous residues 2–14
Q7TYA1	Export membrane protein SecF	Ser ₃₉₆	-	Ambiguous residues 372–407
Q7U241	Probable Phosphoribosylglycinamide	Thr ₂₀₆	-	Thr ₂₀₆
Q7TVC7	Probable peptidoglycan hydrolase	Thr ₄₃	-	Thr ₄₃
Q7TTR2	Long-chain-fatty-acid-AMP FadD32	Thr ₅₅₂	-	Thr ₅₅₂
P0A611	Possible transmembrane cation	Ser ₂₆₈	-	Ser ₂₆₈
P0A611	Single-stranded DNA-binding protein SSB	Ser ₁₅₂	-	Ambiguous residues 123–154
P0A727	Transcriptional regulatory protein PrrA	Thr ₆	-	Thr ₆
P65379	Putative membrane protein mmpS3	Tyr ₇₀	-	Tyr ₇₀
Q7U303	Conserved protein with fha domain	Tyr ₂₃₂	-	Tyr ₂₃₂
		Tyr ₂₁₅	-	Tyr ₂₁₅
P0A521	60kDa Chaperonin 2	Tyr ₃₅₈		Tyr ₃₅₈

^{*} Ser/Thr phosphorylated sites that were previously identified in *M. tuberculosis* H37Rv (Prisic et al., 2010).

^a Uniprot protein accession number.

^b Ser/Thr residue found phosphorylated in the indicated Mycobacterial species.

–, Not detected.

phosphorylation both occur *in vivo* during the exponential phase, at which PknB is most abundant and is thought to be at its maximum activity. Thus, our data reinforces a previous hypothesis suggesting that *in vivo* this enzyme is regulated through an auto-phosphorylation mechanism involving the phosphorylation state of both Thr₁₇₃ and Thr₁₇₁.

Another proposed mechanism of PknB regulation relates to the maintenance of an inactive state *via* the interaction of the juxtamembrane region with the kinase domain. In this model, the auto-phosphorylation of specific residues in the juxtamembrane sequences releases the inhibition by making the sequence available for further interactions with domains of target proteins (Wybenga-Groot et al., 2001). However, previously it was not clear whether Thr₂₉₄ and/or Thr₃₀₉ were the target residues involved so it is notable that our data clearly demonstrate that PknB of *M. bovis* BCG is in fact phosphorylated on Thr₃₀₉.

Our analyses indicate that PknA is phosphorylated in at least one conserved residue, Ser₃₀₉/Ser₃₁₀ (see Table 2). Intriguingly, in this study *M. bovis* BCG PknA was found to be phosphorylated on seven different residues (three Ser and four Thr, respectively), all located in the juxtamembrane region. Unlike PknB, in PknA the juxtamembrane region, encompassing residue 269–338 is indispensable not only for auto-phosphorylation of PknA but also for its substrate phosphorylation ability (Thakur et al., 2008). STPKs exhibit a wide variety of mechanisms for their regulation. Taking into account the degree of phosphorylation verified here in the juxtamembrane region of *M. bovis* BCG PknA compared to that observed in *M. smegmatis* PknA, it is tempting to speculate that this level of phosphorylation of the juxtamembrane region could be in fact limiting the access of PknA to its substrates and this way controlling the action of the enzyme. Importantly, as noted by Chawla et al. (2014), whilst the structure and mode of activation of PknB and PknA have been well established *in vitro*, the structure-function relationships of the various domains have yet to be investigated in the context of mycobacterial growth (Chawla et al., 2014). Here through a MS based phosphoproteomic approach we have established (at the phospho-site level) the phosphorylation state of different domains for both PknA and PknB *in vivo* during growth at exponential phase.

Conserved Tyr Phosphorylated Sites

In our study we have identified nine Tyr p-sites (see Table 1), of which four were also found to be phosphorylated in *M. tuberculosis* (Kusebauch et al., 2014): FHA-domain-containing protein (Tyr₂₁₅ and Tyr₂₃₂), 60 kDa chaperonin 1 (Tyr₃₅₈) and conserved membrane protein mmpS3 (Tyr₇₀) (Figure 1B). FHA-domain-containing protein is a substrate of numerous STPKs, including PknB. Phosphorylation of FHA by PknB has implication in cell wall synthesis with a possible involvement in mycobacterial virulence (Gupta et al., 2009). Likewise both 60 kDa Chaperonin and conserved membrane protein mmpS3 have been implicated in mycobacterial virulence (Wells et al., 2013). Based on our data, we searched for possible conservation of these peptides across other bacterial species. A sequence motif derived from 60 kDa Chaperonin Tyr₃₅₈ (RQEIENSDSDYDREKLQERLA) using Seq2Logo revealed an

overrepresentation of Tyr₃₅₈ (Figure 2). A conserved Tyr₃₆₀ residue on apparently conserved peptide (SDSDYDREKL) was found in three Gram negative pathogenic species, specifically *Shigella* spp., *Klebsiella* spp., and *Salmonella* spp., suggesting that this conserved Tyr phosphorylation site warrants further investigation for possible roles in bacterial pathogenesis.

Phosphoprotein Functional Enrichment

Gene ontology (GO) terms revealed that in both *M. bovis* BCG and *M. smegmatis*, the phosphoproteins/phosphosites were functionally enriched in nine distinct groups, (e.g., ATP binding, translation, kinase activity, cell division, see Figure 2). Of interest, a great deal of phosphorylated proteins in *M. bovis* BCG was clustered into the Transmembrane group (Figure 2). This included a considerable number of multiple phosphorylated proteins and some phosphorylated in internal as well as external regions, like BCG_3967, it is a probable trans-membrane protein and we found it to be phosphorylated four times, at position 10, which like on the flagellin domain and position 801 and 801, the kinase domain. This suggests that there are transmembrane proteins with a potential role in signal transduction. Additionally, it was visible that *M. bovis* BCG phosphoproteome comprised a notable group of phosphoproteins involved in cell division, possible implications of this is discussed below.

Phosphorylation Events Observed in Proteins that Regulate Mechanisms of Growth and Cell Division

Both PknA and PknB are encoded by genes (*pknA* and *pknB*, respectively) located on the same operon as protein phosphatase PstP, RodA (implicated in cell shape control) and PbpA (implicated in peptidoglycan synthesis) (Cole et al., 1998). This locus includes also two FHA (forkhead-associated) domain-containing proteins and in mycobacteria is found near the origin of replication. In *M. bovis* BCG, all proteins referred to above

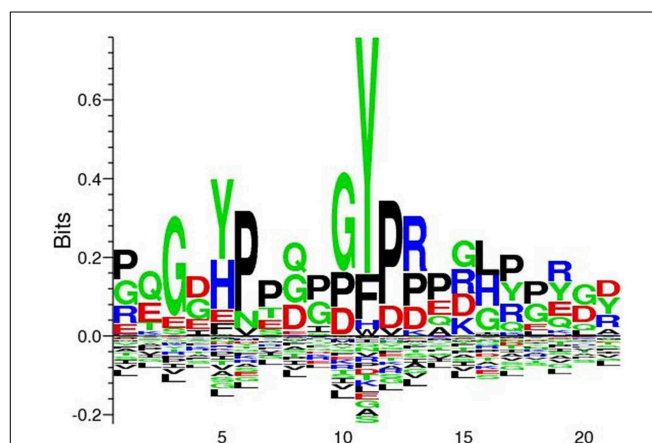


FIGURE 3 | Seq2Logo alignment analysis derived from 60 kDa chaperonin revealed an overrepresentation of Tyr₃₅₈. Seq2Logo analysis indicate that a conserved Tyr_{358–360} is found in additional three pathogenic species, specifically *Shigella* spp., *Klebsiella* spp., and *Salmonella* ssp.

(except PbpA) were found phosphorylated at a total of 15 p-sites: PknA (7); PknB (3); RodA (1); PstP (1) and FHA domain containing protein (3) (see **Supplementary Table S1A**). In *M. smegmatis*, however, only a few proteins were found phosphorylated at a total of 5 p-sites: PknA (2); PknB (2) FHA domain containing protein (1) (see **Supplementary Table S1B**). These observations suggest that the slow growth of *M. bovis* BCG preserves this central set of cell division proteins under a tight regulatory network in which key elements are intimately inter-related by an important series of functional (de)phosphorylation events. For example, PknA and PknB are regulated by PstP-mediated phosphorylation (Boitel et al., 2003; Chopra et al., 2003); additionally, recently it has been shown that both PknA and PknB phosphorylate PstP (Sajid et al., 2011). As discussed above, our results showed that both *M. smegmatis* and *M. bovis* BCG PknB has conserved phosphorylation on Thr₁₇₁ and Thr₁₇₃—both of which sites are known to be substrates for PstP—thus suggesting that in both cases PstP is at least partially inactive. This would make sense considering that during exponential phase PknA and PknB are likely to be at their peak of activity. PstP has been reported to be phosphorylated by PknB on Thr₁₇₃, Thr₁₄₁, Thr₂₉₀, and Thr₁₃₇ in its cytosolic domain and on Thr₁₇₄ by PknA (Sajid et al., 2011). Curiously phosphorylated PstP has been reported to be more active than its unphosphorylated form (Sajid et al., 2011). Here, our results indicate that PstP of *M. bovis* BCG is phosphorylated *in vivo* on the high confidence p-site, Ser₁₅₅ (see **Supplementary Table S1A**). Interestingly, PstP contains three metal-binding centers in its structure (Pullen et al., 2004), sharing the fold and two-metal center of human PP2C α whilst having a third Mn²⁺ in a site created by a large shift in a flap domain next to the active site; this Mn²⁺ occurs at the position of Ser₁₆₀ so it is plausible that phosphorylation of Ser₁₅₅ may directly interfere with PstP activity, thus accounting for our deduction here of reduced PstP activity during exponential phase growth.

Overall, *M. bovis* BCG has 3 times more STPKs and nearly 4 times respective p-sites compared to *M. smegmatis*. Apart from PknA and PknB, the *M. bovis* BCG phosphoproteome is comprised of PknG (Thr₉₅), PknH (Thr₁₇₄), PknE (Ser₃₀₄ and Ser₃₂₆) PknF (Thr₂₈₇). Some of these enzymes have previously been directly implicated in mycobacterial growth [e.g., PknG (Fiuza et al., 2008), PknH (Zheng et al., 2007), PknE and PknF (Gupta et al., 2014)] and it is therefore conceivable that some of the proteins comprising the *M. bovis* BCG phosphoproteome are in fact substrate of some of these phosphorylated protein kinases (*vide infra*). It is worth noting that our study has also identified several Two Component sensory signal transduction proteins as phosphoproteins (e.g., Two component sensory transduction protein regX3 (Thr₁₅₁ and Thr₁₅₃), Two component sensor histidine kinase ppr (Ser₄₄₆), Two component transcriptional regulatory pprA (Ser₂₀). These results are reminiscent of those previously described in *B. subtilis* (Jers et al., 2011) and suggest that in *M. bovis* BCG there may be cross talk between Ser/Thr/Tyr phosphorylation and Two component systems, which would add extra complexity to the overall protein phosphorylation signal transduction pathways regulating exponential growth of *M. bovis* BCG cells.

Phosphorylation Events Observed in Proteins that Regulates Mechanisms of Cell Elongation and Division

In mycobacteria, cell elongation is regulated by a macrocomplex that regulates peptidoglycan remodeling during growth by means of hydrolytic and synthetic roles (as reviewed by (Kieser and Rubin, 2014)). Our data indicate that in *M. bovis* BCG, three important proteins of the macromolecular elongation complex are phosphorylated during exponential growth, namely Wag31 (Ser₂₄₅), CwsA (Thr₇₇) and a putative hydrolase (BCG_0021 involved in peptidoglycan catabolic process) (Thr₄₃). In mycobacteria, Wag31 is phosphorylated by PknA and is essential for correct polar localization and biosynthesis (Jani et al., 2010; Lee et al., 2014); in addition, Wag31 is stabilized by the cell wall protein CwsA. Wag31 is thought to be phosphorylated during exponential phase and remains non- or lowly-phosphorylated during stationary phase (Kang et al., 2005; Park et al., 2008). Interestingly, Wag31, CwsA and the putative peptidoglycan hydrolase were not found amongst the *M. smegmatis* phosphorylated proteins in the present study. Whilst we cannot rule out that our assay did not isolate phosphorylated *M. smegmatis* Wag31, it is perhaps more likely that in the fast growing *M. smegmatis* the elongation complex is regulated by alternative non-phosphorylated mechanism.

Another macromolecular complex, named divisome, is responsible for mycobacterial cell division. Assembly and disassembly of this complex is regulated by protein phosphorylation (Kieser and Rubin, 2014). According to the our data, in *M. bovis* BCG there are five divisome proteins which are phosphorylated, including cell division FtsQ (Thr₂₄), FtsW-like protein (Thr₂₉), CwsA (Thr₇₇) as well as other additional phosphorylated cell division proteins such as RodA (Thr₄₆₃), cell division transmembrane protein FtsK (Thr₃₂₅; Thr₆₄₂) and FtsY (Thr₇₂), strongly suggesting that divisome assembly and indeed cell division in *M. bovis* BCG is subject to a high level of phosphorylation.

Of interest, in our analysis we have detected Hup, a conserved histidine-like protein, phosphorylated on three different p-sites (Thr₄₅, Thr₆₅, and Ser₉₀). In *Mycobacterium* sp., the homolog of HU (Mhpl) is implicated in bacterial adaptation to stress response conditions, possible inhibition of cellular metabolism and reduction of bacterial growth rate through nucleoid reorganization (Lee et al., 1998; Matsumoto et al., 1999; Katsube et al., 2007). Apparently, is expressed in exponentially growing cells of *M. tuberculosis* H37Ra and it is shown to be maximally expressed during stationary phase, while Hup kinases (PknE, PknF, and PknB) were found to be constitutively expressed during exponential phase (Gupta et al., 2014). It has been suggested that the phosphorylation of HupB during the exponential phase by the referred kinases would limit the interaction with DNA (Gupta et al., 2014). In our *M. bovis* BCG data we have identified all the intervenient proteins involved in the described posttranslational regulation mechanism, including the phosphorylation of phosphosite Hup Thr₆₅. It is therefore appropriate to assume that the same mechanism takes place in *M. bovis* BCG cells during exponential growth, and although under limited action it remains possible that the rate of unphosphorylated HupB would have

an impact on the overall growth rate. In contrast, we did not find any evidence to indicate that similar mechanisms operate in *M. smegmatis* cells during exponential growth.

Stress Related Proteins

In rich broth during exponential phase, bacteria experience nearly optimal conditions of growth where there is excess nutrients and little accumulation of by products, in addition to scarce competition between bacterial cells. Surprisingly, under these conditions we observed an unexpected number of chaperones and stress related proteins in the *M. bovis* BCG phosphoproteome: For instance hyperosmotic and heat shock related proteins such as the chaperon protein DnaJ (Thr₁₂₀) chaperon protein DnaK (Ser₅₅₈) and GrpE (Ser₁₂ and Thr₂), multiply phosphorylated 60 kDa chaperonin, 10 kDa chaperonin, and Copper-sensing transcriptional repressor CsoR (Thr₉₃). On the other hand none of these stress related proteins were found in the *M. smegmatis* phosphoproteome, which suggests that even under optimal environmental conditions, slow growing mycobacteria such as *M. bovis* BCG maintain a preventive basal level of stress-related proteins that may act as frontline defense barrier to ensure adequate and prompt response to any sudden change in local environmental conditions. In this scenario protein phosphorylation would keep most of these proteins in an inactive state, whereby dephosphorylation could then immediately recruit these proteins when environmental conditions become unfavorable. A convenient and versatile regulatory mechanism such as this could in fact be a determinant for the survival and persistence of some bacteria.

Conclusion and Perspectives

This study clearly demonstrated that there are major differences between a fast growing and a slow growing mycobacterial phosphoproteome. The *M. smegmatis* phosphoproteome observed here is in many aspects similar to those reported in other soil-dwelling bacterial models and can be viewed as a minimalist phosphoproteome compared to that of *M. bovis* BCG. This latter organism presents a much more complex and sophisticated protein phosphorylation network, regulating important cellular cycle events such as cell wall biosynthesis, elongation, and cell division, as well as apparently being involved in regulating response to stress, which over all would allow a quick cellular

response to abrupt environmental changes. However, this regulatory advantage might be associated with a cost, reflected by reduced metabolic fitness and slower growth rate.

This study demonstrates *M. bovis* BCG is a good model to study aspects of mycobacterial phospho-dependent signal transduction pathways, including those involved in persistence and slow growth, including that associated with drug resistance. By contrast, the substantial differences reported here in the phosphoproteomes of *M. smegmatis* and *M. bovis* BCG suggest that exponentially growing *M. smegmatis* cells *in vitro* are of limited relevance when modeling phosphorylation networks and phospho-regulation events likely to occur in *M. tuberculosis* at the site of disease during an infection.

Acknowledgments

We thank the National Research Foundation (NRF) for their financial support of this research and for a PhD bursary to KCN. NCS and JMB thank the NRF for the South African Research Incentive Funding for Rated Researchers and the Research Chair grants respectively. SG thanks the CSIR for a PhD bursary.

Supplementary Material

The Supplementary Material for this article can be found online at: <http://www.frontiersin.org/journal/10.3389/fmicb.2015.00237/abstract>

Supplementary Figure S1 | Phosphoproteomic workflow diagram.

Mycobacterial strains were harvested at exponential phase, lysed. In-solution digestion was then carried out TIO₂ phosphor enrichment and data acquisition with LC/MS/MS.

Supplementary Figure S2 | (a–f). Total Ion Chromatograms (TIC) and MS summary peptide/phosphopeptides identified in each experiment.

Supplementary S3A | Multiple sequence alignment of *M.bovis* BCG phosphoproteins with their respective *M. smegmatis*.

Supplementary S3B | Multiple sequence alignment of *M. smegmatis* phosphoproteins with their respective *M.bovis* BCG.

Supplementary Table S1A | Spreadsheet of all the identified protein groups, phosphopeptides and phosphoproteins from *M. bovis* BCG.

Supplementary Table S1B | Spreadsheet of all the identified protein groups, phosphopeptides and phosphoproteins from *M. smegmatis*.

References

- Baek, S.-H., Li, A. H., and Sassetti, C. M. (2011). Metabolic regulation of mycobacterial growth and antibiotic sensitivity. *PLoS Biol.* 9:e1001065. doi: 10.1371/journal.pbio.1001065
- Barry, C. E. I. (2001). *Mycobacterium smegmatis*: an absurd model for tuberculosis? Response from Barry III. *Trends Microbiol.* 9, 473–474. doi: 10.1016/S0966-842X(01)02169-2
- Boitel, B., Ortiz-Lombardía, M., Durán, R., Pompeo, F., Cole, S. T., Cerveñansky, C., et al. (2003). PknB kinase activity is regulated by phosphorylation in two Thr residues and dephosphorylation by PstP, the cognate phospho-Ser/Thr phosphatase, in *Mycobacterium tuberculosis*. *Mol. Microbiol.* 49, 1493–1508. doi: 10.1046/j.1365-2958.2003.03657.x
- Calmette, A., Guérin, G., Nègre, L., and Boquet, A. (1921). Prémunition des nouveaux-nés contre la tuberculose par le vaccin BCG. *Ann. Inst. Pasteur.* 40, 89–133.
- Canova, M. J., Veyron-Churlet, R., Zanella-Cleon, I., Cohen-Gonsaud, M., Cozzzone, A. J., Becchi, M., et al. (2008). The *Mycobacterium tuberculosis* serine/threonine kinase PknL phosphorylates Rv2175c: mass spectrometric profiling of the activation loop phosphorylation sites and their role in the recruitment of Rv2175c. *Proteomics* 8, 521–533. doi: 10.1002/pmic.200700442
- Chawla, Y., Upadhyay, S. K., Khan, S., Nagarajan, S. N., Forti, F., and Nandicoori, V. K. (2014). Protein Kinase B (PknB) of *Mycobacterium tuberculosis* is essential for growth of the pathogen *in vitro* as well as for survival within the host. *J. Biol. Chem.* 289, 13858–13875. doi: 10.1074/jbc.M114.563536

- Chopra, P., Singh, B., Singh, R., Vohra, R., Koul, A., Meena, L. S., et al. (2003). Phosphoprotein phosphatase of *Mycobacterium tuberculosis* dephosphorylates serine–threonine kinases PknA and PknB. *Biochem. Biophys. Res. Commun.* 311, 112–120. doi: 10.1016/j.bbrc.2003.09.173
- Cole, S. T., Brosch, R., Parkhill, J., Garnier, T., Churcher, C., Harris, D., et al. (1998). Deciphering the biology of *Mycobacterium tuberculosis* from the complete genome sequence. *Nature* 393, 537–544. doi: 10.1038/31159
- Corper, H. J., and Cohn, M. L. (1933). The viability and virulence of old cultures of tubercle bacilli: studies on twelve year broth cultures maintained at incubator temperatures. *Am. Rev. Tuberc.* 28, 856–874.
- Cowley, S., Ko, M., Pick, N., Chow, R., Downing, K. J., Gordhan, B. G., et al. (2004). The *Mycobacterium tuberculosis* protein serine/threonine kinase PknG is linked to cellular glutamate/glutamine levels and is important for growth *in vivo*. *Mol. Microbiol.* 52, 1691–1702. doi: 10.1111/j.1365-2958.2004.04085.x
- Danilchanka, O., Pavlenok, M., and Niederweis, M. (2008). Role of porins for uptake of antibiotics by *Mycobacterium smegmatis*. *Antimicrob. Agents Chemother.* 52, 3127–3134. doi: 10.1128/AAC.00239-08
- Deol, P., Vohra, R., Saini, A. K., Singh, A., Chandra, H., Chopra, P., et al. (2005). Role of *Mycobacterium tuberculosis* Ser/Thr kinase PknF: implications in glucose transport and cell division. *J. Bacteriol.* 187, 3415–3420. doi: 10.1128/JB.187.10.3415-3420.2005
- Fernandez, P., Saint-Joanis, B., Barilone, N., Jackson, M., Gicquel, B., Cole, S. T., et al. (2006). The Ser/Thr protein kinase PknB is essential for sustaining mycobacterial growth. *J. Bacteriol.* 188, 7778–7784. doi: 10.1128/JB.00963-06
- Fiuza, M., Canova, M. J., Zanella-Cléon, I., Becchi, M., Cozzone, A. J., Mateos, L. M., et al. (2008). From the characterization of the four serine/threonine protein kinases (PknA/B/G/L) of *Corynebacterium glutamicum* toward the role of PknA and PknB in cell division. *J. Biol. Chem.* 283, 18099–18112. doi: 10.1074/jbc.M802615200
- Freschi, L., Osseni, M., and Landry, C. R. (2014). Functional divergence and evolutionary turnover in mammalian phosphoproteomes. *PLoS Genet.* 10:e1004062. doi: 10.1371/journal.pgen.1004062
- Ge, R., and Shan, W. (2011). Bacterial phosphoproteomic analysis reveals the correlation between protein phosphorylation and bacterial pathogenicity. *Genomics Proteomics Bioinformatics* 9, 119–127. doi: 10.1016/S1672-0229(11)60015-6
- Gee, C. L., Papavinasandaram, K. G., Blair, S. R., Baer, C. E., Falick, A. M., King, D. S., et al. (2012). A Phosphorylated Pseudokinase Complex Controls Cell Wall Synthesis in Mycobacteria. *Sci. Signal.* 5, ra7. doi: 10.1126/scisignal.2002525
- Gupta, M., Sajid, A., Arora, G., Tandon, V., and Singh, Y. (2009). Forkhead-associated domain-containing protein Rv0019c and polyketide-associated protein PapA5, from substrates of serine/threonine protein kinase PknB to interacting proteins of *Mycobacterium tuberculosis*. *J. Biol. Chem.* 284, 34723–34734. doi: 10.1074/jbc.M109.058834
- Gupta, M., Sajid, A., Sharma, K., Ghosh, S., Arora, G., Singh, R., et al. (2014). HupB, a nucleoid-associated protein of *Mycobacterium tuberculosis*, is modified by serine/threonine protein kinases *in vivo*. *J. Bacteriol.* 196, 2646–2657. doi: 10.1128/JB.01625-14
- Jani, C., Eoh, H., Lee, J. J., Hamasha, K., Sahana, M. B., Han, J.-S., et al. (2010). Regulation of polar peptidoglycan biosynthesis by Wag31 phosphorylation in mycobacteria. *BMC Microbiol.* 10:327. doi: 10.1186/1471-2180-10-327
- Jers, C., Kobir, A., Søndergaard, E. O., Jensen, P. R., and Mijakovic, I. (2011). *Bacillus subtilis* two-component system sensory kinase DegS is regulated by serine phosphorylation in its input domain. *PLoS ONE* 6:e14653. doi: 10.1371/journal.pone.0014653
- Kang, C. M., Abbott, D. W., Park, S. T., Dascher, C. C., Cantley, L. C., and Husson, R. N. (2005). The *Mycobacterium tuberculosis* serine/threonine kinases PknA and PknB: substrate identification and regulation of cell shape. *Genes Dev.* 19, 1692–704. doi: 10.1101/gad.1311105
- Katsube, T., Matsumoto, S., Takatsuka, M., Okuyama, M., Ozeki, Y., Naito, M., et al. (2007). Control of Cell Wall Assembly by a Histone-Like Protein in Mycobacteria. *J. Bacteriol.* 189, 8241–8249. doi: 10.1128/JB.00550-07
- Kieser, K. J., and Rubin, E. J. (2014). How sisters grow apart: mycobacterial growth and division. *Nat. Rev. Micro.* 12, 550–562. doi: 10.1038/nrmicro3299
- Kusebauch, U., Ortega, C., Ollodart, A., Rogers, R. S., Sherman, D. R., Moritz, R. L., et al. (2014). *Mycobacterium tuberculosis* supports protein tyrosine phosphorylation. *Proc. Natl. Acad. Sci. U.S.A.* 111, 9265–9270. doi: 10.1073/pnas.1323894111
- Lee, B. H., Murugasu-Oei, B., and Dick, T. (1998). Upregulation of a histone-like protein in dormant *Mycobacterium smegmatis*. *Mol. Gen. Genet. MGG* 260, 475–479. doi: 10.1007/s004380050919
- Lee, J. J., Kan, C. M., Lee, J. H., Park, K. S., Jeon, J. H., and Lee, S. H. (2014). Phosphorylation-dependent interaction between a serine/threonine kinase PknA and a putative cell division protein Wag31 in *Mycobacterium tuberculosis*. *New Microbiol.* 37, 525–533.
- Lin, M.-H., Hsu, T.-L., Lin, S.-Y., Pan, Y.-J., Jan, J.-T., Wang, J.-T., et al. (2009). Phosphoproteomics of *Klebsiella pneumoniae* NTUH-K2044 reveals a tight link between tyrosine phosphorylation and virulence. *Mol. Cell. Proteomics* 8, 2613–2623. doi: 10.1074/mcp.M900276-MCP200
- Macek, B., Gnad, F., Soufi, B., Kumar, C., Olsen, J. V., Mijakovic, I., et al. (2008). Phosphoproteome analysis of *E. coli* reveals evolutionary conservation of bacterial Ser/Thr/Tyr phosphorylation. *Mol. Cell. Proteomics* 7, 299–307. doi: 10.1074/mcp.M700311-MCP200
- Marrero, J., Rhee, K. Y., Schnappinger, D., Pethe, K., and Ehrh, S. (2010). Gluconeogenic carbon flow of tricarboxylic acid cycle intermediates is critical for *Mycobacterium tuberculosis* to establish and maintain infection. *Proc. Natl. Acad. Sci. U.S.A.* 107, 9819–9824. doi: 10.1073/pnas.1000715107
- Matsumoto, S., Yukitake, H., Furugen, M., Matsuo, T., Mineta, T., and Yamada, T. (1999). Identification of a Novel DNA-Binding Protein from *Mycobacterium bovis* Bacillus Calmette-Guérin. *Microbiol. Immunol.* 43, 1027–1036. doi: 10.1111/j.1348-0421.1999.tb01232.x
- McKinney, J. D., zu Bentrup, K. H., Munoz-Elias, E. J., Miczak, A., Chen, B., Chan, W.-T., et al. (2000). Persistence of *Mycobacterium tuberculosis* in macrophages and mice requires the glyoxylate shunt enzyme isocitrate lyase. *Nature* 406, 735–738. doi: 10.1038/35021074
- Molle, V., and Kremer, L. (2010). Division and cell envelope regulation by Ser/Thr phosphorylation: mycobacterium shows the way. *Mol. Microbiol.* 75, 1064–1077. doi: 10.1111/j.1365-2958.2009.07041.x
- Park, S. T., Kang, C.-M., and Husson, R. N. (2008). Regulation of the SigH stress response regulon by an essential protein kinase in *Mycobacterium tuberculosis*. *Proc. Natl. Acad. Sci. U.S.A.* 105, 13105–13110. doi: 10.1073/pnas.0801143105
- Prisic, S., Dankwa, S., Schwartz, D., Chou, M. F., Locasale, J. W., Kang, C.-M., et al. (2010). Extensive phosphorylation with overlapping specificity by *Mycobacterium tuberculosis* serine/threonine protein kinases. *Proc. Natl. Acad. Sci. U.S.A.* 107, 7521–7526. doi: 10.1073/pnas.0913482107
- Pullen, K. E., Ng, H.-L., Sung, P.-Y., Good, M. C., Smith, S. M., and Alber, T. (2004). An alternate conformation and a third metal in PstP/Ppp, the *M. tuberculosis* PP2C-Family Ser/Thr protein phosphatase. *Structure* 12, 1947–54. doi: 10.1016/j.str.2004.09.008
- Ramagli, L. S. (1999). Quantifying protein in 2-D PAGE solubilization buffers. *Methods Mol. Biol.* 112, 99–103. doi: 10.1385/1-59259-584-7:99
- Ravichandran, A., Sugiyama, N., Tomita, M., Swarup, S., and Ishihama, Y. (2009). Ser/Thr/Tyr phosphoproteome analysis of pathogenic and non-pathogenic *Pseudomonas* species. *Proteomics* 9, 2764–2775. doi: 10.1002/pmic.2008.00655
- Repaske, R. (1956). Lysis of gram-negative bacteria by lysozyme. *Biochim. Biophys. Acta* 22, 189–191. doi: 10.1016/0006-3002(56)90240-2
- Reyrat, J. M., and Kahn, D. (2001). *Mycobacterium smegmatis*: an absurd model for tuberculosis? *Trends Microbiol.* 9, 472–473. doi: 10.1016/S0966-842X(01)02168-0
- Sajid, A., Arora, G., Gupta, M., Upadhyay, S., Nandicoori, V. K., and Singh, Y. (2011). Phosphorylation of *Mycobacterium tuberculosis* Ser/Thr phosphatase by PknA and PknB. *PLoS ONE* 6:e17871. doi: 10.1371/journal.pone.0017871
- Sassetti, C. M., Boyd, D. H., and Rubin, E. J. (2003). Genes required for mycobacterial growth defined by high density mutagenesis. *Mol. Microbiol.* 48, 77–84. doi: 10.1046/j.1365-2958.2003.03425.x
- Schwartz, D. G. S. (2005). An iterative statistical approach to the identification of protein phosphorylation motifs from large-scale data sets. *Nat. Biotechnol.* 23, 1391–1398. doi: 10.1038/nbt1146
- Shi, L., Pigeonneau, N., Ravikumar, V., Dobrinic, P., Macek, B., Franjevic, D., et al. (2014). Cross-phosphorylation of bacterial serine/threonine and tyrosine protein kinases on key regulatory residues. *Front. Microbiol.* 5:495. doi: 10.3389/fmicb.2014.00495

- Shiloh, M. U., and Champion, P. A. (2010). To catch a killer. what can mycobacterial model teach us about *Mycobacterium tuberculosis* pathogenesis? *Curr. Opin. Microbiol.* 13, 86–92. doi: 10.1016/j.mib.2009.11.006
- Soares, N. C., Spät, P., Krug, K., and Macek, B. (2013). Global dynamics of the *Escherichia coli* proteome and phosphoproteome during growth in minimal medium. *J. Proteome Res.* 12, 2611–2621. doi: 10.1021/pr3011843
- Soares, N. C., Spät, P., Méndez, J. A., Nakedi, K., Aranda, J., and Bou, G. (2014). Ser/Thr/Tyr phosphoproteome characterization of *Acinetobacter baumannii*: comparison between a reference strain and a highly invasive multidrug-resistant clinical isolate. *J. Proteomics* 102, 113–124. doi: 10.1016/j.jprot.2014.03.009
- Sun, X., Ge, F., Xiao, C.-L., Yin, X.-F., Ge, R., Zhang, L.-H., et al. (2009). Phosphoproteomic analysis reveals the multiple roles of phosphorylation in pathogenic bacterium *Streptococcus pneumoniae*. *J. Proteome Res.* 9, 275–282. doi: 10.1021/pr900612v
- Thakur, M., Chaba, R., Mondal, A. K., and Chakraborti, P. K. (2008). Interdomain interaction reconstitutes the functionality of PknA, a eukaryotic type Ser/Thr kinase from *Mycobacterium tuberculosis*. *J. Biol. Chem.* 283, 8023–8033. doi: 10.1074/jbc.M707535200
- Villarino, A., Duran, R., Wehenkel, A., Fernandez, P., England, P., Brodin, P., et al. (2005). Proteomic identification of *M. tuberculosis* protein kinase substrates: PknB recruits GarA, a FHA domain-containing protein, through activation loop-mediated interactions. *J. Mol. Biol.* 350, 953–963. doi: 10.1016/j.jmb.2005.05.049
- Wayne, L. G., and Hayes, L. G. (1996). An *in vitro* model for sequential study of shutdown of *Mycobacterium tuberculosis* through two stages of nonreplicating persistence. *Infect. Immun.* 64, 2062–2069.
- Wells, R. M., Jones, C. M., Xi, Z., Speer, A., Danilchanka, O., Doornbos, K. S., et al. (2013). Discovery of a siderophore export system essential for virulence of *Mycobacterium tuberculosis*. *PLoS Pathog.* 9:e1003120. doi: 10.1371/journal.ppat.1003120
- Wessel, D., and Flügge, U. I. (1984). A method for the quantitative recovery of protein in dilute solution in the presence of detergents and lipids. *Anal. Biochem.* 138, 141–143. doi: 10.1016/0003-2697(84)90782-6
- WHO. (2014). *WHO Global Tuberculosis Report 2014*, Geneva.
- Wybenga-Groot, L. E., Baskin, B., Ong, S. H., Tong, J., Pawson, T., and Sicheri, F. (2001). Structural basis for autoinhibition of the EphB2 receptor tyrosine kinase by the unphosphorylated juxtamembrane region. *Cell* 106, 745–757. doi: 10.1016/S0092-8674(01)00496-2
- Zheng, X., Papavinasundaram, K. G., and Av-Gay, Y. (2007). Novel substrates of *Mycobacterium tuberculosis* PknH Ser/Thr kinase. *Biochem. Biophys. Res. Commun.* 355, 162–168. doi: 10.1016/j.bbrc.2007.01.122

Conflict of Interest Statement: The authors declare that the research was conducted in the absence of any commercial or financial relationships that could be construed as a potential conflict of interest.

Copyright © 2015 Nakedi, Nel, Garnett, Blackburn and Soares. This is an open-access article distributed under the terms of the Creative Commons Attribution License (CC BY). The use, distribution or reproduction in other forums is permitted, provided the original author(s) or licensor are credited and that the original publication in this journal is cited, in accordance with accepted academic practice. No use, distribution or reproduction is permitted which does not comply with these terms.

Phosphoproteome of the cyanobacterium *Synechocystis* sp. PCC 6803 and its dynamics during nitrogen starvation

Philipp Spät¹, Boris Mačák^{2*} and Karl Forchhammer^{1*}

OPEN ACCESS

Edited by:

Ivan Mijakovic,
Chalmers University of Technology,
Sweden

Reviewed by:

Jason Warren Cooley,
University of Missouri, USA
Carsten Jers,
Technical University of Denmark,
Denmark

*Correspondence:

Boris Mačák,
Interfaculty Institute for Cell Biology,
Proteome Center Tuebingen,
University of Tuebingen, Auf der
Morgenstelle 15, D-72076 Tuebingen,
Germany
boris.macek@uni-tuebingen.de;
Karl Forchhammer,
Department of Organismic
Interactions,
Eberhard-Karls-Universität Tübingen,
Auf der Morgenstelle 28, D-72076
Tübingen, Germany
karl.forchhammer@uni-tuebingen.de

Specialty section:

This article was submitted to Microbial
Physiology and Metabolism, a section
of the journal Frontiers in Microbiology

Received: 02 December 2014

Accepted: 13 March 2015

Published: 31 March 2015

Citation:

Spät P, Mačák B and Forchhammer K
(2015) Phosphoproteome of the
cyanobacterium *Synechocystis* sp.
PCC 6803 and its dynamics during
nitrogen starvation.
Front. Microbiol. 6:248.
doi: 10.3389/fmicb.2015.00248

¹ Department of Organismic Interactions, Interfaculty Institute for Microbiology and Infection Medicine, Eberhard-Karls-University Tübingen, Tübingen, Germany, ² Interfaculty Institute for Cell Biology, Proteome Center Tuebingen, Eberhard-Karls-University Tübingen, Tübingen, Germany

Cyanobacteria have shaped the earth's biosphere as the first oxygenic photoautotrophs and still play an important role in many ecosystems. The ability to adapt to changing environmental conditions is an essential characteristic in order to ensure survival. To this end, numerous studies have shown that bacteria use protein post-translational modifications such as Ser/Thr/Tyr phosphorylation in cell signaling, adaptation, and regulation. Nevertheless, our knowledge of cyanobacterial phosphoproteomes and their dynamic response to environmental stimuli is relatively limited. In this study, we applied gel-free methods and high accuracy mass spectrometry toward the detection of Ser/Thr/Tyr phosphorylation events in the model cyanobacterium *Synechocystis* sp. PCC 6803. We could identify over 300 phosphorylation events in cultures grown on nitrate as exclusive nitrogen source. Chemical dimethylation labeling was applied to investigate proteome and phosphoproteome dynamics during nitrogen starvation. Our dataset describes the most comprehensive (phospho)proteome of *Synechocystis* to date, identifying 2382 proteins and 183 phosphorylation events and quantifying 2111 proteins and 148 phosphorylation events during nitrogen starvation. Global protein phosphorylation levels were increased in response to nitrogen depletion after 24 h. Among the proteins with increased phosphorylation, the P_{II} signaling protein showed the highest fold-change, serving as positive control. Other proteins with increased phosphorylation levels comprised functions in photosynthesis and in carbon and nitrogen metabolism. This study reveals dynamics of *Synechocystis* phosphoproteome in response to environmental stimuli and suggests an important role of protein Ser/Thr/Tyr phosphorylation in fundamental mechanisms of homeostatic control in cyanobacteria.

Keywords: cyanobacteria, *Synechocystis* sp. PCC 6803, nitrogen starvation, phosphoproteome, peptide dimethylation labeling, LTQ-Orbitrap

Introduction

Cyanobacteria constitute one of the most widely distributed groups of prokaryotes in the biosphere, where they inhabit almost all illuminated environments. They are oxygenic photoautotrophs, employing photosynthetic machinery that resembles that of plants, due to the endosymbiotic origin

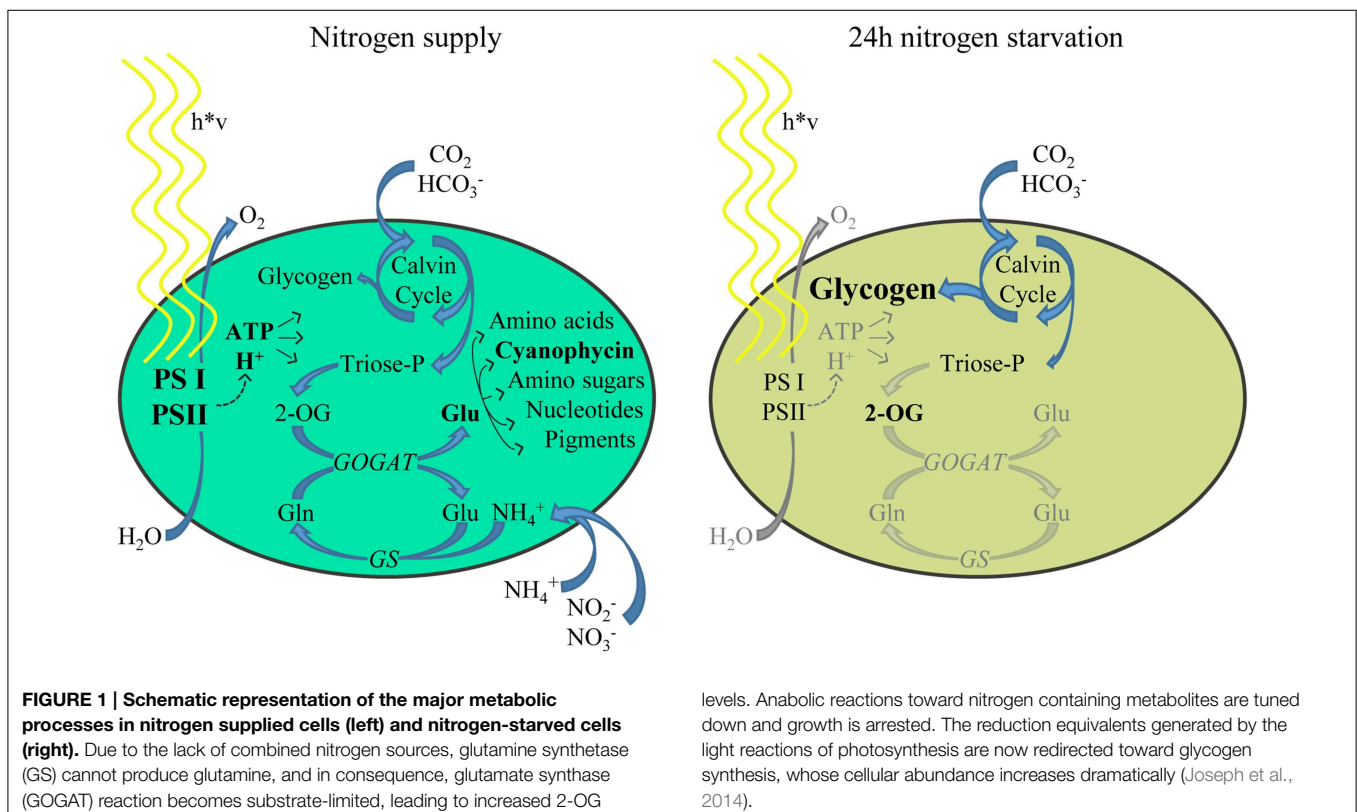
of chloroplasts. The substrate diversity of cyanobacteria is limited since photoautotrophs only need H_2O as an electron donor, CO_2 as a carbon source, and inorganic salts such as nitrogen, phosphorous, sulfur, and iron to fulfill their anabolic needs. Among these, the highest demand is for nitrogen, whose cellular abundance amounts to a carbon to nitrogen ratio of 5:1.

Cyanobacteria encounter many environmental fluctuations, such as changing light conditions, nutrient availability and the ambient physico-chemical properties (osmolarity, temperature etc.). During evolution, these microbes have developed sophisticated regulator systems to adapt cellular processes and maintain metabolic homeostasis in response to these challenges. Nitrogen starvation induces in non-diazotrophic cyanobacteria a highly dynamic response, which can be classified in three phases. Their temporal occurrence depends on many environmental and intrinsic conditions (Schwarz and Forchhammer, 2005). In response to nitrogen depletion, an acclimation process is initiated that is known as chlorosis (Allen and Smith, 1969). Chlorosis is characterized by a rapid degradation of the phycobilisome antenna and a cell cycle arrest after completion of a final cell division (Allen and Smith, 1969; Collier and Grossman, 1992). This initial phase (phase I) is followed by a subsequent gradual and consecutive decrease in photosystem (PS) II and PSI activities (phase II), down-tuning of metabolic activities and proteolytic degradation of cellular proteins. Only after 10–15 days, cells have reached a final resting state, where they are completely bleached (phase III) and can survive for prolonged periods (Görl et al., 1998). **Figure 1** indicates the metabolic changes in the cell

in the phase II chlorosis stage, which starts after 24 h of nitrogen starvation.

Among the short-term acclimation processes, protein phosphorylation plays a prominent role (Biggins and Bruce, 1987; Stock et al., 1989; Hagemann et al., 1993). In bacteria, the two-component sensory transduction pathways have been historically known as the hallmark of bacterial signal transduction, involving protein histidine kinases and response regulators phosphorylated on aspartate residues. These are universally distributed and have been systematically investigated in several cyanobacterial strains (Ashby and Houmard, 2006). Among these, the 47 histidine kinases and 45 response regulators in the unicellular strain *Synechocystis* sp. PCC 6803 substrain Kazusa (hereafter designated as *Synechocystis*) has received the most thorough investigations (Murata and Suzuki, 2006).

Phosphorylation on serine, threonine and tyrosine residues (Ser/Thr/Tyr), referred to as S/T/Y phosphorylation or O-phosphorylation, was initially thought to occur exclusively in eukaryotic signal transduction. However, primarily due to advances in mass spectrometry proteomics technologies, it is now clear that this type of modification frequently occurs in bacteria serving an important role in prokaryotic signal transduction (Macek and Mijakovic, 2011). Most bacterial Ser/Thr kinases resemble those classified in eukaryotes and are termed as Hanks-like kinases, whereas, most bacterial tyrosine (BY)-kinases are unique to prokaryotes (Mijakovic and Macek, 2012; Soufi et al., 2012). Genome sequencing revealed that Hanks-like Ser/Thr kinases, BY-kinases, and protein phosphatases are



globally distributed in the bacterial domain (Pereira et al., 2011). Bacterial S/T/Y phosphorylation is widely involved in signal transduction in response to environmental stimuli and regulates many physiological processes in a bacterial cell (Petranovic et al., 2007; Mijakovic and Macek, 2012).

A survey of the genome of *Synechocystis* revealed the presence of 11 Ser/Thr kinases, one Tyr kinase and seven protein phosphatases (Zhang et al., 2005). Pioneering work in the late 1980s and in the 1990s, employing *in vivo* and *in vitro* labeling experiments using [$\gamma^{32}\text{P}$] phosphate shed the first light on the occurrence of protein phosphorylation events in cyanobacteria (reviewed by Mann, 1994). Protein phosphorylation was shown to be dynamic and to respond to a variety of environmental stimuli, such as changing illumination, nutrient supply, or osmolarity (Sanders et al., 1989; Hagemann et al., 1993).

One of the first discovered and most intensively studied phosphoproteins in cyanobacteria is the signal transduction protein P_{II} (Forchhammer and Tandeau De Marsac, 1994); reviewed in Forchhammer (2004, 2008). The P_{II} signaling protein, a homotrimer of 12.4 kDa, is phosphorylated at the tip of a large, surface exposed loop (termed T-loop) in response to the cellular nitrogen supply. The effector molecule 2-oxoglutarate (2-OG) whose abundance reflects the cellular state of nitrogen assimilation (Muro-Pastor et al., 2001), binds to P_{II} and elicits its phosphorylation on T-loop residue Ser49 (Forchhammer and Tandeau De Marsac, 1995). In its phosphorylated state, P_{II} is not able to bind to and activate the key enzyme of the ornithine/arginine biosynthesis pathway, N-acetyl-L-glutamate kinase (NAGK) (Heinrich et al., 2004). Shifting nitrogen-starved cells back to nitrogen-sufficient conditions, the cellular 2-OG level drops, leading to dephosphorylation of P_{II} (Irmeler and Forchhammer, 2001) with a concomitant activation of NAGK (Maheswaran et al., 2006), thereby feeding nitrogen into the arginine pool.

In addition to P_{II} , the functions of only a few other phosphoproteins have been identified in *Synechocystis*, such as the phosphorylation of phycobiliproteins and phycobilisome linker proteins (Harrison et al., 1991; Piven et al., 2005), or the oscillating phosphorylation of the circadian clock protein KaiC (Nishiwaki et al., 2004). Except these specific investigations focusing on particular phosphoproteins, Mikkat et al. recently published a snapshot of the phosphoproteome of *Synechocystis* based on 2D gel electrophoresis, where the authors identified about 30 phosphoproteins, of which the modified residue could be localized in eight cases. Among these, most previously identified phosphoproteins were included (Mikkat et al., 2014). However, the physiological function of most phosphorylation events remains still unclear.

In the recent years, the analysis of global phosphoproteomes has made dramatic progress due to the development of gel-free workflows and biochemical phosphopeptide enrichment strategies such as titanium dioxide (TiO_2) chromatography coupled to high accuracy mass spectrometry. The development of chemical stable isotope labeling by dimethylation of tryptic peptides enables the application of a cost efficient and reliable quantification strategy also to autotrophic organisms, without

the need of profound genetic manipulation of amino acid metabolic pathways (Boersema et al., 2009). Despite these advantages, the dimethylation approach was never applied in global phosphoproteomic studies in a prokaryotic organism.

The first global study of a cyanobacterial phosphoproteome using gel-free methods was performed in a qualitative manner in the marine unicellular cyanobacterium *Synechococcus* sp. PCC 7002, which resulted in the identification of 410 phosphorylation sites on 245 phosphoproteins (Yang et al., 2013). One general drawback in global studies in cyanobacterial organisms is the high percentage of integral membrane and membrane-associated proteins. Particularly, such membrane proteins are often involved in protein phosphorylation based signal transduction and represent a high potential for phosphorylation (Jers et al., 2008). Therefore, efficient extraction of cytosolic as well as of membrane proteins is essential in order to attain deep phosphoproteome coverage. So far, about 900 known or predicted membrane (associated) proteins have been identified in *Synechocystis* by previous large-scale studies (24.5% of 3672 protein coding genes list on Cyanobase). However, 52.7% of the total protein coding genes was thus far not identified on the proteome level, indicating a need for improvement in protein extraction methods, particularly with respect to hydrophobic (membrane)proteins (Wang et al., 2009).

In the present work, we applied state of the art mass spectrometric analysis to define the phosphoproteome of *Synechocystis*. To ensure an efficient extraction of cytosolic as well as of membrane (phospho)proteins, we compared three common, in gel-free approaches frequently used extraction methods in a qualitative experiment. Here, in total 301 phosphorylation events could be identified, of which 262 could be localized to a specific Ser, Thr, or Tyr residue. This dataset represents the so far most comprehensive qualitative phosphoproteome dataset of *Synechocystis*. It encouraged us to investigate phosphoproteome dynamics in response to nitrogen starvation in a quantitative manner employing for the first time in a bacterial system the method of chemical dimethylation labeling. Extracts from *Synechocystis* cultures grown in the presence of nitrate or ammonia and cultures subjected to nitrogen starvation were dimethyl labeled. Thereby, we could identify altogether 2382 proteins and 183 phosphorylation events. Of those, the dynamics of 2111 proteins and 148 phosphorylation events from two independent experiments could be quantified. The P_{II} signaling protein, which served as a positive control to validate the experiments, showed the highest increase in phosphorylation level upon nitrogen starvation. Other proteins with increased phosphorylation levels comprised functions in photosynthesis and in carbon and nitrogen metabolism, suggesting an important role of protein S/T/Y phosphorylation in such a fundamental acclimation response.

Material and Methods

Cell Culture and Harvest

Wild-type *Synechocystis* sp. PCC 6803 substrain Kazusa was grown photoautotrophically at a constant photon flux density of $40 \mu\text{mol photons m}^{-2} \text{s}^{-1}$ in 5 mM NaHCO_3 and 20 mM

HEPES supplemented BG11 medium (Rippka, 1988), with either 17.6 mM sodium nitrate (NaNO_3) or 5 mM ammonium chloride (NH_4Cl) as exclusive nitrogen source, at 26°C . A stationary culture of *Synechocystis* in BG11 nitrate medium served as a stock for the final inoculation of experimental 500 mL batch cultures in the qualitative experiments. For the quantitative experiment 1, pre-cultures were grown from the stock in fresh nitrate or ammonia medium to optical density (OD_{750}) = 0.6–0.8 and were directly used as inoculum for the experimental 500 mL batch cultures. In experiment 2, the pre-cultures were repeatedly cultivated to OD_{750} = 0.6–0.8 and after five cycles used as inoculum for the experimental 500 mL batch cultures. All experimental cultures were inoculated to an initial OD_{750} = 0.2 and grown to OD_{750} = 0.6 with ambient air bubbling and magnetic stirring. Cultures were harvested by addition of 100 g ice for rapid cooling and centrifugation at $7477 \times g$ for 10 min. The supernatant was removed and cell pellets were resuspended in 50 mL ice cold nitrogen-free BG11 medium and centrifuged again. Cell pellets were quick-frozen in liquid nitrogen. For nitrogen starvation conditions, nitrate grown cells (at OD_{750} = 0.6) were shifted to nitrogen-free BG11 medium by centrifugation with $3500 \times g$ for 8 min at room temperature (RT). The supernatant was decanted, the cell pellet was gently overlaid with nitrogen-free BG11 medium, swirled and decanted again and finally, the cell pellet was resuspended in the same volume as before centrifugation. Cells were kept for 24 h under previous incubation conditions and harvested as described.

Protein Extraction, In-solution Digestion, and Peptide Dimethylation Labeling

Protein extraction method A: Filter Aided Sample Preparation was performed as described previously (Wisniewski et al., 2009) with the following exceptions: In brief, a frozen cell pellet from a nitrate grown culture was resuspended in 2 mL lysis buffer, containing 4% (w/v) sodium dodecyl sulfate (SDS) and 100 mM dithiothreitol (DTT) in 100 mM Tris/HCl, pH 7.5, and each 5 mM of the following phosphatase inhibitors: glycerol-2-phosphate; sodium fluoride (both Sigma-Aldrich) and sodium orthovanadate (Alfa Aesar). The sample was incubated for 10 min at 95°C in a water bath and subsequently sonified on ice for 30 s with a Branson Sonifier 250/Microtip 5 at output control 4 and 40% duty cycle for DNA comminution. The lysate was centrifuged at $13,000 \times g$ for 5 min and the supernatant was transferred onto an Amicon Ultra-15 3 kDa Centrifugal Filter Unit. The lysate was mixed with 5 mL urea buffer (6 M urea/2 M thiourea in 100 mM Tris/HCl; pH 7.5) and centrifuged with $3345 \times g$ for 10 min at RT. This step was repeated once for washing. Alkylation of reduced cysteine disulfide bonds was performed by washing the filter unit with 5 mL urea buffer containing 50 mM iodoacetamide (IAA) and centrifugation for 15 min as before, followed by incubation with 2 mL IAA-urea buffer for 20 min in the dark. The filter was washed for three times with each 2 mL urea buffer and 50 mM NH_4HCO_3 buffer, subsequently. For protein digestion, 50 μg trypsin (MS grade; Thermo Scientific) in 500 μL NH_4HCO_3 buffer, pH 8.0, were added onto the filter and incubated overnight (o.n.) at 37°C . Peptides were collected in a fresh tube by centrifugation as before for 10 min and additional with 500 μL NH_4HCO_3 buffer.

Protein extraction method B: SDS buffer protein extraction and acetone/methanol precipitation: Proteins from frozen cell pellets were extracted with 2 mL lysis buffer (see method A, without DTT), supplemented with 10 mM ethylenediaminetetraacetic acid (EDTA). Cell lysates were sonified on ice as described in method A and subsequently reduced with a final concentration of 10 mM DTT for 1 h at RT under agitation at 650 rpm on a shaker. Alkylation was performed with a final concentration of 5.5 mM IAA for 1 h at RT under agitation in the dark, followed by centrifugation at $13,000 \times g$ for 5 min. Proteins in the supernatant were precipitated by mixing with eight volumes ice cold acetone and one volume ice cold methanol, followed by incubation at -20°C o.n. The precipitate was washed five times with 5 mL ice cold 80% (v/v) acetone in water and centrifugation at $1000 \times g$. The protein pellets were air dried and dissolved in urea buffer.

Protein extraction method C: Protein extraction with Y-PER (Yeast Protein Extraction Reagent; Thermo Scientific) and acetone/methanol precipitation: A frozen cell pellet was resuspended in 2 mL Y-PER, supplemented with 50 $\mu\text{g}/\text{mL}$ lysozyme (from chicken egg, Sigma-Aldrich), cOmplete protease inhibitors (Roche) and phosphatase inhibitors, as described in method A. The suspension was incubated at 37°C for 20 min under agitation at 650 rpm. Cell lysates were sonified on ice and centrifuged as described before. Proteins in the supernatant were acetone/methanol precipitated, washed and dissolved in urea buffer as described in method B. Reduction and alkylation of cysteines was subsequently performed as described in method B.

Protein concentration of samples derived from methods B and C were measured by Bradford assay (Bio-Rad) and subsequently pre-digested with endoproteinase Lys-C (Waco) for 3 h and digested further o.n. with trypsin (MS grade; Thermo Scientific) at RT. The protease/protein ratio was for both enzymes 1:100 (w/w). The resulting peptide mixtures from methods A, B, and C were acidified to pH 2.5 with trifluoroacetic acid (TFA) and desalted by solid phase extraction on Sep-Pak C18 columns (Waters) according to the manufacturer's instructions.

For the quantitative experiments, samples were extracted with method B, in-solution digested and on-column (Sep-Pak C18) dimethylation labeled as described previously (Boersema et al., 2009). In brief, 5 mL of the respective labeling solutions with CH_2O (Sigma-Aldrich) and NaBH_3CN (Fluka) for light-, CD_2O (Sigma-Aldrich) and NaBH_3CN for medium-heavy and $^{13}\text{CD}_2\text{O}$ (Sigma-Aldrich) and NaBD_3CN (Sigma-Aldrich) for heavy labeling were flushed with 15 min contact time through the column. Labeled peptides were washed with 5 mL HPLC Solvent A (0.5% acetic acid) on the column and eluted with HPLC Solvent B (80% acetonitrile in 0.5% acetic acid). For validation of labeling efficiency and correct mixing of the labeled peptides, two times 5 μg of each labeled sample (based on Bradford measurements) were used for separate measurements or mixed 1:1:1 and subjected after purification by C18 stage tips (Ishihama et al., 2006) to pilot LC-MS/MS measurements. Based on the obtained label ratios, correction factors were applied for correct mixing of samples. The labeling efficiencies were in all cases $\geq 94\%$.

Sample Preparation

Sample fractionation for the qualitative proteome experiments was performed on the peptide level by strong anion exchange chromatography (SAX). For quantitative proteome analysis, isoelectric focusing (OffGel fractionation strategy) was performed: For SAX, 100 µg peptides were loaded onto in-house packed SAX column (Empore™) and subsequently eluted stepwise in five pH fractions with 20 mM of acetic-, phosphoric- and boric acid at pH 3, 4, 5, 6 and 8, (pH adjusted with sodium hydroxide), respectively. Each fraction was subsequently purified by C18 stage tips. For OffGel fractionation, 100 µg of the labeled peptide mixture was separated on a linear 13 cm pH 3–10 IEF strip (GE Healthcare) and focused on a OffGel Fractionator 3100 (Agilent), according to the manufacturer's protocol, with 20 kVh at maximum 50 µA. Peptides focused in 12 fractions were separately purified by C18 stage tips.

Phosphopeptide enrichment for qualitative analyses was performed from the digested samples of protein extraction methods A, B and C by TiO₂ chromatography (Soares et al., 2013), with the following exceptions: Obtained peptide solutions from solid phase extraction (pH 2.5) were directly incubated with each 5 mg TiO₂ spheres (10 µm; MZ Analysetechnik), pre-incubated with 2,5-dihydrobenzoic acid (final concentration 30 mg/mL) for five consecutive rounds of 30 min. TiO₂ spheres were washed and eluted as described previously and purified by C18 stage tips. The sample volume was reduced by vacuum centrifugation at RT and subjected to nano-LC-MS/MS analysis.

For the quantitative study, labeled phosphopeptides were enriched by TiO₂ chromatography from each 15 mg peptide mixture. For TiO₂ chromatography, a modified protocol was applied: peptides were eluted from SepPak columns with 80% acetonitrile in 6% TFA and enriched for eight consecutive rounds with each 5 mg TiO₂ spheres (5 µm Sachtopore NP) for 10 min. TiO₂ spheres were washed twice with each 1 mL 80% acetonitrile in 6% TFA for 1 min at 1000 rpm and loaded onto C8 (Empore™) stage tips. The spheres were washed once with 200 µL HPLC Solvent B and phosphopeptides were eluted with 30 µL 5% ammonium hydroxide solution in 60% acetonitrile, pH 11, for 30 min at 4°C into 30 µL 20% TFA in a fresh tube. Eluates were purified by C18 stage tips. The sample volume was reduced by vacuum centrifugation at RT and subjected to nano-LC-MS/MS analysis.

Mass Spectrometry

For nanoLC-MS/MS analyses of proteome and phosphoproteome samples, peptides were loaded onto an in-house packed 15 cm reverse-phase C18 (3 µm; Dr. Maisch) nanoHPLC column on an EasyLC nano-HPLC (Proxeon Biosystems). Separation was performed by 90 min (for OffGel-separated samples) or 130 min (for TiO₂-enriched samples) segmented linear gradients with 5–90% HPLC solvent B. Eluted peptides were directly ionized and measured on a LTQ Orbitrap XL (qualitative study), or LTQ Orbitrap Elite mass spectrometer (quantitative study). Mass spectrometers were operated in the positive ion mode.

The LTQ Orbitrap XL had the following acquisition cycle: one initial full (MS) scan in the Orbitrap mass analyzer was acquired

at resolution 60,000 and scan range of m/z 300–2000, followed by collision induced dissociation (CID) of the 5 (phosphoenrichment) or 15 (proteome) most intense multiply charged ions in the linear ion trap mass analyzer (LTQ). For phosphoproteome analysis, multi stage activation (MSA) in all MS/MS events with neutral losses of phosphoric acid on singly (−97.97 Th), doubly (−48.99 Th) or triply (−33.66 Th) charged precursor ions, was activated.

The LTQ Orbitrap Elite was conducting higher energy collision dissociation (HCD) of the 20 most intense multiply charged ions at the same scan range at resolution 120,000.

Dynamic exclusion of sequenced precursor ions for 90 s and the lock mass option (Olsen et al., 2005) for real time recalibration were enabled on both instruments.

The mass spectrometry proteomics data have been deposited to the ProteomeXchange Consortium (<http://proteomecentral.proteomexchange.org>) via the PRIDE partner repository (Vizcaino et al., 2013) with the dataset identifier PXD001831.

Data Processing and Validation

All raw MS spectra were processed with MaxQuant software suite (version 1.5.1.0) (Cox et al., 2009) and default settings. Identified peaks were searched against the target-decoy databases of *Synechocystis* sp. PCC 6803 from Cyanobase (<http://genome.microbedb.jp/cyanobase>) and Uniprot (<http://www.uniprot.org>), containing 3672 and 3507 protein sequences and 245 common contaminants, with the following database search criteria: Trypsin was defined as cleaving enzyme and up to two missed cleavages were allowed. Carbamido-methylation of cysteines was set as a fixed and methionine oxidation, protein N-termini acetylation and S/T/Y phosphorylation were set as variable modifications. Light-, medium-heavy- and heavy- dimethylation labeling on peptide N-termini and lysine residues was defined for samples from the quantitative experiments. The initial mass tolerance of precursor ions was limited to 6 ppm and 0.5 ppm for fragment ions. False discovery rates (FDRs) of peptides and proteins were set to 1%, respectively. Quantification of dimethylation labeled peptides required at least two ratio counts. Peptides were only allowed with a posterior error probability (PEP) <1% at the peptide- and <5% at the phosphopeptide level. Phosphopeptide MS/MS spectra were further manually filtered and validated with stringent acceptance criteria: Phosphorylation site localization with $\geq 75\%$ localization probability was manually validated as well as comprehensive coverage of b- and y-ion series for CID and HCD spectra as well as a low noise to signal ratio (Supplementary MS Spectra). To exclude quantitation bias of phosphopeptide ratios due to fluctuations of corresponding proteins, phosphopeptide ratios were normalized by division with corresponding protein ratios. Significance analysis of regulated phosphorylation events was performed with Perseus software (version 1.5.0.31), normalized phosphopeptide ratios were log₂ transformed and plotted against the respective log₁₀ transformed phosphopeptide intensities. Significantly regulated phosphorylation events were identified by significance A analysis with a p -value of 0.05.

Immunoblot Analysis

Proteins from 2 mL cell culture aliquots were extracted in 50 mM Tris/HCl, 5 mM EDTA buffer, pH 7.4, with a RiboLysor, conducting five cycles with a speed of 6.5 m s^{-1} for 15 s at 4°C. Protein concentration was measured by Bradford assay and 50 µg or 15 µg total protein content was separated either by SDS- or by non-denaturing clear native polyacrylamide gel electrophoresis (PAGE), respectively. Pre-cast Tris-glycine 4–20% gradient SDS polyacrylamide gels (NuSep) or 4–16% gradient native polyacrylamide gels (Serva) were used according to the manufacturer's protocols. Protein transfer was performed on a semi-dry blotting system (peqlab) onto polyvinylidene fluoride (BioTrace™ PVDF, Pall Corporation) membranes. Membranes were blocked o.n. in TBS and 1% Tween20 at 4°C. Polyclonal primary antibodies against the P_{II} protein (serum, produced in rabbit) or the AtpB protein (Abcam 65378, produced in rabbit) were incubated for 2 h at RT in a 1:5000 dilution in TBS-T after washing of the membrane with TBS-T buffer. Membranes were washed again and peroxidase coupled secondary antibody (Sigma A6154) was added in a 1:2000 dilution for 1 h at RT. Proteins were visualized by Lumi-Light Plus detection reagent (Roche).

Results

As an initial step to systematically approach the global phosphoproteome of *Synechocystis* PCC 6803, we first performed a conventional qualitative gel-free phosphoproteome analysis, based on TiO₂ enrichment of phosphopeptides from a tryptic digest of the crude protein extract, followed by mass spectrometry (MS) analysis. In order to achieve the most comprehensive coverage of the phosphoproteome, we compared three common sample preparation workflows for MS identification of phosphorylation events as well as for total proteome analysis (see below). Based on the obtained results, we applied the most successful protein extraction strategy for a quantitative study to analyze phosphoproteome dynamics in response to nitrogen starvation.

The Qualitative (Phospho)Proteome of *Synechocystis* under Growth on Nitrate

Cells were harvested from a nitrate-grown *Synechocystis* culture at mid exponential growth phase ($\text{OD}_{750} = 0.6$) and split into three equal parts that were subjected to the following workflows: (A) Filter Aided Sample Preparation (FASP), (B) protein extraction as in the FASP protocol in combination with acetone/methanol protein precipitation, and (C) extraction with Y-PER in combination with acetone/methanol protein precipitation (hereafter designated as methods A, B and C, respectively; for details see Materials and Methods). For total proteome analyses, one portion of the sample was fractionated into five fractions by strong anion exchange chromatography. The remaining sample was used for five consecutive rounds of phosphopeptide enrichment by TiO₂ chromatography. All samples were analyzed by nanoLC-MS/MS on an LTQ Orbitrap XL mass spectrometer.

On the proteome level, 2055 proteins were identified in the combined analysis of all three tested sample preparation workflows, including proteins detected in the proteome

measurements and (unmodified) proteins detected from the TiO₂ chromatography. Method A recovered 1835 proteins, method B 2014 proteins and method C 1983 proteins in total (Supplementary Table 1). At the phosphoproteome level, 301 phosphorylation events were identified with high confidence after manual validation of phosphopeptide MS/MS spectra, of which 262 non-redundant phosphorylation events, corresponding to 242 non-redundant phosphopeptides and 188 phosphoproteins, could be located on a specific S/T/Y residue. Additionally, 39 non-redundant phosphorylation events could be located on specific peptides and are referred to as unlocalized. Method A, B or C recovered, respectively, 21, 235, or 67 non-redundant phosphorylation events in total (Supplementary Table 2; Supplementary Information 1).

We concluded that all three methods had a similar performance on the protein level; however, striking differences in the performance were observed on the phosphoproteome level, with method B obviously being the method of choice. These results clearly demonstrate the importance of a potent and suited protein extraction protocol for the analysis of the phosphoproteome in organisms with a high content of membranous compartments such as cyanobacteria. As evidenced here, the overall number of identified proteins did not automatically lead to high numbers of identified phosphorylation events. Since phosphorylation events have in many cases a low occupancy in prokaryotic organisms (Soares et al., 2013), the quantity of specific extracted (phospho)proteins may be crucial, however this issue only can be analyzed in a quantitative experiment.

Quantification of the *Synechocystis* (Phospho)Proteome

The qualitative phosphoproteome analysis of the nitrate-grown *Synechocystis* sp. PCC 6803 cells showed a high abundance of protein S/T/Y phosphorylation; therefore, we were interested in the dynamic response of the (phospho)proteome in response to nitrogen starvation. Since autotrophically growing cyanobacteria are not suitable for metabolic stable isotope labeling, we used a protocol in which samples are labeled after protein digestion, using stable isotope dimethylation of peptides on N-termini and lysine side chains (Boersema et al., 2009). The experimental setup allowed us to analyze and compare three different metabolic conditions: (1) cells exponentially growing on nitrate; (2) cells exponentially growing on ammonia; (3) cells from nitrogen-free medium (nitrogen starvation for 24 h after growth on nitrate). We utilized this approach to perform a global quantitative phosphoproteome study including two experiments with slightly different cultivation settings. In the first experiment, cells from a stationary culture were diluted into fresh medium, grown to an optical density of 0.6 and then used as an inoculum for the final experimental culture. In the second experiment, the cells were pre-adapted to their respective nitrogen source by five cultivation cycles, from where the final experimental culture was started. The exact cultivation conditions for both experiments are described in the Materials and Methods section. The comparison between nitrate and ammonium-grown cells was not further addressed in this study.

Proteins were extracted from cell pellets by “method B” as described in Materials and Methods, precipitated by acetone-methanol mixture and subjected to in-solution digestion by trypsin. Obtained peptide solutions were loaded onto C18 reverse phase columns and subsequently chemically labeled by dimethylation. Different isotopologues of formaldehyde and cyanoborohydride were used: Samples from nitrate grown cultures were light labeled with CH_2O and NaBH_3CN , samples from ammonia grown cultures were medium-heavy labeled with CD_2O and NaBH_3CN and samples from nitrogen starved cells were heavy labeled with $^{13}\text{CD}_2\text{O}$ and NaBD_3CN . Labeling efficiency was in all cases 94% or greater (Supplementary Information 2). Labeled samples from nitrate (NO_3^- ; light), ammonium (NH_4^+ ; medium-heavy), and nitrogen starved (-N; heavy) cells were then mixed in a ratio of 1:1:1 based on the underlying protein amounts. Correct mixing of labeled peptides was validated by a dedicated MS measurement. The mixed sample was used for proteome and phosphoproteome analyses. For proteome analysis, isoelectric focusing (IEF) of the peptide mixtures was performed (OffGel strategy) and phosphopeptide enrichment was conducted by TiO_2 chromatography in two technical replicates. All samples were analyzed by nanoLC-MS/MS on an LTQ Orbitrap Elite mass spectrometer. The experimental workflow is shown in Supplementary Information 3. To exclude quantification bias of phosphorylation events induced by possible alterations in the abundance of the corresponding proteins, measured phosphopeptide ratios were normalized by the respective unmodified protein ratios from the proteome measurements.

Technical Reproducibility of the Experiments

To estimate the technical reproducibility of the phosphoproteome, we analyzed the correlation of phosphorylation event ratios, determined by phosphopeptide enrichments, between the two technical replicates of each experiment. To this end, we calculated Pearson correlation coefficients of 65 and 67 shared quantified phosphorylation events between technical replicates for experiments 1 and 2, respectively. The calculated Pearson correlation coefficients of unnormalized phosphorylation events were 0.905 for $-\text{N}/\text{NO}_3^-$ ratios and 0.937 for $-\text{N}/\text{NH}_4^+$ ratios for the first experiment and 0.948 for $-\text{N}/\text{NO}_3^-$ ratios and 0.913 for $-\text{N}/\text{NH}_4^+$ ratios for the second experiment, revealing a good technical reproducibility and high overlap of phosphorylation events. Correlation plots from technical replicates of phosphopeptide ratios are shown in the supplement (Supplementary Information 4). When comparing the correlation between experiments 1 and 2 in the final dataset, differences on the proteome level as well as on the phosphoproteome level could be observed, which might be accounted to the different pre-culture treatments. On the proteome level, the calculated Pearson correlation coefficients were 0.758 for $-\text{N}/\text{NO}_3^-$ protein ratios and 0.867 for $-\text{N}/\text{NH}_4^+$ protein ratios between experiments 1 and 2. On the phosphoproteome level, the Pearson correlation coefficient were 0.687 for 87 shared $-\text{N}/\text{NO}_3^-$ phosphorylation event ratios and 0.638 for 89 shared $-\text{N}/\text{NH}_4^+$ phosphorylation event ratios between experiments 1 and 2 (Supplementary Information 5).

Protein Phosphorylation Dynamics in Response to Nitrogen Starvation

The combined dataset including proteome and phosphoproteome measurements from all experiments led to the overall identification of 232,924 MS/MS spectra, covering 16,774 non-redundant peptides from 2382 proteins. The estimated false discovery rate (FDR) was 0.18% at the peptide level and 1.04% at the protein level. Of the identified 2382 proteins, 2111 proteins fulfilled the requirement of having at least two quantification events (ratio counts) in at least one of both experiments and were considered as quantified.

Wang and coworkers cataloged the so far identified *Synechocystis* sp. PCC 6803 proteome by combining previously published proteome studies. Thereby, they reported a total of 1738 experimentally identified proteins, which amounts to 47.3% of the possible 3672 protein coding genes listed on Cyanobase (Wang et al., 2009). By comparison, the present quantitative gel-free proteome analysis identified 64.9% of the theoretical *Synechocystis* proteome (2382 of 3672 proteins), with a quantification rate of 57.5% of the total proteome (2111 of 3672). These numbers are presumably close to the completeness of the expressed proteome under the actual experimental conditions, since of the previously identified 1738 proteins, 90.0% (1565) were also identified in the present study. Of the 1935 previously unidentified proteins, 44.3% (857) were identified and 32.0% (620) were even quantified in our combined dataset. In a global transcriptome study, analyzing ten different growth and stress conditions, Kopf and coworkers could recently identify a total of 3101 expressed genes in *Synechocystis*. Under nitrogen starvation and nitrate growth conditions, approximately 75% of these expressed genes were present (approx. 2300) (Kopf et al., 2014). These results match very closely to the number of identified proteins in our MS based analysis (2382).

On the phosphoproteome level, manual inspection of phosphopeptide MS/MS spectra identified in both experiments 183 S/T/Y phosphorylation events with high confidence. Of these, 148 phosphorylation events, corresponding to 86 phosphoproteins, fulfilled the following two criteria: quantification of the phosphorylation event with at least two ratio counts in at least one experiment and normalization by the corresponding protein ratio of the respective experiment. Of these 148 phosphorylation events, 105 were quantified in experiment 1 and 130 in experiment 2, with an overlap of 87 phosphorylation events between both experiments. All detected proteins and phosphopeptides (including unlocalized and localized phosphorylation events) from the quantitative study are shown in the supplement (Supplementary Tables 3, 4).

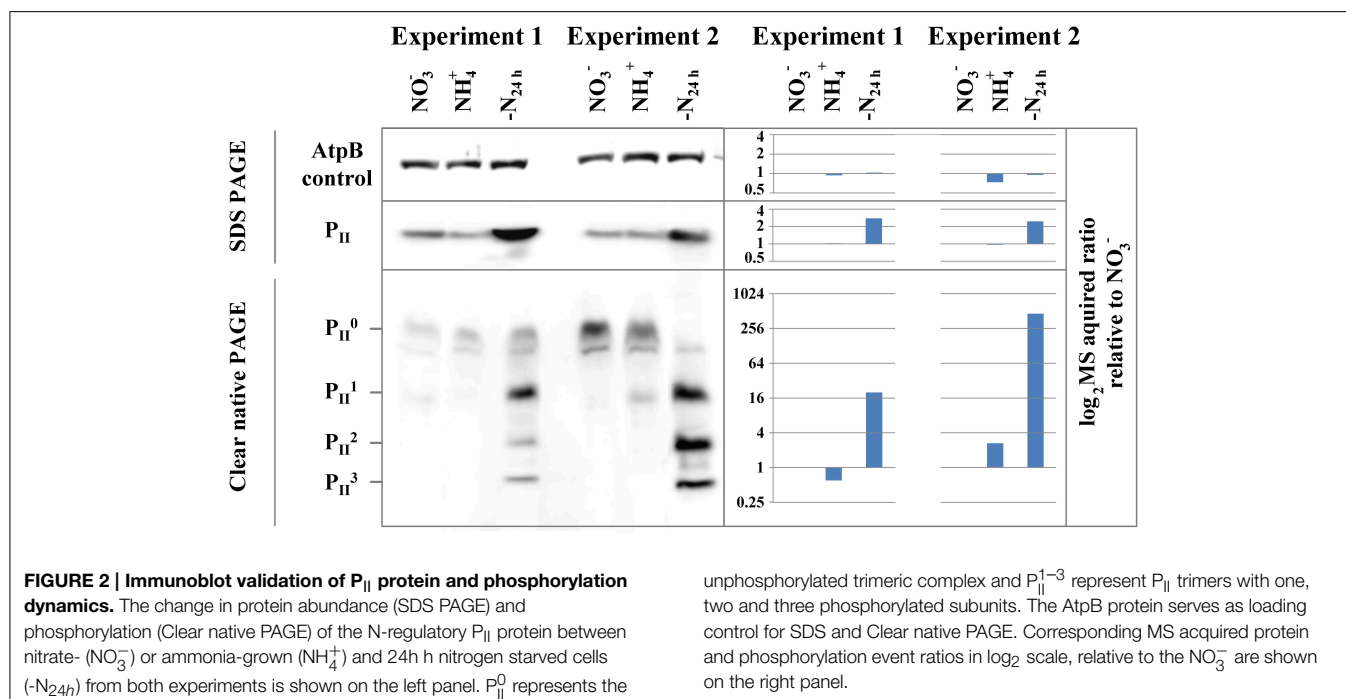
As a test case for our quantitative mass spectrometry acquired (phospho)proteome data, we analyzed the expression profile of the nitrogen regulatory signal protein P_{II} by immunoblot analysis on the protein level by SDS-polyacrylamide gel electrophoresis (PAGE) and on the phosphorylation level by non-denaturing PAGE (Forchhammer and Tandeau De Marsac, 1994). Under nitrogen-limiting conditions, the P_{II} signal protein accumulates, associated with enhanced phosphorylation of residue Ser49 at the apex of the surface exposed T-loop (Forchhammer, 2004). Under nitrogen-depleted conditions, all three subunits of the

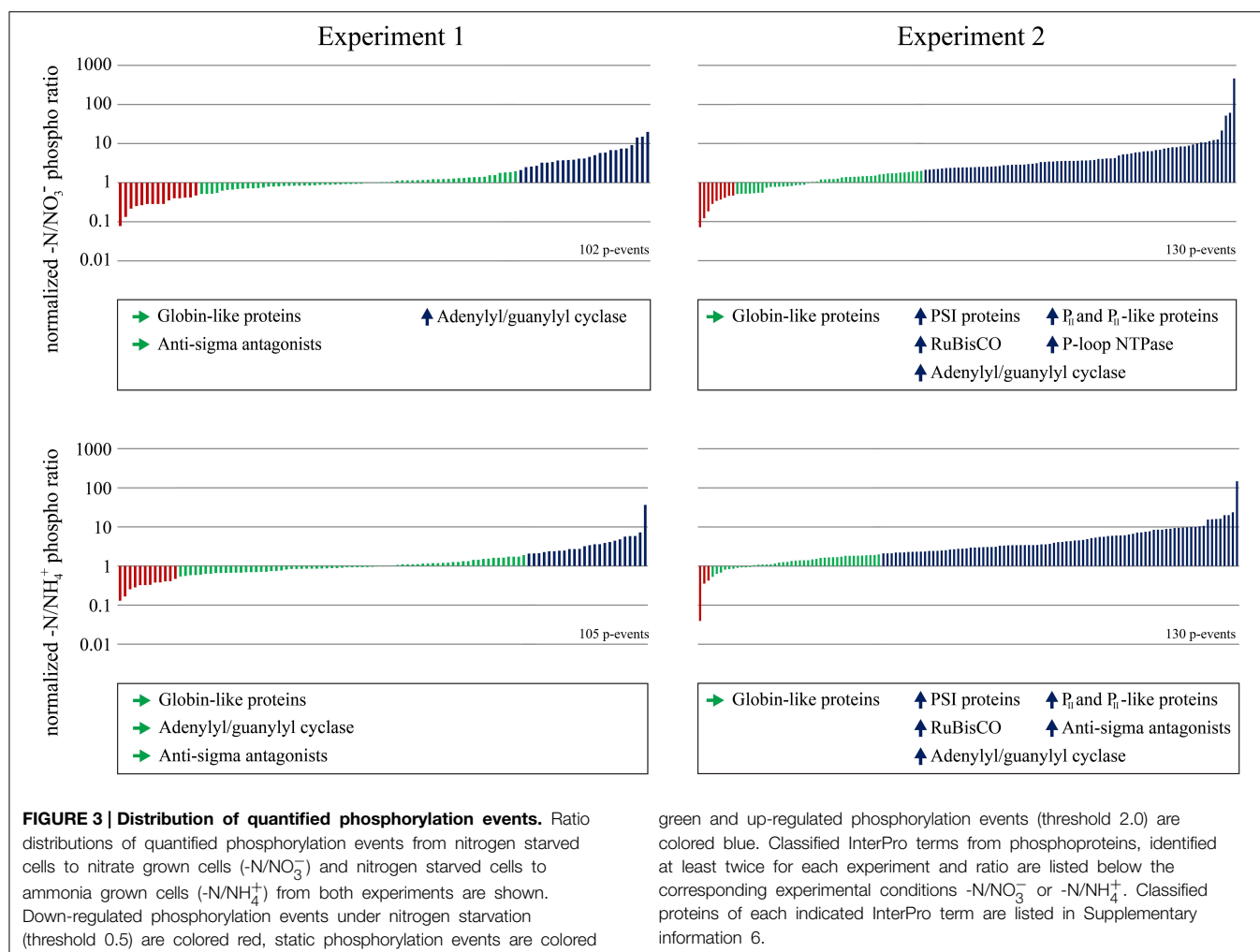
homotrimeric P_{II} protein are phosphorylated (Forchhammer and Tandeau De Marsac, 1994). In the present experiments, P_{II} protein levels were similar between nitrate or ammonium grown cells but increased under nitrogen starvation (Figure 2). This is in accordance with transcription analysis of the *glnB* gene (encoding the P_{II} protein), showing up-regulation under nitrogen starvation (Fadi Aldehni et al., 2003; Aguirre Von Wobeser et al., 2011). The result of the analysis of the P_{II} phosphorylation state by non-denaturing PAGE from both experiments is shown below in the figure. As expected, the Ser49 phosphorylation strongly increased under nitrogen starvation, with the phosphorylated P_{II} trimer isoforms becoming the most prominent bands. The unphosphorylated P_{II} protein is in contrast the most intense band in nitrate and ammonia grown conditions. Overall, MS based quantification of the P_{II} signaling protein with respect to protein abundance as well as on the phosphorylation level, as indicated in the figure, is in good agreement with the immunoblot results, implying that the quantitative MS analysis is valid.

To analyze the response of the *Synechocystis* phosphoproteome to nitrogen starvation, we classified the quantified $-N/NO_3^-$ and $-N/NH_4^+$ phosphorylation event ratios into up- or down-regulated and static patterns, separately for both experiments (Figure 3). Functional assignment of phosphoproteins, comprising all proteins with one or more quantified phosphorylation events in our dataset (proteins with multiple phosphorylation events were only listed once), could be retrieved from InterPro database. InterPro protein terms were obtained for 81 of the 86 phosphoproteins. For classification of phosphorylation event ratios, we defined an arbitrary threshold of a twofold change; phosphorylation events with a ratio below 0.5 were classified as down-regulated; phosphorylation events

with ratios above 2.0 were classified as up-regulated; phosphorylation events with a ratio between 0.5 and 2.0 were classified as static. Interestingly, a difference in the percentage of regulated or static phosphorylation events was observed between both experiments in response to nitrogen starvation (for $-N/NO_3^-$ and $-N/NH_4^+$ ratios). In experiment 1, characterized by a short pre-adaptation to the respective nitrogen sources, the majority of phosphorylation events revealed a static pattern, whereas, in experiment 2, characterized by a long pre-adaptation, the majority revealed up-regulation. In both experiments, down-regulated phosphorylation events revealed the lowest occurrence. The occurrence and frequency of InterPro terms was analyzed in the three classes (down-regulated, static or up-regulated) between $-N/NO_3^-$ and $-N/NH_4^+$ ratios for each experiment (see Figure 3), to reveal whether the phosphorylation pattern correlates with potential protein functions. Whereas, for down-regulated phosphoproteins this analysis did not reveal any results, globin-like proteins (e.g., phycobilisome) revealed in all cases static phosphorylation patterns. In addition, phosphorylation on anti-sigma antagonist proteins was in principal static in the first, but up-regulated in the second experiment. With the exception of the $-N/NH_4^+$ ratios in experiment 1, phosphorylation on adenylyl/guanylyl cyclase proteins was in principal up-regulated. In experiment 2, following proteins showed additionally up-regulated phosphorylation dynamics: proteins of photosystem I (PSI) and RuBisCO, as well as P-loop NTPase and N-regulatory P_{II} and P_{II} -like proteins. However, in experiment 1, these phosphoprotein classes did not fulfill the requirement of having at least two up-regulated evidences. The respective classified proteins are indicated in Supplementary Information 6.

This classification provides a comprehensive overview about general protein functions, which are frequently regulated under



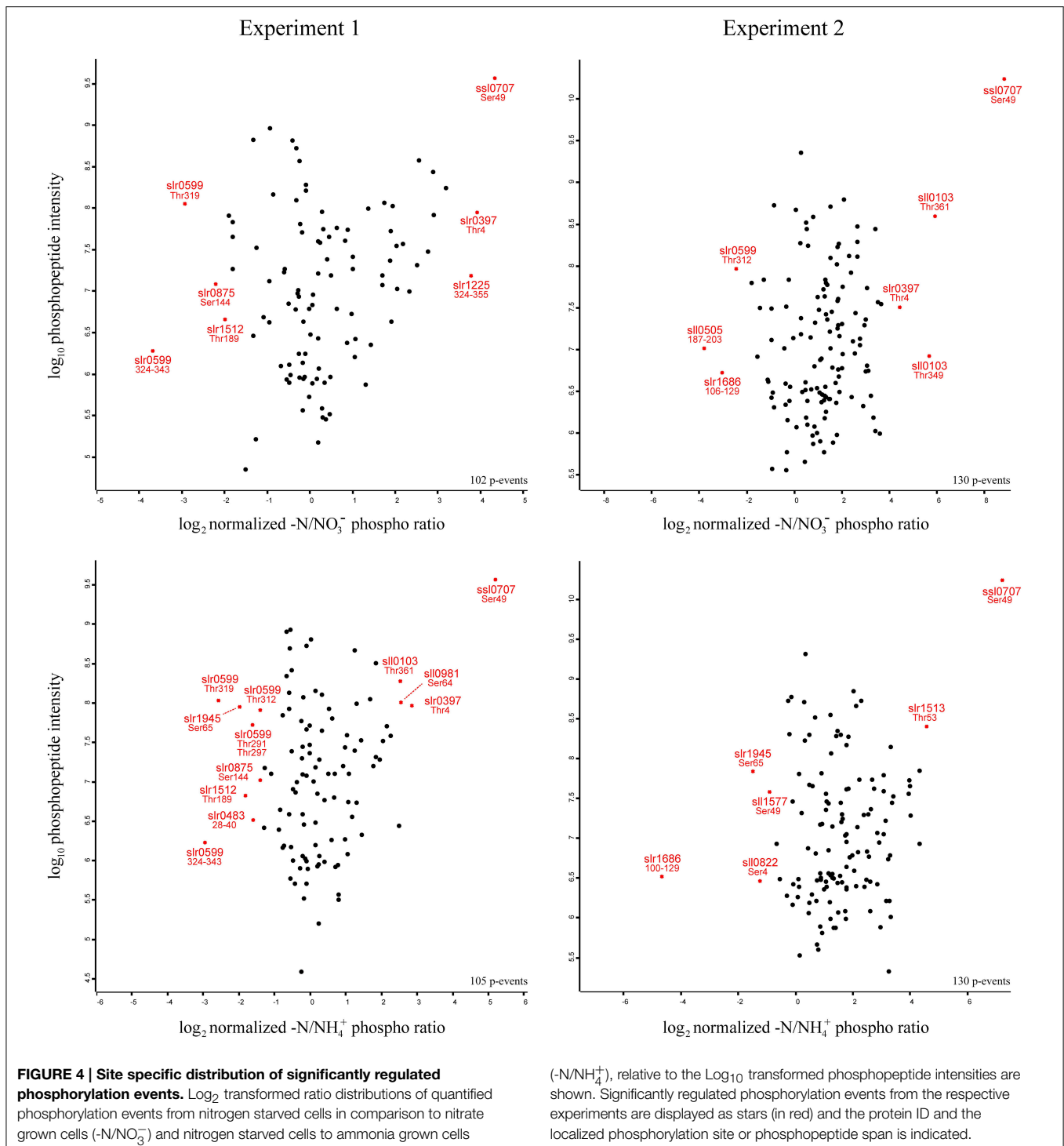


nitrogen starvation by S/T/Y phosphorylation in *Synechocystis*. In order to obtain a more detailed insight about specific phosphorylation events with strong dynamics, and their abundance under the studied conditions, we plotted the quantified phosphorylation event $-N/NO_3^-$ and $-N/NH_4^+$ ratios against the respective phosphopeptide intensities, separately for each experiment (Figure 4). Based on the overall distribution of the specific phosphorylation events, significantly regulated events (both, localized and unlocalized on the detected peptide) were identified by significance analysis, (p -value = 0.05; for details see Materials and Methods). Phosphorylation events revealing significant up- or down-regulation are depicted in the scatter plots as stars (in red), and the respective phosphoprotein and modification site (or phosphopeptide span in case of unlocalized phosphorylation events) is indicated. All significant phosphorylation events (between N/NO_3^- and $-N/NH_4^+$ ratios) from both experiments are listed in Table 1.

As expected from previous studies, P_{II} (Ssl0707) Ser49 phosphorylation exhibited the highest level of increase in phosphorylation and intensity throughout all experiments in response to nitrogen starvation. Interestingly, two Ser/Thr protein kinases with contrary phosphorylation dynamics were identified: The

Ser/Thr protein kinase C (Slr0599) revealed multiple significantly down-regulated phosphorylation events in experiment 1 and for one of them in experiment 2. Four out of five events could be localized on a specific Thr residues (on positions 291, 297, 312, and 319), and one event could be quantified on the phosphopeptide ³²⁴VYTQFTGYTETQEGSPLMK³⁴³. In contrast, the putative Ser/Thr protein kinase F (Slr1225) revealed one significantly up-regulated phosphorylation event, which was quantified on the phosphopeptide ³²⁴APPGATVSTPQGTNTQIQPTPASSASPLTAPK³⁵⁵ for $-N/NO_3^-$ ratios in experiment 1.

Other significantly down-regulated phosphorylation events were detected in experiment 1 on Ser144 of the large-conductance mechanosensitive channel (Slr0875) and on the phosphopeptides ²⁸TDVGPITTPNPQK⁴⁰ and ¹⁸⁷LVAAGVILPLSERSASR²⁰³ of the hypothetical proteins Slr0483 and Sll0505, respectively. The phosphopeptide ¹⁰⁰LQSELSTLEQELAQQDSSPTGPGEEQKSSR¹²⁹, Ser4 and Ser49 of the hypothetical proteins Slr1686 and Sll0822 and the phycocyanin beta subunit (Sll1577), respectively, revealed down-regulated phosphorylation events in experiment 2. Interestingly, down-regulated phosphorylation on Ser65 of



the 2,3-bisphosphoglycerate-independent phosphoglycerate mutase (Slr1945) was detected in both experiments for only $-N/NH_4^+$ ratios. Among other proteins with significantly up-regulated phosphorylation events in our study, Ser64 phosphorylation of the unknown protein Sll0981 was detected in experiment 1, whereas, phosphorylations on Thr4 of the hypothetical protein Slr0397 and Thr349 and Thr361 of the

hypothetical protein Sll0103 were detected in both experiments. Remarkably, the sodium-dependent bicarbonate transporter SbtA (Slr1512) revealed in our study down-regulation of Thr189 phosphorylation in experiment 1, whereas, the neighboring gene product, the P_{II}-like membrane-associated protein SbtB (Slr1513), revealed significant up-regulation on Thr53 in experiment 2 in response to nitrogen starvation. For a complete

TABLE 1 | List of significantly regulated phosphorylation events.

Phospho protein	Phosphopeptide sequence	Significantly regulated phosphorylation events			
		Experiment 1		Experiment 2	
		Down-regulated	Up-regulated	Down-regulated	Up-regulated
Ssl0707	YRGpS ⁴⁹ EYTFEFLQK	-	-N/NO ₃ ⁻ and -N/NH ₄ ⁺	-	-N/NO ₃ ⁻ and -N/NH ₄ ⁺
Slr1945	GQMGNpS ⁶⁵ EVGHLNLGAGR	-N/NH ₄ ⁺	-	-N/NH ₄ ⁺	-
Slr1686	¹⁰⁰ LQSELSTLEQELAQDSSPTG PGEEQKSSR ¹²⁹	-	-	-N/NO ₃ ⁻ and -N/NH ₄ ⁺	-
Slr1513	SSGQPNpT ⁵³ SDIEANIK	-	-	-	-N/NH ₄ ⁺
Slr1512	QPVAAGDYGDQpT ¹⁸⁹ DYPR	-N/NO ₃ ⁻ and -N/NH ₄ ⁺	-	-	-
Slr1225	³²⁴ APPGATVSTPQGTNTQIQPTPAS SASPLTAPK ³⁵⁵	-	-N/NO ₃ ⁻	-	-
Slr0875	LITTLENQSSSpS ¹⁴⁴ Q	-N/NO ₃ ⁻ and -N/NH ₄ ⁺	-	-	-
Slr0599	GDRPGNpT ²⁹¹ VANGKpT ²⁹⁷ K	-N/NH ₄ ⁺	-	-	-
Slr0599	SNHQPTAPTLVVGpT ³¹² PYNANDTQATK	-N/NH ₄ ⁺	-	-N/NO ₃ ⁻	-
Slr0599	SNHQPTAPTLVVGTPYNANDpT ³¹⁹ QATK	-N/NO ₃ ⁻ and -N/NH ₄ ⁺	-	-	-
Slr0599	³²⁴ VYTQFTGYTETQEGSPLMK ³⁴³	-N/NO ₃ ⁻ and -N/NH ₄ ⁺	-	-	-
Slr0483	²⁸ TDVGPIITPNPQK ⁴⁰	-N/NH ₄ ⁺	-	-	-
Slr0397	VLpT ⁴ QFASSPAPPQSFAPNPR	-	-N/NO ₃ ⁻ and -N/NH ₄ ⁺	-	-N/NO ₃ ⁻
Sll1577	ITGNpS ⁴⁹ AIVSNAAR	-	-	-N/NH ₄ ⁺	-
Sll0981	LTLpS ⁶⁴ AQGGNK	-	-N/NH ₄ ⁺	-	-
Sll0822	pS ⁴ NATKPLTGEALLEK	-	-	-N/NH ₄ ⁺	-
Sll0505	¹⁸⁷ LVAAGVILPLSERSASR ²⁰³	-N/NO ₃ ⁻	-	-	-
Sll0103	YRQTQIAEpT ³⁴⁹ K	-	-	-	-N/NO ₃ ⁻
Sll0103	QGAApT ³⁶¹ MLQTAAK	-	-N/NH ₄ ⁺	-	-N/NO ₃ ⁻

overview of the detected phosphorylation events revealing significant regulation in response to nitrogen starvation, see **Table 1**.

Discussion

Sample Preparation and Dimethylation Labeling for Phosphoproteome Quantification

Numerous previous studies revealed insights with regards to the *Synechocystis* proteome and shed first light into the phosphoproteome. However, most of these studies were exclusively focused on specific cellular compartments such as different membrane fractions or the cytoplasm or on specific proteins. Therefore, most previous studies mapped only “snapshots” of either delimited cellular compartments or only one particular metabolic condition of the proteome or the phosphoproteome, mainly performed in a qualitative manner, based on 2D gel strategies. The present study aimed to establish a method to analyze the global dynamic changes of the *Synechocystis* phosphoproteome in a site specific and quantitative manner between distinct metabolic conditions. In the present study, this was exemplified using nitrate and ammonia grown cells in comparison to 24 h nitrogen starved cells.

This study led to a comprehensive detection of the entire expressed proteome, including the identification of 857 and the quantification of 620 previously not identified proteins, and thus far is the largest reported dataset of phosphorylation events in *Synechocystis*. The efficient extraction of phosphoproteins

contributed in combination with a gel-free MS strategy to a high percentage of detections in the qualitative phosphoproteome dataset. Although similar identification numbers were detected on the proteome level, when comparing method B with the detergent buffer based method C (Y-PER), significantly more localized phosphorylation events (235 vs. 67) could be obtained exclusively with method B. This may be due to the fact that the overall extraction efficiency of hydrophobic proteins was higher with method B compared the other methods. In bacteria, phosphorylation events are predominantly present in low occupancy compared to eukaryotes. Therefore, an overall small percentage of phosphoproteins are actually phosphorylated compared to the respective unmodified protein (Soares et al., 2013). When more copies of a certain phosphoprotein with low phosphorylation occupancy are present in the sample, the chances to detect the phosphorylation event or even to localize the modified S/T/Y site are much higher. This becomes especially relevant for quantitative studies, where the corresponding phosphorylation events must be detected in all samples and stages, even if their abundances are strongly fluctuating as in the case of regulated phosphorylation events.

Subsequent to an efficient protein extraction method from the cyanobacterial samples, the quantification technique is crucial. Although many different techniques for quantitative phosphoproteome studies have been reported, SILAC has been established as a precise and robust method firstly in eukaryotic and later in prokaryotic organisms (Ong et al., 2002; Soufi et al.,

2010). Previously, we could detect the phosphoproteome dynamics of the model bacterium *E. coli* K-12 throughout the growth in minimal medium (Soares et al., 2013). However, in autotrophic cyanobacteria species, metabolic SILAC labeling would require severe disruptions in the nitrogen metabolic pathway by knocking out key enzymes of the lysine and/or arginine amino acid synthesis pathways. We decided to bypass this drawback by application of chemical stable isotope labeling based on dimethylation of peptides on a C18 column as described earlier. As mentioned, the methodology was applied before successfully in quantitative phosphoproteome studies, but limited to the eukaryotic domain as reviewed previously (Kovanich et al., 2012).

Here, we expanded this method to the quantitative phosphoproteome analysis in prokaryotic organisms. All validation steps of the labeling methodology confirmed a high quality of the experiments. The labeling efficiency was high ($\geq 94\%$). The correlation between technical replicates of the phosphoproteome revealed high reproducibility and the overlap of quantified phosphorylation events between technical replicates (see Supplementary Information 4) and experiments (see Supplementary Information 5) was high. We conclude that the dimethylation labeling strategy combined with an efficient protein extraction method is highly suitable for systematically detecting phosphoproteome dynamics in (cyano)bacteria.

Dynamics of Protein S/T/Y Phosphorylations Involved in Nitrogen and Carbon Metabolism and Photosynthesis under Nitrogen Starvation

In bacteria, research on protein phosphorylation on Ser/Thr and Tyr residues in the past years led to accumulating evidences revealing this modification as one of the most prominent mechanisms in signal transduction for fast cellular responses to environmental changes (Macek and Mijakovic, 2011; Soufi et al., 2012). Moreover, previous phosphoproteomic studies have revealed that a large portion of these phosphorylation events are associated with key metabolic processes in a cell, however, detailed information of the phosphorylation functions are rare. For cyanobacteria, having an autotrophic lifestyle, fast response to changing environmental conditions that affect the energy-, nitrogen-, and carbon metabolism appears to be essential. This statement agrees with the high numbers of identified and quantified phosphorylation events in our dataset that can be assigned to photosynthesis, carbon and nitrogen uptake and subsequent metabolic pathways.

Of the significantly regulated phosphoproteins, the sensory nitrogen signaling P_{II} protein showed the strongest dynamics in response to nitrogen starvation with Ser49 phosphorylation being strongly up-regulated. This is in agreement with previous studies and emphasizes its role as a marker for nitrogen-limited conditions (Forchhammer and Tandeau De Marsac, 1994, 1995; Mikkat et al., 2014). In *E. coli*, it was reported, that the P_{II} homolog protein GlnK regulates the influx of ammonia from the surrounding medium through the homotrimeric ammonium/methylammonium permease AmtB, and GlnK-AmtB interaction blocks the uptake (Van Heeswijk

et al., 1996). A similar mechanism, although not yet demonstrated, could be assumed in *Synechocystis* between P_{II} and the AmtB homologue Amt1 (Sll0108), with the P_{II} Ser49 phosphorylation preventing this interaction to ensure efficient ammonia uptake under N-limited conditions. Interestingly, we identified Amt1 as a phosphoprotein, which is increasingly phosphorylated under N-limitation. This mechanism could reveal an additional and more sensitive regulative control mechanism to ensure maximum ammonia uptake. Remarkably, the P_{II} -like membrane-associated protein SbtB (Slr1513) revealed significant increasing Thr53 phosphorylation under N-limitation, like the GlnB P_{II} protein. Interestingly, the *sbtB* gene is neighboring the sodium-dependent bicarbonate transporter Slr1512 (*sbtA*) gene on the chromosome, which revealed in our analysis significant decreasing Thr189 phosphorylation under the same conditions. It is thus tempting to speculate that SbtB may be involved in regulation of SbtA activity, in agreement with a recent analysis of the *sbtAB* operon (Du et al., 2014).

Phosphorylation of proteins involved in the inorganic carbon uptake mechanism and the Calvin cycle was also observed: On the carbon dioxide concentrating mechanism (Ccm) proteins M and N (Sll1031 and Sll1032), multiple phosphorylation events were detected, of which three could be quantified and localized on Sll1031 (pSer352, pThr358, and pThr609) and one on Sll1032 (pThr121). These phosphorylation events generally showed either static or slightly increasing phosphorylation under N-depletion, with the most prominent regulation on pThr609, showing up to threefold increase for $-N/NH_4^+$ ratios. More pronounced, phosphorylation of the phosphoribulokinase (Sll1525) on Ser17 increased strongly upon N-starvation. In addition, two phosphorylation events were quantified on the small and large subunits of the ribulose biphosphate carboxylase/oxygenase RuBisCO (Slr0012 and Slr0009), both showing a three- to fourfold increase in response to nitrogen starvation. Both phosphorylation events are localized on seryl-residues, Ser78 on the small and supposedly Ser323 on the large subunit. Interestingly, similar phosphorylation sites were identified in a phosphoproteome study of *Arabidopsis thaliana* on the respective subunits. Here, Ser71 and Ser321 were phosphorylated on the small and large subunits, respectively, besides several other phosphorylation events (Aryal et al., 2011).

Several enzymes involved in the pentose phosphate pathway and in glycolysis were detected as phosphoproteins, generally with static or increasing phosphorylation dynamics toward N-starvation, such as the fructose-bisphosphate aldolase (Sll0018) and the 6-phosphogluconate dehydrogenase (Sll0329). Interestingly, the 2,3-bisphosphoglycerate-independent phosphoglycerate mutase (Slr1945) elicited an opposite response, with the level of Ser65 phosphorylation significantly decreasing under N-depletion.

Cyanobacteria are considered as progenitors of chloroplasts, which explains why the photosynthetic apparatus is highly similar to that of green plants. However, some features are unique to cyanobacteria, such as the phycobilisome light harvesting antenna, transferring light energy to the PSII. Previously, linker proteins from the phycobilisome antenna and ferredoxin-NADPH reductase were identified as

phosphoproteins in *Synechocystis*, and dephosphorylation was driven upon long-term exposure to high light intensities and under nitrogen limitation, initiating proteolytic cleavage and degradation (Piven et al., 2005). In our study, we detected a high abundance of phosphorylation on proteins from the photosynthesis apparatus; we detected in the qualitative dataset 60 phosphorylation events on specific S/T/Y residues from 24 proteins associated with photosynthesis (see Supplementary Table 2). During quantitative analysis, only nine phosphoproteins associated with photosynthesis could be detected. This is in agreement with the general tendency of less identified phosphorylation events in the quantitative dataset.

Among the detected proteins, the most prominent dynamics were observed for PSI, phycocyanin and allophycocyanin proteins. Surprisingly, phosphorylation events on these proteins revealed increasing levels under nitrogen starvation, in contrast to the phycobilisome antenna linker proteins, which were described to undergo dephosphorylation under nitrogen starvation. We were not able to quantify the phosphorylation events on linker proteins. On the proteome level, we detected strong decreasing levels of linker proteins Sll1579 and Sll1471, whereas, all other linker proteins (Slr1459, Slr0335, Sll1580, Slr2051, Ssr3383, and Ssl3093) revealed only slight decreasing or static levels under nitrogen starvation. This result could indicate that either the process of chlorosis has not occurred to a level that is required in order to significantly reduce the level of phycobiliproteins, or phycobiliproteins were only partially degraded and peptide fragments were still present in the cells, which were then detected by MS analysis. To solve this issue, further experiments containing earlier and later time points are required.

Dynamics of Serine/Threonine Kinases

In our quantitative phosphoproteome dataset, we observed an overall trend of increased phosphorylation levels during nitrogen limitation. These dynamics are visualized in **Figures 3, 4**. Overall, there was a higher incidence of increasing than of decreasing phosphorylation in response to nitrogen limitation. This observation is more pronounced in experiment 2, characterized by longer pre-adaption in the respective nitrogen source. Interestingly, two Ser/Thr protein kinases were found among the phosphoproteins with significantly fluctuating phosphorylation dynamics. Ser/Thr protein kinase F (Slr1225) displayed in response to nitrogen starvation increasing phosphorylation of two phosphothreonines on positions 24 and 27 (2–3 fold increased), and on

an unlocalized phosphorylation event on the phosphopeptide ³²⁴APPGATVSTPQGTNTQIQPTPASSASPLTAPK³⁵⁵. Contrary, we identified four phosphothreonines to be significantly decreasing under the same conditions on the Ser/Thr protein kinase C (Slr0599) and one unlocalized phosphorylation event (see **Table 1**). These two Ser/Thr kinases were shown previously *in vitro* by radiolabeling experiments to autophosphorylate (Kamei et al., 2002). Furthermore, both kinases were suggested in combination with Ser/Thr protein kinase K to be required for a phosphorylation cascade resulting in GroES phosphorylation (Zorina et al., 2011). It is conceivable that the phosphorylation dynamics of both kinases are interconnected and could involve a protein phosphatase.

In conclusion, this study reports the first global phosphoproteome analysis of *Synechocystis*, with the highest discovery rate of proteins (2382) and phosphorylation events (301 under nitrogen growth conditions) described thus far. We showed quantitative dynamics of the total proteome in response to nitrogen starvation. This is not only of broad relevance for *Synechocystis* molecular biology, but sets the ground for a comprehensive analysis of the phosphoproteome, with quantified dynamics of 148 phosphorylation events. Using nitrogen starvation acclimation as a test case, this study reveals that protein S/T/Y phosphorylation may play an outstanding regulatory role for metabolic adaptation in the model cyanobacterium *Synechocystis*. This analysis paves the way for an in depth analysis of the role of protein phosphorylation in cyanobacteria, to unravel its contribution to homeostatic control.

Acknowledgments

BM and KF thank the SFB766 of the Deutsche Forschungsgemeinschaft for financial support. Furthermore, we would like to thank all members of the Proteome Center Tuebingen, especially Boumediene Soufi for revising the manuscript, and the Department of Organismic Interactions, especially Khaled Selim for help with immunoblots and Alexander Klotz for help in graphics preparation.

Supplementary Material

The Supplementary Material for this article can be found online at: <http://www.frontiersin.org/journal/10.3389/fmicb.2015.00248/abstract>

References

- Aguirre Von Wobeser, E., Ibelings, B. W., Bok, J., Krasikov, V., Huisman, J., and Matthijs, H. C. P. (2011). Concerted changes in gene expression and cell physiology of the cyanobacterium *Synechocystis* sp. Strain PCC 6803 during transitions between nitrogen and light-limited growth. *Plant Physiol.* 155, 1445–1457. doi: 10.1104/pp.110.165837
- Allen, M., and Smith, A. (1969). Nitrogen chlorosis in blue-green algae. *Arch. Mikrobiol.* 69, 114–120. doi: 10.1007/BF00409755
- Aryal, U. K., Krochko, J. E., and Ross, A. R. S. (2011). Identification of phosphoproteins in *Arabidopsis thaliana* leaves using polyethylene glycol fractionation, immobilized metal-ion affinity chromatography, two-dimensional gel electrophoresis and mass spectrometry. *J. Proteome Res.* 11, 425–437. doi: 10.1021/pr200917t
- Ashby, M. K., and Houmard, J. (2006). Cyanobacterial two-component proteins: structure, diversity, distribution, and evolution. *Microbiol. Mol. Biol. Rev.* 70, 472–509. doi: 10.1128/MMBR.00046-05
- Biggins, J., and Bruce, D. (1987). "The relationships between protein kinase activity and chlorophyll a fluorescence changes in thylakoids from the cyanobacterium

- Synechococcus 6301," in *Progress in Photosynthesis Research*, ed J. Beggins (Dordrecht: Springer), 773–776.
- Boersma, P. J., Rajmakers, R., Lemeer, S., Mohammed, S., and Heck, A. J. R. (2009). Multiplex peptide stable isotope dimethyl labeling for quantitative proteomics. *Nat. Protoc.* 4, 484–494. doi: 10.1038/nprot.2009.21
- Collier, J. L., and Grossman, A. R. (1992). Chlorosis induced by nutrient deprivation in *Synechococcus* sp. strain PCC 7942: not all bleaching is the same. *J. Bacteriol.* 174, 4718–4726.
- Cox, J., Matic, I., Hilger, M., Nagaraj, N., Selbach, M., Olsen, J. V., et al. (2009). A practical guide to the MaxQuant computational platform for SILAC-based quantitative proteomics. *Nat. Protoc.* 4, 698–705. doi: 10.1038/nprot.2009.36
- Du, J., Förster, B., Rourke, L., Howitt, S. M., and Price, G. D. (2014). Characterisation of cyanobacterial bicarbonate transporters in *E. coli* shows that SbtA homologs are functional in this heterologous expression system. *PLoS ONE* 9:e115905. doi: 10.1371/journal.pone.0115905
- Fadi Aldehni, M., Sauer, J., Spielhaupter, C., Schmid, R., and Forchhammer, K. (2003). Signal transduction protein P(II) Is required for NtcA-regulated gene expression during nitrogen deprivation in the cyanobacterium *Synechococcus elongatus* strain PCC 7942. *J. Bacteriol.* 185, 2582–2591. doi: 10.1128/JB.185.8.2582-2591.2003
- Forchhammer, K. (2004). Global carbon/nitrogen control by PII signal transduction in cyanobacteria: from signals to targets. *FEMS Microbiol. Rev.* 28, 319–333. doi: 10.1016/j.femsre.2003.11.001
- Forchhammer, K. (2008). PII signal transducers: novel functional and structural insights. *Trends Microbiol.* 16, 65–72. doi: 10.1016/j.tim.2007.11.004
- Forchhammer, K., and Tandeau De Marsac, N. (1994). The PII protein in the cyanobacterium *Synechococcus* sp. strain PCC 7942 is modified by serine phosphorylation and signals the cellular N-status. *J. Bacteriol.* 176, 84–91.
- Forchhammer, K., and Tandeau De Marsac, N. (1995). Phosphorylation of the PII protein (glnB gene product) in the cyanobacterium *Synechococcus* sp. strain PCC 7942: analysis of *in vitro* kinase activity. *J. Bacteriol.* 177, 5812–5817.
- Görl, M., Sauer, J., Baier, T., and Forchhammer, K. (1998). Nitrogen-starvation-induced chlorosis in *Synechococcus* PCC 7942: adaptation to long-term survival. *Microbiology* 144, 2449–2458. doi: 10.1099/00221287-144-9-2449
- Hagemann, M., Golldack, D., Biggins, J., and Erdmann, N. (1993). Salt-dependent protein phosphorylation in the cyanobacterium *Synechocystis* PCC 6803. *FEMS Microbiol. Lett.* 113, 205–209. doi: 10.1111/j.1574-6968.1993.tb06515.x
- Harrison, M. A., Tsinoremas, N. F., and Allen, J. F. (1991). Cyanobacterial thylakoid membrane proteins are reversibly phosphorylated under plastoquinone-reducing conditions *in vitro*. *FEBS Lett.* 282, 295–299. doi: 10.1016/0014-5793(91)80499-S
- Heinrich, A., Maheswaran, M., Ruppert, U., and Forchhammer, K. (2004). The *Synechococcus elongatus* PII signal transduction protein controls arginine synthesis by complex formation with N-acetyl-L-glutamate kinase. *Mol. Microbiol.* 52, 1303–1314. doi: 10.1111/j.1365-2958.2004.04058.x
- Irmeler, A., and Forchhammer, K. (2001). A PP2C-type phosphatase dephosphorylates the PII signaling protein in the cyanobacterium *Synechocystis* PCC 6803. *Proc. Natl. Acad. Sci. U.S.A.* 98, 12978–12983. doi: 10.1073/pnas.231254998
- Ishihama, Y., Rappsilber, J., and Mann, M. (2006). Modular stop and go extraction tips with stacked disks for parallel and multidimensional peptide fractionation in proteomics. *J. Proteome Res.* 5, 988–994. doi: 10.1021/pr050385q
- Jers, C., Soufi, B., Grangeasse, C., Deutscher, J., and Mijakovic, I. (2008). Phosphoproteomics in bacteria: towards a systemic understanding of bacterial phosphorylation networks. *Expert Rev. Proteomics* 5, 619–627. doi: 10.1586/14789450.5.4.619
- Joseph, A., Aikawa, S., Sasaki, K., Teramura, H., Hasunuma, T., Matsuda, F., et al. (2014). Rre37 stimulates accumulation of 2-oxoglutarate and glycogen under nitrogen starvation in *Synechocystis* sp. PCC 6803. *FEBS Lett.* 588, 466–471. doi: 10.1016/j.febslet.2013.12.008
- Kamei, A., Yuasa, T., Geng, X., and Ikeuchi, M. (2002). Biochemical examination of the potential eukaryotic-type protein kinase genes in the complete genome of the unicellular cyanobacterium *Synechocystis* sp. PCC 6803. *DNA Res.* 9, 71–78. doi: 10.1093/dnares/9.3.71
- Kopf, M., Klähn, S., Scholz, I., Matthiessen, J. K. F., Hess, W. R., and Voß, B. (2014). Comparative analysis of the primary transcriptome of *Synechocystis* sp. PCC 6803. *DNA Res.* 21, 527–539. doi: 10.1093/dnares/dsu018
- Kovanich, D., Cappadona, S., Rajmakers, R., Mohammed, S., Scholten, A., and Heck, A. R. (2012). Applications of stable isotope dimethyl labeling in quantitative proteomics. *Anal. Bioanal. Chem.* 404, 991–1009. doi: 10.1007/s00216-012-6070-z
- Macek, B., and Mijakovic, I. (2011). Site-specific analysis of bacterial phosphoproteomes. *Proteomics* 11, 3002–3011. doi: 10.1002/pmic.201100012
- Maheswaran, M., Ziegler, K., Lockau, W., Hagemann, M., and Forchhammer, K. (2006). P(II)-Regulated arginine synthesis controls accumulation of cyanophycin in *Synechocystis* sp. Strain PCC 6803. *J. Bacteriol.* 188, 2730–2734. doi: 10.1128/JB.188.7.2730-2734.2006
- Mann, N. H. (1994). Protein phosphorylation in cyanobacteria. *Microbiology* 140, 3207–3215. doi: 10.1099/13500872-140-12-3207
- Mijakovic, I., and Macek, B. (2012). Impact of phosphoproteomics on studies of bacterial physiology. *FEMS Microbiol. Rev.* 36, 877–892. doi: 10.1111/j.1574-6976.2011.00314.x
- Mikkat, S., Fulda, S., and Hagemann, M. (2014). A 2D gel electrophoresis-based snapshot of the phosphoproteome in the cyanobacterium *Synechocystis* sp. strain PCC 6803. *Microbiology* 160, 296–306. doi: 10.1099/mic.0.074443-0
- Murata, N., and Suzuki, I. (2006). Exploitation of genomic sequences in a systematic analysis to access how cyanobacteria sense environmental stress. *J. Exp. Bot.* 57, 235–247. doi: 10.1093/jxb/erj005
- Muro-Pastor, M. I., Reyes, J. C., and Florencio, F. J. (2001). Cyanobacteria perceive nitrogen status by sensing intracellular 2-oxoglutarate levels. *J. Biol. Chem.* 276, 38320–38328. doi: 10.1074/jbc.M105297200
- Nishiwaki, T., Satomi, Y., Nakajima, M., Lee, C., Kiyohara, R., Kageyama, H., et al. (2004). Role of KaiC phosphorylation in the circadian clock system of *Synechococcus elongatus* PCC 7942. *Proc. Natl. Acad. Sci. U.S.A.* 101, 13927–13932. doi: 10.1073/pnas.0403906101
- Olsen, J. V., De Godoy, L. M. F., Li, G., Macek, B., Mortensen, P., Pesch, R., et al. (2005). Parts per Million Mass Accuracy on an Orbitrap Mass Spectrometer via Lock Mass Injection into a C-trap. *Mol. Cell. Proteomics* 4, 2010–2021. doi: 10.1074/mcp.T500030-MCP200
- Ong, S.-E., Blagoev, B., Kratchmarova, I., Kristensen, D. B., Steen, H., Pandey, A., et al. (2002). Stable isotope labeling by amino acids in cell culture, SILAC, as a simple and accurate approach to expression proteomics. *Mol. Cell. Proteomics* 1, 376–386. doi: 10.1074/mcp.M200025-MCP200
- Pereira, S. F. F., Goss, L., and Dworkin, J. (2011). Eukaryote-like serine/threonine kinases and phosphatases in bacteria. *Microbiol. Mol. Biol. Rev.* 75, 192–212. doi: 10.1128/MMBR.00042-10
- Petranovic, D., Michelsen, O., Zahradka, K., Silva, C., Petranovic, M., Jensen, P. R., et al. (2007). *Bacillus subtilis* strain deficient for the protein-tyrosine kinase PtkA exhibits impaired DNA replication. *Mol. Microbiol.* 63, 1797–1805. doi: 10.1111/j.1365-2958.2007.05625.x
- Piven, I., Ajlani, G., and Sokolenko, A. (2005). Phycobilisome linker proteins are phosphorylated in *Synechocystis* sp. PCC 6803. *J. Biol. Chem.* 280, 21667–21672. doi: 10.1074/jbc.M412967200
- Rippka, R. (1988). "[1] Isolation and purification of cyanobacteria," in *Methods in Enzymology*, ed A. N. G. Lester Packer (Academic Press), 3–27.
- Sanders, C. E., Melis, A., and Allen, J. F. (1989). *In vivo* phosphorylation of proteins in the cyanobacterium *Synechococcus* 6301 after chromatic acclimation to Photosystem I or Photosystem II light. *Biochim. Biophys. Acta Bioenerg.* 976, 168–172. doi: 10.1016/S0005-2728(89)80226-9
- Schwarz, R., and Forchhammer, K. (2005). Acclimation of unicellular cyanobacteria to macronutrient deficiency: emergence of a complex network of cellular responses. *Microbiology* 151, 2503–2514. doi: 10.1099/mic.0.27883-0
- Soares, N. C., Spät, P., Krug, K., and Macek, B. (2013). Global dynamics of the *Escherichia coli* proteome and phosphoproteome during growth in minimal medium. *J. Proteome Res.* 12, 2611–2621. doi: 10.1021/pr3011843
- Soufi, B., Kumar, C., Gnad, F., Mann, M., Mijakovic, I., and Macek, B. (2010). Stable isotope labeling by amino acids in cell culture (SILAC) applied to quantitative proteomics of *Bacillus subtilis*. *J. Proteome Res.* 9, 3638–3646. doi: 10.1021/pr100150w
- Soufi, B., Soares, N. C., Ravikumar, V., and Macek, B. (2012). Proteomics reveals evidence of cross-talk between protein modifications in bacteria: focus on acetylation and phosphorylation. *Curr. Opin. Microbiol.* 15, 357–363. doi: 10.1016/j.mib.2012.05.003
- Stock, J. B., Ninfa, A. J., and Stock, A. M. (1989). Protein phosphorylation and regulation of adaptive responses in bacteria. *Microbiol. Rev.* 53, 450–490.

- Van Heeswijk, W. C., Hoving, S., Molenaar, D., Stegeman, B., Kahn, D., and Westerhoff, H. V. (1996). An alternative PII protein in the regulation of glutamine synthetase in *Escherichia coli*. *Mol. Microbiol.* 21, 133–146. doi: 10.1046/j.1365-2958.1996.6281349.x
- Vizcaíno, J. A., Côté, R. G., Csordas, A., Dienes, J. A., Fabregat, A., Foster, J. M., et al. (2013). The proteomics identifications (PRIDE) database and associated tools: status in 2013. *Nucleic Acids Res.* 41, D1063–D1069. doi: 10.1093/nar/gks1262
- Wang, Y., Xu, W., and Chitnis, P. (2009). Identification and bioinformatic analysis of the membrane proteins of synechocystis sp. PCC 6803. *Proteome Sci.* 7, 11. doi: 10.1186/1477-5956-7-11
- Wisniewski, J. R., Zougman, A., Nagaraj, N., and Mann, M. (2009). Universal sample preparation method for proteome analysis. *Nat. Methods* 6, 359–362. doi: 10.1038/nmeth.1322
- Yang, M.-K., Qiao, Z.-X., Zhang, W.-Y., Xiong, Q., Zhang, J., Li, T., et al. (2013). Global phosphoproteomic analysis reveals diverse functions of serine/threonine/tyrosine phosphorylation in the model cyanobacterium *Synechococcus* sp. Strain PCC 7002. *J. Proteome Res.* 12, 1909–1923. doi: 10.1021/pr4000043
- Zhang, C. C., Jang, J., Sakr, S., and Wang, L. (2005). Protein phosphorylation on ser, thr and tyr residues in cyanobacteria. *J. Mol. Microbiol. Biotechnol.* 9, 154–166. doi: 10.1159/000089644
- Zorina, A., Stepanchenko, N., Novikova, G. V., Sinetova, M., Panichkin, V. B., Moshkov, I. E., et al. (2011). Eukaryotic-like Ser/Thr protein kinases SpkC/F/K are involved in phosphorylation of GroES in the cyanobacterium *Synechocystis*. *DNA Res.* 18, 137–151. doi: 10.1093/dnares/dsr006
- Conflict of Interest Statement:** The Guest Associate Editor Ivan Mijakovic declares that, despite having coauthored an article with the author Boris Macek in 2014, the review process was handled objectively. The authors declare that the research was conducted in the absence of any commercial or financial relationships that could be construed as a potential conflict of interest.

Copyright © 2015 Spät, Maček and Forchhammer. This is an open-access article distributed under the terms of the Creative Commons Attribution License (CC BY). The use, distribution or reproduction in other forums is permitted, provided the original author(s) or licensor are credited and that the original publication in this journal is cited, in accordance with accepted academic practice. No use, distribution or reproduction is permitted which does not comply with these terms.

Redox regulation by reversible protein S-thiolation in bacteria

Vu Van Loi, Martina Rossius and Haike Antelmann *

Institute of Microbiology, Ernst-Moritz-Arndt-University of Greifswald, Greifswald, Germany

OPEN ACCESS

Edited by:

Jörg Stülke,
Georg-August-Universität Göttingen,
Germany

Reviewed by:

Ulrike Kappler,
University of Queensland, Australia
Jan Maarten Van Dijk,
University of Groningen and University
Medical Center Groningen,
Netherlands

*Correspondence:

Haike Antelmann,
Institute of Microbiology,
Ernst-Moritz-Arndt-University of
Greifswald,
Friedrich-Ludwig-Jahnstr. 15,
Greifswald, Germany
antelman@uni-greifswald.de

Specialty section:

This article was submitted to Microbial Physiology and Metabolism, a section of the journal Frontiers in Microbiology

Received: 25 November 2014

Accepted: 20 February 2015

Published: 16 March 2015

Citation:

Loi VV, Rossius M and Antelmann H (2015) Redox regulation by reversible protein S-thiolation in bacteria. *Front. Microbiol.* 6:187. doi: 10.3389/fmicb.2015.00187

Low molecular weight (LMW) thiols function as thiol-redox buffers to maintain the reduced state of the cytoplasm. The best studied LMW thiol is the tripeptide glutathione (GSH) present in all eukaryotes and Gram-negative bacteria. Firmicutes bacteria, including *Bacillus* and *Staphylococcus* species utilize the redox buffer bacillithiol (BSH) while Actinomycetes produce the related redox buffer mycothiol (MSH). In eukaryotes, proteins are post-translationally modified to S-glutathionylated proteins under conditions of oxidative stress. S-glutathionylation has emerged as major redox-regulatory mechanism in eukaryotes and protects active site cysteine residues against overoxidation to sulfonic acids. First studies identified S-glutathionylated proteins also in Gram-negative bacteria. Advances in mass spectrometry have further facilitated the identification of protein S-bacillithiolations and S-mycothiolation as BSH- and MSH-mixed protein disulfides formed under oxidative stress in Firmicutes and Actinomycetes, respectively. In *Bacillus subtilis*, protein S-bacillithiolation controls the activities of the redox-sensing OhrR repressor and the methionine synthase MetE *in vivo*. In *Corynebacterium glutamicum*, protein S-mycothiolation was more widespread and affected the functions of the maltodextrin phosphorylase MalP and thiol peroxidase (Tpx). In addition, novel bacilliredoxins (Brx) and mycoredoxins (Mrx1) were shown to function similar to glutaredoxins in the reduction of BSH- and MSH-mixed protein disulfides. Here we review the current knowledge about the functions of the bacterial thiol-redox buffers glutathione, bacillithiol, and mycothiol and the role of protein S-thiolation in redox regulation and thiol protection in model and pathogenic bacteria.

Keywords: oxidative stress, protein S-thiolation, thiol-redox buffer, glutathione, bacillithiol, mycothiol

Introduction

The cytoplasm is a reducing environment and protein thiols are maintained in their reduced state by low molecular weight (LMW) thiol-redox buffers and enzymatic thiol-disulfide oxidoreductases, including the thioredoxin and glutaredoxin systems (Fahey, 2013; Van Laer et al., 2013). In their natural environment or during infections, bacteria encounter different reactive species, such as reactive oxygen, nitrogen, chlorine, and electrophilic species (ROS, RNS, RCS, RES) (Antelmann and Helmman, 2011; Gray et al., 2013a). These reactive species cause different post-translational thiol-modifications in proteins and activate or inactivate specific transcription factors resulting in expression of detoxification pathways. LMW thiol-redox buffers function in detoxification of different reactive species and are often present in millimolar concentrations in the cytoplasm.

The best studied LMW thiol is glutathione (GSH) present in eukaryotes and Gram-negative bacteria (Fahey, 2013). Most Gram-positive bacteria do not produce GSH. Instead, the Actinomycetes

utilize mycothiol (MSH) as thiol-redox buffer (Jothivasan and Hamilton, 2008; Newton et al., 2008). In *Bacillus megaterium*, *Bacillus cereus*, and *Staphylococcus aureus*, coenzyme A (CoASH) serves as an abundant LMW thiol (Newton et al., 1996). Many Firmicutes bacteria, including *Bacillus* and *Staphylococcus* species utilize bacillithiol (BSH) and cysteine as major thiol-redox buffers (Newton et al., 2009). Alternative LMW thiols include also the betaine-histidine derivative ergothioneine that compensates for the absence of MSH in *Mycobacterium smegmatis* *mshA* mutants (Ta et al., 2011). Cysteine is used for alternative S-thiolations in the absence of BSH and MSH in *Bacillus subtilis* and *Corynebacterium glutamicum* since S-cysteinylated proteins were identified in *bsh* and *msh* mutants (Chi et al., 2011, 2014).

The protozoa *Leishmania* and *Trypanosoma* produce the glutathione-derivative trypanothione (bis-glutathionylspermidine or TSH₂). In *Escherichia coli*, glutathionylspermidine (GSP) was detected during the stationary phase (Fahey, 2013). Some microaerophilic γ -proteobacteria utilize glutathione amide (GASH) which forms a persulfide (GASSH) during photoautotrophic growth on high concentrations of sulfide (Bartsch et al., 1996).

Under conditions of oxidative stress, LMW thiols form mixed disulfides with protein thiols which is termed protein S-thiolation. In eukaryotes, protein S-glutathionylation has emerged as major redox-regulatory mechanism that controls the activity of redox sensing transcription factors and protects active site Cys residues against irreversible oxidation to sulfonic acids (Dalle-Donne et al., 2009). S-glutathionylation controls numerous physiological processes, such as cellular growth and differentiation, cell cycle progression, transcriptional activity, cytoskeletal function, cellular metabolism, and apoptosis (Klatt and Lamas, 2000; Ghezzi, 2005, 2013; Dalle-Donne et al., 2007, 2009). S-glutathionylation must meet several criteria to function as redox-control mechanism: (1) reversibility, (2) specificity to active site Cys, (3) change in protein function/activity, and (4) induction by ROS or RNS. S-glutathionylation serves as a form of GSH storage to prevent the export of GSSG under oxidative stress (Dalle-Donne et al., 2009). Many eukaryotic proteins, like α -ketoglutarate dehydrogenase, glyceraldehyde 3-phosphate dehydrogenase, ornithine δ -aminotransferase, pyruvate kinase, heat specific chaperones, and regulatory proteins (c-Jun, NF- κ B) are reversibly inactivated or activated by S-glutathionylation (Dalle-Donne et al., 2009; Kehr et al., 2011). However, the regulatory role of protein S-thiolation for bacterial physiology has only recently been investigated. Here we review the current knowledge about the functions of the bacterial redox buffers GSH, MSH, and BSH and their roles for protein S-thiolations in GSH-, MSH- and BSH-producing bacteria.

Sources of Reactive Oxygen, Electrophile, and Chlorine Species (ROS, RES, RCS)

Bacteria encounter ROS during respiration or by the oxidative burst of activated neutrophils during infections (Imlay, 2003, 2008, 2013). The incomplete stepwise reduction of molecular oxygen (O₂) leads to generation of superoxide anions (O₂^{•−}),

hydrogen peroxide (H₂O₂) and the highly reactive hydroxyl radical (OH[•]) (Figure 1). Superoxide anion and H₂O₂ are also produced by autoxidation of flavoenzymes (Mishra and Imlay, 2012; Imlay, 2013). Superoxide dismutases (SOD) convert O₂^{•−} to H₂O₂. Several peroxide scavenging enzymes, such as catalases and peroxidases catalyze the detoxification of H₂O₂. H₂O₂ reacts with ferrous iron (Fe²⁺) in the Fenton reaction generating the highly toxic hydroxyl radical (OH[•]) which can damage all cellular macromolecules (Imlay, 2003, 2008). H₂O₂ destroys the Fe-S-cluster of dehydratases and inactivates single ferrous iron-centers of redox enzymes (Mishra and Imlay, 2012; Imlay, 2013).

During the oxidative burst, activated neutrophils release O₂^{•−}, H₂O₂, nitric oxide (NO), and hypochlorous acid (HOCl) with the aim to kill invading pathogenic bacteria (Forman and Torres, 2001; Winterbourn and Kettle, 2013). The neutrophil NADPH oxidase (NOX) shuttles electrons from NADPH to O₂ in the phagosomal lumen and generates around 20 μ M superoxide anion. Myeloperoxidase (MPO) is released upon degranulation in millimolar concentrations. MPO catalyzes the dismutation of O₂^{•−} to H₂O₂ and subsequent conversion of H₂O₂ and chloride to HOCl (Figure 1) (Winterbourn and Kettle, 2013). NO is generated in neutrophils by the inducible nitric oxide synthase (iNOS) catalyzing the oxidation of L-arginine to L-citrulline. The reaction of NO with O₂^{•−} leads to formation of peroxynitrite (ONOO[−]). Thus, neutrophils release ROS, RNS, and the highly reactive HOCl as antimicrobial defense mechanism.

Reactive electrophilic species (RES) have electron-deficient centers and can react with the nucleophilic Cys thiol group via the thiol-S-alkylation chemistry (Figure 2) (Antelmann and Helmman, 2011). RES include quinones, aldehydes, epoxides, diamide and α,β -unsaturated dicarbonyl compounds. RES are often generated as secondary reactive intermediates from oxidation products of amino acids, lipids or carbohydrates (Marnett et al., 2003; Rudolph and Freeman, 2009). Quinones are lipid-electron carriers of the respiratory chain, including

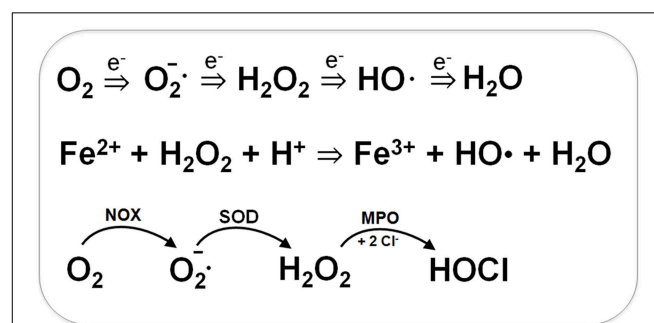


FIGURE 1 | Generation of Reactive Oxygen Species (ROS) during respiration and HOCl production by activated neutrophils during infections. ROS are generated in bacteria during respiration by stepwise one-electron transfer to O₂ producing superoxide anion, hydrogen peroxide and hydroxyl radical. The highly reactive hydroxyl radical is also produced from H₂O₂ and Fe²⁺ in the Fenton reaction. During infections, activated neutrophils generate superoxide anion by the NADPH oxidase (NOX) that is converted to H₂O₂ by the superoxide dismutase (SOD). Myeloperoxidase (MPO) is released upon degranulocytosis producing the highly reactive hypochlorous acids (HOCl) from H₂O₂ and Cl[−] as potent killing agent for pathogenic bacteria.

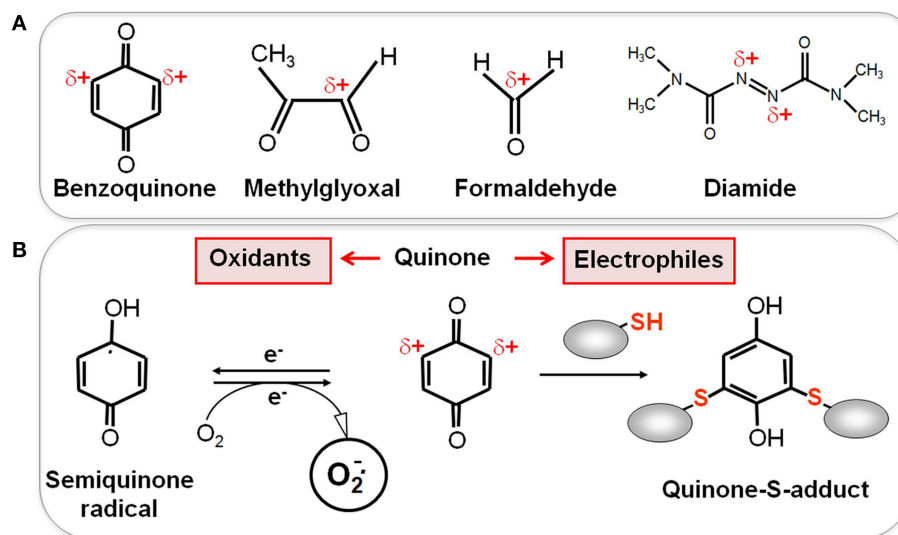


FIGURE 2 | Reactive Electrophilic Species (RES) with partial positive charges (δ^+) (A) and the reaction of quinones with thiols via the S-alkylation and oxidation chemistry (B). (A) In quinones and aldehydes the electrons are drawn to carbonyl oxygen leaving the partial positive charges at neighboring carbon atoms that become electrophilic. Diamide is

an electrophilic azocompound that causes disulfide stress. **(B)** Quinones can react as electrophiles with the nucleophilic thiol group of Cys residues via thiol-S-alkylation leading to irreversible thiol-S-adduct formation. In the oxidative mode, quinones are incompletely reduced to semiquinone radicals that generate superoxide anions and can oxidize protein thiols to disulfides.

ubiquinone and menaquinone (Farrand and Taber, 1974). Soil bacteria encounter quinones as redox active components of humic substances and in dissolved organic matter (Ratasuk and Nanny, 2007). The toxic dicarbonyl compound methylglyoxal is produced in all organisms from triose-phosphate intermediates as byproduct of the glycolysis and can be generated also from amino acids metabolism (Ferguson et al., 1998; Booth et al., 2003; Kalapos, 2008). Bacteria also have to cope with the carbonyl compound formaldehyde. Formaldehyde is an intermediate in the C_1 -metabolism of methanotrophic and methylotrophic bacteria and is ubiquitously distributed in the environment. Thus, bacteria have evolved conserved pathways for detoxification of formaldehyde and methylglyoxal that involve LMW thiols.

In eukaryotic cells, RES are implicated in many pathophysiological processes and modulate signaling pathways (Mackay and Knock, 2015). Eukaryotic cells produce lipid-derived RES, such as malondialdehyde (MDA) and 4-hydroxy-2-nonenal (HNE) (Rudolph and Freeman, 2009). HNE is generated from polyunsaturated fatty acids in biological membranes by a radical-based peroxidation chain reaction (Jacobs and Marnett, 2010). Furthermore, 15-deoxy- $\Delta^{12,14}$ -prostaglandin J₂ (15d-PGJ₂) is generated from arachidonic acid during inflammation and 2-trans-hexadecenal (2-HD) is produced during sphingolipid metabolism which promotes apoptosis (Wang et al., 2014). Bacterial membrane lipids also contain unsaturated fatty acids which are synthesized at higher levels during adaptation to cold shock to maintain the fluidity of the membrane (De Mendoza, 2014). These unsaturated fatty acids in bacterial membrane lipids could be the target for ROS leading to lipid peroxidation products in bacteria. Lipid hydroperoxides, such as linoleic acid hydroperoxide are sensed by the redox-sensing MarR-type repressor OhrR.

OhrR regulates the peroxiredoxin OhrA that functions in detoxification of organic hydroperoxides (Atichartpongkul et al., 2001; Fuangthong et al., 2001). However, the fatty acid-derived peroxidation product which is sensed by OhrR *in vivo* remains to be identified.

Post-Translational Thiol-Modifications of Proteins by ROS, RES, and RCS in Bacteria

ROS, RES, and RCS can damage all cellular macromolecules including proteins, nucleic acids or carbohydrates (Imlay, 2008, 2013; Jacobs and Marnett, 2010; Gray et al., 2013a). However, in eukaryotes low levels of ROS and RES act also as second messengers to modulate signal transduction pathways (Rudolph and Freeman, 2009; Mackay and Knock, 2015). Bacterial transcription factors often use redox-sensitive Cys residues for sensing of ROS, RES, and RCS to control the expression of specific detoxification pathways (Antelmann and Helmann, 2011; Gray et al., 2013a). The thiol group of cysteine is subject to reversible and irreversible post-translational thiol-modifications that lead to inactivation or activation of the transcription factor. Protein thiols can be reversibly oxidized to protein disulfides and irreversibly overoxidized to sulfinic or sulfonic acids by ROS (Antelmann and Helmann, 2011). ROS lead first to oxidation of protein thiols to Cys sulfenic acids as unstable intermediates (R-SOH) (Figure 3). Cys sulfenic acid rapidly reacts further with other thiols to form intramolecular and intermolecular protein disulfides or mixed disulfides with LMW thiols, collectively termed as S-thiolations (e.g., S-cysteinylation, S-glutathionylation, S-mycothiolation, and S-bacillithiolation). Protein S-thiolations protect the thiol groups against the irreversible overoxidation to

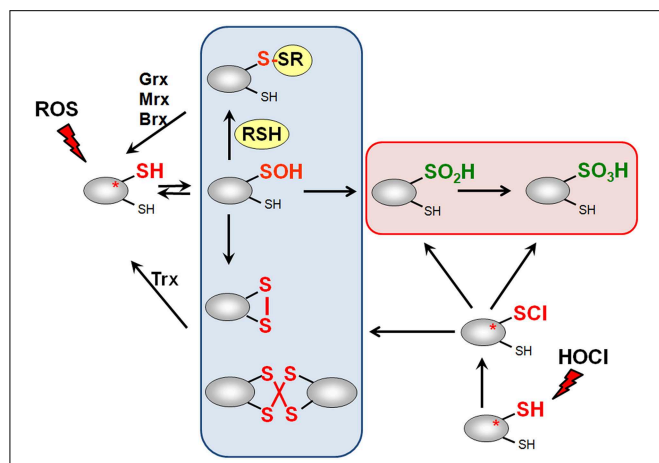


FIGURE 3 | Thiol-chemistry of ROS and HOCl with thiol-containing proteins. The Cys thiol group is oxidized by ROS to an unstable Cys sulfenic acid intermediate (Cys-SOH) that reacts further with proximal thiols to form intramolecular and intermolecular disulfides or mixed disulfides with LMW thiols (RSH), such as glutathione, bacillithiol or cysteine, termed as S-thiolations. HOCl leads to chlorination of protein thiols to sulfinylchloride intermediates (Cys-SCI) that react further to form disulfides. In the absence of proximal thiols, the chlorinated Cys is overoxidized to Cys sulfinic and sulfonic acids. Disulfides function as redox switches to control protein activity and protect thiol groups against overoxidation to Cys sulfinic and sulfonic acids.

Cys sulfinic (R-SO₂H) and sulfonic acid (R-SO₃H). This is particularly important for essential and abundant proteins whose overoxidation would lead to loss of cell viability and requires new protein synthesis to replace inactivated proteins. However, eukaryotic sulfiredoxins are able to reduce sulfinic acids in 2-Cys peroxiredoxins, but sulfiredoxins are not present in bacteria (Lowther and Haynes, 2011).

Hypochlorous acid (HOCl) is a strong two-electron oxidant and chlorinating agent with a high redox potential [E^0 (HOCl/Cl⁻) = 1.28 mV] (Davies, 2011). HOCl targets most strongly the sulfur-containing amino acids cysteine and methionine with the second-order rate constant of $k = 3 \times 10^7 \text{ M}^{-1} \text{ s}^{-1}$ (Hawkins et al., 2003). HOCl first chlorinates the thiol group to form the unstable sulfinylchloride intermediate that reacts further with another thiol group to disulfides. In the absence of another thiol, the chlorinated thiol group is overoxidized very rapidly to sulfinic or sulfonic acids (Hawkins et al., 2003) (Figure 3). We confirmed that strong disulfide stress responses are caused by HOCl in different Gram-positive bacteria *in vivo* and detected mixed protein disulfides with Cys, BSH, and MSH as major oxidation products (Chi et al., 2011, 2013, 2014).

RNS cause reversible thiol-modifications: nitric oxide (NO) leads to S-nitrosothiol formation (RS-NO) and peroxynitrite (ONOO⁻) causes S-nitrothiol (RS-NO₂) formation. Alternatively, S-nitrosothiol (e.g., GSNO or MSNO) can be formed by direct reaction of NO with LMW thiols (Antelmann and Helmann, 2011).

RES can react via the thiol-S-alkylation chemistry with Cys thiols. However, quinones have two modes of action, an oxidation and an alkylation mode. In the oxidation mode, the

one-electron reduction of quinones generates the highly reactive semiquinone radical leading to generation of superoxide anions (Figure 2). The electrophilic reaction of quinones involves the 1,4-reductive Michael-type addition of thiols to quinones (Marriott et al., 2003). Quinones lead to irreversible thiol-S-alkylation and protein aggregation to deplete protein thiols in the proteome *in vivo* (Liebeke et al., 2008). However, non-toxic quinone concentrations resulted in reversible thiol-disulfide switches in RES-sensing redox regulators (e.g., YodB, CatR, QsrR, NemR) to activate the expression of specific quinone detoxification pathways (Antelmann and Helmann, 2011; Gray et al., 2013a; Lee et al., 2013). Methylglyoxal reacts with nucleophilic centers of the DNA and with the amino acids arginine, lysine and cysteine causing advanced glycation end-products (Bourajjaj et al., 2003). The lipid-derived electrophiles MDA and HNE were shown to alkylate DNA bases and protein thiols leading to DNA and membrane damages in eukaryotes (Rudolph and Freeman, 2009).

Biosynthesis and Functions of Major LMW Thiol-Redox Buffers in Bacteria

Biosynthesis, Uptake, and Functions of Glutathione in Bacteria

The tripeptide glutathione (γ -glutamylcysteinyl-glycine; GSH) is utilized as major LMW thiol-redox buffer in Gram-negative bacteria and in some Gram-positive Firmicutes bacteria, including *Streptococcus agalactiae*, *Listeria monocytogenes*, and *Clostridium acetobutylicum* (Figure 4). In *E. coli*, GSH biosynthesis occurs in two steps: The γ -glutamylcysteine ligase (GshA) catalyzes the formation of γ -glutamylcysteine (γ -Glu-Cys) from glutamate and cysteine. In the second step, ligation of glycine to γ -Glu-Cys is catalyzed by glutathione synthase (GshB) (Meister, 1995; Anderson, 1998). In *S. agalactiae* and *L. monocytogenes*, a bifunctional fusion protein GshF is present that exhibits both GshA and GshB activities (Gopal et al., 2005; Janowiak and Griffith, 2005). Interestingly, *Lactococcus lactis*, *Streptococcus pneumoniae* and *Haemophilus influenzae* do not synthesize GSH, but encode GSH-uptake mechanisms. In *S. pneumoniae*, the GSH-uptake from the host is mediated by the ABC transporter binding protein GshT (Potter et al., 2012; Vergauwen et al., 2013). In addition, the cystine importer TcyBC was shown to be primed for GSH import by GshT. In *H. influenzae*, GSH import is mediated by the ABC-transporter DppBCDF and requires the periplasmic GSH-binding protein GbpA (Vergauwen et al., 2010). Strikingly, these pathogens utilize host-derived GSH as protection mechanism against the host immune defense.

GSH is present in millimolar concentrations in the cytoplasm of *E. coli* (Masip et al., 2006; Fahey, 2013). GSH maintains protein thiols in the reduced state and serves as a storage form of cysteine. In contrast to cysteine, GSH is resistant to metal-catalyzed autooxidation because of its bound Cys amino and carboxyl groups that prevent ligation of heavy metal ions (Fahey, 2013). During the bacterial growth and under oxidative stress, GSH is oxidized to glutathione disulfide (GSSG). The NADPH-dependent glutathione reductase (Gor) keeps GSH in its reduced state to maintain a high GSH/GSSG ratio ranging

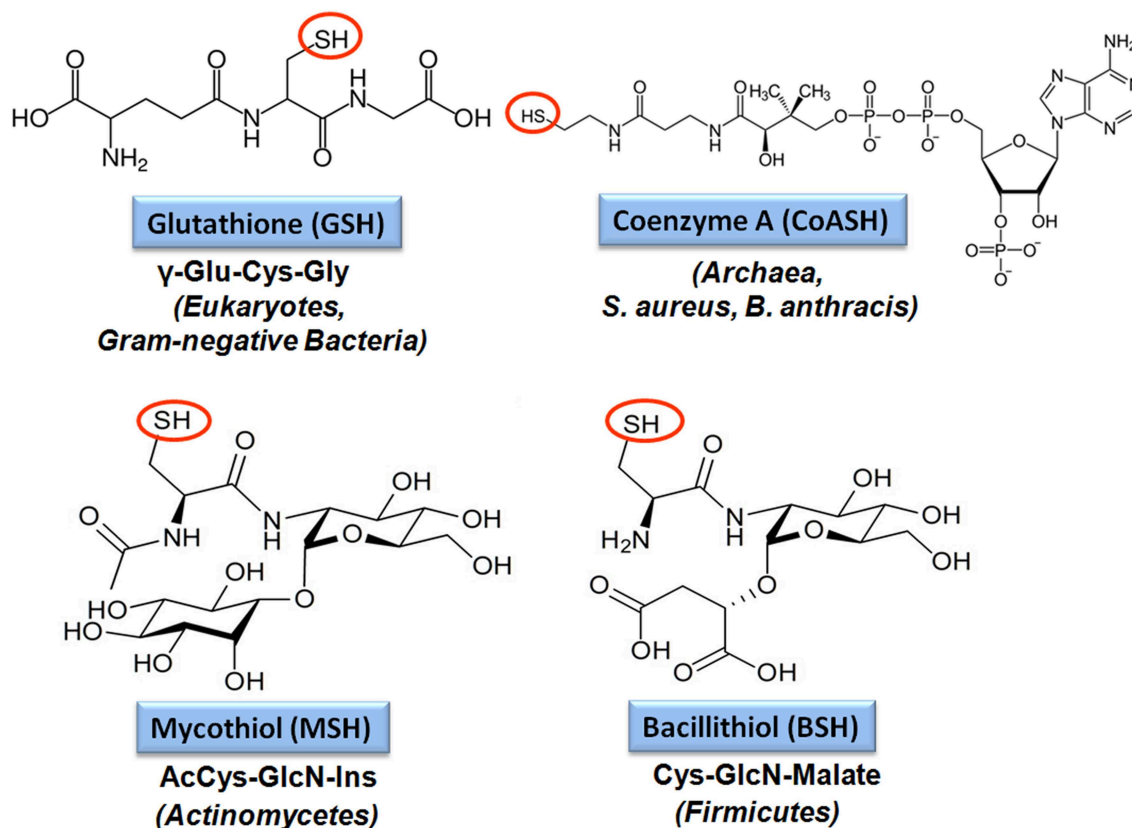


FIGURE 4 | Structures of major bacterial low molecular weight (LMW) thiols. Major LMW thiols are glutathione (GSH) in eukaryotes and Gram-negative bacteria, mycothiol (MSH) in Actinomycetes and

bacillithiol (BSH) in Firmicutes. Coenzyme A (CoASH) also serves as a LMW thiol-redox buffer in some bacteria, like in *S. aureus* and *B. anthracis*.

from 30:1 to 100:1 in the cytoplasm. The standard thiol-disulfide redox potential of the GSH redox couple was calculated as $E^{0'}(\text{GSSG}/\text{GSH}) = -240 \text{ mV}$ at physiological pH values (Hwang et al., 1995; Van Laer et al., 2013).

The various detoxification functions of GSH have been extensively studied in *E. coli gsh* mutants. In *E. coli*, GSH functions in detoxification of ROS, RES, RCS, RNS, xenobiotics, antibiotics, toxic metals, and metalloids (Masip et al., 2006) (Table 1). Detoxification of xenobiotics, electrophiles and antibiotics by GSH occurs either spontaneously by S-conjugation or by the catalytic activity of GSH-S-transferases (Fahey, 2013). The GSH-S-conjugates are usually excreted from the cell as non-toxic mercapturic acid derivatives. GSH was shown to function as a cofactor in methylglyoxal detoxification in *E. coli*. The major pathway for methylglyoxal detoxification in *E. coli* is the GSH-dependent glyoxalase pathway. The glyoxalase-I (GloA) catalyzes formation of S-lactoyl-GSH from GSH-hemithioacetal and glyoxalase-II (GloB) converts S-lactoyl-GSH to D-lactate (Ferguson et al., 1998; Booth et al., 2003). In addition, glyoxalase-III operates GSH-independently to convert methylglyoxal to lactate. The glyoxalase-I encoding *gloA* gene and the *nemRA* operon are redox-regulated by the NemR repressor under methylglyoxal, quinone and HOCl stress (Gray et al., 2013b; Lee et al.,

2013; Ozyamak et al., 2013). The glyoxalase GloA and the oxidoreductase NemA are important for methylglyoxal survival and confer resistance to methylglyoxal in *E. coli* (Ozyamak et al., 2013). The resistance to methylglyoxal is also linked to the activation of potassium efflux by the S-lactoyl-GSH intermediate leading to cytoplasmic acidification (Ferguson et al., 1998; Booth et al., 2003). The cytoplasmic acidification limits the interaction of methylglyoxal with DNA bases. Thus, potassium efflux and detoxification by GloA protect against methylglyoxal toxicity in *E. coli*.

Interestingly, expression of the *E. coli gshAB* genes in the industrial important *Clostridium acetobutylicum* enhances robustness and alcohol production as a promising strategy for engineering industrial production strains. Thus, GSH protects also against large-scale ethanol and butanol production in *C. acetobutylicum* during fermentation (Hou et al., 2013).

Functions of Glutathione in the Virulence of Pathogenic Bacteria

GSH has many detoxification functions to maintain the redox balance of the cytoplasm, but only recently the role of GSH for the control of virulence functions has been explored in the pathogenic bacteria *S. pneumoniae*, *L. monocytogenes*, and

TABLE 1 | Functions of the bacterial redox buffers glutathione, bacillithiol, and mycothiol.

Redox buffer	Organism	Functions of thiol-redox buffers and thiol-dependent enzymes	References
Glutathione	<i>Escherichia coli</i>	GSH functions in detoxification of ROS, RES, RCS, RNS, xenobiotics, antibiotics, toxic metals, metalloids	Masip et al., 2006 Potter et al., 2012
	<i>Salmonella Typhimurium</i>	Gor: GSSG reductase Gpx: GSH-dependent peroxidase Gst: GSH S-transferases required for conjugation of alkylating agents and antibiotics Grx: Glutaredoxins for reduction of S-glutathionylated proteins GloA/GloB: glyoxalase-I/II for GSH-dependent conversion of methylglyoxal to lactate	
Bacillithiol	<i>Bacillus subtilis</i>	BSH involved in detoxification of hypochlorite, diamide, methylglyoxal, ROS (paraquat, H ₂ O ₂), alkylating agents and fosfomycin	Gaballa et al., 2010 Chi et al., 2011 Ma et al., 2014 Gaballa et al., 2010 Lamers et al., 2012 Roberts et al., 2013 Thompson et al., 2013, 2014 Newton et al., 2011 Perera et al., 2014 Gaballa et al., 2014 Chandrangu et al., 2014
	<i>Staphylococcus aureus</i>	BSH provides a Zn buffer for labile Zn pool YpdA: possible BSSB reductase FosB: BSH-dependent epoxide hydrolase for fosfomycin detoxification YfiT/BstA: DinB-family BSH S-transferases required for conjugation of alkylating agents (monochlorobimane, 1-chloro-2,4-dinitrobenzene and cerulenin) BrxA/BrxB: Bacilliredoxins for reduction of S-bacillithiolated proteins GlxA/GlxB: glyoxalase-I/II for BSH-dependent conversion of methylglyoxal to lactate	
Mycothiol	<i>Streptomyces coelicolor</i>	MSH protects against ROS, RES, NO, toxins, antibiotics (erythromycin, vancomycin, rifampicin), heavy metals, maleylpyruvate, ethanol, gentisate, glyphosate, arsenate in Actinomycetes	Newton et al., 2008 Fahey, 2013 Liu et al., 2013
	<i>Mycobacterium tuberculosis</i>	Mtr: MSSM reductase Tpx, AhpE, Mpx: MSH-dependent peroxidases	
	<i>Corynebacterium glutamicum</i>	Mst: DinB-family MSH S-transferases required for conjugation of alkylating agents and antibiotics (monochlorobimane, DTNB, rifampicin, cerulenin) LmbT, LmbV and LmbE: MSH S-transferases for biosynthesis of the lincosamide antibiotic lincosycin in <i>S. lincolnensis</i> Mca: S-conjugate amidase cleaves MSH-S-conjugates to mercapturic acids Mrx1: Mycoredoxin-1 for reduction of S-mycothiolations MscR/AdhE/FadH: MSNO reductase/ formaldehyde dehydrogenase	Chi et al., 2014 Hugo et al., 2014 Newton et al., 2012 Zhao et al., 2015 Newton et al., 2008, 2011 Van Laer et al., 2012 Newton et al., 2008 Lessmeier et al., 2013 Witthoff et al., 2013 Feng et al., 2006
		Cg3349: maleylpyruvate isomerase for maleylpyruvate detoxification in <i>C. glutamicum</i> ArsC1/C2: MSH-dependent arsenate reductases	
			Ordenez et al., 2009

Salmonella Typhimurium (Potter et al., 2012; Song et al., 2013; Reniere et al., 2015) (Table 2). In *S. pneumoniae*, the glutathione reductase Gor and the GSH-importer GshT were required for oxidative stress protection and metal ion resistance. Moreover, the *gshT* mutant was attenuated in colonization and invasion in a mouse model of pneumococcal infection (Potter et al., 2012). Thus, GSH protects against the host immune defense and contributes to fitness of *S. pneumoniae*.

The intracellular pathogen *L. monocytogenes* is able to synthesize GSH via the *gshF* fusion protein, but GSH can be also imported from the host (Reniere et al., 2015). The *L. monocytogenes gshF* mutant was two-fold less virulent compared to the wild type in a mice model. In addition, the *gshF* mutant was sensitive to oxidative stress, contains lower levels of ActA and formed small plaques in tissue culture assays that measure cell-to-cell spread (Reniere et al., 2015). The Actin assembly-inducing protein ActA is controlled by the virulence regulator PrfA and used by *L. monocytogenes* to move through the host cells (Freitag et al., 2009). It was shown that the virulence phenotype of the *gshF* mutant is caused by the lack of PrfA activation by bacterial and

host-derived GSH (Reniere et al., 2015). Interestingly, activation of PrfA is mediated by an allosteric binding of GSH to PrfA, but not by S-glutathionylation. Thus, GSH plays a role as signaling molecule to activate virulence gene expression in an intracellular pathogen.

In *S. Typhimurium*, GSH antagonizes the bacteriostatic effects of RNS *in vivo* and *gshA* mutants were sensitive to ROS and RNS (Song et al., 2013). Thus, GSH presents a first line defense against ROS and RNS produced by the host immune system. This was shown in an acute model of salmonellosis in mice expressing the wild-type NRAMP1^R allele (natural resistance-associated macrophage protein 1) which is linked to high NO production of the macrophages. The *gshA* and *gshB* mutants were attenuated in this acute model of salmonellosis. It was further shown that GSH protects against ROS and RNS produced by the NADPH phagocyte oxidase and inducible nitric oxide synthase (iNOS) in this mice model (Song et al., 2013). These recent studies highlight the important roles of GSH in the control of virulence functions, expression of virulence factors and pathogen fitness under infection conditions in *S. pneumoniae*, *L. monocytogenes*, and

TABLE 2 | The role of thiol-redox buffers for virulence in pathogenic bacteria.

Redox buffer	Organism	Genes for biosynthesis or uptake	Virulence phenotypes of mutants	References
Glutathione (uptake)	<i>Streptococcus pneumoniae</i>	<i>gshT</i> (GSH importer)	<i>gshT</i> mutant attenuated in colonization and invasion in a mouse model of pneumococcal infection	Potter et al., 2012
Glutathione (biosynthesis and uptake)	<i>Listeria monocytogenes</i>	<i>gshF</i> (γ -Glu-Cys ligase/GSH synthase)	Virulence defect of the <i>gshF</i> mutant caused the lack of PrfA activation and lower <i>actA</i> expression by bacterial and host GSH	Reniere et al., 2015
Glutathione (biosynthesis)	<i>Salmonella</i> Typhimurium	<i>gshA</i> (γ -Glu-Cys ligase) <i>gshB</i> (GSH synthase)	<i>gshA</i> and <i>gshB</i> mutants attenuated in acute model of salmonellosis in NRAMP1 ^R mice; GSH protects against ROS and RNS produced by NOX in mice	Song et al., 2013
Bacillithiol (biosynthesis)	<i>Staphylococcus aureus</i>	<i>bshA</i> (glycosyltransferase) <i>bshB</i> (deacetylase) <i>bshC</i> (Cys ligase)	COL and USA300 <i>bshA</i> mutants impaired in human whole-blood survival assays; SH1000 natural <i>bshC</i> mutant survival defect in macrophage phagocytosis assays	Posada et al., 2014 Pöther et al., 2013
Mycothioliol (biosynthesis)	<i>Mycobacterium tuberculosis</i>	<i>mshA1</i> (glycosyltransferase) <i>mshA2</i> (phosphatase) <i>mshB</i> (deacetylase) <i>mshC</i> (Cys ligase) <i>mshD</i> (acetyltransferase)	<i>mshC</i> mutant impaired in growth and survival in mouse model of infection	Sareen et al., 2003; Sassetti and Rubin, 2003

S. Typhimurium. As shown for *L. monocytogenes*, GSH might play similar roles to activate virulence gene expression by redox control of virulence gene regulators in other pathogens which remains to be elucidated.

Redox Proteomic Methods to Study Protein S-Glutathionylation at a Global Scale

Advances in probe design and mass spectrometry-based thiol-trapping approaches have facilitated the detection of specific reversible thiol-modifications, including sulfenylation, nitrosylation, glutathionylation, and sulphydrations of proteins at a global scale (Leonard and Carroll, 2011; Pan and Carroll, 2013; Paulsen and Carroll, 2013; Gupta and Carroll, 2014; Zhang et al., 2014). Different methods have been applied for specific detection of S-glutathionylations in eukaryotic cells, including the use of GSH-specific antibodies and the labeling of S-thiolations with ³⁵S-cysteine followed by 2D gel electrophoresis and phosphoimaging (Fratelli et al., 2002, 2003, 2004). However, the specificity of the GSH antibodies is questionable and the gel-based detection of S-thiolations using ³⁵S-cysteine does not distinguish between S-cysteinylations and S-glutathionylations or other forms of S-thiolations. Hence, more sensitive mass spectrometry-based redox proteomics methods have been developed, including the glutaredoxin-coupled NEM-biotin switch assay and the treatment of cell extracts with N,N-biotinyl glutathione disulfide (BioGSSG) (Lind et al., 2002; Brennan et al., 2006; Kehr et al., 2011; Zaffagnini et al., 2012a) (Figure 5). Both methods make use of the specific streptavidin enrichment of biotinylated peptides that improve the identification of S-glutathionylated peptides using mass spectrometry. The NEM biotin-switch assay was successfully applied to detect protein S-glutathionylation in eukaryotic endothelial cells and

malaria parasites which applies glutaredoxin for reduction of protein-SSG followed by NEM-biotin alkylation and enrichment using streptavidin columns (Lind et al., 2002; Kehr et al., 2011). The biotin-GSSG approach has been applied to identify S-glutathionylated proteins in the green algae *Chlamydomonas reinhardtii* (Zaffagnini et al., 2012a) and in the photosynthetic cyanobacterium *Synechocystis* sp. PCC6803 (Chardonnet et al., 2015). In total, 383 S-glutathionylated proteins were identified in *Synechocystis* sp. PCC6803 and 125 glutathionylation sites were mapped by mass spectrometry. In addition, the peroxiredoxin PrxII (S11621) and the 3-phosphoglycerate dehydrogenase PGDH (S11908) could be S-glutathionylated by BioGSSG *in vitro* (Chardonnet et al., 2015).

In another approach, biotinyl-spermine (biotine-spm) and *in vivo* expressed *E. coli* GspS have been applied for mammalian cells to convert GSH to biotin-glutathionylspermidine (biotin-Gsp) which subsequently modified proteins by Biotin-Gsp-S-thiolation (Chiang et al., 2012; Lin et al., 2015). The biotine-spm is removed enzymatically by GspA from the enriched biotin-Gsp-S-thiolated peptides and the GSS-peptides are identified by mass spectrometry. This approach allows the identification of S-glutathionylation sites without the biotin-tag and enhances the coverage for S-glutathionylated proteins. In mammalian cells, 1409 S-glutathionylated cysteines in 913 proteins were identified using the Gsp-biotin approach (Chiang et al., 2012; Lin et al., 2015). This makes the application of this chemoenzymatic approach using the GspS enzyme attractive for global and specific studies of S-glutathionylated proteins.

In *S. Typhimurium*, protein S-glutathionylation has been studied at a global scale by top-down and bottom-up proteomic approaches (Ansong et al., 2013). Top-down proteomics uses whole proteins for separation and fragmentation directly

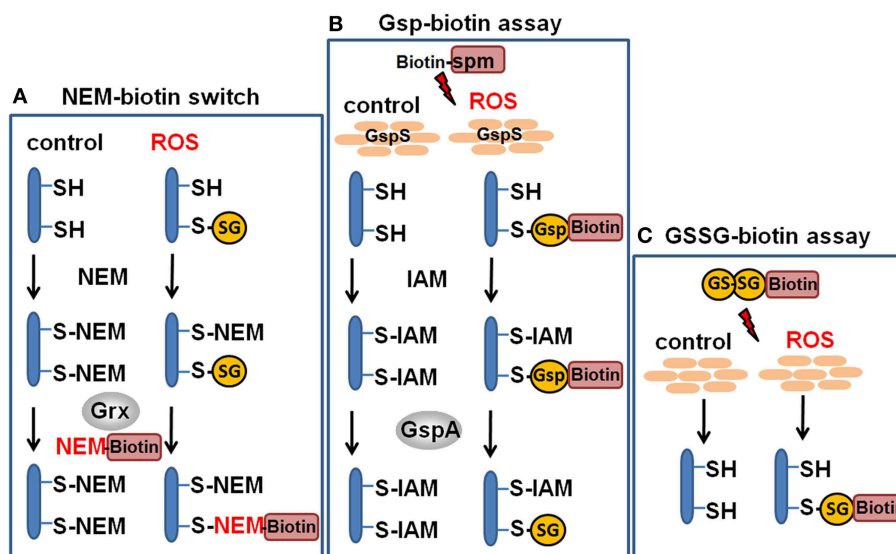


FIGURE 5 | Redox proteomics methods to study protein S-glutathionylation at a global scale. Mass spectrometry-based methods for identification of S-glutathionylations include the glutaredoxin-coupled NEM-biotin switch assay (A), the biotin-Gsp assay (B) or the N,N-biotinyl glutathione disulfide (BioGSSG) assay (C) (Lind et al., 2002; Brennan et al., 2006; Kehr et al., 2011; Zaffagnini et al., 2012a). In the biotin-Gsp assay, E.

coli GspS is expressed in mammalian cells and converts GSH and biotinyl-spermine (biotin-spm) to biotin-glutathionylspermidine (biotin-Gsp). Proteins in ROS-treated cells are modified by biotin-Gsp-S-thiolation (Chiang et al., 2012; Lin et al., 2015). The biotin-spm is removed from the enriched biotin-Gsp-S-thiolated peptides by GspA and the GSS-peptides are identified by mass spectrometry.

in the mass spectrometer. In bottom-up proteomics approaches proteins are digested by a protease and the peptide mixtures are analyzed by mass spectrometry to identify proteins at the peptide level. The top-down proteomic approach identified 563 proteins with 1665 post-translational modifications in *S. Typhimurium*. The authors identify 25 S-thiolated proteins in cells grown in complete LB medium including 16 S-glutathionylated proteins and nine S-cysteinylated proteins. Interestingly, a subset of nine S-glutathionylated are modified by S-cysteinylated in infection-like minimal LPM medium (Table 3). This could indicate a shift from S-glutathionylation to S-cysteinylated under infection-like conditions in *S. Typhimurium*. These S-thiolated proteins include phosphoglycerate kinase (Pgk), elongation factor (Tuf) and enolase (Eno) that are also targets for S-glutathionylations in endothelial cells (Fratelli et al., 2002). The top-down proteomics results were verified by bottom-up proteomics approaches to identify the specific S-thiolated Cys peptides (Ansong et al., 2013). Structural analysis revealed that S-glutathionylation occurred mostly at buried Cys residues and not at surface-exposed Cys. S-glutathionylation on buried Cys was also shown for the enolase whose activity is known to be modified by S-thiolation in human cells (Fratelli et al., 2002). It is postulated that *S. Typhimurium* switches from S-glutathionylation to S-cysteinylated during infection conditions as novel redox-control mechanism. In agreement with the proteome data, transcriptome results point to an up-regulation of Cys biosynthesis and down-regulation of GSH biosynthesis under infection-like conditions. However, the physiological role of this S-thiolation switch for redox control of the identified protein targets under ROS stress remains to be elucidated.

Furthermore, no blocking of reduced thiols with NEM or IAM was performed to avoid artificial disulfide formation. Thus, it remains to be verified that the observed S-thiolations are not caused by artificial thiol-disulfide exchange. Previous studies have also shown that *L. monocytogenes* is able to both import and synthesize GSH (Reniere et al., 2015). Furthermore, the non-GSH-utilizing *S. aureus* was shown to import GSH during growth in LB medium (Pöthner et al., 2013). Thus, the possible uptake of GSH in *S. Typhimurium* from LB-medium could contribute to the observed S-glutathionylations which needs to be investigated.

The Regulatory Potential of Protein S-Glutathionylation in Gram-negative Bacteria

The role of protein S-glutathionylation for redox control has been studied in few Gram-negative bacteria, including *E. coli*, *S. Typhimurium*, *Neisseria meningitidis*, *Pseudomonas aeruginosa*, and *Synechocystis* sp. PCC6803 (Table 3). In *E. coli*, the peroxide-sensing regulator OxyR is activated by S-glutathionylation at its redox-sensing Cys199 *in vitro* (Kim et al., 2002). In addition, the activities of glyceraldehyde-3-phosphate dehydrogenase, methionine synthase and the PAPS reductase are inhibited by S-glutathionylation in *E. coli* (Lillig et al., 2003; Hondorp and Matthews, 2004; Brandes et al., 2009). A recent study provides a model for the S-glutathionylation of the conserved active site Cys in GapDH and explains the reactivity of the active site toward H_2O_2 (Peralta et al., 2015). Reaction of the active site Cys with H_2O_2 is catalyzed by a mechanism which stabilizes the transition state and promotes leaving group departure by providing a proton relay. This model suggests the conserved

TABLE 3 | Targets for protein S-thiolation by bacterial thiol-redox buffers.

Redox buffer	Organism	Functions of S-thiolated proteins	S-thiolated Cys	References
Glutathione	<i>Salmonella</i> Typhimurium	16 protein-SSG and nine protein-SSCys identified in LB medium cultures		Ansong et al., 2013
		nine protein-SSG in LB switch to protein-SSCys in minimal medium: DnaK (chaperone) CspD (cold shock protein) HNS (transcription regulator) MinE (cell division factor) Ndk (nucleoside diphosphate kinase) GrxC (glutaredoxin) RplC (50S ribosomal protein) YifE (unknown function) YjgF (translation inhibitor)	Cys15 Cys19 Cys21 Cys16 Cys139 Cys66 Cys199 Cys64 Cys107	
Glutathione	<i>Escherichia coli</i>	OxyR (peroxide sensor) Gap (glyceraldehyde-3-phosphate DH) MetE (methionine synthase) PpaC (PAPS reductase)	Cys199 redox-sensing Cys152 active site Cys645 not conserved Cys239 active site	Kim et al., 2002 Brandes et al., 2009 Hondorp and Matthews, 2004 Lillig et al., 2003
Glutathione	<i>Neisseria meningitidis</i>	EstD (esterase)	Cys54 substrate binding	Chen et al., 2013
Glutathione	<i>Pseudo-alteromonas haloplanktis</i>	PhSOD (iron-superoxide dismutase)	Cys57 conserved	Castellano et al., 2008
Glutathione	<i>Synechocystis</i> sp. PCC6803	383 total protein-SSG 125 S-glutathionylation sites: Inorganic pyrophosphatase Phosphoribulokinase PAPS reductase Triose phosphate isomerase IMP dehydrogenase ADP-glucose pyrophosphorylase RubisCo MerA (mercury reductase) AbrB (repressor of hydrogenase operon)	Cys164 Cys19 Cys230 Cys127 Cys222 Cys55 Cys422, Cys242 Cys78 active site Cys34 redox-sensing	Chardonnet et al., 2015 Marteyn et al., 2013 Cassier-Chauvat et al., 2014
Bacillithiol	<i>Bacillus subtilis</i>	54 total protein-SSB including eight conserved protein-SSB: MetE (methionine synthase) PpaC (Mn-dependent inorganic pyrophosphatase) SerA (D-3-phosphoglycerate DH) AroA (chorismate mutase) TufA (Elongation factor Tu) GuaB (IMP dehydrogenase) YphP/BrxA (bacilliredoxin) YumC (Ferrodoxin-NADP reductase2)	Cys730 active site Cys158 active site Cys410 conserved Cys126 conserved Cys83 GTP-binding site Cys308 active site Cys53 active site Cys85 active site	Chi et al., 2011 Chi et al., 2013
	<i>Bacillus pumilus</i> <i>Bacillus amyloliquefaciens</i> <i>Staphylococcus carnosus</i>			
Mycothioli	<i>Corynebacterium glutamicum</i>	25 total protein-SSM identified: MalP (Maltodextrin phosphorylase) MetE (Methionine synthase) Hom (Homoserine DH) Ino-1 (Myo-inositol-1-P-synthase) Fba (Fructose-bisphosphate aldolase) SerA (Phosphoglycerate DH) Pta (Phosphate acetyltransferase) XylB (pentulose/hexulose kinase) GuaB1/2 (IMP dehydrogenase) NadC (Nicotinate-nucleotide pyrophosphorylase)	Cys180 conserved Cys713 active site Cys239 Cys79 Cys332 Cys266 Cys367 Cys338 Cys302/Cys317 active site Cys114	

(Continued)

TABLE 3 | Continued

Redox buffer	Organism	Functions of S-thiolated proteins	S-thiolated Cys	References
Mycothioli	<i>Corynebacterium glutamicum</i>	PurL (Phosphoribosyl formylglycinamide synthase)	Cys716	Chi et al., 2014
		TheD/ThiD2 (Thiamine biosynthesis)	Cys451 active site/Cys111	
		Tpx (Thiol peroxidase)	Cys60 active site/Cys94 resolving	
		Mpx (Mycothioli peroxidase)	Cys36 active site	
		MsrA (Met-SO reductase)	Cys91 conserved	
		HmuO (Heme oxygenase)	Cys165	
		RpsC/F/M, RplM (ribosomal proteins)	Cys153/67/50/86	
		Tuf (translation elongation factor)	Cys277 conserved	
		PheT (Phe-tRNA synthetase)	Cys89 tRNA binding	

redox-regulation of GapDH by S-thiolation of its active site Cys across all domains of life.

In *Neisseria meningitidis*, an esterase EstD acts together with the GSH-dependent alcohol dehydrogenase AdhC in formaldehyde detoxification. EstD is inactivated via S-glutathionylation at its conserved Cys54 by its substrate S-formyl-GSH during formaldehyde detoxification *in vitro* (Chen et al., 2013). In the psychrophilic bacterium *Pseudoalteromonas haloplanktis*, S-glutathionylation of the iron-superoxide dismutase PhSOD at the single Cys57 protected the enzyme from tyrosine nitration and peroxynitrite inactivation *in vitro* and *in vivo* (Castellano et al., 2008).

In *Synechocystis* sp. PCC6803, a MerA-like enzyme that functions in mercury and uranium reduction was shown to be redox-controlled by S-glutathionylation (Marteyn et al., 2013). MerA was S-glutathionylated at Cys78 that is required for mercury reduction resulting in inhibition of MerA activity. MerA redox regulation and reactivation required reduction by glutaredoxin-1 (Grx1). The active site Cys31 and Cys86 of Grx-1 operate in MerA interactions and both Cys are required for MerA reactivation. Furthermore, S-glutathionylation was shown to control the activity of the transcription factor AbrB2 in *Synechocystis* sp. PCC6803 (Cassier-Chauvat et al., 2014). AbrB2 is a repressor of the hydrogenase-encoding *hoxEFUYH* operon and also down-regulates antioxidant genes, such as *cydAB* encoding the cytochrome bd-quinol oxidase and *norB* encoding the nitric oxide reductase. The production of hydrogen is thought to be an antioxidant mechanism to eliminate electrons for oxygen reduction and ROS generation. AbrB2 contains a conserved single cysteine that is essential for redox-regulation and oligomerisation of AbrB2 as shown in C34S mutants. S-glutathionylation of Cys34 affected the binding of AbrB2 to the *hox* promoter and the stability of AbrB2 *in vitro*. In conclusion, S-glutathionylation has been shown to function in the redox-control of two transcriptional regulators, OxyR and AbrB2 in Gram-negative bacteria *in vitro*. However, compared to the many targets for S-glutathionylation that have been studied in eukaryotic organisms, there is much to be discovered about the regulatory potential of S-glutathionylation in bacteria.

Protein S-glutathionylation is a reversible redox switch mechanism. The glutaredoxin (Grx)/GSH/GSH reductase (Gor) system catalyzes specific de-glutathionylation of S-glutathionylated proteins (Fernandes and Holmgren, 2004; Inaba, 2009). Grx

were first discovered in *E. coli* (Holmgren, 1976) where they have important functions as electron donors for ribonucleotide reductase (RNR), adenosine-5'-phosphosulfate (APS) reductase, 3'-phosphoadenosine-5'-phosphosulfate (PAPS) reductase and arsenate reductases (Holmgren, 1981; Aslund et al., 1994). Grx are structurally classified into the classical di-thiol Grxs with a CPTC redox active site and the monothiol Grx containing a CGPS redox active site (Lillig et al., 2008). In *E. coli*, three di-thiol Grx proteins (Grx1, Grx2, and Grx3) and one monothiol protein (Grx4) have been characterized.

The de-glutathionylation by Grx enzymes involves thiol-disulfide exchange reactions with GSH via nucleophilic double displacement (ping-pong) mechanisms and occurs via mono- or di-thiol mechanisms. Most di-thiol Grx use monothiol mechanisms that take place in two steps: In the first step, the nucleophilic thiolate anion attacks the S-glutathionylated substrate protein, resulting in reduction of the mixed disulfide and the S-glutathionylated Grx (Grx-SSG) intermediate. This Grx-SSG intermediate is regenerated by GSH and Gor at expense of NADPH (Allen and Mieyal, 2012). The di-thiol mechanism involves a second active site Cys that forms an intramolecular disulfide to resolve the Grx-SSG intermediate that has been shown for some plant Grx enzymes (Zaffagnini et al., 2012b). However, this di-thiol mechanism of Grx is less efficient for protein de-glutathionylation and more involved in the reduction of intermolecular protein disulfides (Lillig et al., 2008; Allen and Mieyal, 2012). Thus far, the knowledge about Grx functions and substrates in most GSH-producing bacteria is scarce and remains an important subject for future studies.

Biosynthesis and Regulation of Bacillithiol in Gram-Positive Firmicutes Bacteria

Bacillithiol (BSH) is composed of Cys-GlcN-malate and serves as major LMW thiol in many Firmicutes bacteria, including *Bacillus* and *Staphylococcus* species, *Deinococcus radiodurans*, and *Streptococcus agalactiae* (Newton et al., 2009) (Figure 4). The BSH biosynthesis pathway was first identified in *B. subtilis*. In the first step, the glycosyltransferase BshA couples UDP-GlcNAc to L-malic acid for generation GlcNAc-Mal (Ruane et al., 2008; Gaballa et al., 2010; Parsonage et al., 2010). The deacetylase BshB1 catalyzes deacetylation of GlcNAc-Mal to GlcN-Mal. The last step involves the putative cysteine ligase YIIA (BshC) that presumably adds Cys to GlcN-Mal (Gaballa et al., 2010). BshB1 has a

paralog BshB2 and both enzymes have deacetylase activity. The functional redundancy of BshB1 and BshB2 in *B. subtilis* suggests that BshB2 might function as BSH-S-conjugate amidase Bca in detoxification of RES similar to the MSH-S-conjugate amidase Mca (Parsonage et al., 2010). The functions of the BshB1/2 homologs of *B. anthracis* (BA1557 and BA3888) and *B. cereus* (BC1534 and BC3461) in the deacetylation of GlcNAc-Mal have been demonstrated *in vitro*. In addition, BA3888 was shown to function as BSH-S-conjugate amidase (Bca) (Fang et al., 2013). In contrast to BshA and BshB, the activity of the putative cysteine ligase BshC has never been demonstrated biochemically *in vitro*. The structure of BshC was resolved revealing a core Rossmann fold with connecting peptide motifs (CP1 and CP2) and an α -helical coiled-coil domain required for dimerization (Vanduinen et al., 2015). BshC was crystallized with citrate and glycerol in the canonical active site and ADP bound in a second binding pocket that is different from the ADP-binding pocket in the related MshC structure. The active sites are solvent exposed and open for possible interactions with a protein, substrate or cofactor that remain to be elucidated to understand the catalytic mechanism of BshC (Vanduinen et al., 2015).

The regulation of the BSH biosynthesis genes has been studied in *B. subtilis*. The *bshA* and *bshB1* genes belong to a large operon of seven genes including *mgsA* which encodes a methylglyoxal synthase. The *bshB2* and *bshC* genes are encoded by two different operons. The *bshA*, *bshB*, and *bshC* genes are induced under conditions of disulfide stress provoked by diamide or NaOCl and positively controlled by the disulfide stress regulator Spx (Chi et al., 2011; Rochat et al., 2012; Gaballa et al., 2013). Consistent with the Spx-dependent control of the BSH biosynthesis genes, lower BSH levels were detected in the *spx* mutant using thiol-metabolomics (Chi et al., 2011; Rochat et al., 2012; Gaballa et al., 2013). It is interesting to note, that the Trx pathway and BSH biosynthesis genes are both regulated by the major disulfide stress regulator Spx in *B. subtilis* (Zuber, 2004, 2009; Chi et al., 2011; Rochat et al., 2012; Gaballa et al., 2013).

Functions of Bacillithiol and BSH-Dependent Detoxification Enzymes

BSH is predominantly present in its reduced form in the cytoplasm with BSH/BSSB ratios ranging from 100:1 to 400:1 in *B. subtilis* indicating the presence of an efficient bacillithiol disulfide reductase (Sharma et al., 2013). The FAD-dependent pyridine nucleotide disulfide oxidoreductase YpdA (IPR023856) was suggested to function as BSSB reductase because of its phylogenetic relationship to the BSH biosynthesis enzymes as revealed by a STRING search (Gaballa et al., 2010). However, the function of YpdA has not yet been demonstrated.

The standard thiol-redox potential of BSH was calculated as E° (BSSB/BSH) = -221 mV which is higher than the GSH redox potential [E° (GSSG/GSH) = -240 mV] (Sharma et al., 2013). The microscopic pK_a values of the thiol group of BSH were determined as $pK_a = 7.97$ when the amino group of the Cys is protonated and as $pK_a = 9.55$ in the presence of the deprotonated amino group of Cys (Sharma et al., 2013). Thus, the thiol group in BSH is more acidic compared to the thiol group in Cys suggesting an enhanced level and reactivity of the BSH thiolate anions

to detoxify reactive species. The BSH concentrations in *B. subtilis* vary during the growth in LB medium and increase strongly during the stationary phase to 3.5–5.2 mM. In contrast, the cellular Cys concentration is kept at a relatively low level (0.13–0.28 mM). Thus, BSH concentrations are ~ 17 -fold higher compared to the level of Cys (Sharma et al., 2013). Similar concentrations of BSH (2 mM) were measured in *Bacillus pumilus* during growth. In *B. pumilus*, BSH levels increased under peroxide stress to 6 mM which is caused by an increased *bshB* expression (Handtke et al., 2014). BSH levels are also two-fold increased under diamide and NaOCl stress in *B. subtilis* due to Spx-dependent induction of *bshA*, *bshB*, and *bshC* (Chi et al., 2013; Gaballa et al., 2013). In *S. aureus*, the BSH levels are lower (0.3–1 mM) in the different clinical isolates (COL, USA300, Mu50, or N315) and BSH levels are not up-regulated during the stationary phase (Posada et al., 2014).

The physiological functions of BSH were studied in *bsh* mutants of *B. subtilis* and *S. aureus* (Table 1). Phenotype analyses showed increased sensitivities of *bsh* mutants toward hypochlorite, diamide, methylglyoxal, ROS (paraquat, H_2O_2), osmotic, and acidic stress, alkylating agents and fosfomycin in *B. subtilis* (Gaballa et al., 2010; Chi et al., 2011). The fosfomycin-sensitive phenotype of *bsh* mutants depends on the epoxide hydrolase FosB that requires BSH as a cofactor to open the ring structure for fosfomycin detoxification (Lamers et al., 2012; Roberts et al., 2013; Thompson et al., 2013) (Figure 6). FosB shows a preference for BSH as thiol cofactor and does only work poorly with Cys. The biochemical activity has been demonstrated for various *Bacillus* and *Staphylococcus* FosB homologs (Lamers et al., 2012; Roberts et al., 2013; Thompson et al., 2013). In *B. subtilis* and *S. aureus*, both FosB and BSH confer resistance to fosfomycin treatment in survival assays *in vivo* (Gaballa et al., 2010; Thompson et al., 2014). Co-crystallization of *S. aureus* FosB with L-Cys or BSH revealed a mixed disulfide at the active site Cys9 of FosB which is unique in FosB from *S. aureus* (Thompson et al., 2014).

Reactive electrophiles, such as monobromobimane are detoxified by direct conjugation to BSH or by conjugation reactions catalyzed by BSH S-transferases. BSH functions as a cofactor for DinB-family S-transferases that are widely distributed among GSH-, BSH-, and MSH-producing bacteria (Newton et al., 2011; Perera et al., 2014). The *B. subtilis* DinB-family YfiT protein was active as S-transferase with BSH to conjugate monochlorobimane, but inactive with MSH or GSH (Newton et al., 2011). The *yfiT* gene is flanked by *yfiS* and *yfiU* encoding putative efflux transporters for mercapturic acids produced during electrophile detoxification. The YfiT-homolog of *S. aureus* BstA catalyzed the conjugation of BSH to monochlorobimane, 1-chloro-2,4-dinitrobenzene and cerulenin, while rifampicin was BstA-independently conjugated to BSH (Perera et al., 2014).

BSH is involved in methylglyoxal detoxification and functions as a cofactor for BSH-dependent glyoxalases in *B. subtilis* (Chandrangsu et al., 2014). Methylglyoxal rapidly depletes BSH leading to BSH-hemithioacetal formation that is converted to S-lactoyl BSH by the glyoxalase-I (GlxA). The glyoxalase-II (GlxB) catalyzes conversion of S-lactoyl-BSH to lactate (Figure 6). Phenotype studies further indicated that BSH can detoxify heavy metal ions, such as tellurite and selenite in *B. subtilis* (Helmann, 2011).

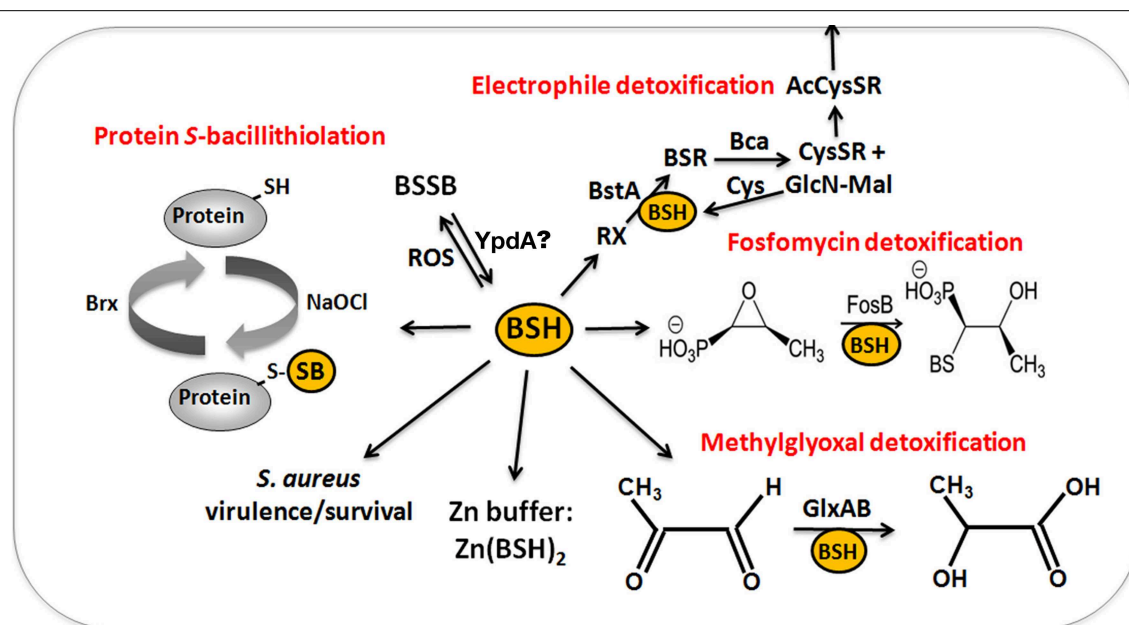


FIGURE 6 | The functions of bacillithiol (BSH) in *B. subtilis* and *S. aureus*. Bacillithiol functions in detoxification of ROS, RES, HOCl, and antibiotics (fosfomycin, rifampicin) in *B. subtilis* and *S. aureus*. BSH is oxidized by ROS to bacillithiol disulfide (BSSB). Electrophiles (RX) are conjugated to BSH by the BSH S-transferase BstA to form BS-electrophiles (BSR) which are cleaved by the BSH S-conjugate amidase Bca to CysSR and mercapturic acids (AcCysSR) that are exported from the cell. BSH serves as a cofactor for the epoxide hydrolase FosB which adds BSH to fosfomycin to open the ring structure

for its detoxification. BSH functions in methylglyoxal detoxification as a cofactor for the glyoxalases I/II (GlxA and GlxB) in *B. subtilis*. GlxA converts BSH-hemithioacetal to S-lactoyl-BSH that is further converted by GlxB to D-lactate. BSH serves as Zn buffer under conditions of Zn excess in *B. subtilis*. In *S. aureus*, BSH is important under infection-related conditions and increased the survival of *S. aureus* in phagocytosis assays using murine macrophages. Under conditions of NaOCl stress, proteins are oxidized to mixed disulfides with BSH, termed as S-bacillithiolations which is reversed by bacilliredoxins.

In addition, BSH functions as Zn buffer in metal ion homeostasis (Ma et al., 2014). The Cys thiol and carboxylate moieties of BSH can bind and store Zn(II) as BSH_2Zn complex under conditions of Zn(II) stress (Ma et al., 2014). BSH binding to Zn(II) occurred at much higher affinity compared to GSH. Mutants lacking BSH are more sensitive to Zn(II) stress and induced the Zn efflux CadA system at lower Zn levels compared to the wild type. BSH also protected against Zn(II) toxicity in cells lacking Zn efflux pumps. In addition, Zn efflux is elevated under conditions of diamide stress when the pool of reduced BSH is depleted. These results establish a new role of BSH as buffer for the labile Zn pool that are likely important for related pathogens under infection conditions.

In conclusion, functional analyses of *bsh* mutants established important roles of BSH as GSH surrogate in Firmicutes bacteria, including similar detoxification functions and BSH-dependent enzymes, such as DinB-family S-transferases and glyoxalases that are widely conserved across bacteria. However, the conserved role of FosB as BSH-dependent fosfomycin hydrolase and the function of BSH as Zn buffer have been described only in BSH-producing bacteria.

Functions of Bacillithiol in the Virulence of *Staphylococcus aureus*

Phenotype analyses of *S. aureus* *bsh* mutants were conducted for different clinical isolates of methicillin-resistant *S. aureus*

strains (MRSA) that revealed a role of BSH for stress resistance and under infection conditions (Pöther et al., 2013; Posada et al., 2014) (Table 2). In survival assays, *S. aureus* USA300 LAC transposon *bsh* mutants were more sensitive to alkylating agents (iodoacetamide and CDNB), methylglyoxal, peroxide and superoxide stress, diamide, fosfomycin, cerulenin, rifampicin and metals ions, like copper and cadmium (Rajkarnikar et al., 2013). In *S. aureus* COL and USA300 backgrounds, *bshA* and *fosB* mutants with clean deletions showed increased sensitivities to fosfomycin, diamide and H_2O_2 and the levels of NADPH and BSH were decreased in *fosB* mutants suggesting a function of FosB as S-transferase in the oxidative stress resistance (Posada et al., 2014). The *S. aureus* COL and USA300 *bshA* mutants showed a decreased survival in human whole-blood survival assays (Posada et al., 2014). Microarray analyses of the *bshA* mutant further revealed that staphyloxanthin biosynthetic genes are induced while the level of staphyloxanthin was strongly decreased in the *S. aureus* *bshA* mutant. Interestingly, the widely used strains of the *S. aureus* NCTC8325 lineage including SH1000 harbor natural *yllA* (*bshC*) null mutations that are caused by a 8 bp duplication in the *bshC* gene and these strains do not produce BSH (Gaballa et al., 2010; Newton et al., 2012; Posada et al., 2014). In contrast, *S. aureus* Newman encodes a functional *bshC* gene and produces BSH as revealed by thiol metabolomics (Newton et al., 2012; Pöther et al., 2013). BSH biosynthesis in *S. aureus* SH1000 could be restored by plasmid-encoded expression of the

bshC gene (Pöther et al., 2013; Posada et al., 2014). In phagocytosis assays using murine macrophages and human epithelial cell lines the survival of the SH1000 strain was decreased compared to the *bshC* complemented *S. aureus* strain (Pöther et al., 2013; Posada et al., 2014). Thus, BSH is involved in the defense against the host-immune system and contributes to pathogen fitness in *S. aureus* clinical MRSA isolates under infection-related conditions. It will be exciting to unravel the regulatory mechanisms that contribute to virulence control by BSH in *S. aureus*.

The Role of Protein S-Bacillithiolation in Gram-Positive Firmicutes Bacteria

Protein S-bacillithiolation was recently discovered as a widespread thiol protection and redox-regulatory mechanism in different Firmicutes bacteria (Chi et al., 2011, 2013) (Figure 7). S-bacillithiolation functions as a redox-switch mechanism to control the activity of redox-sensing transcription factors and metabolic enzymes, including OhrR and MetE (Lee et al., 2007; Chi et al., 2011) (Table 3). S-bacillithiolation of the OhrR repressor occurs at its lone Cys15 residue leading to inactivation of OhrR and expression of the thiol-dependent OhrA peroxiredoxin for detoxification of organic hydroperoxides and NaOCl (Fuangthong et al., 2001; Chi et al., 2011). S-bacillithiolation is also widespread among other Firmicutes

with eight common and 29 unique S-bacillithiolated proteins identified in *B. subtilis*, *Bacillus amyloliquefaciens*, *Bacillus pumilus*, *B. megaterium*, and *Staphylococcus carnosus* (Chi et al., 2011, 2013). The S-bacillithiolome contains mainly biosynthetic enzymes for amino acids (methionine, cysteine, branched chain and aromatic amino acids), cofactors (thiamine), nucleotides (GTP), as well as translation factors, chaperones, redox, and antioxidant proteins. Among the most conserved protein-SSB were abundant and essential proteins like TufA, MetE, GuaB that are targets for S-thiolation also in MSH-producing bacteria (Chi et al., 2014).

The methionine synthase MetE is the most abundant S-bacillithiolated protein in *Bacillus* species after NaOCl exposure. S-bacillithiolation of MetE occurs at its Zn-binding active site Cys730 and at the non-essential surface-exposed Cys719, leading to methionine starvation in NaOCl-treated cells (Chi et al., 2011). Similarly, methionine auxotrophy is caused by S-glutathionylation of MetE in *E. coli* after diamide stress (Hondorp and Matthews, 2004). The active site Zn center of MetE is also S-mycothiolated in *C. glutamicum* (Chi et al., 2014). Since formyl methionine is required for initiation of translation, MetE inactivation could stop translation during the time of hypochlorite detoxification. This translation arrest caused by S-bacillithiolation is supported by the strong repression of the

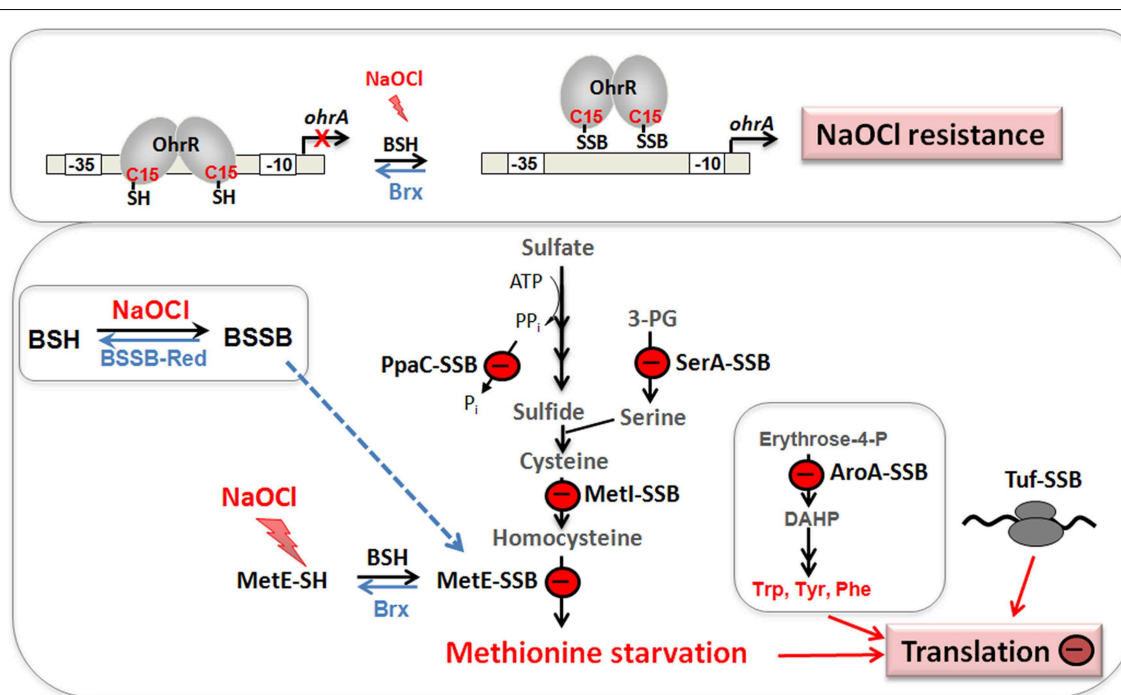


FIGURE 7 | Physiological roles of S-bacillithiolations in *B. subtilis* and other Firmicutes. NaOCl leads to S-bacillithiolation of OhrR, MetE, YxjG, PpaC, SerA, AroA, GuaB, YumC, TufA, and YphP in *B. subtilis* (Chi et al., 2011). S-bacillithiolation of OhrR inactivates the repressor and causes induction of the OhrA peroxiredoxin that confers NaOCl resistance. S-bacillithiolation of the methionine synthase MetE at its active site Cys730 and other enzymes of the Cys and Met biosynthesis pathway (YxjG, PpaC, SerA, MetI) leads to methionine auxotrophy (Chi et al., 2011, 2013). In

addition, other amino acids biosynthesis enzymes, translation factors and ribosomal proteins are S-bacillithiolated in Firmicutes bacteria. Thus, we hypothesize that S-bacillithiolation leads to a transient translation stop during the time of NaOCl detoxification to prevent further protein damage. NaOCl stress causes oxidation of BSH to BSSB and a two-fold decreased BSH/BSSB redox ratio that possibly contributes to S-bacillithiolation. The reduction of MetE-SSB and OhrR-SSB is catalyzed by bacilliredoxins (BrxA/Brx) in *B. subtilis*.

stringent response RelA regulon under NaOCl stress, which includes genes for ribosomal proteins and translation factors (Chi et al., 2011).

Our studies revealed that S-bacillithiolations were observed under diamide and NaOCl stress, but not under control conditions. This confirms previous results about the mechanisms of S-glutathionylations which requires activation of protein thiols by ROS. S-glutathionylation can be caused via thiol-disulfide exchange with GSSG and by activation of thiols to sulfenic acid, sulfenylamides, thiyl radicals, thiosulfinate or S-nitrosyl intermediates (Gallogly and Mieyal, 2007; Mieyal et al., 2008; Allen and Mieyal, 2012; Mieyal and Chock, 2012). Hypochlorite leads to chlorination of the thiol group to form sulfenylchloride that is unstable and rapidly reacts further to form mixed BSH protein disulfides (Hawkins et al., 2003; Davies, 2011). The increased BSSB level under NaOCl-stress might also contribute to S-bacillithiolation via thiol-disulfide exchange.

Among the S-bacillithiolated proteins, the thioredoxin-like proteins YtxJ, YphP, and YqiW were identified in *B. subtilis* and *Staphylococcus* that occur only in BSH-producing bacteria (Chi et al., 2013). These Trx-like enzymes were suggested to function as bacilliredoxins (Brx) in the de-bacillithiolation process. YtxJ could function as monothiol Brx and contains a single Cys in the conserved TCPIS motif. YphP (BrxA) and YqiW (BrxB) are paralogs of the uncharacterized DUF1094 family (53% identity) with unusual CGC active sites (Gaballa et al., 2010). YphP has also weak thiol-disulfide isomerase activity and a relatively high standard redox potential of $E^0' = -130$ mV (Derewenda et al., 2009). It was demonstrated that BrxA and BrxB function in the reduction of the S-bacillithiolated substrates MetE and OhrR *in vitro* (Gaballa et al., 2014) (Figure 8). The BrxBCxA resolving Cys mutant protein was able to reduce

S-bacillithiolated OhrR to restore the DNA-binding activity of OhrR. However, the BrxBCxA mutant was unable to reduce S-cysteinylated OhrR. These results provide first evidence for the function of glutaredoxin-like enzymes in BSH-producing bacteria. However, phenotype analyses revealed that both, BrxA and BrxB are not essential and rather dispensable for oxidative stress resistance under conditions of S-bacillithiolations in *B. subtilis* (Gaballa et al., 2014). Thus, the bacilliredoxin pathway is redundant with other thiol-disulfide oxidoreductases or the thioredoxin pathway *in vivo* for reduction of BSH mixed disulfides. In conclusion, the redox regulation of enzymes and transcription regulators by S-bacillithiolation and bacilliredoxins has been studied in detail in the model bacterium *B. subtilis*. Future studies should be directed to elucidate if S-bacillithiolation and bacilliredoxins control virulence functions and pathogen fitness in the major pathogen *S. aureus*.

Biosynthesis and Regulation of Mycothiol in Actinomycetes

Mycothiol (MSH) is composed of N-Acetyl-Cys-GlcN-myo-inositol (Figure 4) and is present in high-GC Gram-positive Actinomycetes, such as Streptomycetes, Mycobacteria and Corynebacteria (Jothivasan and Hamilton, 2008; Newton et al., 2008). The biosynthesis of MSH proceeds from myo-inositol-1-phosphate, UDP-GlcNAc and cysteine and occurs in five steps (Jothivasan and Hamilton, 2008; Newton et al., 2008). The glycosyltransferase MshA conjugates myo-inositol-1-P to UDP-GlcNAc and produces GlcNAc-Ins-P. Dephosphorylation of GlcNAc-Ins-P by the phosphatase MshA2 generates GlcNAc-Ins which is the substrate for the deacetylase MshB. The MshB enzyme is homologous to the MSH S-conjugate amidase (Mca), and has both deacetylase and amidase activities. The cysteine

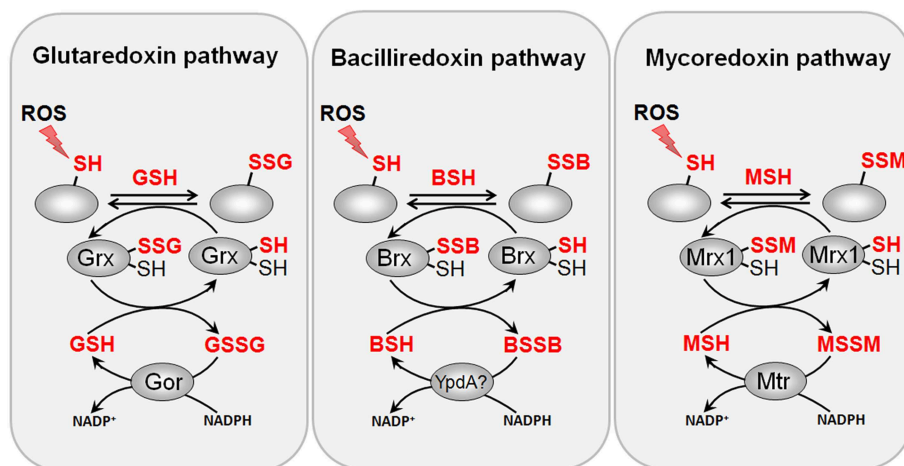


FIGURE 8 | Reduction of protein S-glutathionylations, S-bacillithiolations and S-mycothiolations by glutaredoxin, bacilliredoxin and mycoredoxin pathways. The S-glutathionylated proteins are reduced by glutaredoxins (Grx) leading to a Grx-SSG intermediate that is reduced by GSH leading to GSSG which is recycled back to GSH by the NADPH-dependent GSSG reductase (Gor). Analogous bacilliredoxin and mycoredoxin pathways have been characterized in BSH-

and MSH-utilizing Gram-positive bacteria. The S-bacillithiolated proteins are reduced by bacilliredoxins (Brx) leading to Brx-SSB formation. Brx-SSB is reduced by BSH with the generation of BSSB that likely requires the NADPH-dependent BSSB reductase YpdA for regeneration of BSH. In Actinomycetes, mycoredoxin1 catalyzes reduction of S-mycothiolated proteins leading to Mrx1-SSM generation that is recycled by MSH and the NADPH-dependent MSSM reductase Mtr.

ligase MshC adds Cys to GlcN-Ins to generate Cys-GlcN-Ins. The final acetylation of the Cys is catalyzed by the acetyltransferase MshD to produce MSH (Jothivasan and Hamilton, 2008; Newton et al., 2008). The structure of MSH is similar to that of BSH and the glycosyltransferase BshA and deacetylase BshB of *B. subtilis* are homologs of the MshA and MshB enzymes of *Mycobacteria*.

MSH biosynthesis enzymes in *Streptomyces* are redox-controlled under diamide stress by the disulfide stress specific σ^R ECF sigma factor/RsrA anti sigma factor system (Kim et al., 2012). σ^R is sequestered by its redox-sensitive anti sigma factor RsrA in non-stressed cells. RsrA is oxidized at redox-sensing Cys residues in the Zn-binding site under disulfide stress that leads to relief of σ^R . Free σ^R transcribes genes required to maintain the thiol-redox homeostasis, including the genes for TrxAB and MSH biosynthesis, such as *mshA*, *mshB*, *mshC*, *mshD*, *mca* (Bae et al., 2004; Newton and Fahey, 2008; Park and Roe, 2008). In *C. glutamicum*, the homologous ECF sigma factor σ^H /RshA system controls the disulfide stress response genes for the Trx/TrxR system (*trxB*, *trxB1*, *trxC*) and for MSH biosynthesis and recycling (*mshC*, *mca*, *mtr*) (Ehira et al., 2009; Busche et al., 2012). The regulation of the Trx and MSH pathways by σ^R /RsrA or σ^H /RshA is conserved among Actinomycetes (Park and Roe, 2008; Antelmann and Helmann, 2011; Kim et al., 2012). Thus, it is common in Gram-positive bacteria that the genes for BSH and MSH biosynthesis pathways are under redox-control of the major disulfide stress regulators, Spx in Firmicutes bacteria and RsrA/RshA in Actinomycetes, respectively.

Functions of Mycothiol and MSH-Dependent Enzymes in Actinomycetes

MSH serves as the major thiol-redox buffer in Actinomycetes. MSH is oxidized to MSH disulfide (MSSM) under oxidative stress conditions. The mycothiol disulfide reductase Mtr maintains MSH in its reduced state at the expense of NADPH. MSH is involved in protection against oxidative and electrophile stress, alkylating agents, toxins, antibiotics (erythromycin, vancomycin, rifampin, azithromycin), heavy metal stress, aromatic compounds, ethanol and glyphosate in *Streptomyces*, *Mycobacteria* and *Corynebacteria* (Buchmeier et al., 2003, 2006; Rawat et al., 2007; Newton et al., 2008; Liu et al., 2013) (Table 1). MSH is used as a cofactor for MSH-dependent enzymes during detoxification of toxins, electrophiles and antibiotics in Actinomycetes (Figure 9, Table 1). MSH forms conjugates with xenobiotics and antibiotics either spontaneously or by the DinB-family MSH S-transferases (Newton et al., 2011). The MSH S-transferase Mst of *M. smegmatis* was shown to catalyze the conjugation of monochlorobimane and DTNB to MSH but its natural substrate is not known (Newton et al., 2011). MSH-S-conjugates are rapidly cleaved by the MSH-S-conjugate amidase (Mca) to glucoseamine-myoinositol (GlcN-Ins) and mercapturic acid derivatives (AcCysSR) that are excreted from the cell. Mca is the major detoxification enzyme for MSH S-conjugates with antibiotics, including cerulenin and rifamycin in *Mycobacteria* (Newton et al., 2008, 2011). Interestingly, MSH and the Mca-homologs LmbT, LmbV and LmbE play also a direct role in the biosynthesis of the sulfur-containing lincosamide antibiotic

lincomycin in *Streptomyces lincolnensis* (Zhao et al., 2015). MSH functions as the sulfur donor for incorporation of the methylmercapto group into lincomycin after thiol exchange. In addition, ergothioneine (EGT), that is utilized as another thiol by Actinomycetes, acts as a carrier for the assembly of the N-methylated 4-propyl-L-proline (PPL) and lincosamide moieties to form lincomycin. EGT and MSH were shown to function in lincomycin biosynthesis through unusual S-glycosylations documenting a first biochemical role of LMW thiols in bacteria. Since the biosynthetic pathways for many sulfur-containing natural compounds include Mca homologs, the involvement of LMW thiols in natural product biosynthesis might be a common mechanism (Zhao et al., 2015).

MSH functions as a cofactor for many redox enzymes that are involved in the detoxification of peroxides, electrophiles (formaldehyde), NO, aromatic compounds (maleylpyruvate) and arsenate (Fahey, 2013) (Table 1). There is evidence for a MSH-peroxidase Mpx involved in peroxide detoxification that was identified as S-mycothiolated Gpx-homolog under oxidative stress in *C. glutamicum* (Chi et al., 2014). The MSH-dependent alcohol dehydrogenase MscR (MSNO reductase/formaldehyde dehydrogenase) catalyzes the detoxification of formaldehyde and S-nitrosyl-mycothiol (MSNO) (Newton et al., 2008). MSH reacts with formaldehyde to MS-CH₂OH that is converted to formate by MscR. MscR also converts MSNO to MSH sulfonamide (MSONH₂). In *C. glutamicum*, a similar MSH-dependent pathway for formaldehyde oxidation by the MSH-dependent formaldehyde dehydrogenase AdhE/FadH has been characterized (Lessmeier et al., 2013; Witthoff et al., 2013). In *C. glutamicum*, MSH is further involved in degradation of aromatic compounds, including gentisate, 3-hydroxybenzoate, maleylpyruvate, resorcinol, and naphthalene and *msh* mutants were unable to grow on these substrates (Liu et al., 2013). MSH functions as a cofactor for the maleylpyruvate isomerase in the gentisate ring-cleavage pathway to catalyze the isomerization of maleylpyruvate to fumaryl pyruvate in *C. glutamicum* (Feng et al., 2006). Similarly, MSH was suggested as a cofactor for enzymes of the naphthalene and resorcinol degradation pathway (Liu et al., 2013).

MSH confers resistance to metal ions, such as Cr(VI), Zn(II), Cd(II), Co(II), and Mn(II) in *C. glutamicum* (Liu et al., 2013). The detoxification of arsenate [As(V)] to arsenite [As(III)] depends on the MSH-dependent arsenate reductases ArsC1/C2 (Ordóñez et al., 2009). ArsC1/C2 function similar to S-transferases in arsenate detoxification by formation of an arseno-MSH conjugate that requires the mycoredoxin-1/MSH/Mtr electron pathway for reduction. In contrast, another arsenate reductase Cg_ArsC1' detoxifies arsenate with electrons from the Trx pathway (Viladangos et al., 2011).

MSH enhanced also the robustness of *C. glutamicum* during industrial production of glutamate and L-lysine (Liu et al., 2014). The overexpression of *mshA* resulted in increased MSH biosynthesis and higher resistance of *C. glutamicum* to peroxides, methylglyoxal, antibiotics (erythromycin and streptomycin), metal ions, organic acids, furfural and ethanol (Liu et al., 2014). Thus, the increased biosynthesis of LMW thiol redox buffers, as shown for GSH in *C. acetobutylicum* and MSH in

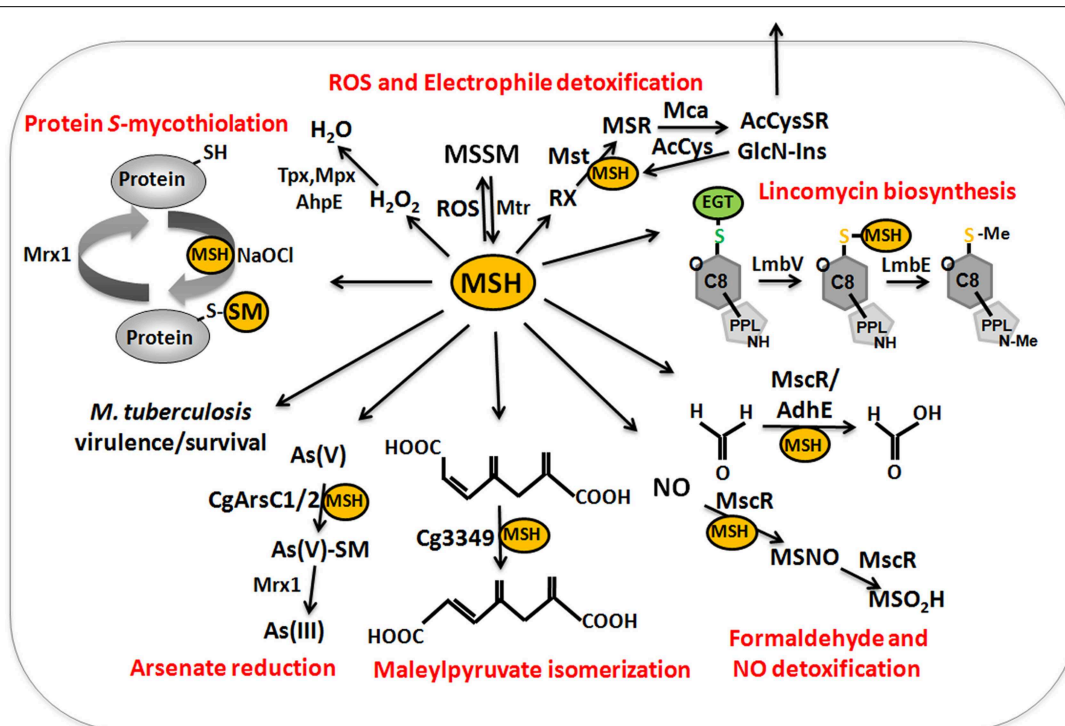


FIGURE 9 | The functions of mycothiol (MSH) in Mycobacteria and Corynebacteria. Mycothiol (MSH) is oxidized by ROS to mycothiol disulfide (MSSM). MSSM is reduced back to MSH by the mycothiol disulfide reductase Mtr on expense of NADPH. MSH-dependent peroxidases, such as Mpx, Tpx, and AhpE function in peroxide detoxification. Electrophiles (RX) are conjugated to MSH by the MSH S-transferase Mst to form MS-electrophiles (MSR) which are cleaved by the MSH S-conjugate amidase Mca to mercapturic acids (AcCysSR) that are exported from the cell. The Mca-homologs LmbT, LmbV, and LmbE function also in the assembly and biosynthesis of the sulfur-containing lincosamide antibiotic lincomycin in

Streptomyces lincolnensis (Zhao et al., 2015). MSH serves as a cofactor for the alcohol dehydrogenase AdhE/MscR in Mycobacteria and Corynebacteria for detoxification of formaldehyde to formate and MSNO to MSO₂H. MSH functions in detoxification of maleylpyruvate as a cofactor for maleylpyruvate isomerase in *C. glutamicum*. Arsenate reductases CgArsC1 and CgArsC2 conjugate MSH and arsenate As(V) to form As(V)-SM that is reduced to As(III) by Mrx1. In *M. tuberculosis*, MSH is important under infection conditions and for growth and survival. Under conditions of NaOCl stress, proteins are oxidized to mixed disulfides with MSH, termed as S-mycothiolations which is reversed by mycoredoxins.

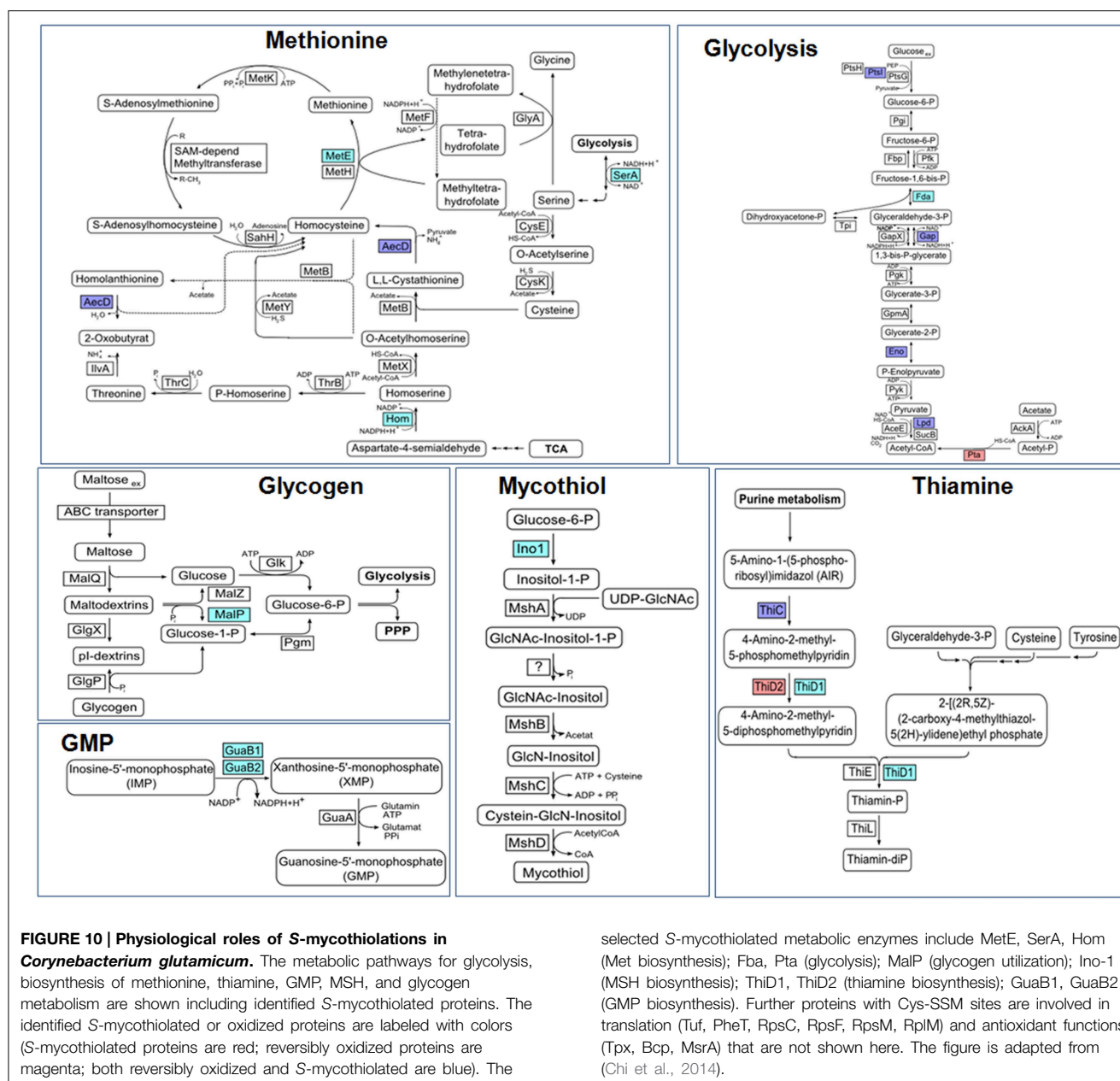
C. glutamicum, might be a promising strategy to engineer robust industrial production strains.

In *Mycobacterium tuberculosis*, MSH is essential for growth and survival of *M. tuberculosis* under infection conditions (Sareen et al., 2003; Sassetti and Rubin, 2003). In addition, MSH is required to activate the antituberculosis prodrug isoniazid and hence *M. tuberculosis mshA* mutants are resistant to isoniazid (Buchmeier et al., 2003). Tuberculosis (TB) causes still nearly 2 million death each year and multiple and extensive drug resistant strains occur that require new targets for antituberculosis drugs. Thus, inhibitors of MSH biosynthesis enzymes are promising candidates for antituberculosis drug developments. Several MSH biosynthesis inhibitors have been applied that target the MSH-S-conjugate amidase Mca, the deacetylase MshB, the cysteine ligase MshC and the MSSM reductase Mtr that are attractive antituberculosis drug targets (Nilewar and Kathiravan, 2014).

The Role of Protein S-Mycothiolation in Gram-Positive Actinomycetes

Protein S-mycothiolation was first studied in *C. glutamicum* and 25 S-mycothiolated proteins could be identified under NaOCl

stress by mass spectrometry (Chi et al., 2014) (Table 3). The thiol-peroxidase Tpx and the putative MSH peroxidase Mpx were S-mycothiolated under control and NaOCl stress conditions at their active site Cys residues. The fragment ion spectra of the S-mycothiolated Cys-peptides are characterized by diagnostic myoinositol-loss precursor ions (−180 Da) that serve as markers for identification. The 25 S-mycothiolated proteins overlap with 16 NaOCl-sensitive proteins identified in the fluorescent-label thiol-redox proteome. These include Tuf, GuaB1, GuaB2, SerA, and MetE as conserved abundant targets for S-thiolations across Gram-positive bacteria (Chi et al., 2013). The S-mycothiolated proteins are involved in the metabolism of carbohydrates, such as glycolysis (Fba, Pta, XylB), glycogen and maltodextrin degradation (MalP) and several biosynthesis pathways for serine, cysteine, methionine (SerA, Hom, MetE), nucleotides and thiamine (GuaB1, GuaB2, PurL, NadC, ThiD1, and ThiD2) and myo-inositol-1-phosphate (Ino-1 or Cg3323) (Figure 10). Further protein-SSM function in peroxide detoxification (Tpx, Gpx), methionine sulfoxide reduction (MsrA), heme degradation for iron mobilization (HmuO) and protein translation (RpsF, RpsC, RpsM, RplM, Tuf). The glycogen phosphorylase MalP is one of



the most abundantly S-mycothioliated proteins in NaOCl-treated cells (Chi et al., 2014). S-mycothioliation of MalP is important for oxidative stress resistance in *C. glutamicum* since the *malP* deletion mutant is NaOCl-sensitive in growth assays. MalP functions in glycogen degradation during the stationary phase. S-mycothioliation of MalP may prevent glycogen degradation under NaOCl stress since the glycogen content remained stable despite a strongly decreased glucose uptake rate.

The mycoredoxin-1 (Mrx1) has been characterized as glutaredoxin-homolog of Actinomycetes in reduction of MSH mixed disulfides (Van Laer et al., 2012) (Figure 8). Mrx-1 has a typical Trx-like fold with a CGYC motif and a *cis*-Pro57 in a groove that presumable binds MSH. The redox potential of

Mrx-1 was calculated as $E^{\circ} = -218 \text{ mV}$ and the pK_a of the active site Cys17 was 5.1–5.6. Mrx-1 catalyzed de-mycothioliation in a hydroxyethyl disulfide (HED) assay and is coupled to the MSH/Mtr/NADPH pathway. Mrx-1 operates via a monothiol reaction mechanism in the de-mycothioliation reaction analogous to most glutaredoxins that are involved in de-glutathionylation. The first Mrx1 substrate was identified as the thiol-peroxidase Tpx that was S-mycothioliated at its active site Cys60 and resolving site Cys94 in *C. glutamicum* *in vivo* under hypochlorite stress (Chi et al., 2014). Tpx showed NADPH-linked peroxidase activity and reduced H_2O_2 in a Trx/TrxR-coupled electron assay. S-mycothioliation of Tpx inhibits the peroxidase activity which was restored after reduction by the Mrx1/MSH/Mtr pathway. Thus,

S-mycothiolation controls Tpx activity and protects the peroxidic Cys against overoxidation. In *M. tuberculosis*, Mrx1 has been shown to reduce the one-Cys peroxiredoxin AhpE (Hugo et al., 2014). AhpE is a membrane-associated peroxidase that detoxifies peroxinitrite and fatty acid hydroperoxides as preferred substrates (Hugo et al., 2009; Reyes et al., 2011). AhpE is oxidized by peroxides to form a sulfenic acid intermediate (AhpE-SOH) that can be reduced directly by Mrx1. Alternatively, AhpE-SOH can react with MSH to S-mycothiolated AhpE-SSM which is reduced by the Mrx1/MSH/Mtr electron pathway (Hugo et al., 2014). The direct AhpE-SOH reduction may occur in the membrane when MSH is not available and the formation of AhpE-SSM and subsequent Mrx1-reduction was suggested to predominate in the cytosol. Interestingly, the reducing mechanism of AhpE-SSM is similar to the detoxification of arsenate by CgArsC1 and CgArsC2. Arsenate reacts with MSH to an arseno-(V)-MSH complex that is reduced by Mrx1 releasing As(III) and Mrx1-SSM that is recycled by the MSH/Mtr/NADPH electron pathway (Ordonez et al., 2009; Villadangos et al., 2011). It remains to be shown if AhpE is mycothiolated under oxidative stress in *M. tuberculosis* cells *in vivo*. These results show that Mrx1 functions as glutaredoxin homolog in *C. glutamicum* and *M. tuberculosis* in the reduction of S-mycothiolated peroxiredoxins (Tpx and AhpE), when coupled to the MSH/Mtr/NADPH electron pathway and as electron donor for arsenate reductase in arsenate detoxification.

Recently, Mrx1 has been coupled to redox sensitive GFP (roGFP2) to construct a new genetically encoded biosensor for dynamic measurements of the MSH redox potential in different *M. tuberculosis* strains (Bhaskar et al., 2014). This study revealed phenotypic redox heterogeneity of E^0 (MSSM/MSH) within Mycobacteria inside infected macrophages that are caused by sub-vacuolar compartments. Those sub-populations with higher E^0 (MSSM/MSH) were more susceptible to clinical relevant antibiotics whereas populations with lower MSH redox potentials were resistant to antibiotics. The results further show that several anti-TB drugs induce oxidative stress in *M. tuberculosis* during infections. In conclusion, this Mrx1-roGFP2 biosensor is a promising tool to study MSH redox potential changes of *M. tuberculosis* under infections and antibiotic treatments. This is the first example for a genetically encoded redox biosensor that measures dynamic changes of the mycothiol redox potential in bacteria. Future studies should be directed to apply similar biosensors in other pathogenic bacteria to study the dynamics of redox potential changes during infections.

Conclusion and Perspectives for Future Research

In this review, we provide an overview about the biosynthesis pathways and functions of the bacterial redox buffers glutathione, bacillithiol and mycothiol and their regulatory roles for protein S-thiolations. Bacterial redox buffers maintain the reduced state of the cytoplasm and function as cofactors of conserved enzymes for detoxification of ROS, RES, chlorines, antibiotics and xenobiotics. These thiol-dependent enzymes include

NADPH-dependent disulfide reductases (Gor, Mtr, YpdA) and related glutaredoxin-like enzymes (Grx, Mrx, Brx), DinB-family S-transferases (Gst, Mst, BstA), S-conjugate amidases (Mca, Bca) and glyoxalases (GloAB, GlxAB). However, some detoxification enzymes still need to be characterized in BSH-utilizing bacteria, including the BSH-dependent formaldehyde reductase (AdhA), the putative BSH peroxidase (Bpx) or thiol-dependent dioxygenases (MhqA, MhqE and MhqO) (Antelmann et al., 2008). The discovery of the biochemical functions of MSH, EGT and S-transferases in the lincomycin antibiotic biosynthesis opens perspectives to characterize the roles of thiol-redox buffers in the biosynthesis of sulfur-containing co-factors, natural compounds and antibiotics in other bacteria.

The structures of BSH and MSH are similar and the BSH biosynthesis enzymes BshA, BshB and BshC are homologous to the MSH biosynthesis enzymes MshA, MshB, and MshC. However, the crystal structure of BshC has revealed significant differences compared to MshC which requires further studies to understand the still unknown cysteine ligation mechanism of BshC (Vanduinen et al., 2015). It is further interesting, that the levels of BSH and MSH vary strongly between Firmicutes and Actinomycetes and also during growth and stress conditions. While Mycobacteria produce up to 20 mM MSH, the levels of BSH are much lower reaching 1–6 mM in Firmicutes bacteria. The differences in BSH and MSH levels during growth and under stress can be explained by the redox control of the BSH and MSH biosynthesis enzymes by the major thiol-based redox sensors (Spx and RsrA/RshA), presumably to enhance the redox buffer capacity under certain conditions to keep the reduced state of the cytoplasm. In contrast, redox regulation of GSH biosynthesis genes has not been shown. However, the pathogen *L. monocytogenes* is able to synthesize GSH and to import host-derived GSH as adaptation strategy under infection conditions (Reniere et al., 2015). Importantly, synthesized and host-derived GSH both contribute to virulence factor regulation in *L. monocytogenes*, while GSH-import was required for full virulence in *S. pneumoniae* (Potter et al., 2012; Reniere et al., 2015). Overall, the roles of GSH, BSH and MSH for virulence and pathogen fitness have been shown for many important human pathogens, including *L. monocytogenes*, *S. pneumoniae*, *S. Typhimurium*, *S. aureus*, and *M. tuberculosis*. Future studies in the field of infection biology should be directed to understand the molecular mechanisms of virulence factor regulation by thiol-redox buffers that might involve also protein S-thiolation mechanisms. The GSH, BSH and MSH biosynthesis enzymes, GSH uptake systems as well as S-thiolated proteins could be promising drug targets for the development of novel anti-infectives against emerging drug resistant strains of *S. pneumoniae*, *S. aureus* and *M. tuberculosis*. Thus, the large scale identification and quantification of S-thiolated proteins in pathogens is an important topic for future research.

Advances in mass spectrometry and chemical probe design have facilitated the development of more sensitive redox proteomics methods, such as the NEM-biotin switch assay or the Gsp-biotin assay to study targets for protein S-glutathionylation at a global scale (Lind et al., 2002; Kehr et al., 2011; Lin et al.,

2015). In addition, numerous BSH- and MSH-mixed protein disulfides have been identified recently under disulfide stress conditions, such as NaOCl and diamide. However, more quantitative MS-based redox proteomics approaches are required to determine the level of mixed BSH- and MSH-protein disulfides by combining the direct shotgun approach with OxICAT or the NEM-biotin switch assay coupled to Brx or Mrx1 (Leichert et al., 2008; Kehr et al., 2011). In addition, the regulatory roles for only few S-bacillithiolated and S-mycothiolated proteins have been studied thus far, including the redox regulator OhrR and the methionine synthase MetE (Lee et al., 2007; Chi et al., 2011). However, many interesting metabolic enzymes, redox-sensing transcription factors or virulence factors might be controlled by

protein S-thiolations in the pathogenic bacteria *S. aureus* and *M. tuberculosis* that remain to be elucidated in future research. Thus, it is an exciting field for new frontiers of science to unravel the regulatory potential of emerging protein S-thiolations in bacteria.

Acknowledgments

This work was supported by grants from the Deutsche Forschungsgemeinschaft (DFG) AN746/3-1 and AN746/4-1 within the DFG priority program SPP1710, by the DFG Research Training Group GRK1947, project [C1] and by an ERC Consolidator Grant (GA 615585) MYCOTHIOLOME to H.A.

References

- Allen, E. M., and Mieyal, J. J. (2012). Protein-thiol oxidation and cell death: regulatory role of glutaredoxins. *Antioxid. Redox Signal.* 17, 1748–1763. doi: 10.1089/ars.2012.4644
- Anderson, M. E. (1998). Glutathione: an overview of biosynthesis and modulation. *Chem. Biol. Interact.* 111–112, 1–14. doi: 10.1016/S0009-2797(97)00146-4
- Ansong, C., Wu, S., Meng, D., Liu, X., Brewer, H. M., Deatherage Kaiser, B. L., et al. (2013). Top-down proteomics reveals a unique protein S-thiolation switch in *Salmonella* Typhimurium in response to infection-like conditions. *Proc. Natl. Acad. Sci. U.S.A.* 110, 10153–10158. doi: 10.1073/pnas.1221210110
- Antelmann, H., Hecker, M., and Zuber, P. (2008). Proteomic signatures uncover thiol-specific electrophile resistance mechanisms in *Bacillus subtilis*. *Expert Rev. Proteomics* 5, 77–90. doi: 10.1586/14789450.5.1.77
- Antelmann, H., and Helmann, J. D. (2011). Thiol-based redox switches and gene regulation. *Antioxid. Redox Signal.* 14, 1049–1063. doi: 10.1089/ars.2010.3400
- Aslund, F., Ehn, B., Miranda-Vizuete, A., Pueyo, C., and Holmgren, A. (1994). Two additional glutaredoxins exist in *Escherichia coli*: glutaredoxin 3 is a hydrogen donor for ribonucleotide reductase in a thioredoxin/glutaredoxin 1 double mutant. *Proc. Natl. Acad. Sci. U.S.A.* 91, 9813–9817. doi: 10.1073/pnas.91.21.9813
- Atichartpongkul, S., Loprasert, S., Vattanaviboon, P., Whangsuk, W., Helmann, J. D., and Mongkolsuk, S. (2001). Bacterial Ohr and OsmC paralogues define two protein families with distinct functions and patterns of expression. *Microbiology* 147, 1775–1782.
- Bae, J. B., Park, J. H., Hahn, M. Y., Kim, M. S., and Roe, J. H. (2004). Redox-dependent changes in RsrA, an anti-sigma factor in *Streptomyces coelicolor*: zinc release and disulfide bond formation. *J. Mol. Biol.* 335, 425–435. doi: 10.1016/j.jmb.2003.10.065
- Bartsch, R. G., Newton, G. L., Sherrill, C., and Fahey, R. C. (1996). Glutathione amide and its perthiol in anaerobic sulfur bacteria. *J. Bacteriol.* 178, 4742–4746.
- Bhaskar, A., Chawla, M., Mehta, M., Parikh, P., Chandra, P., Bhawe, D., et al. (2014). Reengineering redox sensitive GFP to measure mycothiol redox potential of *Mycobacterium tuberculosis* during infection. *PLoS Pathog.* 10:e1003902. doi: 10.1371/journal.ppat.1003902
- Booth, I. R., Ferguson, G. P., Miller, S., Li, C., Gunasekera, B., and Kinghorn, S. (2003). Bacterial production of methylglyoxal: a survival strategy or death by misadventure? *Biochem. Soc. Trans.* 31, 1406–1408.
- Bourajjaj, M., Stehouwer, C. D., Van Hinsbergh, V. W., and Schalkwijk, C. G. (2003). Role of methylglyoxal adducts in the development of vascular complications in diabetes mellitus. *Biochem. Soc. Trans.* 31, 1400–1402. doi: 10.1042/BST0311400
- Brandes, N., Schmitt, S., and Jakob, U. (2009). Thiol-based redox switches in eukaryotic proteins. *Antioxid. Redox Signal.* 11, 997–1014. doi: 10.1089/ars.2008.2285
- Brennan, J. P., Miller, J. I., Fuller, W., Wait, R., Begum, S., Dunn, M. J., et al. (2006). The utility of N,N-biotinyl glutathione disulfide in the study of protein S-glutathiolation. *Mol. Cell. Proteomics* 5, 215–225. doi: 10.1074/mcp.M500212-MCP200
- Buchmeier, N. A., Newton, G. L., and Fahey, R. C. (2006). A mycothiol synthase mutant of *Mycobacterium tuberculosis* has an altered thiol-disulfide content and limited tolerance to stress. *J. Bacteriol.* 188, 6245–6252. doi: 10.1128/JB.00393-06
- Buchmeier, N. A., Newton, G. L., Koledin, T., and Fahey, R. C. (2003). Association of mycothiol with protection of *Mycobacterium tuberculosis* from toxic oxidants and antibiotics. *Mol. Microbiol.* 47, 1723–1732. doi: 10.1046/j.1365-2958.2003.03416.x
- Busche, T., Silar, R., Picmanova, M., Patek, M., and Kalinowski, J. (2012). Transcriptional regulation of the operon encoding stress-responsive ECF sigma factor SigH and its anti-sigma factor RshA, and control of its regulatory network in *Corynebacterium glutamicum*. *BMC Genomics* 13:445. doi: 10.1186/1471-2164-13-445
- Cassier-Chauvat, C., Veaudor, T., and Chauvat, F. (2014). Advances in the function and regulation of hydrogenase in the cyanobacterium *Synechocystis* PCC6803. *Int. J. Mol. Sci.* 15, 19938–19951. doi: 10.3390/ijms151119938
- Castellano, I., Ruocco, M. R., Cecere, F., Di Maro, A., Chambery, A., Michniewicz, A., et al. (2008). Glutathionylation of the iron superoxide dismutase from the psychrophilic eubacterium *Pseudoalteromonas haloplanktis*. *Biochim. Biophys. Acta* 1784, 816–826. doi: 10.1016/j.bbapap.2008.02.003
- Chandrangsu, P., Dusi, R., Hamilton, C. J., and Helmann, J. D. (2014). Methylglyoxal resistance in *Bacillus subtilis*: contributions of bacillithiol-dependent and independent pathways. *Mol. Microbiol.* 91, 706–715. doi: 10.1111/mmi.12489
- Chardonnet, S., Sakr, S., Cassier-Chauvat, C., Le Marechal, P., Chauvat, F., Lemaire, S. D., et al. (2015). First proteomic study of S-glutathionylation in cyanobacteria. *J. Proteome Res.* 14, 59–71. doi: 10.1021/pr500625a
- Chen, N. H., Counago, R. M., Djoko, K. Y., Jennings, M. P., Apicella, M. A., Kobe, B., et al. (2013). A glutathione-dependent detoxification system is required for formaldehyde resistance and optimal survival of *Neisseria meningitidis* in biofilms. *Antioxid. Redox Signal.* 18, 743–755. doi: 10.1089/ars.2012.4749
- Chi, B. K., Busche, T., Van Laer, K., Basell, K., Becher, D., Clermont, L., et al. (2014). Protein S-mycothiolation functions as redox-switch and thiol protection mechanism in *Corynebacterium glutamicum* under hypochlorite stress. *Antioxid. Redox Signal.* 20, 589–605. doi: 10.1089/ars.2013.5423
- Chi, B. K., Gronau, K., Mader, U., Hessling, B., Becher, D., and Antelmann, H. (2011). S-bacillithiolation protects against hypochlorite stress in *Bacillus subtilis* as revealed by transcriptomics and redox proteomics. *Mol. Cell. Proteomics* 10, M111.009506. doi: 10.1074/mcp.M111.009506
- Chi, B. K., Roberts, A. A., Huyen, T. T., Basell, K., Becher, D., Albrecht, D., et al. (2013). S-bacillithiolation protects conserved and essential proteins against hypochlorite stress in firmicutes bacteria. *Antioxid. Redox Signal.* 18, 1273–1295. doi: 10.1089/ars.2012.4686
- Chiang, B. Y., Chou, C. C., Hsieh, F. T., Gao, S., Lin, J. C., Lin, S. H., et al. (2012). In vivo tagging and characterization of S-glutathionylated proteins by a chemoenzymatic method. *Angew. Chem. Int. Ed Engl.* 51, 5871–5875. doi: 10.1002/anie.201200321
- Dalle-Donne, I., Rossi, R., Colombo, G., Giustarini, D., and Milzani, A. (2009). Protein S-glutathionylation: a regulatory device from bacteria to humans. *Trends Biochem. Sci.* 34, 85–96. doi: 10.1016/j.tibs.2008.11.002

- Dalle-Donne, I., Rossi, R., Giustarini, D., Colombo, R., and Milzani, A. (2007). S-glutathionylation in protein redox regulation. *Free Radic. Biol. Med.* 43, 883–898. doi: 10.1016/j.freeradbiomed.2007.06.014
- Davies, M. J. (2011). Myeloperoxidase-derived oxidation: mechanisms of biological damage and its prevention. *J. Clin. Biochem. Nutr.* 48, 8–19. doi: 10.3164/jcbn.11-006FR
- De Mendoza, D. (2014). Temperature sensing by membranes. *Annu. Rev. Microbiol.* 68, 101–116. doi: 10.1146/annurev-micro-091313-103612
- Derewenda, U., Boczek, T., Gorres, K. L., Yu, M., Hung, L. W., Cooper, D., et al. (2009). Structure and function of *Bacillus subtilis* YphP, a prokaryotic disulfide isomerase with a CXC catalytic motif. *Biochemistry* 48, 8664–8671. doi: 10.1021/bi900437z
- Ehira, S., Teramoto, H., Inui, M., and Yukawa, H. (2009). Regulation of *Corynebacterium glutamicum* heat shock response by the extracytoplasmic-function sigma factor SigH and transcriptional regulators HspR and HrcA. *J. Bacteriol.* 191, 2964–2972. doi: 10.1128/JB.00112-09
- Fahey, R. C. (2013). Glutathione analogs in prokaryotes. *Biochim. Biophys. Acta* 1830, 3182–3198. doi: 10.1016/j.bbagen.2012.10.006
- Fang, Z., Roberts, A. A., Weidman, K., Sharma, S. V., Claiborne, A., Hamilton, C. J., et al. (2013). Cross functionalities of *Bacillus deacetylases* involved in bacillithiol biosynthesis and bacillithiol-S-conjugate detoxification pathways. *Biochem. J.* doi: 10.1042/BJ20130415
- Farrand, S. K., and Taber, H. W. (1974). Changes in menaquinone concentration during growth and early sporulation in *Bacillus subtilis*. *J. Bacteriol.* 117, 324–326.
- Feng, J., Che, Y., Milse, J., Yin, Y. J., Liu, L., Ruckert, C., et al. (2006). The gene ncgl2918 encodes a novel maleylpyruvate isomerase that needs mycothiol as cofactor and links mycothiol biosynthesis and gentisate assimilation in *Corynebacterium glutamicum*. *J. Biol. Chem.* 281, 10778–10785. doi: 10.1074/jbc.M513192200
- Ferguson, G. P., Totemeyer, S., Maclean, M. J., and Booth, I. R. (1998). Methylglyoxal production in bacteria: suicide or survival? *Arch. Microbiol.* 170, 209–218.
- Fernandes, A. P., and Holmgren, A. (2004). Glutaredoxins: glutathione-dependent redox enzymes with functions far beyond a simple thioredoxin backup system. *Antioxid. Redox Signal.* 6, 63–74. doi: 10.1089/152308604771978354
- Forman, H. J., and Torres, M. (2001). Redox signaling in macrophages. *Mol. Aspects Med.* 22, 189–216. doi: 10.1016/S0098-2997(01)00010-3
- Fratelli, M., Demol, H., Puype, M., Casagrande, S., Eberini, I., Salmons, M., et al. (2002). Identification by redox proteomics of glutathionylated proteins in oxidatively stressed human T lymphocytes. *Proc. Natl. Acad. Sci. U.S.A.* 99, 3505–3510. doi: 10.1073/pnas.052592699
- Fratelli, M., Demol, H., Puype, M., Casagrande, S., Villa, P., Eberini, I., et al. (2003). Identification of proteins undergoing glutathionylation in oxidatively stressed hepatocytes and hepatoma cells. *Proteomics* 3, 1154–1161. doi: 10.1002/pmic.200300436
- Fratelli, M., Gianazza, E., and Ghezzi, P. (2004). Redox proteomics: identification and functional role of glutathionylated proteins. *Expert Rev. Proteomics* 1, 365–376. doi: 10.1586/14789450.1.3.365
- Freitag, N. E., Port, G. C., and Miner, M. D. (2009). *Listeria monocytogenes* – from saprophyte to intracellular pathogen. *Nat. Rev. Microbiol.* 7, 623–628. doi: 10.1038/nrmicro2171
- Fuangthong, M., Atichartpongkul, S., Mongkolsuk, S., and Helmann, J. D. (2001). OhrR is a repressor of ohrA, a key organic hydroperoxide resistance determinant in *Bacillus subtilis*. *J. Bacteriol.* 183, 4134–4141. doi: 10.1128/JB.183.14.4134-4141.2001
- Gaballa, A., Antelmann, H., Hamilton, C. J., and Helmann, J. D. (2013). Regulation of *Bacillus subtilis* bacillithiol biosynthesis operons by SpX. *Microbiology* 159, 2025–2035. doi: 10.1099/mic.0.070482-0
- Gaballa, A., Chi, B. K., Roberts, A. A., Becher, D., Hamilton, C. J., Antelmann, H., et al. (2014). Redox regulation in *Bacillus subtilis*: the bacilliredoxins BrxA(YphP) and BrxB(YqiW) function in de-bacillithiolation of S-bacillithiolated OhrR and MetE. *Antioxid. Redox Signal.* 21, 357–367. doi: 10.1089/ars.2013.5327
- Gaballa, A., Newton, G. L., Antelmann, H., Parsonage, D., Upton, H., Rawat, M., et al. (2010). Biosynthesis and functions of bacillithiol, a major low-molecular-weight thiol in *Bacilli*. *Proc. Natl. Acad. Sci. U.S.A.* 107, 6482–6486. doi: 10.1073/pnas.1000928107
- Gallooly, M. M., and Mieyal, J. J. (2007). Mechanisms of reversible protein glutathionylation in redox signaling and oxidative stress. *Curr. Opin. Pharmacol.* 7, 381–391. doi: 10.1016/j.coph.2007.06.003
- Ghezzi, P. (2005). Regulation of protein function by glutathionylation. *Free Radic. Res.* 39, 573–580. doi: 10.1080/10715760500072172
- Ghezzi, P. (2013). Protein glutathionylation in health and disease. *Biochim. Biophys. Acta* 1830, 3165–3172. doi: 10.1016/j.bbagen.2013.02.009
- Gopal, S., Borovok, I., Ofer, A., Yanku, M., Cohen, G., Goebel, W., et al. (2005). A multidomain fusion protein in *Listeria monocytogenes* catalyzes the two primary activities for glutathione biosynthesis. *J. Bacteriol.* 187, 3839–3847. doi: 10.1128/JB.187.11.3839-3847.2005
- Gray, M. J., Wholey, W. Y., and Jakob, U. (2013a). Bacterial responses to reactive chlorine species. *Annu. Rev. Microbiol.* 67, 141–160. doi: 10.1146/annurev-micro-102912-142520
- Gray, M. J., Wholey, W. Y., Parker, B. W., Kim, M., and Jakob, U. (2013b). NemR is a bleach-sensing transcription factor. *J. Biol. Chem.* 288, 13789–13798. doi: 10.1074/jbc.M113.454421
- Gupta, V., and Carroll, K. S. (2014). Sulfenic acid chemistry, detection and cellular lifetime. *Biochim. Biophys. Acta* 1840, 847–875. doi: 10.1016/j.bbagen.2013.05.040
- Handtke, S., Schroeter, R., Jurgen, B., Methling, K., Schluter, R., Albrecht, D., et al. (2014). *Bacillus pumilus* reveals a remarkably high resistance to hydrogen peroxide provoked oxidative stress. *PLoS ONE* 9:e85625. doi: 10.1371/journal.pone.0085625
- Hawkins, C. L., Pattison, D. I., and Davies, M. J. (2003). Hypochlorite-induced oxidation of amino acids, peptides and proteins. *Amino Acids* 25, 259–274. doi: 10.1007/s00726-003-0016-x
- Helmann, J. D. (2011). Bacillithiol, a new player in bacterial redox homeostasis. *Antioxid. Redox Signal.* 15, 123–133. doi: 10.1089/ars.2010.3562
- Holmgren, A. (1976). Hydrogen donor system for *Escherichia coli* ribonucleoside-diphosphate reductase dependent upon glutathione. *Proc. Natl. Acad. Sci. U.S.A.* 73, 2275–2279. doi: 10.1073/pnas.73.7.2275
- Holmgren, A. (1981). Regulation of ribonucleotide reductase. *Curr. Top. Cell. Regul.* 19, 47–76. doi: 10.1016/B978-0-12-152819-5.50019-1
- Hondorp, E. R., and Matthews, R. G. (2004). Oxidative stress inactivates cobalamin-independent methionine synthase (MetE) in *Escherichia coli*. *PLoS Biol.* 2:e336. doi: 10.1371/journal.pbio.0020336
- Hou, X., Peng, W., Xiong, L., Huang, C., Chen, X., and Zhang, W. (2013). Engineering *Clostridium acetobutylicum* for alcohol production. *J. Biotechnol.* 166, 25–33. doi: 10.1016/j.jbiotec.2013.04.013
- Hugo, M., Turell, L., Manta, B., Botti, H., Monteiro, G., Netto, L. E., et al. (2009). Thiol and sulfenic acid oxidation of AhpE, the one-cysteine peroxiredoxin from *Mycobacterium tuberculosis*: kinetics, acidity constants, and conformational dynamics. *Biochemistry* 48, 9416–9426. doi: 10.1021/bi901221s
- Hugo, M., Van Laer, K., Reyes, A. M., Vertommen, D., Messens, J., Radi, R., et al. (2014). Mycothiol/mycoredoxin 1-dependent reduction of the peroxiredoxin AhpE from *Mycobacterium tuberculosis*. *J. Biol. Chem.* 289, 5228–5239. doi: 10.1074/jbc.M113.510248
- Hwang, C., Lodish, H. F., and Sinskey, A. J. (1995). Measurement of glutathione redox state in cytosol and secretory pathway of cultured cells. *Meth. Enzymol.* 251, 212–221. doi: 10.1016/0076-6879(95)51123-7
- Imlay, J. A. (2003). Pathways of oxidative damage. *Annu. Rev. Microbiol.* 57, 395–418. doi: 10.1146/annurev-micro.57.030502.090938
- Imlay, J. A. (2008). Cellular defenses against superoxide and hydrogen peroxide. *Annu. Rev. Biochem.* 77, 755–776. doi: 10.1146/annurev.biochem.77.061606.161055
- Imlay, J. A. (2013). The molecular mechanisms and physiological consequences of oxidative stress: lessons from a model bacterium. *Nat. Rev. Microbiol.* 11, 443–454. doi: 10.1038/nrmicro3032
- Inaba, K. (2009). Disulfide bond formation system in *Escherichia coli*. *J. Biochem.* 146, 591–597. doi: 10.1093/jb/mvp102
- Jacobs, A. T., and Marnett, L. J. (2010). Systems analysis of protein modification and cellular responses induced by electrophile stress. *Acc. Chem. Res.* 43, 673–683. doi: 10.1021/ar900286y
- Janowiak, B. E., and Griffith, O. W. (2005). Glutathione synthesis in *Streptococcus agalactiae*. One protein accounts for gamma-glutamylcysteine synthetase and glutathione synthetase activities. *J. Biol. Chem.* 280, 11829–11839. doi: 10.1074/jbc.M414326200

- Jothivasan, V. K., and Hamilton, C. J. (2008). Mycothiol: synthesis, biosynthesis and biological functions of the major low molecular weight thiol in actinomycetes. *Nat. Prod. Rep.* 25, 1091–1117. doi: 10.1039/b616489g
- Kalapos, M. P. (2008). The tandem of free radicals and methylglyoxal. *Chem. Biol. Interact.* 171, 251–271. doi: 10.1016/j.cbi.2007.11.009
- Kehr, S., Jortzik, E., Delahunty, C., Yates, J. R. III, Rahlfs, S., and Becker, K. (2011). Protein S-glutathionylation in malaria parasites. *Antioxid. Redox Signal.* 15, 2855–2865. doi: 10.1089/ars.2011.4029
- Kim, M. S., Dufour, Y. S., Yoo, J. S., Cho, Y. B., Park, J. H., Nam, G. B., et al. (2012). Conservation of thiol-oxidative stress responses regulated by SigR orthologues in actinomycetes. *Mol. Microbiol.* 85, 326–344. doi: 10.1111/j.1365-2958.2012.08115.x
- Kim, S. O., Merchant, K., Nudelman, R., Beyer, W. F. Jr., Keng, T., Deangelo, J., et al. (2002). OxyR: a molecular code for redox-related signaling. *Cell* 109, 383–396. doi: 10.1016/S0092-8674(02)00723-7
- Klatt, P., and Lamas, S. (2000). Regulation of protein function by S-glutathiolation in response to oxidative and nitrosative stress. *Eur. J. Biochem.* 267, 4928–4944. doi: 10.1046/j.1432-1327.2000.01601.x
- Lamers, A. P., Keithly, M. E., Kim, K., Cook, P. D., Stec, D. F., Hines, K. M., et al. (2012). Synthesis of bacillithiol and the catalytic selectivity of FosB-type fosfomycin resistance proteins. *Org. Lett.* 14, 5207–5209. doi: 10.1021/ol302327t
- Lee, C., Shin, J., and Park, C. (2013). Novel regulatory system nemRA-gloA for electrophile reduction in *Escherichia coli* K-12. *Mol. Microbiol.* 88, 395–412. doi: 10.1111/mmi.12192
- Lee, J. W., Soonsanga, S., and Helmann, J. D. (2007). A complex thiolate switch regulates the *Bacillus subtilis* organic peroxide sensor OhrR. *Proc. Natl. Acad. Sci. U.S.A.* 104, 8743–8748. doi: 10.1073/pnas.0702081104
- Leichert, L. I., Gehrke, F., Gudiseva, H. V., Blackwell, T., Ilbert, M., Walker, A. K., et al. (2008). Quantifying changes in the thiol redox proteome upon oxidative stress *in vivo*. *Proc. Natl. Acad. Sci. U.S.A.* 105, 8197–8202. doi: 10.1073/pnas.0707723105
- Leonard, S. E., and Carroll, K. S. (2011). Chemical 'omics' approaches for understanding protein cysteine oxidation in biology. *Curr. Opin. Chem. Biol.* 15, 88–102. doi: 10.1016/j.cbpa.2010.11.012
- Lessmeier, L., Hoefener, M., and Wendisch, V. F. (2013). Formaldehyde degradation in *Corynebacterium glutamicum* involves acetaldehyde dehydrogenase and mycothiol-dependent formaldehyde dehydrogenase. *Microbiology* 159, 2651–2662. doi: 10.1099/mic.0.072413-0
- Liebeke, M., Pother, D. C., Van Duy, N., Albrecht, D., Becher, D., Hochgrafe, F., et al. (2008). Depletion of thiol-containing proteins in response to quinones in *Bacillus subtilis*. *Mol. Microbiol.* 69, 1513–1529. doi: 10.1111/j.1365-2958.2008.06382.x
- Lillig, C. H., Berndt, C., and Holmgren, A. (2008). Glutaredoxin systems. *Biochim. Biophys. Acta* 1780, 1304–1317. doi: 10.1016/j.bbagen.2008.06.003
- Lillig, C. H., Potamitou, A., Schwenn, J. D., Vlamis-Gardikas, A., and Holmgren, A. (2003). Redox regulation of 3'-phosphoadenylylsulfate reductase from *Escherichia coli* by glutathione and glutaredoxins. *J. Biol. Chem.* 278, 22325–22330. doi: 10.1074/jbc.M302304200
- Lin, J. C., Chiang, B. Y., Chou, C. C., Chen, T. C., Chen, Y. J., and Lin, C. H. (2015). Glutathionylspermidine in the modification of protein SH groups: the enzymology and its application to study protein glutathionylation. *Molecules* 20, 1452–1474. doi: 10.3390/molecules20011452
- Lind, C., Gerdes, R., Hammell, Y., Schuppe-Koistinen, I., Von Lowenhillem, H. B., Holmgren, A., et al. (2002). Identification of S-glutathionylated cellular proteins during oxidative stress and constitutive metabolism by affinity purification and proteomic analysis. *Arch. Biochem. Biophys.* 406, 229–240. doi: 10.1016/S0003-9861(02)00468-X
- Liu, Y. B., Chen, C., Chaudhry, M. T., Si, M. R., Zhang, L., Wang, Y., et al. (2014). Enhancing *Corynebacterium glutamicum* robustness by over-expressing a gene, mshA, for mycothiol glycosyltransferase. *Biotechnol. Lett.* 36, 1453–1459. doi: 10.1007/s10529-014-1501-x
- Liu, Y. B., Long, M. X., Yin, Y. J., Si, M. R., Zhang, L., Lu, Z. Q., et al. (2013). Physiological roles of mycothiol in detoxification and tolerance to multiple poisonous chemicals in *Corynebacterium glutamicum*. *Arch. Microbiol.* 195, 419–429. doi: 10.1007/s00203-013-0889-3
- Lowther, W. T., and Haynes, A. C. (2011). Reduction of cysteine sulfinic acid in eukaryotic, typical 2-Cys peroxiredoxins by sulfiredoxin. *Antioxid. Redox Signal.* 15, 99–109. doi: 10.1089/ars.2010.3564
- Ma, Z., Chandransu, P., Helmann, T. C., Romsang, A., Gaballa, A., and Helmann, J. D. (2014). Bacillithiol is a major buffer of the labile zinc pool in *Bacillus subtilis*. *Mol. Microbiol.* 94, 756–770. doi: 10.1111/mmi.12794
- Mackay, C. E., and Knock, G. A. (2015). Control of vascular smooth muscle function by Src-family kinases and reactive oxygen species in health and disease. *J. Physiol. (Lond)*. doi: 10.1113/jphysiol.2014.285304
- Marnett, L. J., Riggins, J. N., and West, J. D. (2003). Endogenous generation of reactive oxidants and electrophiles and their reactions with DNA and protein. *J. Clin. Invest.* 111, 583–593. doi: 10.1172/JCI200318022
- Marteyn, B., Sakr, S., Farci, S., Bedhomme, M., Chardonnet, S., Decottignies, P., et al. (2013). The *Synechocystis* PCC6803 MeraA-like enzyme operates in the reduction of both mercury and uranium under the control of the glutaredoxin 1 enzyme. *J. Bacteriol.* 195, 4138–4145. doi: 10.1128/JB.00272-13
- Masip, L., Veeravalli, K., and Georgiou, G. (2006). The many faces of glutathione in bacteria. *Antioxid. Redox Signal.* 8, 753–762. doi: 10.1089/ars.2006.8.753
- Meister, A. (1995). Glutathione biosynthesis and its inhibition. *Meth. Enzymol.* 252, 26–30. doi: 10.1016/0076-6879(95)52005-8
- Mieyal, J. J., and Chock, P. B. (2012). Posttranslational modification of cysteine in redox signaling and oxidative stress: focus on S-glutathionylation. *Antioxid. Redox Signal.* 16, 471–475. doi: 10.1089/ars.2011.4454
- Mieyal, J. J., Gallogly, M. M., Qanungo, S., Sabens, E. A., and Shelton, M. D. (2008). Molecular mechanisms and clinical implications of reversible protein S-glutathionylation. *Antioxid. Redox Signal.* 10, 1941–1988. doi: 10.1089/ars.2008.2089
- Mishra, S., and Imlay, J. (2012). Why do bacteria use so many enzymes to scavenge hydrogen peroxide? *Arch. Biochem. Biophys.* 525, 145–160. doi: 10.1016/j.abb.2012.04.014
- Newton, G. L., Arnold, K., Price, M. S., Sherrill, C., Delcardayre, S. B., Aharonowitz, Y., et al. (1996). Distribution of thiols in microorganisms: mycothiol is a major thiol in most actinomycetes. *J. Bacteriol.* 178, 1990–1995.
- Newton, G. L., Buchmeier, N., and Fahey, R. C. (2008). Biosynthesis and functions of mycothiol, the unique protective thiol of Actinobacteria. *Microbiol. Mol. Biol. Rev.* 72, 471–494. doi: 10.1128/MMBR.00008-08
- Newton, G. L., and Fahey, R. C. (2008). Regulation of mycothiol metabolism by sigma(R) and the thiol redox sensor anti-sigma factor RsrA. *Mol. Microbiol.* 68, 805–809. doi: 10.1111/j.1365-2958.2008.06222.x
- Newton, G. L., Fahey, R. C., and Rawat, M. (2012). Detoxification of toxins by bacillithiol in *Staphylococcus aureus*. *Microbiology* 158, 1117–1126. doi: 10.1099/mic.0.055715-0
- Newton, G. L., Leung, S. S., Wakabayashi, J. I., Rawat, M., and Fahey, R. C. (2011). The DinB superfamily includes novel mycothiol, bacillithiol, and glutathione S-transferases. *Biochemistry* 50, 10751–10760. doi: 10.1021/bi201460j
- Newton, G. L., Rawat, M., La Clair, J. J., Jothivasan, V. K., Budiarto, T., Hamilton, C. J., et al. (2009). Bacillithiol is an antioxidant thiol produced in Bacilli. *Nat. Chem. Biol.* 5, 625–627. doi: 10.1038/nchembio.189
- Nilewar, S. S., and Kathiravan, M. K. (2014). Mycothiol: a promising antitubercular target. *Bioorg. Chem.* 52, 62–68. doi: 10.1016/j.bioorg.2013.11.004
- Ordonez, E., Van Belle, K., Roos, G., De Galan, S., Letek, M., Gil, J. A., et al. (2009). Arsenate reductase, mycothiol, and mycoredoxin concert thiol/disulfide exchange. *J. Biol. Chem.* 284, 15107–15116. doi: 10.1074/jbc.M900877200
- Ozyamak, E., De Almeida, C., De Moura, A. P., Miller, S., and Booth, I. R. (2013). Integrated stress response of *Escherichia coli* to methylglyoxal: transcriptional readthrough from the nemRA operon enhances protection through increased expression of glyoxalase I. *Mol. Microbiol.* 88, 936–950. doi: 10.1111/mmi.12234
- Pan, J., and Carroll, K. S. (2013). Persulfide reactivity in the detection of protein S-sulfhydration. *ACS Chem. Biol.* 8, 1110–1116. doi: 10.1021/cb4001052
- Park, J. H., and Roe, J. H. (2008). Mycothiol regulates and is regulated by a thiol-specific antisigma factor RsrA and sigma(R) in *Streptomyces coelicolor*. *Mol. Microbiol.* 68, 861–870. doi: 10.1111/j.1365-2958.2008.06191.x
- Parsonage, D., Newton, G. L., Holder, R. C., Wallace, B. D., Paige, C., Hamilton, C. J., et al. (2010). Characterization of the N-acetyl-alpha-D-glucosaminyl 1-malate synthase and deacetylase functions for bacillithiol biosynthesis in *Bacillus anthracis*. *Biochemistry* 49, 8398–8414. doi: 10.1021/bi100698n
- Paulsen, C. E., and Carroll, K. S. (2013). Cysteine-mediated redox signaling: chemistry, biology, and tools for discovery. *Chem. Rev.* 113, 4633–4679. doi: 10.1021/cr300163e
- Peralta, D., Bronowska, A. K., Morgan, B., Doka, E., Van Laer, K., Nagy, P., et al. (2015). A proton relay enhances H2O2 sensitivity of GAPDH to facilitate

- metabolic adaptation. *Nat. Chem. Biol.* 11, 156–163. doi: 10.1038/nchem-bio.1720
- Perera, V. R., Newton, G. L., Parnell, J. M., Komives, E. A., and Pogliano, K. (2014). Purification and characterization of the *Staphylococcus aureus* bacillithiol transferase BstA. *Biochim. Biophys. Acta* 1840, 2851–2861. doi: 10.1016/j.bbagen.2014.05.001
- Posada, A. C., Kolar, S. L., Dusi, R. G., Francois, P., Roberts, A. A., Hamilton, C. J., et al. (2014). Importance of bacillithiol in the oxidative stress response of *Staphylococcus aureus*. *Infect. Immun.* 82, 316–332. doi: 10.1128/IAI.01074-13
- Pöther, D. C., Gierok, P., Harms, M., Mostertz, J., Hochgrafe, F., Antelmann, H., et al. (2013). Distribution and infection-related functions of bacillithiol in *Staphylococcus aureus*. *Int. J. Med. Microbiol.* 303, 114–123. doi: 10.1016/j.ijmm.2013.01.003
- Potter, A. J., Trappetti, C., and Paton, J. C. (2012). *Streptococcus pneumoniae* uses glutathione to defend against oxidative stress and metal ion toxicity. *J. Bacteriol.* 194, 6248–6254. doi: 10.1128/JB.01393-12
- Rajkarnikar, A., Strankman, A., Duran, S., Vargas, D., Roberts, A. A., Barretto, K., et al. (2013). Analysis of mutants disrupted in bacillithiol metabolism in *Staphylococcus aureus*. *Biochem. Biophys. Res. Commun.* 436, 128–133. doi: 10.1016/j.bbrc.2013.04.027
- Ratasuk, N., and Nanny, M. A. (2007). Characterization and quantification of reversible redox sites in humic substances. *Environ. Sci. Technol.* 41, 7844–7850. doi: 10.1021/es071389u
- Rawat, M., Johnson, C., Cadiz, V., and Av-Gay, Y. (2007). Comparative analysis of mutants in the mycothiol biosynthesis pathway in *Mycobacterium smegmatis*. *Biochem. Biophys. Res. Commun.* 363, 71–76. doi: 10.1016/j.bbrc.2007.08.142
- Reniere, M. L., Whiteley, A. T., Hamilton, K. L., John, S. M., Lauer, P., Brennan, R. G., et al. (2015). Glutathione activates virulence gene expression of an intracellular pathogen. *Nature* 517, 170–173. doi: 10.1038/nature14029
- Reyes, A. M., Hugo, M., Trostchansky, A., Capece, L., Radi, R., and Trujillo, M. (2011). Oxidizing substrate specificity of *Mycobacterium tuberculosis* alkyl hydroperoxide reductase E: kinetics and mechanisms of oxidation and overoxidation. *Free Radic. Biol. Med.* 51, 464–473. doi: 10.1016/j.freeradbiomed.2011.04.023
- Roberts, A. A., Sharma, S. V., Strankman, A. W., Duran, S. R., Rawat, M., and Hamilton, C. J. (2013). Mechanistic studies of FosB: a divalent-metal-dependent bacillithiol-S-transferase that mediates fosfomycin resistance in *Staphylococcus aureus*. *Biochem. J.* 451, 69–79. doi: 10.1042/BJ20121541
- Rochat, T., Nicolas, P., Delumeau, O., Rabatnova, A., Korelusova, J., Leduc, A., et al. (2012). Genome-wide identification of genes directly regulated by the pleiotropic transcription factor Spx in *Bacillus subtilis*. *Nucleic Acids Res.* 40, 9571–9583. doi: 10.1093/nar/gks755
- Ruane, K. M., Davies, G. J., and Martinez-Fleites, C. (2008). Crystal structure of a family GT4 glycosyltransferase from *Bacillus anthracis* ORF BA1558. *Proteins* 73, 784–787. doi: 10.1002/prot.22171
- Rudolph, T. K., and Freeman, B. A. (2009). Transduction of redox signaling by electrophile-protein reactions. *Sci Signal* 2:re7. doi: 10.1126/scisignal.290re7
- Sareen, D., Newton, G. L., Fahey, R. C., and Buchmeier, N. A. (2003). Mycothiol is essential for growth of *Mycobacterium tuberculosis* Erdman. *J. Bacteriol.* 185, 6736–6740. doi: 10.1128/JB.185.22.6736-6740.2003
- Sassetti, C. M., and Rubin, E. J. (2003). Genetic requirements for mycobacterial survival during infection. *Proc. Natl. Acad. Sci. U.S.A.* 100, 12989–12994. doi: 10.1073/pnas.2134250100
- Sharma, S. V., Arbach, M., Roberts, A. A., Macdonald, C. J., Groom, M., and Hamilton, C. J. (2013). Biophysical features of bacillithiol, the glutathione surrogate of *Bacillus subtilis* and other firmicutes. *Chembiochem* 14, 2160–2168. doi: 10.1002/cbic.201300404
- Song, M., Husain, M., Jones-Carson, J., Liu, L., Henard, C. A., and Vazquez-Torres, A. (2013). Low-molecular-weight thiol-dependent antioxidant and antinutrosative defences in *Salmonella pathogenesis*. *Mol. Microbiol.* 87, 609–622. doi: 10.1111/mmi.12119
- Ta, P., Buchmeier, N., Newton, G. L., Rawat, M., and Fahey, R. C. (2011). Organic hydroperoxide resistance protein and ergothioneine compensate for loss of mycothiol in *Mycobacterium smegmatis* mutants. *J. Bacteriol.* 193, 1981–1990. doi: 10.1128/JB.01402-10
- Thompson, M. K., Keithly, M. E., Goodman, M. C., Hammer, N. D., Cook, P. D., Jagessar, K. L., et al. (2014). Structure and function of the genomically encoded fosfomycin resistance enzyme, FosB, from *Staphylococcus aureus*. *Biochemistry* 53, 755–765. doi: 10.1021/bi4015852
- Thompson, M. K., Keithly, M. E., Harp, J., Cook, P. D., Jagessar, K. L., Sulikowski, G. A., et al. (2013). Structural and chemical aspects of resistance to the antibiotic fosfomycin conferred by FosB from *Bacillus cereus*. *Biochemistry* 52, 7350–7362. doi: 10.1021/bi4009648
- Van Laer, K., Buts, L., Foloppe, N., Vertommen, D., Van Belle, K., Wahni, K., et al. (2012). Mycoredoxin-1 is one of the missing links in the oxidative stress defence mechanism of Mycobacteria. *Mol. Microbiol.* 86, 787–804. doi: 10.1111/mmi.12030
- Van Laer, K., Hamilton, C. J., and Messens, J. (2013). Low-molecular-weight thiols in thiol-disulfide exchange. *Antioxid. Redox Signal.* 18, 1642–1653. doi: 10.1089/ars.2012.4964
- Vanduinen, A. J., Winchell, K. R., Keithly, M. E., and Cook, P. D. (2015). X-ray crystallographic structure of BshC, a unique enzyme involved in bacillithiol biosynthesis. *Biochemistry* 54, 100–103. doi: 10.1021/bi501394q
- Vergauwen, B., Elegheert, J., Dansercoer, A., Devreese, B., and Savvides, S. N. (2010). Glutathione import in *Haemophilus influenzae* Rd is primed by the periplasmic heme-binding protein HbpA. *Proc. Natl. Acad. Sci. U.S.A.* 107, 13270–13275. doi: 10.1073/pnas.1005198107
- Vergauwen, B., Verstraete, K., Senadheera, D. B., Dansercoer, A., Cvitkovitch, D. G., Guedon, E., et al. (2013). Molecular and structural basis of glutathione import in Gram-positive bacteria via GshT and the cystine ABC importer TcyBC of *Streptococcus mutans*. *Mol. Microbiol.* 89, 288–303. doi: 10.1111/mmi.12274
- Villadangos, A. F., Van Belle, K., Wahni, K., Dufe, V. T., Freitas, S., Nur, H., et al. (2011). *Corynebacterium glutamicum* survives arsenic stress with arsenate reductases coupled to two distinct redox mechanisms. *Mol. Microbiol.* 82, 998–1014. doi: 10.1111/j.1365-2958.2011.07882.x
- Wang, C., Weerapana, E., Blewett, M. M., and Cravatt, B. F. (2014). A chemoproteomic platform to quantitatively map targets of lipid-derived electrophiles. *Nat. Methods* 11, 79–85. doi: 10.1038/nmeth.2759
- Winterbourn, C. C., and Kettle, A. J. (2013). Redox reactions and microbial killing in the neutrophil phagosome. *Antioxid. Redox Signal.* 18, 642–660. doi: 10.1089/ars.2012.4827
- Witthoff, S., Muhlroth, A., Marienhagen, J., and Bott, M. (2013). C1 metabolism in *Corynebacterium glutamicum*: an endogenous pathway for oxidation of methanol to carbon dioxide. *Appl. Environ. Microbiol.* 79, 6974–6983. doi: 10.1128/AEM.02705-13
- Zaffagnini, M., Bedhomme, M., Groni, H., Marchand, C. H., Puppo, C., Gontero, B., et al. (2012a). Glutathionylation in the photosynthetic model organism *Chlamydomonas reinhardtii*: a proteomic survey. *Mol. Cell. Proteomics* 11:M111.014142. doi: 10.1074/mcp.M111.014142
- Zaffagnini, M., Bedhomme, M., Lemaire, S. D., and Trost, P. (2012b). The emerging roles of protein glutathionylation in chloroplasts. *Plant Sci.* 185–186, 86–96. doi: 10.1016/j.plantsci.2012.01.005
- Zhang, D., Macinkovic, I., Devarie-Baez, N. O., Pan, J., Park, C. M., Carroll, K. S., et al. (2014). Detection of protein S-sulphydration by a tag-switch technique. *Angew. Chem. Int. Ed Engl.* 53, 575–581. doi: 10.1002/anie.201305876
- Zhao, Q., Wang, M., Xu, D., Zhang, Q., and Liu, W. (2015). Metabolic coupling of two small-molecule thiols programs the biosynthesis of lincomycin A. *Nature* 518, 115–119. doi: 10.1038/nature14137
- Zuber, P. (2004). Spx-RNA polymerase interaction and global transcriptional control during oxidative stress. *J. Bacteriol.* 186, 1911–1918. doi: 10.1128/JB.186.7.1911-1918.2004
- Zuber, P. (2009). Management of oxidative stress in *Bacillus*. *Annu. Rev. Microbiol.* 63, 575–597. doi: 10.1146/annurev.micro.091208.073241

Conflict of Interest Statement: The authors declare that the research was conducted in the absence of any commercial or financial relationships that could be construed as a potential conflict of interest.

Copyright © 2015 Loi, Rossius and Antelmann. This is an open-access article distributed under the terms of the Creative Commons Attribution License (CC BY). The use, distribution or reproduction in other forums is permitted, provided the original author(s) or licensor are credited and that the original publication in this journal is cited, in accordance with accepted academic practice. No use, distribution or reproduction is permitted which does not comply with these terms.



Identification of essential amino acid residues in the nisin dehydratase NisB

Rustem Khusainov^{1†}, Auke J. van Heel¹, Jacek Lubelski¹, Gert N. Moll² and Oscar P. Kuipers^{1,3*}

¹ Department of Molecular Genetics, Groningen Biomolecular Sciences and Biotechnology Institute, University of Groningen, Groningen, Netherlands

² LanthioPharma, Groningen, Netherlands

³ Kluyver Centre for Genomics of Industrial Fermentation, Groningen, Netherlands

Edited by:

Ivan Mijakovic, Chalmers University of Technology, Sweden

Reviewed by:

George-John Nychas, Agricultural University of Athens, Greece
Thomas Hindré, University J. Fourier, France

*Correspondence:

Oscar P. Kuipers, Department of Molecular Genetics, Groningen Biomolecular Sciences and Biotechnology Institute, University of Groningen, Nijenborgh 7, 9747 AG, Groningen, Netherlands
e-mail: o.p.kuipers@rug.nl

† Present address:

Rustem Khusainov, Circassia Ltd., The Oxford Science Park, Oxford, UK

Nisin is a posttranslationally-modified antimicrobial peptide that has the ability to induce its own biosynthesis. Serines and threonines in the modifiable core peptide part of precursor nisin are dehydrated to dehydroalanines and dehydrobutyrines by the dehydratase NisB, and subsequently cysteines are coupled to the dehydroamino acids by the cyclase NisC. In this study, we applied extensive site-directed mutagenesis, together with direct binding studies, to investigate the molecular mechanism of the dehydratase NisB. We use a natural nisin-producing strain as a host to probe mutant-NisB functionality. Importantly, we are able to differentiate between intracellular and secreted fully dehydrated precursor nisin, enabling investigation of the NisB properties needed for the release of dehydrated precursor nisin to its devoted secretion system NisT. We report that single amino acid substitutions of conserved residues, i.e., R83A, R83M, and R87A result in incomplete dehydration of precursor nisin and prevention of secretion. Single point NisB mutants Y80F and H961A, result in a complete lack of dehydration of precursor nisin, but do not abrogate precursor nisin binding. The data indicate that residues Y80 and H961 are directly involved in catalysis, fitting well with their position in the recently published 3D-structure of NisB. We confirm, by *in vivo* studies, results that were previously obtained from *in vitro* experiments and NisB structure elucidation and show that previous findings translate well to effects seen in the original production host.

Keywords: NisB, dehydratase, posttranslational modifications, mechanism, NisC, lanthionine, lantibiotics, nisin

INTRODUCTION

Lantibiotics are ribosomally synthesized polycyclic peptides. The rings contain post-translationally introduced thioether-bridged amino acids, so called lanthionines. The most studied lantibiotic, which has also found commercial application, is nisin. Nisin has been successfully used for over 50 years as a food preservative without significant resistance development in food pathogens (Gravesen et al., 2001; Kramer et al., 2008).

Precursor nisin is composed of a 23 amino acid leader peptide followed by a modifiable 34 amino acid core peptide part (Figure 1). The leader peptide is a recognition signal for the modification enzymes NisB and NisC (Xie et al., 2004; Mavaro et al., 2011; Khusainov et al., 2013a) and the transporter NisT (van der Meer et al., 1994). It furthermore keeps the fully modified precursor nisin inactive (Kuipers et al., 1993b; van der Meer et al., 1994). Nisin contains one lanthionine ring and four (methyl)lanthionine rings that are introduced enzymatically. Analysis of truncated nisin variants has shown that the presence of at least the three N-terminal rings ABC is necessary for nisin variants to exert some antimicrobial activity (Chan et al., 1996).

NisB is a dehydratase of about 117.5 kDa (Kuipers et al., 1993a). It is the first enzyme to come into play during the modification by dehydrating serines and threonines in the core peptide part of precursor nisin, to form dehydroalanines and

dehydrobutyrines, respectively (Figure 1). Moreover, *in vitro* activity studies have indicated a possible mechanism for the dehydration reaction, involving glutamylation of Ser and Thr residues (Garg et al., 2013). Recently the structure of NisB was solved implicating an un-expected cofactor namely glutamyl-tRNA^{Glu} (Ortega et al., 2015). This study gives insight in the mechanism of action of NisB and also revealed the location of its active sites, the glutamylation domain and the glutamate elimination domain. Dehydrated amino acids are coupled to cysteines by a second enzyme, NisC, in a regio- and stereospecific manner, to generate lanthionine rings (Figure 1). A model of the catalytic mechanism of NisC has been proposed based on *in vitro* studies and the crystal structure of NisC (Li and van der Donk, 2007).

Modified precursor nisin is transported via the dedicated ABC transporter NisT and the nisin leader peptide is extracellularly cleaved off by the protease NisP, liberating active nisin (Kuipers et al., 1993a). While nisin itself is renowned for its strong antimicrobial and autoinducer activity, the nisin modification enzymes have additional relevance because of their influence on the extent of modification. NisB, NisC, and NisT can also modify and transport peptides unrelated to nisin provided that the nisin leader peptide is present at the N-terminus (Kuipers et al., 2004; Kluskens et al., 2005; Rink et al., 2007; Majchrzykiewicz et al., 2010; van Heel et al., 2013). In this way lanthionines can

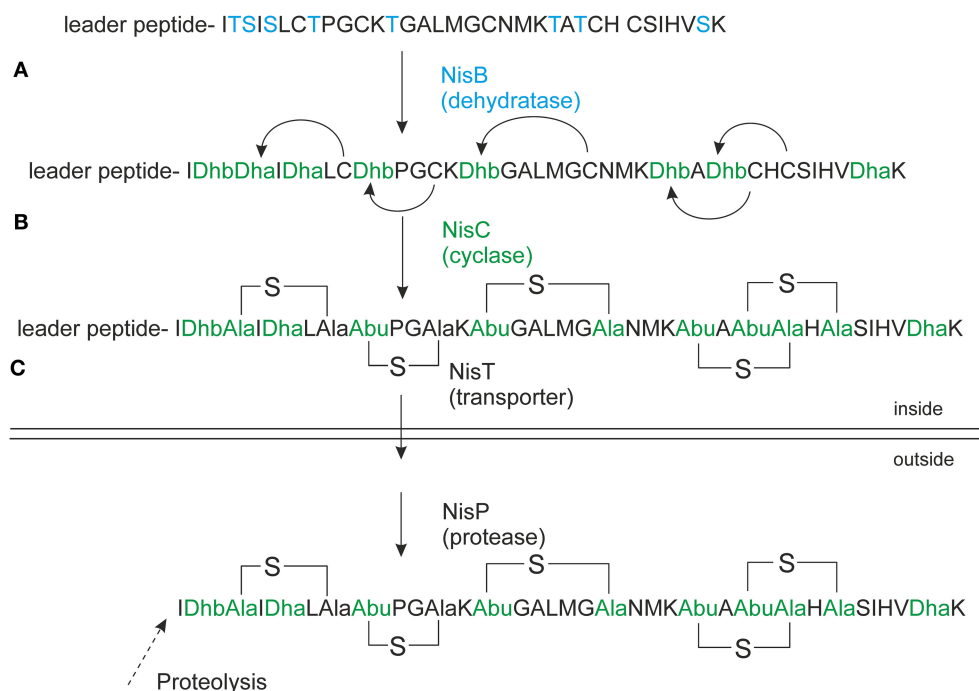


FIGURE 1 | Nisin biosynthesis. NisA is ribosomally synthesized in a form of precursor nisin. **(A)** NisB dehydrates underlined Ser/Thr's (in bold), the resulted dehydrated precursor nisin contains dehydroalanines (Dha) and dehydrobutyrines (Dhb); **(B)** NisC forms thioether bridges between dehydrated residues and cysteines resulting in fully modified precursor nisin.

(C) NisT transports the fully modified precursor nisin outside the cell. NisP cleaves off the nisin leader extracellularly to liberate active nisin. The Figure is in accordance with recent recommendations for a universal nomenclature for ribosomally synthesized and posttranslationally modified peptide natural products (Arnison et al., 2013).

be introduced into medically relevant peptides. By imposing a conformational constraint, the lanthionines confer resistance to breakdown by peptidases (Rink et al., 2010), enable in specific cases oral and pulmonary delivery (de Vries et al., 2010) and allow to select for peptides with optimal receptor interaction, thus strongly enhancing their therapeutic potential (Kluskens et al., 2005, 2009; van Heel et al., 2011). LanB enzymes do not share significant sequence homology to members of known protein families, thus representing a unique family of enzymes. Recent studies have shown that the process of dehydration by NisB and cyclization by NisC can alternate at the nisin precursor peptide (Kuipers et al., 2008; Lubelski et al., 2009). This appears to proceed from the N- to the C-terminus for class I enzymes (Lubelski et al., 2009), as well as for class II enzymes (Lee et al., 2009). A complex of the nisin biosynthesis enzymes has been isolated consisting of NisB, NisC, and NisT (Khusainov et al., 2011). Moreover, NisB has been demonstrated to have stronger interactions with precursor nisin than NisC has (Khusainov et al., 2011). Interestingly, the nisin leader is not absolutely required for class I lantibiotic biosynthesis *in vivo* (Khusainov and Kuipers, 2012), however, its addition *in trans* increases the efficiency of modification (Khusainov and Kuipers, 2012). Recently, it has been shown that synthetic nisin variants lacking Ser/Thr's in the core structure still bind NisB and synthetic nisin variant lacking Cys in the core structure bind NisC (Khusainov and Kuipers, 2013b). Increasing the number of negatively charged amino acids in the core peptide part of precursor nisin does not abolish binding of

the nisin modification enzymes to these unnatural nisin variants (Khusainov and Kuipers, 2013b).

Nisin's N-terminal lanthionine ring binds to the cell wall precursor lipid II that is considered to act as a docking molecule (Breukink et al., 1999; Hasper et al., 2006). Nisin exerts at least two modes of antimicrobial action: it displaces lipid II from the septum thereby inhibiting cell wall synthesis and it forms hybrid pores composed of nisin and lipid II, which permeabilize the target cell membrane (Hasper et al., 2006; Lubelski et al., 2008).

Four classes of lanthipeptides have been distinguished (Xie et al., 2004; Goto et al., 2010; Mueller et al., 2010). Nisin belongs to class I, in which precursor peptides are dehydrated by LanB enzymes and cyclized by LanC enzymes. (Methyl)lanthionines in classes II, III, and IV are installed by the bi- or multifunctional enzymes LctM, RamC/LabKC, or LanL, respectively, that perform both dehydration and cyclization reactions (Xie et al., 2004; Goto et al., 2010; Mueller et al., 2010). We here applied extensive protein engineering of NisB to elucidate the potential mechanistic roles of highly and less conserved residues. We identified two likely catalytic site residues, i.e., Y80 and H961 and several regions for substrate binding and discuss these results in conjunction with the recently published NisB 3D-structure (Ortega et al., 2015).

MATERIALS AND METHODS

BACTERIAL STRAINS AND GROWTH CONDITIONS

Table S1 (supplementary material) lists the strains and plasmids that were used in this study. *Lactococcus lactis* was used as a host

for the overexpression plasmids pNZnisA-E3 or pNZnisA-H6 expressing precursor nisin or His-tagged precursor nisin, respectively. Mutated versions of NisB as well as of wild type NisC and NisT were overexpressed using the pIL3BTC plasmid (Rink et al., 2005). Cells were grown as described previously (Khusainov et al., 2011) at 30°C in M17 medium (Difco) supplemented with 0.5% (w/v) glucose and antibiotics at 5 µg/ml chloramphenicol and 5 µg/ml erythromycin, where appropriate. When both chloramphenicol and erythromycin were used, 4 µg/ml of each was applied. Prior to mass spectrometric analyses, cells were cultured in minimal medium as previously described (Rink et al., 2005).

RECOMBINANT DNA TECHNIQUES

Standard genetic manipulations were essentially performed as described by Sambrook and Russell (2001). Plasmid pIL3BTC (Rink et al., 2005) served as a template for PCR in order to obtain site-specific NisB mutants. The round PCR method was performed as described earlier (Rink et al., 2005). In brief, the primers used were 5'-phosphorylated to allow ligation of the amplicon ends after PCR. The primers were oriented in the reverse direction to allow amplification of the whole plasmid. The mismatches were in the 5'-ends of either the forward or the reverse primer. Standard PCR was performed with these primers according to the Phusion DNA-polymerase manufacture (Finnzymes). After PCR, the PCR product was purified with the PCR-purification kit (Roche). Subsequently, DNA ligation was performed with T4 DNA ligase (Thermo Scientific). Plasmid isolation was performed by means of the Plasmid DNA Isolation Kit (Roche Applied Science). Restriction analysis was performed with restriction enzymes from Thermo Scientific.

PROTEIN EXPRESSION AND PURIFICATION

C-terminal His-tagged precursor nisin was purified as described before (Khusainov et al., 2011). *L. lactis* NZ9000 (de Ruyter et al., 1996) containing mutated versions of *nisB* together with wild type *nisTC* and *nisA* containing the C-terminal sequence for the His-tag, was grown overnight followed by 1:50 dilution in GM17 (M17 (Difco) supplemented with 0.5% (w/v) Glucose). Growth was continued until OD₆₆₀ = 0.6, followed by induction with 0.5 ng/ml of nisin for 2 h. Cells were collected by centrifugation, and lysed by use of 10 µg ml⁻¹ freshly prepared lysozyme solution, followed by the addition of 10 mM MgSO₄ and 100 µg ml⁻¹ Dnase I (Sigma). Cells were disrupted by several rounds of freeze thaw cycles with liquid nitrogen in cases when 0.5 L of culture was used. Cells were disrupted by French Pressure treatment (15,400 psi) in case 2 L cultures were used, and remaining debris was removed by low speed centrifugation (13,000 × g for 15 min at 4°C; Sorvall SS34 rotor).

MASS SPECTROMETRIC ANALYSIS

In order to conduct mass spectrometric analysis of the produced peptides we used crude supernatants from bacteria grown on minimal medium. Prior to the mass spectrometric analysis, samples were ZipTipped (C18 ZipTip, Millipore) essentially as described before (Khusainov et al., 2011). In short, ZipTips were equilibrated with 100% acetonitrile and washed with 0.1% trifluoroacetic acid. Subsequently, the supernatant containing the

peptides was mixed with 0.1% trifluoroacetic acid and applied to a ZipTip. Bound peptides were washed with 0.2% trifluoroacetic acid and eluted with 50% acetonitrile and 0.1% trifluoroacetic acid. The eluent was mixed in a ratio of 1:1 with matrix (10 mg/ml α-cyano-4-hydroxycinnamic acid) and 1.5 µl was spotted on the target and allowed to dry. Mass spectra were recorded with a Voyager-DE Pro (Applied Biosystems) MALDI-time-of-flight mass spectrometer. In order to increase the sensitivity and the accuracy, external calibration was applied with six different peptides (Protein MALDI-MS Calibration Kit, Sigma).

INTERACTION ANALYSIS OF PRECURSOR NISIN WITH THE MODIFICATION ENZYMES NisB AND NisC

To investigate the binding of NisB mutants to precursor nisin a previously described pull-down method of the nisin biosynthesis complex, using His-tagged precursor nisin as bait, was applied (Khusainov et al., 2011).

RESULTS

Amino acid sequence alignment of 36 LanB protein sequences resulted in the identification of several conserved residues (Figure 2) (Schuster-Bockler et al., 2004). We selected 25 (semi) conserved residues for site-directed mutagenesis. NisB mutants harboring single amino acid substitutions residues were generated (Table 1). The expression of the NisB mutants and their integrity were checked by, either mass spectrometric determination of nisin in the supernatant, or by SDS-PAGE and Western blot analysis (Figure S1). NisB is about 117.5 kDa and is known to have a natural N-terminal degradation product of ~90 kDa (Khusainov et al., 2011).

L. lactis strain NZ9000, expressing simultaneously *nisA*, *nisTC* and in each case a different mutant version of the *nisB* gene, was used to study the functionality of mutants of NisB. Wild type precursor nisin is naturally secreted out of the cell by NisT. In this study, the secreted precursor nisin variants were purified from the supernatant by ZipTip purification (Millipore) and subsequently analyzed by MALDI-TOF mass spectrometry (Tables 1, S2, Figure 3). Those precursor nisin variants that were not secreted, were His-tagged and Ni-NTA purified and subsequently analyzed by MALDI-TOF mass spectrometry (Tables 1, S2, Figure 3).

MUTATIONS IN NisB THAT HAVE NO MAJOR IMPACT ON THE SECRETION AND MODIFICATION OF NISIN

To gain insight in the mechanism of action of NisB 25 different mutations were made in the sequence. The mutations were selected to modify different conserved residues based on an alignment of LanB-type dehydratases. Throughout the sequence of NisB, we observed several repetitions of conserved leucine and isoleucine residues or islands of adjacent leucine-isoleucine residues. To investigate the role of these conserved leucine and isoleucine residues, we performed a substitution of a single isoleucine (I298A) and a double substitution of adjacent leucine-isoleucine residues (L223A, I224A). Both mutants resulted in the secretion of fully modified nisin. Further NisB mutants F342A, Y346F, D648A, P639A, R775A, Y827F, D843A, S844A, S958A,

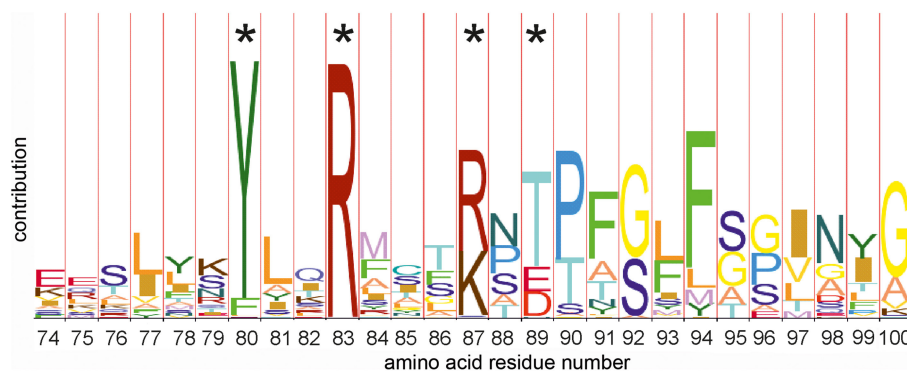


FIGURE 2 | HMM-logo of the N-terminal amino acid alignment of thirty six members of the dehydratase LanB family. The hidden markov model (HMM) shows a number of conserved amino acid residues. Residues marked with an asterisk have been (among others)

mutated in this study. Other mutations have been selected on the basis of the full models of the C (PFAM PF04738 <http://pfam.xfam.org/family/PF04738>) and the N terminal domains (PFAM PF04737 http://pfam.xfam.org/family/Lant_dehyd_N).

Table 1 | Dehydration pattern of precursor nisin modified by NisB mutants.

Mutated residue in NisB	Dehydrations observed*	Secretion of NisA
(L223A, I224A), I298A, F342A, Y346F, P639A, R775A, Y827F, D843A, S844A, S958A, R966A, E975Q,	8 , 7, (6)	+
D121A, D299A, D648A	8, 7 , (6)	+
T89A	7, 6 , 5	+
R784A	7	+
R83A, R83M	0, 1, 2, (3)	—
R87A	4, 5, 6, 7	—
R14A, W616A (Khusainov et al., 2011)	0, 1, 2, 3, 4, 5, 6, 7	—
Y80F, H961A	0	—

+Demonstrated by the NisA-H6 pull-down assay (Figure S1).

*Most prominent mass peak observed is indicated with the bold number.

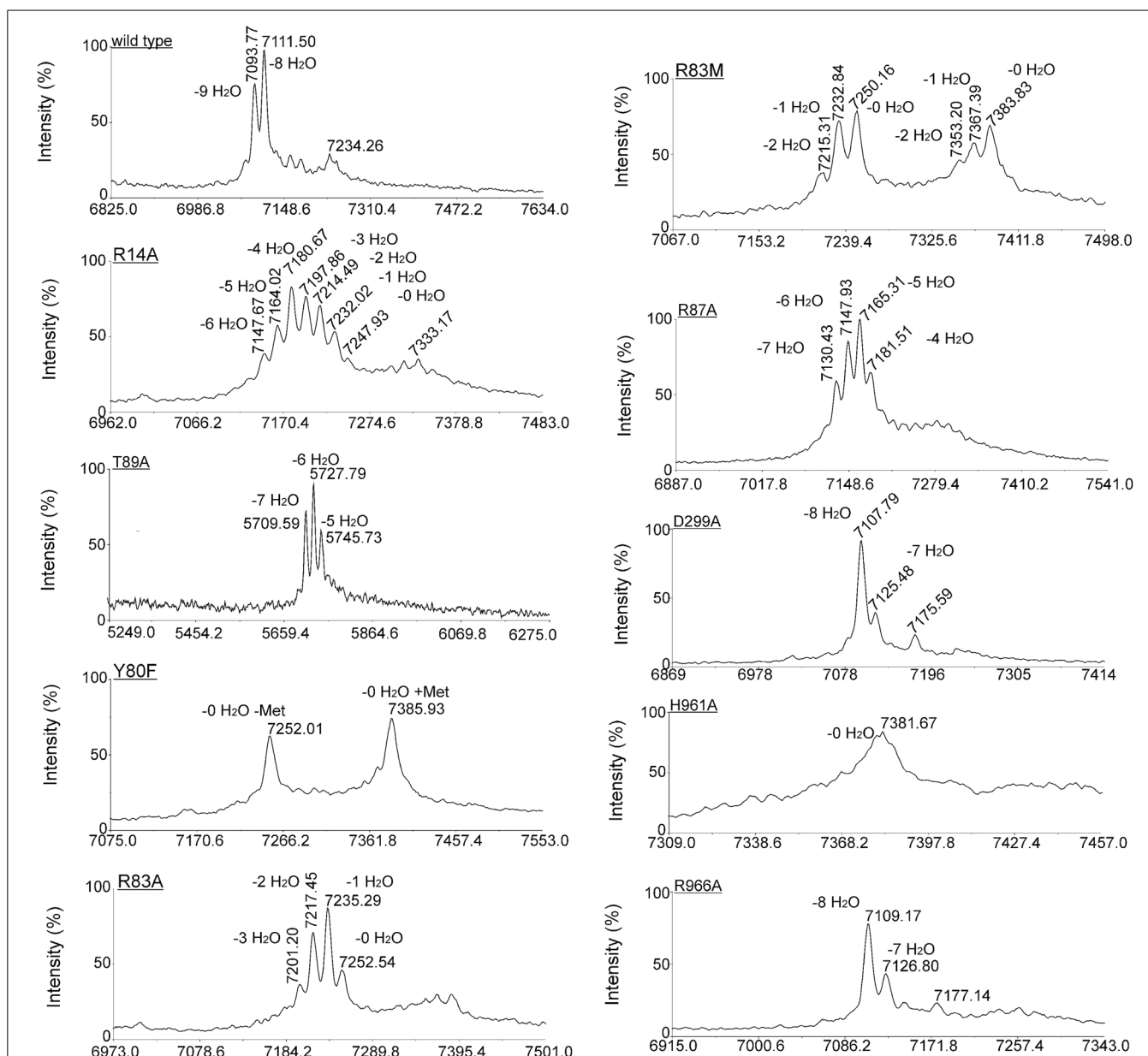
R966A, E975Q also resulted in the secretion of fully modified precursor nisin identical to the wild type precursor nisin. In all these samples the most prominent mass peak corresponded to the 8-fold dehydrated nisin as is normal for the wild type nisin. Therefore, these mutations appear not to affect NisB-precursor nisin interactions and NisB-catalyzed dehydration. The dehydration pattern of precursor nisin, modified and secreted by wild type NisB enzymes, harbors 8, 7, and 6 dehydrated residues, with 8 being the most predominant peak in the mass spectra. For the mutant R784A, the only peak observed corresponded to the 7 times dehydrated NisA, indicating a slightly reduced modification efficiency and possibly a slightly lower production level since no peaks corresponding to the 6 and 8 times dehydrated substrate were observed. The analyzed dehydration pattern of precursor nisin which was modified by the NisB mutants where aspartate was changed to alanine (D121A, D299A, D648A) showed a similar pattern to that of wild type. Although all three expected

dehydration species were present, i.e., 8, 7 and 6, the major peak observed corresponded, unlike in wild type precursor nisin, to a 7-fold dehydrated precursor nisin. This indicates that the dehydration efficiency of the above Asp?Ala NisB mutants was slightly decreased.

Intriguingly, the mutation T89A led to a secreted precursor nisin containing exactly one dehydration less than usually observed for wild type NisB. Mass spectrometry demonstrated a dehydration pattern of precursor nisin with 7, 6 and 5 dehydrations, while the 6-fold dehydration peak was the most prominent peak (Table 1, Figure 3). T89 is not very remote from the likely catalytic residue Y80 (vide infra).

MUTATIONS IN NisB THAT ABOLISH SECRETION OF MODIFIED PRECURSOR NISIN (TABLE 1)

Notably, several single NisB mutations at conserved positions, i.e., R14A, Y80F, R83A, R83M, R87A, H961A (Table 1; Figure S1) and the previously reported W616A (Khusainov et al., 2011) resulted in a lack of secretion of modified precursor nisin to the outside of the cell, thus hampering the evaluation of mutant NisB-mediated dehydration. To analyze these intracellularly-trapped precursor nins, His-tagged precursor nisin variants were constructed, used and purified by Ni-NTA columns from the cell extract (Figure S1). To break the cells (Figure S1), we used several rounds of liquid nitrogen freeze-thaw cycles, which lead to cell lysis. However, application of this method may result in differences in the efficiency of *L. lactis* cell lysis. For this reason, results presented here should be interpreted qualitatively only. Subsequently, these modified precursor nisin mutants were analyzed by MALDI-TOF mass spectrometry (Tables 1, S1, Figure 3). A previously developed pull-out assay, which relies on interaction of His-tagged precursor nisin with its modification enzymes (Khusainov et al., 2011) demonstrated that all these NisB mutants could still bind precursor nisin (Figure S1). Since unmodified precursor nisin can also be exported via NisT (Kuipers et al., 2004), the NisB mutants leading to intracellularly trapped precursor nisin apparently have a reduced capacity to release their substrate. Furthermore, these data clearly demonstrate that the specific NisB mutants that cause



version of precursor nisin was purified out of the cytoplasm of the cell. Cells containing plasmid pL3BTC and a plasmid encoding for NisA with C-terminal extension and a His6 tag were grown until OD 0.6, induced with 0.5 ng/ml nisin and let grow for two additional hours. Subsequently, cells were harvested, disrupted by French press and purified precursor nisin was analyzed by MALDI-TOF MS.

a lack of secretion of precursor nisin, have a reduced dehydration capacity.

NisB SINGLE MUTANTS R83A, R83M, AND R87A HAVE SEVERELY REDUCED DEHYDRATION CAPACITIES

Interestingly, R83A and R83M were severely hampered in their dehydration capacity and led to intermediate dehydration patterns: up to 3 or 2-fold dehydration of precursor nisin. R87A resulted in 4, 5, 6, and 7 dehydrations. This suggests that these

residues are important for possible positioning of the partially dehydrated peptide into the active site.

CATALYTIC RESIDUES OF NisB

Site-directed mutagenesis of Y80F and H961A resulted in a lack of secreted precursor nisin. This result is consistent with recent studies (Garg et al., 2013; Ortega et al., 2015), where mutagenesis of the NisB H961 residue also resulted in a non-dehydrated precursor nisin and was shown to be part of the active site of the

glutamate elimination domain. Applying the previously described modification enzyme co-purification binding assay (Khusainov et al., 2011) we showed that the NisB mutants Y80F and H961A are still able to bind precursor nisin (Figure S1). MALDI-TOF MS analysis resulted in one major peak, corresponding to fully unmodified precursor nisin for both NisB mutants (Table S2, Figure 3). These results strongly suggest that Y80 and H961 are directly involved in catalysis, since no dehydration at all was observed.

DISCUSSION

The class I dehydratase NisB is a remarkable catalyst that breaks 16 bonds by modifying 3 Ser and 5 Thr residues in precursor nisin. To investigate the effect of mutations in NisB on its activity, we applied extensive site-directed mutagenesis of its conserved residues without prior knowledge of its later published structure. This resulted in the identification of residues in NisB that are important for catalysis and/or for the efficiency of dehydration.

The effects of the mutations that we observed can be classified into three groups: (1) mutations that resulted in a wild type extent of dehydration and secretion, (2) mutations that resulted in non-secreted peptides with intermediate dehydration patterns, and (3) mutations that resulted in non-secreted and unmodified precursor nisin.

The NisB mutants from the groups 2 and 3 prevented export of precursor nisin. However, NisT has been demonstrated of being capable of exporting unmodified precursor nisin in the absence of NisB (Kuipers et al., 2004). It can be speculated that the absence of the export might be caused by strongly reduced release of precursor nisin from a mutant NisB. Another explanation might be that lack of secretion is observed because NisB and NisC are acting alternately (Lubelski et al., 2009). Incomplete dehydration might disturb this delicate process leading to complexes that do not release the product, which might block the export.

Mechanistic *in vitro* investigations of the dehydration reaction of the bifunctional and multifunctional LctM, RamC/LabKC, and LanL enzymes demonstrated that LctM, RamC/LabKC, and LanL phosphorylate Ser and Thr in the substrate peptide, as was evidenced by MALDI-TOF MS, which identified peaks with a mass shift of +80 Da differences (Chatterjee et al., 2005; Goto et al., 2010; Mueller et al., 2010). The class II LanM enzymes have been shown to use ATP as an energy source. Notably, the class III labyrinthopeptin A2 modification enzyme LabKC has been recently demonstrated to require GTP for the phosphorylation and dehydration reaction of serines (Mueller et al., 2010). The recently published reconstitution of the *in vitro* activity of class I NisB (Garg et al., 2013), shows that the dehydration by class I lantibiotic enzymes happens via glutamylation of Ser/Thr and not by phosphorylation. It is not clear why class I lantibiotic enzymes use different mechanism for dehydration, however this might be due different evolutionary lineages that these enzymes followed.

In the *in vitro* study of Garg et al., individual replacement of residues Arg14, Arg83, Arg87, Thr89, Asp121, Asp299, Arg464, and Arg966 with Ala and subsequent expression and purification of these NisB mutants in *E. coli* resulted in abolishment of dehydration (Garg et al., 2013). In our *in vivo* study in its native host *L. lactis*, the NisB mutants Arg14, Arg83, Arg87, Thr89, Asp121,

Asp299, and Arg966 resulted in partial dehydration of the precursor nisin (Table 1). These differences are most likely due to the differences in the host (*E. coli* vs. *L. lactis*) or due to the differences between *in vivo* and *in vitro* conditions. However, both of the studies pinpoint the importance of these residues for the dehydration reaction. Moreover, we identified one more residue of crucial importance: i.e., Y80. The mutant Y80F most likely interferes with the glutamylation domain that was recently identified (Ortega et al., 2015). Furthermore, we show that NisB R14A, Y80F, R83A, R83M, R87A, H961A, and W616A mutants result in a lack of transport of precursor nisin.

Here we present data that is perfectly in line with the recent publication of the structure of NisB (Ortega et al., 2015) as can be seen in Figure 4, indicating the relation between position and effect of the mutation in the 3D-structure of NisB. With our *in vivo* results we can confirm conclusions made on the basis of experiments that were performed *in vitro* using heterologously expressed enzymes and substrates.

In the structure of NisB four specific domains have been identified, a glutamylation domain, a glutamate elimination domain, a tRNA interaction domain and a region likely to interact with the nisin and its leader. We investigated several mutants that lie within the proximity of the glutamylation domain (Figure 4A), of which only H961A resulted in complete loss of activity. All other mutants showed normal dehydration patterns indicating a certain degree of structural freedom around the active site. The glutamate elimination domain shows a different picture (Figure 4B). The mutant Y80F resulted in total loss of activity but also many mutations in the vicinity (R83A/M, R87A, R14A, and T89A) had a detrimental effect on the activity. Although in Figure 4B, D648 seems to be in the proximity of the active site, this is actually not the case (2D vs. 3D artifact) and therefore it is explainable that mutating it into Ala had no effect on the activity. The glutamate elimination site contains several conserved residues that are less tolerant to amino acid changes. No mutants close to the tRNA interaction domain were investigated. Close to the putative nisin leader interaction site (<10 Å) only one double mutant (I223A, I224A) was investigated which resulted in normal activity. Although the NisA interaction region of the structure was not extensively probed in this study, it can be expected that there is a high degree of tolerance to amino acid substitutions since many different substrates can be modified by NisB.

From the mutants we tested only the single mutants, i.e., NisB Y80F and NisB H961A result in non-modified precursor nisin, and importantly these mutants still bind precursor nisin and are able to co-purify NisB in the precursor nisin co-purification assay. Overall, we can conclude that R14, R83, R87, and W616 (Khusainov et al., 2011) in NisB play an important, though not direct catalytic role, in the dehydration reaction of class I lantibiotics, since their substitution leads to a reduced extent of dehydration, without completely abolishing it and a lack of secretion. The (novel) single point mutation Y80F and the single point mutation H961A in NisB lead to unmodified and non-secreted precursor nisin. Notably, NisB residues that resulted in an intermediate dehydration pattern also resulted in a lack of secretion of precursor nisin. This observation suggests that the NisB mutants that result in unsecreted precursor nisin either do not release

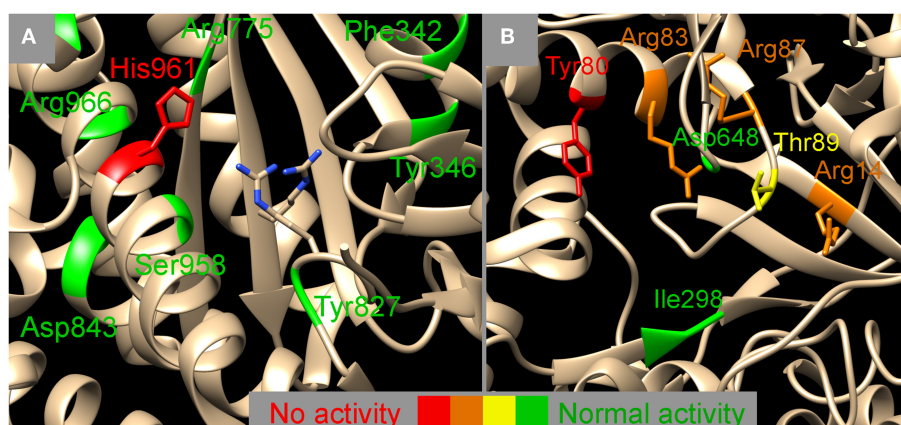


FIGURE 4 | Mapping the NisB mutants on two functional domains, the glutamylation domain (A) and the glutamate elimination domain (B) (PDB 4WD9, Ortega et al., 2015). Colors indicate the effect of the mutation on the dehydratase activity, red, no activity observed; orange, activity severely hampered; yellow, activity slightly hampered; green, normal activity. The exact nature of the mutation can be looked up in **Table 1**. (A) Next to the

sidechain of His961 also the sidechains of Arg826 and Arg786 are indicated which have been indicated to be important for glutamylation previously (Garg et al., 2013). The vicinity of the glutamylation domain (A) seems to allow for some amino acid changes whereas the surrounding of the glutamate elimination domain (B) seems to be more strictly determined. Image was created using UCSF chimera version 1.10.1 (Pettersen et al., 2004).

the substrate precursor nisin or a subsequent cyclization reaction by NisC is significantly slowed down, preventing the export. This observation indicates that the modification and the transport processes are linked to each other, in line with a previous publication (van den Berg van Saparoea et al., 2008), possibly through the complex formation that has recently been described (Khusainov et al., 2011).

ACKNOWLEDGMENTS

Liang Zhou is acknowledged for critical reading of the manuscript. We are thankful to Arjan Narbad, Institute of Food Research, Norwich, for providing NisB antibodies. Rustem Khusainov received financial support from the Dutch Science Council ALW: ALW 816.02.005.

SUPPLEMENTARY MATERIAL

The Supplementary Material for this article can be found online at: <http://www.frontiersin.org/journal/10.3389/fmicb.2015.00102/abstract>

REFERENCES

- Arnison, P. G., Bibb, M. J., Bierbaum, G., Bowers, A. A., Bugni, T. S., Bulaj, G., et al. (2013). Ribosomally synthesized and post-translationally modified peptide natural products: overview and recommendations for a universal nomenclature. *Nat. Prod. Rep.* 30, 108–160. doi: 10.1039/c2np20085f
- Breukink, E., Wiedemann, I., van Kraaij, C., Kuipers, O. P., Sahl, H. G., and de Kruijff, B. (1999). Use of the cell wall precursor lipid II by a pore-forming peptide antibiotic. *Science* 286, 2361–2364. doi: 10.1126/science.286.5448.2361
- Chan, W. C., Leyland, M., Clark, J., Dodd, H. M., Lian, L. Y., Gasson, M. J., et al. (1996). Structure-activity relationships in the peptide antibiotic nisin: antibacterial activity of fragments of nisin. *FEBS Lett.* 390, 129–132. doi: 10.1016/0014-5793(96)00638-2
- Chatterjee, C., Miller, L. M., Leung, Y. L., Xie, L. L., Yi, M. S., Kelleher, N. L., et al. (2005). Lactacin 481 synthetase phosphorylates its substrate during lantibiotic production. *J. Am. Chem. Soc.* 127, 15332–15333. doi: 10.1021/ja0543043
- de Ruyter, P. G., Kuipers, O. P., and de Vos, W. M. (1996). Controlled gene expression systems for *Lactococcus lactis* with the food-grade inducer nisin. *Appl. Environ. Microbiol.* 62, 3662–3667
- de Vries, L., Reitzema-Klein, C. E., Meter-Arkema, A., van Dam, A., Rink, R., Moll, G. N., et al. (2010). Oral and pulmonary delivery of thioether-bridged angiotensin-(1-7) Peptides 31, 893–898. doi: 10.1016/j.peptides.2010.02.015
- Garg, N., Salazar-Ocampo, L. M., and van der Donk, W. A. (2013). *In vitro* activity of the nisin dehydratase NisB. *Proc. Natl. Acad. Sci. U.S.A.* 110, 7258–7263. doi: 10.1073/pnas.1222488110
- Goto, Y., Li, B., Claesen, J., Shi, Y., Bibb, M. J., and van der Donk, W. A. (2010). Discovery of unique lanthionine synthetases reveals new mechanistic and evolutionary insights. *PLoS Biol.* 8:e1000339. doi: 10.1371/journal.pbio.1000339
- Gravesen, A., Sorensen, K., Aarestrup, F. M., and Knochel, S. (2001). Spontaneous nisin-resistant *listeria monocytogenes* mutants with increased expression of a putative penicillin-binding protein and their sensitivity to various antibiotics. *Microb. Drug. Resist.* 7, 127–135. doi: 10.1089/10766290152045002
- Hasper, H. E., Kramer, N. E., Smith, J. L., Hillman, J. D., Zachariah, C., Kuipers, O. P., et al. (2006). An alternative bactericidal mechanism of action for lantibiotic peptides that target lipid II. *Science* 313, 1636–1637. doi: 10.1126/science.1129818
- Khusainov, R., Heils, R., Lubelski, J., Moll, G. N., and Kuipers, O. P. (2011). Determining sites of interaction between prenisin and its modification enzymes NisB and NisC. *Mol. Microbiol.* 82, 706–718. doi: 10.1111/j.1365-2958.2011.07846.x
- Khusainov, R., and Kuipers, O. P. (2012). When the leader gets loose: *in vivo* biosynthesis of a leaderless prenisin is stimulated by a trans-acting leader peptide. *Chembiochem* 13, 2433–2438. doi: 10.1002/cbic.201200437
- Khusainov, R., and Kuipers, O. P. (2013b). The presence of modifiable residues in the core peptide part of precursor nisin is not crucial for precursor nisin interactions with NisB- and NisC. *PLoS ONE* 8:e74890. doi: 10.1371/journal.pone.0074890
- Khusainov, R., Moll, G. N., and Kuipers, O. P. (2013a). Identification of distinct nisin leader peptide regions that determine interactions with the modification enzymes NisB and NisC. *FEBS Open Bio.* 3, 237–242. doi: 10.1016/j.fob.2013.05.001
- Kluskens, L. D., Kuipers, A., Rink, R., de Boef, E., Fekken, S., Driessen, A. J., et al. (2005). Post-translational modification of therapeutic peptides by NisB, the dehydratase of the lantibiotic nisin. *Biochemistry* 44, 12827–12834. doi: 10.1021/bi050805p
- Kluskens, L. D., Nelemans, S. A., Rink, R., de Vries, L., Meter-Arkema, A., Wang, Y., et al. (2009). Angiotensin-(1-7) with thioether bridge: An angiotensin-converting enzyme-resistant, potent angiotensin-(1-7) analog. *J. Pharmacol. Exp. Ther.* 328, 849–854. doi: 10.1124/jpet.108.146431
- Kramer, N. E., Hasper, H. E., van den Bogaard, P. T. C., Morath, S., de Kruijff, B., Hartung, T., et al. (2008). Increased D-alanylation of lipoteichoic

- acid and a thickened septum are main determinants in the nisin resistance mechanism of *Lactococcus lactis*. *Microbiology* 154, 1755–1762. doi: 10.1099/mic.0.2007/015412-0
- Kuipers, A., de Boef, E., Rink, R., Fekken, S., Kluskens, L. D., Driessen, A. J. M., et al. (2004). NisT, the transporter of the lantibiotic nisin, can transport fully modified, dehydrated, and unmodified prenisin and fusions of the leader peptide with non-lantibiotic peptides. *J. Biol. Chem.* 279, 22176–22182. doi: 10.1074/jbc.M312789200
- Kuipers, A., Meijer-Wierenga, J., Rink, R., Kluskens, L. D., and Moll, G. N. (2008). Mechanistic dissection of the enzyme complexes involved in biosynthesis of lactacin 3147 and nisin. *Appl. Environ. Microbiol.* 74, 6591–6597. doi: 10.1128/AEM.01334-08
- Kuipers, O. P., Beerthuyzen, M. M., Siezen, R. J., and de Vos, W. M. (1993b). Characterization of the nisin gene cluster nisABTCIPR of *Lactococcus lactis*. Requirement of expression of the nisA and nisI genes for development of immunity. *Eur. J. Biochem.* 216, 281–291. doi: 10.1111/j.1432-1033.1993.tb18143.x
- Kuipers, O. P., Rollema, H. S., Devos, W. M., and Siezen, R. J. (1993a). Biosynthesis and secretion of a precursor of nisin-Z by *Lactococcus lactis*, directed by the leader peptide of the homologous lantibiotic subtilin from *Bacillus subtilis*. *FEBS Lett.* 330, 23–27. doi: 10.1016/0014-5793(93)80911-D
- Lee, M. V., Ihnken, L. A. F., You, Y. O., McClerren, A. L., van der Donk, W. A., and Kelleher, N. L. (2009). Distributive and directional behavior of lantibiotic synthetases revealed by high-resolution tandem mass spectrometry. *J. Am. Chem. Soc.* 131, 12258–12264. doi: 10.1021/ja9033507
- Li, B., and van der Donk, W. A. (2007). Identification of essential catalytic residues of the cyclase NisC involved in the biosynthesis of nisin. *J. Biol. Chem.* 282, 21169–21175. doi: 10.1074/jbc.M701802200
- Lubelski, J., Khusainov, R., and Kuipers, O. P. (2009). Directionality and coordination of dehydration and ring formation during biosynthesis of the lantibiotic nisin. *J. Biol. Chem.* 284, 25962–25972. doi: 10.1074/jbc.M109.026690
- Lubelski, J., Rink, R., Khusainov, R., Moll, G. N., and Kuipers, O. P. (2008). Biosynthesis, immunity, regulation, mode of action and engineering of the model lantibiotic nisin. *Cell. Mol. Life. Sci.* 65, 455–476. doi: 10.1007/s00018-007-7171-2
- Majchrzykiewicz, J. A., Lubelski, J., Moll, G. N., Kuipers, A., Bijlsma, J. J. E., Kuipers, O. P., et al. (2010). Production of a class II two-component lantibiotic of *Streptococcus pneumoniae* using the class I nisin synthetic machinery and leader sequence. *Antimicrob. Agents. Chemother.* 54, 1498–1505. doi: 10.1128/AAC.00883-09
- Mavaro, A., Abts, A., Bakkes, P. J., Moll, G. N., Driessen, A. J. M., Smits, S. H. J., et al. (2011). Substrate recognition and specificity of the NisB protein, the lantibiotic dehydratase involved in nisin biosynthesis. *J. Biol. Chem.* 286, 30552–30560. doi: 10.1074/jbc.M111.263210
- Mueller, W. M., Schmiederer, T., Ensle, P., and Suessmuth, R. D. (2010). *In vitro* biosynthesis of the prepeptide of type-III lantibiotic labyrinthopeptin A2 including formation of a C–C bond as a post-translational modification. *Angew. Chem. Int. Ed. Engl.* 49, 2436–2440. doi: 10.1002/anie.200905909
- Ortega, M. A., Hao, Y., Zhang, Q., Walker, M. C., van der Donk, W. A., and Nair, S. K. (2015). Structure and mechanism of the tRNA-dependent lantibiotic dehydratase NisB. *Nature* 517, 509–512. doi: 10.1038/nature13888
- Pettersen, E. F., Goddard, T. D., Huang, C. C., Couch, G. S., Greenblatt, D. M., Meng, E. C., et al. (2004). UCSF Chimera—a visualization system for exploratory research and analysis. *J. Comput. Chem.* 25, 1605–1612. doi: 10.1002/jcc.20084
- Rink, R., Arkema-Meter, A., Baudoin, I., Post, E., Kuipers, A., Nelemans, S. A., et al. (2010). To protect peptide pharmaceuticals against peptidases. *J. Pharmacol. Toxicol. Methods* 61, 210–218. doi: 10.1016/j.vascn.2010.02.010
- Rink, R., Kluskens, L. D., Kuipers, A., Driessen, A. J. M., Kuipers, O. P., and Moll, G. N. (2007). NisC, the cyclase of the lantibiotic nisin, can catalyze cyclization of designed nonlantibiotic peptides. *Biochemistry* 46, 13179–13189. doi: 10.1021/bi700106z
- Rink, R., Kuipers, A., de Boef, E., Leenhouts, K. J., Driessen, A. J., Moll, G. N., et al. (2005). Lantibiotic structures as guidelines for the design of peptides that can be modified by lantibiotic enzymes. *Biochemistry* 44, 8873–8882. doi: 10.1021/bi050081h
- Sambrook, J., and Russell, D. W. (2001). *Molecular Cloning: A Laboratory Manual*. Cold Spring Harbor, NY: Cold Spring Harbor Laboratory Press
- Schuster-Bockler, B., Schultz, J., and Rahmann, S. (2004). HMM Logos for visualization of protein families. *BMC Bioinformatics* 5:7. doi: 10.1186/1471-2105-5-7
- van den Berg van Saparoea, H. B., Bakkes, P. J., Moll, G. N., and Driessen, A. J. M. (2008). Distinct contributions of the nisin biosynthesis enzymes NisB and NisC and transporter NisT to prenisin production by *Lactococcus lactis*. *Appl. Environ. Microbiol.* 74, 5541–5548. doi: 10.1128/AEM.00342-08
- van der Meer, J., Rollema, H., Siezen, R., Beerthuyzen, M., Kuipers, O., and De Vos, W. (1994). Influence of amino acid substitutions in the nisin leader peptide on biosynthesis and secretion of nisin by *Lactococcus lactis*. *J. Biol. Chem.* 269, 3555–3562.
- van Heel, A. J., Montalban-Lopez, M., and Kuipers, O. P. (2011). Evaluating the feasibility of lantibiotics as an alternative therapy against bacterial infections in humans. *Expert. Opin. Drug. Metab. Toxicol.* 7, 675–680. doi: 10.1517/17425255.2011.573478
- van Heel, A. J., Mu, D., Montalban-Lopez, M., Hendriks, D., and Kuipers, O. P. (2013). Designing and producing modified, new-to-nature peptides with antimicrobial activity by use of a combination of various lantibiotic modification enzymes. *ACS Synth. Biol.* 2, 397–404. doi: 10.1021/sb3001084
- Xie, L., Miller, L. M., Chatterjee, C., Averin, O., Kelleher, N. L., and van der Donk, W. A. (2004). Lactacin 481: *in vitro* reconstitution of lantibiotic synthetase activity. *Science* 303, 679–681. doi: 10.1126/science.1092600

Conflict of Interest Statement: The authors declare that the research was conducted in the absence of any commercial or financial relationships that could be construed as a potential conflict of interest.

Received: 23 October 2014; accepted: 27 January 2015; published online: 26 February 2015.

Citation: Khusainov R, van Heel AJ, Lubelski J, Moll GN and Kuipers OP (2015) Identification of essential amino acid residues in the nisin dehydratase NisB. *Front. Microbiol.* 6:102. doi: 10.3389/fmicb.2015.00102

This article was submitted to *Microbial Physiology and Metabolism*, a section of the journal *Frontiers in Microbiology*.

Copyright © 2015 Khusainov, van Heel, Lubelski, Moll and Kuipers. This is an open-access article distributed under the terms of the Creative Commons Attribution License (CC BY). The use, distribution or reproduction in other forums is permitted, provided the original author(s) or licensor are credited and that the original publication in this journal is cited, in accordance with accepted academic practice. No use, distribution or reproduction is permitted which does not comply with these terms.



Characterization of the *E. coli* proteome and its modifications during growth and ethanol stress

Boumediene Soufi, Karsten Krug, Andreas Harst[†] and Boris Macek*

Proteome Center Tuebingen, University of Tuebingen, Tuebingen, Germany

Edited by:

Ivan Mijakovic, Chalmers University of Technology, Sweden

Reviewed by:

Céline Henry, Institut National de la Recherche Agronomique, France
Chunaram Choudhary, University of Copenhagen, Denmark

*Correspondence:

Boris Macek, Proteome Center Tuebingen, University of Tuebingen, Auf der Morgenstelle 15, 72076 Tuebingen, Germany
e-mail: boris.macek@uni-tuebingen.de

[†] Present address:

Andreas Harst, Ruhr-Universität Bochum, Bochum, Germany

We set out to provide a resource to the microbiology community especially with respect to systems biology based endeavors. To this end, we generated a comprehensive dataset monitoring the changes in protein expression, copy number, and post translational modifications in a systematic fashion during growth and ethanol stress in *E. coli*. We utilized high-resolution mass spectrometry (MS) combined with the Super-SILAC approach. In a single experiment, we have identified over 2300 proteins, which represent approximately 88% of the estimated expressed proteome of *E. coli* and estimated protein copy numbers using the Intensity Based Absolute Quantitation (iBAQ). The dynamic range of protein expression spanned up to six orders of magnitude, with the highest protein copy per cell estimated at approximately 300,000. We focused on the proteome dynamics involved during stationary phase growth. A global up-regulation of proteins related to stress response was detected in later stages of growth. We observed the down-regulation of the methyl directed mismatch repair system containing MutS and MutL of *E. coli* growing in long term growth cultures, confirming that higher incidence of mutations presents an important mechanism in the increase in genetic diversity and stationary phase survival in *E. coli*. During ethanol stress, known markers such as alcohol dehydrogenase and aldehyde dehydrogenase were induced, further validating the dataset. Finally, we performed unbiased protein modification detection and revealed changes of many known and unknown protein modifications in both experimental conditions. Data are available via ProteomeXchange with identifier PXD001648.

Keywords: Super-SILAC, quantitative proteomics, absolute quantitation, stress response, *E. coli*, post translational modifications

INTRODUCTION

E. coli serves as an excellent model to study general features of prokaryotic proteome, such as its dynamics under various physiological conditions, its dynamic range of expression and its modifications. Despite the significant progress made toward the understanding of bacterial regulatory processes, the scale and dynamics of the global protein expression during bacterial growth and stress response has not been addressed systematically. During growth in batch culture, bacteria have to constantly monitor changes and make adjustments on the molecular level during different stages of bacterial growth (Nystrom, 2004). For example, long term growing *E. coli* in stationary phase have developed specific mechanisms encouraging certain genetic mutations to occur in order to cope with the numerous stresses encountered during stationary phase, better known as the growth advantage in stationary phase (GASP) phenotype (Finkel, 2006). *E. coli* is an excellent organism to use when studying ethanol stress response, as it is a commonly used industrial strain in many processes including bio-ethanol production (Woodruff et al., 2013). Ethanol stress in *E. coli* is known to cause a variety of different physiological responses such as the inhibition of peptidoglycan biosynthesis (Buttke and Ingram, 1978), and fatty acid biosynthesis (Clark and Beard, 1979). Despite the fact that previous studies monitored bacterial proteome changes in response to various

stresses and growth conditions (Bernhardt et al., 2003; Lee et al., 2006; Soufi et al., 2010; Soares et al., 2013), a systematic and comprehensive analysis of proteome changes during growth, and ethanol stress in *E. coli* has not been performed. Monitoring these changes and processes on the level of the proteome, will allow for a much better understanding into the adaptive mechanisms bacteria undertake during changes in their environment.

Quantitative mass spectrometry (MS) based proteomics has become an invaluable tool utilized to study protein expression and dynamics in a global fashion (Aebersold and Mann, 2003). Technologies developed in this field have evolved quite dramatically within the last decade, especially in context of advanced methodologies in the metabolic labeling of proteins using stable isotopes such as ¹⁵N labeling (Gouw et al., 2011) and Stable isotope labeling of amino acids in cell culture (SILAC) (Ong et al., 2002). SILAC has been used before in studies of bacterial growth; however, its classical application allows for comparison of only three conditions at a time (Soares et al., 2013). One extension of SILAC, known as the Super-SILAC approach, involves mixing samples from different experimental conditions labeled with the same SILAC-label to obtain an internal standard. This labeled standard can then be added into several samples and used for their indirect quantitative comparison. This approach can be used to produce a quantitative analysis of a wide range of biological and

environmental samples (Geiger et al., 2010) and has been applied primarily in eukaryotic systems for quantification of many different types of cancer and tumor cell lines (Deeb et al., 2012; Geiger et al., 2012; Lund et al., 2012; Boersema et al., 2013; Schweppe et al., 2013); only one application of this approach has been reported in prokaryotic systems so far (Berghoff et al., 2013).

In this study, we employ the Super-SILAC approach to study proteome dynamics in bacteria during growth and ethanol stress. We investigate the absolute and relative proteome dynamics on the global scale at seven distinct growth phases in *E. coli* cultured in minimal medium. We identify 2303 proteins with 1604 proteins being absolutely quantified in all seven growth phases, and achieve good reproducibility between biological replicates. We extend this approach to monitor ethanol stress response in *E. coli* at two distinct time points leading to the identification of 2251 and quantification of 1804 proteins. Distinct global proteome changes were observed in both analyzed conditions with good correlation between biological replicates in all experiments. In terms of an unbiased detection of protein post translational modification changes, we detected numerous types of modifications depending on the growth state employed.

MATERIALS AND METHODS

BACTERIAL STRAIN

The *E. coli* BW25113 strain was employed in all experiments conducted in this study.

BACTERIAL CELL CULTURE AND SILAC LABELING

Each experiment was performed in two biological replicates. *E. coli* cells were grown in a 2L flask containing 500 ml of minimal M9 media with stable isotope-labeled (heavy) L-Lysine-13C6, 15N2 in batch culture. Aliquots of batch culture were removed at each specific growth stage (7 time points) in the growth experiment or collected at pre stress, 10 min, and 2 h post ethanol stress in the ethanol stress experiment (Supplementary Figure 1). Separately, 1.25L of cells were grown in a 5L flask with M9 medium containing unlabeled (light) L-Lysine-12C6, 14N2 at the exact seven different phases of growth or collected at 10 min and 2 h post ethanol stress. For ethanol stress experiments, 4% v/v of ethanol was added when cells had reached an OD600 of 0.4.

PROTEIN EXTRACTION AND MIXING

The cells were harvested by centrifugation at 4000 g for 10 min, media was removed and cells were snap-frozen in liquid nitrogen and stored at -80°C . The cell pellets were resuspended in the appropriate amount of the commercially available YPER lysis buffer (Thermo Scientific), plus 50 $\mu\text{g}/\text{ml}$ lysozyme. Cell wall lysis was performed at 37°C for 20 min, followed by brief sonication on ice (1 min at 40% amplitude) to remove DNA. Cellular debris was removed by centrifugation at 13000 g for 30 min. The crude protein extract was precipitated via the methanol/chloroform approach and the proteins were resuspended in denaturation buffer containing 6 M urea/2 M thiourea in 10 mM Tris. Protein concentration was measured by Bradford assay (Bio-Rad, Munich, Germany). Protein extracts obtained from L-Lysine-13C6, 15N2 labeled cells were mixed 1:1:1:1:1:1:1

for growth, and 1:1:1 for ethanol stress to obtain the Super-SILAC standard (SSS) for each respective experiment. Proteins labeled with L-Lysine-12C6, 14N2 (50 μg) were then mixed in an equimolar ratio with the SSS (50 μg), resulting in 7 protein samples per biological replicate.

IN-SOLUTION DIGESTION

A total of 100 μg (50 μg SSS and 50 μg light) of crude protein extract in denaturation buffer were digested via in-solution prior to peptide separation. Briefly, proteins were reduced with 1 mM dithiothreitol for 1 h shaking at room temperature, alkylated with 5.5 mM iodoacetamide for 1 h shaking at room temperature in the dark, predigested with 1:100 (w/w) endoproteinase Lys-C for 3 h at room temperature, diluted with 4 volumes of 20 mM ammonium bicarbonate followed by an overnight digestion step 1:100 (w/w) endoproteinase Lys-C at room temperature. The protein digest was acidified using trifluoroacetic acid (TFA) to a final concentration of 0.1% (v/v) to stop the protein digestion. In the case of samples fractionated using Off-Gel fractionation no TFA was added. For the intensity-based absolute quantification of proteins (iBAQ), the UPS2 Proteomics Dynamic Range Standard set (Sigma-Aldrich) was spiked in prior to digestion.

ISOELECTRIC FOCUSING

Hundred microgram of peptides were separated using the OFFGEL 3100 Fractionator (Agilent) following the experimental steps as previously reported (Hubner et al., 2008). Separation was performed on a 13 cm Immobiline DryStrip (GE Healthcare) with a pH separation gradient of 3–13 to a maximum of 50 μA for 20 kVh. Peptides were acidified using an acidic solution (30% ACN, 5% Acetic acid, 10%TFA), followed by a cleanup step using Stage-Tips loaded with C18 material (Rappsilber et al., 2007).

SDS-PAGE AND IN-GEL DIGESTION

Protein separation via SDS-PAGE followed by an In-Gel digestion was used for one biological replicate from each Super-SILAC experiment. Briefly, 100 μg (50 μg SSS and 50 μg light) of crude protein extracts were separated on a NuPage Bis-Tris 4–12% gradient gel (Invitrogen). After staining the gel with Coomassie Blue, protein lanes were cut into 12 equal slices. Coomassie Blue stain was subsequently removed from each gel slice via washing with 10 mM ammonium bicarbonate (ABC) and acetonitrile (ACN) (1:1, v/v). Protein slices were reduced with 10 mM dithiothreitol (DTT) in 20 mM (ABC) for 45 min at 56°C and alkylated with 55 mM iodoacetamide IAA in 20 mM ABC for 30 min in the dark at room temperature. Gel slices were washed twice with 5 mM ABC, followed by a dehydration step by incubating with 100% ACN at room temperature. Proteins were digested with Lys-C (Wako) (12.5 ng/ μL in 20 mM ABC) at 37°C overnight. Digested peptides were recovered from each gel slice using three consecutive extraction steps: (I) 3% TFA in 30% ACN (II) 0.5% acetic acid in 80% ACN (III) 100% ACN. Resulting peptides were desalted using StageTips (Ishihama et al., 2006).

LC-MS/MS ANALYSIS

All samples were measured on an EASY-nLC II nano-LC (Proxeon Biosystems) coupled to an Orbitrap Elite mass spectrometer (Thermo Fisher Scientific). Peptides were further separated

chromatographically using a 15 cm PicoTip fused silica emitter with an inner diameter of 75 μm (New Objective) packed in-house with reversed-phase ReproSil-Pur C18-AQ 3 μm resin (Dr. Maisch GmbH). A total of 2 μg of peptides were injected into the column, using the intelligflow technology with solvent A (0.5% acetic acid) at a rate of 200 nL/min to a maximum pressure of 280 Bar. Peptides were then eluted using a 90 min segmented gradient of 5–50% solvent B (80% ACN in 0.5% acetic acid). The mass spectrometer was operated on a data-dependent positive ion mode. Peptide fragmentation (MS/MS) was induced using either collision induced dissociation (CID) or higher-energy collisional dissociation (HCD). Survey spectral full-scans were recorded between 300 and 2000 Thomson at a resolution of 120,000 with a target value of 1E6 charges in the LTQ mass analyzer. The 20 most intense peaks from the survey scans were selected for fragmentation using CID with a normalized collision energy of 35% at a target value of 5000 charges. The dynamic exclusion window was set at 90 s. For operation via HCD, normalized collision energy of 40 eV requiring a minimum signal of 1000 and a target value of 4E4 charges was employed. The spectra were acquired in the Orbitrap mass analyzer with a resolution of 7500. The 15 most intense peaks from the survey scans were selected for fragmentation using HCD.

DATA PROCESSING

All acquired MS data was processed with the MaxQuant software suite (Cox and Mann, 2008) version 1.2.2.9. Briefly, the SILAC labeling parameter was set to a multiplicity of Two (Lys0, Lys8). After all peptides were quantified, a database search was performed using the MaxQuant internal search engine Andromeda (Cox et al., 2011). Full enzyme specificity was required, with an allowance of up to two missed cleavages. Lys-C was specified as the protease. MS/MS spectra were searched against the Uniprot *Escherichia coli* K12 database (taxonomy reference: 833333), complete proteome set containing 4303 protein entries, downloaded Dec 24, 2012. For absolute protein quantification analysis, MS/MS spectra were also searched against another FASTA file containing the Proteomics Dynamic Range Standard (UPS2, Sigma) with a total of 48 entries. Methionine oxidation and protein N-terminal acetylation were defined as variable modifications. Cysteine carbamidomethylation was defined as a fixed modification. MS scan mass tolerance was set to 6 ppm. For CID fragmentation, the MS/MS tolerance was 0.5 Da, whereas for HCD fragmentation the mass tolerance was set to 20 ppm. Peptides and assembled proteins were searched at a false discovery rate (FDR) of 1%. A minimum of two quantified peptides per protein were required for protein quantitation.

RELATIVE PROTEIN QUANTITATION

SILAC ratios of proteins (“light” to “heavy”) were transformed to log2 scale and only proteins that were quantified in all seven growth phases (growth) or all three time points (ethanol stress) were considered for further quantitative analysis. The magnitude of fluctuation was expressed by calculating the standard deviation of the log-transformed ratios across the growth phases or time points. The resulting quartiles of the distribution were used to

bin proteins according to the extent of fluctuation. Those belonging to the quartile with the highest standard deviation (75–100%) were defined as “fluctuating” or dynamic, whereas those belonging to the quartile with the lowest standard deviation (0–25%) were defined as “non-fluctuating” or static.

BACTERIAL CELL COUNTING

As part of the protein copy number /cell calculation, the total number of *E. coli* cells were counted. Briefly, *E. coli* cells were grown in minimal M9 media supplemented with 0.5% glucose at an OD600 = 0.5 (TP3) and 1.0 (TP5) were grown in minimal media. Experiments were performed in biological triplicates and replicates at an OD600 of 0.5 and 1.0, respectively. 500 μl of cells were mixed with 50 μl 25% para-formaldehyde (20 mM MOPS PS = 7) and 50 μl 2.5% glutaraldehyde, followed by an incubation period of 15 min at room temperature. Cells were counted using Fluorescence-activated Cell Sorting (FACS). In brief, the BD LSR Fortessa FACS instrument was used. Standard settings were employed (log scale acquisition, Threshold: 400 FCS, Acquisition speed: low). Gating settings were set according to cell size in order to remove background noise in the form of cellular aggregates and debris. *E. coli* cells were diluted 1:20 for more accurate counts (5 μl cells, 95 μl water). Each biological replicate was measured 3 times (technical replicates) and averaged in order to obtain the final cell count at each growth phase. The exact number of cells was derived from the total volume of cells taken for protein extraction, and calculated for the amount of input protein material that was used for digestion (50 μg).

ABSOLUTE PROTEIN QUANTITATION

The absolute protein copy number per cell was calculated for the Super-SILAC growth experiment in two stages of growth: logarithmic and early stationary. To this end, the intensity based absolute quantitation approach (iBAQ) supported by the MaxQuant Software suite was employed as previously shown. The absolute amount of protein is proportional to the absolute molar amounts of the UPS2 protein standard spiked into the protein sample. All acquired iBAQ values were divided by 4, due to the fact that 1/4 of the UPS2 protein was spiked in the log and early stationary Super-SILAC growth experimental samples. The total number of cells counted via FACS (N_{cells}), was used to calculate the absolute protein copy numbers ($\text{CN}_{\text{protein}}$) by utilizing the calculation as previously described (Carpy et al., 2014):

$$\text{CN}_{\text{protein}} = \frac{N_A (\text{iBAQ}_{\text{protein}} * 10^{-15})}{N_{\text{cells}}}$$

N_A represents Avogadro’s number. The absolute protein amounts calculated for the super-SILAC standard together with corresponding SILAC ratios were used to calculate the absolute amount for each protein in all seven stages of growth in the growth analysis experiment.

PEAK TIME INDEX CALCULATION

For each protein we determined the experimental condition of its highest expression (“peak time index”) as described in Olsen et al. (2010). Briefly, the SILAC ratios for each protein were normalized

to the maximal change across the experiment. We then calculated the weighted mean of the expression ratio in a particular condition with respect to the normalized ratios of adjacent conditions, i.e., adjacent growth phases or time points upon ethanol stress. We slightly modified the peak time index calculation as described in Olsen et al. (2010) to account for the acyclicity of our experiments. To assign the resulting “peak time index” of every protein to a specific growth phase respective time point, we applied hierarchical clustering on these values using the Euclidian distance and a defined cluster numbers of seven (growth phase) or three (ethanol stress).

FUNCTIONAL ENRICHMENT ANALYSIS

We retrieved Gene Ontology (GO) annotation of *E. coli* from the UniProt-GOA database (downloaded on April 18, 2012). To test whether specific annotation terms are enriched or depleted within a set of proteins of interest we applied Fisher’s exact test using the theoretical *E. coli* proteome as background. Derived *p*-values were further adjusted to address multiple hypothesis testing using the method proposed by Benjamini and Hochberg (1995).

UNBIASED DETECTION OF PROTEIN MODIFICATIONS

All acquired MS data was processed with the MaxQuant software suite (Cox and Mann, 2008) version 1.2.2.9. Briefly, the SILAC labeling parameter was set to a multiplicity of Two (Lys0, Lys8), or as unlabeled (in order to serve as quality control for dependent peptide (DP) function). All other parameters were the same as described above, except that the DP function was enabled in order to search for modified peptides that were not identified. Briefly, MaxQuant compares all identified MS/MS to all unidentified MS/MS spectra. The precursor mass differences are calculated between identified spectra (“base peptides”) and unidentified spectra with similar MS/MS features (“dependent peptides”) and corresponding possible modifications are reported.

RESULTS AND DISCUSSION

ABSOLUTE QUANTIFICATION OF *E. COLI* PROTEOME

In total, we identified 2303 proteins at a false discovery rate (FDR) of 1% of which 1604 were quantified in all seven stages of growth (Table 1, Table S1). We applied the iBAQ MS based strategy (Schwanhauser et al., 2011) to estimate copy numbers of proteins in the analyzed conditions. To this end, we used an internal standard containing absolute molar amount of proteins (standard) spiked into the protein samples. The iBAQ standard was spiked in the *E. coli* Super-SILAC experiment at two time points (TP3 & TP5). This led to the estimates of protein copy numbers for 1587 proteins during growth in minimal medium (Table S2). Moreover, we applied the protein copy numbers from the growth dataset (T3 time point) to the proteins quantified in

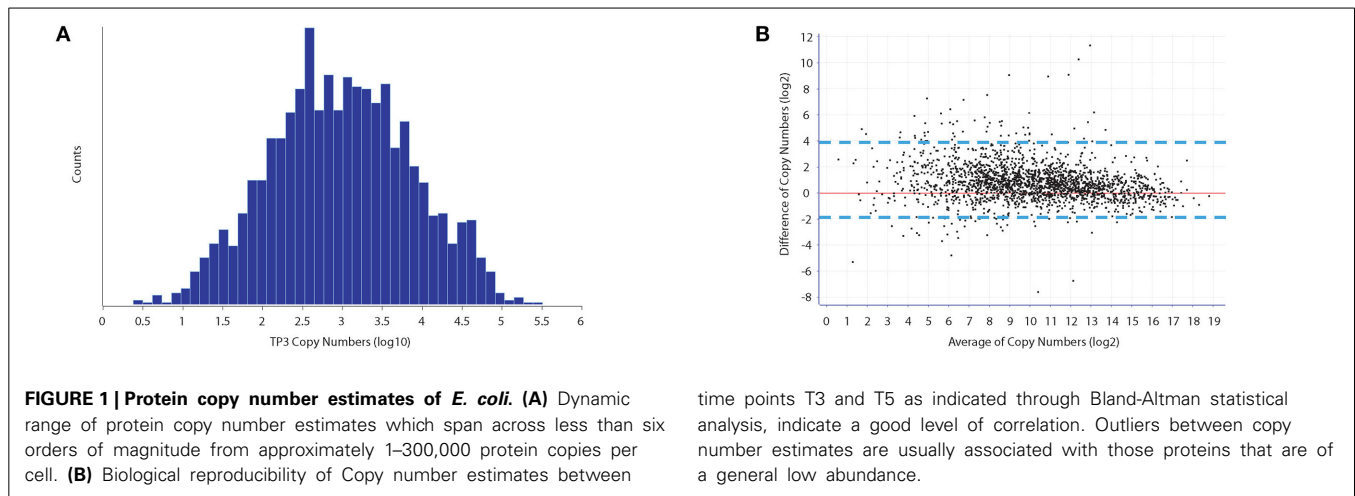
order to assess protein abundance changes during ethanol stress, which lead to protein copy number estimates for 1620 proteins (Table S7).

Despite the fact that MS based strategies have been increasingly used in determining protein copy numbers in living organisms, there is a large discrepancy between previous studies that have estimated protein copy numbers from bacteria to eukaryotes. Possible reasons have been recently discussed in detail (Milo, 2013) and include loss of material during sample preparation (cell lysis, protein digestion etc), the inherent detection limits of mass spectrometers toward low abundant proteins, and errors in MS quantitation methodologies. Furthermore, in bacteria, the total amount of protein moieties per cell and the number of cells can differ greatly depending on the strain and growth conditions employed. Therefore, cell counting was recently identified as one of the main reasons for inaccuracies in estimation of protein copy numbers. To address this, we carefully determined the number of cells that existed in the exact experimental conditions that were employed. To this end, we performed multiple biological and technical measurements of the total *E. coli* cell counts using FACS which showed excellent reproducibility (Table S4, Supplementary Figure 12). We also employed orthogonal methods of determining the number of *E. coli* cells, such as CFU counting and microscopy-based methods, however with much lower level of reproducibility and accuracy than FACS (data not shown). The FACS-derived total cell count was then used to derive the absolute protein copies per cell.

Bland-Altman analysis of replicate UPS standard measurements (difference of the copy numbers between TP3 and TP5 vs the average), revealed a small standard deviation (Figure 1B). Therefore, the average of protein copy numbers between TP3 and TP5 was used to obtain copy numbers for all time points in both growth and ethanol stress datasets. We observed a good level of reproducibility between the protein intensities derived from both the UPS2 internal standard as well as their iBAQ intensities for all proteins between TP3 and TP5 (Supplementary Figure 2). We deduced no significant difference between the total protein moieties/cell in different growth stages (Table S5), which demonstrates an overall balance of protein synthesis and degradation at different points during growth to maintain an overall level of cellular homeostasis. Our results showed that an *E. coli* cell under tested conditions has an average of 10,761,042 protein molecules with a dynamic range of protein copy number within 6 orders of magnitude (Figure 1A). Many of the higher abundant proteins were ribosomal, membrane and carbohydrate metabolism related proteins. For example, previous studies have shown that the most abundant lipomembrane protein in *E. coli* is the Braun lipoprotein found in the outer membrane with approximately 200,000 copies per cell (Braun, 1975). Our studies revealed similar protein copy number estimates of the Braun lipoprotein at 167,568/118,072 copies per cell at TP3 and TP5 respectively which is within the same range of magnitude as previously reported. Elongation factor Tu1 was found to be the most abundant protein with 327,934 and 301,731 copies per cell at TP3 and TP5, respectively. The least abundant classes of proteins (<500 copies/cell) for both TP3 and TP5 were enriched toward membrane and membrane associated proteins (inner, outer, plasma etc). This is

Table 1 | Total number of identified and quantified proteins.

	Growth	Ethanol Stress
Identified	2303	2260
Quantified (all phases)	1604	1984
Absolutely quantified	1587	1620



due to the fact that membrane proteins typically pose problems during a typical cell lysis procedure without specific membrane protein enrichment, thus difficult to accurately detect.

The economics of protein synthesis becomes especially important during extended periods of growth as the bacterial cells need to prioritize and conserve their energy toward those biological processes that are essential in order to sustain the growth and survival when facing conditions of nutrient starvation and harsh stress conditions. For example, we observed that most Glycolytic/Gluconeogenic enzymes (essential proteins required in environmental growth conditions employed) stay the same or increase in abundance whereas non-essential proteins such as cold shock proteins (respond to specific stress conditions) decrease during the later stages of growth as their synthesis would be a waste or precious energy in which the bacterial cell cannot afford (Supplementary Figures 3A, B). Furthermore, we estimated protein copy numbers for all 299 gene products of *E. coli* that are considered essential which showed a high level of correlation between TP3 and TP5. This is as expected, as essential proteins need to be constantly present in order to maintain cellular viability.

In order to validate the absolute quantification data, we investigated known protein complexes in *E. coli*. Protein complexes serve as a very important role as they act together in order to implement numerous biological functions ultimately regulating complex metabolic pathways. Recently, a study analyzed the synthetic rates of a total of 64 well characterized (in terms of stoichiometry) *E. coli* multiprotein complexes (Li et al., 2014). We took the protein stoichiometries reported from this study to compare with our copy number estimates. We would expect that those protein complexes with similar stoichiometries should have similar copy numbers. We observed that absolute levels of proteins with predicted high copy numbers/cell (>10,000) are more accurate (with respect to their stoichiometry) than those with low copy numbers (<500). This is to be expected as the errors tend to become larger with low copy number proteins due to their lower intensities during MS analysis. All stoichiometries and their copy numbers of the 64 protein complexes (that were identified/quantified) can be seen in Supplementary File 1.

time points T3 and T5 as indicated through Bland-Altman statistical analysis, indicate a good level of correlation. Outliers between copy number estimates are usually associated with those proteins that are of a general low abundance.

RELATIVE DYNAMICS OF *E. COLI* PROTEOME DURING GROWTH

For relative quantitation, we assessed the extent of protein fluctuation during different stages of growth and ethanol stress, using the standard deviation of SILAC ratios as described previously (Carpy et al., 2014). To this end we calculated the standard deviations of the log₂-transformed protein ratios measured across the analyzed points and binned the proteins into a total of four quartiles (See Experimental Procedures for details). We then performed a functional enrichment analysis for the proteome data (GO analysis) in order to gain insights into which classes of proteins are dynamic and which are static (Supplementary Figure 4). Hierarchical clustering was performed in order to gain a better understanding on significantly changing protein profiles (quartile with top 25% changing proteins) cluster together during the seven different stages of growth (Figure 2A). Enrichment analysis of GO terms revealed association of certain protein clusters with distinct cellular processes (Supplementary Figure 5). For example, during later stages of stationary phase growth in batch culture, an increased expression of multiple universal stress proteins and other proteins involved in stress response occurred (Figure 2B). These proteins continue to increase into the later stages of stationary phase (TP7) despite the fact that the cells are under an enormous amount of growth perturbations, *E. coli* attempts to maintain cellular homeostasis by expressing high levels of stress response proteins. The same is true for protein peak time index (Supplementary Figure 6A), which indicates that proteins associated with stress response are peaking during stationary phase (Supplementary Figure 6B). Furthermore, during stationary phase we observed an increase in the *pspA* protein which helps maintain cellular growth during alkaline and nutrient depleted environmental conditions typically associated with stationary phase growth (Weiner and Model, 1994).

E. coli as well as other bacterial species have the ability to maintain viability during extended periods of growth during stationary phase. This phenomena is known as the GASP phenotype (Zambrano and Kolter, 1996). This occurs in many Gram negative bacterial species including *E. coli*, and is normally defined as growth in culture for 10 days or longer (Zambrano and Kolter, 1996). As the bacterial cells are encountering several stresses and

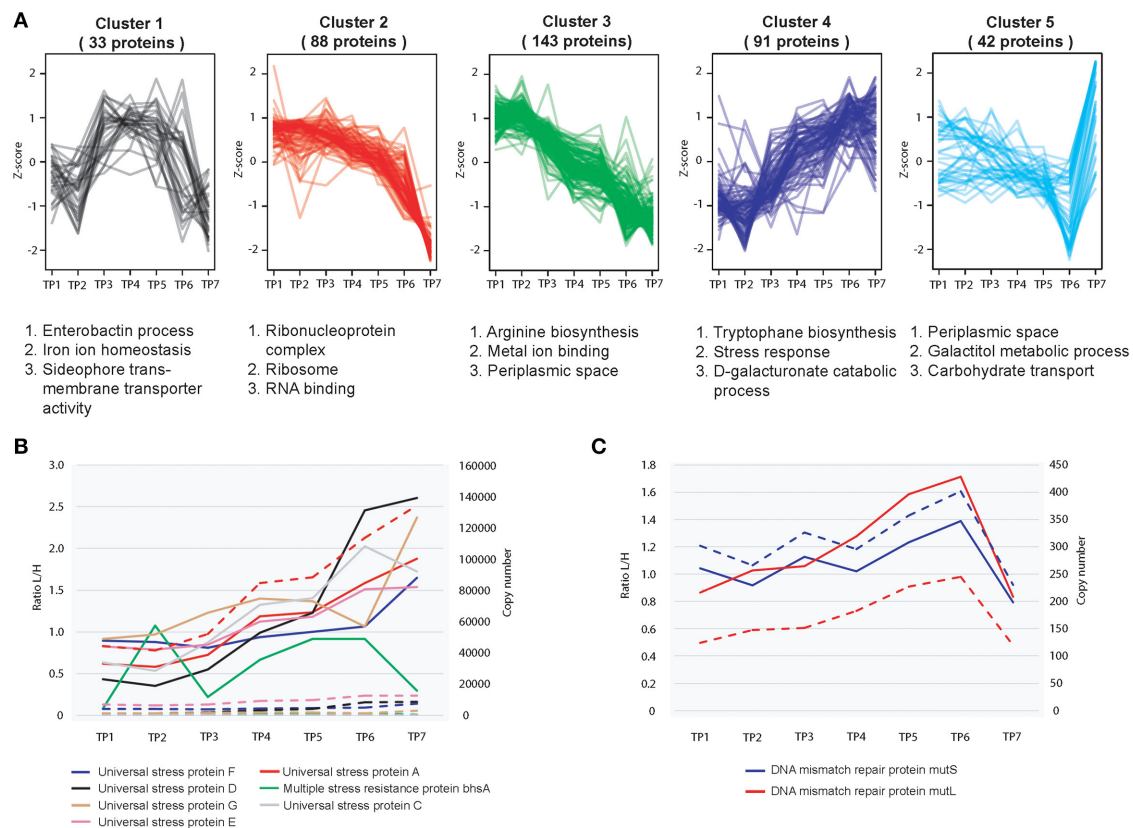


FIGURE 2 | Relative proteome dynamics during growth in *E. coli*. (A)

Hierarchical clustering analysis of fluctuating proteins reveals distinct growth stage specific changes, resulting in five distinct clusters. Examples of representative classes of proteins based on GO enrichments are depicted below each cluster. **(B)** Relative (solid line) and absolute dynamics (dashed

line) of detected universal stress response proteins reveals an increased level of expression during later stages of stationary phase (TP7) **(C)** Relative (solid line) and absolute dynamics (dashed line) of detected mismatch repair proteins mutS and mutL reveals a decreased level of expression during later stages of growth.

starvation conditions during extended periods of growth, the bacterial cells are developing increased tolerance toward these harsh environmental conditions through mutations on certain genes, thereby increasing the cellular fitness of these mutants thus enabling a small proportion of the cellular population to survive. Although we did not sample *E. coli* cells growing for a period longer than 10 days, there was evidence of protein activity associated with the GASP phenotype at TP7 (4 days growth). For example, MutS and MutL act as part of the *E. coli* methyl directed mismatch repair system and remove wrongly incorporated bases to ensure both a high fidelity and a low mutation rate of the global protein pool. In the GASP phenotype, lowering the levels of these proteins will increase the gene mutation rate of the bacteria (Finkel, 2006). This promotes a higher level of genetic diversity leading to a greater chance of survival for the bacteria. To this end, expression levels of MutS, MutL decreased during extended growth periods in stationary phase (TP7) (Figure 2C). It has also previously been reported that Dps plays an important role during starvation conditions in *E. coli*, has a significant increase in its synthetic rate during long term growth (6–7 days) (Farrell and Finkel, 2003). Interestingly we observed an approximate 4 fold increase in the levels of Dps between 30 h and 4 days of stationary phase growth, which suggests that this protein could

also play an important role in maintaining the cellular integrity of *E. coli* at much earlier periods of stationary phase than previously reported.

Dps is induced by the gene product of the σ^S RNA polymerase better known as the *rpoS* gene. *RpoS* serves as a major regulator of multiple genes associated with stress response typically associated with nutrient starvation (Lacour and Landini, 2004). Moreover, many of these Sigma-S dependent genes were found to be specifically induced during the initial onset of stationary phase growth (Lacour and Landini, 2004). Since we did not observe an increase of Dps synthesis (induced by RpoS) until TP7, this prompted us to look for other RpoS regulated targets and observe their proteome dynamics during growth. We observed an increased level of the *tnaA* encoded tryptophanase enzyme, which acts as an important signaling molecule during stationary phase growth and is also regulated by RpoS (Lacour and Landini, 2004). These observations could suggest that these RpoS regulated proteins have a more important role in extended periods of stationary phase growth rather than at the onset of stationary phase. It is important to note that not all RpoS regulated targets showed this profile type which could be due to the fact that these proteins are specifically induced and regulated by RpoS under different environmental or growth conditions.

Interestingly, we also noticed a dramatic increase in the abundance of the novel aldo-keto reductase protein yghZ (Grant et al., 2003). It is known to assist with methylglyoxal toxicity, a product that is produced in *E. coli* by methylglyoxal synthase (mgsA) which assists to prevent the accumulation of phosphorylated sugars. Despite that fact that we do see a steady increase of mgsA production from TP1-TP7, since its dynamics are similar to those of tnaA and DPs could suggest that it might play an important role during later stages of stationary growth.

RELATIVE PROTEOME DYNAMICS DURING ETHANOL STRESS

In response to alcohol stress, bacteria undergo many changes on both the physical and physiological levels. This includes but is not limited to changes in fatty acid composition, loss of ions from membrane leakage, an increase in membrane fluidity, and a decreased level of translation (Ingram, 1990). We extended the Super-SILAC approach to study the global changes of the proteome upon stress with ethanol. Hierarchical clustering analysis reveals very distinct changes on the proteome upon 10 min and 2 h post ethanol stress as opposed to pre stress conditions (Figure 3A). This is as expected, as with an acute and rapid perturbation such as ethanol stress, many physiological changes will be employed by *E. coli* in a rapid fashion. Peak time index analysis of the top 25% most changing proteins revealed that those proteins belonging to general stress response and heat shock response had the highest increase in expression levels during extended periods of ethanol stress (2 h) in both biological replicates (Supplementary Figure 7). Heat shock proteins are commonly known to be up-regulated during many different types of stresses including but not limited to ethanol stress.

Supplementary Figure 8A shows many heat shock proteins are induced upon ethanol stress.

The alcohol dehydrogenase YqhD and aldehyde dehydrogenase AldB were highly induced upon ethanol stress as expected. In mesophilic bacteria, it has been previously reported that when submitted to alcohol stresses, they attempt to make a balance between stress response and growth (Huffer et al., 2011). In this dataset, we observed that many stress response pathways such as the universal stress proteins (Supplementary Figure 8B), and multiple stress resistance proteins (ex BhsA, RpoH etc) were induced. However, key pathways critical for growth such as the glycolysis/gluconeogenesis pathways overall remained at a constant level. Figure 3B depicts all alcohol dehydrogenases identified in this study. As expected the main alcohol dehydrogenase yqhD is highly induced upon the addition of ethanol, however it appears that once yqhD is activated other alcohol dehydrogenases such as the propanol preferring alcohol dehydrogenase are down-regulated suggesting a type of a highly controlled network by different alcohol dehydrogenase members.

Many proteins involved in carbohydrate synthesis and transport were also found to be significantly regulated during exposure to ethanol. Interestingly, many of these regulated genes were also previously found to be over expressed during response to butanol (Rutherford et al., 2010) suggesting that many of these proteins play a role in responding to general solvent stress. For example, the manXYZ system is known to play a role in tolerating solvent stress in *E. coli* (Okochi et al., 2007). To this end, we also observed an up-regulation of manX and manZ upon ethanol stress at virtually identical levels which is expected since they are expressed from the same operon, and fall within the same range in terms

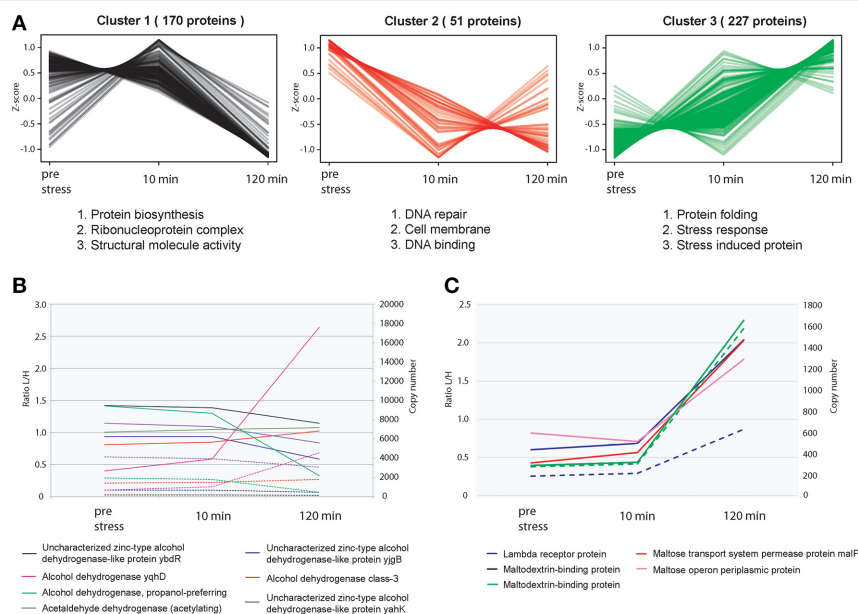


FIGURE 3 | Relative proteome dynamics during ethanol stress in *E. coli*.

(A) Hierarchical clustering analysis of fluctuating proteins reveals distinct specific changes at each time point, resulting in three distinct clusters. Examples of representative classes of proteins based on GO enrichments are depicted below each cluster. (B) Relative (solid line) and absolute dynamics

(dashed line) of detected alcohol dehydrogenases confirms that upon ethanol stress, the alcohol dehydrogenase of *E. coli* (yqhD) has the highest level of expression compared to other alcohol dehydrogenases. (C) Relative (solid line) and absolute dynamics (dashed line) of detected proteins associated with the binding and transport of maltose.

of protein copies/cell. Unfortunately no quantification data could be obtained for ManY. We also detected an up-regulation of the maltose-binding protein MalE as well as other proteins related to the transport of Maltose into the cell (**Figure 3C**). Maltose is known to exhibit certain properties similar to that of chaperones, in an attempt to prevent the aggregation of proteins during heat shock stress (Richarme and Caldas, 1997).

Another noteworthy observation is with regards to the YehU/YehT system in *E. coli*. This two component signaling transduction system was never characterized until very recently where this system was reported to be involved in the stationary phase control network of *E. coli* (Kraxenberger et al., 2012). Moreover, it showed that currently the only known and exclusive substrate of YehT is YjiY, an inner membrane protein that is a member of the CstA transporter superfamily (Kraxenberger et al., 2012). This superfamily is typically associated with the transport of peptides and amino acids. The authors reported that upon the onset of stationary phase, YjiY is strongly induced. An up regulation of YjiY was observed during late stationary phase growth and ethanol stress in both biological replicates, however YjiY was the most strongly induced protein after 10 min post ethanol stress. Currently the exact function of YjiY is not known. Therefore, from these observations one could speculate that perhaps YjiY (an inner membrane transporter) acts as a general stress response protein or perhaps also very specific to ethanol stress itself. Upon stress it could be feasible that it removes peptides and amino acids caused from misfolded proteins and degraded proteins via proteases. Further experimental validation on the potential role and function of YjiY during ethanol stress is required in order to understand the exact function of this protein.

How well bacteria can maintain their membrane integrity is a critical survival factor during ethanol stress. Upon ethanol stress, a common phenomenon is that the bacterial membrane increases in fluidity. This results in a sudden loss in the control of solute transportation (Huffer et al., 2011). This can cause a detrimental effect on the viability and stability of bacteria due to the rapid loss of many important ions such as magnesium (Ingram, 1976). In *E. coli*, membrane fluidity increases approximately 15% upon ethanol treatment (Huffer et al., 2011). One strategy that many bacteria employ to circumvent this increase in fluidity is known as lipid mixing. The bacteria replace the lipid content with stronger more complex unsaturated fatty acids in an attempt to maintain cell membrane rigidity. In *E. coli*, the key genes involved in unsaturated fatty acid synthesis are *faba* and *fabb* (Feng and Cronan, 2009). We observed that these proteins as well as many other members of the fab protein family exhibited minor changes during ethanol stress (Supplementary Figure 8C). This observation could be one of the reasons why the *E. coli* membrane increases in fluidity hence ceasing the growth of WT *E. coli* strains upon ethanol stress. For further insights with respect to this section, please refer to the Supplemental text section.

UNBIASED DETECTION OF PROTEIN MODIFICATIONS DURING GROWTH AND ETHANOL STRESS

To perform a global screen of protein modifications during growth and ethanol stress we employed the “DP” algorithm which is a part of the MaxQuant software suite. This algorithm

can identify co-translational and post translational modifications, modifications encountered during sample preparation, unknown modifications, as well as amino acid substitutions in a systematic and unbiased fashion. To this end, MaxQuant uses all MS/MS spectra that were identified during the regular database search and compares them to all unidentified MS/MS spectra. It then calculates precursor mass differences between identified spectra (“base peptides”) and unidentified spectra with similar MS/MS features (“dependent peptides”). Therefore, the algorithm reports mass differences that correspond to possible modifications on dependent peptides. This can be used as a powerful approach to detect various modifications without specifically searching for them, and thus has great potential for discovering novel protein modifications. This algorithm works in a similar way as previously reported (Savitski et al., 2006).

Since our dataset contained SILAC label we first tested the accuracy of the algorithm by processing the data without defining any SILAC labels. As expected, DP analysis revealed high number of dependent peptides that contained a Lys8 label (Supplementary Files 2, 3). We then implemented this feature in our experiments in order to elucidate which modifications are present during growth and ethanol stress, and whether these modifications are growth state dependent or ethanol stress dependent.

In all experiments, we observed more than 50 distinct mass differences that were detected in more than 50 MS/MS spectra. Most of them corresponded to known modifications that most likely result from sample preparation (e.g., deamidation, methionine oxidation, carbamidomethylation, etc.), as well as other known and unknown PTMs that could potentially have a biological or regulatory relevance (Tables S8, S9). For both growth and ethanol stress datasets, we compiled the 10 annotated modifications that occurred with highest frequency (**Table 2**). Utilizing a pairwise comparison of each growth stage relative to TP3 (Supplementary File 2), and each ethanol stress time point relative to pre stress (Supplementary File 3). We did observe subtle changes of many different PTMs, which could be due to both the specific environmental/biological growth condition, or technical variations due to sample preparation (Supplementary Files 2, 3). There was very little detection of some known regulatory modifications, such as protein phosphorylation, stressing the importance of enrichment steps prior to MS analysis for those PTMs that are of low abundance and stoichiometry.

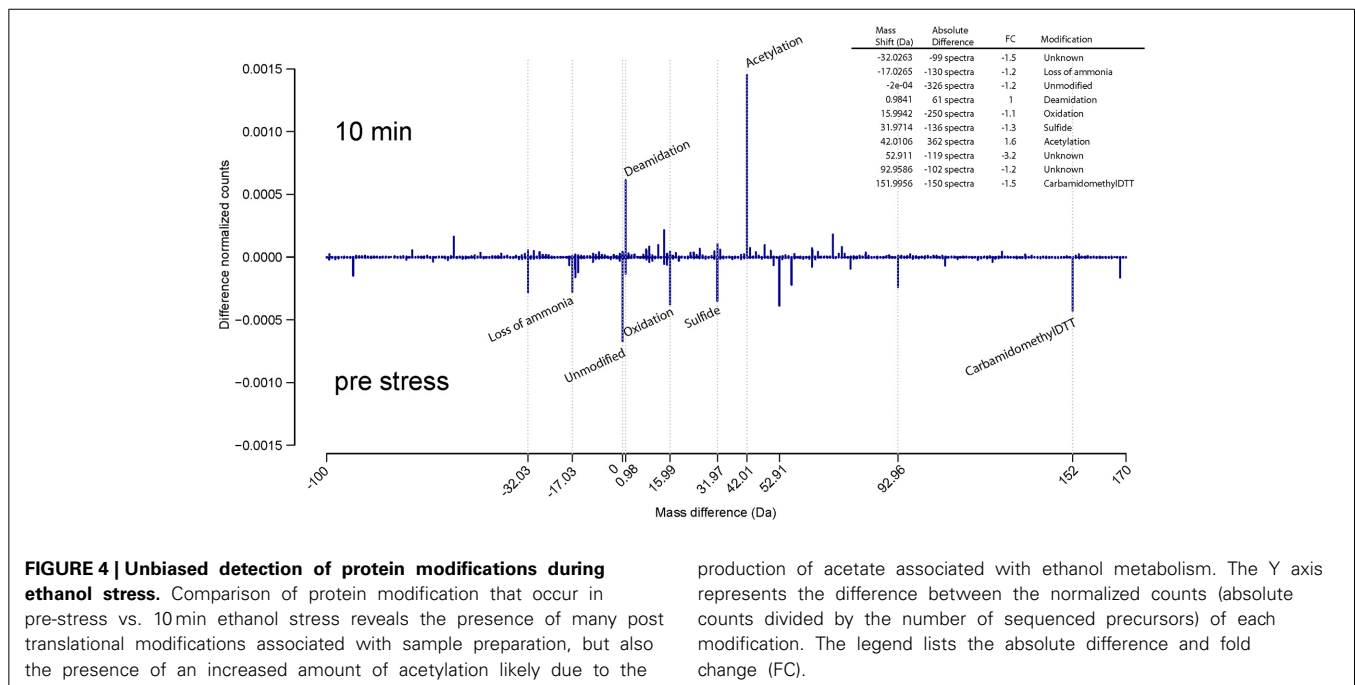
Interestingly, during ethanol stress, already after 10 min post stress, a strong increase in the level of acetylation was encountered relative to pre stressed *E. coli* cells (**Figure 4**). A similar pattern was detected after 2 h post ethanol stress treatment. This increased level of protein acetylation during ethanol stress in a bacteria is a novel observation, likely resulting from conversion of ethanol into acetate, which can then bind randomly to amino acid residues of the protein in a non-enzymatic fashion. However, further experiments will be needed to confirm this.

CONCLUSIONS AND FUTURE PERSPECTIVES

In this study, we used the Super-SILAC approach to investigate global relative proteome dynamics in *E. coli* during growth and ethanol stress grown in minimal medium. Moreover,

Table 2 | Frequent annotated modifications observed during growth and ethanol stress.

Modification (Growth)	Average mass shift (Da)	Most frequent amino acid	Max# dependent peptides (growth)	Max# dependent peptides (stress)
Deamidation	0.984	Asparagine	2031	1675
Carbamidomethyl DTT	151.995	n-terminal	814	475
di-Oxidation	31.988	Tryptophan	1851	1023
Sulfide	31.971	Cysteine	401	586
Acetylation	42.010	n-terminal	1116	1289
Oxidation	15.994	Tyrosine	3951	2172
Loss of ammonia	-17.026	n-terminal	999	795
Loss of water	-18.010	n-terminal	1044	1046
Formylation	27.994	n-terminal	319	123
Acetaldehyde	26.015	n-terminal	392	795



we estimated the absolute protein copy number per cell in *E. coli* using the iBAQ. To this end, we identified 2303 proteins which represents approximately 88% of the estimated expressed proteome of *E. coli*. The estimates of protein copy numbers of over 2000 proteins were derived. Unbiased detection of protein modifications revealed an increased level of protein acetylation after only 10 min post ethanol stress. Overall, this dataset represents the most comprehensive relative and absolute quantitative analysis of bacterial growth during normal and ethanol stress conditions at the proteome level and implicates both known as well as novel observations of *E. coli* proteome dynamics during growth and ethanol stress in minimal medium.

AUTHOR CONTRIBUTIONS

BS and BM designed the experiments. BS and AH performed bacterial cell culture/ counting, MS measurements, proteome analysis and data processing. BS and KK performed bioinformatics analysis. BS and BM wrote the manuscript.

production of acetate associated with ethanol metabolism. The Y axis represents the difference between the normalized counts (absolute counts divided by the number of sequenced precursors) of each modification. The legend lists the absolute difference and fold change (FC).

ACKNOWLEDGMENTS

Authors wish to thank Katharina Fuchs for help with FACS analysis, and Alejandro Carpy for advice on protein copy number analysis. We also wish to thank the Juniorprofessoren-Programm of the BW-Stiftung, the PRIME-XS Consortium, the German Research Foundation (DFG) and the SFB-766 for funding. The mass spectrometry proteomics data have been deposited to the ProteomeXchange Consortium (<http://proteomecentral.proteomexchange.org>) via the PRIDE partner repository with the dataset identifier PXD001648.

SUPPLEMENTARY MATERIAL

The Supplementary Material for this article can be found online at: <http://www.frontiersin.org/journal/10.3389/fmicb.2015.00103/abstract>

REFERENCES

Abersold, R., and Mann, M. (2003). Mass spectrometry-based proteomics. *Nature* 422, 198–207. doi: 10.1038/nature01511

- Benjamini, Y., and Hochberg, Y. (1995). Controlling the false discovery rate: a practical and powerful approach to multiple testing. *J. R. Statist. Soc. B* 57, 289–300.
- Berghoff, B. A., Konzer, A., Mank, N. N., Looso, M., Rische, T., Förstner, K. U., et al. (2013). Integrative “omics”-approach discovers dynamic and regulatory features of bacterial stress responses. *PLoS Genet.* 9:e1003576. doi: 10.1371/journal.pgen.1003576
- Bernhardt, J., Weibezahn, J., Scharf, C., and Hecker, M. (2003). *Bacillus subtilis* during feast and famine: visualization of the overall regulation of protein synthesis during glucose starvation by proteome analysis. *Genome Res.* 13, 224–237. doi: 10.1101/gr.905003
- Boersem, P. J., Geiger, T., Wiśniewski, J. R., and Mann, M. (2013). Quantification of the N-glycosylated secretome by super-silac during breast cancer progression and in human blood samples. *Mol. Cell. Proteomics* 12, 158–171. doi: 10.1074/mcp.M112.023614
- Braun, V. (1975). Covalent lipoprotein from the outer membrane of *Escherichia coli*. *Biochim. Biophys. Acta* 415, 335–377. doi: 10.1016/0304-4157(75)90013-1
- Buttke, T. M., and Ingram, L. O. N. (1978). Mechanism of ethanol-induced changes in lipid composition of *Escherichia coli*: inhibition of saturated fatty acid synthesis *in vivo*. *Biochemistry* 17, 637–644. doi: 10.1021/bi00597a012
- Carpy, A., Krug, K., Graf, S., Koch, A., Popic, S., Hauf, S., et al. (2014). Absolute proteome and phosphoproteome dynamics during the cell cycle of fission yeast. *Mol. Cell. Proteomics* 13, 1925–1936. doi: 10.1074/mcp.M113.035824
- Clark, D. P., and Beard, J. P. (1979). Altered phospholipid composition in mutants of *Escherichia coli* sensitive or resistant to organic solvents. *J. Gen. Microbiol.* 113, 267–274. doi: 10.1099/00221287-113-2-267
- Cox, J., and Mann, M. (2008). MaxQuant enables high peptide identification rates, individualized p.p.b.-range mass accuracies and proteome-wide protein quantification. *Nat. Biotechnol.* 26, 1367–1372. doi: 10.1038/nbt.1511
- Cox, J. R., Neuhauser, N., Michalski, A., Scheltema, R. A., Olsen, J. V., and Mann, M. (2011). Andromeda: a peptide search engine integrated into the maxquant environment. *J. Proteome Res.* 10, 1794–1805. doi: 10.1021/pr101065j
- Deeb, S. J., D’Souza, R. C. J., Cox, J., Schmidt-Supprian, M., and Mann, M. (2012). Super-silac allows classification of diffuse large b-cell lymphoma subtypes by their protein expression profiles. *Mol. Cell. Proteomics* 11, 77–89. doi: 10.1074/mcp.M111.015362
- Farrell, M. J., and Finkel, S. E. (2003). The growth advantage in stationary-phase phenotype conferred by rpoS mutations is dependent on the pH and nutrient environment. *J. Bacteriol.* 185, 7044–7052. doi: 10.1128/JB.185.24.7044-7052.2003
- Feng, Y., and Cronan, J. E. (2009). *Escherichia coli* unsaturated fatty acid synthesis: complex transcription of the fabA gene and *in vivo* identification of the essential reaction catalyzed by FabB. *J. Biol. Chem.* 284, 29526–29535. doi: 10.1074/jbc.M109.023440
- Finkel, S. E. (2006). Long-term survival during stationary phase: evolution and the GASP phenotype. *Nat. Rev. Microbiol.* 4, 113–120. doi: 10.1038/nrmicro1340
- Geiger, T., Cox, J., Ostasiewicz, P., Wisniewski, J. R., and Mann, M. (2010). Super-SILAC mix for quantitative proteomics of human tumor tissue. *Nat. Methods* 7, 383–385. doi: 10.1038/nmeth.1446
- Geiger, T., Wehner, A., Schaab, C., Cox, J., and Mann, M. (2012). Comparative proteomic analysis of eleven common cell lines reveals ubiquitous but varying expression of most proteins. *Mol. Cell. Proteomics* 11:M111.014050. doi: 10.1074/mcp.M111.014050
- Gouw, J., Tops, B. J., and Krijgsveld, J. (2011). Metabolic labeling of model organisms using heavy nitrogen (¹⁵N). *Methods Mol. Biol.* 753, 29–42. doi: 10.1007/978-1-61779-148-2_2
- Grant, A. W., Steel, G., Waugh, H., and Ellis, E. M. (2003). A novel aldo-keto reductase from *Escherichia coli* can increase resistance to methylglyoxal toxicity. *FEMS Microbiol. Lett.* 218, 93–99. doi: 10.1111/j.1574-6968.2003.tb11503.x
- Hubner, N. C., Ren, S., and Mann, M. (2008). Peptide separation with immobilized pI strips is an attractive alternative to in-gel protein digestion for proteome analysis. *Proteomics* 8, 4862–4872. doi: 10.1002/pmic.200800351
- Huffer, S., Clark, M. E., Ning, J. C., Blanch, H. W., and Clark, D. S. (2011). Role of alcohols in growth, lipid composition, and membrane fluidity of yeasts, bacteria, and archaea. *Appl. Environ. Microbiol.* 77, 6400–6408. doi: 10.1128/AEM.00694-11
- Ingram, L. O. (1976). Adaptation of membrane lipids to alcohols. *J. Bacteriol.* 125, 670–678.
- Ingram, L. O. (1990). Ethanol tolerance in bacteria. *Crit. Rev. Biotechnol.* 9, 305–319. doi: 10.3109/07388558909036741
- Ishihama, Y., Rappsilber, J., and Mann, M. (2006). Modular stop and go extraction tips with stacked disks for parallel and multidimensional Peptide fractionation in proteomics. *J. Proteome Res.* 5, 988–994. doi: 10.1021/pr050385q
- Kraxenberger, T., Fried, L., Behr, S., and Jung, K. (2012). First insights into the unexplored two-component system YehU/YehT in *Escherichia coli*. *J. Bacteriol.* 194, 4272–4284. doi: 10.1128/JB.00409-12
- Lacour, S., and Landini, P. (2004). SigmaS-dependent gene expression at the onset of stationary phase in *Escherichia coli*: function of sigmaS-dependent genes and identification of their promoter sequences. *J. Bacteriol.* 186, 7186–7195. doi: 10.1128/JB.186.21.7186-7195.2004
- Lee, K. J., Bae, S. M., Lee, M. R., Yeon, S. M., Lee, Y. H., and Kim, K. S. (2006). Proteomic analysis of growth phase-dependent proteins of *Streptococcus pneumoniae*. *Proteomics* 6, 1274–1282. doi: 10.1002/pmic.200500415
- Li, G. W., Burkhardt, D., Gross, C., and Weissman, J. S. (2014). Quantifying absolute protein synthesis rates reveals principles underlying allocation of cellular resources. *Cell* 157, 624–635. doi: 10.1016/j.cell.2014.02.033
- Lund, R. R., Terp, M. G., Lænkholm, A.-V., Jensen, O. N., Leth-Larsen, R., and Ditzel, H. J. (2012). Quantitative proteomics of primary tumors with varying metastatic capabilities using stable isotope-labeled proteins of multiple histogenic origins. *Proteomics* 12, 2139–2148. doi: 10.1002/pmic.201100490
- Milo, R. (2013). What is the total number of protein molecules per cell volume? A call to rethink some published values. *Bioessays* 35, 1050–1055. doi: 10.1002/bies.201300066
- Nystrom, T. (2004). Stationary-phase physiology. *Annu. Rev. Microbiol.* 58, 161–181. doi: 10.1146/annurev.micro.58.030603.123818
- Okochi, M., Kurimoto, M., Shimizu, K., and Honda, H. (2007). Increase of organic solvent tolerance by overexpression of manXYZ in *Escherichia coli*. *Appl. Microbiol. Biotechnol.* 73, 1394–1399. doi: 10.1007/s00253-006-0624-y
- Olsen, J. V., Vermeulen, M., Santamaria, A., Kumar, C., Miller, M. L., Jensen, L. J., et al. (2010). Quantitative phosphoproteomics reveals widespread full phosphorylation site occupancy during mitosis. *Sci. Signal.* 3, ra3. doi: 10.1126/scisignal.2000475
- Ong, S. E., Blagoev, B., Kratchmarova, I., Kristensen, D. B., Steen, H., Pandey, A., et al. (2002). Stable isotope labeling by amino acids in cell culture, SILAC, as a simple and accurate approach to expression proteomics. *Mol. Cell. Proteomics* 1, 376–386. doi: 10.1074/mcp.M200025-MCP200
- Rappsilber, J., Mann, M., and Ishihama, Y. (2007). Protocol for micro-purification, enrichment, pre-fractionation and storage of peptides for proteomics using StageTips. *Nat. Protocols* 2, 1896–1906. doi: 10.1038/nprot.2007.261
- Richarme, G., and Caldas, T. D. (1997). Chaperone properties of the bacterial periplasmic substrate-binding proteins. *J. Biol. Chem.* 272, 15607–15612. doi: 10.1074/jbc.272.25.15607
- Rutherford, B. J., Dahl, R. H., Price, R. E., Szmidt, H. L., Benke, P. I., Mukhopadhyay, A., et al. (2010). Functional genomic study of exogenous n-butanol stress in *Escherichia coli*. *Appl. Environ. Microbiol.* 76, 1935–1945. doi: 10.1128/AEM.02323-09
- Savitski, M. M., Nielsen, M. L., and Zubarev, R. A. (2006). ModifiComb, a new proteomic tool for mapping substoichiometric post-translational modifications, finding novel types of modifications, and fingerprinting complex protein mixtures. *Mol. Cell. Proteomics* 5, 935–948. doi: 10.1074/mcp.T500034-MCP200
- Schwanhauser, B., Busse, D., Li, N., Dittmar, G., Schuchhardt, J., Wolf, J., et al. (2011). Global quantification of mammalian gene expression control. *Nature* 473, 337–342. doi: 10.1038/nature10098
- Schweppe, D. K., Rigas, J. R., and Gerber, S. A. (2013). Quantitative phosphoproteomic profiling of human non-small cell lung cancer tumors. *J. Proteomics* 91, 286–296. doi: 10.1016/j.jprot.2013.07.023
- Soares, N. C., Spat, P., Krug, K., and Macek, B. (2013). Global dynamics of the *Escherichia coli* proteome and phosphoproteome during growth in minimal medium. *J. Proteome Res.* 12, 2611–2621. doi: 10.1021/pr3011843
- Soufi, B., Kumar, C., Gnad, F., Mann, M., Mijakovic, I., and Macek, B. (2010). Stable isotope labeling by amino acids in cell culture (SILAC) applied to quantitative proteomics of *Bacillus subtilis*. *J. Proteome Res.* 9, 3638–3646. doi: 10.1021/pr100150w
- Weiner, L., and Model, P. (1994). Role of an *Escherichia coli* stress-response operon in stationary-phase survival. *Proc. Natl. Acad. Sci. U.S.A.* 91, 2191–2195. doi: 10.1073/pnas.91.6.2191
- Woodruff, L. B., Pandhal, J., Ow, S. Y., Karimpour-Fard, A., Weiss, S. J., Wright, P. C., et al. (2013). Genome-scale identification and characterization of ethanol tolerance genes in *Escherichia coli*. *Metab. Eng.* 15, 124–133. doi: 10.1016/j.ymben.2012.10.007

Zambrano, M. M., and Kolter, R. (1996). GASping for life in stationary phase. *Cell* 86, 181–184. doi: 10.1016/S0092-8674(00)80089-6

Conflict of Interest Statement: The Guest Associate Editor Ivan Mijakovic declares that, despite having coauthored an article with the authors Boris Macek and Karsten Krug in 2014, the review process was handled objectively. The authors declare that the research was conducted in the absence of any commercial or financial relationships that could be construed as a potential conflict of interest.

Received: 28 November 2014; accepted: 27 January 2015; published online: 18 February 2015.

Citation: Soufi B, Krug K, Harst A and Macek B (2015) Characterization of the E. coli proteome and its modifications during growth and ethanol stress. *Front. Microbiol.* 6:103. doi: 10.3389/fmicb.2015.00103

This article was submitted to *Microbial Physiology and Metabolism*, a section of the journal *Frontiers in Microbiology*.

Copyright © 2015 Soufi, Krug, Harst and Macek. This is an open-access article distributed under the terms of the Creative Commons Attribution License (CC BY). The use, distribution or reproduction in other forums is permitted, provided the original author(s) or licensor are credited and that the original publication in this journal is cited, in accordance with accepted academic practice. No use, distribution or reproduction is permitted which does not comply with these terms.



Post-translational modifications are key players of the *Legionella pneumophila* infection strategy

Céline Michard^{1,2,3,4,5} and Patricia Doublet^{1,2,3,4,5} *

¹ Legionella Pathogenesis Group, International Center for Infectiology Research, Université de Lyon, Lyon, France

² INSERM U1111, Lyon, France

³ Ecole Normale Supérieure de Lyon, Lyon, France

⁴ Centre International de Recherche en Infectiologie, Université Lyon 1, Lyon, France

⁵ Centre National de la Recherche Scientifique, UMR5308, Lyon, France

Edited by:

Christophe Grangeasse, Centre National de la Recherche Scientifique, France

Reviewed by:

Buchrieser Carmen, Institut Pasteur, France

Nelson Cruz Soares, University of Cape Town, South Africa

*Correspondence:

Patricia Doublet, Legionella Pathogenesis Group, International Center for Infectiology Research, Université de Lyon, Bat A. Lwoff, 10 rue Dubois, 69622 Villeurbanne cedex, Lyon, France
e-mail: patricia.doublet@univ-lyon1.fr

Post-translational modifications (PTMs) are widely used by eukaryotes to control the enzymatic activity, localization or stability of their proteins. Traditionally, it was believed that the broad biochemical diversity of the PTMs is restricted to eukaryotic cells, which exploit it in extensive networks to fine-tune various and complex cellular functions. During the last decade, the advanced detection methods of PTMs and functional studies of the host–pathogen relationships highlight that bacteria have also developed a large arsenal of PTMs, particularly to subvert host cell pathways to their benefit. *Legionella pneumophila*, the etiological agent of the severe pneumonia legionellosis, is the paradigm of highly adapted intravacuolar pathogens that have set up sophisticated biochemical strategies. Among them, *L. pneumophila* has evolved eukaryotic-like and rare/novel PTMs to hijack host cell processes. Here, we review recent progress about the diversity of PTMs catalyzed by *Legionella*: ubiquitination, prenylation, phosphorylation, glycosylation, methylation, AMPylation, and de-AMPylation, phosphocholination, and de-phosphocholination. We focus on the host cell pathways targeted by the bacteria catalyzed PTMs and we stress the importance of the PTMs in the *Legionella* infection strategy. Finally, we highlight that the discovery of these PTMs undoubtedly made significant breakthroughs on the molecular basis of *Legionella* pathogenesis but also lead the way in improving our knowledge of the eukaryotic PTMs and complex cellular processes that are associated to.

Keywords: post-translational modification, *Legionella pneumophila*, Dot/Icm effectors, host cell pathways hijacking, *Legionella* virulence

INTRODUCTION

Post-translational modifications (PTMs) are widely used by eukaryotes to control quickly, locally and specifically the enzymatic activity, localization or stability of their proteins, and thus to fine-tune key factors of the cellular biology to environmental changes. Eukaryotic PTMs involve diverse modifications of specific residues of the protein by the covalent addition of simple or complex chemical groups; they include the addition of chemical group (e.g., phosphate, methyl, or acetate), more complex molecules (e.g., carbohydrates or lipids), the covalent linkage of small proteins (e.g., ubiquitin), and the irreversible hydrolysis of a specific peptide bond between two amino acids, or proteolysis (for review, see Walsh et al., 2005). PTMs are catalyzed by specific enzymes and most of them are reversed by antagonistic catalytic activities. Traditionally, it was believed that the broad biochemical diversity of the PTMs is restricted to complex eukaryotic cells, which exploit it in extensive networks to control various and complex cellular functions. During the last decade, the advanced detection methods of PTMs, including the modified peptides enrichment combined with high accuracy mass spectrometry, the pathogen genomes sequencing that predicts PTMs activities, and the functional studies of the host–pathogen relationships highlight that bacteria have also developed

a large arsenal of PTMs, particularly to subvert host cell pathways to their benefit, to escape to the host defences, and finally to promote their replication (for review, see Ribet and Cossart, 2010a,b).

Legionella pneumophila, the etiological agent of the severe pneumonia legionellosis, is a paradigm of highly adapted intravacuolar pathogens that have set up sophisticated biochemical strategies to hijack host cell processes. *Legionella* pathogenic strains (i) emerge from the environment after intracellular multiplication in protozoans, especially in amoebae; (ii) are disseminated by contaminated aerosols; and (iii) can infect alveolar macrophages of its accidental human host. Within environmental phagocytic cells and human macrophages, *L. pneumophila* evades endocytic degradation (Horwitz and Maxfield, 1984; Clemens et al., 2000), controls the innate immune response, especially the NF- κ B pathway (Schmeck et al., 2007; Shin et al., 2008), and triggers the biogenesis of a *Legionella*-containing vacuole (LCV), a rough endoplasmic reticulum-like compartment permissive for its intracellular replication (Horwitz, 1983; Kagan and Roy, 2002). Crucial for hijacking host cell vesicle trafficking necessary for LCV biogenesis, and subsequently for intracellular multiplication of *L. pneumophila*, is the Dot/Icm Type 4 Secretion System (T4SS; Marra et al., 1992; Andrews et al., 1998) that

translocates into the host cell cytosol over 275 bacterial proteins, named effectors (Zhu et al., 2011). Many Dot/Icm effectors harbor eukaryotic domains (Cazalet et al., 2004), such as protein–protein interaction domains and enzymatic activity-associated domains, in particular for PTMs such as methylation, phosphorylation, ubiquitination, and glycosylation, which support that *L. pneumophila* has evolved eukaryotic-like PTMs to hijack host cell processes.

Here, we review recent progress about the diversity of PTMs catalyzed by *Legionella*. We focus on the host cell pathways targeted by the bacteria-catalyzed PTMs and we stress the importance of the PTMs in the *Legionella* infection strategy.

DIVERSITY OF PTMs CATALYZED BY *L. pneumophila*

A key finding of the *L. pneumophila* genome analysis was the identification of a large number of proteins similar to eukaryotic proteins. The wide variety of these proteins includes enzymatic activity-associated domains for various PTMs such as phosphorylation, glycosylation, methylation, prenylation, ubiquitination, reversible AMPylation, and phosphocholination of host cell proteins to modulate cellular functions (Table 1).

PROTEIN PHOSPHORYLATION

Phosphorylation–dephosphorylation of proteins represents a powerful regulatory mechanism of cellular activity. Indeed, intensive research has revealed that eukaryotes contain numerous interconnected signal transduction networks in which protein phosphorylation plays a dominant role for controlling essential functions, such as growth, cell cycle and apoptosis, in response to extracellular stimuli and stresses. It consists in the reversible covalent addition of a phosphate group, from the phosphate donor ATP, to specific residues of a target protein, the most frequent being hydroxyl groups of serine, threonine or tyrosine residues. The phosphoester bond is catalyzed by eukaryotic protein kinases that share a common catalytic domain characterized by 11 conserved Hanks's subdomains (Hanks, 2003). Conversely, phosphatases hydrolyze the phosphoester bond, thereby releasing the phosphate group and restoring the acceptor amino acid in its unphosphorylated form.

The genomes of the six sequenced *L. pneumophila* strains, Philadelphia, Lens, Paris, Corby, Alcoy, and 130b, have been reported to encode four putative eukaryotic-like serine/threonine kinases, named LegK1–LegK4 (Cazalet et al., 2004; de Felipe et al., 2005; D'Auria et al., 2010; Schroeder et al., 2010). Alignment with several eukaryotic protein kinases revealed residues that are highly conserved in the Hanks' subdomains, including the glycine-rich loop and the invariant lysine in subdomains I and II, which are essential for binding and correct orientation of the phosphate donor ATP. *In vitro* phosphorylation assays confirmed that these kinases were functional for autophosphorylation and/or phosphorylation of the classical substrate for eukaryotic kinases Myelin-basic protein (Hervet et al., 2011; Table 1).

PROTEIN ALKYLATION

Protein alkylation consists in the addition of alkyl substituents on specific amino acids. The common alkyl groups transferred are the methyl (C1) or the C15 (farnesyl)/C20 (geranyl–geranyl) isoprenyl

groups, leading to protein methylation and protein prenylation, respectively.

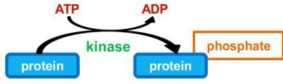

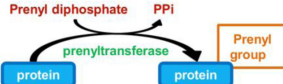
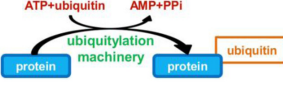
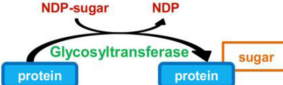
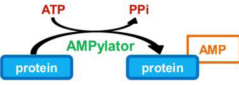
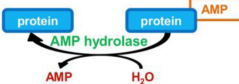
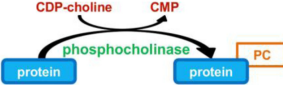

Protein methylation typically takes place on arginine or lysine residues in the protein sequence. Arginine can be methylated once or twice, with either both methyl groups on one terminal nitrogen (asymmetric dimethylated arginine) or one on both nitrogens (symmetric dimethylated arginine) by peptidylarginine methyltransferases (PRMTs). Lysine can be methylated once, twice, or three times by lysine methyltransferases (Walsh et al., 2005). Protein methylation has been extensively studied in the histones. The transfer of methyl groups from S-adenosyl methionine (SAM) to histones is catalyzed by SET domain-containing proteins. This protein family is characterized by an ~130 amino acid-long SET domain that possesses catalytic activity toward the ϵ -amino group of lysine residues. *In vivo*, lysine methylation can be dynamically regulated by the opposing actions of lysine methyltransferases and lysine demethylases (Herz et al., 2013). *L. pneumophila* genome analysis revealed that all the five strains Philadelphia, Lens, Paris, Corby, and Alcoy encode each an orthologous protein encoding a SET domain that show 95–100% sequence identity over the entire length (Cazalet et al., 2004). *In vitro* assays recently demonstrated that Lpp1683 in Paris strain and Lpg1718 in Philadelphia strain, display histone methyltransferase activity toward the histone H3 substrate (Li et al., 2013; Rolando et al., 2013b; Table 1).

Prenylation, i.e., addition of a farnesyl (C15) or a geranyl–geranyl (C20) group, is a PTM that covalently links a lipid moiety at the cysteine residue of the CAAX motif in the C-terminal region of proteins (where C represents cysteine and A an aliphatic amino acids). The Ras GTPases, Rab small GTPases, and protein kinases superfamilies have members that can be prenylated on cysteine thiolate side chains. The lipid anchors drive the modified proteins to partition more to membranes, thus controlling their subcellular localization (Walsh et al., 2005). Interestingly, bioinformatic approaches identified 11–12 (depending on the strains) different *Legionella* proteins containing a CAAX motif in the C terminus, which have been so called Pel proteins for Prenylated effectors of *Legionella* (Ivanov et al., 2010; Price et al., 2010a,b). Six of these proteins had highly conserved homologs across all *Legionella* strains, whereas four of the proteins were unique for either the Philadelphia or Lens strain. Host farnesyltransferase and class I geranylgeranyltransferase were both involved in the lipidation of the *Legionella* CAAX motif proteins, among which AnkB from *L. pneumophila* AA100 and Philadelphia Lp01 (Ivanov et al., 2010; Price et al., 2010a,b; Table 1).

PROTEIN UBIQUITINATION

Ubiquitination consists in the addition of one or several ubiquitins on a target protein, most frequently on lysine residue, although linkages on cysteine, serine or threonine, or on the N-terminal amino group have also been reported. Ubiquitin is a small protein of 9 kDa, which contains itself seven lysines; all of these lysine residues can be used as a target for the addition of another ubiquitin moiety, thus leading to polyubiquitination. Polyubiquitin chains built up through Lys48 side chains are commonly associated with proteasome binding and degradation of the modified protein, whereas chains tethered through

Table 1 | Diversity of PTMs catalyzed by Dot/Icm effectors of *Legionella pneumophila*.

PTMs	Mechanism	Effector name	Motif	Target	Reference
Phosphorylation		LegK1 LegK2 LegK3 LegK4	STPK STPK STPK STPK	IκB	Ge et al. (2009), Hervet et al. (2011) Hervet et al. (2011) Hervet et al. (2011) Hervet et al. (2011)
Methylation		LegAS4/RomA	SET domain	H3	Li et al. (2013), Rolando et al. (2013b)
Prenylation		AnkB /LegAU13 /Ceg27	CAAX		Price et al. (2010a)
Ubiquitination		LubX /LegU2 AnkB /LegAU13 /Ceg27 LegU1 SidC	U-box F-box F-box	Clk1 /SidH Skp1/ParvB BAT3	Kubori et al. (2008) Price et al. (2009), Lomma et al. (2010) Ensminger and Isberg (2010) Hsu et al. (2014)
Glycosylation		Lgt1 Lgt2 Lgt3 /Legc5 SetA	Coiled- coil Coiled- coil Coiled- coil	eEF1A eEF1A eEF1A	Belyi et al. (2006) Belyi et al. (2008), Aktories (2011) Belyi et al. (2008), Aktories (2011) Heidtman et al. (2009)
AMPylation		SidM /DrrA		Rab1	Müller et al. (2010)
DeAMPylation		SidD		Rab1	Neunuebel et al. (2011), Tan et al. (2011)
Phosphocholination		AnkX /AnkN /LegA8	Ankyrin	Rab1	Mukherjee et al. (2011)
Dephosphocholination		Lem3		Rab1	Tan et al. (2011)

STPK, Ser/Thr protein kinase.

Lys63 participate in signal transduction, vesicular trafficking or DNA repair (Hochstrasser, 2009). The conjugation of ubiquitin requires different enzymes (**Figure 1**): E1 activating enzymes that bind ubiquitin in a ATP dependent manner; E2 conjugation enzymes that bind ubiquitin in a thioester bond; E3 ubiquitin ligases are then required to catalyze the efficient transfer of the

activated ubiquityl protein tag to Lys side chains of target proteins. There are two different families of E3 ubiquitin ligases, the HECT family and the RING/U-Box family. In the RING family, some of the enzyme 3 are multicomponent catalysts, such as the SCF E3s that consist in four subunits: the invariable subunit Skp1, the central core component Cullin, the RING finger

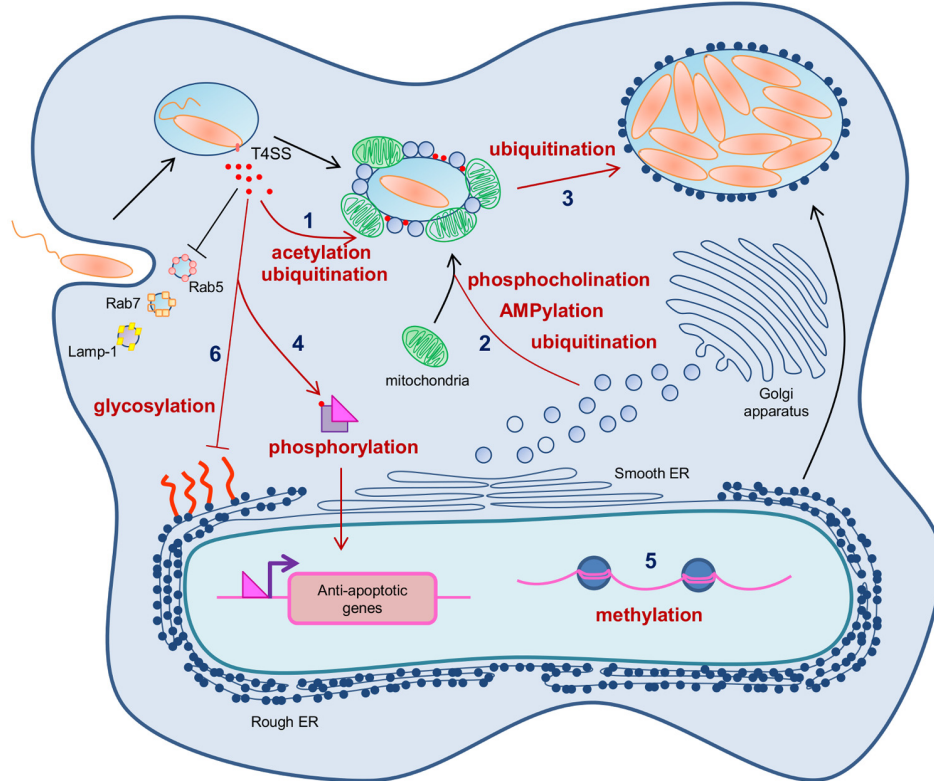


FIGURE 2 | Post-translational modifications controlling various infectious cycle steps of *Legionella pneumophila*. Immediately after uptake of the bacteria, *L. pneumophila* secretes a high number of Dot/Icm effectors into the host cell cytosol. (1) *L. pneumophila* exploits the host prenylation apparatus to alkylate some of these effectors and target them to the LCV surface. The effector LubX is able to ubiquitinate some effectors thus addressing them to proteasomal degradation and controlling their temporal presence on the LCV during infection. (2) Four Dot/Icm effectors reversibly AMPylate and phosphocholinate the host Rab1 small GTPase, thus controlling its activity to promote ER recruitment on the LCV, a prerequisite feature to make the phagosome a replicative niche. SidC and its paralog SdcA monoubiquitinate Rab1 and catalyze

polyubiquitin chains formation necessary for ER recruitment on the LCV. (3) The Dot/Icm effector AnkB functions as a platform for the docking of polyubiquitinated proteins to the LCV membrane, thus promoting proteasome-mediated generation of free amino acids essential as energy and carbon sources for *L. pneumophila* intracellular proliferation. (4) The Dot/Icm effector LegK1 phosphorylates IκB, thus mimicking the host IKKs, and triggering the activation of the NF-κB pathway and the transcription of NF-κB dependent genes. (5) The Dot/Icm effector LegAS4/RomA trigger the methylation of the histone H3, thus inducing epigenetic changes and subsequent transcriptional control of host genes. (6) Several Dot/Icm effectors exhibit glycosidase activity toward eEF1A, thus inhibiting the host cell translation.

exhibits structural similarities with the C-terminal domain of the glutamine synthase adenylyl transferase, which leads the authors to speculate that the N-terminal region of SidM might have AMPylase activity toward the small GTPase Rab1, the substrate of its GEF domain. Indeed, *in vitro* assays and mass spectrometry analysis demonstrates that SidM, more precisely its N-terminal domain, AMPylates Rab1 on the Tyr77 residue (Müller et al., 2010; Table 1).

AMPylation is a reversible process. Two independent groups simultaneously identified SidD from *L. pneumophila* as the first protein exhibiting a deAMPyase activity, by using two distinct approaches. Neunuebel et al. (2011) observed that a whole cell lysate from *L. pneumophila* but not from *E. coli* efficiently removes *in vitro* radiolabeled AMP from AMPylated Rab1. Given that genes of functionally linked proteins tend to be clustered on bacterial genomes, they deleted the immediately nearby *sidM* gene, namely *sidD* gene, and they observed that the whole cell lysate from the *sidD* mutant was not able anymore to deAMPyate SidM

(Neunuebel et al., 2011). On the other hand, Tan and Luo identified SidD as a protein capable of suppressing the toxicity of the AMPylase SidM to yeast (Tan and Luo, 2011). Both groups demonstrated that SidD removes the AMP moiety from Tyr77 of Rab1, thus reversing the effect of SidM on this small GTPase activity (Table 1).

REVERSIBLE PHOSPHOCHOLINATION

As mentioned above, the Fic domain is associated to enzymes that trigger AMPylation of target proteins. *In silico* analysis revealed that another protein from *L. pneumophila*, namely AnkX, contains a Fic domain. However, mass spectrometry demonstrated that AnkX promotes a novel PTM, namely phosphocholination rather than AMPylation (Mukherjee et al., 2011). Phosphocholination consists in the covalent link of a phosphocholine group to a serine residue (Table 1). More precisely, AnkX catalyzes the phosphocholination of Ser76 of the small GTPase Rab1, immediately upstream the Tyr77 AMPylated by SidM (Mukherjee et al., 2011).

Like AMPylation, phosphocholination is a reversible PTM. Tan et al. (2011) recently identified the Dot/Icm effector Lem3 as a protein capable to rescue the growth of yeast transformed by AnkX expression vector, which suggested that Lem3 was able to antagonize the activity of phosphocholination of AnkX. Indeed, *in vitro* assays demonstrated that Lem3 reverses the AnkX-dependent phosphocholination of Rab1 by removing the phosphocholine moiety from Rab1 (Tan et al., 2011; **Table 1**).

PTMs FOR *Legionella* CONTAINING VACUOLE BIOGENESIS

Legionella-containing vacuole biogenesis is a main trait of *Legionella* intracellular fate that allows the bacteria to generate a niche permissive for intracellular replication. Within 15 min of uptake, the LCV is surrounded and fused with ER-derived smooth vesicles and mitochondria (Horwitz, 1983), and 4 h post-contact it is decorated by host cell ribosomes (Horwitz and Silverstein, 1981; Roy and Tilney, 2002), thus resulting in a replication-permissive vacuole (**Figure 2**). *Legionella*-containing vacuole biogenesis mobilizes complex molecular mechanisms that are strictly dependent on the Dot/Icm T4SS and its exceptionally high number of effectors. PTMs of both host cell proteins and Dot/Icm effectors play a key role in the fine-tuned orchestration of this infection step.

Dot/Icm EFFECTORS ACETYLATION AND UBIQUITINATION SPATIO-TEMPORALLY CONTROL THEIR RECRUITMENT ON THE LCV

Given the high number of effectors, it could be assumed that both translocation into the host cell cytosol, organelles addressing, and degradation of each effector must be controlled such that it could sequentially participate to the LCV biogenesis. Many Dot/Icm effectors are targeted to the LCV surface. *L. pneumophila* uses [PI(4)P] to anchor some Dot/Icm substrates, such as SidC and SidM to the cytoplasmic face of LCV (Ragaz et al., 2008; Brombacher et al., 2009). Another way for *L. pneumophila* to address injected effectors to the LCV membrane, is the exploitation of the host cell prenylation apparatus (Ivanov et al., 2010; Price et al., 2010a). The Dot/Icm substrate AnkB, of strains *L. pneumophila* AA100 and Philadelphia Lp01, contains a CAAX motif. During infection, the CAAX motif of AnkB is modified by the host farnesylation machinery (Ivanov et al., 2010; Price et al., 2010a). Expression of a CAAX substituted-variant results in defective anchoring of AnkB to the LCV, severe defects in intracellular replication, and attenuation of intrapulmonary proliferation in a mouse model, thus demonstrating that the farnesyl-dependent vacuolar location of AnkB is essential to its role in the infectious cycle of *L. pneumophila* (Price et al., 2009).

In addition to the appropriate addressing of Dot/Icm effectors, a specific temporal control of their stability in the host cell is carried out during *L. pneumophila* infection. In that purpose, *L. pneumophila* interferes with the ubiquitin system to address some effectors to proteasomal degradation. LubX is a Dot/Icm effector containing two U-box domains and functions as a E3 ubiquitin ligase toward the cellular Clk1 protein. However, cellular consequences of ubiquitination of Clk1 remain unknown (Kubori et al., 2008). LubX was also shown to bind and polyubiquitinate *in vitro* SidH, another Dot/Icm effector. It mediates proteasomal

degradation of SidH in infected cells. Thus, LubX is considered like a metaeffector that controls in space and time, the presence of another effector, by using ubiquitination PTM (Kubori et al., 2010).

AMPylation AND PHOSPHOCHOLINATION CONTROLS THE GTPase Rab1 ACTIVATION FOR ER RECRUITMENT ON THE LCV

One main characteristic of the LCV is that it is fused with ER-derived vesicles. The manipulation of host cell vesicular trafficking by *L. pneumophila* is strictly dependent of the Dot/Icm T4SS. In particular, some of Dot/Icm substrates target host cell small GTPases. Among them, the effector SidM interacts with Rab1, and its GEF and GDI activities result in Rab1 release from GDI (Ingmundson et al., 2007), and in LCV membrane associated GTP-coupled Rab1 (Arasaki et al., 2012), respectively (**Figure 3**). An additional PTM-associated enzymatic activity of the multifunctional protein SidM has recently been revealed. The N-terminal domain of SidM, which exhibits similarities with the catalytic domain of glutamin synthetase adenyl transferase, modifies the tyrosine 77 of Rab1 by AMPylation or adenylation, i.e., the addition of a AMP moiety (Müller et al., 2010). This PTM inhibits GAP-stimulated GTP hydrolysis, thus locking Rab1 in the GTP-bound active state, and finally allows ER recruitment at the surface of the LCV (**Figure 3**).

The activation of Rab1 by SidM is counteracted by two others Dot/Icm effectors, SidD and LepB (**Figure 3**). SidD removes AMP from Tyr77 of Rab1 (Neunuebel et al., 2011; Tan and Luo, 2011) by a protein phosphatase-like catalytic mechanism, as suggested by structural analysis (Rigden, 2011). DeAMPylation of Rab1 makes it accessible for GAP activities, such as that exhibited by LepB. Despite any similarity with eukaryotic Rab-GAPs, LepB harbors a Rab1-specific GAP activity that promotes GTP hydrolysis and subsequent removal of Rab1 from the LCV (Ingmundson et al., 2007; Mihai Gazdag et al., 2013). Consistent with the SidD-dependent action of LepB, the phenotype of a *lepB* mutant is similar to that of a *sidD* mutant, i.e., a prolonged localization of Rab1 on the LCV (Neunuebel et al., 2011).

Two additional Dot/Icm effectors target the Rab1 GTPase for PTM and participate to the temporal control of its activation during *Legionella* infection cycle. AnkX harbors a novel PTM activity, namely phosphocholination, that transfers a phosphocholine moiety from CDP-choline to serine 76 of Rab1, preceding the SidM-modified tyrosine (Mukherjee et al., 2011; **Figure 3**). Although the biological effect of this PTM of Rab1 is not completely deciphered, it results in the same biochemical consequence as the SidM-mediated AMPylation, i.e., locking Rab1 in the active form. Like AMPylation, phosphocholination is reversible. The Dot/Icm effector Lem3 has been recently shown to possess an antagonistic activity to that of AnkX by removing the phosphocholine from the Ser76 of Rab1 (Tan et al., 2011; Goody et al., 2012). Thus, Rab1 is directly targeted and its activity is controlled by four different Dot/Icm effectors that catalyze different PTMs.

It is noteworthy that ubiquitination, mediated by the Dot/Icm effectors SidC and SdcA, could also participate to ER recruitment on the LCV. The Dot/Icm effector SidC and its paralog SdcA were

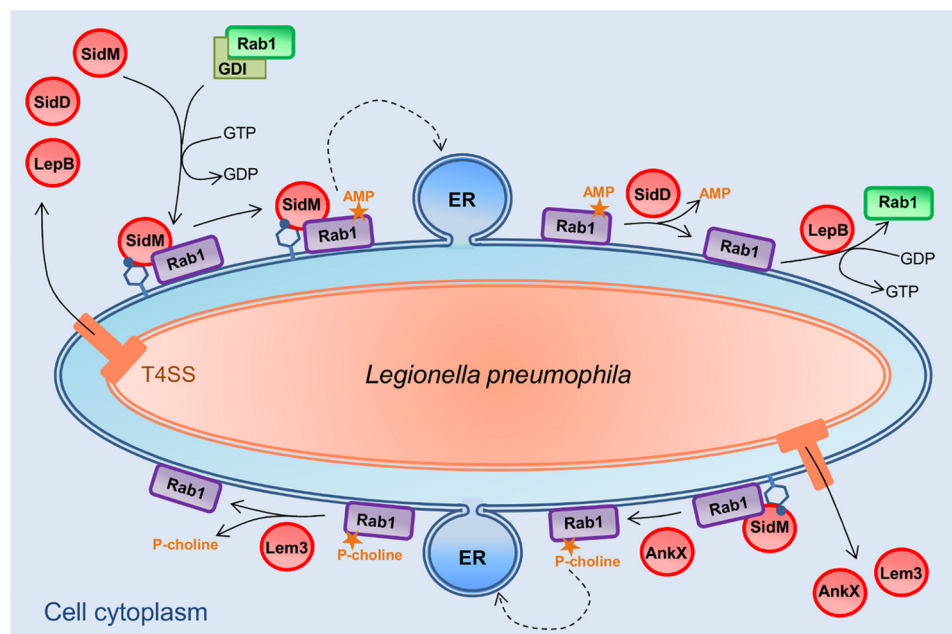


FIGURE 3 | Post-translational modifications of small GTPase Rab1 by *L. pneumophila* for LCV biogenesis. The ER recruitment on the LCV is orchestrated by four Dot/Icm effectors-mediated PTMs. SidM releases Rab1 from GDI with its GEF activity. SidM then modifies Rab1 by AMPylation, i.e., the addition of a AMP moiety. This PTM locks Rab1 in the GTP-bound active state, and finally allows ER recruitment at the surface of the LCV. SidD removes AMP from Rab1, making it accessible

for GAP activities, such as that exhibited by LepB. LepB promotes GTP hydrolysis of Rab1, removing it from the LCV. AnkX harbors a novel PTM activity, the phosphocholination, that transfers a phosphocholine moiety to Rab1, resulting in the same effect that the SidM-mediated AMPylation, i.e., locking Rab1 in the active form. The Dot/Icm effector Lem3 possesses an antagonistic activity to that of AnkX by removing the phosphocholine from Rab1.

proposed to function as vesicle fusion tethering factors involved in the recruitment of ER vesicles on the LCV (Luo and Isberg, 2004; Ragaz et al., 2008). Recently, infection by a WT *L. pneumophila* strain was shown to mediate the mono-ubiquitination of Rab1 on lysine 187 (Horenkamp et al., 2014). Given that cells infected with the double mutant *sdca-sidC* did not exhibit this Rab1 PTM, it was assumed that Rab1 ubiquitination required the Dot/Icm effectors SidC and Sdca. However, ectopic expression of SidC or Sdca alone in HEK293 cells did not result in Rab1 ubiquitination, which suggests that neither SidC nor Sdca are E3 ubiquitin ligases. By contrast, another study demonstrated that the N-terminal domain of SidC exhibits ubiquitin ligase activity that catalyzes polyubiquitin chains formation and is necessary for ER recruitment on the LCV (Hsu et al., 2014). According to the authors, SidC does not seem to directly target Rab1 but more likely triggers a remodeling of proteins composition at the surface of the LCV. Although the mono-ubiquitination of Rab1 would be mediated by an indirect unknown mechanism and that the substrates and impact of the SidC/Sdca-catalyzed polyubiquitination remains unclear, both these studies highlight the role of ubiquitination in ER recruitment on the LCV.

UBIQUITINATION OF BAT3 COULD MITIGATE THE EFFECTS OF DISRUPTING NORMAL VESICULAR TRAFFICKING

Legionella pneumophila co-opts host vesicular trafficking during infection, in particular to recruit ER on the LCV. It can be assumed that some Dot/Icm substrates are translocated to protect

host cells against the cytotoxic stress generated by the ER traffic hijacking. Among them, the Dot/Icm effector LegU1 contains an F-box domain and interferes with ubiquitin signaling. It can be integrated into the functional SCF1 complex that confers E3 ubiquitin ligase activity. It specifically targets the host chaperone protein BAT3, a key regulator of the ER stress response. LegU1 associates with BAT3 and mediates its polyubiquitination *in vitro* (Ensminger and Isberg, 2010). Moreover, another translocated *L. pneumophila* protein, Lpg2160, plays a role in this complex by binding both the SCF complex and BAT3. These results suggest that this multicomplex formation leads to BAT3 ubiquitination, probably to modulate the ER stress response during infection (Ensminger and Isberg, 2010).

PTMs FOR SUSTAINING *Legionella* INTRACELLULAR REPLICATION

In the rough ER-like compartment of the LCV, *L. pneumophila* proliferates in a so-called replicative form until vacuolar nutrients become limiting. Polyubiquitination of host cell proteins mediated by a *Legionella* effector has been recently proposed to be a bacterial strategy dedicated to generate sources of carbon and energy needed for microbial proliferation *in vivo* (Price et al., 2011). Indeed, in addition to the CAAX farnesylation motif described above, AnkB from *L. pneumophila* Philadelphia strain harbors two ankyrin (ANK) protein-protein interaction domains and a F-box domain. In both macrophages and protozoa, AnkB functions as a bona fide F-box protein where it recruits Skp1,

thus subverting the host SCF1 complex and functioning as a platform for the docking of polyubiquitinated proteins to the LCV membrane. The polyubiquitinated proteins assembled by AnkB on the LCV are preferentially enriched for Lys48-linked polyubiquitinated proteins, which is a hallmark for proteasomal degradation, that generate 2–24 amino acid peptides (Price et al., 2011). Interestingly, substitution of Lys48 to Arg abolishes the decoration of the LCV with polyubiquitinated proteins and blocks intracellular proliferation. Moreover, inhibition of proteasome, or host amino- and oligo-peptidases that degrade the short peptides generated by proteasomal degradation, blocks intracellular proliferation (Price et al., 2011). However, both inhibitions are bypassed by excess amino acid supplementation. Together these data strongly support that AnkB promotes proteasome-mediated generation of free amino acids essential as energy and carbon sources for *L. pneumophila* intracellular proliferation (Figure 2).

It is noteworthy that in some *L. pneumophila* strains such as the strain Paris, AnkB does not contain the CAAX motif. Given they do not localize to the LCV, these AnkB homologues might not be key effectors of *L. pneumophila* that generate nutrients for intracellular growth. A yeast two-hybrid screen and co-immunoprecipitation analysis identified ParvB as one target of the *L. pneumophila* F-box protein AnkB encoded by strain Paris. ParvB, or affixin, is known to play important roles in focal adhesion, cell spreading and motility. Surprisingly, expression of AnkB led to a decrease of ubiquitination of ParvB. Thus, it was proposed that *L. pneumophila* modulates ubiquitination of ParvB by competing with eukaryotic E3 ligases for the specific protein–protein interaction site of ParvB. However, the role of AnkB in the infectious cycle of *L. pneumophila* strain Paris remains unknown (Lomma et al., 2010).

PTMs FOR CONTROLLING HOST CELL GENES EXPRESSION

PHOSPHORYLATION OF I κ B FOR CONTROLLING THE NF- κ B DEPENDENT GENES TRANSCRIPTION

After phagocytosis, *L. pneumophila* resides and replicates in the LCV within the host cytosol. Consequently, survival of the host cell is necessary for successful replication. To prevent cell death, some Dot/Icm translocated substrates interfere with pro-death pathways (Laguna et al., 2006; Banga et al., 2007). A second mechanism of preventing host cell death during infection is to stimulate the NF- κ B pathway, which results in up-regulation of genes encoding anti-apoptotic proteins (Karin and Lin, 2002). NF- κ B homo- and heterodimers are master transcription regulators of the mammalian innate immune response that control the expression of almost 400 genes (Karin and Lin, 2002; Ahn and Aggarwal, 2005; Hayden and Ghosh, 2008). NF- κ B activation can result from sensing of pathogen associated molecular patterns (PAMPs) by the pattern recognition receptors (PRRs), which leads to activation of I κ B kinases (IKKs). Once activated, IKKs phosphorylate I κ B family members, inhibitory proteins that are bound to NF- κ B subunits in the cell cytoplasm, thus triggering I κ B ubiquitination, I κ B degradation, and subsequent translocation of NF- κ B into the nucleus (Hayden and Ghosh, 2008). *L. pneumophila* infection results in increased Dot/Icm-dependent transcription of NF- κ B subunits as well as NF- κ B regulated genes

including pro-inflammatory cytokines and antagonists of apoptosis (Losick and Isberg, 2006; Abu-Zant et al., 2007; Shin et al., 2008). Besides the engagement of PRRs with PAMPs, direct targeting of the pathway by a Dot/Icm effector, namely LegK1, has been demonstrated (Ge et al., 2009; Figure 2). LegK1 efficiently phosphorylates I κ B on Ser-32 and Ser-36 both *in vitro* and in cells, thus mimicking the host IKKs. Ectopic expression of the protein in mammalian cells results in activation of an NF- κ B-dependent promoter. The kinase activity is necessary for this activation, as a point mutation in the ATP binding domain or a catalytic residue abolishes NF- κ B activity (Ge et al., 2009; Losick et al., 2010), and cell-free reconstitution revealed that LegK1 stimulated NF- κ B activation in the absence of IKKs (Ge et al., 2009).

METHYLATION OF HISTONES FOR CONTROLLING HOST CELL GENE TRANSCRIPTION

Legionella-containing vacuoles are studded with an increasing number of ribosomes during the first 8 h after bacterial internalization, after which the bacteria start to replicate in the vacuole. Besides, transcription of rRNA genes (rDNAs) in the nucleolus is known to be regulated by epigenetic chromatin modifications including histone H3 lysine (de)methylation. Recently, the Dot/Icm LegAS4 from *L. pneumophila* Philadelphia strain was shown to localize in the host nucleolus and promoted rDNA transcription (Li et al., 2013; Figure 2). LegAS4 contains an active SET-domain-sharing 35% sequence identity with eukaryotic NSD2/3 Lys Histone Methyltransferases of the SET2 family. *In vitro* studies on histone H3 substrate, using methylation-specific H3 antibodies, show that LegAS4 catalyses dimethylation of histone H3 on Lys4 (H3K4me2). Consistently, ectopic expression of LegAS4 in human cells is associated with increased levels of H3K4me2 at rDNA promoters and the activation of the transcription of these genes. LegAS4's association with rDNA chromatin is mediated by interaction with host HP1a/c. Docking of LegAS4 to these regions through binding to HP1, and subsequent methylation of H3K4, might convert the epigenetically silent state of rDNA genes to an active state methylated H3. Stimulation of rDNA transcription might contribute to bacterial replication in two flavors. The enforced higher proliferation potential of infected cells, resulting from activation of rDNA transcription, could provide a better niche for bacterial replication. On the other hand, intracellular bacteria could exploit host ribosome activity for its own survival advantages (Li et al., 2013).

Interestingly, mass spectrometry analysis revealed that the equivalent effector of LegAS4 from the *L. pneumophila* strain Paris, named RomA (for regulator of methylation A) trimethylates *in vitro* Lys14 of H3 (H3K14me3), a histone mark not previously described in mammals (Rolando et al., 2013b). This epigenetic mark was confirmed by systematic site-directed mutagenesis of the lysine residues in the N-terminal tail of H3. It is noteworthy that while H3 methylation was almost completely decreased when H3 was mutated on K14, RomA enzymatic activity appeared to be also reduced on H3 carrying a mutated K4. However, no H3K4 methylation was revealed in western-blot probed with anti-H3K4me2 or H3K4me3 antibodies, thus suggesting that RomA

only targets K14 of H3 and that H3K4 methylation could influence H3K14 methylation by being part of the motif required by RomA to bind to its substrate (Rolando et al., 2013b). By promoting a burst of H3K14me₃, RomA decreases H3K14 acetylation, which is an activating mark, thus leading to repression of host gene expression. In addition, ChIP-seq analysis identified 4,870 H3K14 methylated promoter regions, including at innate immune genes, during *Legionella* infection.

Recently, the H3K14-specific methylation was shown to be conserved in cells infected by seven different strains of *L. pneumophila*, including the Philadelphia 1 (Lp02) strain (Rolando and Buchrieser, 2014). Thus, there is more likely no different specificity of the methylation activities of LegAS4 and RomA, and despite slight discrepancies about the biochemistry and the biological effect of these effectors, both these studies highlight the key role of histone PTMs during *Legionella* infection (Figure 2).

GLYCOSYLATION OF EF1A FOR INHIBITING THE HOST CELL TRANSLATION

In addition to controlling the host cell gene transcription, *L. pneumophila* is able to inhibit the overall host cell translation. *L. pneumophila* encodes three Dot/Icm effectors, namely Lgt1, Lgt2, and Lgt3, that monoglycosylate the serine residue Ser53 of the GTPase domain of the host translational factor eEF1A (eukaryotic Elongation Factor 1A), leading to the inhibition of protein synthesis, and consequently to the death of the host cell (Belyi et al., 2006). Although EF1A glycosylation seems to promote *L. pneumophila* pathogenesis, the biological role of this PTM remains to be addressed. Because their activities cause the host cell death, glycosyltransferases are usually considered like bacterial toxins rather than molecular tools that hijack host cell pathways to the benefit of the bacteria. However, it can be assumed that the inhibition of host cell protein synthesis leads to the overall decrease of the host metabolism, which promotes the ability of the bacteria to overcome the cellular response and consequently to replicate (Belyi et al., 2011). Moreover, it has been recently shown that Lgt1, Lgt2, Lgt3 plus two others Dot/Icm effectors, SidI and SidL that respectively, interacts with eEF1A and eEF1B (Shen et al., 2009) and inhibit protein synthesis by an unknown mechanism, are critical to control the host cell transcription response to *Legionella* infection (Fontana et al., 2011). In fact, these Dot/Icm effectors decrease the overall translation of host cell proteins, among which the NF- κ B inhibitor I κ B, thus promoting the activation of the NF- κ B pathway. In that way, glycosylation of eEF1A by these effectors and thus inhibition of host cell translation could potentiate the activation of the NF- κ B pathway, already controlled by the I κ B phosphorylation by LegK1, as described above.

CONCLUSION

Given PTMs play key roles in the cellular biology, it is not surprising that interference with host PTMs is a strategy widely used by bacterial pathogens to not only escape from host cell defences but also to hijack host cell pathways to their benefit. However, recent technological progresses in the detection of PTMs and advanced functional studies of the host–bacteria relationship highlighted an unexpected diversity of the PTMs triggered by bacteria and the

complexity of these processes in host–pathogen interactions, thus making studies of bacteria-mediated PTMs an emerging field of research.

Legionella pneumophila is a paradigm of a pathogenic bacteria that evolved sophisticated biochemical strategies to successfully infect and replicate into professional bacteria killer phagocytic cells. In fact, *L. pneumophila* is a unique example for the co-evolution of a bacterium with environmental hosts, namely amoeba, that results in the acquisition of many genes encoding proteins that can be secreted by the Dot/Icm T4SS and trigger diverse PTMs into the host cells. Indeed, the large repertoire of Dot/Icm effectors enables the bacteria to phosphorylate, alkylate, ubiquitinate, glycosylate, AMPylate, and phosphocholinate specific host cell proteins. Noteworthy, *L. pneumophila* also catalyze PTMs of its own proteins, namely some of Dot/Icm effectors, to control their localization and/or their stability in the host cell, and subsequently their activity during the infection. Importantly, despite PTMs are usually catalyzed by eukaryotic-like proteins, some of them are performed by enzymes that do not exhibit similarity with their eukaryotic counterparts. More interestingly, research on Dot/Icm effectors functional roles lead to the discovery of a new PTM, namely the reversible phosphocholination, that may also be used by eukaryotic cells to modulate cellular functions, as previously suggested by studies that detected phosphoryl-choline substituted peptides secreted by nematodes and from mammalian cells residing in the placenta (Lovell et al., 2007; Grabitzki et al., 2008). AMPylation had been also discovered by studying infections by *V. parahaemolyticus* and *H. somni*, a human pathogen and the causal agent of septicemia in cattle, respectively (Worby et al., 2009; Yarbrough et al., 2009). These discoveries reveal that studies of the relationship between pathogenic bacteria and their host cells could lead the way to improve our knowledge of the eukaryotic PTMs and complex cellular processes that are associated to.

Interestingly, *L. pneumophila* targets host proteins that have been already described to be preferential targeted for bacterial-induced PTMs. This is the case of regulators of the NF- κ B pathway, which allows the bacteria to control both anti-apoptotic genes and host immune response, like previously demonstrated for *Shigella flexneri* (Kim et al., 2005), *Salmonella typhimurium* (Le Nègrate et al., 2008), *L. monocytogenes* (Gouin et al., 2010), and *Yersinia* species (Mittal et al., 2006). Moreover, *L. pneumophila* joins those bacteria that secrete effectors manipulating PTMs at histones tails, allowing a fine-tuned regulation of host genes transcription (Hamon and Cossart, 2008; Bierne, 2013; Rolando et al., 2013a). These recent insights highlight the key role of both these processes and their control by PTMs in the pathogenic bacteria–host relationships.

ACKNOWLEDGMENTS

The Ph.D. grant of Céline Michard was provided by the Programme Avenir Lyon Saint-Etienne (ANR-11-IDEX-0007) of Université de Lyon, within the program “Investissements d’Avenir” operated by the French National Research Agency (ANR). We apologize to authors whose works cannot be cited here because of space limitations.

REFERENCES

- Abu-Zant, A., Jones, S., Asare, R., Suttles, J., Price, C., Graham, J., et al. (2007). Anti-apoptotic signalling by the Dot/Icm secretion system of *L. pneumophila*. *Cell Microbiol.* 9, 246–264. doi: 10.1111/j.1462-5822.2006.00785.x
- Ahn, K. S., and Aggarwal, B. B. (2005). Transcription factor NF-kappaB: a sensor for smoke and stress signals. *Ann. N. Y. Acad. Sci.* 1056, 218–233. doi: 10.1196/annals.1352.026
- Aktories, K. (2011). Bacterial protein toxins that modify host regulatory GTPases. *Nat. Rev. Microbiol.* 9, 487–498. doi: 10.1038/nrmicro2592
- Andrews, H. L., Vogel, J. P., and Isberg, R. R. (1998). Identification of linked *Legionella pneumophila* genes essential for intracellular growth and evasion of the endocytic pathway. *Infect. Immun.* 66, 950–958.
- Arasaki, K., Toomre, D. K., and Roy, C. R. (2012). The *Legionella pneumophila* effector DrrA is sufficient to stimulate SNARE-dependent membrane fusion. *Cell Host Microbe* 11, 46–57. doi: 10.1016/j.chom.2011.11.009
- Banga, S., Gao, P., Shen, X., Fiscus, V., Zong, W. X., Chen, L., et al. (2007). *Legionella pneumophila* inhibits macrophage apoptosis by targeting pro-death members of the Bcl2 protein family. *Proc. Natl. Acad. Sci. U.S.A.* 104, 5121–5126. doi: 10.1073/pnas.0611030104
- Belyi, I., Popoff, M. R., and Cianciotto, N. P. (2003). Purification and characterization of a UDP-glucosyltransferase produced by *Legionella pneumophila*. *Infect. Immun.* 71, 181–186. doi: 10.1128/IAI.71.1.181-186.2003
- Belyi, Y., Jank, T., and Aktories, K. (2011). Effector glycosyltransferases in *Legionella*. *Front. Microbiol.* 2:76. doi: 10.3389/fmicb.2011.00076
- Belyi, Y., Niggeweg, R., Opitz, B., Vogelsang, M., Hippenstiel, S., Wilm, M., et al. (2006). *Legionella pneumophila* glucosyltransferase inhibits host elongation factor 1A. *Proc. Natl. Acad. Sci. U.S.A.* 103, 16953–16958. doi: 10.1073/pnas.0601562103
- Belyi, Y., Tabakova, I., Stahl, M., and Aktories, K. (2008). Lgt: a family of cytotoxic glucosyltransferases produced by *Legionella pneumophila*. *J. Bacteriol.* 190, 3026–3035. doi: 10.1128/JB.01798-07
- Bierne, H. (2013). Nuclear microbiology—bacterial assault on the nucleolus. *EMBO Rep.* 14, 663–664. doi: 10.1038/embor.2013.105
- Brombacher, E., Urwyler, S., Ragaz, C., Weber, S. S., Kami, K., Overduin, M., et al. (2009). Rab1 guanine nucleotide exchange factor sidm is a major phosphatidylinositol 4-phosphate-binding effector protein of *Legionella pneumophila*. *J. Biol. Chem.* 284, 4846–4856. doi: 10.1074/jbc.M807505200
- Cazalet, C., Rusniok, C., Bruggemann, H., Zidane, N., Magnier, A., Ma, L., et al. (2004). Evidence in the *Legionella pneumophila* genome for exploitation of host cell functions and high genome plasticity. *Nat. Genet.* 36, 1165–1173. doi: 10.1038/ng1447
- Clemens, D. L., Lee, B. Y., and Horwitz, M. A. (2000). *Mycobacterium tuberculosis* and *Legionella pneumophila* phagosomes exhibit arrested maturation despite acquisition of Rab7. *Infect. Immun.* 68, 5154–5166. doi: 10.1128/IAI.68.9.5154-5166.2000
- D'Auria, G., Jiménez-Hernández, N., Peris-Bondia, F., Moya, A., and Latorre, A. (2010). *Legionella pneumophila* pangenome reveals strain-specific virulence factors. *BMC Genomics* 11:181. doi: 10.1186/1471-2164-11-181
- de Felipe, K. S., Pampou, S., Jovanovic, O. S., Pericone, C. D., Ye, S. F., Kalachikov, S., et al. (2005). Evidence for acquisition of *Legionella* type IV secretion substrates via interdomain horizontal gene transfer. *J. Bacteriol.* 187, 7716–7726. doi: 10.1128/JB.187.22.7716-7726.2005
- Ensminger, A. W., and Isberg, R. R. (2010). E3 ubiquitin ligase activity and targeting of BAT3 by multiple *Legionella pneumophila* translocated substrates. *Infect. Immun.* 78, 3905–3919. doi: 10.1128/IAI.00344-10
- Fontana, M. F., Banga, S., Barry, K. C., Shen, X., Tan, Y., Luo, Z. Q., et al. (2011). Secreted bacterial effectors that inhibit host protein synthesis are critical for induction of the innate immune response to virulent *Legionella pneumophila*. *PLoS Pathog.* 7:e1001289. doi: 10.1371/journal.ppat.1001289
- Ge, J., Xu, H., Li, T., Zhou, Y., Zhang, Z., Li, S., et al. (2009). A *Legionella* type IV effector activates the NF-kappaB pathway by phosphorylating the IkappaB family of inhibitors. *Proc. Natl. Acad. Sci. U.S.A.* 106, 13725–13730. doi: 10.1073/pnas.0907200106
- Goody, P. R., Heller, K., Oesterlin, L. K., Müller, M. P., Itzen, A., and Goody, R. S. (2012). Reversible phosphocholination of Rab proteins by *Legionella pneumophila* effector proteins. *EMBO J.* 31, 1774–1784. doi: 10.1038/emboj.2012.16
- Gouin, E., Adib-Conquy, M., Balestrino, D., Nahori, M. A., Villiers, V., Colland, F., et al. (2010). The *Listeria monocytogenes* InlC protein interferes with innate immune responses by targeting the I{kappa}B kinase subunit IKK{alpha}. *Proc. Natl. Acad. Sci. U.S.A.* 107, 17333–17338. doi: 10.1073/pnas.1007765107
- Grabitzki, J., Ahrend, M., Schachter, H., Geyer, R., and Lochnit, G. (2008). The PCome of *Caenorhabditis elegans* as a prototypic model system for parasitic nematodes: identification of phosphorylcholine-substituted proteins. *Mol. Biochem. Parasitol.* 161, 101–111. doi: 10.1016/j.molbiopara.2008.06.014
- Hamon, M. A., and Cossart, P. (2008). Histone modifications and chromatin remodeling during bacterial infections. *Cell Host Microbe* 4, 100–109. doi: 10.1016/j.chom.2008.07.009
- Hanks, S. (2003). Genomic analysis of the eukaryotic protein kinase superfamily: a perspective. *Genome Biol.* 4, 111. doi: 10.1186/gb-2003-4-5-111
- Hayden, M. S., and Ghosh, S. (2008). Shared principles in NF-kappaB signaling. *Cell* 132, 344–362. doi: 10.1016/j.cell.2008.01.020
- Heidtmann, M., Chen, E. J., Moy, M. Y., and Isberg, R. R. (2009). Large-scale identification of *Legionella pneumophila* Dot/Icm substrates that modulate host cell vesicle trafficking pathways. *Cell Microbiol.* 11, 230–248. doi: 10.1111/j.1462-5822.2008.01249.x
- Hervet, E., Charpentier, X., Vianney, A., Lazzaroni, J.-C., Gilbert, C., Atlan, D., et al. (2011). Protein kinase LegK2 is a type IV secretion system effector involved in endoplasmic reticulum recruitment and intracellular replication of *Legionella pneumophila*. *Infect. Immun.* 79, 1936–1950. doi: 10.1128/IAI.00805-10
- Herz, H. M., Garruss, A., and Shilatfard, A. (2013). SET for life: biochemical activities and biological functions of SET domain-containing proteins. *Trends Biochem. Sci.* 38, 621–639. doi: 10.1016/j.tibs.2013.09.004
- Hochstrasser, M. (2009). Origin and function of ubiquitin-like proteins. *Nature* 458, 422–429. doi: 10.1038/nature07958
- Horenkamp, F. A., Mukherjee, S., Alix, E., Schauder, C. M., Hubber, A. M., Roy, C. R., et al. (2014). *Legionella pneumophila* subversion of host vesicular transport by SidC effector proteins. *Traffic* 15, 488–499. doi: 10.1111/tra.12158
- Horwitz, M. A. (1983). Formation of a novel phagosome by the Legionnaires' disease bacterium (*Legionella pneumophila*) in human monocytes. *J. Exp. Med.* 158, 1319–1331. doi: 10.1084/jem.158.4.1319
- Horwitz, M. A., and Maxfield, F. R. (1984). *Legionella pneumophila* inhibits acidification of its phagosome in human monocytes. *J. Cell Biol.* 99, 1936–1943. doi: 10.1083/jcb.99.6.1936
- Horwitz, M. A., and Silverstein, S. C. (1981). Interaction of the Legionnaires' disease bacterium (*Legionella pneumophila*) with human phagocytes. I. *L. pneumophila* resists killing by polymorphonuclear leukocytes, antibody, and complement. *J. Exp. Med.* 153, 386–397. doi: 10.1084/jem.153.2.386
- Hsu, F., Luo, X., Qiu, J., Teng, Y. B., Jin, J., Smolka, M. B., et al. (2014). The *Legionella* effector SidC defines a unique family of ubiquitin ligases important for bacterial phagosomal remodeling. *Proc. Natl. Acad. Sci. U.S.A.* 111, 10538–10543. doi: 10.1073/pnas.1402605111
- Ingmundson, A., Delprato, A., Lambright, D., and Roy, C. (2007). *Legionella pneumophila* proteins that regulate Rab1 membrane cycling. *Nature* 450, 365–369. doi: 10.1038/nature06336
- Ivanov, S. S., Charron, G., Hang, H. C., and Roy, C. R. (2010). Lipidation by the host prenyltransferase machinery facilitates membrane localization of *Legionella pneumophila* effector proteins. *J. Biol. Chem.* 285, 34686–34698. doi: 10.1074/jbc.M110.170746
- Kagan, J., and Roy, C. (2002). *Legionella* phagosomes intercept vesicular traffic from endoplasmic reticulum exit sites. *Nat. Cell Biol.* 4, 945–954. doi: 10.1038/ncb883
- Karin, M., and Lin, A. (2002). NF-kappaB at the crossroads of life and death. *Nat. Immunol.* 3, 221–227. doi: 10.1038/ni0302-221
- Kim, D. W., Lenzen, G., Page, A. L., Legrain, P., Sansonetti, P. J., and Parsot, C. (2005). The *Shigella flexneri* effector OspG interferes with innate immune responses by targeting ubiquitin-conjugating enzymes. *Proc. Natl. Acad. Sci. U.S.A.* 102, 14046–14051. doi: 10.1073/pnas.0504466102
- Kinch, L. N., Yarbrough, M. L., Orth, K., and Grishin, N. V. (2009). Fido, a novel AMPylation domain common to fic, doc, and AvrB. *PLoS ONE* 4:e5818. doi: 10.1371/journal.pone.0005818
- Komano, T., Utsumi, R., and Kawamukai, M. (1991). Functional analysis of the fic gene involved in regulation of cell division. *Res. Microbiol.* 142, 269–277. doi: 10.1016/0923-2508(91)90040-H
- Kubori, T., Hyakutake, A., and Nagai, H. (2008). *Legionella* translocates an E3 ubiquitin ligase that has multiple U-boxes with distinct functions. *Mol. Microbiol.* 67, 1307–1319. doi: 10.1111/j.1365-2958.2008.06124.x

- Kubori, T., Shinzawa, N., Kanuka, H., and Nagai, H. (2010). *Legionella* metaeffector exploits host proteasome to temporally regulate cognate effector. *PLoS Pathog.* 6:e1001216. doi: 10.1371/journal.ppat.1001216
- Laguna, R. K., Creasey, E. A., Li, Z., Valtz, N., and Isberg, R. R. (2006). A *Legionella pneumophila*-translocated substrate that is required for growth within macrophages and protection from host cell death. *Proc. Natl. Acad. Sci. U.S.A.* 103, 18745–18750. doi: 10.1073/pnas.0609012103
- Le Negrate, G., Faustin, B., Welsh, K., Loeffler, M., Krajewska, M., Hasegawa, P., et al. (2008). *Salmonella* secreted factor L deubiquitinase of *Salmonella typhimurium* inhibits NF-kappaB, suppresses IkappaBalpha ubiquitination and modulates innate immune responses. *J. Immunol.* 180, 5045–5056. doi: 10.4049/jimmunol.180.7.5045
- Li, T., Lu, Q., Wang, G., Xu, H., Huang, H., Cai, T., et al. (2013). SET-domain bacterial effectors target heterochromatin protein 1 to activate host rDNA transcription. *EMBO Rep.* 14, 733–740. doi: 10.1038/embor.2013.86
- Lomma, M., Dervins-Ravault, D., Rolando, M., Nora, T., Newton, H. J., Sansom, F. M., et al. (2010). The *Legionella pneumophila* F-box protein Lpp2082 (AnkB) modulates ubiquitination of the host protein parvin B and promotes intracellular replication. *Cell Microbiol.* 12, 1272–1291. doi: 10.1111/j.1462-5822.2010.01467.x
- Lorick, K. L., Jensen, J. P., Fang, S., Ong, A. M., Hatakeyama, S., and Weissman, A. M. (1999). RING fingers mediate ubiquitin-conjugating enzyme (E2)-dependent ubiquitination. *Proc. Natl. Acad. Sci. U.S.A.* 96, 11364–11369. doi: 10.1073/pnas.96.20.11364
- Losick, V. P., Haessler, E., Moy, M. Y., and Isberg, R. R. (2010). LnaB: a *Legionella pneumophila* activator of NF-kappaB. *Cell Microbiol.* 12, 1083–1097. doi: 10.1111/j.1462-5822.2010.01452.x
- Losick, V. P., and Isberg, R. R. (2006). NF-kappaB translocation prevents host cell death after low-dose challenge by *Legionella pneumophila*. *J. Exp. Med.* 203, 2177–2189. doi: 10.1084/jem.20060766
- Lovell, T. M., Woods, R. J., Butlin, D. J., Brayley, K. J., Manyonda, I. T., Jarvis, J., et al. (2007). Identification of a novel mammalian post-translational modification, phosphocholine, on placental secretory polypeptides. *J. Mol. Endocrinol.* 39, 189–198. doi: 10.1677/JME-07-0007
- Luo, Z. Q., and Isberg, R. R. (2004). Multiple substrates of the *Legionella pneumophila* Dot/Icm system identified by interbacterial protein transfer. *Proc. Natl. Acad. Sci. U.S.A.* 101, 841–846. doi: 10.1073/pnas.0304916101
- Marra, A., Blander, S. J., Horwitz, M. A., and Shuman, H. A. (1992). Identification of a *Legionella pneumophila* locus required for intracellular multiplication in human macrophages. *Proc. Natl. Acad. Sci. U.S.A.* 89, 9607–9611. doi: 10.1073/pnas.89.20.9607
- Mihai Gazdag, E., Streller, A., Haneburger, I., Hilbi, H., Vetter, I. R., Goody, R. S., et al. (2013). Mechanism of Rab1b deactivation by the *Legionella pneumophila* GAP LepB. *EMBO Rep.* 14, 199–205. doi: 10.1038/embor.2012.211
- Mittal, R., Peak-Chew, S. Y., and McMahon, H. T. (2006). Acetylation of MEK2 and I kappa B kinase (IKK) activation loop residues by YopJ inhibits signaling. *Proc. Natl. Acad. Sci. U.S.A.* 103, 18574–18579. doi: 10.1073/pnas.0608995103
- Mukherjee, S., Liu, X., Arasaki, K., McDonough, J., Galán, J. E., and Roy, C. R. (2011). Modulation of Rab GTPase function by a protein phosphocholine transferase. *Nature* 477, 103–106. doi: 10.1038/nature10335
- Müller, M. P., Peters, H., Blümer, J., Blankenfeldt, W., Goody, R. S., and Itzen, A. (2010). The *Legionella* effector protein DrrA AMPylates the membrane traffic regulator Rab1b. *Science* 329, 946–949. doi: 10.1126/science.1192276
- Neunuebel, M. R., Chen, Y., Gaspar, A. H., Backlund, P. S., Yergey, A., and Machner, M. P. (2011). De-AMPylation of the small GTPase Rab1 by the pathogen *Legionella pneumophila*. *Science* 333, 453–456. doi: 10.1126/science.1207193
- Price, C. T., Al-Khodori, S., Al-Quadan, T., Santic, M., Habyarimana, F., Kalia, A., et al. (2009). Molecular mimicry by an F-box effector of *Legionella pneumophila* hijacks a conserved polyubiquitination machinery within macrophages and protozoa. *PLoS Pathog.* 5:e1000704. doi: 10.1371/journal.ppat.1000704
- Price, C. T., Al-Quadan, T., Santic, M., Jones, S. C., and Abu Kwaik, Y. (2010a). Exploitation of conserved eukaryotic host cell farnesylation machinery by an F-box effector of *Legionella pneumophila*. *J. Exp. Med.* 207, 1713–1726. doi: 10.1084/jem.20100771
- Price, C. T., Jones, S. C., Amundson, K. E., and Kwaik, Y. A. (2010b). Host-mediated post-translational prenylation of novel dot/icm-translocated effectors of *legionella pneumophila*. *Front. Microbiol.* 1:131. doi: 10.3389/fmicb.2010.00131
- Price, C. T., Al-Quadan, T., Santic, M., Rosenshine, I., and Abu Kwaik, Y. (2011). Host proteasomal degradation generates amino acids essential for intracellular bacterial growth. *Science* 334, 1553–1557. doi: 10.1126/science.1212868
- Price, C. T., and Kwaik, Y. A. (2010). Exploitation of host polyubiquitination machinery through molecular mimicry by eukaryotic-like bacterial F-box effectors. *Front. Microbiol.* 1:122. doi: 10.3389/fmicb.2010.00122
- Ragaz, C., Pietsch, H., Urwyler, S., Tiaden, A., Weber, S., and Hilbi, H. (2008). The *Legionella pneumophila* phosphatidylinositol-4 phosphate-binding type IV substrate SidC recruits endoplasmic reticulum vesicles to a replication-permissive vacuole. *Cell Microbiol.* 10, 2416–2433. doi: 10.1111/j.1462-5822.2008.01219.x
- Ribet, D., and Cossart, P. (2010a). Pathogen-mediated posttranslational modifications: a re-emerging field. *Cell* 143, 694–702. doi: 10.1016/j.cell.2010.11.019
- Ribet, D., and Cossart, P. (2010b). Post-translational modifications in host cells during bacterial infection. *FEBS Lett.* 584, 2748–2758. doi: 10.1016/j.febslet.2010.05.012
- Rigden, D. J. (2011). Identification and modelling of a PPM protein phosphatase fold in the *Legionella pneumophila* deAMPylase SidD. *FEBS Lett.* 585, 2749–2754. doi: 10.1016/j.febslet.2011.08.006
- Rolando, M., and Buchrieser, C. (2014). *Legionella pneumophila* type IV effectors hijack the transcription and translation machinery of the host cell. *Trends Cell Biol.* 24, 771–778. doi: 10.1016/j.tcb.2014.06.002
- Rolando, M., Rusniok, C., Margueron, R., and Buchrieser, C. (2013a). [Host epigenetic targeting by *Legionella pneumophila*]. *Med. Sci. (Paris)* 29, 843–845. doi: 10.1051/medsci/20132910010
- Rolando, M., Sanulli, S., Rusniok, C., Gomez-Valero, L., Bertholet, C., Sahr, T., et al. (2013b). *Legionella pneumophila* effector RomA uniquely modifies host chromatin to repress gene expression and promote intracellular bacterial replication. *Cell Host Microbe* 13, 395–405. doi: 10.1016/j.chom.2013.03.004
- Roy, C. R., and Mukherjee, S. (2009). Bacterial FIC Proteins AMP Up Infection. *Sci. Signal.* 2, pe14. doi: 10.1126/scisignal.262pe14
- Roy, C. R., and Tilney, L. G. (2002). The road less traveled: transport of *Legionella* to the endoplasmic reticulum. *J. Cell Biol.* 158, 415–419. doi: 10.1083/jcb.2002.05011
- Schmuck, B., N'Guessan, P. D., Ollomang, M., Lorenz, J., Zahlten, J., Opitz, B., et al. (2007). *Legionella pneumophila*-induced NF-kappaB- and MAPK-dependent cytokine release by lung epithelial cells. *Eur. Respir. J.* 29, 25–33. doi: 10.1183/09031936.00141005
- Schroeder, G. N., Petty, N. K., Mousnier, A., Harding, C. R., Vogrin, A. J., Wee, B., et al. (2010). *Legionella pneumophila* strain 130b possesses a unique combination of type IV secretion systems and novel Dot/Icm secretion system effector proteins. *J. Bacteriol.* 192, 6001–6016. doi: 10.1128/JB.00778-10
- Shen, X., Banga, S., Liu, Y., Xu, L., Gao, P., Shamovsky, I., et al. (2009). Targeting eEF1A by a *Legionella pneumophila* effector leads to inhibition of protein synthesis and induction of host stress response. *Cell Microbiol.* 11, 911–926. doi: 10.1111/j.1462-5822.2009.01301.x
- Shin, S., Case, C. L., Archer, K. A., Nogueira, C. V., Kobayashi, K. S., Flavell, R. A., et al. (2008). Type IV secretion-dependent activation of host MAP kinases induces an increased proinflammatory cytokine response to *Legionella pneumophila*. *PLoS Pathog.* 4:e1000220. doi: 10.1371/journal.ppat.1000220
- Tan, Y., Arnold, R. J., and Luo, Z. Q. (2011). *Legionella pneumophila* regulates the small GTPase Rab1 activity by reversible phosphorylation. *Proc. Natl. Acad. Sci. U.S.A.* 108, 21212–21217. doi: 10.1073/pnas.1114023109
- Tan, Y., and Luo, Z. Q. (2011). *Legionella pneumophila* SidD is a deAMPylase that modifies Rab1. *Nature* 475, 506–509. doi: 10.1038/nature10307
- Walsh, C. T., Garneau-Tsodikova, S., and Gatto, G. J. (2005). Protein posttranslational modifications: the chemistry of proteome diversifications. *Angew. Chem. Int. Ed. Engl.* 44, 7342–7372. doi: 10.1002/anie.200501023
- Worby, C. A., Mattoo, S., Kruger, R. P., Corbeil, L. B., Koller, A., Mendez, J. C., et al. (2009). The fic domain: regulation of cell signaling by adenylation. *Mol. Cell.* 34, 93–103. doi: 10.1016/j.molcel.2009.03.008
- Yarborough, M. L., Li, Y., Kinch, L. N., Grishin, N. V., Ball, H. L., and Orth, K. (2009). AMPylation of Rho GTPases by *Vibrio* VopS disrupts effector

- binding and downstream signaling. *Science* 323, 269–272. doi: 10.1126/science.1166382
- Yarbrough, M. L., and Orth, K. (2009). AMPylation is a new post-translational modification. *Nat. Chem. Biol.* 5, 378–379. doi: 10.1038/nchembio0609-378
- Zhu, W., Banga, S., Tan, Y., Zheng, C., Stephenson, R., Gately, J., et al. (2011). Comprehensive identification of protein substrates of the Dot/Icm type IV transporter of *Legionella pneumophila*. *PLoS ONE* 6:e17638. doi: 10.1371/journal.pone.0017638

Conflict of Interest Statement: The authors declare that the research was conducted in the absence of any commercial or financial relationships that could be construed as a potential conflict of interest.

Received: 27 November 2014; accepted: 23 January 2015; published online: 10 February 2015.

Citation: Michard C and Doublet P (2015) Post-translational modifications are key players of the *Legionella pneumophila* infection strategy. *Front. Microbiol.* 6:87. doi: 10.3389/fmicb.2015.00087

This article was submitted to Microbial Physiology and Metabolism, a section of the journal *Frontiers in Microbiology*.

Copyright © 2015 Michard and Doublet. This is an open-access article distributed under the terms of the Creative Commons Attribution License (CC BY). The use, distribution or reproduction in other forums is permitted, provided the original author(s) or licensor are credited and that the original publication in this journal is cited, in accordance with accepted academic practice. No use, distribution or reproduction is permitted which does not comply with these terms.



Phosphoproteomics analysis of a clinical *Mycobacterium tuberculosis* Beijing isolate: expanding the mycobacterial phosphoproteome catalog

Suereta Fortuin¹, Gisele G. Tomazella², Nagarjuna Nagaraj³, Samantha L. Sampson¹, Nicolaas C. Gey van Pittius¹, Nelson C. Soares⁴, Harald G. Wiker^{2†}, Gustavo A. de Souza^{5†} and Robin M. Warren^{1*†}

¹ Division of Molecular Biology and Human Genetics, Faculty Medicine and Health Sciences, DST/NRF Centre of Excellence for Biomedical Tuberculosis Research, SAMRC Centre for Tuberculosis Research, Stellenbosch University, Cape Town, South Africa

² The Gade Research Group for Infection and Immunity, Department of Clinical Science, University of Bergen, Bergen, Norway

³ Max Planck Institute for Biochemistry, Munich, Germany

⁴ Faculty of Health Sciences, Institute of Infectious Disease and Molecular Medicine, University of Cape Town, Cape Town, South Africa

⁵ Norway Proteomics Core Facility, Department of Immunology, Oslo University, Oslo, Norway

Edited by:

Ivan Mijakovic, Chalmers University of Technology, Sweden

Reviewed by:

Lei Shi, Chalmers University of Technology, Sweden

Boumediene Soufi, Proteome Center Tuebingen, Germany

*Correspondence:

Robin M. Warren, Division of Molecular Biology and Human Genetics, Faculty Medicine and Health Sciences, DST/NRF Centre of Excellence for Biomedical Tuberculosis Research, SAMRC Centre for Tuberculosis Research, Stellenbosch University, Francie van Zijl drive, Tygerberg, Cape Town 7505, South Africa
e-mail: rw1@sun.ac.za

[†] These authors have contributed equally to this work.

Reversible protein phosphorylation, regulated by protein kinases and phosphatases, mediates a switch between protein activity and cellular pathways that contribute to a large number of cellular processes. The *Mycobacterium tuberculosis* genome encodes 11 Serine/Threonine kinases (STPKs) which show close homology to eukaryotic kinases. This study aimed to elucidate the phosphoproteomic landscape of a clinical isolate of *M. tuberculosis*. We performed a high throughput mass spectrometric analysis of proteins extracted from an early-logarithmic phase culture. Whole cell lysate proteins were processed using the filter-aided sample preparation method, followed by phosphopeptide enrichment of tryptic peptides by strong cation exchange (SCX) and Titanium dioxide (TiO₂) chromatography. The MaxQuant quantitative proteomics software package was used for protein identification. Our analysis identified 414 serine/threonine/tyrosine phosphorylated sites, with a distribution of S/T/Y sites; 38% on serine, 59% on threonine and 3% on tyrosine; present on 303 unique peptides mapping to 214 *M. tuberculosis* proteins. Only 45 of the S/T/Y phosphorylated proteins identified in our study had been previously described in the laboratory strain H₃₇Rv, confirming previous reports. The remaining 169 phosphorylated proteins were newly identified in this clinical *M. tuberculosis* Beijing strain. We identified 5 novel tyrosine phosphorylated proteins. These findings not only expand upon our current understanding of the protein phosphorylation network in clinical *M. tuberculosis* but the data set also further extends and complements previous knowledge regarding phosphorylated peptides and phosphorylation sites in *M. tuberculosis*.

Keywords: *M. tuberculosis*, phosphoproteomics, tyrosine phosphorylation, serine phosphorylation, threonine phosphorylation

INTRODUCTION

According to the World Health Organization (WHO), tuberculosis (TB) ranks as the second leading cause of death from an infectious disease worldwide, after HIV (WHO|Global tuberculosis report 2014, 2014). It is estimated that one third of the world's population is infected with *Mycobacterium tuberculosis*, the causative agent of TB and 8.6 million new TB cases were reported in 2012 alone (WHO|Global tuberculosis report 2013, 2013). In order to control this epidemic there is a critical need for the development of effective and affordable anti-TB therapy and diagnostic tools.

Harnessing the power of the field of proteomics provides a unique opportunity to identify novel protein candidates for diagnosis and drug targets of pathogenic bacteria. Of particular

interest is the identification of proteins with post-translational modifications (PTMs) as these modifications are often critical to protein functions, such as regulating protein-protein interactions, subcellular localization or modification of catalytic sites (Seo and Lee, 2004; Gupta et al., 2007). Protein phosphorylation is an important reversible PTM that directly or indirectly regulates signal transduction cascades linking the intracellular and extracellular environments. In bacteria, protein phosphorylation plays a fundamental role in the regulation of key processes ranging from metabolism and cellular homeostasis to cellular signaling which can be mediated by two classes of phosphorylation events (Cozzone, 1998). The underlying molecular mechanisms regulating protein phosphorylation and dephosphorylation is of great physiological importance due to its ability to ultimately

affect protein activity, function, half-life or subcellular localization (McConnell and Wadzinski, 2009). Until recently it was thought that histidine/aspartate phosphorylation was the main mediator of signal transduction in bacteria (Frasch and Dworkin, 1996). However, with the advancement of mass spectrometry-based analyses serine/threonine and tyrosine kinases have been identified in a number of different bacteria (Macek et al., 2007; Macek and Mijakovic, 2011; Mijakovic and Macek, 2012).

The *M. tuberculosis* genome encodes 11 Serine/Threonine kinases (STPK's) (PknA, PknB, PknD, PknE, PknF, PknG, PknH, PknI, PknJ, PknK, PknL), two tyrosine phosphatases (PtpA, PtpB) and 11 two-component systems, highlighting the complexity of signaling network mediated by protein phosphorylation and thereby their potential as drug targets (Chopra et al., 2003; Koul et al., 2004; Sharma et al., 2004; Sala and Hartkoorn, 2011). Prisic et al. described the Serine/Threonine (S/T) phosphorylation profiles of the laboratory strain *M. tuberculosis* H₃₇Rv under 6 different culture conditions (Prisic et al., 2010). This study identified 301 phosphorylated proteins after combining data from six different culture conditions (Prisic et al., 2010) and identified four phosphorylated STPKs, ribosomal and ribosome-associated proteins as well as phosphorylated substrates which suggest that protein phosphorylation provides a mechanism for regulating key physiological process during infection. A more recent study of H₃₇Rv further expanded the knowledge of the phosphoproteome by identifying novel tyrosine (Y) phosphorylated proteins in *M. tuberculosis* further supporting the broad regulation of its physiology by phosphorylation (Kusebauch et al., 2014).

In this study we report the phosphoproteome of a previously described clinical Beijing genotype *M. tuberculosis* isolate at early-logarithmic growth phase in liquid culture to provide further insight the influence of S/T/Y phosphorylation events on bacterial growth and virulence (de Souza et al., 2010). We used a combination of strong cation exchange (SCX) with Titanium dioxide (TiO₂) enrichment in a mass spectrometry-based phosphoproteomic analysis of a hyper-virulent clinical *M. tuberculosis* isolate (de Souza et al., 2010). We confirmed the presence of previously described *M. tuberculosis* phosphorylated proteins and also identified novel phosphorylated proteins and sites. In addition, this dataset identified novel tyrosine phosphorylation events, and thereby confirmed that there are multiple tyrosine kinase targets in this clinically relevant *M. tuberculosis* strain.

MATERIALS AND METHODS

CELL CULTURE AND LYSATE PREPARATION

A previously described hyper-virulent clinical Beijing genotype *Mycobacterium tuberculosis* isolate, SAW5527, isolated from a TB patient attending a primary health care clinic in the Western Cape province, South Africa was used for this phosphoproteomics analysis (de Souza et al., 2010). Secondary cultures were inoculated into 50 ml 7H9 Middlebrooks medium supplemented with Dextrose and Catalase and incubated at 37°C until early-logarithmic phase (OD₆₀₀ between 0.6 and 0.7). Mycobacterial cells were collected by centrifugation (2000 × g for 10 min at 4°C) and washed two times with cold lysis buffer containing 10 mM Tris-HCl (pH 7.4), 0.1% Tween-80, Complete Protease inhibitor cocktail (Roche, Mannheim Germany) and Phosphatase inhibitor

cocktail (Roche, Mannheim Germany). An equal amount of 0.1 mm glass beads (Biospec Products Inc., Bartlesville, OK) was added to the cell pellet after centrifugation together with cold 300 µl lysis buffer and 10 µl DNaseI (2U/ml) (NEB, New England Laboratories). Lysis was achieved by mechanical bead-beating in a Rylolyser (Bio101 SAVANT, Vista, CA) for 6 cycles of 20 s at a speed of 4.0 m.s⁻¹, with 1 min cooling periods on ice. The whole cell lysates were filter-sterilized with a sterile 0.22 µm pore acrodisc 25 mm PF syringe filter (Pall Life Sciences, Pall Corporation, Ann Arbor, MI) and stored at -80°C. The protein concentration of the whole cell lysate was determined using the RC DC Protein assay according to manufacturer's instructions (BioRad). A single biological replicate was analyzed in triplicate for downstream phosphoproteomic analysis.

FILTER AIDED SAMPLE PREPARATION AND TRYPSIN DIGESTION

Four milligrams of concentrated whole cell lysate proteins was heated in 4% SDS buffer and 0.1 M dithiothreitol (DTT) in 100 mM Tris/HCl pH 7.5. The samples were processed using Filter Aided Sample Preparation (FASP) (Wiśniewski et al., 2009). In brief, 4 mg dried whole cell lysate protein was resuspended in 250 µl of urea (UA) and loaded onto a 15 ml Amicon filtration device (30 kDa MWCO) and centrifuged at 2000 × g for 40 min at 25°C. After centrifugation, the flow-through was collected in a clean falcon tube and discarded. The concentrated whole cell lysate proteins in the filter unit were diluted in 2 ml 8 M Urea in 0.1 M Tris/HCl (pH 8.5) and re-centrifuged to remove the SDS. The flow-through was discarded and the remaining proteins in the filter unit were alkylated by mixing with 1.5 ml 50 mM iodoacetamide (IAA) and incubated in the dark for 20 min to irreversibly modify cysteine. The alkylated proteins were equilibrated with 2 ml 50 mM ammonium bicarbonate (ABC) and digested with trypsin (Promega) in a protein to enzyme ratio of 100:1 at 37°C overnight. After trypsin digestion the filter unit is transferred to a clean collection tube and the peptides were eluted by centrifuged at 14 000 × g for 10 min. The eluted peptides were diluted in 50 µl water to avoid desalting for further processing of the peptide and acidified with trifluoroacetic acid (TFA).

FRACTIONATION OF PEPTIDES BY STRONG CATION EXCHANGE (SCX)

Extracted trypsin digested peptides were diluted to a volume of 7 ml in Solvent A (5 mM monopotassium phosphate (KH₂PO₄) 30% acetonitrile (ACN), pH 2.7). The pH of the diluted peptide samples was adjusted to 2.7 and made up to a volume of 10 ml with 100% ACN. The respective peptide samples were then separated at pH 2.7 by strong cation exchange (SCX) by loading each peptide mixture onto a cation exchanger column (3.0 mm × 20 cm) (Poly LC, Columbia, MD) containing 5 µm polysulfoethyl aspartamine beads with a 200 Å pore size and a flow rate of 350 µl/min⁻¹ equilibrated with SCX solvent A. The flow-through was collected and the bound peptides were eluted from the columns using an increasing salt gradient (0–30%) containing 5 mM KH₂PO₄ pH and 150 mM KCl. A total of 9 fractions were collected; 5 fractions generated by SCX based on UV absorbance (220 and 280), 3 from the flow-through and 1 salvage fraction (containing washes from the cation exchanger column) from the SCX column as an additional fraction.

ENRICHMENT OF PHOSPHOPEPTIDES WITH TiO₂ BEADS

All nine fractions (5 SCX, 3 SCX flow-through, 1 salvage fraction) were subjected to Titanium dioxide (TiO₂) phosphopeptide enrichment. The TiO₂-beads, 10 µm in size, (GL Sciences, Inc., Japan) was resuspended 30 mg/ml dihydrobenzoic acid (DHB) (Sigma) to prevent non-specific binding. Each of the 9 fractions was incubated 4 times with TiO₂ at a peptide to bead ratio of 1:2–1:8. Each fraction was rotated for 30 min, and then briefly centrifuged (14,000 g × 30 s). The supernatants were aspirated and transferred to a new labeled tube and the phosphopeptides bound to the TiO₂ beads were washed twice with 30% ACN and 3% TFA followed by washing twice with 75% ACN and 0.3% TFA. The enriched phosphorylated peptides were eluted with elution buffer containing 25% ammonia and ACN pH10. The eluted phosphopeptides were desalted using in house prepared C₁₈ Stage tips.

LC-MS/MS ANALYSIS

The peptides were separated on a column packed in-house with C₁₈ beads (reprosil-AQ Pur, Rd Maisch) on an Proxeon Easy-nLC system (Proxeon Biosystems, Odense, Denmark) using a binary gradient with buffer A (0.5% acetic acid in water) and buffer B (0.5% acetic acid and 80% ACN). The 4 µl of the enriched phosphopeptides from each of the 9 fractions were injected 3 times and were loaded directly without any trapping column with buffer A at a flow rate of 500 nl/min. Elution was carried out at a flow rate of 250 nl/min, with a linear gradient from 10 to 35% buffer B over a period of 95 min followed by 50% buffer B for 15 min. At the end of the gradient the column was washed with 90% buffer B and equilibrated with 5% buffer B for 10 min. The LC system was directly coupled in-line with the LTQ-Orbitrap Velos instrument (Thermo Fisher Scientific) via the Proxeon Biosystems nano-electrospray source. The mass spectrometer was programmed to acquire in a data-dependant mode with a resolution of 30,000 at 400 m/z with lock mass option enabled for the 445.120025. However, the target lock mass abundance was set to 0% in order to save the injection time for lock mass. For full scans 1E6 ions were accumulated within a maximum injection time of 250 ms in the C trap and detected in the Orbitrap mass analyser. The 10 most intense ions with charge states ≥ 2 were sequentially isolated and fragmented by high-energy collision dissociation (HCD) mode in the collision cell with normalized collision energy of 40% and detected in the Orbitrap analyser at 75,000 resolution. For HCD based method, the activation time option in the Xcalibur file was set to 0.1 ms. For the high-low strategy, full scans were acquired in the Orbitrap analyser at 60,000 resolution as parallel acquisition is enabled in the high-low mode. Up to the 10 most intense peaks with charge states ≥ 2 were selected for sequencing to a target value of 5000 with a maximum injection time of 25 ms and fragmented in the ion trap by HCD with normalized collision energy of 35%, activation of 0.25 and activation time of 10 ms.

DATABASE SEARCH

The raw data acquired were processed using MaxQuant software version (1.4.1.2) and processed as per default workflow. Since HCD spectra were acquired in profile mode, deisotoping was performed similar to survey MS scans to obtain singly charged

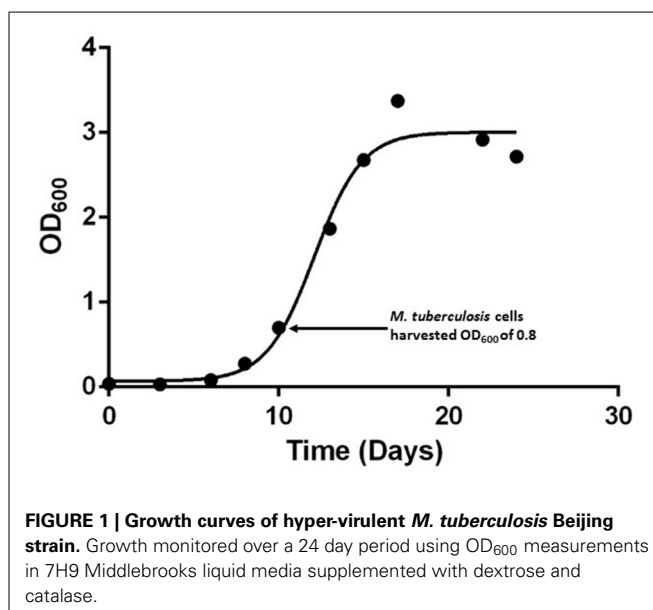


FIGURE 1 | Growth curves of hyper-virulent *M. tuberculosis* Beijing strain. Growth monitored over a 24 day period using OD₆₀₀ measurements in 7H9 Middlebrooks liquid media supplemented with dextrose and catalase.

peak lists and searched against the *M. tuberculosis* H₃₇Rv protein database (version R11 tuberculist.epfl.ch). The search included cysteine carbamidomethylation as a fixed modification while N-acetylation, oxidation of methionine and phosphorylation at serine, threonine and tyrosine were set as variable modifications. Up to two missed cleavages were allowed for protease digestion and a peptide had to be fully tryptic. Identifications were filtered at 1% FDR at three levels namely; site, peptide and protein using reversed sequences. As such there is no fixed cut-off score threshold but instead spectra were accepted until the 1% false discovery rate (FDR) is reached. Only peptides with a minimum length of 7 amino acids were considered for identification and detected in at least one or more of the replicates. All phosphopeptide spectra were manually validated by applying stringent acceptance criteria: only phosphorylation events on S/T/Y with a localization probability of ≥ 0.75 and PEP ≤ 0.01 were used for further analysis and reported as high confidence localized phosphosites.

GENE ONTOLOGY ANALYSIS

The categorization of identified phosphorylated proteins in terms of functional categorization, molecular function, biological processes and cellular components was carried out using TubercuList-*Mycobacterium tuberculosis* Database.

RESULTS

In this study we set out to analyse the phosphoproteome of a hyper-virulent Beijing genotype *M. tuberculosis* isolate by extracting whole cell lysate proteins at early-logarithmic growth (OD₆₀₀ of 0.8) (Figure 1) which resulted in the identification of 619 MS/MS spectra. The 274 LC-MS/MS spectra that fulfilled the criteria for high confidence phosphosites identified a total of 414 (38:59:3%) S/T/Y phosphorylation sites present in 214 *M. tuberculosis* H₃₇Rv proteins (Supplementary Table S2; Supplementary Figure S1).

Table 1 | List of phosphopeptides identified in this and previous studies of *M. tuberculosis*.

Rv numbers	Protein name	Phosphopeptides	Phospho-residue	References
Rv0007	Rv0007	FISGASAPVTGPAAAVR	Not known	Prisic et al., 2010
		FIS*GAS*APVT*GPAAAVR	S; T	This study
		FIS*GASAPVT*GPAAAVR	S; T	This study
Rv0014c	PknB	AIADSGNSVTQTAAVIGTAQYLSPEQAR	Not known	Prisic et al., 2010
		AIADSGNSVT*QT*AAVIGTAQYLSPEQAR	T	This study
		AIADSGNS*VT*QTAAVIGTAQYLSPEQAR	S; T	This study
		TSLSSAAGNLSGPRTDPLPR	Not known	Prisic et al., 2010
		TSLSSAAGNLS*GPRTDPLPR	S	This study
		TSLSSAAGNLSGPRT*DPLPR	T	This study
Rv0015c	PknA	RPFAGDGALT\$VAMK	T	Prisic et al., 2010; This study
Rv0020c	FhaA	FEQSSNLHTGQFR	Not known	Prisic et al., 2010
		FEQS*SNLHT*GQFR	S; T	This study
		HPDQGDY\$PEQIGYPDQGGYPEQR	Y	Kusebauch et al., 2014; This study
		QDYGGGADY\$TR	Y	Kusebauch et al., 2014; This study
		VPGY\$APQGGGYAEPAGR	Y	Kusebauch et al., 2014; This study
Rv0175	Rv0175	AADSAESDAGADQTGPQVK	Not known	Prisic et al., 2010
		AADSAESDAGADQT*GPQVK	T	This study
Rv0204c	Rv0204c	DPPT\$DPNLR		Prisic et al., 2010; This study
Rv0227c	Rv0227c	GGFEFVPGAEAEETKLPTQRPDFPR	Not known	Prisic et al., 2010
		GGFEFVPGAEAEET\$EK	T	Prisic et al., 2010; This study
Rv0351	GrpE	RIDPET#GEVR	T	Prisic et al., 2010
		IDPET*GEVR	T	This study
Rv0389	PurT	AAGHQVQPQT\$GGVSPR	T	Prisic et al., 2010; This study
Rv0410c	PknG	SGPGTQPADAQTAT#SATVRPL	T	O'Hare et al., 2008
		S*GPGT*QPADAQTSATSATVR	S; T	This study
		SGPGTQPADAQTAT*S*ATVRPLSTQAVFR	S; T	This study
		SGPGTQPADAQTAT*SAT*VR	T	This study
		PLST#QAVFRPDFGDEDNFPHTLGPDTPEQDR	T	O'Hare et al., 2008
		PLS*T*QAVFR	S; T	This study
Rv0421c	Rv0421c	GLAEGPLIAGGHS#YGGRR	S	Prisic et al., 2010
		GLAEGPLIAGGHS*Y*GGR	S; Y	This study
Rv0440	GroEL2	KWGAPTIT\$NDGVSIK	T	Molle et al., 2006
		WGAPTIT*NDGVSIK	T	This study
		AVEKVT#ETLLK	T	Molle et al., 2010
		VTET*LLK	T	This study
Rv0497	Rv0497	RGDSDAITVAELT\$GEIPIIR	T	Prisic et al., 2010; This study
		T*GPHPETESSGNR	T	This study
Rv0685	Tuf	PDLNET\$KAFDQ	T	Sajid et al., 2011
		VLHDKFPDLNET*K	T	This study
Rv0733	Adk	LGIPQISTGELFR	Not known	Prisic et al., 2010
		LGIPQIS*TGELFR	S	This study
Rv0822c	Rv0822c	VHDDADDQODTEAIAIPAHSLEFLSELPDLR	Not Known	Prisic et al., 2010
		VHDDADDQODT*EAIAIPAHSLEFLSELPDLR	T	This study
Rv0896	GltA2	ADTDDT\$ATLR	T	Prisic et al., 2010; This study
Rv0931c	PknD	PGLTQT\$GTAVG	T	Durán et al., 2005; This study
		AASDPGLT*QT*GTAVGTYNMAPER	T	This study
		WSPGDS*AT*VAGPLAADSR	S; T	This study
		WSPGDSATVAGPLAADSR	Not known	Prisic et al., 2010
		WSPGDS*AT*VAGPLAADSR	S; T	This study
		WSPGDS*ATVAGPLAADS*R	S	This study
Rv1388	MihF	AQEIMTELEIAPT\$RR	T	Prisic et al., 2010; This study
Rv1719	Rv1719	S\$GGIQVIAR	S	Prisic et al., 2010; This study

(Continued)

Table 1 | Continued

Rv numbers	Protein name	Phosphopeptides	Phospho-residue	References
Rv1746	PknF	DDTRVS ^S QPVAV	S	Durán et al., 2005; This study
Rv1747	Rv1747	YPTGGQQLWPPSGPQR	T	Prisic et al., 2010
		YPT*GGQQLWPPS*GPQR	S; T	This study
		IPAAPPSGPQPR	Not known	Prisic et al., 2010
		IPAAPPS*GPQPR	S	This study
Rv1820	IlvG	STDTPAQTMHAGR	Not Known	Prisic et al., 2010
		STD*TAQTMHAGR	T	This study
Rv1827	GarA	DQTSDEVTVETTSVFR	Not known	Prisic et al., 2010
		DQTSDEVT*VET*T*SVFR	T	This study
		VTVETT ^S SVFRA	T	Prisic et al., 2010; This study
		DQTSDEVTVET ^S TSVFR	T	Villarino et al., 2005; This study
		DQT*SDEVTVET*TSVFR	T	This study
		DQTSDEVT*VET*TSVFR	T	This study
		DQTSDEVTVET*T*SVFR	T	This study
		DQTSDEVT*VET*T*SVFR	T	This study
Rv2094c	TatA	VDPSAASGQDS*T*EARPA	S; T	This study
		AEASITPTPVQSQR	Not known	Prisic et al., 2010
		AEAS*ITPTPVQSQR	S	This study
		AEASITPT*PVQSQR	T	Prisic et al., 2010; This study
		VDPSAASGQDSTEAPRA	Not known	Chou et al., 2012
		VDPSAASGQDST*EARPA	T	This study
Rv2127	AnsP1	ERLGH ^T SGPFAVANPPVR	T	Prisic et al., 2010; This study
Rv2151c	FtsQ	VADDAADEEAVT*EPLATESK	T	Prisic et al., 2010; This study
Rv2197c	Rv2197c	MAEAEPATRPT*GASVR	T	Prisic et al., 2010; This study
		MAEAEPAT* ^R RPTGASVR	T	Prisic et al., 2010
		MAEAEPAT* ^R RPT*GASVR	T	This study
Rv2198c	MmpS3	ASGNHLPVAGGGDKLPSDQTGETDAYSR	Not known	Prisic et al., 2010
		ASGNHLPVAGGGDKLPSDQT*GETDAY ^S SR	T; Y	Kusebauch et al., 2014; This study
Rv2536	Rv2536	ADDSPTGEMQVAQPEAQTAAVATVER	Not known	Prisic et al., 2010
		AADTDVFSVR	Not known	Prisic et al., 2010
		AADT*DVFS*AVR	T	This study
Rv2536	Rv2536	EAPT ^S EVIR	T	Prisic et al., 2010; This study
		ADDSPT*GEMQVAQPEAQTAAVAT*VER	T	This study
		ADDS*PTGEMQVAQPEAQTAAVATVER	S	This study
Rv2606c	SnzP	MDPAGNPATGT ^S AR	T	Prisic et al., 2010; This study
		MDPAGNPAT*GTAR	T	This study
Rv2694c	Rv2694c	RIPGIDT ^S GR	T	Prisic et al., 2010; This study
Rv2696c	Rv2696c	EAAAAQADT* ^R QRQAAGVAR	T	Prisic et al., 2010
		EAAAAQADT* ^R QR	T	This study
Rv2921	FtsY	IDTSGLPVAGDDATVPR	Not known	Prisic et al., 2010
		IDTS*GLPAVGDDATVPR	S	This study
		IDT*SGLPVAGDDAT*VPR	T	This study
		IDT*SGLPVAGDDAT*VPR	T	This study
Rv2940c	Mas	ALAQYLADTLAEEQAAAPAS ^S	S	Prisic et al., 2010; This study
Rv2996c	SerA1	SATTVDAEVLAAAPK	Not known	Prisic et al., 2010
		SAT*TVDAEVLAAAPK	T	This study
		S*ATTVDAEVLAAAPK	S	This study
Rv3181c	Rv3181c	LAALDST* ^R DTLER	T	Prisic et al., 2010
		LAALDST* ^R DT*LER	T	This study
Rv3197	Rv3197	S ^R KDEVTAELMEK	S	Prisic et al., 2010
Rv3200c	Rv3200c	QSGADTVVSS ^S ETAGR	S	Prisic et al., 2010; This study
		QSGADTVVVS*SETAGR	S	This study

(Continued)

Table 1 | Continued

Rv numbers	Protein name	Phosphopeptides	Phospho-residue	References
Rv3248c	SahH	GVTEETTTGVLR	Not known	Prisic et al., 2010
		GVTEET*T*GVLR	T	This study
		GVTEET*TTGVLR	T	This study
Rv3604c	Rv3604c	TADTPPDDSGGLHAR	Not known	Prisic et al., 2010
		TADTPPDDSGGLHAR	S	This study
		DPLTGGQSVADLMAR	Not known	Prisic et al., 2010
		DPLT [§] GGQSVADLMAR	T	Prisic et al., 2010; This study
Rv3801c	FadD32	FDPEDTSEQLVIVGER	Not known	Prisic et al., 2010
		FDPEDT*SEQLVIVGER	T	This study
Rv3817	Rv3817	LWQAEDDS*S*R	S	This study
		RLWQAEDDSSR	Not known	Prisic et al., 2010
Rv3868	EccA1	LAQVLIDIT [§] LDEDLRLR	T	Prisic et al., 2010; This study

* Novel phosphorylated amino acid identified in this study.

Phosphorylated residue identified in previous studies.

§ Phosphorylated residue identified in current and previous studies.

Of the 401 serine/threonine phosphorylation sites (pS/T), only 156 had been previously described for *M. tuberculosis* (Table 1). Only 6 of 13 tyrosine phosphorylation sites (pY) has been previously described for *M. tuberculosis* (Kusebauch et al., 2014). The remaining 245 pS/T and 7 pY were uniquely identified in this study (Supplemental Table S2). To determine whether phosphorylated proteins were differentially represented in any particular cellular process, we grouped the phosphorylated proteins based on their functional category according to Tuberculist (Lew et al., 2011) (Figure 2). One hundred and seventy (79.4%) of the phosphorylated proteins had an annotated function, while the remaining 59 phosphorylated proteins (20.5%) were assigned as hypothetical. The biological function of the annotated proteins varied from transcription, translation, protein biosynthesis, fatty acid metabolism to phosphorylation. Our analysis identified phosphorylated forms of the 9 of the 11 *M. tuberculosis* STPKs: PknA, PknB, PknD, PknF, PknG, PknE, PknH, PknJ, and PknL (Table 2). Of these, phosphorylated forms of PknE, PknH, PknJ, and PknL had not been previously described in *M. tuberculosis*.

We detected 13 Y phosphorylation sites located on 10 proteins in *M. tuberculosis* during early-logarithmic growth. Six of the 13 Y phosphorylation sites (Table 3) were located on two proteins, FhaA and MmpS3 (Kusebauch et al., 2014) and have recently been described in a *M. tuberculosis* H37Rv at stationary growth phase. The remaining 7 Y phosphorylated sites were uniquely identified in this study. Amongst these with known annotations were 2 virulence factors (GroS and GroEL2) and Ppa involved in macromolecule biosynthesis.

A large number of proteins involved in intermediary metabolism and respiration processes such as lipid and fatty acid metabolism (KasB, FadD32, AccD4, and MmaA3) were found to be phosphorylated in this study (Supplemental Table S2). In addition, several proteins from the ESX-1 type seven secretion system (T7SS) in *M. tuberculosis* including EspR, EccA, CFP10, EspI, EspL, EspB were amongst the identified phosphorylated proteins (Supplemental Table S1). We also identified virulence factors such Pks15, AceA5, FadD5, EsxB, KatG, GlpX, Rv2032, and PtbB that

were phosphorylated in this hyper-virulent *M. tuberculosis* strain (Supplemental Table S2).

Of the 21 phosphorylated proteins involved in information pathways, we identified 6 phosphorylated ribosomal proteins; two phosphorylated small subunit (30S) ribosomal proteins (S3, S19), and four large subunit (50S) ribosomal proteins (L3, L24, L29, L31) with a total of 8 S/T phosphorylation sites. In addition, phosphorylated sites on the ribosomal proteins RpsS and RplX were also identified (Table 4).

DISCUSSION

Here we report 214 phosphorylated proteins extracted during early-logarithmic growth phase from a hyper-virulent clinical Beijing genotype *Mycobacterium tuberculosis* isolate. These proteins can be categorized into different biological functions according to Tuberculist (Lew et al., 2011). The impact of phosphorylation on these Hank's type Ser/Thr kinases (STPKs), phosphatases and their substrates, and the functional role of phosphorylated residues still remains to be elucidated. However, as in previous studies, the identification of phosphorylated residues clearly suggests functional importance.

REGULATORY PROTEINS

In recent years, bacterial S/T/Y kinases and phosphatases have been extensively investigated, with indications that they might play a crucial role in pathogenicity. These Hank's type kinases have the ability to short-circuit the host defense mechanism since they are mostly involved in key biological processes. We identified phosphopeptides from 9 of the 11 STPKs encoded by the *M. tuberculosis* genome. This included both previously described S/T phosphorylation sites (Boitel et al., 2003; Young et al., 2003; Durán et al., 2005; Villarino et al., 2005; Molle et al., 2006; O'Hare et al., 2008; Prisic et al., 2010; Sajid et al., 2011; Chou et al., 2012; Kusebauch et al., 2014) and novel sites on these STPKs thereby highlighting the complexity of the signal transduction mechanism of this pathogen. Phosphorylated peptides were not detected for PknI and PknK. However MS/MS spectra for these peptides

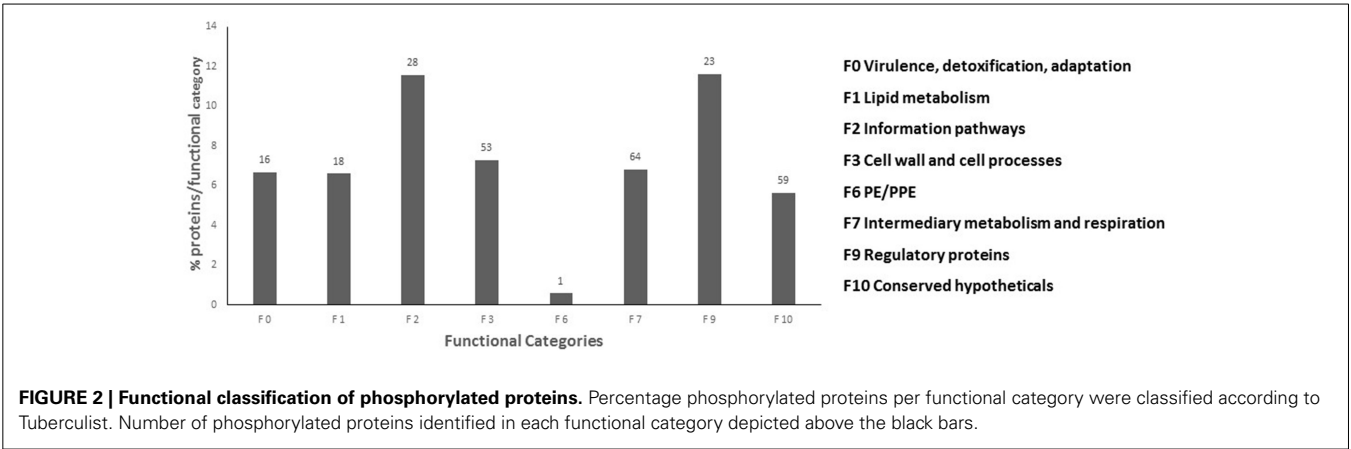


Table 2 | Serine/threonine kinases and their phosphorylation sites identified in this study.

STPK	Phosphorylated residue (position in protein)	Phosphopeptides	References
PknA	T ⁸ , S ¹⁰ , T ²²⁴ , S ²⁹⁹ , T ³⁰¹ , T ³⁰²	AAPAAIPS*GT*T*AR VGVT*LS*GR RPFAGDGALT#VAMK	This study This study Prisic et al., 2010
PknB	S ¹⁶⁹ , T ¹⁷¹ , T ¹⁷³ , S ³⁰⁵ , T ³⁰⁹	AIADSGNS*VT*QTAAVIGTAQYLSPEQAR TSLSSAAGNLS*GPRTDPLPR AIADSGNSVT*QT*AAVIGTAQYLSPEQAR TSLSSAAGNLSGPRT*DPLPR	This study This study This study This study
PknD	T ¹⁶⁹ , T ¹⁷¹ , S ³³² , T ³³⁴ , S ³⁴³ , S ³⁵⁰	GGNWPS*QTGHSPAVPNALQASLGHAVPPAGNK WSPGDS*AT*VAGPLAADS WSPGDS*ATVAGPLAADS*R AASDPGLT*QT*GTAVGTYNYMAPER	This study This study This study This study
PknE	S ³⁰⁴	LPVPSTHPVS*PGTR	This study
PknF	T ²⁸⁹ , S ²⁹⁰	LGGAGDPDDT*RVS*QPVAVAAPAK	This study
PknG	S ¹⁰ , T ¹⁴ , T ²³ , S ²⁴ , T ²⁶ , S ³¹ , T ³² , T ⁵⁵	PLS*T*QAVFR S*GPGT*QPADAQTATSATVR SGPGTQPADAQTAT*S*ATVRPLSTQAVFR PDFGDEDNFPHTLGPD*EPQDR SGPGTQPADAQTAT*SAT*VR	This study This study This study This study This study
PknH	T ¹⁷⁴	LTQLGT*AVGTWK	This study
PknJ	S ⁴⁹⁸	HLADLAS*IWRR	This study
PknL	S ³⁰⁶ , T ³⁰⁹	S*RIT*QQGQLGAK	This study

* Novel phosphorylation sites identified in this study.
Phosphorylated residue identified in previous studies.

for these proteins were detected with mass spectrometry thereby confirming the presence of these proteins (data not shown). Of the phosphorylated STPKs, PknA, PknB, and PknG have been shown to be essential for *in vitro* growth (Sasseti et al., 2003) and to regulate cell growth and cell division and interfere with host signaling pathways (Fernandez et al., 2006). PknE, PknH, PknJ, and PknL have been implicated in the adaptation to the extracellular environment or intracellular survival of *M. tuberculosis* (Sharma et al., 2006; Lakshminarayan, 2009; Arora et al., 2010; Parandhaman et al., 2014) which is in agreement with reports that during early growth the bacilli undergo a period of adaptation to their external environment (Stock et al., 1989; Soares et al., 2013). PknE is involved in the suppression

of apoptosis during nitrate stress (Kumar and Narayanan, 2012) and intracellular survival and adaptation to hostile environments (Parandhaman et al., 2014). In *M. tuberculosis*, PknH controls the expression of a variety of cell wall related enzymes and regulates *in vivo* growth in mice (Zheng et al., 2007). PknJ undergoes autophosphorylation and phosphorylates the Thr¹⁶⁸, Thr¹⁷¹, and Thr¹⁷³ residues of Embr (a transcriptional regulator), MmaA4/Hma (a methyltransferase involved in mycolic acid biosynthesis) and PepE (a peptidase located adjacent to the *pknJ* gene in the *M. tuberculosis* genome), respectively (Jang et al., 2010). Lastly, PknL is involved in an adaptive response to nutrient starvation. This kinase regulates transcription which allows the bacilli to maintain metabolic activity without sourcing energy

Table 3 | Tyrosine phosphorylation sites identified.

Rv number	Protein name	Tyrosine phosphopeptides	Biological Function	References
Rv0020c	FhaA	GGQGQGRPDEY*YDDR GGYPPEGGYPPQPGY*PRPR HEEGSY*VPSGPPGPPEQR HPDQGDY [§] PEQIGYPDQGGYPEQR QDYGGGADY [§] TR VPGY [§] APQGGGYAEPAGR	Signal transduction	This study This study This study Kusebauch et al., 2014; This study Kusebauch et al., 2014; This study Kusebauch et al., 2014; This study
Rv0421c	Rv0421c	GLAEGPLIAGGHS*Y*GGR	Hypothetical	This study
Rv0440	GroEL2	QEIENSDSDY [§] DREK	Protein refolding	Kusebauch et al., 2014; This study
Rv0613c	RecC	IVLAGY*DEELLER	Exonuclease V gamma chain	This study
Rv1513	Rv1513	HQDAFPANY*VGAQR	Hypothetical	This study
Rv2198c	MmpS3	ASGNHLPPVAGGGDKLPSDQT*GETDAY*SR AYS*APESEHVTGGPY [§] VPADLR AYS*APESEHVT*GGPY*VPADLR	Integral Membrane protein	This study Kusebauch et al., 2014 This study
Rv3418c	GroS	Y*GGTEIK	Response to stress	This study
Rv3628	Ppa	HFFVHY*K	Phosphate metabolic process	This study

[#] Previously identified pY site.

^{*} Novel pY site identified in this study.

[§] pY site identified in current and previous studies.

Table 4 | List of phosphorylated ribosomal proteins identified in this study and other bacteria.

Protein name	Protein name	Phosphopeptides	Phospho-residue	References
<i>rpsC</i>	<i>Streptomyces coelicolor</i> <i>M. tuberculosis</i>	Not known NPES*QAQLVAQGVAEQLSNR AAGGEEAAPDAAAPVEAQSTES*	Not known S S	Mikulik et al., 2011 This study This study
<i>rpsS</i>	<i>M. tuberculosis</i>	HVPVFVTES*MVGHK	S	This study
<i>rplC</i>	<i>Streptomyces coelicolor</i> <i>Streptococcus pneumonia</i> <i>Halobacterium salinarum</i> <i>M. tuberculosis</i>	Not known Not known Not known IVVEVCSQCHPFYT*GK	Not known Not known Not known T	Mikulik et al., 2011 Zhang et al., 2000 Aivaliotis et al., 2009 This study
<i>rplX</i>	<i>M. tuberculosis</i>	S*GGIVTQEAPIHVSNNVMVDSGKPTR	S	This study
<i>rpmC</i>	<i>Streptococcus agalatae</i> <i>Streptomyces coelicolor</i> <i>Listeria monocytogenes</i> <i>Lactococcus lactis</i> <i>M. tuberculosis</i>	FQAAAGQLEKT*AR RERELGIET*VESA FQLATGQLENT*AR DLSTTEIQDQEK MKLSETK ELGLATGPDGKES*	T T T Not known Not known S	Burnside et al., 2011 Manteca et al., 2011 Misra et al., 2011 Misra et al., 2011 Soufi et al., 2008 This study
<i>rpmE</i>	<i>Klebsiella pneumonia</i> <i>Halobacterium salinarum</i> <i>M. tuberculosis</i>	S*TVGHDLNLDVCGK ASSEFDDRFTVPLRDVTK T*GGLVMVR	S Not known T	Lin et al., 2009 Aivaliotis et al., 2009 This study

^{*} Novel pY site identified in this study.

from elsewhere (Lakshminarayan, 2009). Furthermore, we identified a number of STPK substrates that were phosphorylated in clinical hyper-virulent *M. tuberculosis* strain (list not shown) thereby highlighting the complexity of the phosphorylation regulatory network in *M. tuberculosis*. Even though the role of STPKs in bacterial physiology is not yet fully understood the data presented here could underpin a targeted approach to improving our understanding of STPK-mediated signal transduction mechanisms in *M. tuberculosis*.

TYROSINE PHOSPHORYLATION

The *M. tuberculosis* genome encodes for two putative tyrosine phosphatases (PtpA and PtpB) but is not predicted to encode tyrosine kinases (Cole et al., 1998; Bach et al., 2009). Most bacterial phosphorylation sites are on serine and threonine; a survey of 11 bacterial phosphoproteomes revealed that S/T phosphorylation accounted for an average of 48 and 40% of phosphorylated sites, respectively, while tyrosine phosphorylation events account for less than 10% of the overall phosphoproteome (Ge

and Shan, 2011). Tyrosine phosphorylated proteins have been previously shown to play important regulatory roles through their involvement in biological functions such as exopolysaccharide production, DNA metabolism, stress responses (Ge et al., 2011; Whitmore and Lamont, 2012). Recently, Kusebauch et al. identified tyrosine phosphorylated proteins in *M. tuberculosis* and demonstrated that a number of STPKs can phosphorylate tyrosine in either *cis* or *trans* (Kusebauch et al., 2014). This suggests that STPKs have the ability to phosphorylate S/T/Y. In this study we identified 13 tyrosine phosphorylation sites in 8 proteins (Table 3). An overlap of three proteins (FhaA, MmpS3, and GroES) and 6 tyrosine phosphorylated sites we similar between this and the previous study (Kusebauch et al., 2014). Five of the tyrosine phosphorylated proteins (FhaA, GroEL2, MmpS3, GroES, and Ppa) identified in this study are essential for *in vitro* growth (Sasseti et al., 2003; Griffin et al., 2011) and involved in a variety of functions.

This study confirmed and expanded work by Kusebauch et al., where multiple tyrosine phosphopeptides were identified for FhaA. FhaA is a regulatory protein which has been implicated in cell wall biosynthesis (Fernandez et al., 2006) and has a strong association with PknA and PknB (Pallen et al., 2002; Roumestand et al., 2011). We found that the highly S/T/Y phosphorylated FHA-domain contained 6 tyrosine phosphopeptides of which 4 were previously been identified in H₃₇Rv (Kusebauch et al., 2014). FhaA is a major substrate of PknB and has been implicated in the formation of a regulatory complex with MviN required for peptidoglycan biosynthesis (Warner and Mizrahi, 2012). In our dataset, we found that all three of the proteins (PknB, FhaA, and MviN) in the regulator complex were phosphorylated.

We also confirm the presence of a previously reported Y phosphopeptide of MmpS3 and identified a second phosphopeptide. MmpS3 forms part of the mycobacterial membrane protein small family and is an essential protein for mycobacterial growth and cholesterol metabolism (Griffin et al., 2012). The role of phosphorylation of this protein has yet to be determined.

The two proteins GroEL2 and GroES have been identified as potential candidates for antituberculosis treatment (Al-Attayah et al., 2006). We confirmed the presence of the Y phosphopeptide in GroEL2 identified in H₃₇Rv (Kusebauch et al., 2014). Recently it has been shown that the antigen GroES is sufficient to protect BALB/c mice against challenge infection (Lima et al., 2003) and up-regulated in kanamycin and amikacin resistant isolates (Kumar et al., 2013). Ppa is an inorganic pyrophosphate and is involved in macromolecule biosynthesis. The *M. tuberculosis* Ppa is highly similar to a well conserved homolog of *Legionella pneumophila* PPase which is induced in macrophages, although the *M. tuberculosis* Ppa promoter is not responsive to any specific intracellular triggers (Triccas and Gicquel, 2001).

VIRULENCE FACTORS

The identification of virulence factors is crucial in order to improve our understanding of the mechanisms involved in pathogenesis of *M. tuberculosis*. Several of the phosphorylated virulence

factors identified in this study were found to be involved in basic metabolic pathways such a lipid and fatty acid metabolism, secretion systems and response and adaptation to environmental changes. The virulence factor KasB and key enzymes (FadD32, AccD4, and MmaA3) in the mycolic acids biosynthesis pathway were phosphorylated in this hyper-virulent *M. tuberculosis* strain. The *kasB* gene is not essential for growth, however, the deletion mutant, $\Delta kasB$, resulted in an alteration in growth morphology and loss of acid-fast staining (Bhatt et al., 2007). This suggests that modification of this protein could influence the synthesis of mycolic acids and thereby the pathogenicity of the bacilli.

The specialized ESX-1 Type VII secretion system (T7SS), unique to pathogenic mycobacteria is responsible for the secretion of two culture filtrate proteins EsxA and EsxB (ESAT-6 and CFP-10). These secretion systems have been shown to be involved in virulence and are critical for intracellular survival (Bitter and Kuijl, 2014) due to their ability to secrete proteins that lack classical signal peptides across the complex cell envelope to host cells during infection (Houben et al., 2014, p. 5). *M. tuberculosis* have several different ESX regions (ESX-1 to ESX-5) (Daleke et al., 2012) with varying gene numbers and size for each of these secretion machinery. In this study we found 6 T7SS proteins to be phosphorylated in the hyper-virulent strain. In a previous study, proteomics of whole cell extracts of this hyper-virulent *M. tuberculosis* strain revealed an under-representation of virulence factors such as ESAT-6 and Esx-like proteins (de Souza et al., 2010). The authors showed the abundance of ESAT-6 gene expression was reduced in the hyper-virulent *M. tuberculosis* suggesting that the low levels of this protein might be as a result of its ability to export these proteins more efficiently into the extracellular environment (de Souza et al., 2010).

PROTEIN SYNTHESIS AND INTERACTIONS

The impact of phosphorylation on the functionality of ribosomal proteins is not fully understood. Mikulik et al. hypothesized that phosphorylation of ribosomal proteins induces or stabilizes conformational changes during proteins synthesis which could allow modification of subunit association or changes in interactions with proteins and RNAs (Mikulik et al., 2011). According to the protein phosphorylation database, phosphopeptides of RpmC have been identified in four different bacteria (Soufi et al., 2008; Burnside et al., 2011; Manteca et al., 2011; Misra et al., 2011). The implication of phosphorylation on RpmC has not been investigated. However, in *E. coli*, RpmC, RplW and Trigger factor are located at the exit tunnel in the ribosome, suggesting that phosphorylation may impact on multiple stages of transcription (Kramer et al., 2002). In our study we identified phosphopeptides for 7 ribosomal proteins. We also identified unique phosphopeptides on ribosomal proteins RpsS and RplX (Table 3).

OVERLAP OF PHOSPHORYLATED PROTEINS WITH OTHER BACTERIA

Twenty-five of phosphorylated proteins identified in our study were also identified in phosphoproteomics studies of other bacteria such as *Klebsiella pneumonia* (Lin et al., 2009), *Helicobacter pylori* (Ge et al., 2011), *Streptococcus pneumonia* (Sun et al., 2010),

Bacillus subtilis (Macek et al., 2007), *Halobacterium salinarum* (Aivaliotis et al., 2009), etc. (Table 4). In our dataset the distribution of S/T/Y seem to be bias toward pT and is in accordance with previously described phosphoproteomes of *M. tuberculosis* (Prisic et al., 2010; Kusebauch et al., 2014). Manual evaluation of the genome found an over-representation of Threonine relative to Serine (52:48%). This compared to other bacteria such as *Acinetobacter baumannii* (Soares et al., 2014), *Bacillus subtilis* (Macek et al., 2007), *Escherichia coli* (Macek et al., 2008; Soares et al., 2013) and *Halobacterium salinarum* (Aivaliotis et al., 2009), *Pseudomonas aeruginosa* (Ravichandran et al., 2009), and *Streptomyces coelicolor* (Parker et al., 2010) which demonstrate a bias toward pS.

Forty-five of the phosphorylated proteins identified in our study were previously described for *M. tuberculosis* H₃₇Rv (Boitel et al., 2003; Young et al., 2003; Molle et al., 2004, 2006; Durán et al., 2005; Kang et al., 2005; Villarino et al., 2005; O'Hare et al., 2008; Thakur et al., 2008; Prisic et al., 2010; Sajid et al., 2011; Gee et al., 2012). The reason for not identifying all of the previously identified phosphorylated proteins in the protein phosphorylation database could be ascribed to different genetic backgrounds of the analyzed *M. tuberculosis* strains, culture conditions, sample preparation and different MS-based proteomics approaches used in each of the studies. Our analysis was performed on a hyper-virulent clinical isolate of *M. tuberculosis* and a member of the Beijing genotype which is genetically distinct from the laboratory strain *M. tuberculosis* H₃₇Rv analyzed by Prisic et al. and Kusebauch et al. In addition, the Prisic et al. study reported on the combined phosphoproteome from 6 different conditions (5 different culture conditions and 2 different growth phases) (Prisic et al., 2010) while Kusebauch et al. reported on the phosphoproteome of late-logarithmic phase cultures (Kusebauch et al., 2014), whereas our study analyzed early-logarithmic phase cultures. Even though the overlap between our study of clinical *M. tuberculosis* and that of the previously described laboratory *M. tuberculosis* H₃₇Rv is low this work substantially extends our knowledge of the *M. tuberculosis* phosphoproteome. During logarithmic growth phase of bacterial growth the cells are adapting to the environment of the growth media and biological process such as RNA synthesis, DNA replication and synthesis of micro- and macromolecules are up-regulated. It is important to note that in this study the whole cell lysate proteins were enriched for phosphopeptides and we detected a number of phosphorylated proteins involved in these biological processes such as fatty acid- and lipid biosynthetic metabolism; RNA modification and translation; DNA repair, replication and modification. It is believed that environmental conditions, cell density and growth phase influence the expression of virulence factors by a pathogen (McIver et al., 1995). This is consistent other bacterial phosphoproteomes, thereby emphasizing that S/T/Y phosphorylation is an important process required for the regulation of numerous cellular processes.

CONCLUSION

Recent developments in the methodology and mass spectrometry technology for phosphoproteomics have highlighted the need to explore the involvement of phosphorylation in disease

development and progression. However, the impact of the protein phosphorylation cascade on the physiology of pathogenic bacteria such as *M. tuberculosis* has yet to be fully elucidated. Improved preparative techniques and more sensitive instrumentation are required to fully appreciate the complexity of protein modification. This can only be achieved if concomitant methods are developed to elucidate the impact of phosphorylation on protein function. Although this qualitative study was done in clinical hyper-virulent *M. tuberculosis*, without any follow-up validation studies it still provides a valuable resource for further investigating and understanding the impact of protein phosphorylation regulation in *M. tuberculosis*.

ACKNOWLEDGMENTS

This work was sponsored by the National Research Foundation Norway/RSA research cooperation programme, the Medical research Council of South Africa, DST/NRF Centre of Excellence for Biomedical Tuberculosis Research Stellenbosch University (Professor Paul van Helden). We further want to acknowledge Prof. M. Mann who permitted us to use the proteomics and mass spectrometry facilities at the Max Planck Institute, Munich, Germany.

SUPPLEMENTARY MATERIAL

The Supplementary Material for this article can be found online at: <http://www.frontiersin.org/journal/10.3389/fmicb.2015.00006/abstract>

REFERENCES

- Aivaliotis, M., Macek, B., Gnad, F., Reichelt, P., Mann, M., and Oesterhelt, D. (2009). Ser/Thr/Tyr protein phosphorylation in the archaeon *Halobacterium salinarum*—a representative of the third domain of life. *PLoS ONE* 4:e4777. doi: 10.1371/journal.pone.0004777
- Al-Attayah, R., Madi, N. M., El-Shamy, A. M., Wiker, H. G., Andersen, P., and Mustafa, A. S. (2006). Cytokine profiles in tuberculosis patients and healthy subjects in response to complex and single antigens of *Mycobacterium tuberculosis*. *FEMS Immunol. Med. Microbiol.* 47, 254–261. doi: 10.1111/j.1574-695X.2006.00110.x
- Arora, G., Sajid, A., Gupta, M., Bhaduri, A., Kumar, P., Basu-Modak, S., et al. (2010). Understanding the role of PknJ in *Mycobacterium tuberculosis*: biochemical characterization and identification of novel substrate pyruvate kinase A. *PLoS ONE* 5:10772. doi: 10.1371/journal.pone.0010772
- Bach, H., Wong, D., and Av-Gay, Y. (2009). *Mycobacterium tuberculosis* PtkA is a novel protein tyrosine kinase whose substrate is PtpA. *Biochem. J.* 420, 155–160. doi: 10.1042/BJ20090478
- Bhatt, A., Fujiwara, N., Bhatt, K., Gurucha, S. S., Kremer, L., Chen, B., et al. (2007). Deletion of kasB in *Mycobacterium tuberculosis* causes loss of acid-fastness and subclinical latent tuberculosis in immunocompetent mice. *Proc. Natl. Acad. Sci. U.S.A.* 104, 5157–5162. doi: 10.1073/pnas.0608654104
- Bitter, W., and Kuijl, C. (2014). Targeting bacterial virulence: the coming out of type VII secretion inhibitors. *Cell Host Microbe* 16, 430–432. doi: 10.1016/j.chom.2014.09.010
- Boitel, B., Ortiz-Lombardía, M., Durán, R., Pompeo, F., Cole, S. T., Cerveñansky, C., et al. (2003). PknB kinase activity is regulated by phosphorylation in two Thr residues and dephosphorylation by PstP, the cognate phospho-Ser/Thr phosphatase, in *Mycobacterium tuberculosis*. *Mol. Microbiol.* 49, 1493–1508. doi: 10.1046/j.1365-2958.2003.03657.x
- Burnside, K., Lembo, A., Harrell, M. L., Gurney, M., Xue, L., BinhTran, N.-T., et al. (2011). Serine/threonine phosphatase Stp1 mediates post-transcriptional regulation of hemolysin, autolysis, and virulence of group B *Streptococcus*. *J. Biol. Chem.* 286, 44197–44210. doi: 10.1074/jbc.M111.313486
- Chopra, P., Meena, L. S., and Singh, Y. (2003). New drug targets for *Mycobacterium tuberculosis*. *Indian J. Med. Res.* 117, 1–9.

- Chou, M. F., Prisc, S., Lubner, J. M., Church, G. M., Husson, R. N., and Schwartz, D. (2012). Using bacteria to determine protein kinase specificity and predict target substrates. *PLoS ONE* 7:e52747. doi: 10.1371/journal.pone.0052747
- Cole, S. T., Brosch, R., Parkhill, J., Garnier, T., Churcher, C., Harris, D., et al. (1998). Deciphering the biology of *Mycobacterium tuberculosis* from the complete genome sequence. *Nature* 393, 537–544. doi: 10.1038/31159
- Cozzzone, A. J. (1998). Post-translational modification of proteins by reversible phosphorylation in prokaryotes. *Biochimie* 80, 43–48.
- Daleke, M. H., Ummels, R., Bawono, P., Heringa, J., Vandenbroucke-Grauls, C. M. J. E., Luirink, J., et al. (2012). General secretion signal for the mycobacterial type VII secretion pathway. *Proc. Natl. Acad. Sci. U.S.A.* 109, 11342–11347. doi: 10.1073/pnas.1119453109
- de Souza, G. A., Fortuin, S., Aguilar, D., Pando, R. H., McEvoy, C. R. E., van Helden, P. D., et al. (2010). Using a label-free proteomics method to identify differentially abundant proteins in closely related hypo- and hypervirulent clinical *Mycobacterium tuberculosis* Beijing isolates. *Mol. Cell. Proteomics* 9, 2414–2423. doi: 10.1074/mcp.M900422-MCP200
- Durán, R., Villarino, A., Bellinzoni, M., Wehenkel, A., Fernandez, P., Boitel, B., et al. (2005). Conserved autophosphorylation pattern in activation loops and juxtamembrane regions of *Mycobacterium tuberculosis* Ser/Thr protein kinases. *Biochem. Biophys. Res. Commun.* 333, 858–867. doi: 10.1016/j.bbrc.2005.05.173
- Fernandez, P., Saint-Joanis, B., Barilone, N., Jackson, M., Gicquel, B., Cole, S. T., et al. (2006). The Ser/Thr protein kinase PknB is essential for sustaining mycobacterial growth. *J. Bacteriol.* 188, 7778–7784. doi: 10.1128/JB.00963-06
- Frasch, S. C., and Dworkin, M. (1996). Tyrosine phosphorylation in *Mycobacterium xanthus*, a multicellular prokaryote. *J. Bacteriol.* 178, 4084–4088.
- Ge, R., and Shan, W. (2011). Bacterial phosphoproteomic analysis reveals the correlation between protein phosphorylation and bacterial pathogenicity. *Genomics Proteomics Bioinformatics* 9, 119–127. doi: 10.1016/S1672-0229(11)60015-6
- Ge, R., Sun, X., Xiao, C., Yin, X., Shan, W., Chen, Z., et al. (2011). Phosphoproteome analysis of the pathogenic bacterium *Helicobacter pylori* reveals over-representation of tyrosine phosphorylation and multiply phosphorylated proteins. *Proteomics* 11, 1449–1461. doi: 10.1002/pmic.201000649
- Gee, C. L., Papavinasandaram, K. G., Blair, S. R., Baer, C. E., Falick, A. M., King, D. S., et al. (2012). A phosphorylated pseudokinase complex controls cell wall synthesis in *Mycobacteria*. *Sci. Signal.* 5, ra7. doi: 10.1126/scisignal.2002525
- Griffin, J. E., Gawronski, J. D., DeJesus, M. A., Ioerger, T. R., Akerley, B. J., and Sassetti, C. M. (2011). High-resolution phenotypic profiling defines genes essential for *Mycobacterium tuberculosis* growth and cholesterol catabolism. *PLoS Pathog.* 7:e1002251. doi: 10.1371/journal.ppat.1002251
- Griffin, J. E., Pandey, A. K., Gilmore, S. A., Mizrahi, V., McKinney, J. D., Bertozzi, C. R., et al. (2012). Cholesterol catabolism by *Mycobacterium tuberculosis* requires transcriptional and metabolic adaptations. *Chem. Biol.* 19, 218–227. doi: 10.1016/j.chembiol.2011.12.016
- Gupta, N., Tanner, S., Jaitly, N., Adkins, J. N., Lipton, M., Edwards, R., et al. (2007). Whole proteome analysis of post-translational modifications: applications of mass-spectrometry for proteogenomic annotation. *Genome Res.* 17, 1362–1377. doi: 10.1101/gr.6427907
- Houben, E. N. G., Korotkov, K. V., and Bitter, W. (2014). Take five—Type VII secretion systems of *Mycobacteria*. *Biochim. Biophys. Acta* 1843, 1707–1716. doi: 10.1016/j.bbamcr.2013.11.003
- Jang, J., Stella, A., Boudou, F., Levillain, F., Darthuy, E., Vaubourgeix, J., et al. (2010). Functional characterization of the *Mycobacterium tuberculosis* serine/threonine kinase PknJ. *Microbiol. Read. Engl.* 156, 1619–1631. doi: 10.1099/mic.0.038133-0
- Kang, C.-M., Abbott, D. W., Park, S. T., Dascher, C. C., Cantley, L. C., and Husson, R. N. (2005). The *Mycobacterium tuberculosis* serine/threonine kinases PknA and PknB: substrate identification and regulation of cell shape. *Genes Dev.* 19, 1692–1704. doi: 10.1101/gad.1311105
- Koul, A., Herget, T., Klebl, B., and Ullrich, A. (2004). Interplay between mycobacteria and host signalling pathways. *Nat. Rev. Microbiol.* 2, 189–202. doi: 10.1038/nrmicro840
- Kramer, G., Rauch, T., Rist, W., Vorderwülbecke, S., Patzelt, H., Schulze-Specking, A., et al. (2002). L23 protein functions as a chaperone docking site on the ribosome. *Nature* 419, 171–174. doi: 10.1038/nature01047
- Kumar, B., Sharma, D., Sharma, P., Katoch, V. M., Venkatesan, K., and Bisht, D. (2013). Proteomic analysis of *Mycobacterium tuberculosis* isolates resistant to kanamycin and amikacin. *J. Proteomics* 94, 68–77. doi: 10.1016/j.jprot.2013.08.025
- Kumar, D., and Narayanan, S. (2012). pknE, a serine/threonine kinase of *Mycobacterium tuberculosis* modulates multiple apoptotic paradigms. *Infect. Genet. Evol. J. Mol. Epidemiol. Evol. Genet. Infect. Dis.* 12, 737–747. doi: 10.1016/j.meegid.2011.09.008
- Kusebauch, U., Ortega, C., Olloidal, A., Rogers, R. S., Sherman, D. R., Moritz, R. L., et al. (2014). *Mycobacterium tuberculosis* supports protein tyrosine phosphorylation. *Proc. Natl. Acad. Sci. U.S.A.* 111, 9265–9270. doi: 10.1073/pnas.1323894111
- Lakshminarayan, H. (2009). Involvement of serine threonine protein kinase PknL, from *Mycobacterium tuberculosis* H37Rv in starvation response of *Mycobacteria*. *J. Microb. Biochem. Technol.* 1, 30–36.
- Lew, J. M., Kapopoulou, A., Jones, L. M., and Cole, S. T. (2011). TubercuList—10 years after. *Tuberc. Edinb. Scotl.* 91, 1–7. doi: 10.1016/j.tube.2010.09.008
- Lima, K. M., Santos, S. A., Lima, V. M. F., Coelho-Castelo, A. A. M., Rodrigues, J. M., and Silva, C. L. (2003). Single dose of a vaccine based on DNA encoding mycobacterial hsp65 protein plus TDM-loaded PLGA microspheres protects mice against a virulent strain of *Mycobacterium tuberculosis*. *Gene Ther.* 10, 678–685. doi: 10.1038/sj.gt.3301908
- Lin, M.-H., Hsu, T.-L., Lin, S.-Y., Pan, Y.-J., Jan, J.-T., Wang, J.-T., et al. (2009). Phosphoproteomics of *Klebsiella pneumoniae* NTUH-K2044 reveals a tight link between tyrosine phosphorylation and virulence. *Mol. Cell. Proteomics* 8, 2613–2623. doi: 10.1074/mcp.M900276-MCP200
- Macek, B., Gnad, F., Soufi, B., Kumar, C., Olsen, J. V., Mijakovic, I., et al. (2008). Phosphoproteome analysis of *E. coli* reveals evolutionary conservation of bacterial Ser/Thr/Tyr phosphorylation. *Mol. Cell. Proteomics* 7, 299–307. doi: 10.1074/mcp.M700311-MCP200
- Macek, B., and Mijakovic, I. (2011). Site-specific analysis of bacterial phosphoproteomes. *Proteomics* 11, 3002–3011. doi: 10.1002/pmic.201100012
- Macek, B., Mijakovic, I., Olsen, J. V., Gnad, F., Kumar, C., Jensen, P. R., et al. (2007). The serine/threonine/tyrosine phosphoproteome of the model bacterium *Bacillus subtilis*. *Mol. Cell. Proteomics* 6, 697–707. doi: 10.1074/mcp.M600464-MCP200
- Manteca, A., Ye, J., Sánchez, J., and Jensen, O. N. (2011). Phosphoproteome analysis of *Streptomyces* development reveals extensive protein phosphorylation accompanying bacterial differentiation. *J. Proteome Res.* 10, 5481–5492. doi: 10.1021/pr200762y
- McConnell, J. L., and Wadzinski, B. E. (2009). Targeting protein serine/threonine phosphatases for drug development. *Mol. Pharmacol.* 75, 1249–1261. doi: 10.1124/mol.108.053140
- McIver, K. S., Heath, A. S., and Scott, J. R. (1995). Regulation of virulence by environmental signals in group A streptococci: influence of osmolarity, temperature, gas exchange, and iron limitation on emm transcription. *Infect. Immun.* 63, 4540–4542.
- Mijakovic, I., and Macek, B. (2012). Impact of phosphoproteomics on studies of bacterial physiology. *FEMS Microbiol. Rev.* 36, 877–892. doi: 10.1111/j.1574-6976.2011.00314.x
- Mikulík, K., Bobek, J., Ziková, A., Smětáková, M., and Bezoušková, S. (2011). Phosphorylation of ribosomal proteins influences subunit association and translation of poly (U) in *Streptomyces coelicolor*. *Mol. Biosyst.* 7, 817–823. doi: 10.1039/c0mb00174k
- Misra, S. K., Milohanic, E., Aké, F., Mijakovic, I., Deutscher, J., Monnet, V., et al. (2011). Analysis of the serine/threonine/tyrosine phosphoproteome of the pathogenic bacterium *Listeria monocytogenes* reveals phosphorylated proteins related to virulence. *Proteomics* 11, 4155–4165. doi: 10.1002/pmic.201100259
- Molle, V., Brown, A. K., Besra, G. S., Cozzzone, A. J., and Kremer, L. (2006). The condensing activities of the *Mycobacterium tuberculosis* type II fatty acid synthase are differentially regulated by phosphorylation. *J. Biol. Chem.* 281, 30094–30103. doi: 10.1074/jbc.M601691200
- Molle, V., Leiba, J., Zanella-Cléon, I., Becchi, M., and Kremer, L. (2010). An improved method to unravel phosphoacceptors in Ser/Thr protein kinase-phosphorylated substrates. *Proteomics* 10, 3910–3915. doi: 10.1002/pmic.201000316
- Molle, V., Soulat, D., Jault, J.-M., Grangeasse, C., Cozzzone, A. J., and Prost, J.-F. (2004). Two FHA domains on an ABC transporter, Rv1747, mediate its phosphorylation by PknF, a Ser/Thr protein kinase from *Mycobacterium tuberculosis*. *FEMS Microbiol. Lett.* 234, 215–223. doi: 10.1016/j.femsle.2004.03.033

- O'Hare, H. M., Durán, R., Cerveñansky, C., Bellinzoni, M., Wehenkel, A. M., Pritsch, O., et al. (2008). Regulation of glutamate metabolism by protein kinases in mycobacteria. *Mol. Microbiol.* 70, 1408–1423. doi: 10.1111/j.1365-2958.2008.06489.x
- Pallen, M., Chaudhuri, R., and Khan, A. (2002). Bacterial FHA domains: neglected players in the phospho-threonine signalling game? *Trends Microbiol.* 10, 556–563. doi: 10.1016/S0966-842X(02)02476-9
- Parandhaman, D. K., Hanna, L. E., and Narayanan, S. (2014). PknE, a serine/threonine protein kinase of *Mycobacterium tuberculosis* initiates survival crosstalk that also impacts HIV coinfection. *PLoS ONE* 9:e83541. doi: 10.1371/journal.pone.0083541
- Parker, J. L., Jones, A. M. E., Serazetdinova, L., Saalbach, G., Bibb, M. J., and Naldrett, M. J. (2010). Analysis of the phosphoproteome of the multicellular bacterium *Streptomyces coelicolor* A3(2) by protein/peptide fractionation, phosphopeptide enrichment and high-accuracy mass spectrometry. *Proteomics* 10, 2486–2497. doi: 10.1002/pmic.201000090
- Prisic, S., Dankwa, S., Schwartz, D., Chou, M. F., Locasale, J. W., Kang, C.-M., et al. (2010). Extensive phosphorylation with overlapping specificity by *Mycobacterium tuberculosis* serine/threonine protein kinases. *Proc. Natl. Acad. Sci. U.S.A.* 107, 7521–7526. doi: 10.1073/pnas.0913482107
- Ravichandran, A., Sugiyama, N., Tomita, M., Swarup, S., and Ishihama, Y. (2009). Ser/Thr/Tyr phosphoproteome analysis of pathogenic and non-pathogenic *Pseudomonas* species. *Proteomics* 9, 2764–2775. doi: 10.1002/pmic.200800655
- Roumestand, C., Leiba, J., Galoppe, N., Margeat, E., Padilla, A., Bessin, Y., et al. (2011). Structural insight into the *Mycobacterium tuberculosis* Rv0202c protein and its interaction with the PknB kinase. *Structure* 19, 1525–1534. doi: 10.1016/j.str.2011.07.011
- Sajid, A., Arora, G., Gupta, M., Singhal, A., Chakraborty, K., Nandicoori, V. K., et al. (2011). Interaction of *Mycobacterium tuberculosis* elongation factor Tu with GTP is regulated by phosphorylation. *J. Bacteriol.* 193, 5347–5358. doi: 10.1128/JB.05469-11
- Sala, C., and Hartkoorn, R. C. (2011). Tuberculosis drugs: new candidates and how to find more. *Future Microbiol.* 6, 617–633. doi: 10.2217/fmb.11.46
- Sassetti, C. M., Boyd, D. H., and Rubin, E. J. (2003). Genes required for mycobacterial growth defined by high density mutagenesis. *Mol. Microbiol.* 48, 77–84. doi: 10.1046/j.1365-2958.2003.03425.x
- Seo, J., and Lee, K.-J. (2004). Post-translational modifications and their biological functions: proteomic analysis and systematic approaches. *J. Biochem. Mol. Biol.* 37, 35–44. doi: 10.5483/BMBRep.2004.37.1.035
- Sharma, K., Chopra, P., and Singh, Y. (2004). Recent advances towards identification of new drug targets for *Mycobacterium tuberculosis*. *Expert Opin. Ther. Targets* 8, 79–93. doi: 10.1517/14728222.8.2.79
- Sharma, K., Gupta, M., Pathak, M., Gupta, N., Koul, A., Sarangi, S., et al. (2006). Transcriptional control of the mycobacterial embCAB operon by PknH through a regulatory protein, EmbR, *in vivo*. *J. Bacteriol.* 188, 2936–2944. doi: 10.1128/JB.188.8.2936-2944.2006
- Soares, N. C., Spät, P., Ménédez, J. A., Nokedi, K., Aranda, J., and Bou, G. (2014). Ser/Thr/Tyr phosphoproteome characterization of *Acinetobacter baumannii*: comparison between a reference strain and a highly invasive multidrug-resistant clinical isolate. *J. Proteomics* 102, 113–124. doi: 10.1016/j.jpro.2014.03.009
- Soufi, B., Gnad, F., Jensen, P. R., Petranovic, D., Mann, M., Mijakovic, I., et al. (2008). The Ser/Thr/Tyr phosphoproteome of *Lactococcus lactis* IL1403 reveals multiply phosphorylated proteins. *Proteomics* 8, 3486–3493. doi: 10.1002/pmic.200800069
- Stock, J. B., Ninfa, A. J., and Stock, A. M. (1989). Protein phosphorylation and regulation of adaptive responses in bacteria. *Microbiol. Rev.* 53, 450–490.
- Sun, X., Ge, F., Xiao, C.-L., Yin, X.-F., Ge, R., Zhang, L.-H., et al. (2010). Phosphoproteomic analysis reveals the multiple roles of phosphorylation in pathogenic bacterium *Streptococcus pneumoniae*. *J. Proteome Res.* 9, 275–282. doi: 10.1021/pr900612v
- Thakur, M., Chaba, R., Mondal, A. K., and Chakraborti, P. K. (2008). Interdomain interaction reconstitutes the functionality of PknA, a eukaryotic type Ser/Thr kinase from *Mycobacterium tuberculosis*. *J. Biol. Chem.* 283, 8023–8033. doi: 10.1074/jbc.M707535200
- Triccas, J. A., and Gicquel, B. (2001). Analysis of stress- and host cell-induced expression of the *Mycobacterium tuberculosis* inorganic pyrophosphatase. *BMC Microbiol.* 1:3. doi: 10.1186/1471-2180-1-3
- Villarino, A., Duran, R., Wehenkel, A., Fernandez, P., England, P., Brodin, P., et al. (2005). Proteomic identification of *M. tuberculosis* protein kinase substrates: PknB recruits GarA, a FHA domain-containing protein, through activation loop-mediated interactions. *J. Mol. Biol.* 350, 953–963. doi: 10.1016/j.jmb.2005.05.049
- Warner, D. F., and Mizrahi, V. (2012). A pseudokinase debut at the mycobacterial cell wall. *Sci. Signal.* 5, pe3–pe3. doi: 10.1126/scisignal.2002785
- Whitmore, S. E., and Lamont, R. J. (2012). Tyrosine phosphorylation and bacterial virulence. *Int. J. Oral Sci.* 4, 1–6. doi: 10.1038/ijos.2012.6
- WHO/Global tuberculosis report 2013. (2013). WHO. Available online at: <http://www.who.int/tb/publications/globalreport/en/> [Accessed October 1, 2014].
- WHO/Global tuberculosis report 2014. (2014). WHO/Global Tuberculosis Report 2014, Geneva.
- Wiśniewski, J. R., Zougman, A., Nagaraj, N., and Mann, M. (2009). Universal sample preparation method for proteome analysis. *Nat. Methods* 6, 359–362. doi: 10.1038/nmeth.1322
- Young, T. A., Delagoutte, B., Endrizzi, J. A., Falick, A. M., and Alber, T. (2003). Structure of *Mycobacterium tuberculosis* PknB supports a universal activation mechanism for Ser/Thr protein kinases. *Nat. Struct. Mol. Biol.* 10, 168–174. doi: 10.1038/nsb897
- Zhang, W., Li, L., Jiang, W., Zhao, G., Yang, Y., and Chiao, J. (2000). A novel transmembrane serine/threonine protein kinase gene from a rifamycin SV-producing amycolatopsis mediterranei U32. *Eur. J. Biochem. FEBS* 267, 3744–3752. doi: 10.1046/j.1432-1327.2000.01410.x
- Zheng, X., Papavinasundaram, K. G., and Av-Gay, Y. (2007). Novel substrates of *Mycobacterium tuberculosis* PknH Ser/Thr kinase. *Biochem. Biophys. Res. Commun.* 355, 162–168. doi: 10.1016/j.bbrc.2007.01.122

Conflict of Interest Statement: The authors declare that the research was conducted in the absence of any commercial or financial relationships that could be construed as a potential conflict of interest.

Received: 31 October 2014; accepted: 04 January 2015; published online: 10 February 2015.

Citation: Fortuin S, Tomazella GG, Nagaraj N, Sampson SL, Gey van Pittius NC, Soares NC, Wiker HG, de Souza GA and Warren RM (2015) Phosphoproteomics analysis of a clinical *Mycobacterium tuberculosis* Beijing isolate: expanding the mycobacterial phosphoproteome catalog. *Front. Microbiol.* 6:6. doi: 10.3389/fmicb.2015.00006

This article was submitted to *Microbial Physiology and Metabolism*, a section of the journal *Frontiers in Microbiology*.

Copyright © 2015 Fortuin, Tomazella, Nagaraj, Sampson, Gey van Pittius, Soares, Wiker, de Souza and Warren. This is an open-access article distributed under the terms of the Creative Commons Attribution License (CC BY). The use, distribution or reproduction in other forums is permitted, provided the original author(s) or licensor are credited and that the original publication in this journal is cited, in accordance with accepted academic practice. No use, distribution or reproduction is permitted which does not comply with these terms.



The length of a lantibiotic hinge region has profound influence on antimicrobial activity and host specificity

Liang Zhou, Auke J. van Heel and Oscar P. Kuipers*

Department of Molecular Genetics, Groningen Biomolecular Sciences and Biotechnology Institute, University of Groningen, Groningen, Netherlands

Edited by:

Ivan Mijakovic, Chalmers University of Technology, Sweden

Reviewed by:

Thomas Hindré, University J. Fourier - Centre National de la Recherche Scientifique, France
Susanne Gebhard, University of Bath, UK

*Correspondence:

Oscar P. Kuipers, Department of Molecular Genetics, Groningen Biomolecular Sciences and Biotechnology Institute, University of Groningen, Groningen, Nijenborgh 7, 9747 AG, Netherlands
e-mail: o.p.kuipers@rug.nl

Lantibiotics are ribosomally synthesized (methyl)lanthionine containing peptides which can efficiently inhibit the growth of Gram-positive bacteria. As lantibiotics kill bacteria efficiently and resistance to them is difficult to be obtained, they have the potential to be used in many applications, e.g., in pharmaceutical industry or food industry. Nisin can inhibit the growth of Gram-positive bacteria by binding to lipid II and by making pores in their membrane. The C-terminal part of nisin is known to play an important role during translocation over the membrane and forming pore complexes. However, as the thickness of bacterial membranes varies between different species and environmental conditions, this property could have an influence on the pore forming activity of nisin. To investigate this, the so-called “hinge region” of nisin (residues NMK) was engineered to vary from one to six amino acid residues and specific activity against different indicators was compared. Antimicrobial activity in liquid culture assays showed that wild type nisin is most active, while truncation of the hinge region dramatically reduced the activity of the peptide. However, one or two amino acids extensions showed only slightly reduced activity against most indicator strains. Notably, some variants (+2, +1, -1, -2) exhibited higher antimicrobial activity than nisin in agar well diffusion assays against *Lactococcus lactis* MG1363, *Listeria monocytogenes*, *Enterococcus faecalis* VE14089, *Bacillus sporothermodurans* IC4 and *Bacillus cereus* 4153 at certain temperatures.

Keywords: lantibiotics, nisin, hinge region, membrane, diffusion

INTRODUCTION

The increasing occurrence of multi-drug resistance (Davies and Davies, 2010) has made the development of new antibiotics a priority. Lantibiotics (lanthionine-containing antibiotics) display strong activity against Gram-positive pathogens and can become a valuable addition to traditional antibiotics (van Heel et al., 2011). Nisin (Figure 1), is the prototype lantibiotic from *Lactococcus lactis* and it is active against Gram-positive bacteria at the nanomolar range. The biosynthesis of nisin involves ribosomal peptide synthesis, dehydration of serine and threonine residues, cyclization via sulfhydryl addition of cysteine to a dehydrated residue, transportation of the precursor peptide and proteolytic activation (Lubelski et al., 2008b). After ribosomal synthesis, nisin has a leader peptide part in front of the core peptide and is called prenisin. The leader peptide guides prenisin to NisB that dehydrates serines and threonines to form dehydroalanines (Dha) and dehydrobutyrines (Dhb). NisC can couple cysteines to dehydrated residues by an addition reaction, resulting in five (methyl)lanthionine rings in the structure of nisin. Subsequently, NisT transports the modified prenisin to the outside of the cell. Prenisin can be activated by cutting off the leader, a process that is catalyzed by the dedicated proteinase NisP.

Nisin has two inhibition mechanisms (Wiedemann et al., 2001; Breukink and de Kruijff, 2006): it binds to lipid II and causes pore formation. Lipid II is located in the membrane and

plays an essential role in cell wall synthesis. Nisin can pass the peptidoglycan layer of Gram-positive bacteria and can bind to lipid II with the first two rings, which inhibits cell wall synthesis and bacterial growth. After binding, the C-terminal part of nisin will insert into the lipid bilayer, and subsequently a nisin-lipid II complex will be assembled (8:4) to form a pore complex in the membrane, eventually killing the bacterium (Hasper et al., 2004).

The so-called hinge region of nisin consisting of 3 amino acids (NMK) is located between the first three rings and the last two rings of nisin (see Figure 1). This region has been implicated to play an important role during insertion of the C-terminus of nisin into the membrane (Hasper et al., 2004). Mutagenesis of the hinge region has been studied intensively (Lubelski et al., 2008b; Ross and Vederas, 2011). The most recent research was conducted by Healy et al. (2013). Two mutants (AAA and SAA) were rationally designed based on random mutagenesis results, and the mutants showed enhanced activity against specific indicator strains such as *Lactococcus lactis* HP, *Streptococcus agalactiae* ATCC 13813, *Mycobacterium smegmatis* MC2155 and *Staphylococcus aureus* RF122.

So far, there has been no systematic study performed on the influence of the length of the hinge region on activity and spectrum. Nisin has to bend into the membrane and form a stable pore complex, and the membrane thickness of the bacteria might affect the activity of nisin. As we know, the thicknesses of bacterial

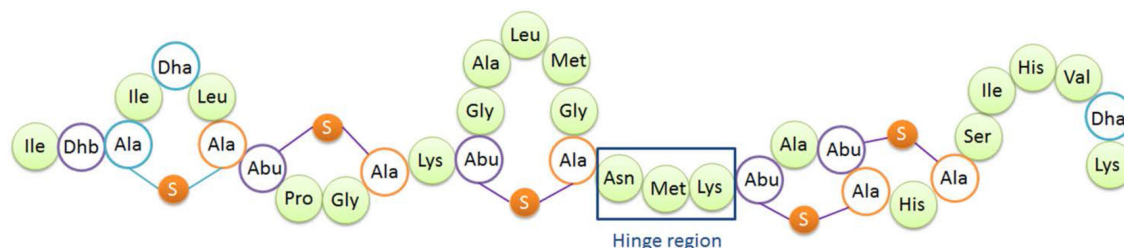


FIGURE 1 | Structure of nisin A. Dha, dehydroalanine; Dhb, dehydrobutyrine; Ala-S-Ala, lanthionine; Abu-S-Ala, β -methyllanthionine. The hinge region (Asn-Met-Lys) is indicated.

membranes are affected by temperature (Cybulski et al., 2010) and different species can have different membrane thicknesses. To modulate the activity of nisin against bacteria with different membrane thicknesses, varying the length of the peptide could be effective. In the paper of Lubelski et al. (2008a), one to four alanines were added behind lysine 22 of nisin and the activities of these variants against *L. lactis* were tested, but the inhibition spectrum was not shown. In this current paper, the length of the nisin hinge region was varied from 1 to 6 amino acids. The variants were characterized by MS and activity assays on 10 different indicator strains. Profound effects of the length of the hinge region on the activity of the resulting peptides were demonstrated. This study represents a first trial on the rational design of the length of the hinge region assuming the difference in membrane thickness of targeted bacteria is important for effective membrane insertion.

MATERIALS AND METHODS

BACTERIAL STRAINS AND GROWTH CONDITIONS

The bacterial strains used in this study are listed in **Table 1**. *L. lactis* strains were cultured in M17 broth supplemented with 0.5% (w/v) glucose (GM17) or GM17 agar for genetic manipulation or in minimal expression medium (MEM) for protein expression at 30°C (Rink et al., 2005). *E. faecalis*, *S. aureus*, *S. pneumoniae*, and *L. monocytogenes* were grown in GM17 at 37°C or GM17 agar at different temperatures for agar diffusion assay. *M. luteus* was grown in Luria-Bertani broth shaken (200 rpm) at 30°C or LB agar at 20°C for agar diffusion assay. *Bacillus* strains were cultured in Brain Heart Infusion (BHI) shaken (200 rpm) or BHI agar at different temperatures for agar diffusion assay.

MOLECULAR CLONING

To obtain the hinge region variants, primers were designed to modify the DNA sequence of specific amino acids. With these primers (containing the modification on the 5' end), the full plasmid was amplified. Phusion High-Fidelity DNA Polymerase (Thermo Scientific) was used to perform the PCR (Sambrook and Russell, 2001). PCR products were purified (Roche Switzerland) and ligated according to the manufacturer of the ligase (Thermo Scientific). The DNA sequence encoding the +3 variant was synthesized commercially (Life Technologies). Preparation of competent cells and transformation were performed as described previously (Holo and Nes, 1995).

EXPRESSION, TCA PRECIPITATION AND TRICINE SDS-PAGE

The expression strain *L. lactis* NZ9000 contained plasmids pIL3EryBTC and pNZnisA harboring different variants of the hinge region. Cells were cultured at 30°C first in GM17 medium with 4 μ g/ml chloramphenicol and 4 μ g/ml erythromycin until OD (600 nm) reached 0.7, then centrifuged and resuspended in MEM medium with 0.5% (w/v) glucose, 3 μ g/ml chloramphenicol, 3 μ g/ml erythromycin and 2 nM nisin to induce. After 3 h induction, the supernatant was harvested. The supernatant of small volume of fermentation (<10 ml) was concentrated by TCA precipitation (Sambrook and Russell, 2001) and the concentrated peptides were loaded on Tricine SDS-PAGE gel (Schägger, 2006) to check the amount and purity.

PURIFICATION, CHARACTERIZATION AND QUANTIFICATION

>100 microgram of prenisin variants were purified by cation-ion exchange, desalting and freeze-drying (van Heel et al., 2013). The freeze dried peptides were dissolved and cut by trypsin overnight at 37°C in 50 mM Tris-HCl (pH 6.8) to separate the leader and core peptide. The digested product was further purified by HPLC (Agilent 1260 Infinity LC) equipped with a semi-preparative C12 column (Phenomenex 250 \times 10 mm). The fractions were collected, tested for activity against *L. lactis* and analyzed with MALDI-TOF (van Heel et al., 2013). The active, fully dehydrated and pure fractions were freeze-dried. The freeze-dried peptides were dissolved with 0.05% acetic acid and first quantified by BCA (Thermo Scientific), using pure nisin as standard. The preliminary normalized peptides were further quantified with HPLC with an analytical C12 column (Phenomenex 250 \times 4.60 mm). The concentration of the peptide was calculated by comparing the area of absorption peak at 226 nm with the area of different amount of pure nisin.

DETERMINATION OF THE MINIMUM INHIBITORY CONCENTRATION (MIC)

The indicator strains were cultured until OD (600 nm) reached 0.5. Before MIC value test, the culture was diluted 1000 times to make the concentration of cells around 5×10^5 per milliliter. The test was performed using a temperature controlled plate reader [Tecan200 (Tecan Group AG)] and 96 well plate (Greiner Bio-one). 180 μ l indicator strain culture mixed with 20 μ l hinge region analogs with final concentration from 0.031 μ g/ml–32 μ g/ml was incubated at 30°C or 37°C for 18 h. OD (600 nm) was checked every 30 min. For aerobic strains, 2 min of shaking

Table 1 | Strains and plasmids used in this study.

Strain or plasmids	Characteristics	References
STRAIN		
<i>Lactococcus lactis</i> NZ9000	<i>nisRK</i>	Kuipers et al., 1997
PLASMIDS		
pIL3EryBTC	<i>nisBTC</i> , encoding nisin modification machinery, EryR ^a	van Heel et al., 2013
pNZ8048	Nisin inducible promoter in shuttle vector	de Ruyter et al., 1996
pNZnisA	<i>nisA</i> , encoding nisin, CmR ^a , inserted in pNZ8048	van Heel et al., 2013
pNZnisA H-2	<i>nisA</i> , encoding nisin, with methionine and lysine in the hinge region deleted	This study
pNZnisA H-1	<i>nisA</i> , encoding nisin, with methionine in the hinge region deleted	This study
pNZnisA H+1L	<i>nisA</i> , encoding nisin, with leucine inserted behind asparagine in the hinge region	This study
pNZnisA H+1V	<i>nisA</i> , encoding nisin, with valine inserted behind asparagine in the hinge region	This study
pNZnisA H+1I	<i>nisA</i> , encoding nisin, with isoleucine inserted behind asparagine in the hinge region	This study
pNZnisA H+2	<i>nisA</i> , encoding nisin, with isoleucine and valine inserted behind asparagine in the hinge region	This study
pNZnisA H+3	<i>nisA</i> , encoding nisin, with isoleucine, valine and leucine inserted behind asparagine in the hinge region	This study
Indicator strains		
<i>Lactococcus lactis</i> MG1363	Nisin sensitive indicator	Gasson, 1983
<i>Enterococcus faecalis</i> VE14089	Nisin sensitive indicator	Rigottier-Gois et al., 2011
<i>Staphylococcus aureus</i>	Nisin sensitive indicator	Lab collection
<i>Micrococcus luteus</i>	Nisin sensitive indicator	Lab collection
<i>Streptococcus pneumonia</i> R6	Nisin sensitive indicator	Lab collection
<i>Listeria monocytogenes</i>	Nisin sensitive indicator	Lab collection
<i>Bacillus sporothermodurans</i> IC4	Nisin sensitive indicator	TIFN collection
<i>Bacillus cereus</i> (L29) 16	Nisin sensitive indicator	TIFN collection
<i>Bacillus cereus</i> 4147	Nisin sensitive indicator	TIFN collection
<i>Bacillus cereus</i> 4153	Nisin sensitive indicator	TIFN collection

^a EryR, erythromycin resistance; CmR, chloramphenicol resistance.

was performed before every check. The concentration of peptide without observed growth of indicator strains was considered as the MIC value.

AGAR WELL DIFFUSION ASSAY

For the agar well diffusion assay, the same cultures as in the MIC value test were used and diluted 200 times with solid media. Identical sizes of wells (7.5 mm diameter) were made and 2 µg of hinge region analogs dissolved in 20 µl 0.05% acetic acid were added. The plates were incubated at different temperatures for at least 1 day until apparent halos appeared. For activity test at low temperature, the indicators were diluted in the same way but poured into smaller plates (52 mm diameter). The plates were incubated at 4°C overnight before the peptides were added. *B. sporothermodurans* IC4 and *B. cereus* 4153 were first incubated with the peptides at 4°C for 2 weeks then moved to 30°C and incubated overnight. The diameters of the halos were measured.

RESULTS

THE HINGE REGION WAS VARIED FROM ONE TO SIX AMINO ACIDS

The hinge region is a positively charged and flexible part of nisin. According to previous mutagenesis results, incorporating negatively charged amino acids into the hinge region will greatly reduce the activity, while small, polar, hydrophobic or positively charged amino acids incorporation did not reduce the activity dramatically (Ross and Vederas, 2011). Therefore for

Table 2 | Sequence of the hinge region variants.

Name	Hinge region
–2	N
–1	NK
Wild type	NMK
+1	NLMK
	NVMK
	NIMK
+2	NIVMK
+3	NIVLMK

this research, the nonpolar and hydrophobic amino acids valine, leucine and isoleucine were chosen to elongate the hinge region and inserted between the asparagine residue and methionine residue. In the two amino acids truncation variant, methionine and lysine were deleted. And in the one amino acid truncation variant, methionine was deleted. Table 2 shows the sequence of the hinge-region variants.

THE HINGE REGION VARIANTS SHOW DIFFERENT EXTRACELLULAR EXPRESSION LEVELS

The nisin-inducible two plasmids expression and modification system (Kluskens et al., 2005) was used to express nisin and the

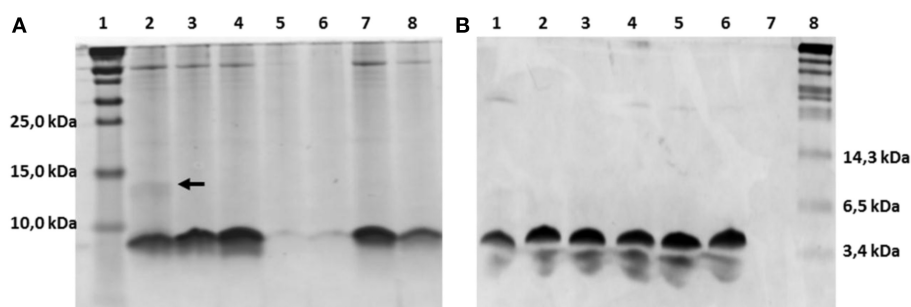


FIGURE 2 | Comassie stained tricine SDS-PAGE gel. (A) TCA precipitated hinge region analogs. 1.8 ml supernatant was concentrated to 100 μ l solution by TCA precipitation and 15 μ l was loaded on the gel. Lane 1, protein marker (Thermo Scientific), the molecular weight are indicated on the left, from low to high are 10kDa, 15kDa and 25kDa; Lane 2–8, hinge region analogs. Lane 2, –2; Lane 3, –1; Lane 4, wild type; Lane 5, +1(valine); Lane 6,

+1(leucine); Lane 7, +2; Lane 8, +3. The dimer of the –2 variant is indicated by an arrow. **(B)** Purified hinge region analogs (3 μ g peptides were loaded per well). From left to right are –2 (lane 1), –1 (lane 2), wild type (lane 3), +1 (leucine) (lane 4), +2 (lane 5), +3 (lane 6) and the protein marker (Biolabs) (lane 8). The molecular weight of the marker are indicated, from low to high 3.4kDa, 6.5kDa, and 14.3kDa.

hinge region variants. In **Figure 2A** the production of different hinge region variants is compared by loading TCA precipitated supernatants on a tricine SDS-PAGE gel. From lane 4 we can see that nisin is produced at a good amount. The –2 (lane 3), –1 (lane 2) and +2 (lane 7) variants showed an almost equal level of production compared to nisin. The +3 (lane 8) variant showed about half the amount of production. However, the +1 (lane 5 and lane 6) variants showed about 100 times lower production than wild type. And this deficiency did not change when the inserted amino acid was changed from isoleucine (data not shown) to valine or leucine. As the leucine insertion analog showed a slightly improved production level, in the following experiments, the +1L was used.

VARIATION OF THE HINGE REGION DOES NOT CHANGE THE DEGREE OF DEHYDRATION OF THE PEPTIDE EXCEPT FOR THE –2 PEPTIDE

The dehydrated residues and the (methyl)lanthionine rings are very important for the activity of lantibiotics. And these modifications are catalyzed by NisB and NisC (Lubelski et al., 2008b). However, varying the length of the hinge region can change the distance between the modifiable residues and the leader and affect the behavior of NisB and NisC. To make sure the variants were fully modified, MALDI-TOF was used to assess the dehydration extent of the peptides (**Table 3**). The mass of the TCA precipitated peptides indicated that the –2 peptide was dehydrated 7 times and other analogs were fully dehydrated ($-8 \text{ H}_2\text{O}$). Also the –2 analog has more tendency to form a dimer (see arrow in **Figure 2A**), and this has been confirmed by western blot (data not shown). However, by large scale purification, the 8 times dehydrated –2 variant was also obtained through isolation by HPLC (**Table 3**). **Figure 2B** shows the purified peptides.

VARYING THE LENGTH OF THE HINGE REGION CHANGES THE ANTIMICROBIAL ACTIVITY OF NISIN, IN A TARGET-SPECIFIC WAY

The MIC values of 10 different indicator strains were assessed for the hinge region mutants and wild type. Literature indicates that *Staphylococcus* and *Micrococcus* commonly have thinner membranes, while *Streptococcus* and *Lactococcus lactis* have a thicker

Table 3 | Molecular mass of hinge region analogs detected by MALDI-TOF.

Hinge region analogs	Number of dehydration	TCA precipitated prepeptides		Peptides after large scale purification (without leader)	
		Predicted mass(Da)	Observed mass(Da)	Predicted mass(Da)	Observed mass(Da)
–2	8	5427.9		3095.7	3093.1
	7	5445.9	5447.5	3113.7	
–1	8	5556.1	5560.1	3223.9	3224.2
WT	8	5687.3	5686.9	3355.1	3353.5
+1L	8	5800.7	5800.7	3468.5	3467.4
+2	8	5899.6	5899.2	3567.4	3564.4
+3	8	6012.8	6013.8	3680.6	3681.0

membrane (Bierbaum and Sahl, 2009). In **Table 4**, the strain-specific activities of hinge region variants are shown. To compare activity of all analogs, the residual activity of analogs of nisin were calculated. From the ratio, we can see wild type nisin has the best activity against all indicators. The –2 variant lost most of the activity. One amino acid deletion was also detrimental for the activity, but against *S. pneumoniae* and *B. sporothermodurans*, which grow slowly, the –1 variant showed less reduced activity than other analogs. One or two amino acids elongation changed the activity only modestly. Against *Enterococcus faecalis*, the +1 showed better activity than +2, while against *Listeria monocytogenes*, *Bacillus cereus* 4147 and 4153, the +2 variant showed relatively higher activity. Activity against *Staphylococcus aureus* was dramatically reduced when changing the length of the hinge region.

ACTIVITY OF HINGE REGION ANALOGUES IN SOLID MEDIA

The antimicrobial activity of the hinge region analogs in solid media were tested by an agar well diffusion assay. The diameters of the halos were measured and the residual activity of the analogs were estimated according to the formula of the relationship

Table 4 | Minimum inhibitory concentration (MIC) of the hinge-region variants against representative Gram-positive strains, determined in liquid culture.

Indicators	MIC value ($\mu\text{g/ml}$)						Residual activity of variants compared to nisin (%) ^a					
	–2	–1	WT	+1	+2	+3	–2	–1	WT	+1	+2	+3
<i>Enterococcus faecalis</i> VE14089	>32	>32	1.7	4	5.3	>8	<6	<6	100	37	30	<21
<i>Listeria monocytogenes</i>	>8	>8	2	8	4	>8	<25	<25	100	25	50	<25
<i>Bacillus cereus</i> 4147	>32	>32	4	16	8	16	<13	<13	100	25	50	25
<i>Bacillus cereus</i> 4153	>32	>32	4	16	8	32	<13	<13	100	25	50	13
<i>Lactococcus lactis</i> MG1363	0.5	1	0.03	0.125	0.125	0.25	6	3	100	25	25	13
<i>Bacillus cereus</i> (L'29) 16	>32	>32	4	16	16	32	<13	<13	100	25	25	13
<i>Micrococcus luteus</i>	>8	>8	2	8	8	8	<25	<25	100	25	25	25
<i>Streptococcus pneumoniae</i> R6	8	4	1	6	4	8	13	25	100	17	25	13
<i>Bacillus sporothermodurans</i> IC4	3	0.75	0.375	1	1	2	13	50	100	33	33	17
<i>Staphylococcus aureus</i>	>16	16	0.5	8	>8	>16	<3	3	100	6	<6	<3

^a The percentage of residual activity was calculated by dividing the MIC value of nisin by that of the analogs.

between the concentration of nisin and the sizes of halos. We made use of the fact that the size of the halo is directly related to the log of nisin concentration. Of course this is an estimate of activity of the variants because any changes in diffusion of the variant bacteriocin or growth rates of indicator bacteria during the assay could also affect the size of the halo. (Table 5 and Supplementary Figure 1). The plates were shown in supplementary data (Supplementary Figures 2–8). As we can see, nisin did not always show the best activity. More specifically, against *L. lactis*, *L. monocytogenes* and *E. faecalis*, the +2 variant showed a higher or equal activity compared to nisin. And the +1 variant, which is not as efficient as the +2, also displayed almost equal or better activity than nisin. In contrast to the MIC value test in liquid culture, the –2 variant showed large halos in the plate activity test against these three strains. And against *L. lactis* at 20°C, the inhibition zone was larger than nisin. The –1 variant showed about 30% residual activity against *L. lactis* and *L. monocytogenes* at all tested temperatures. However, against *E. faecalis*, the –1 variant showed an increased activity when the temperature goes higher (from 21 to 140%). Notably, against *B. sporothermodurans*, the –1 variant showed an apparently larger halo than nisin, which is in accordance with the MIC value test. And the +2 variant also showed higher activity than nisin. The *Bacillus cereus* are difficult to be inhibited by nisin, and the +2 variant displayed either equal or higher plate activity than nisin at 30°C (Supplementary Figure 8). The *M. luteus* grows quite fast at room temperature and only the +2 variant retained 55% of the activity of nisin. Against *S. aureus*, the analogs displayed dramatically reduced activity. And in this case, the +1 variant displayed relatively higher activity than the +2 variant. In all the cases, the +3 variant displayed dramatically reduced activity.

THE INHIBITION CAPABILITY OF NISIN AND +2 VARIANT AT LOW TEMPERATURE

Some food spoilage bacteria e.g., *Bacillus cereus* and *Listeria monocytogenes*, can grow at low temperature. In this research, several kinds of bacteria were chosen to test their sensitivity to nisin and the hinge region analog +2 at low temperatures (Figure 3).

The *L. lactis* and *L. monocytogenes* grow well at 4°C. After 1 week, big halos can be seen in the plates. Against *L. lactis*, nisin showed an apparently larger halo than the +2 variant, which are different from the results at higher temperature. Against *L. monocytogenes*, both wild type and the +2 displayed high activity but the wild type can inhibit the growth of bacteria a bit more efficiently than +2. *B. cereus* 4147 cannot grow at 4°C but grow well at 12°C. However, the +2 variant also showed lower activity than nisin at this temperature. As the *Bacillus* did not show apparent growth after incubated with the peptides at 4°C for 2 weeks, the plates were moved to 30°C and incubated overnight. In this case, the *Bacillus* grow fast and various sizes of colonies were shown. As the figure shows, the wild type displayed significantly higher activity than +2 against *B. sporothermodurans*, while against *B. cereus* 4153, the +2 variant showed a modestly larger halo than nisin.

DISCUSSION

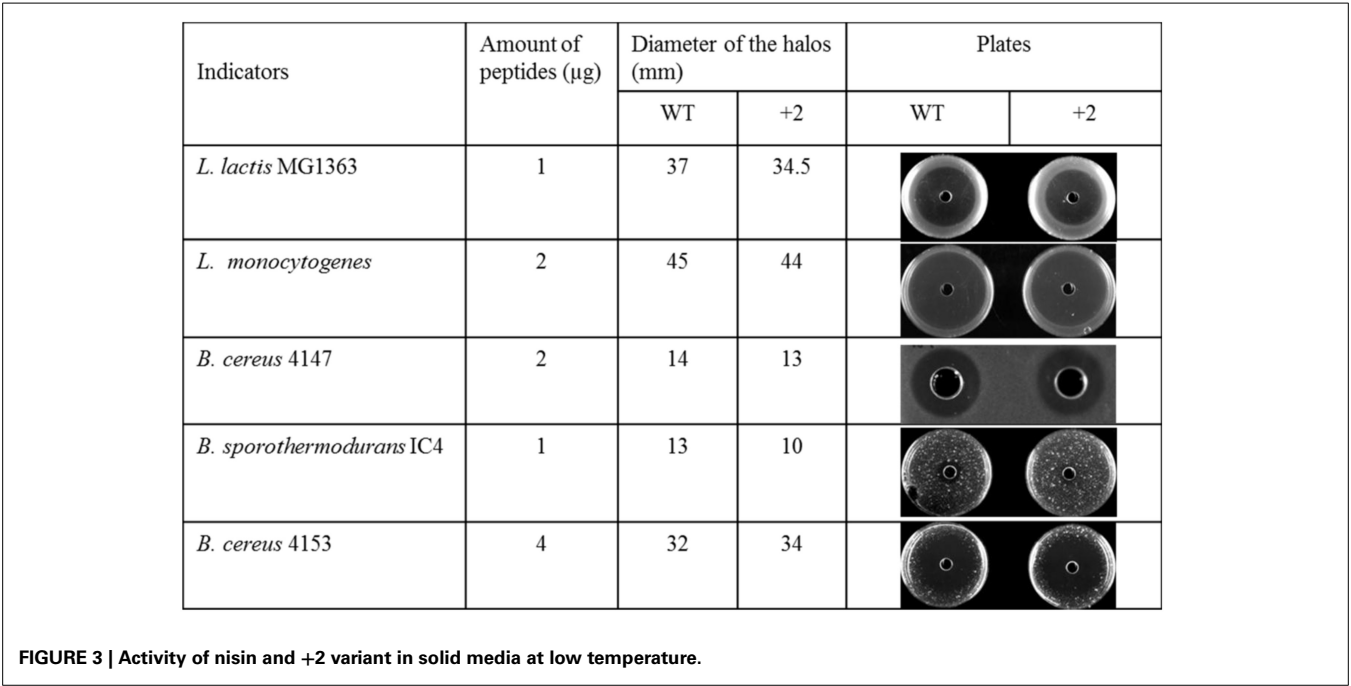
Nisin inhibits the growth of Gram-positive bacteria by binding to lipid II, inserting into the membrane and forming stable pores in the membrane. However, the thicknesses of the membrane vary between different species and growth conditions. This difference can affect the activity of the peptide. For example, some lantibiotics with shorter length, e.g., epidermin (Bonelli et al., 2006), gallidermin (Bonelli et al., 2006), mutacin 1140 (Smith et al., 2008) and bovicin HC5 (Paiva et al., 2011), display lipid II binding activity but only form pores when the targeted bacteria or liposomes have a thinner membrane (not exceeding 40 Å). These results indicate that the length of the lantibiotics, especially at the C-terminal part, could be optimized to efficiently inhibit growth of bacteria with different membrane thicknesses. In this paper, the length of the hinge region of nisin was varied to make the peptides have different lengths of C-terminus.

Three similar amino acids (I, V, L) were used to elongate the hinge region at the same position (between N20 and M21). Notably, all +1 variants showed an extremely low production level. Since the dehydration extent of the +1 variant was normal and since this peptide showed good activity, the modification machinery seems to work properly. To understand the reasons for

Table 5 | Activities of the hinge region analogs in agar well diffusion assay.

Indicators	T (°C)	Diameter of the halos (mm)						T (°C)	Residual activity (%) ^a					
		−2	−1	wt	+1	+2	+3		−2	−1	wt	+1	+2	+3
<i>L. lactis</i> MG1363	20	16.0	14.0	15.5	15.8	16.2	11.0	20	120	33	100	122	140	5
	20	16.8	14.9	16.8	n.d.	17.1	12.5	30	91	17	100		114	3
	30	15.8	13.5	16.1	n.d.	16.3	11.0							
	30	16.1	13.4	16.1	n.d.	16.3	n.d.							
<i>L. monocytogenes</i>	20	17.0	14.8	17.3	16.8	17.8	11.8	20	82	19	100	72	139	3
	30	15.8	13.8	15.8	n.d.	16.0	11.0	30	76	29	100		114	3
	30	15.0	14.2	16.0	n.d.	n.d.	10.2							
<i>E. faecalis</i> VE14089	20	17.5	16.5	19.0	18.5	19.5	15.0	20	36	21	100	72	144	6
	20	17.6	17.0	19.2	n.d.	19.8	14.5	30	77	72	100		88	9
	30	15.0	14.9	15.4	n.d.	15.2	11.7	37	76	140	100	82	101	14
	37	12.3	13.6	13.3	n.d.	13.1	10.2							
	37	13.3	14.0	13.3	13.0	13.5	10.5							
<i>M. luteus</i>	20	7.5	7.5	12.1	8.5	11.2	8.0	20	0	0	100	9	55	7
<i>S. aureus</i>	20	8.0	8.0	10.8	8.8	8.5	7.5	20	16	16	100	27	22	0
<i>B. sporothermodurans</i> IC4	30	n.d.	15.0	12.5	n.d.	13.8	9.0	30		522	100		236	10

^a The residual activity is estimated according to a standard curve of various nisin concentrations plotted against diameter (halo diameter is directly related to log of nisin concentration). Improvements in residual activity are indicated in gray. n.d.: not determined.



the low production level, additional different amino acids could be inserted at different positions of the hinge region. Especially since previously it was shown that inserting an alanine at the end of the hinge region (NMKA) did not affect the production level (Lubelski et al., 2008a).

Specific activity of the variants was tested against different indicators. As the hinge region connects the first three rings and the intertwined rings of nisin, deletion of one or two amino acids will reduce the flexibility of the peptide and the pore formation

activity will be weakened or abolished. The results show that these truncations are detrimental for activity against all indicators, which proves that the flexibility of the hinge region is important for the activity of nisin. This has also been shown before by proline-proline containing variants (Kuipers et al., 1996). Elongation of the hinge region can potentially enhance the activity of peptides against those bacteria with thicker membrane. In this paper, one or two amino acids extensions only modestly reduced the activity. This indicated that a slightly longer

hinge region did not greatly affect the function of nisin and the pore formation activity could still be performed. The relatively lower activity is probably because the addition of leucine (+1), or isoleucine and valine (+2) changed the amphipathicity of the C-terminus of nisin, due to which the peptide cannot perform the pore formation efficiently. If the added amino acids and position of the insertion can be randomly changed, probably higher activity can be obtained. According to the literatures, some point mutants in the hinge region showed enhanced or modestly reduced activity, e.g., N20 (P,K), M21(V,K,G), K22(T,S) (Yuan et al., 2004; Field et al., 2008) and the combinations of AAK, NAI, SLS, AAA and SAA have been shown to have high activity (Healy et al., 2013). These residues can be good candidates to elongate the hinge region. Furthermore, the elongated variants showed 16 times or more reduced activity against *Staphylococcus aureus*, which indicates significant strain specificity of the +1 and +2 variants. This bacterium was described to have a thinner membrane (Bonelli et al., 2006), but whether longer peptides have reduced activities against bacteria with thinner membranes needs to be further proven.

As it can be seen, the peptides showed different inhibition capability in the solid media compared to the MIC value test. This can be related to the growth differences of the strain and diffusion rate of the peptides. Against some indicators (e.g., *M. luteus*, *S. aureus*), the hinge region analogs did not show any advantages compared to nisin, and nisin showed much better activity than the +2 variant at low temperatures, which indicate that after a long time of evolution, nisin has more advantages than the analogs in most of the conditions.

Increasing the activity of nisin is very hard, because it is already evolutionary optimized against its natural targets. But engineering of nisin can change the properties of the peptide and the analogs can be applied against specific targets. To be used as a valuable antimicrobial reagent, the production level is very important. The +1 variant is not suited in this respect although the activity is relatively high. The −2 variant is also not a good candidate for application because of the incomplete dehydration. The +2 variant showed good properties and can be specifically used to inhibit growth of *L. lactis* MG1363 and *L. monocytogenes* at room temperature or higher, *B. cereus* 4153 in refrigerator or at 30°C in solid media. Both the +2 and −1 variant can be used to inhibit growth of *B. sporothermodurans* IC4 at 30°C in solid media. It has been shown that the thickness of the lipid bilayer is affected by temperature and the membrane will become thinner as the temperature goes up (Szekely et al., 2011). In this research, the activities of hinge region analogs against *E. faecalis* showed temperature dependence in the agar well diffusion assay. As the temperature goes up, the peptide with a shorter hinge region (−1 variant) displayed higher activity. So the −1 variant can be applied at 37°C in solid media against *E. faecalis*. At room temperature, this bacterium grows more slowly, and then the +2 variant can inhibit its growth more efficiently. This study shows that by engineering the length of the hinge region of nisin, variants with a changed host range can be obtained, but that the effects are very host range- and temperature dependent. Moreover, some variants display better activity in a solid test medium, while being worse in liquid culture. Thus, the choice of wild-type or variant

nisin will depend on the specific application, temperature and matrix.

ACKNOWLEDGMENTS

We are grateful to Antonina Krawczyk for the gift of *Bacillus* strains. Liang Zhou is supported by the Chinese Scholarship Council (CSC) and State Key Laboratory of Microbial Technology, School of Life Sciences, Shandong University, Jinan, P. R. China.

SUPPLEMENTARY MATERIAL

The Supplementary Material for this article can be found online at: <http://www.frontiersin.org/journal/10.3389/fmicb.2015.00011/abstract>

REFERENCES

- Bierbaum, G., and Sahl, H.-G. (2009). Lantibiotics: mode of action, biosynthesis and bioengineering. *Curr. Pharm. Biotechnol.* 10, 2–18. doi: 10.2174/138920109787048616
- Bonelli, R. R., Schneider, T., Sahl, H.-G., and Wiedemann, I. (2006). Insights into *in vivo* activities of lantibiotics from gallidermin and epidermin mode-of-action studies. *Antimicrob. Agents Chemother.* 50, 1449–1457. doi: 10.1128/AAC.50.4.1449-1457.2006
- Breukink, E., and de Kruijff, B. (2006). Lipid II as a target for antibiotics. *Nat. Rev. Drug Discov.* 5, 321–332. doi: 10.1038/nrd2004
- Cybulski, L. E., Martin, M., Mansilla, M. C., Fernández, A., and de Mendoza, D. (2010). Membrane thickness cue for cold sensing in a bacterium. *Curr. Biol.* 20, 1539–1544. doi: 10.1016/j.cub.2010.06.074
- Davies, J., and Davies, D. (2010). Origins and evolution of antibiotic resistance. *Microbiol. Mol. Biol. Rev.* 74, 417–433. doi: 10.1128/MMBR.00016-10
- de Ruyter, P. G., Kuipers, O. P., and de Vos, W. M. (1996). Controlled gene expression systems for *Lactococcus lactis* with the food-grade inducer nisin. *Appl. Environ. Microbiol.* 62, 3662–3667.
- Field, D., Connor, P. M. O., Cotter, P. D., Hill, C., and Ross, R. P. (2008). The generation of nisin variants with enhanced activity against specific Gram-positive pathogens. *Mol. Microbiol.* 69, 218–230. doi: 10.1111/j.1365-2958.2008.06279.x
- Gasson, M. J. (1983). Plasmid complements of *Streptococcus lactis* NCDO 712 and other lactic streptococci after protoplast-induced curing. *J. Bacteriol.* 154, 1–9.
- Hasper, H. E., de Kruijff, B., and Breukink, E. (2004). Assembly and stability of nisin-lipid II pores. *Biochemistry* 43, 11567–11575. doi: 10.1021/bi049476b
- Healy, B., Field, D., O'Connor, P. M., Hill, C., Cotter, P. D., and Ross, R. P. (2013). Intensive mutagenesis of the nisin hinge leads to the rational design of enhanced derivatives. *PLoS ONE* 8:e79563. doi: 10.1371/journal.pone.0079563
- Holo, H., and Nes, I. F. (1995). Transformation of *Lactococcus* by electroporation. *Methods Mol. Biol.* 47, 195–199.
- Kluskens, L. D., Kuipers, A., Rink, R., de Boef, E., Fekken, S., Driessen, A. J. M., et al. (2005). Post-translational modification of therapeutic peptides by NisB, the dehydratase of the lantibiotic nisin. *Biochemistry* 44, 12827–12834. doi: 10.1021/bi050805p
- Kuipers, O. P., Bierbaum, G., Ottenwälder, B., Dodd, H. M., Horn, N., Metzger, J., et al. (1996). Protein engineering of lantibiotics. *Antonie Van Leeuwenhoek* 69, 161–169. doi: 10.1007/BF00399421
- Kuipers, O. P., de Ruyter, P. G., Kleerebezem, M., and de Vos, W. M. (1997). Controlled overproduction of proteins by lactic acid bacteria. *Trends Biotechnol.* 15, 135–140. doi: 10.1016/S0167-7799(97)01029-9
- Lubelski, J., Overkamp, W., Kluskens, L. D., Moll, G. N., and Kuipers, O. P. (2008a). Influence of shifting positions of Ser, Thr, and Cys residues in prenisin on the efficiency of modification reactions and on the antimicrobial activities of the modified prepeptides. *Appl. Environ. Microbiol.* 74, 4680–4685. doi: 10.1128/AEM.00112-08
- Lubelski, J., Rink, R., Khusainov, R., Moll, G. N., and Kuipers, O. P. (2008b). Biosynthesis, immunity, regulation, mode of action and engineering of the model lantibiotic nisin. *Cell. Mol. Life Sci.* 65, 455–476. doi: 10.1007/s00018-007-7171-2

- Paiva, A. D., Breukink, E., and Mantovani, H. C. (2011). Role of lipid II and membrane thickness in the mechanism of action of the lantibiotic bovicin HC5. *Antimicrob. Agents Chemother.* 55, 5284–5293. doi: 10.1128/AAC.00638-11
- Rigottier-Gois, L., Alberti, A., Houel, A., Taly, J.-F., Palcy, P., Manson, J., et al. (2011). Large-Scale screening of a targeted *Enterococcus faecalis* mutant library identifies envelope fitness factors. *PLoS ONE* 6:e29023. doi: 10.1371/journal.pone.0029023
- Rink, R., Kuipers, A., de Boef, E., Leenhouts, K. J., Driessen, A. J. M., Moll, G. N., et al. (2005). Lantibiotic structures as guidelines for the design of peptides that can be modified by lantibiotic enzymes. *Biochemistry* 44, 8873–8882. doi: 10.1021/bi050081h
- Ross, A. C., and Vederas, J. C. (2011). Fundamental functionality: recent developments in understanding the structure-activity relationships of lantibiotic peptides. *J. Antibiot. (Tokyo)* 64, 27–34. doi: 10.1038/ja.2010.136
- Sambrook, J., and Russell, D. W. (2001). *Molecular Cloning: A Laboratory Manual, Third Edition. 3rd Edn.* Cold Spring Harbor, NY: Cold Spring Harbor Laboratory Press.
- Schägger, H. (2006). Tricine-SDS-PAGE. *Nat. Protoc.* 1, 16–22. doi: 10.1038/nprot.2006.4
- Smith, L., Hasper, H., Breukink, E., Novak, J., Cerkasov, J., Hillman, J. D., et al. (2008). Elucidation of the antimicrobial mechanism of mutacin 1140. *Biochemistry* 47, 3308–3314. doi: 10.1021/bi701262z
- Szekely, P., Dvir, T., Asor, R., Resh, R., Steiner, A., Szekely, O., et al. (2011). Effect of temperature on the structure of charged membranes. *J. Phys. Chem. B* 115, 14501–14506. doi: 10.1021/jp207566n
- van Heel, A. J., Montalbán-López, M., and Kuipers, O. P. (2011). Evaluating the feasibility of lantibiotics as an alternative therapy against bacterial infections in humans. *Expert Opin. Drug Metab. Toxicol.* 7, 675–680. doi: 10.1517/17425255.2011.573478
- van Heel, A. J., Mu, D., Montalbán-López, M., Hendriks, D., and Kuipers, O. P. (2013). Designing and producing modified, new-to-nature peptides with antimicrobial activity by use of a combination of various lantibiotic modification enzymes. *ACS Synth. Biol.* 2, 397–404. doi: 10.1021/sb3001084
- Wiedemann, I., Breukink, E., van Kraaij, C., Kuipers, O. P., Bierbaum, G., de Kruijff, B., et al. (2001). Specific binding of nisin to the peptidoglycan precursor lipid II combines pore formation and inhibition of cell wall biosynthesis for potent antibiotic activity. *J. Biol. Chem.* 276, 1772–1779. doi: 10.1074/jbc.M006770200
- Yuan, J., Zhang, Z.-Z., Chen, X.-Z., Yang, W., and Huan, L.-D. (2004). Site-directed mutagenesis of the hinge region of nisinZ and properties of nisinZ mutants. *Appl. Microbiol. Biotechnol.* 64, 806–815. doi: 10.1007/s00253-004-1599-1

Conflict of Interest Statement: The authors declare that the research was conducted in the absence of any commercial or financial relationships that could be construed as a potential conflict of interest.

Received: 23 October 2014; accepted: 06 January 2015; published online: 29 January 2015.

Citation: Zhou L, van Heel AJ and Kuipers OP (2015) The length of a lantibiotic hinge region has profound influence on antimicrobial activity and host specificity. *Front. Microbiol.* 6:11. doi: 10.3389/fmicb.2015.00011

This article was submitted to *Microbial Physiology and Metabolism*, a section of the journal *Frontiers in Microbiology*.

Copyright © 2015 Zhou, van Heel and Kuipers. This is an open-access article distributed under the terms of the Creative Commons Attribution License (CC BY). The use, distribution or reproduction in other forums is permitted, provided the original author(s) or licensor are credited and that the original publication in this journal is cited, in accordance with accepted academic practice. No use, distribution or reproduction is permitted which does not comply with these terms.



Protein-tyrosine phosphorylation in *Bacillus subtilis*: a 10-year retrospective

Ivan Mijakovic^{1*} and Josef Deutscher^{2,3*}

¹ Systems and Synthetic Biology, Department of Chemical and Biological Engineering, Chalmers University of Technology, Göteborg, Sweden

² Centre National de la Recherche Scientifique, FRE3630 Expression Génétique Microbienne, Institut de Biologie Physico-Chimique, Paris, France

³ UMR1319 Microbiologie de l'Alimentation au Service de la Santé Humaine, Institut National de la Recherche Agronomique/AgroParisTech, Jouy en Josas, France

Edited by:

Jörg Stülke,
Georg-August-Universität
Göttingen, Germany

Reviewed by:

Haïke Antelmann, University of
Greifswald, Germany
Jörg Stülke, Georg-August-
Universität Göttingen, Germany

*Correspondence:

Ivan Mijakovic, Systems and
Synthetic Biology, Department of
Chemical and Biological
Engineering, Chalmers University of
Technology, Kemivägen 10,
Göteborg SE-41296, Sweden
e-mail: ivan.mijakovic@chalmers.se;
Josef Deutscher, UMR1319
Microbiologie de l'Alimentation au
Service de la Santé Humaine,
Institut National de la Recherche
Agronomique/AgroParisTech,
Bâtiment CBAI, Avenue Lucien
Bretignières, Thiverval-Grignon,
FR-78850, France
e-mail: josef.deutscher@grignon.inra.fr

The discovery of tyrosine-phosphorylated proteins in *Bacillus subtilis* in the year 2003 was followed by a decade of intensive research activity. Here we provide an overview of the lessons learned in that period. While the number of characterized kinases and phosphatases involved in reversible protein-tyrosine phosphorylation in *B. subtilis* has remained essentially unchanged, the number of proteins known to be targeted by this post-translational modification has increased dramatically. This is mainly due to phosphoproteomics and interactomics studies, which were instrumental in identifying new tyrosine-phosphorylated proteins. Despite their structural similarity, the two *B. subtilis* protein-tyrosine kinases (BY-kinases), PtkA and PtkB (EpsB), seem to accomplish different functions in the cell. The PtkB is encoded by a large operon involved in exopolysaccharide production, and its main role appears to be the control of this process. The PtkA seems to have a more complex role; it phosphorylates and regulates a large number of proteins involved in the DNA, fatty acid and carbon metabolism and engages in physical interaction with other types of kinases (Ser/Thr kinases), leading to mutual phosphorylation. PtkA also seems to respond to several activator proteins, which direct its activity toward different substrates. In that respect PtkA seems to function as a highly connected signal integration device.

Keywords: protein phosphorylation, BY-kinase, phosphotyrosine-protein phosphatase, regulatory network, substrate specificity

***Bacillus subtilis* POSSESSES 2 BY-KINASES (PtkA AND PtkB), ONE COGNATE PHOSPHATASE (PtpZ), AND TWO PUTATIVE PHOSPHOTYROSINE-PROTEIN PHOSPHATASES YfkJ AND YwIe**

The first report of proteins being phosphorylated on tyrosine residues by a protein-tyrosine kinase in *Bacillus subtilis* was published by Mijakovic et al. (2003). At the time it was known that some other bacteria, such as *Escherichia coli* and *Streptococcus pneumoniae*, encode proteins that autophosphorylate on tyrosine residues in their C-terminal domains (Vincent et al., 1999; Morona et al., 2000). These autokinases were shown to be implicated in regulating the synthesis of extracellular polysaccharides (Wugeditsch et al., 2001; Bender et al., 2003), and were later named BY-kinases (abbreviation of “bacterial tyrosine kinases”; Grangeasse et al., 2007). Proteins belonging to the BY-kinase family exhibit a surprisingly low degree of sequence homology, with the only conserved features being the catalytic site composed of the Walker A, A' and B motifs and the autophosphorylation region in their C-termini (Shi et al., 2014b). BY-kinases were identified in *B. subtilis* based on sequence homology with *E. coli* Wzc and

S. pneumoniae CpsB (Mijakovic et al., 2003). *B. subtilis* possesses two BY-kinases, originally known as YwqD and YveL, which were renamed PtkA and PtkB, respectively (Mijakovic et al., 2005a). PtkB is also known as EpsB (Kearns et al., 2005). One finding that emerged during the initial functional characterization of the *B. subtilis* BY-kinases had a broad impact on the field: BY-kinases not only can autophosphorylate, they can also phosphorylate other cellular proteins, and thus regulate their functions. The first reported BY-kinase substrate was the UDP-glucose dehydrogenase Ugd (YwqF), which was found to be phosphorylated by the *B. subtilis* PtkA (Mijakovic et al., 2003). The Ugd homolog in *E. coli* was also found to be phosphorylated by the PtkA homolog, Wzc (Grangeasse et al., 2003). The second *B. subtilis* BY-kinase, PtkB, was initially not biochemically characterized due to its insolubility (Mijakovic et al., 2003). Genes encoding PtkA and PtkB are adjacent to genes encoding their respective transmembrane activators, TkmA (YwqC) and TkmB (YveK). These proteins have two transmembrane helices with a large extracellular loop between them, and short cytosolic termini, responsible for the interaction with the cytosolic kinase. Structures of some BY-kinases have been resolved, and notably that of CapB from

Staphylococcus aureus (Olivares-Illana et al., 2008) has provided a number of important structural and functional insights. BY-kinases from *Firmicutes* form octamers, in which the C-terminus of one subunit enters the active site of the adjacent subunit where it gets phosphorylated. Upon trans-autophosphorylation, the BY-kinase octamers dissociate, and this may have important functional consequences, which are discussed in the next section.

Bacillus subtilis possesses one polyhistidinol phosphatase-like phosphotyrosine-protein phosphatase, PtpZ (YwqE; Mijakovic et al., 2005a), which dephosphorylates PtkA and its known substrates. PtkA and PtpZ are encoded by the same operon, and thus seem to act in concert. In addition to PtpZ, there are two low molecular weight phosphotyrosine-protein phosphatases in *B. subtilis*: YwLE and YfkJ (Musumeci et al., 2005). YfkJ and YwLE were both suggested to play a role in ethanol stress resistance in *B. subtilis*, but the exact mechanism of this regulation has not been clarified (Musumeci et al., 2005). The crystal structure of YwLE has recently been solved (Xu et al., 2006), and this phosphatase has also been reported to dephosphorylate arginine-phosphorylated CtsR (Fuhrmann et al., 2009). There is overwhelming recent evidence in support of its role in dephosphorylating arginine-phosphorylated proteins (Schmidt et al., 2014).

The last review of the state-of-the art concerning protein-tyrosine phosphorylation in *B. subtilis*, comprising the above mentioned findings, was published almost a decade ago (Mijakovic et al., 2005b). In the perspectives section of that paper it was argued that the next step in the field should be a systematic search for tyrosine-phosphorylated proteins, exploring the possibility that kinases phosphorylate multiple substrates. Another highlighted perspective was the possibility that kinases cross-react with alternative activator proteins and possibly other kinases. As will be discussed in the following sections, these predictions have been to a large extent validated by recent developments in the field.

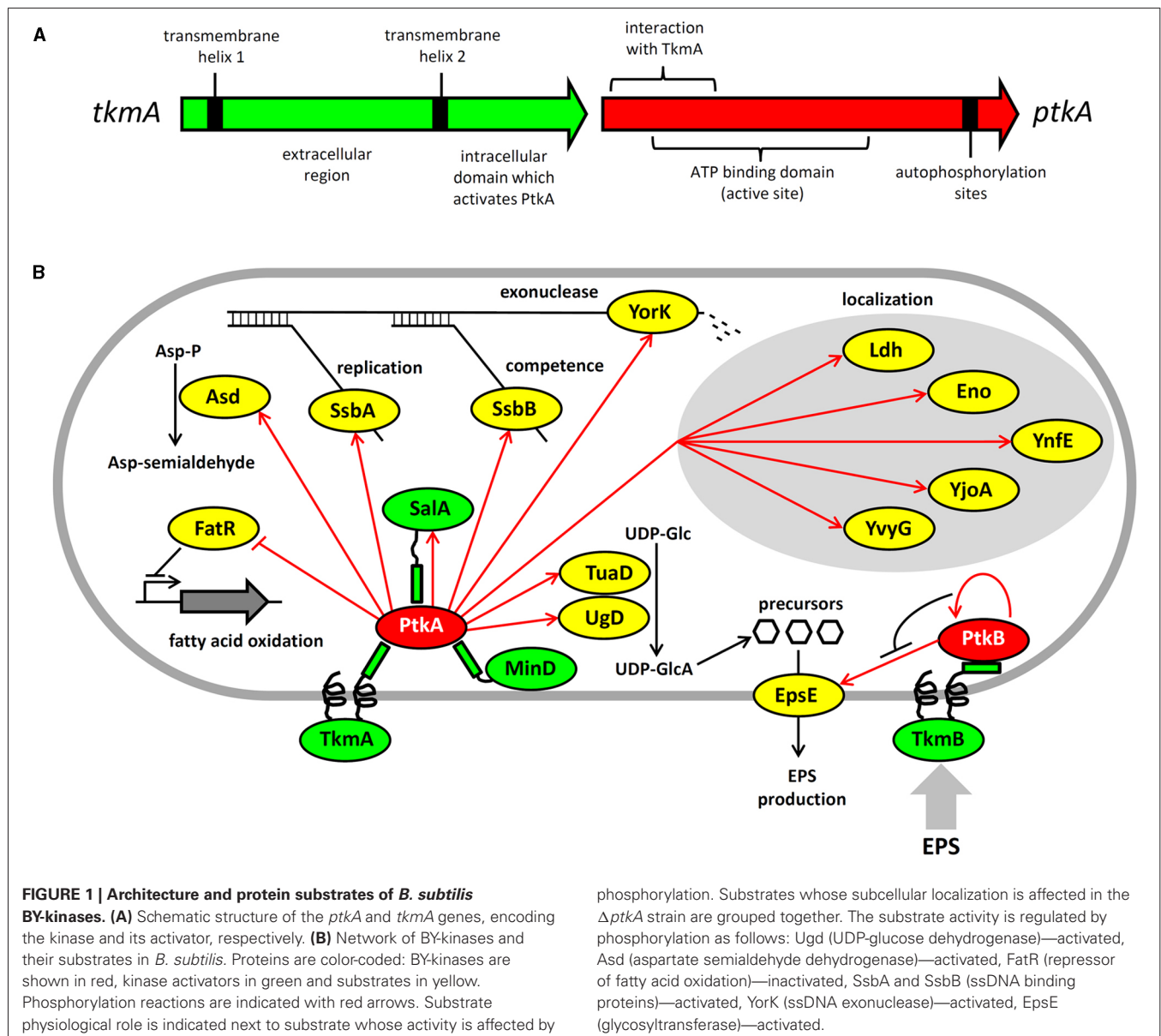
LESSONS LEARNED OVER THE LAST DECADE: PtkA IS A HIGHLY CONNECTED REGULATORY DEVICE, PHOSPHORYLATING MANY SUBSTRATES AND REGULATING VARIOUS CELLULAR PROCESSES

Investigations of the *B. subtilis* phosphoproteome started in the era of gel-based proteomics (Lévine et al., 2006), but the first identification of tyrosine-phosphorylated sites came with the gel-free site-specific phosphoproteomics (Macek et al., 2007). Subsequently, a number of phosphoproteomics studies mapped an increasing number of tyrosine-phosphorylated proteins (Eymann et al., 2007; Soufi et al., 2010; Ravikumar et al., 2014). All of the mentioned site-specific phosphoproteome studies, except for Ravikumar et al. (2014), focused on a single experimental point, typically in exponential stage, but in different media. For example, the dataset in Macek et al. (2007) was obtained in LB, Soufi et al. (2010) report the data for the minimal medium with phosphate starvation, etc. The overlap among the reported phosphorylation sites in these different studies is very limited. This can be partly explained by the diversity of the *B. subtilis* phosphoproteome in different stages of growth, which was reported by Ravikumar

et al. (2014), highlighting the highly dynamic nature of this reversible modification (Nicolas et al., 2012). But it is also plausible to presume that the reported phosphoproteomes are far from exhaustive due to technical limitations of our current approaches. Ongoing phosphoproteomics studies indicate that the size of the detected bacterial phosphoproteomes is likely to increase dramatically due to new methods for phosphopeptide enrichment. The incompleteness of published phosphoproteomes, and the apparent low level of conservation of phosphorylation sites, seriously limit the performance of available predictors of protein phosphorylation (Iakoucheva et al., 2004; Miller et al., 2009).

The phosphoproteomics results immediately invited the question whether PtkA or PtkB could phosphorylate any of these newly-identified tyrosine-phosphorylated proteins. There are no known motifs for substrate recognition by PtkA and PtkB, thus the only way to answer this question was to examine the substrate-kinase relationships experimentally. *In vitro* follow-up studies indicated that PtkA can indeed phosphorylate many of them (Mijakovic et al., 2006; Jers et al., 2010; **Figure 1**). Nevertheless, tyrosine kinases different from BY-kinases are likely to be present in bacteria. For example, phosphoproteome studies with *Listeria monocytogenes*, a close relative of *B. subtilis*, revealed about a dozen tyrosine-phosphorylated peptides (Misra et al., 2011, 2014). However, no protein resembling BY-kinases is present in this pathogen.

The consequences of PtkA-dependent phosphorylation vary considerably depending on its substrate. Phosphorylation of Ugd led to an increase in its UDP-glucose dehydrogenase activity, and thus production of UDP-glucuronate (Mijakovic et al., 2003; Petranovic et al., 2007). Unphosphorylated tyrosine 70 occupies the active site of Ugd and thus obstructs substrate binding. Phosphorylation displaces tyrosine 70 from the active site and hence activates Ugd function (Petranovic et al., 2009). PtkA also phosphorylates and activates the aspartate dehydrogenase Asd, which converts aspartyl-phosphate to a semi-aldehyde (Jers et al., 2010). A number of substrates phosphorylated and activated by PtkA are involved in single-stranded DNA-metabolism; these include the ssDNA-binding proteins SsbA (Ssb) and SsbB (YwpH; Mijakovic et al., 2006) and the ssDNA-specific exonuclease YorK (Jers et al., 2010). Phosphorylation of these proteins has been linked to the cell cycle and DNA replication phenotype of the Δ ptkA mutant (Petranovic et al., 2007), although the details of the underlying mechanism are not clear. PtkA-dependent phosphorylation directly regulates the activity of the protein substrates mentioned above (Ugd, Asd, SsbA, SsbB, YorK), but that is not the only possible outcome of substrate phosphorylation. In case of other tyrosine-phosphorylated proteins revealed by phosphoproteomics: Ldg, Eno, YnfE, YjoA, and YvyG, the PtkA did not control their activity, but seems to be required for their proper cellular localization (Jers et al., 2010). There are also cases where PtkA-dependent phosphorylation had no detectable effect on either activity or localization; such is the case of the peptide transport protein OppA (Jers et al., 2010). PtkA and its cognate phosphatase PtpZ have also been linked with biofilm formation, although their precise roles in this process remain elusive (Kiley and Stanley-Wall, 2010).



While the phosphoproteomics studies continue to provide a growing list of tyrosine-phosphorylated proteins, they do not provide direct evidence for physiological links between these phosphoproteins and kinases and phosphatases responsible for their phosphorylation state. Another global approach, the interactomics, has recently provided important insights in that direction (Shi et al., 2014a). A global two-hybrid interactomics study focused on *B. subtilis* BY-kinases and cognate phosphatases as initial baits revealed a large network of 137 interactions, linking 82 proteins. The capacity of the network to reveal new BY-kinase substrates was demonstrated immediately. The first such characterized substrate was the fatty acid-regulated transcriptional factor FatR, which interacted with TkmA in two hybrid experiments. The transcription regulator was subsequently shown to be phosphorylated by PtkA/TkmA on a tyrosine residue, which plays a key role in FatR interaction with its DNA binding site

(Derouiche et al., 2013). Phosphorylation of FatR led to a loss of interaction with DNA, and derepression of its target operon involved in hydroxylation of polyunsaturated fatty acids. Further substrates of PtkA revealed by interactomics were the general recombinase RecA and the cell division protein DivIVA (Shi et al., 2014a), but these have not yet been characterized beyond the *in vitro* phosphorylation studies. The interaction network also provided a number of proteins interacting with both a kinase and a phosphatase, strongly indicating that they may be the substrates of both.

Interestingly, not all BY-kinase interacting proteins turned out to be substrates. The BY-kinases and their respective activators are encoded by a single gene, and thus exist as fusion proteins in Proteobacteria. In Firmicutes, they are encoded by separate genes, and thus theoretically capable of dissociating from one another. Based on this, we have been speculating for some time

that BY-kinases may indeed dissociate from their canonical transmembrane activators and interact with other proteins, which may act as alternative activators (Shi et al., 2010). The interaction network in *B. subtilis* provided first evidence for this. We have previously pointed out that PtkA exhibits significant homology with two other Walker motif-containing proteins, MinD and SalA (Mijakovic et al., 2005b). Both MinD and SalA were revealed as PtkA interactants (Shi et al., 2014a). While neither MinD nor SalA possess kinase activity, they both exhibit the capacity to activate PtkA kinase function (Shi et al., 2014a). MinD specifically activates kinase autophosphorylation (Shi et al., 2014a). Our recent results suggest that SalA behaves more like the canonical modulator TkmA, it activates both kinase autophosphorylation and substrate phosphorylation, but the Ptk/SalA complex exhibits different substrate specificity than the PtkA/TkmA complex. This suggests that the purpose of alternative activators for PtkA could be to expand and diversify its substrate pool. Protein localization studies also support the notion that PtkA cycles among different activators in the cell. When *ptkA* and *tkmA* were jointly overexpressed as fluorescent protein fusions, they co-localized at the membrane during the exponential phase, but PtkA left the membrane and became cytosolic in the stationary phase (Jers et al., 2010). In the absence of overexpression, PtkA localized at a single cell pole in a significant fraction of cells in the exponential phase, and this localization was MinD dependent (Shi et al., 2014a). It therefore seems plausible that TkmA, MinD, and SalA represent three alternative anchoring points for PtkA, directing its localization and activity toward different substrates throughout the cell cycle.

PtkB: AN INSULATED REGULATORY DEVICE, REGULATING ONLY EXOPOLYSACCHARIDE PRODUCTION?

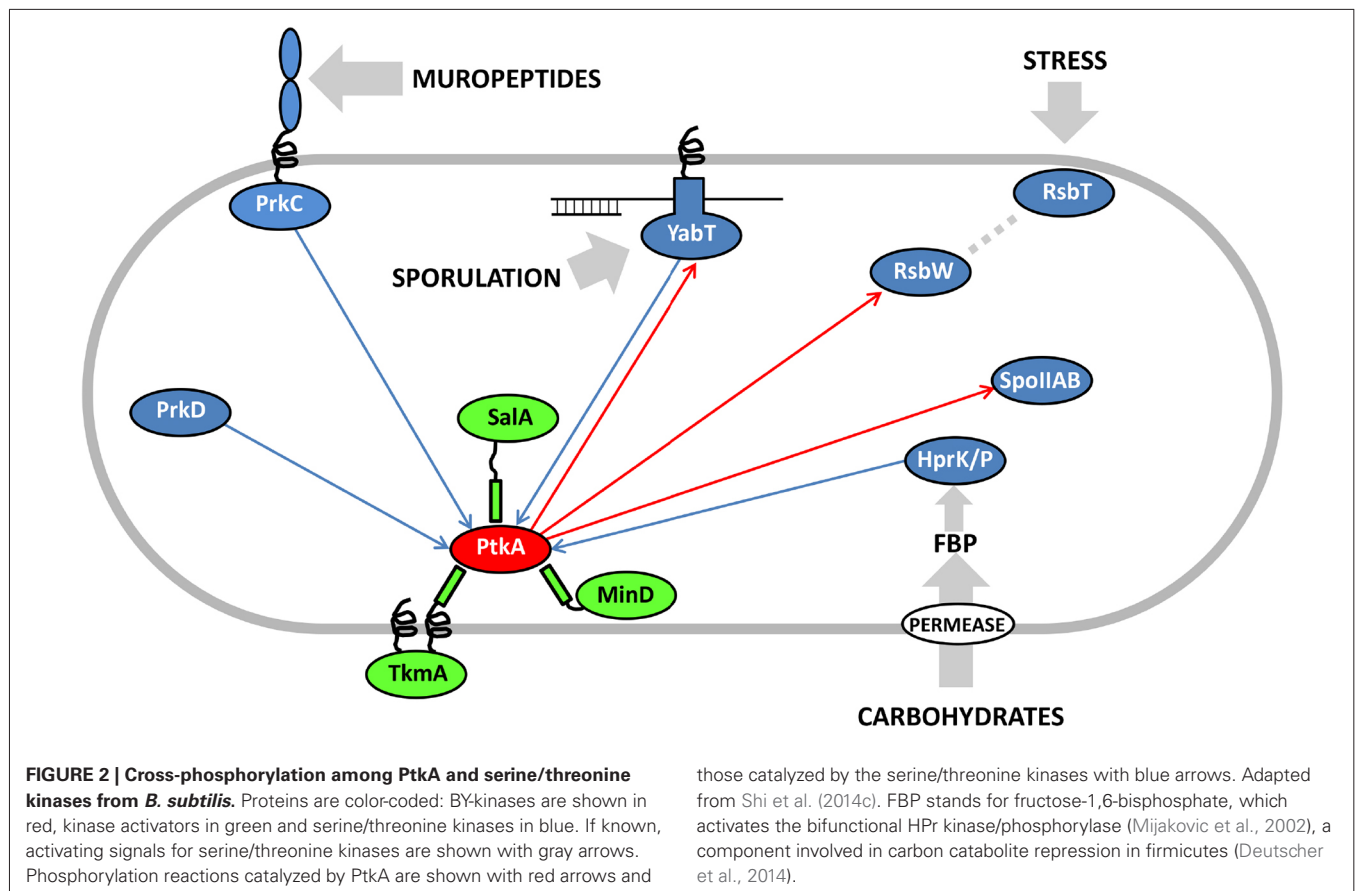
PtkB is encoded by a large *eps* operon involved in production of exopolysaccharides (Elsholz et al., 2014) and biofilm development (Gerwig et al., 2014). PtkB phosphorylates at least one enzyme encoded by the same operon, the glycosyl-transferase EpsE (Elsholz et al., 2014). This phosphorylation mechanism has been described as a positive feedback loop, in which exopolysaccharides act through the transmembrane activator protein TkmB (EpsA, YveK). According to Elsholz et al. (2014), in the presence of exopolysaccharides TkmB prevents autophosphorylation of PtkB and diverts its activity toward the substrate: EpsE. Phosphorylated EpsE is activated, and consequently the production and export of exopolysaccharides increases. This is a very surprising finding, since it has never been reported that autophosphorylation and substrate phosphorylation can be mutually antagonistic in any BY-kinase. In fact, the structural data suggest quite the opposite. The octamer structure of the BY-kinases represents the conformation in which the kinase active sites are inaccessible to substrates (Olivares-Illana et al., 2008). Autophosphorylation triggers octamer dissociation, and theoretically renders the active sites of the kinase accessible to substrates. It will therefore be very interesting to investigate the structural context of PtkB inactivation by autophosphorylation. Whatever the mechanism of PtkB regulation is, the phenotype of $\Delta ptkB$ and the present studies suggest its involvement uniquely in a single process, the production of extracellular polysaccharides during biofilm development

(Elsholz et al., 2014; Gerwig et al., 2014). However, one should not prematurely conclude that PtkB is an insulated regulatory device. Firstly, the role of PtkB is partially complemented by PtkA with respect to biofilm development (Gerwig et al., 2014). Further, interactomics data suggest the ability of Tkm/PtkA and TkmB/PtkB to switch partners, at least at the protein-protein interaction level (Shi et al., 2014a). This suggests a possibility of promiscuity also at the level of substrate phosphorylation. Finally, in the two hybrid screen PtkB interacted directly with MinD, PolA, RpoB, and MutL, which are the key players of housekeeping processes such as division, replication, transcription, and damage repair (Shi et al., 2014a). These interactions in a high confidence network are very likely to have physiological significance, and thus suggest that PtkB may be involved in coordinating exopolysaccharide synthesis with other key cellular processes.

EMERGING PROPERTIES OF THE BY-KINASE REGULATORY NETWORK IN *B. subtilis*: RAPIDLY EVOLVING BY-KINASES ADOPT NEW SUBSTRATES AND ENGAGE IN INTERACTION WITH OTHER TYPES OF KINASES

A recent study compared the sequences of BY-kinases from all available bacterial genomes, in an attempt to understand their evolutionary history (Shi et al., 2014b). One surprising finding of that study was the apparent hyper-mutability of BY-kinase genes. The synonymous substitution rate in BY-kinase genes was comparable to other bacterial genes. However, the non-synonymous substitution rate in BY-kinase genes was about threefold higher compared to the control. This indicates that BY-kinases accumulate mutations at an increased rate. One direct consequence of this phenomenon is no detectable co-evolution between kinases and their known substrates. This lack of co-evolution means that BY-kinases are promiscuous and can phosphorylate substrate homologs from different bacteria (Shi et al., 2014b). This promiscuity toward substrates thus seems to be “hard-wired” in the evolutionary setup of BY-kinases. Why would bacteria maintain such promiscuous regulatory devices? One possible explanation that was put forward is the maintenance of BY-kinases as rapidly evolving regulators, which can readily adopt new substrates when environmental changes impose selective pressure for rapid evolution of new regulatory modules (Shi et al., 2014b). In that sense, BY-kinases should be seen as sensing/regulatory devices at the forefront of rapid adaptation.

Eukaryal serine/threonine and tyrosine kinases are known to form complex cascades of mutual activation, in which one kinase phosphorylates another (cross-phosphorylation), and which serve as signal integration and amplification devices (Nishida and Gotoh, 1993). No evidence of such cascades existed in bacteria until two very recent studies, in *Mycobacterium tuberculosis* (Baer et al., 2014) and *B. subtilis* (Shi et al., 2014c). Baer et al. (2014) reported cross-phosphorylation among mycobacterial serine/threonine kinases of the Hanks type, while Shi et al. (2014c) detected extensive cross-phosphorylation among serine/threonine kinases of several distinct families (Hanks type, two-component-like, HprK/P) and the BY-kinases. The BY-kinase PtkA thus engages in extensive cross-phosphorylation interplay with other kinases. In addition to being able to switch activators



with PtkB, it also phosphorylates the following serine/threonine kinases: YabT, RsbW and SpoIIAB *in vitro* (Figure 2). In turn, it is phosphorylated by PrkC, PrkD, YabT, and HprK/P. It has not yet been clearly established whether all these cross-phosphorylation events have regulatory roles, but the existing data seem to favor that notion. In the case of phosphorylation of the Hanks-type kinase YabT by PtkA, three phosphorylated tyrosines were detected by mass spectrometry (Shi et al., 2014c). Two of them (Y28 and Y92) are putatively involved in YabT dimerization and the third one (Y254) is in the region essential for DNA binding. DNA binding is the key signal which activates YabT (Bidnenko et al., 2013), and phosphorylation of Y254 is likely to prevent this activation. In the case of PtkA phosphorylation by PrkC, the target residue is S223 (Shi et al., 2014c). The phosphorylated S223 is adjacent to the C-terminal cluster of tyrosines (Y225, Y227, and Y228) which constitute PtkA autophosphorylation sites. As mentioned previously, PtkA autophosphorylation in this region triggers the dissociation of the octameric ring (Olivares-Illana et al., 2008). In agreement with this finding, it has been observed that PtkA autophosphorylation *in vivo* gets strongly enhanced in the $\Delta prkC$ strain (Ravikumar et al., 2014). Therefore the PrkC-dependent phosphorylation of PtkA could constitute a signal to tune PtkA autophosphorylation levels, and by extension its oligomerization state and access to substrates.

In conclusion, the picture of the regulatory network that emerges around the BY-kinase PtkA is an extremely complex one,

with many degrees of connectivity. This kinase phosphorylates and regulates over a dozen cellular substrates, including three other protein kinases (YabT, RsbW, and SpoIIAB). It interacts with three activator proteins: TkmA, MinD, and Sala, but apparently not at the same time, nor the same place. These activators can respectively transmit to PtkA the inputs regarding the presence of exopolysaccharides at the surface, progression of the cell cycle and the exoprotease activity. They also influence the choice of substrates that PtkA can phosphorylate. Finally, PtkA is phosphorylated by four other kinases: PrkC, YabT, HprK/P, and PrkD, which are likely to transmit signals relative to germination, sporulation and sugar availability. The emergent picture is that of a signal integration device that receives a large number of inputs and distributes the outputs via regulation of relevant downstream processes via substrate phosphorylation. From the pleiotropic phenotype of $\Delta ptkA$ (Petranovic et al., 2007), early on it could be imagined that its cellular role will be complex. Untangling this web of interactions and sorting them out spatially and temporally will require significant additional efforts. PtkB should also not be forgotten in this network reconstruction, as preliminary evidence indicates that it could also be more promiscuous than presently believed. In order to fully explain the roles of PtkA and PtkB in *B. subtilis* physiology, the attention should now be turned to in-depth physiological characterization of all the connected signaling pathways. This effort should be supported by more time-resolved quantitative phosphoproteomics, which should be able to capture

the dynamic aspect of these regulatory events. Lessons learned in *B. subtilis* are likely to be of interest for the studies of BY-kinases in pathogenic bacteria, as they are known to play important roles in bacterial virulence (Cozzone, 2009).

ACKNOWLEDGMENTS

This work was supported by a grant from the Chalmers University of Technology (to Ivan Mijakovic) and by the Agence Nationale de la Recherche (ANR) project N° ANR-09-BLAN-0273 (to Josef Deutscher).

REFERENCES

- Baer, C. E., Iavarone, A. T., Alber, T., and Sassetti, C. M. (2014). Biochemical and spatial coincidence in the provisional Ser/Thr protein kinase interaction network of *Mycobacterium tuberculosis*. *J. Biol. Chem.* 289, 20422–20433. doi: 10.1074/jbc.M114.559054
- Bender, M. H., Cartee, R. T., and Yother, J. (2003). Positive correlation between tyrosine phosphorylation of CpsD and capsular polysaccharide production in *Streptococcus pneumoniae*. *J. Bacteriol.* 185, 6057–6066. doi: 10.1128/JB.185.20.6057-6066.2003
- Bidnenko, V., Shi, L., Kobir, A., Ventroux, M., Pigeonneau, N., Henry, C., et al. (2013). *Bacillus subtilis* serine/threonine protein kinase YabT is involved in spore development via phosphorylation of a bacterial recombinase. *Mol. Microbiol.* 88, 921–935. doi: 10.1111/mmi.12233
- Cozzone, A. J. (2009). Bacterial tyrosine kinases: novel targets for antibacterial therapy? *Trends Microbiol.* 17, 536–543. doi: 10.1016/j.tim.2009.09.005
- Derouiche, A., Bidnenko, V., Grenha, R., Pigeonneau, N., Ventroux, M., Franz-Wachtel, M., et al. (2013). Interaction of bacterial fatty-acid-displaced regulators with DNA is interrupted by tyrosine phosphorylation in the helix-turn-helix domain. *Nucleic Acids Res.* 41, 9371–9381. doi: 10.1093/nar/gkt709
- Deutscher, J., Aké, F. M., Derkaoui, M., Zébré, A. C., Cao, T. N., Bouraoui, H., et al. (2014). The bacterial phosphoenolpyruvate: carbohydrate phosphotransferase system: regulation by protein phosphorylation and phosphorylation-dependent protein–protein interactions. *Microbiol. Mol. Biol. Rev.* 78, 231–256. doi: 10.1128/MMBR.00001-14
- Elsholz, A. K. W., Wacker, S. A., and Losick, R. (2014). Self-regulation of exopolysaccharide production in *Bacillus subtilis* by a tyrosine kinase. *Genes Dev.* 28, 1710–1720. doi: 10.1101/gad.246397.114
- Eymann, C., Becher, D., Bernhardt, J., Gronau, K., Klutzny, A., and Hecker, M. (2007). Dynamics of protein phosphorylation on Ser/Thr/Tyr in *Bacillus subtilis*. *Proteomics* 7, 3509–3526. doi: 10.1002/pmic.200700232
- Fuhrmann, J., Schmidt, A., Spiess, S., Lehner, A., Turgay, K., Mechtler, K., et al. (2009). McsB is a protein arginine kinase that phosphorylates and inhibits the heat-shock regulator CtsR. *Science* 324, 1323–1327. doi: 10.1126/science.1170088
- Gerwig, J., Kiley, T. B., Gunka, K., Stanley-Wall, N., and Stülke, J. (2014). The protein tyrosine kinases EpsB and PtkA differentially affect biofilm formation in *Bacillus subtilis*. *Microbiology* 160, 682–691. doi: 10.1099/mic.0.074971-0
- Grangeasse, C., Cozzone, A. J., Deutscher, J., and Mijakovic, I. (2007) Tyrosine phosphorylation: an emerging regulatory device of bacterial physiology. *Trends Biochem. Sci.* 32, 86–94. doi: 10.1016/j.tibs.2006.12.004
- Grangeasse, C., Obadia, B., Mijakovic, I., Deutscher, J., Cozzone, A. J., and Doublet, P. (2003). Autophosphorylation of the *Escherichia coli* protein kinase Wzc regulates tyrosine phosphorylation of Ugd, a UDP-glucose dehydrogenase. *J. Biol. Chem.* 278, 39323–39329. doi: 10.1074/jbc.M305134200
- Iakoucheva, L. M., Radivojac, P., Brown, C. J., O'Connor, T. R., Sikes, J. G., Obradovic, Z., et al. (2004). Intrinsic disorder and protein phosphorylation. *Nucleic Acids Res.* 32, 1037–1049. doi: 10.1093/nar/gkh253
- Jers, C., Pedersen, M. M., Paspaliari, D. K., Schütz, W., Johnsson, C., Soufi, B., et al. (2010). *Bacillus subtilis* BY-kinase PtkA controls enzyme activity and localization of its protein substrates. *Mol. Microbiol.* 77, 287–299. doi: 10.1111/j.1365-2958.2010.07227.x
- Kearns, D. B., Chu, F., Branda, S. S., Kolter, R., and Losick, R. (2005). A master regulator for biofilm formation by *Bacillus subtilis*. *Mol. Microbiol.* 55, 739–749. doi: 10.1111/j.1365-2958.2004.04440.x
- Kiley, T. B., and Stanley-Wall, N. R. (2010). Post-translational control of *Bacillus subtilis* biofilm formation mediated by tyrosine phosphorylation. *Mol. Microbiol.* 78, 947–963. doi: 10.1111/j.1365-2958.2010.07382.x
- Lévine, A., Vannier, F., Absalon, C., Kuhn, L., Jackson, P., Scrivener, E., et al. (2006). Analysis of the dynamic *Bacillus subtilis* Ser/Thr/Tyr phosphoproteome implicated in a wide variety of cellular processes. *Proteomics* 6, 2157–2173. doi: 10.1002/pmic.200500352
- Macek, B., Mijakovic, I., Olsen, J. V., Gnad, F., Kumar, C., Jensen, P. R., et al. (2007). The serine/threonine/tyrosine phosphoproteome of the model bacterium *Bacillus subtilis*. *Mol. Cell. Proteomics* 6, 697–707. doi: 10.1074/mcp.M600464-MCP200
- Mijakovic, I., Musumeci, L., Tautz, L., Petranovic, D., Edwards, R. A., Jensen, P. R., et al. (2005a). In vitro characterization of the *Bacillus subtilis* protein tyrosine phosphatase YwqE. *J. Bacteriol.* 187, 3384–3390. doi: 10.1128/JB.187.10.3384-3390.2005
- Mijakovic, I., Petranovic, D., Bottini, N., Deutscher, J., and Jensen, P. R. (2005b). Protein-tyrosine phosphorylation in *Bacillus subtilis*. *J. Mol. Microbiol. Biotechnol.* 9, 189–197. doi: 10.1159/000089647
- Mijakovic, I., Petranovic, D., Macek, B., Cepo, T., Mann, M., Davies, J., et al. (2006). Bacterial single-stranded DNA-binding proteins are phosphorylated on tyrosine. *Nucleic Acids Res.* 34, 1588–1596. doi: 10.1093/nar/gkj514
- Mijakovic, I., Poncet, S., Boël, G., Mazé, A., Gillet, S., Jamet, E., et al. (2003). Transmembrane modulator-dependent bacterial tyrosine kinase activates UDP-glucose dehydrogenases. *EMBO J.* 22, 4709–4718. doi: 10.1093/emboj/cdg458
- Mijakovic, I., Poncet, S., Galinier, A., Monedero, V., Fieulaine, S., Janin, J., et al. (2002). Pyrophosphate-producing protein dephosphorylation by HPr kinase/phosphorylase: a relic of early life? *Proc. Natl. Acad. Sci. U.S.A.* 99, 13442–13447. doi: 10.1073/pnas.212410399
- Miller, M. L., Soufi, B., Jers, C., Blom, N., Macek, B., and Mijakovic, I. (2009). NetPhosBac—a predictor for Ser/Thr phosphorylation sites in bacterial proteins. *Proteomics* 9, 116–125. doi: 10.1002/pmic.200800285
- Misra, S. K., Aké, F., Wu, Z., Milohanic, E., Cao, T. N., Cossart, P., et al. (2014). Quantitative proteome analyses identify PrfA-responsive proteins and phosphoproteins in *Listeria monocytogenes*. *J. Proteome Res.* 13, 6046–6057. doi: 10.1021/pr500929u
- Misra, S. K., Milohanic, E., Aké, F., Mijakovic, I., Deutscher, J., Monnet, V., et al. (2011). Analysis of the serine/threonine/tyrosine phosphoproteome of the pathogenic bacterium *Listeria monocytogenes* reveals phosphorylated proteins related to virulence. *Proteomics* 11, 4155–4165. doi: 10.1002/pmic.201100259
- Morona, J. K., Paton, J. C., Miller, D. C., and Morona, R. (2000). Tyrosine phosphorylation of CpsD negatively regulates capsular polysaccharide biosynthesis in *Streptococcus pneumoniae*. *Mol. Microbiol.* 35, 1431–1442. doi: 10.1046/j.1365-2958.2000.01808.x
- Musumeci, L., Bongiorno, C., Tautz, L., Edwards, R. A., Osterman, A., Perego, M., et al. (2005). Low-molecular-weight protein tyrosine phosphatases of *Bacillus subtilis*. *J. Bacteriol.* 187, 4945–4956. doi: 10.1128/JB.187.14.4945-4956.2005
- Nicolas, P., Mäder, U., Dervyn, E., Rochat, T., Leduc, A., Pigeonneau, N., et al. (2012). Condition-dependent transcriptome reveals high-level regulatory architecture in *Bacillus subtilis*. *Science* 335, 1103–1106. doi: 10.1126/science.1206848
- Nishida, E., and Gotoh, Y. (1993). The MAP kinase cascade is essential for diverse signal transduction pathways. *Trends Biochem. Sci.* 18, 128–131. doi: 10.1016/0968-0004(93)90019-J
- Olivares-Illana, V., Meyer, P., Bechet, E., Gueguen-Chaignon, V., Soulat, D., Lazereg-Riquier, S., et al. (2008). Structural basis for the regulation mechanism of the tyrosine kinase CapB from *Staphylococcus aureus*. *PLoS Biol.* 6:e143. doi: 10.1371/journal.pbio.0060143
- Petranovic, D., Grangeasse, C., Macek, B., Abdillatef, M., Gueguen-Chaignon, V., Nessler, S., et al. (2009). Activation of *Bacillus subtilis* Ugd by the BY-kinase PtkA proceeds via phosphorylation of its residue tyrosine 70. *J. Mol. Microbiol. Biotechnol.* 17, 83–89. doi: 10.1159/000206635
- Petranovic, D., Michelsen, O., Zahradka, K., Silva, C., Petranovic, M., Jensen, P. R., et al. (2007). *Bacillus subtilis* strain deficient for the protein-tyrosine kinase PtkA exhibits impaired DNA replication. *Mol. Microbiol.* 63, 1797–1805. doi: 10.1111/j.1365-2958.2007.05625.x
- Ravikumar, V., Shi, L., Derouiche, A., Jers, C., Cousin, C., et al. (2014). Quantitative phosphoproteome analysis of *Bacillus subtilis* reveals novel substrates of the kinase PrkC and phosphatase PrpC. *Mol. Cell. Proteomics* 13, 1965–1978. doi: 10.1074/mcp.M113.035949

- Schmidt, A., Trentini, D. B., Spiess, S., Fuhrmann, J., Ammerer, G., Mechtler, K., et al. (2014). Quantitative phosphoproteomics reveals the role of protein arginine phosphorylation in the bacterial stress response. *Mol. Cell. Proteomics* 13, 537–550. doi: 10.1074/mcp.M113.032292
- Shi, L., Kobir, A., Jers, C., and Mijakovic, I. (2010). Bacterial protein-tyrosine kinases. *Curr. Proteomics* 7, 188–194. doi: 10.2174/157016410792928198
- Shi, L., Pigeonneau, N., Ventroux, M., Derouiche, A., Bidnenko, V., Mijakovic, I., et al. (2014a). Protein-tyrosine phosphorylation interaction network in *Bacillus subtilis* reveals new substrates, kinase activators and kinase cross-talk. *Front. Microbiol.* 5:538. doi: 10.3389/fmicb.2014.00538
- Shi, L., Ji, B., Kolar-Znika, L., Boskovic, A., Jadeau, F., Combet, C., et al. (2014b). Evolution of bacterial protein-tyrosine kinases and their relaxed specificity toward substrates. *Genome Biol. Evol.* 6, 800–817. doi: 10.1093/gbe/evu056
- Shi, L., Pigeonneau, N., Ravikumar, V., Dobrinic, P., Macek, B., Franjevic, D., et al. (2014c). Cross-phosphorylation of bacterial serine/threonine and tyrosine protein kinases on key regulatory residues. *Front. Microbiol.* 5:495. doi: 10.3389/fmicb.2014.00495
- Soufi, B., Kumar, C., Gnad, F., Mann, M., Mijakovic, I., and Macek, B. (2010). Stable isotope labeling by amino acids in cell culture (SILAC) applied to quantitative proteomics of *Bacillus subtilis*. *J. Proteome Res.* 9, 3638–3646. doi: 10.1021/pr100150w
- Vincent, C., Doublet, P., Grangeasse, C., Vaganay, E., Cozzzone, A. J., and Duclos, B. (1999). Cells of *Escherichia coli* contain a protein-tyrosine kinase, Wzc, and a phosphotyrosine-protein phosphatase, Wzb. *J. Bacteriol.* 181, 3472–3477.
- Wugeditsch, T., Paiment, A., Hocking, J., Drummelsmith, J., Forrester, C., and Whitfield, C. (2001). Phosphorylation of Wzc, a tyrosine autokinase, is essential for assembly of group 1 capsular polysaccharides in *Escherichia coli*. *J. Biol. Chem.* 276, 2361–2371. doi: 10.1074/jbc.M009092200
- Xu, H., Xia, B., and Jin, C. (2006). Solution structure of a low-molecular-weight protein tyrosine phosphatase from *Bacillus subtilis*. *J. Bacteriol.* 188, 1509–1517. doi: 10.1128/JB.188.4.1509-1517.2006

Conflict of Interest Statement: The authors declare that the research was conducted in the absence of any commercial or financial relationships that could be construed as a potential conflict of interest.

Received: 07 November 2014; accepted: 07 January 2015; published online: 23 January 2015.

Citation: Mijakovic I and Deutscher J (2015) Protein-tyrosine phosphorylation in *Bacillus subtilis*: a 10-year retrospective. *Front. Microbiol.* 6:18. doi: 10.3389/fmicb.2015.00018

This article was submitted to Microbial Physiology and Metabolism, a section of the journal Frontiers in Microbiology.

Copyright © 2015 Mijakovic and Deutscher. This is an open-access article distributed under the terms of the Creative Commons Attribution License (CC BY). The use, distribution or reproduction in other forums is permitted, provided the original author(s) or licensor are credited and that the original publication in this journal is cited, in accordance with accepted academic practice. No use, distribution or reproduction is permitted which does not comply with these terms.



Activity of the response regulator CiaR in mutants of *Streptococcus pneumoniae* R6 altered in acetyl phosphate production

Patrick Marx[†], Marina Meiers and Reinhold Brückner*

Department of Microbiology, University of Kaiserslautern, Kaiserslautern, Germany

Edited by:

Jörg Stülke,
Georg-August-Universität Göttingen,
Germany

Reviewed by:

Anne Galinier, Centre National de la
Recherche Scientifique, France
Oscar P. Kuipers, University of
Groningen, Netherlands

*Correspondence:

Reinhold Brückner, Department of
Microbiology, University of
Kaiserslautern, Paul Ehrlich Straße
23, D-67663 Kaiserslautern,
Germany
e-mail: rbrueckn@rhrk.uni-kl.de

[†]Present address:

Patrick Marx, Department of
Restorative Dentistry, Oregon
Health and Science University,
Portland, OR, USA

The two-component regulatory system (TCS) CiaRH of *Streptococcus pneumoniae* is implicated in competence, β -lactam resistance, maintenance of cell integrity, bacteriocin production, host colonization, and virulence. Depending on the growth conditions, CiaR can be highly active in the absence of its cognate kinase CiaH, although phosphorylation of CiaR is required for DNA binding and gene regulation. To test the possibility that acetyl phosphate (AcP) could be the alternative phosphodonator, genes involved in pyruvate metabolism were disrupted to alter cellular levels of acetyl phosphate. Inactivating the genes of pyruvate oxidase SpxB, phosphotransacetylase Pta, and acetate kinase AckA, resulted in very low AcP levels and in strongly reduced CiaR-mediated gene expression in CiaH-deficient strains. Therefore, alternative phosphorylation of CiaR appears to proceed via AcP. The AcP effect on CiaR is not detected in strains with CiaH. Attempts to obtain elevated AcP by preventing its degradation by acetate kinase AckA, were not successful in CiaH-deficient strains with a functional SpxB, the most important enzyme for AcP production in *S. pneumoniae*. The *ciaH-spxB-ackA* mutant producing intermediate amounts of AcP could be constructed and showed a promoter activation, which was much higher than expected. Since activation was dependent on AcP, it can apparently be used more efficiently for CiaR phosphorylation in the absence of AckA. Therefore, high AcP levels in the absence of CiaH and AckA may cause extreme overexpression of the CiaR regulon leading to synthetic lethality. AckA is also involved in a regulatory response, which is mediated by CiaH. Addition of acetate to the growth medium switch CiaH from kinase to phosphatase. This switch is lost in the absence of AckA indicating metabolism of acetate is required, which starts with the production of AcP by AckA. Therefore, AckA plays a special regulatory role in the control of the CiaRH TCS.

Keywords: *Streptococcus pneumoniae*, two-component regulatory system CiaRH, acetyl phosphate, alternative phosphorylation, pyruvate oxidase, acetate kinase

INTRODUCTION

The two-component regulatory system (TCS) Competence Induction and Altered cefotaxime susceptibility (CiaRH) of the human pathogen *Streptococcus pneumoniae* is a pleiotropic regulatory device, which is involved in controlling a variety of physiological processes such as genetic competence (Sebert et al., 2005; Cassone et al., 2012), maintenance of cell integrity (Dagkessamanskaia et al., 2004; Mascher et al., 2006a), β -lactam resistance (Guenzi et al., 1994; Müller et al., 2011), bacteriocin production (Dawid et al., 2009; Kochan and Dawid, 2013), and virulence (Throup et al., 2000; Sebert et al., 2002; Ibrahim et al., 2004). CiaR belonging to the OmpR family of response regulators (Martínez-Hackert and Stock, 1997) and the periplasmic-sensing EnvZ-PhoQ-type (Mascher et al., 2006b) histidine kinase CiaH constitute a prototypical TCS. The response regulator CiaR controls directly 16 promoters, 15 positively and one negatively (Halfmann et al., 2007b; Denapate et al., 2012). These promoters drive transcription of 29 genes, among them five genes specifying

small non-coding RNAs (csRNAs, *c*ia-controlled small RNAs) (Halfmann et al., 2007b). The csRNAs in turn are implicated in autolysis (Halfmann et al., 2007b), competence (Tsui et al., 2010; Schnorpfeil et al., 2013), β -lactam resistance (Schnorpfeil et al., 2013), and virulence (Mann et al., 2012). In addition, a gene product of another member of the CiaR regulon, the serine protease HtrA, participates in regulating most of the above mentioned phenotypes (Ibrahim et al., 2004; Cassone et al., 2012; Kochan and Dawid, 2013).

TCSs with transcription regulators as output domains typically turn gene expression on and off in response to the presence of certain stimuli (Gao and Stock, 2009; Krell et al., 2010). CiaRH however, was found to be highly active under a variety of laboratory growth conditions (Halfmann et al., 2011), but also in animal models analyzing colonization and virulence (Throup et al., 2000; Marra et al., 2002; Sebert et al., 2002; Ibrahim et al., 2004). Moreover, the system is active in various *S. pneumoniae* clinical isolates (Sebert et al., 2002; Lanie et al., 2007; Kumar

et al., 2010; Tsui et al., 2010), not only in strain R6 used in this study.

Even in the absence of CiaH, CiaR-dependent promoters are still active and their strength may even be higher than with a functional CiaH under certain growth conditions (Halfmann et al., 2011). On the other hand, purified CiaR did not bind to promoter fragments unless acetyl phosphate (AcP) was added prior to the gel shift assay (Halfmann et al., 2011). A mutant form of CiaR containing an alanine instead of aspartic acid at position 51 was no longer able to activate gene expression and did not bind efficiently to promoter fragments even in the presence of AcP (Halfmann et al., 2011). Therefore, *in vitro* and *in vivo* evidence strongly suggests that the phosphorylated form of CiaR is active in DNA binding and transcriptional regulation. Nevertheless, high CiaR-dependent promoter activity is detected in the absence of CiaH indicating that CiaR must be able to obtain its phosphate from other sources.

Two ways are conceivable how CiaR could be phosphorylated in the absence of cognate CiaH kinase: Phosphorylation by another histidine kinase by cross-talk (Laub and Goulian, 2007), or cross-phosphorylation by small molecular weight high-energy donors such as AcP (Lukat et al., 1992; Wanner, 1992; Wolfe, 2010). Since *in vitro* CiaR DNA binding activity could be stimulated by AcP, CiaR may indeed be phosphorylated by this molecule *in vivo*.

Synthesis of AcP in *S. pneumoniae* depends on three enzymes, pyruvate oxidase SpxB, phosphotransacetylase Pta, and acetate kinase AckA (Spellerberg et al., 1996; Pericone et al., 2003; Ramos-Montanez et al., 2010; Carvalho et al., 2013). SpxB uses oxygen and inorganic phosphate to produce AcP and H₂O₂ directly from pyruvate. AcP production by Pta proceeds via acetyl-coenzyme A, which is produced by pyruvate-formate lyase (Yesilkaya et al., 2009). Finally, AckA converts AcP to acetate, which is excreted, and generates ATP. The enzyme is also able to catalyze the reverse reaction but the equilibrium is far toward ATP formation.

In the present study, we examined the hypothesis that AcP could be the phosphoryl donor for CiaR by creating mutants in the *spxB*, *pta*, and *ackA* AcP biosynthesis genes and subsequent measurements of CiaR-mediated gene expression in the presence or absence of CiaH. The results of these experiments provide strong evidence that AcP is important for CiaR phosphorylation in the absence of CiaH. They also reveal a special role of AckA in this regulation.

MATERIALS AND METHODS

BACTERIAL STRAINS, PLASMIDS, GROWTH CONDITIONS, AND TRANSFORMATION

The *S. pneumoniae* strains used in this study are derivatives of *S. pneumoniae* R6 (Ottolenghi and Hotchkiss, 1962) and are listed in Table 1. *S. pneumoniae* was grown at 37°C in static cultures without aeration in C-medium (Lacks and Hotchkiss, 1960) supplemented with 0.1% yeast extract (C+Y) or brain-heart infusion (BHI). BHI was purchased from Becton Dickinson, France. The cultures for all experiments had a volume of 10 ml and were kept in glass tubes with a diameter of 1.4 mm. Therefore, *S. pneumoniae* was grown under semi-aerobic conditions, identical to

Table 1 | *S. pneumoniae* strains used in this study.

Strain ^a	Characteristics	Sources or references
R6	Wild type	Ottolenghi and Hotchkiss, 1962
RCH	<i>ciaH::aad9</i>	Halfmann et al., 2011
RKL95	<i>spxB::ermB</i>	This work
RKL399	<i>spxB::ermB, pta::cat</i>	This work
RKL369	<i>spxB::ermB, pta::cat, ackA::aphIII</i>	This work
RKL394	<i>spxB::ermB, ackA::aphIII</i>	This work
RKL380	<i>pta::cat</i>	This work
RKL416	<i>pta::cat, ackA::aphIII</i>	This work
RKL379	<i>ackA::aphIII</i>	This work
RKL400	<i>ciaH::aad9, spxB::ermB</i>	This work
RKL410	<i>ciaH::aad9, spxB::ermB, pta::cat</i>	This work
RKL373	<i>ciaH::aad9, spxB::ermB, pta::cat, ackA::aphIII</i>	This work
RKL401	<i>ciaH::aad9, spxB::ermB, ackA::aphIII</i>	This work
RKL385	<i>ciaH::aad9, pta::cat</i>	This work
RKL168	<i>ciaH306, rpsL41^b</i>	Müller et al., 2011
RKL162	<i>ciaH202, rpsL41</i>	Müller et al., 2011
RKL163	<i>ciaH305, rpsL41</i>	Müller et al., 2011
RKL164	<i>ciaH208, rpsL41</i>	Müller et al., 2011
RKL165	<i>ciaH408, rpsL41</i>	Müller et al., 2011
RKL243	<i>ciaH232, rpsL41</i>	Müller et al., 2011
RKL245	<i>ciaH556, rpsL41</i>	Müller et al., 2011
RKL246	<i>ciaH1057, rpsL41</i>	Müller et al., 2011
RKL244	<i>ciaHT_{PT}, rpsL41</i>	Müller et al., 2011

^a All strains are R6 derivatives.

^b Strains contain *rpsL41* (*streptR*) because *ciaH* alleles were introduced by the Janus counter-selection procedure (Sung et al., 2001).

our previous experiments. For the acetate experiments, C+Y-medium and BHI-medium have been modified. The standard C+Y-medium contains 12.5 mM sodium acetate (Lacks and Hotchkiss, 1960). Modified C+Y medium contained no sodium acetate, 25 mM or 50 mM. Sodium acetate was added from a 3M stock solution, which had been adjusted to pH 7.8, the pH of C+Y medium. BHI was treated similarly, except that a 3M sodium acetate stock solution of pH 7.4 was used according to the pH of this medium. Growth of *S. pneumoniae* was monitored by measuring optical density of 600 nm (OD₆₀₀). *S. pneumoniae* and its derivatives were grown at 37°C on plates containing D-blood agar (Alloing et al., 1996). Strains with inactivated *ackA* were kept in an air proof candle jar containing 5% oxygen and 10% carbon dioxide.

The promoter probe plasmids with *E. coli lacZ* as a reporter gene pPP2 containing *htrA*, *spr0931*, and *ccnA* promoters, respectively, were described previously (Halfmann et al., 2007b). The plasmids were multiplied in *E. coli* DH5α [φ80d*lacZ*ΔM15 Δ(*lacZYA-argF*) *recA1 endA1 hsdR17 supE44 thi-1 gyrA96 phoA relA1*] and subsequently transferred to *S. pneumoniae* strains as

described (Halfmann et al., 2007b). Natural competent cells of *S. pneumoniae* were only used for the wild type R6 and the *ciaH* mutant RCH. The other mutant strains described in this study were transformed by the addition of CSP as described (Schnorpfel et al., 2013), since their competence development has not been thoroughly studied. *E. coli* strains were grown in LB medium and transformed according to Hanahan (1983).

GENE INACTIVATIONS

The oligonucleotides used for the gene inactivations are listed in **Table 2**. The construction of the *ciaH* mutant (*ciaH::aad9*) has been described previously (Halfmann et al., 2011). The *spxB* inactivation construct was obtained in strain *S. pneumoniae* D39 and its construction has been described elsewhere (Böttig and Mühlemann, 2008). The *spxB* gene inactivated by an erythromycin resistance gene (*spxB::ermB*) was amplified by primer pair *spxB_fwd2*, *spxB_rev2* and transferred to *S. pneumoniae* R6 and its derivatives by selection on 0.5 µg/µl erythromycin. Integration was confirmed by PCR. The *spxB* mutant of R6 was designated RKL95 (**Table 1**).

To construct the *pta* mutant, a direct PCR cloning approach has been performed to replace nucleotides 9 to 366 of the *pta* coding region by the chloramphenicol resistance cassette *cat*. The *pta* coding region consists of 974 bp and is followed immediately downstream by two IS-elements (Hoskins et al., 2001). To allow specific homologous recombination, the 3'-part of *pta* was kept. The *cat* gene fragment was generated by primer pair *cat1*, *cat2* using plasmid puc18-VegM-CAT2 as template (Halfmann et al., 2007b). The upstream fragment of *pta* was amplified by primers *pta1*, *pta2*, the downstream fragment containing the 3'-end of *pta* by primers *pta3*, *pta4*. Each of the primers incorporate recognition sequences for the restriction enzymes *SphI* and *SpeI*. The amplicons were ligated subsequent to their cleavage.

The ligation was re-amplified by primer pair *pta1* and *pta2* and *S. pneumoniae* R6 transformants were selected on 3 µg/ml chloramphenicol to obtain strain RKL380 (*pta::cat*). Integration was confirmed by PCR and sequencing. Subsequently, DNA of strain RKL380 was used as template to amplify the *pta::cat* deletion construct with primers *pta3* and *pta4*. The amplicon was then used to move the *pta* deletion to different *S. pneumoniae* strains.

The *ackA* mutant has been constructed by replacement of the entire gene coding region with the kanamycin resistance gene *aphIII* (Halfmann et al., 2007b). The *aphIII* fragment was generated with primers *ackAf2B* and *ackAr2B*. The upstream fragment of *ackA* was amplified with *ackAf1* and *ackAr1B* while the downstream fragment was amplified with primers *ackAf3B* and *ackAr3*. Each of the primers contained recognition sequences for the restriction enzymes *SphI* and *BamHI*. The amplicons were ligated subsequently to their cleavage. The entire ligation was amplified using primer pair *ackAf1*, *ackAr3r*. Since problems have been reported inactivating *ackA* in *S. pneumoniae* D39 (Ramos-Montanez et al., 2010), this fragment was transferred first to the *spxB* mutant strain RKL95. Selection occurred on 100 µg/ml kanamycin containing blood agar plates incubated in an atmosphere with reduced oxygen (5%) and 10% CO₂. Integration was confirmed by PCR and sequencing. Chromosomal DNA of this strain was then used to amplify the *ackA::aphIII* fragment to transform *S. pneumoniae* R6 to yield strain RKL379 and the other *ackA* deletion strains (**Table 1**).

Inactivation of *ackA* was generally performed as the latest step in strain constructions. In the presence of *ciaRH*, no problems were encountered during *ackA* inactivation. Since genetic instability of *ackA* mutants was described for D39, the predecessor of R6, the genes found to be mutated in this study, *spxB* and *spxR* (Ramos-Montanez et al., 2010), were sequenced in several colonies of our *ackA* mutant strains. No alterations were detected. In the *ciaH::aad9* mutant strain however, *ackA* inactivation could not be achieved in the presence of a functional *SpxB*. The transformation efficiency with the *ackA::aphIII* fragment dropped in RCH (*ciaH::aad9*) or in RKL385 (*ciaH::aad9*, *pta::cat*, **Table 1**) by about four orders of magnitude compared to the corresponding strains with *ciaRH* (R6, RKL80, **Table 1**) or strains with inactivated *spxB* (RKL400, RKL410, **Table 1**). Since the strains with intact *spxB* that could not be obtained efficiently produced large amounts of H₂O₂, katalase was added to the agar. However, transformation efficiency did not improve. The bacteria recovered in these transformations were subsequently found to have suppressor mutations in *spxR*, but also in *ciaR*.

Mutations in *ciaR* were intriguing, since it suggested that an intact *ciaR* is detrimental in this genetic constellation. And indeed, a *ciaR* mutant could be efficiently transformed with the *ackA::aphIII* fragment. Sequencing *spxB* in a couple of transformants revealed no mutations. Thus, inactivation of *ciaH* and *ackA* causes synthetic lethality, which can be suppressed by mutation of *spxB*, but also by *ciaR* inactivation.

Since the non-coding csRNAs and the protease HtrA were implicated in regulating various processes in *S. pneumoniae* (Sebert et al., 2002; Dawid et al., 2009; Schnorpfel et al., 2013), inactivation of these genes were tested for suppression of the lethal phenotype. Deletion of the csRNA genes had no effect,

Table 2 | Oligonucleotides used in this study.

Primer ^a	Sequence
<i>spxB_fwd2</i>	CGGTTTCAGGTTTCATCGAACGCTC
<i>spxB_rev2</i>	CAACTGGGTTTACTTTGTCAAGG
<i>cat1</i>	GCGACTAGTCTTGACTCCTGTTGATAGATCC
<i>cat2</i>	GGCGCATGCGACAAAAATGGACTGAACAAGTCAG
<i>pta1</i>	CGCAGATGAACATGTCAAGG
<i>pta2</i>	GCGACTAGTCTTCCATGAGTTTCTCCTTTAAG
<i>pta3</i>	GCGGCATGCGGAGCGATTCACTCAACAGC
<i>pta4</i>	GCGGCATGCGGAGCGATTCACTCAACAGC
<i>ackAf2B</i>	GCGGCATGCGGAGCGATTCACTCAACAGC
<i>ackAr2B</i>	GCGGCATGCGGAGCGATTCACTCAACAGC
<i>ackAf1</i>	TCTGGATGGTGAACTGAGC
<i>ackAr1B</i>	GCGGCATGCGGAGCGATTCACTCAACAGC
<i>ackAf3B</i>	GCGGCATGCGGAGCGATTCACTCAACAGC
<i>ackAr3</i>	CCTGGATATTGTTCTCGAAGC
<i>ackAf4</i>	GTGGAGCAGCAAGCAATCAAG
<i>ackAr4</i>	TGTGCCTGTACTACGGCCTCG

^a Recognition sites for restriction enzymes are underlined.

but *htrA* inactivation resulted in about 200-fold more transformants. Deletion of the *csRNA* genes and *htrA* together further improved transformation tenfold. However, these transformants also acquired suppressor mutations in *spxB* and *ciaR*.

DETERMINATION OF AcP AMOUNTS

Determination of cellular levels of AcP was carried out according to described methods (Prüss and Wolfe, 1994; Pericone et al., 2003). All steps have been performed on ice or at 4°C, respectively. Ten ml cultures of the desired strains have been grown to mid-exponential phase (OD₆₀₀ 0.4) and subsequently centrifuged at 9000 rpm for 10 min at 4°C. Cell pellets were resuspended in 1 ml ice cold luciferase buffer (100 mM Tris, 4 mM EDTA, pH 7.6) and transferred into 1.5 ml tubes. The cells were lysed for 2 min at 95°C. Within that time, no degradation of AcP was observed in tests using purified AcP (Sigma Aldrich). The cells were quickly cooled on ice, kept for 10 min and then centrifuged at 10,000 rpm for 2 min at 4°C. The supernatant was transferred to a 2 ml tube and mixed with 50 mg/ml powdered activated charcoal (Sigma Aldrich) to remove small compounds like ADP and ATP. After incubation on ice for 15 min, the samples have been filtered (0.22 µm pore-size) to remove the charcoal. The remaining AcP in the samples was enzymatically converted into ATP by acetate kinase. Samples of 100 µl were mixed with the following compounds in the indicated final concentration: 20 mM MgCl₂, 30 mM ADP (Sigma Aldrich), 0.5 U/µl acetate kinase from *B. stearothermophilus* (Sigma Aldrich). Samples containing acetate kinase have been prepared as duplicates and one sample was prepared without acetate kinase as negative control and a control for ATP removal as well. The reaction mixtures were incubated at 30°C for 4 h. The generated ATP was determined by measuring luminescence using the ATP Bioluminescence Assay Kit CLS II (Roche) following the manufacturers' instructions. Luciferase Reagent was added to the acetate kinase reaction mixtures at the ratio of 1. Samples were incubated at room temperature for 2 min and ATP was determined in a BioOrbit 1253 luminometer. Data obtained from samples with acetate kinase were taken as means and subtracted from data obtained from samples without acetate kinase. ATP amounts were determined by comparison with standard curves. Standard curves were generated using known AcP amounts in concentrations between 0.2 and 50 µM, which were converted to ATP as described above. Protein content of the samples was determined as described (Halfmann et al., 2007a) to relate AcP levels to protein.

DETERMINATION OF β-GALACTOSIDASE ACTIVITY

To assess the activity of CiaR, strains harboring CiaR-dependent promoter-β-galactosidase gene (*lacZ*) fusions in the genome (Halfmann et al., 2007b) were assayed for β-galactosidase activity as described (Halfmann et al., 2007a). Units are expressed in nmol nitrophenol released per min and mg of protein.

RESULTS

ACETYL PHOSPHATE LEVELS IN *S. PNEUMONIAE* R6 AND MUTANTS WITH ALTERED PYRUVATE METABOLISM

Since the enzymes pyruvate oxidase SpxB, phosphotransacetylase Pta, and acetate kinase AckA are the key determinants for

AcP production in *S. pneumoniae* (Figure 1), inactivation of their genes should substantially alter AcP levels. Therefore, the respective genes were inactivated by resistance cassettes alone or in combination as described in Materials and Methods. To start with this genetic analysis the wild type strain R6 was used carrying an intact *ciaRH* system. The mutants were grown in C+Y medium, the medium supporting high levels of CiaR activity in the absence CiaH (Halfmann et al., 2011), and AcP was measured as described in Materials and Methods. As shown in Figure 2A, pyruvate oxidase SpxB is the major enzyme involved in AcP production, a result consistent with earlier work (Pericone et al., 2003; Ramos-Montanez et al., 2008, 2010). The AcP level in the *spxB* mutant of R6 strain dropped about 20-fold, which is a larger reduction than in *S. pneumoniae* D39 (Pericone et al., 2003; Ramos-Montanez et al., 2008, 2010). This difference is most likely the consequence of an *spxB* polymorphism detected in both strains (Belanger et al., 2004; Ramos-Montanez et al., 2008). The enzyme is apparently more active in R6 (Belanger et al., 2004). Single inactivation of *pta* encoding phosphotransacetylase had no significant effect, but without SpxB and acetate kinase AckA a contribution of Pta to AcP production is detectable. Inactivation of *ackA* in an SpxB-deficient strain increased the low level of AcP about 14-fold (Figure 2A), because conversion of AcP to acetate by AckA is blocked and AcP can accumulate (Wolfe, 2005). In the *spxB-pta* double mutant however, *ackA* mutation did not result in the elevation of AcP. Thus, some AcP had been produced by Pta in the absence of SpxB. Why Pta is not significantly contributing to AcP production in the presence of SpxB is not clear at the moment.

Growth was differently affected in the mutant strains (Table S1). The single mutants in *spxB* or *ackA* grew almost like the wild type, all other mutant strains were slower with doubling

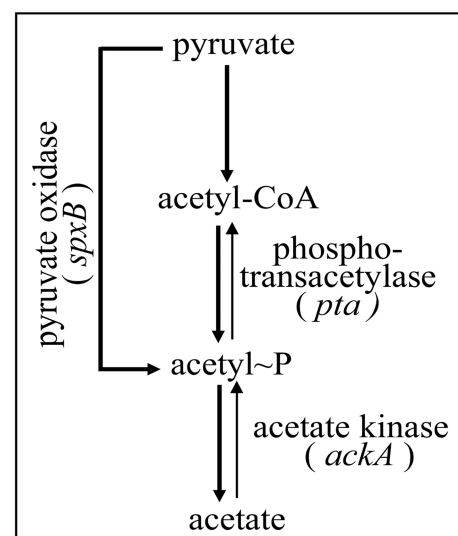


FIGURE 1 | Acetyl phosphate production in *S. pneumoniae*. The part of pyruvate metabolism relevant for this study is shown. Three enzymes, SpxB, Pta, and AckA, are implicated in AcP production as detailed in the introduction. Acetyl-CoA is produced from pyruvate by pyruvate formate lyase (Yesilkaya et al., 2009).

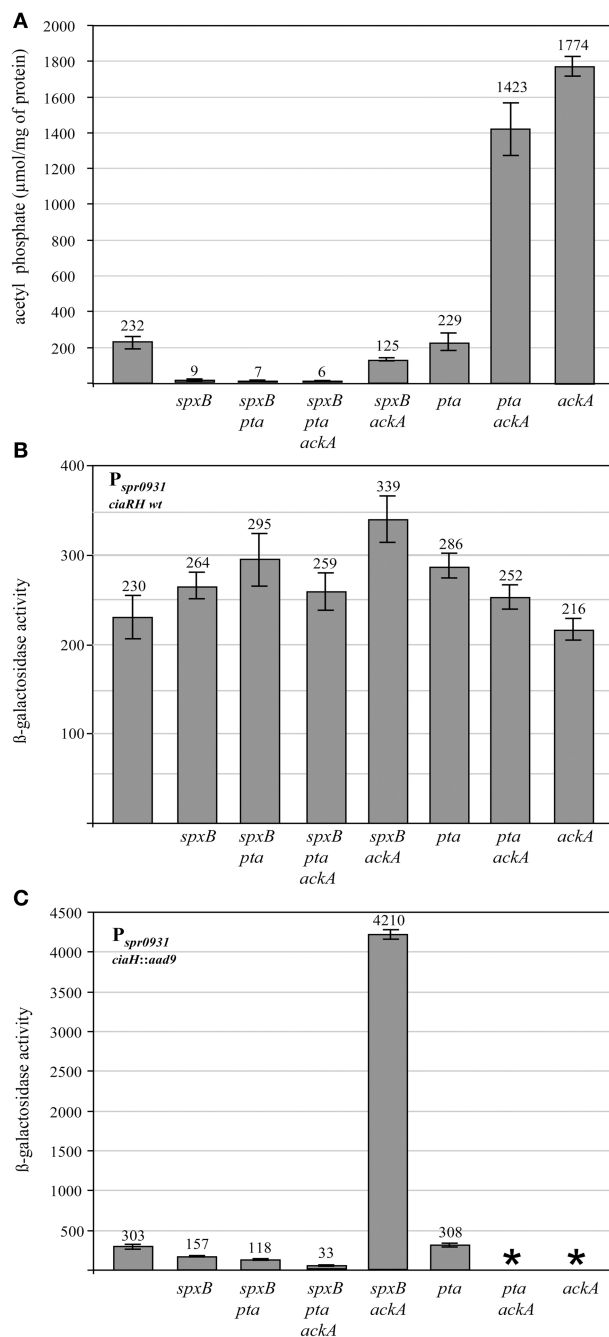


FIGURE 2 | Acetyl phosphate levels and promoter activities in pyruvate metabolism mutants of *S. pneumoniae* R6. (A) Acetyl phosphate in pyruvate metabolism mutants. The strains were grown in C+Y medium to mid-exponential growth phase (OD₆₀₀ 0.4) and acetyl phosphate was determined from 10 ml of the cultures. The strains used in these determinations were (from left to right): R6, RKL95 (*spxB::ermB*), RKL399 (*spxB::ermB, pta::cat*), RKL369 (*spxB::ermB, pta::cat, ackA::aphIII*), RKL394 (*spxB::ermB, ackA::aphIII*), RKL380 (*pta::cat*), RKL416 (*pta::cat, ackA::aphIII*), RKL379 (*ackA::aphIII*). All strains are derivatives of R6 and harbor wild type *ciaRH*. The inactivated genes are indicated. AcP was determined in at least two independent cultures and the values are shown along with standard deviations. **(B)** CiaR-dependent promoter activity in pyruvate metabolism mutants harboring *ciaRH* wild type. The strains were

(Continued)

FIGURE 2 | Continued

grown in C+Y medium to an OD₆₀₀ of 0.4 and β-galactosidase activity was determined. The strains were (from left to right): R6, RKL95 (*spxB::ermB*), RKL399 (*spxB::ermB, pta::cat*), RKL369 (*spxB::ermB, pta::cat, ackA::aphIII*), RKL394 (*spxB::ermB, ackA::aphIII*), RKL380 (*pta::cat*), RKL416 (*pta::cat, ackA::aphIII*), RKL379 (*ackA::aphIII*). All strains contained a P_{spr0931} promoter *lacZ* fusion in the genome (*bgaA::tetM-P_{spr0931}-lacZ*). The promoter of *spr0931* is activated by CiaR and its activity is strictly CiaR-dependent. Two other promoters, P_{htrA} and P_{ccnA}, reacted as P_{spr0931} and a CiaR-independent promoter P_{vegM} showed no change in activity. The inactivated genes are indicated. Values of at least three independent cultures are shown along with standard deviations. β-galactosidase units are expressed in nmol nitrophenol released per min and mg of protein. **(C)** CiaR-dependent promoter activity in pyruvate metabolism mutants harboring inactivated *ciaH*. The strains were (from left to right): RCH (*ciaH::aad9*), RKL400 (*ciaH::aad9, spxB::ermB*), RKL410 (*ciaH::aad9, spxB::ermB, pta::cat*), RKL373 (*ciaH::aad9, spxB::ermB, pta::cat, ackA::aphIII*), RKL401 (*ciaH::aad9, spxB::ermB, ackA::aphIII*), RKL385 (*ciaH::aad9, pta::cat*). *Indicates that these strains could not be constructed. All strains had a P_{spr0931} promoter *lacZ* fusion in the genome (*bgaA::tetM-P_{spr0931}-lacZ*). The promoter of *spr0931* is shown as a representative for CiaR-dependent promoters. The control promoter P_{vegM} was not affected. All strains are CiaH-deficient. The inactivated genes are indicated. Values of at least three independent cultures are shown along with standard deviations. β-galactosidase units are expressed in nmol nitrophenol released per min and mg of protein.

times ranging between 45 and 55 min compared to 37 min of the wild type.

The AcP determinations in this series of *S. pneumoniae* R6 pyruvate metabolism mutants largely confirmed what could be expected from the literature (Pericone et al., 2003; Wolfe, 2005; Ramos-Montanez et al., 2010). Without SpxB and Pta, AcP production is virtually absent. AcP produced by SpxB or Pta accumulates, when *ackA* is inactivated. Consequently, R6 derivatives are available covering a wide range of AcP levels. Since the AcP synthesis mutants were constructed to analyze the connection of AcP to CiaRH-mediated gene expression, it was of interest to determine whether CiaRH could influence AcP levels. AcP determinations in CiaR-, and CiaH-deficient as well as in CiaRH hyperactive strains (Müller et al., 2011) did not reveal an influence (Figure S1).

CiaR-MEDIATED GENE EXPRESSION IN AcP SYNTHESIS MUTANTS IN THE PRESENCE OF CiaH

During the initial characterization of the CiaR regulon (Halfmann et al., 2007b), all CiaR-controlled promoters were cloned into an integrative reporter plasmid (Halfmann et al., 2007a). These constructs are well-suited to analyze CiaR-dependent gene expression (Halfmann et al., 2007b; Müller et al., 2011). Therefore, three of these promoter fusions, P_{spr0931}, P_{htrA}, and P_{ccnA}, were introduced into the mutant strains described above as representatives of the CiaR regulon. They were chosen because their activity is strongly dependent on CiaR and there is no evidence that they are controlled by other regulators (Halfmann et al., 2007b). Measuring the promoter activities in C+Y medium revealed only subtle changes in an almost identical range for all promoters (data not shown). As a representative example, P_{spr0931} mediated β-galactosidase expression determined in the middle of exponential growth (OD₆₀₀ 0.4) is

shown in **Figure 2B**. In general, promoter activities are slightly higher in almost all mutant strains. The *ackA-pta* mutant showed the strongest activation with an increase of 1.5-fold. Similar results were obtained measuring earlier (OD₆₀₀ 0.2) or later (OD₆₀₀ 0.8). Considering that AcP levels vary more than 100-fold (**Figure 2A**), one can conclude that CiaR-dependent promoters are not influenced by AcP under these conditions. The strains used in this series of experiments carried wild type *ciaRH*. Therefore, CiaH will predominantly control the phosphorylation status of CiaR and thereby promoter activities.

CiaR-MEDIATED GENE EXPRESSION IN AcP SYNTHESIS MUTANTS IN THE ABSENCE OF CiaH

Since cross-phosphorylation or cross-talk in TCSs is quite often only detected in the absence of cognate histidine kinases (Laub and Goulian, 2007), it was of interest to determine promoter activities in the AcP synthesis mutants without CiaH. And indeed, drastic changes were detected in the *ciaH* mutant strains (**Figure 2C**), quite in contrast to the strains carrying *ciaRH* wild type (**Figure 2B**). Inactivation of *spxB* resulted in a twofold reduction of P_{spr0931} activity. The other CiaR-dependent promoters reacted accordingly (data not shown). While *pta* inactivation in the *spxB* mutant resulted in a further 2.5-fold reduction, promoter activity dropped about tenfold in the *spxB-pta-ackA* triple mutant. Therefore, inactivation of the genes of pyruvate metabolism, which resulted in the reduction of AcP (**Figure 2A**) clearly diminished CiaR-dependent transcription. Accordingly, no change was observed in the *pta* mutant (**Figure 2C**), which had wild type AcP levels (**Figure 2A**).

A surprising result, however, has been obtained in the *spxB-ackA* mutant strain (**Figure 2C**). Although AcP is about twofold reduced compared to the wild type (**Figure 2A**), transcription from CiaR-dependent promoters is tremendously increased. P_{spr0931} activity rose about 14-fold (**Figure 2C**). In addition, inactivation of *ackA* in strains with intact *spxB*, which are characterized by a high amount of AcP (**Figure 2A**) could not be achieved. Disruption of the same genes was possible in strains with a functional CiaH, but also in the absence of CiaR (see Materials and Methods). Considering the very strong P_{spr0931} activation in the *spxB-ackA-ciaH* mutant strain, it appears that the inability to introduce mutations in *ackA* to strains with a functional SpxB in the absence of CiaH is caused by extreme activation of the CiaR regulon. We have shown previously that strong activation of the CiaR regulon by mutations in *ciaH* could impair growth (Müller et al., 2011). It is therefore conceivable, that higher activation of CiaR-mediated transcription in the AckA-deficient strains could lead to lethality.

The results of these experiments clearly demonstrate a strong influence of the pyruvate metabolism on CiaR-mediated gene expression, provided the cognate kinase CiaH was absent. Promoter activation was strongly reduced in strains producing low amounts of AcP, which would be consistent with AcP as the alternative route of phosphorylation for CiaR in the absence of CiaH. The experiments also show that there is no strict correlation between the AcP level and promoter activation. Especially in the absence of AckA in the *spxB* mutant background, CiaR is disproportionately activated.

THE INFLUENCE OF ACETATE IN THE GROWTH MEDIUM ON CiaR-MEDIATED GENE EXPRESSION

In contrast to the growth of *S. pneumoniae* in C+Y medium, which supports high levels of CiaR-dependent transcription in the absence of CiaH, the same promoters are only weakly active in brain heart infusion (BHI) medium (Halfmann et al., 2011). Measuring AcP in BHI medium revealed an almost threefold reduction ($81 \pm 9 \mu\text{mol/mg}$ of protein) compared to C+Y medium (**Figure 1**), again indicating that AcP levels modulate CiaR activity in the absence of CiaH. This medium was therefore well-suited to test if exogenously added acetate could enhance CiaR activation in the absence of CiaH. As shown in **Figure 3**, P_{spr0931} activity could be nicely stimulated. Adding 12.5 mM sodium acetate, the concentration found in C+Y medium, activation was moderate (1.5 fold), but twofold (25 mM) or fourfold (50 mM) more sodium acetate enhanced the promoter activity seven- and thirtyfold, respectively (**Figure 3**). The addition of potassium acetate had the same effect, while sodium chloride did not change P_{spr0931} activity (**Figure S2**). In conclusion, the observed effect appears to be specific for acetate. Repeating these experiments in C+Y medium with altered acetate concentration yielded in principle the same results, but the change in expression was less pronounced (**Figure S3**). Unexpectedly, measuring AcP in BHI supplemented with acetate, did not reveal a significant increase, not even with the highest concentration.

Another surprising result was obtained measuring promoter activities in the wild type *ciaRH* strain as control. In this strain, addition of acetate to 50mM reduced the promoter activity about twofold compared to the values obtained without acetate supplementation (**Figure 3**). In comparison with the activity measured without CiaH however, promoter strength is tenfold reduced. This comparison strongly suggests that CiaH acts as a phosphatase when acetate concentrations are high in the growth medium. Modifying acetate concentrations in C+Y medium altered CiaR-mediated expression similarly, but again less pronounced (**Figure S4**), indicating that CiaR is dephosphorylated under these conditions. These results are in accordance with the previous notion that CiaH acts as a phosphatase in standard C+Y medium (Halfmann et al., 2011).

The effect of acetate on CiaH activity could be caused directly by binding to CiaH, or indirectly, which would require metabolism of acetate. In the latter case, regulation should depend on AckA, since internalized acetate must be phosphorylated for further metabolism. Therefore, the *ackA* mutant strain was tested in BHI medium and in BHI with 50 mM sodium acetate. The acetate effect was virtually gone upon *ackA* inactivation (**Figure S5**). Therefore, the change of CiaH activity is not caused by acetate itself. Metabolism is required to produce a signal that may then be detected by CiaH.

RESPONSE TO ACETATE IN THE GROWTH MEDIUM BY VARIANTS OF CiaH

Since CiaH appeared to respond to a signal produced by metabolism of acetate, it was of interest to test variants of CiaH, which have been analyzed in some detail previously (Müller et al., 2011). The majority of these *ciaH* mutants (**Table 1**) have been obtained in screens aimed at isolating β -lactam resistant mutants

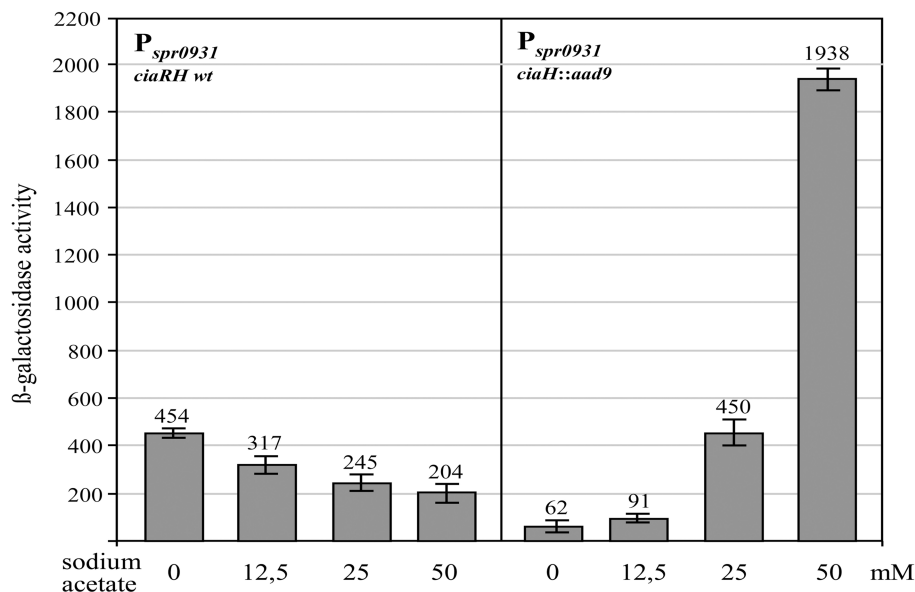


FIGURE 3 | Effect of acetate supplementation of the growth medium on CiaR-dependent promoter activity. The strains were grown in BHI medium containing the indicated concentrations of sodium acetate to an OD₆₀₀ of 0.4 and β-galactosidase was measured. The comparison of the promoter activities of the R6 wild type harboring *ciaRH* (four measurements from the left) with those

found in the CiaH-deficient mutant RCH (*ciaH::aad9*) is shown. All strains had a $P_{spr0931}$ promoter *lacZ* fusion in the genome (*bgaA::tetM-P_{spr0931}-lacZ*). The concentrations of sodium acetate are indicated. Values of at least three independent cultures are shown along with standard deviations. β-galactosidase units are expressed in nmol nitrophenol released per min and mg of protein.

of *S. pneumoniae* R6 (Guenzi et al., 1994; Zähler et al., 2002), but a few were also detected in *ciaH* genes of clinical isolates (Müller et al., 2011). Common to all these *ciaH* alleles, with one exception, is their ability to enhance CiaR-mediated gene expression to higher levels compared to the wild type R6. In some cases, hyperactivation of CiaR is the consequence of the mutations in *ciaH* (Müller et al., 2011).

Promoter activities were measured in these strains in BHI and BHI with 50 mM sodium acetate. As shown in Figure 4, the response to acetate is quite variable. In the mutants obtained in the laboratory, reduction of promoter activities was not observed. In three of these strains, promoter strength was even slightly higher. Quite in contrast, three CiaH variants from clinical isolates reacted more strongly than the wild type (Figure 4), with repression rates of fourfold (*ciaH556*, *ciaH1057*) or even higher (*ciaH232*). The latter allele is the only one which did not enhance CiaR-mediated gene expression (Müller et al., 2011). One clinical variant (*ciaHTpVT*) behaved like the wild type. Interestingly, three CiaH variants, CiaH305, CiaH408, and CiaH232, reacting differently, have alterations in the extracytoplasmic part of the protein. Binding of an unknown factor may have been affected by these mutations. In any case, the differential response of several CiaH variants to acetate in the medium is a strong indication that the effect is specifically mediated by CiaH.

DISCUSSION

Genetic inactivation of genes involved in the production of AcP (Figure 1) resulted in *S. pneumoniae* strains producing drastically different amounts of AcP (Figure 2A). While the double mutant

in *spxB* and *pta* produced very little or perhaps no AcP, inactivation of *ackA* alone or in combination with *pta*, raised AcP to very high levels (Figure 2A). Under latter conditions, concomitant inactivation of *ciaH* was not possible. Measuring CiaR-dependent promoters in an *spxB-ackA* background, a strain producing intermediate AcP amounts (Figure 2A), revealed a very strong increase in promoter activity (Figure 2C). It appears therefore, that the inability to construct *ackA-ciaH* and *ackA-pta-ciaH* mutants is caused by overactivation of CiaR and consequently overexpression of the CiaR regulon. And indeed, the *ackA* mutation could be combined with an inactivated *ciaR* gene (*ciaR::aad9*) and could be constructed in *ciaRH* wild type. In this strain, CiaH is able to reduce CiaR-dependent gene expression back to wild type levels (Figure 2B). Interestingly, in a study to determine the role of AcP in the regulation of the orphan response regulator DegU in *Listeria monocytogenes*, *ackA* inactivation could not be achieved unless *pta* was also inactivated (Gueriri et al., 2008).

The strains in which *ackA* could not be inactivated together with *ciaH* produce high amounts of H₂O₂ because of the activity of SpxB (Spellerberg et al., 1996; Pericone et al., 2003; Ramos-Montanez et al., 2008). H₂O₂ production alone cannot account for the lethality, since CiaRH does not affect *spxB* expression (own unpublished observations). The detrimental concerted action of H₂O₂ and one or more overexpressed members of the CiaR regulon remains a possibility. The stress protease HtrA appears to be one of these factors.

In contrast to the problems with *ackA* inactivation detailed above and also contrary to the strong activation of CiaR-dependent promoters in the *spxB-ackA* mutant strain, *ackA*

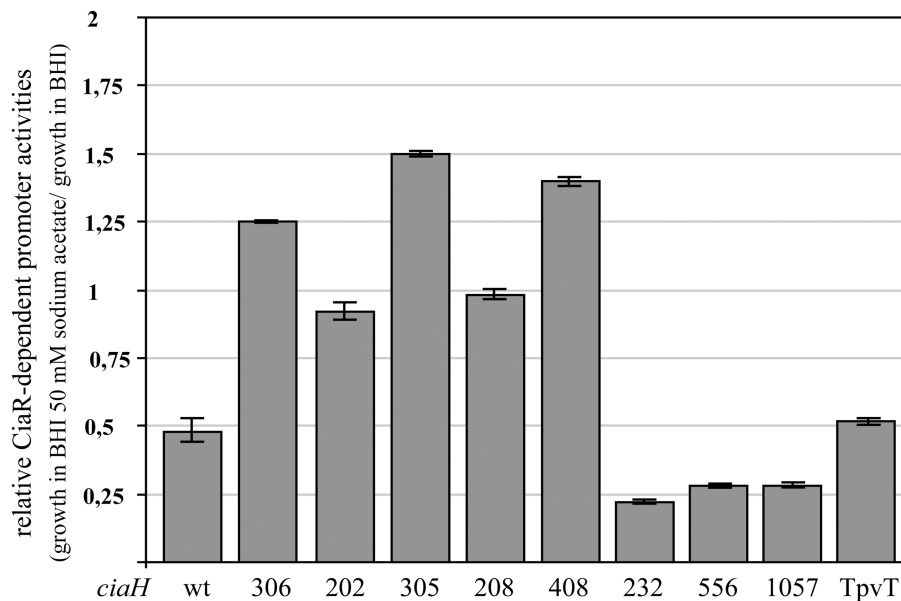


FIGURE 4 | Change of CiaR-dependent promoter activities upon acetate supplementation in strains harboring variants of *ciaH*.

The strains were grown in BHI medium containing 50 mM of sodium acetate or BHI without the addition of acetate to an OD₆₀₀ of 0.4 and β-galactosidase was measured. Activities of two promoters, *P_{htrA}* and *P_{spr0931}*, were determined under both growth conditions and the relative expression rate was calculated by dividing the value of the acetate supplemented culture by the value of the

untreated sample. All strains contained promoter fusions in the genome (*bgaA::tetM-P_{spr0931}-lacZ* or *bgaA::tetM-P_{htrA}-lacZ*). The following strains were used (from left to right): R6, RKL168 (*ciaH306*), RKL162 (*ciaH202*), RKL163 (*ciaH305*), RKL164 (*ciaH208*), RKL165 (*ciaH408*), RKL243 (*ciaH232*), RKL245 (*ciaH556*), RKL246 (*ciaH1057*), RKL244 (*ciaH_{TpvT}*). The *ciaH* allele numbers are indicated. Values of at least two independent cultures of each promoter harboring strain are shown along with standard deviations.

mutation in a *spxB-pta* mutant background was readily achieved and promoted only low levels of CiaR-mediated gene expression (Figure 2C). Reducing AcP levels by sequential inactivation of *spxB*, *pta*, and *ackA* concomitantly lowered CiaR-dependent promoter activities tenfold in the absence of CiaH (Figure 2C). Therefore, CiaR clearly responds to AcP levels. Since phosphorylation is needed for CiaR activity and CiaR binding to promoter fragments *in vitro* is stimulated by AcP (Halfmann et al., 2011), combined evidence suggests that AcP may indeed serve as alternative source of phosphorylation for CiaR. One can always argue that an unknown histidine kinase phosphorylates CiaR by cross-talk in response to varying levels of AcP, but we consider this possibility less likely than AcP-dependent phosphorylation.

Although reduced AcP levels resulted in lower activity of CiaR, the response is not always proportional. The *ciaH-spxB-ackA* mutant produced about half of the AcP found in the wild type (Figure 2A), but promoter activities raised more than tenfold. In addition, *ackA* mutants with functional SpxB are not viable (see above). On the other hand, *ackA* inactivation did not increase promoter activities in strains producing spurious amounts of AcP (*spxB-pta*; Figure 2C). Thus, the effect of AckA on CiaR activity is dependent on AcP. It appears, that CiaR can use AcP as phosphodonor more efficiently in the absence of AckA. At the current stage of knowledge, it is impossible to offer conclusive explanations. An attractive hypothesis, however, would be a direct interaction between AckA and CiaR, which according to our data should lead to reduced phosphorylation of CiaR by AcP. Enzymes

with additional roles in other processes are rather widespread also in bacteria (Wang et al., 2013). Prominent examples of these so-called moon-lighting proteins in bacteria are glycolytic enzymes serving also as receptors for various molecules on the bacterial surface (Wang et al., 2013). Furthermore, a number of enzymes play regulatory roles in complex physiological processes and were proposed to be called trigger enzymes (Commichau and Stülke, 2008). According to our hypothesis, AckA could be such a trigger enzyme. Interestingly, a number of bacteria possess two *ackA* genes, but the analysis of their physiological roles has just started (Chan et al., 2014; Puri et al., 2014). Intriguingly, gene duplication events are quite often associated with trigger enzymes leading to speciation of variants acting then as enzymes or as regulators (Commichau and Stülke, 2008).

The experiments to enhance CiaR-mediated gene regulation by the addition of acetate to the BHI medium constitutes another example, in which AcP levels do not correlate with promoter activities. Although the CiaR-dependent promoters were stimulated about 30-fold by the addition of 50 mM sodium acetate (Figure 3), AcP levels were not significantly elevated under these conditions. Promoter activation was completely lost (Figure S5), when a *ciaR* mutant (*ciaR152*) was tested, which expressed a non-phosphorylatable D51A variant of CiaR (Halfmann et al., 2011). Therefore, phosphorylation of CiaR is required to see the acetate effect. Without higher amounts of acetate in BHI medium, CiaR is apparently not able to use the AcP efficiently that is present in BHI grown cells. Since almost the same effects of acetate addition were observed in C+Y medium (Figure S3),

this regulatory event appears to be general and not specific for BHI, where it is detected best.

To take up again our hypothesis of CiaR-AckA interaction, these results may indicate that this interaction could be regulated according to the activity of AckA or to the availability of the substrates AcP and acetate. It is clearly too early to speculate further on this type of regulation, especially because extremely little is known in *S. pneumoniae* about *ackA* expression or regulation of AckA activity, which has been shown in other organisms to be subject to allosteric control (Puri et al., 2014). In *Borrelia burgdorferi*, an orphan response regulator Rrp2 was also strongly stimulated by acetate in the growth medium, but AcP levels have not been determined (Xu et al., 2010).

A further effect of acetate addition to BHI medium was detected in the wild type (Figure 3). In the presence of CiaH, the promoter stimulating effect observed in the absence of CiaH is converted to a reduction (Figure 3). It appears that the phosphatase activity of CiaH is stimulated under these conditions. Without added acetate CiaH acts as a kinase, but with 25 or 50 mM acetate as a phosphatase. Since this regulation is also dependent on AckA (Figure S5), it is very unlikely that acetate itself serves as the signal for CiaH. Rather, acetate should be metabolized to produce a signal that is sensed by CiaH. Since CiaH is lacking a recognizable intracellular sensing domain, this unknown stimulus should be located outside the cell. And indeed, three of the CiaH mutants (CiaH305, 408, 232) showing a different response compared to the wild type have amino acid substitutions in the extracytoplasmic sensing domain.

What could be the signal CiaH is responding to? Considering that CiaRH is implicated in β -lactam resistance and maintenance of cell integrity (Guenzi et al., 1994; Mascher et al., 2006a) and that CiaR responds to AcP levels, a tempting candidate would be acetylated peptidoglycan (Vollmer, 2008). In *S. pneumoniae*, acetylation of peptidoglycan could be quite variable since mainly N-acetylglucosamine and to a lesser extent N-acetylmuramic acid can be deacetylated (Vollmer and Tomasz, 2000) and N-acetylmuramic acid is additionally O-acetylated (Crisostomo et al., 2006). Both processes are not essential for peptidoglycan synthesis and could be regulated and variable.

In a simple scenario, high levels of AcP, which can phosphorylate CiaR and raise its activity to high levels, would lead to more peptidoglycan acetylation, which could turn on CiaH phosphatase activity reducing CiaR activation virtually back to wild type levels. How higher peptidoglycan acetylation could be achieved by AcP is an open question. However, recent evidence clearly demonstrates that the role of AcP in acetylation at least of proteins is much more prominent than anticipated (Verdin and Ott, 2013; Weinert et al., 2013; Kuhn et al., 2014). It remains a possibility that AcP may also be a determinant in the acetylation of other compounds.

Acetylation can also be involved in the additional control of TCSs (Barak et al., 2006; Lima et al., 2011, 2012; Hu et al., 2013; Kuhn et al., 2014) and as mentioned above, AcP can serve as an acetyl donor in protein acetylation. Therefore, protein acetylation should also be altered in the *S. pneumoniae* AcP synthesis mutants described in this study. Could then acetylation explain the CiaR-related fluctuations in gene expression phenotypes rather than

phosphorylation? The response of CiaR is clearly dependent on phosphorylation and CiaH is in complete control, but the strength of the change in activity may be additionally modified by protein acetylation. The genetic arguments for a special role of AckA in the process of CiaR activation remain the same. In the absence of AckA, CiaR is disproportionally active. Assuming this overactivation is caused by phosphorylation and acetylation, the underlying mechanisms would be more complicated than our proposed model.

The *S. pneumoniae* strain used throughout this study is the laboratory strain R6 derived from *S. pneumoniae* D39, which was used to identify DNA as the genetic material (Avery et al., 1944). Considering the great variety between strains of bacterial species, it is always the question whether findings in one strain also apply to others. In microarray studies of AcP production mutants in D39 it was reported that expression of several members of the CiaR regulon is reduced in a triple *spxB-pta-ackA* harboring *ciaRH* (Ramos-Montanez et al., 2010). In our study, expression went down only in the absence of *ciaH*. Strain D39 and R6 show about 80 differences, among them *spxB* (Lanie et al., 2007). But even considering the higher activity of SpxB in R6 (Belanger et al., 2004; Ramos-Montanez et al., 2008), we cannot offer an explanation for the observed difference. Curiously, two D39 variants that were kept separately for some time differed in their CiaRH-mediated gene regulation (Lanie et al., 2007). Therefore, it appears that strain-specific variations in regulatory circuits may be encountered quite frequently.

CiaRH and at least one major player in the regulatory processes analyzed in this study, SpxB, can be regarded as virulence factors (Spellerberg et al., 1996; Ibrahim et al., 2004). The human pathogen *S. pneumoniae* faces varying concentrations of oxygen and different carbohydrates in its natural host, which will inevitably change AcP levels. Since CiaRH appears to have evolved to maintain high levels of regulon expression under a variety of conditions, it would be reasonable to safeguard high expression by AcP-mediated CiaR phosphorylation, in case no appropriate signal to stimulate CiaH kinase activity is available. Since all *S. pneumoniae* genomes sequenced so far harbor *ciaRH* and *spxB*, this scenario may indeed be important for survival of *S. pneumoniae* in its natural host.

ACKNOWLEDGMENTS

We thank Regine Hakenbeck for her continuous interest and support. We also thank A. J. Wolfe for helpful discussions during the preparation of the manuscript. We acknowledge the contributions of Ulrike Günzler, Jennifer Grün, Lisa König, and especially Alexander Halfmann to the project.

SUPPLEMENTARY MATERIAL

The Supplementary Material for this article can be found online at: <http://www.frontiersin.org/journal/10.3389/fmicb.2014.00772/abstract>

REFERENCES

- Alloing, G., Granadel, C., Morrison, D. A., and Claverys, J. P. (1996). Competence pheromone, oligopeptide permease, and induction of competence in *Streptococcus pneumoniae*. *Mol. Microbiol.* 21, 471–478. doi: 10.1111/j.1365-2958.1996.tb02556.x

- Avery, O. T., Macleod, C. M., and McCarty, M. (1944). Studies on the chemical nature of the substance inducing transformation of pneumococcal types: induction of transformation by a desoxyribonucleic acid fraction isolated from pneumococcus type III. *J. Exp. Med.* 79, 137–158. doi: 10.1084/jem.79.2.137
- Barak, R., Yan, J., Shainskaya, A., and Eisenbach, M. (2006). The chemotaxis response regulator CheY can catalyze its own acetylation. *J. Mol. Biol.* 359, 251–265. doi: 10.1016/j.jmb.2006.03.033
- Bättig, P., and Mühlemann, K. (2008). Influence of the *spxB* gene on competence in *Streptococcus pneumoniae*. *J. Bacteriol.* 190, 1184–1189. doi: 10.1128/JB.01517-07
- Belanger, A. E., Clague, M. J., Glass, J. I., and Leblanc, D. J. (2004). Pyruvate oxidase is a determinant of Avery's rough morphology. *J. Bacteriol.* 186, 8164–8171. doi: 10.1128/JB.186.24.8164-8171.2004
- Carvalho, S. M., Farshchi Andisi, V., Gradstedt, H., Neef, J., Kuipers, O. P., Neves, A. R., et al. (2013). Pyruvate oxidase influences the sugar utilization pattern and capsule production in *Streptococcus pneumoniae*. *PLoS ONE* 8:e68277. doi: 10.1371/journal.pone.0068277
- Cassone, M., Gagne, A. L., Spruce, L. A., Seeholzer, S. H., and Seibert, M. E. (2012). The HtrA Protease from *Streptococcus pneumoniae* digests both denatured proteins and the competence-stimulating peptide. *J. Biol. Chem.* 287, 38449–38459. doi: 10.1074/jbc.M112.391482
- Chan, S. H., Norregaard, L., Solem, C., and Jensen, P. R. (2014). Acetate kinase isozymes confer robustness in acetate metabolism. *PLoS ONE* 9:e92256. doi: 10.1371/journal.pone.0092256
- Commichau, F. M., and Stülke, J. (2008). Trigger enzymes: bifunctional proteins active in metabolism and in controlling gene expression. *Mol. Microbiol.* 67, 692–702. doi: 10.1111/j.1365-2958.2007.06071.x
- Crisostomo, M. I., Vollmer, W., Kharat, A. S., Inhulsen, S., Gehre, F., Buckenmaier, S., et al. (2006). Attenuation of penicillin resistance in a peptidoglycan O-acetyl transferase mutant of *Streptococcus pneumoniae*. *Mol. Microbiol.* 61, 1497–1509. doi: 10.1111/j.1365-2958.2006.05340.x
- Dagkessamanskaia, A., Moscoso, M., Henard, V., Guiral, S., Overweg, K., Reuter, M., et al. (2004). Interconnection of competence, stress and CiaR regulons in *Streptococcus pneumoniae*: competence triggers stationary phase autolysis of *ciaR* mutant cells. *Mol. Microbiol.* 51, 1071–1086. doi: 10.1111/j.1365-2958.2003.03892.x
- Dawid, S., Seibert, M. E., and Weiser, J. N. (2009). Bacteriocin activity of *Streptococcus pneumoniae* is controlled by the serine protease HtrA via posttranscriptional regulation. *J. Bacteriol.* 191, 1509–1518. doi: 10.1128/JB.01213-08
- Denapaite, D., Brückner, R., Hakenbeck, R., and Vollmer, W. (2012). Biosynthesis of teichoic acids in *Streptococcus pneumoniae* and closely related species: lessons from genomes. *Microb. Drug. Resist.* 18, 344–358. doi: 10.1089/mdr.2012.0026
- Gao, R., and Stock, A. M. (2009). Biological insights from structures of two-component proteins. *Annu. Rev. Microbiol.* 63, 133–154. doi: 10.1146/annurev.micro.091208.073214
- Guenzi, E., Gasc, A. M., Sicard, M. A., and Hakenbeck, R. (1994). A two-component signal-transducing system is involved in competence and penicillin susceptibility in laboratory mutants of *Streptococcus pneumoniae*. *Mol. Microbiol.* 12, 505–515. doi: 10.1111/j.1365-2958.1994.tb01038.x
- Gueriri, I., Bay, S., Dubrac, S., Cyncynatus, C., and Msadek, T. (2008). The Pta-AckA pathway controlling acetyl phosphate levels and the phosphorylation state of the DegU orphan response regulator both play a role in regulating *Listeria monocytogenes* motility and chemotaxis. *Mol. Microbiol.* 70, 1342–1357. doi: 10.1111/j.1365-2958.2008.06496.x
- Halfmann, A., Hakenbeck, R., and Brückner, R. (2007a). A new integrative reporter plasmid for *Streptococcus pneumoniae*. *FEMS Microbiol. Lett.* 268, 217–224. doi: 10.1111/j.1574-6968.2006.00584.x
- Halfmann, A., Kovács, M., Hakenbeck, R., and Brückner, R. (2007b). Identification of the genes directly controlled by the response regulator CiaR in *Streptococcus pneumoniae*: five out of 15 promoters drive expression of small non-coding RNAs. *Mol. Microbiol.* 66, 110–126. doi: 10.1111/j.1365-2958.2007.05900.x
- Halfmann, A., Schnorpfel, A., Müller, M., Marx, P., Günzler, U., Hakenbeck, R., et al. (2011). Activity of the two-component regulatory system CiaRH in *Streptococcus pneumoniae* R6. *J. Mol. Microbiol. Biotechnol.* 20, 96–104. doi: 10.1159/000324893
- Hanahan, D. (1983). Studies on transformation of *Escherichia coli* with plasmids. *J. Mol. Biol.* 166, 557–580. doi: 10.1016/S0022-2836(83)80284-8
- Hoskins, J., Alborn, W. E. Jr., Arnold, J., Blaszcak, L. C., Burgett, S., Dehoff, B. S., et al. (2001). Genome of the Bacterium *Streptococcus pneumoniae* Strain R6. *J. Bacteriol.* 183, 5709–5717. doi: 10.1128/JB.183.19.5709-5717.2001
- Hu, L. I., Chi, B. K., Kuhn, M. L., Filippova, E. V., Walker-Peddakotla, A. J., Basell, K., et al. (2013). Acetylation of the response regulator RcsB controls transcription from a small RNA promoter. *J. Bacteriol.* 195, 4174–4186. doi: 10.1128/JB.00383-13
- Ibrahim, Y. M., Kerr, A. R., McCluskey, J., and Mitchell, T. J. (2004). Control of virulence by the two-component system CiaR/H is mediated via HtrA, a major virulence factor of *Streptococcus pneumoniae*. *J. Bacteriol.* 186, 5258–5266. doi: 10.1128/JB.186.16.5258-5266.2004
- Kochan, T. J., and Dawid, S. (2013). The HtrA protease of *Streptococcus pneumoniae* controls density-dependent stimulation of the bacteriocin *blp* locus via disruption of pheromone secretion. *J. Bacteriol.* 195, 1561–1572. doi: 10.1128/JB.01964-12
- Krell, T., Lacal, J., Busch, A., Silva-Jimenez, H., Guazzaroni, M. E., and Ramos, J. L. (2010). Bacterial sensor kinases: diversity in the recognition of environmental signals. *Annu. Rev. Microbiol.* 64, 539–559. doi: 10.1146/annurev.micro.112408.134054
- Kuhn, M. L., Zemaitaitis, B., Hu, L. I., Sahu, A., Sorensen, D., Minasov, G., et al. (2014). Structural, kinetic and proteomic characterization of acetyl phosphate-dependent bacterial protein acetylation. *PLoS ONE* 9:e94816. doi: 10.1371/journal.pone.0094816
- Kumar, R., Shah, P., Swiatlo, E., Burgess, S. C., Lawrence, M. L., and Nanduri, B. (2010). Identification of novel non-coding small RNAs from *Streptococcus pneumoniae* TIGR4 using high-resolution genome tiling arrays. *BMC Genomics* 11:350. doi: 10.1186/1471-2164-11-350
- Lacks, S., and Hotchkiss, R. D. (1960). A study of the genetic material determining an enzyme in *Pneumococcus*. *Biochim. Biophys. Acta* 39, 508–518. doi: 10.1016/0006-3002(60)90205-5
- Lanie, J. A., Ng, W. L., Kazmierczak, K. M., Andrzejewski, T. M., Davidsen, T. M., Wayne, K. J., et al. (2007). Genome sequence of Avery's virulent serotype 2 strain D39 of *Streptococcus pneumoniae* and comparison with that of unencapsulated laboratory strain R6. *J. Bacteriol.* 189, 38–51. doi: 10.1128/JB.01148-06
- Laub, M. T., and Goulian, M. (2007). Specificity in two-component signal transduction pathways. *Annu. Rev. Genet.* 41, 121–145. doi: 10.1146/annurev.genet.41.042007.170548
- Lima, B. P., Antelmann, H., Gronau, K., Chi, B. K., Becher, D., Brinsmade, S. R., et al. (2011). Involvement of protein acetylation in glucose-induced transcription of a stress-responsive promoter. *Mol. Microbiol.* 81, 1190–1204. doi: 10.1111/j.1365-2958.2011.07742.x
- Lima, B. P., Thanh Huyen, T. T., Basell, K., Becher, D., Antelmann, H., and Wolfe, A. J. (2012). Inhibition of acetyl phosphate-dependent transcription by an acetylable lysine on RNA polymerase. *J. Biol. Chem.* 287, 32147–32160. doi: 10.1074/jbc.M112.365502
- Lukat, G. S., Mcclary, W. R., Stock, A. M., and Stock, J. B. (1992). Phosphorylation of bacterial response regulator proteins by low molecular weight phosphodonor. *Proc. Natl. Acad. Sci. U. S. A.* 89, 718–722. doi: 10.1073/pnas.89.2.718
- Mann, B., Van Opijnen, T., Wang, J., Obert, C., Wang, Y. D., Carter, R., et al. (2012). Control of virulence by small RNAs in *Streptococcus pneumoniae*. *PLoS Pathog.* 8:e1002788. doi: 10.1371/journal.ppat.1002788
- Marra, A., Asundi, J., Bartilson, M., Lawson, S., Fang, F., Christine, J., et al. (2002). Differential fluorescence induction analysis of *Streptococcus pneumoniae* identifies genes involved in pathogenesis. *Infect. Immun.* 70, 1422–1433. doi: 10.1128/IAI.70.3.1422-1433.2002
- Martinez-Hackert, E., and Stock, A. M. (1997). Structural relationships in the OmpR family of winged-helix transcription factors. *J. Mol. Biol.* 269, 301–312. doi: 10.1006/jmbi.1997.1065
- Mascher, T., Heintz, M., Zähler, D., Merai, M., and Hakenbeck, R. (2006a). The CiaRH system of *Streptococcus pneumoniae* prevents lysis during stress induced by treatment with cell wall inhibitors and mutations in *pbp2x* involved in β -lactam resistance. *J. Bacteriol.* 188, 1959–1978. doi: 10.1128/JB.188.5.1959-1968.2006
- Mascher, T., Helmann, J. D., and Unden, G. (2006b). Stimulus perception in bacterial signal-transducing histidine kinases. *Microbiol. Mol. Biol. Rev.* 70, 910–938. doi: 10.1128/MMBR.00020-06
- Müller, M., Marx, P., Hakenbeck, R., and Brückner, R. (2011). Effect of new alleles of the histidine kinase gene *ciaH* on the activity of the response

- regulator CiaR in *Streptococcus pneumoniae* R6. *Microbiology* 157, 3104–3112. doi: 10.1099/mic.0.053157-0
- Ottolenghi, E., and Hotchkiss, R. D. (1962). Release of genetic transforming agent from pneumococcal cultures during growth and disintegration. *J. Exp. Med.* 116, 491–519. doi: 10.1084/jem.116.4.491
- Pericone, C. D., Park, S., Imlay, J. A., and Weiser, J. N. (2003). Factors contributing to hydrogen peroxide resistance in *Streptococcus pneumoniae* include pyruvate oxidase (SpxB) and avoidance of the toxic effects of the fenton reaction. *J. Bacteriol.* 185, 6815–6825. doi: 10.1128/JB.185.23.6815-6825.2003
- Prüss, B. M., and Wolfe, A. J. (1994). Regulation of acetyl phosphate synthesis and degradation, and the control of flagellar expression in *Escherichia coli*. *Mol. Microbiol.* 12, 973–984. doi: 10.1111/j.1365-2958.1994.tb01085.x
- Puri, P., Goel, A., Bochynska, A., and Poolman, B. (2014). Regulation of acetate kinase isozymes and its importance for mixed-acid fermentation in *Lactococcus lactis*. *J. Bacteriol.* 196, 1386–1393. doi: 10.1128/JB.01277-13
- Ramos-Montanez, S., Kazmierczak, K. M., Hentchel, K. L., and Winkler, M. E. (2010). Instability of *ackA* (Acetate Kinase) mutations and their effects on acetyl phosphate (AcP) and ATP Amounts in *Streptococcus pneumoniae* D39. *J. Bacteriol.* 192, 6390–6400. doi: 10.1128/JB.00995-10
- Ramos-Montanez, S., Tsui, H. C., Wayne, K. J., Morris, J. L., Peters, L. E., Zhang, E., et al. (2008). Polymorphism and regulation of the *spxB* (pyruvate oxidase) virulence factor gene by a CBS-HotDog domain protein (SpxR) in serotype 2 *Streptococcus pneumoniae*. *Mol. Microbiol.* 67, 729–746. doi: 10.1111/j.1365-2958.2007.06082.x
- Schnorpfeil, A., Kranz, M., Kovacs, M., Kirsch, C., Gartmann, J., Brunner, I., et al. (2013). Target evaluation of the non-coding csRNAs reveals a link of the two-component regulatory system CiaRH to competence control in *Streptococcus pneumoniae* R6. *Mol. Microbiol.* 89, 334–349. doi: 10.1111/mmi.12277
- Sebert, M. E., Palmer, L. M., Rosenberg, M., and Weiser, J. N. (2002). Microarray-based identification of *htrA*, a *Streptococcus pneumoniae* gene that is regulated by the CiaRH two-component system and contributes to nasopharyngeal colonization. *Infect. Immun.* 70, 4059–4067. doi: 10.1128/IAI.70.8.4059-4067.2002
- Sebert, M. E., Patel, K. P., Plotnick, M., and Weiser, J. N. (2005). Pneumococcal HtrA protease mediates inhibition of competence by the CiaRH two-component signaling system. *J. Bacteriol.* 187, 3969–3979. doi: 10.1128/JB.187.12.3969-3979.2005
- Spellerberg, B., Cundell, D. R., Sandros, J., Pearce, B. J., Idanpaan-Heikkilä, I., Rosenow, C., et al. (1996). Pyruvate oxidase, as a determinant of virulence in *Streptococcus pneumoniae*. *Mol. Microbiol.* 19, 803–813. doi: 10.1046/j.1365-2958.1996.425954.x
- Sung, C. K., Li, H., Claverys, J. P., and Morrison, D. A. (2001). An *rpsL* cassette, janus, for gene replacement through negative selection in *Streptococcus pneumoniae*. *Appl. Environ. Microbiol.* 67, 5190–5196. doi: 10.1128/AEM.67.11.5190-5196.2001
- Throup, J. P., Koretke, K. K., Bryant, A. P., Ingraham, K. A., Chalker, A. F., Ge, Y., et al. (2000). A genomic analysis of two-component signal transduction in *Streptococcus pneumoniae*. *Mol. Microbiol.* 35, 566–576. doi: 10.1046/j.1365-2958.2000.01725.x
- Tsui, H. C., Mukherjee, D., Ray, V. A., Sham, L. T., Feig, A. L., and Winkler, M. E. (2010). Identification and characterization of noncoding small RNAs in *Streptococcus pneumoniae* serotype 2 strain D39. *J. Bacteriol.* 192, 264–279. doi: 10.1128/JB.01204-09
- Verdin, E., and Ott, M. (2013). Acetylphosphate: a novel link between lysine acetylation and intermediary metabolism in bacteria. *Mol. Cell.* 51, 132–134. doi: 10.1016/j.molcel.2013.07.006
- Vollmer, W. (2008). Structural variation in the glycan strands of bacterial peptidoglycan. *FEMS Microbiol. Rev.* 32, 287–306. doi: 10.1111/j.1574-6976.2007.00088.x
- Vollmer, W., and Tomasz, A. (2000). The *pgdA* gene encodes for a peptidoglycan N-acetylglucosamine deacetylase in *Streptococcus pneumoniae*. *J. Biol. Chem.* 275, 20496–20501. doi: 10.1074/jbc.M910189199
- Wang, G., Xia, Y., Cui, J., Gu, Z., Song, Y., Chen, Y. Q., et al. (2013). The roles of moonlighting proteins in bacteria. *Curr. Issues Mol. Biol.* 16, 15–22.
- Wanner, B. L. (1992). Is cross regulation by phosphorylation of two-component response regulator proteins important in bacteria? *J. Bacteriol.* 174, 2053–2058.
- Weinert, B. T., Iesmantavicius, V., Wagner, S. A., Scholz, C., Gummeson, B., Beli, P., et al. (2013). Acetyl-phosphate is a critical determinant of lysine acetylation in *E. coli*. *Mol. Cell* 51, 265–272. doi: 10.1016/j.molcel.2013.06.003
- Wolfe, A. J. (2005). The acetate switch. *Microbiol. Mol. Biol. Rev.* 69, 12–50. doi: 10.1128/MMBR.69.1.12-50.2005
- Wolfe, A. J. (2010). Physiologically relevant small phosphodonors link metabolism to signal transduction. *Curr. Opin. Microbiol.* 13, 204–209. doi: 10.1016/j.mib.2010.01.002
- Xu, H., Caimano, M. J., Lin, T., He, M., Radolf, J. D., Norris, S. J., et al. (2010). Role of acetyl-phosphate in activation of the Rrp2-RpoN-RpoS pathway in *Borrelia burgdorferi*. *PLoS Pathog* 6:e1001104. doi: 10.1371/annotation/88293342-3534-4b8b-8800-c63a8c86bf6d
- Yesilkaya, H., Spissu, F., Carvalho, S. M., Terra, V. S., Homer, K. A., Benisty, R., et al. (2009). Pyruvate formate lyase is required for pneumococcal fermentative metabolism and virulence. *Infect. Immun.* 77, 5418–5427. doi: 10.1128/IAI.00178-09
- Zähner, D., Kaminski, K., Van Der Linden, M., Mascher, T., Merai, M., and Hakenbeck, R. (2002). The *ciaR/ciaH* regulatory network of *Streptococcus pneumoniae*. *J. Mol. Microbiol. Biotechnol.* 4, 211–216.

Conflict of Interest Statement: The authors declare that the research was conducted in the absence of any commercial or financial relationships that could be construed as a potential conflict of interest.

Received: 08 November 2014; accepted: 17 December 2014; published online: 15 January 2015.

Citation: Marx P, Meiers M and Brückner R (2015) Activity of the response regulator CiaR in mutants of *Streptococcus pneumoniae* R6 altered in acetyl phosphate production. *Front. Microbiol.* 5:772. doi: 10.3389/fmicb.2014.00772

This article was submitted to Microbial Physiology and Metabolism, a section of the journal *Frontiers in Microbiology*.

Copyright © 2015 Marx, Meiers and Brückner. This is an open-access article distributed under the terms of the Creative Commons Attribution License (CC BY). The use, distribution or reproduction in other forums is permitted, provided the original author(s) or licensor are credited and that the original publication in this journal is cited, in accordance with accepted academic practice. No use, distribution or reproduction is permitted which does not comply with these terms.



Post-translational hydroxylation by 2OG/Fe(II)-dependent oxygenases as a novel regulatory mechanism in bacteria

Laura M. van Staaldouin and Zongchao Jia*

Department of Biomedical and Molecular Sciences, Queen's University, Kingston, ON, Canada

Edited by:

Ivan Mijakovic, Chalmers University of Technology, Sweden

Reviewed by:

Haike Antelmann,
Ernst-Moritz-Arndt-Universität
Greifswald, Germany
Michael Suits, Wilfrid Laurier
University, Canada

*Correspondence:

Zongchao Jia, Department of
Biomedical and Molecular Sciences,
Queen's University, Botterell Hall,
18 Stuart Street, Kingston,
ON K7L 3N6, Canada
e-mail: jia@queensu.ca

Protein hydroxylation has been well-studied in eukaryotic systems. The structural importance of hydroxylation of specific proline and lysine residues during collagen biosynthesis is well established. Recently, key roles for post-translational hydroxylation in signaling and degradation pathways have been discovered. The function of hydroxylation in signaling is highlighted by its role in the hypoxic response of eukaryotic cells, where oxygen dependent hydroxylation of the hypoxia inducible transcription factor both targets it for degradation and blocks its activation. In contrast, the role of protein hydroxylation has been largely understudied in prokaryotes. Recently, an evolutionarily conserved class of ribosomal oxygenases (ROX) that catalyze the hydroxylation of specific residues in the ribosome has been identified in bacteria. ROX activity has been linked to cell growth, and has been found to have a direct impact on bulk protein translation. This discovery of ribosomal protein hydroxylation in bacteria could lead to new therapeutic targets for regulating bacterial growth, as well as, shed light on new prokaryotic hydroxylation signaling pathways. In this review, recent structural and functional studies will be highlighted and discussed, underscoring the regulatory potential of post-translational hydroxylation in bacteria.

Keywords: 2-oxoglutarate/Fe(II)-dependent oxygenase, post-translational hydroxylation, ribosomal oxygenase (ROX), prokaryote, YcfD

INTRODUCTION

Of the commonly observed post-translational modifications, post-translational hydroxylation represents the smallest change. However, despite its diminutive nature, this modification may have significant effects on protein production and we are just beginning to discover its potential as a regulatory mechanism. Since the discovery of enzyme-catalyzed hydroxylation of prolyl residues during collagen biosynthesis, the importance of post-translational hydroxylation of proteins has been well established (Stetten, 1949; Hutton et al., 1966). More recently roles for protein hydroxylation in cell signaling and degradation pathways have been identified, expanding the significance of this post-translational modification. While important roles for protein hydroxylation have been observed, in comparison with other post-translational modifications such as phosphorylation, their full extent has yet to be determined (Loenarz and Schofield, 2011). Although not likely to be as widespread as others, new functions of protein hydroxylation are being discovered that indicate it may have a larger role than previously thought.

The post-translational hydroxylation of collagen, one of the most abundant structural proteins in animals, has been extensively studied. The discovery that the hydroxylation of prolyl and lysyl residues in collagen as a result of an oxygenase catalyzed modification provided the first evidence of the importance of enzyme catalyzed post-translational hydroxylation (Stetten, 1949; Hutton et al., 1966; Jenkins and Raines, 2002). Three different post-translational hydroxylations are present in collagen: 4R-hydroxy-L-proline, 3S-hydroxy-L-proline and 5R-hydroxy-L-lysine, with the 4R-hydroxy-L-proline being the most commonly

observed (Myllyharju and Kivirikko, 2001). These hydroxylations are vital for the structure of collagen, which is comprised uniquely of three left-handed helices wound together around a central-axis to form a triple stranded right-handed tertiary structure, with multiple collagen molecules cross-linked to form connective tissues. The stability and strength of this structure is dependent upon a Gly-Xaa-Yaa repeating motif, where Xaa is typically L-proline and Yaa is typically 4R-hydroxy-L-proline (Engel and Bächinger, 2005). The hydroxylation of proline residues in collagen is catalyzed by procollagen prolyl 3- and 4-hydroxylases (P3H and P4H) to form the 3S-hydroxy-L-proline and 4R-hydroxy-L-proline, respectively (Figure 1A; Myllyharju, 2003; Vranka et al., 2004). The hydroxylated 4R-hydroxy-L-proline in the Yaa position is critical for stabilizing the structure, partly through essential hydrogen bonds and partly by the stereoelectric gauche effect (Prockop and Kivirikko, 1995; Myllyharju and Kivirikko, 2004). In contrast to the stabilizing effect of the 4R-hydroxy-L-proline, the rare 3S-hydroxy-L-proline has a less defined role, with initial evidence indicating a slight destabilizing effect (Jenkins et al., 2003). Evidence has now been found that this modification mediates inter-helical interactions and helps the assembly of the collagen triple helix (Weis et al., 2010). Mature collagen molecules are assembled by tissue specific cross-linking of domains flanking the triple stranded helical domain. This cross-linking is mediated by the presence of hydroxylysine, the formation of which is catalyzed by procollagen lysyl 5-hydroxylase (PLOD; Figure 1B; Yamauchi and Sricholpech, 2012). Defects in all three types of collagen hydroxylation have been linked to number of diseases, highlighting the importance of this post-translational modification.

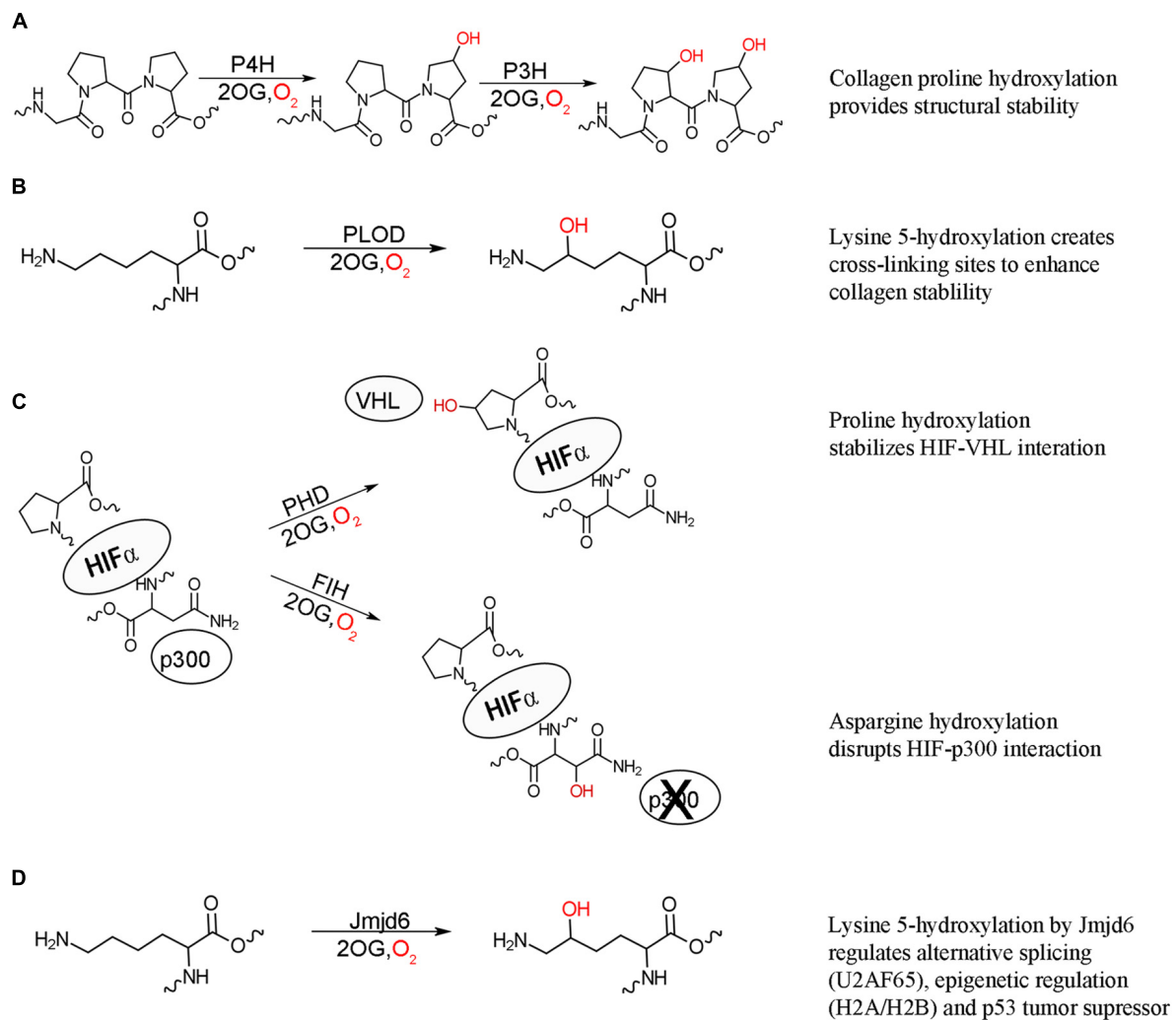


FIGURE 1 | 2-oxoglutarate oxygenase catalyzed hydroxylation and their biochemical effects. (A) Hydroxylation of proline residues of collagen by procollagen prolyl 4-hydroxylase (P4H) and prolyl 3-hydroxylase (P3H) increase the structural stability of collagen. **(B)** Hydroxylation of collagen lysine residues by procollagen lysine 5-hydroxylase (PLOD) provides further stability through creating cross-linking sites. **(C)** Hydroxylation of HIF proline residues by prolyl hydroxylase domain (PHD) enzymes stabilizes the

interaction between HIF and von Hippel Lindau (VHL) protein targeting HIF for degradation, while asparaginyl hydroxylation of HIF by factor inhibiting HIF (FIH) acts to inhibit transcriptional activity by disrupting the interaction of HIF with p300. Both hydroxylation events result in suppression of the hypoxic response. **(D)** Lysyl hydroxylation of a variety of proteins by hydroxylase Jmjd6 has effects on alternative splicing (U2AF65), epigenetic regulation (histones H2A/H2B and H3/H4), and p53 tumor suppressor activity.

Post-translational hydroxylation is now known to be involved, not only in protein structural stability, but also in cellular signaling. The transcription factor hypoxia inducible factor (HIF) is critical for the initiation of the hypoxic response, which occurs when multicellular organisms are subjected to low oxygen levels (Palmer and Clegg, 2014). HIF is a constitutively expressed, heterodimeric protein, comprised of HIF1 α and HIF1 β subunits (Wang et al., 1995). The HIF1 β subunit resides in the nucleus while, under hypoxic conditions, the HIF1 α subunit is translocated into the nucleus and the active heterodimer recruits the transcriptional coactivator p300, initiating transcription of genes required for hypoxic response (reviewed in Hewitson and Schofield, 2004). Under normal oxygen levels, the HIF1 α subunit is not detectable in the cell implicating oxygen regulated

suppression of HIF α lifetime and activity in the cell (Huang et al., 1996). It is now known that post-translational hydroxylation occurs at three separate sites on HIF1 α under normoxic conditions. The oxygen dependent post-translational hydroxylation of two critical proline residues by a family of three closely related prolyl hydroxylases (PHD1-3) results in the recruitment of HIF1 α to the E3 ubiquitin ligase complex and subsequent degradation of HIF1 α (Figure 1C; Ivan et al., 2001; Jaakkola et al., 2001; Masson et al., 2001; Yu et al., 2001). Another level of HIF inhibition under normal oxygen levels is the post-translational hydroxylation of an asparaginyl residue by the hydroxylase: factor inhibiting HIF (FIH). This hydroxylation blocks the interaction of HIF1 α with p300, thus inhibiting transcriptional activity (Figure 1C; Lando et al., 2002). This hydroxylase-mediated control

of the hypoxic response is the first comprehensively described instance of post-translational hydroxylation as a regulatory mechanism.

Following the discovery that HIF activity is regulated by hydroxylation, the possibility of similar systems being regulated by hydroxylation was investigated and revealed post-translational hydroxylation of lysine residues in the splicing factor U2 small nuclear ribonucleoprotein auxiliary factor 65-kDa subunit (U2AF65) catalyzed by the FIH related hydroxylase Jumonji domain 6 protein (Jmjd6; Webby et al., 2009). Jmjd6 was originally identified as a histone arginine demethylase (Chang et al., 2007); however, large scale analysis of Jmjd6 interacting proteins revealed that its predominate function is lysyl hydroxylation (Figure 1D; Webby et al., 2009). Hydroxylation of U2AF65 was found to change alternative RNA splicing for some genes indicating a role in the regulation of gene splicing, with knockdown of Jmjd6 resulting in similar splicing patterns to those observed under hypoxic conditions (Webby et al., 2009). Jmjd6 is now known to regulate alternative gene splicing through interaction with a number of splicing factors, as well as the pre-RNA itself, though the exact conditions and physiological role for hydroxylation have yet to be identified (Heim et al., 2014). Jmjd6 was subsequently found to also hydroxylate lysine residues on the histones H2A/H2B and H3/H4 (Unoki et al., 2013). The hydroxylated lysines were found to inhibit both *N*-acetylation and *N*-methylation of histone peptides *in vitro*. Conversely, both *N*-acetylation and *N*-methylation of lysine residues blocked Jmjd6 catalyzed hydroxylation. Combined these results suggest a role of post-translational histone hydroxylation in the epigenetic regulation of gene expression and chromosomal rearrangement. Most recently, Jmjd6 was found to catalyze the lysyl hydroxylation of the tumor suppressor p53, decreasing p53 activity, and promoting colon carcinogenesis (Wang et al., 2014). Jmjd6 hydroxylation of p53 reveals a connection between oxygen levels, cell cycle control, and apoptosis.

PROTEIN HYDROXYLASES

Post-translational hydroxylation involves the oxidative conversion of a C–H bond to a C–OH group on an amino acid side chain. Protein hydroxylases, the enzymes responsible for catalyzing this conversion, are found to belong to the 2-oxoglutarate (2OG)/Fe²⁺-dependent oxygenase (2OG oxygenase) superfamily of proteins (Loenarz and Schofield, 2011). The majority of these enzymes use a Fe²⁺ cofactor and 2OG and dioxygen as co-substrates. 2OG oxygenases are widely distributed evolutionarily conserved enzymes involved in many biologically important processes such as DNA repair, protein modification, lipid metabolism, and secondary metabolite production in plants and microbes. The enzymes catalyze a diverse array of oxidative reactions, including desaturation, ring formation or expansion, epimerization, and carbon–carbon bond cleavage. However, the most common reaction they catalyze is hydroxylation (Hausinger, 2004). 2OG oxygenases are known to catalyze the hydroxylation of a variety of substrates ranging from small molecules to macromolecular molecules, including both proteins and DNA.

Proteins belonging to the 2OG oxygenase family are identified by a conserved HXD/EX_nH sequence motif, where the histidine and aspartate/glutamate residues are involved in coordinating the metal cofactor (Clifton et al., 2006). The three-dimensional structures of many 2OG oxygenases, including a number of post-translational hydroxylases have been determined. All 2OG oxygenases are found to have a conserved core structure of eight β-strands, which form two anti-parallel β-sheets that come together in a right-handed double-stranded β-helix (DSBH) or jelly roll (Figure 2; Roach et al., 1995; Clifton et al., 2006). The conserved sequence motif is found within the DSBH, and marks the location of the enzyme active site where Fe²⁺ is brought together with the substrates. The DSBH forms a very robust active site allowing for the accommodation of the different substrates of the 2OG oxygenases, and for the catalysis of complex oxidative reactions. Structural data, combined with kinetic and spectroscopic analysis suggest that the 2OG oxygenases share a common enzymatic mechanism wherein the Fe²⁺-bound enzyme interacts with 2OG, triggering reaction with dioxygen, which leads to the formation of a ferryl intermediate that acts as a reactive oxidizing species formed upon oxidative decarboxylation of 2OG (Holme, 1975; Chowdhury et al., 2014). The ferryl intermediate is then poised to react with the substrate. This is where the mechanisms diverge depending on the type of reaction being catalyzed, accounting for the breadth, and versatility of this class of enzyme.

RIBOSOMAL OXYGENASES

With the discovery of the importance of hydroxylation of HIF and splicing relating proteins by 2OG oxygenases in eukaryotes, the question of whether oxygenase catalyzed post-translational hydroxylation has a role in prokaryotic cells was raised. The *Escherichia coli* gene of unknown function, *ycfD*, was identified as a potential 2OG oxygenase, which was confirmed by the observation of YcfD bound to the 2OG as a co-substrate (van Staaldouin et al., 2014) and catalyzed 2OG turnover in the absence of substrate (Ge et al., 2012). A peptide screen combined with co-immunoprecipitation analyses revealed that YcfD hydroxylated the β carbon of arginine 81 of ribosomal protein L-16 (Rpl16; Ge et al., 2012). Interaction with Rpl16 was independently confirmed and shown to be highly specific by glutathione S-transferase pull-down experiments (van Staaldouin et al., 2014). Consistent with the close link between translation and growth, alteration of YcfD expression has been shown to have dramatic effects on cell growth. Comparison of wild-type cell growth to that of a strain lacking the *ycfD* gene (*ΔycfD*) showed that, under normal conditions, there was no difference between the two cell lines. However, under nutrient-limiting conditions, the growth of *ΔycfD* cells was significantly reduced, which correlated with a reduction in bulk protein translation by three- and fourfold (Ge et al., 2012). Overexpression of YcfD was also shown to significantly inhibit *E. coli* colony formation under standard growth conditions, indicating a clear role for YcfD in *E. coli* cell growth regulation (van Staaldouin et al., 2014). Two human homologs to YcfD, Mina53 and NO66, were also identified to hydroxylate ribosomal proteins, and have similar effects on cell proliferation (Tsuneoka et al., 2002; Teye et al.,

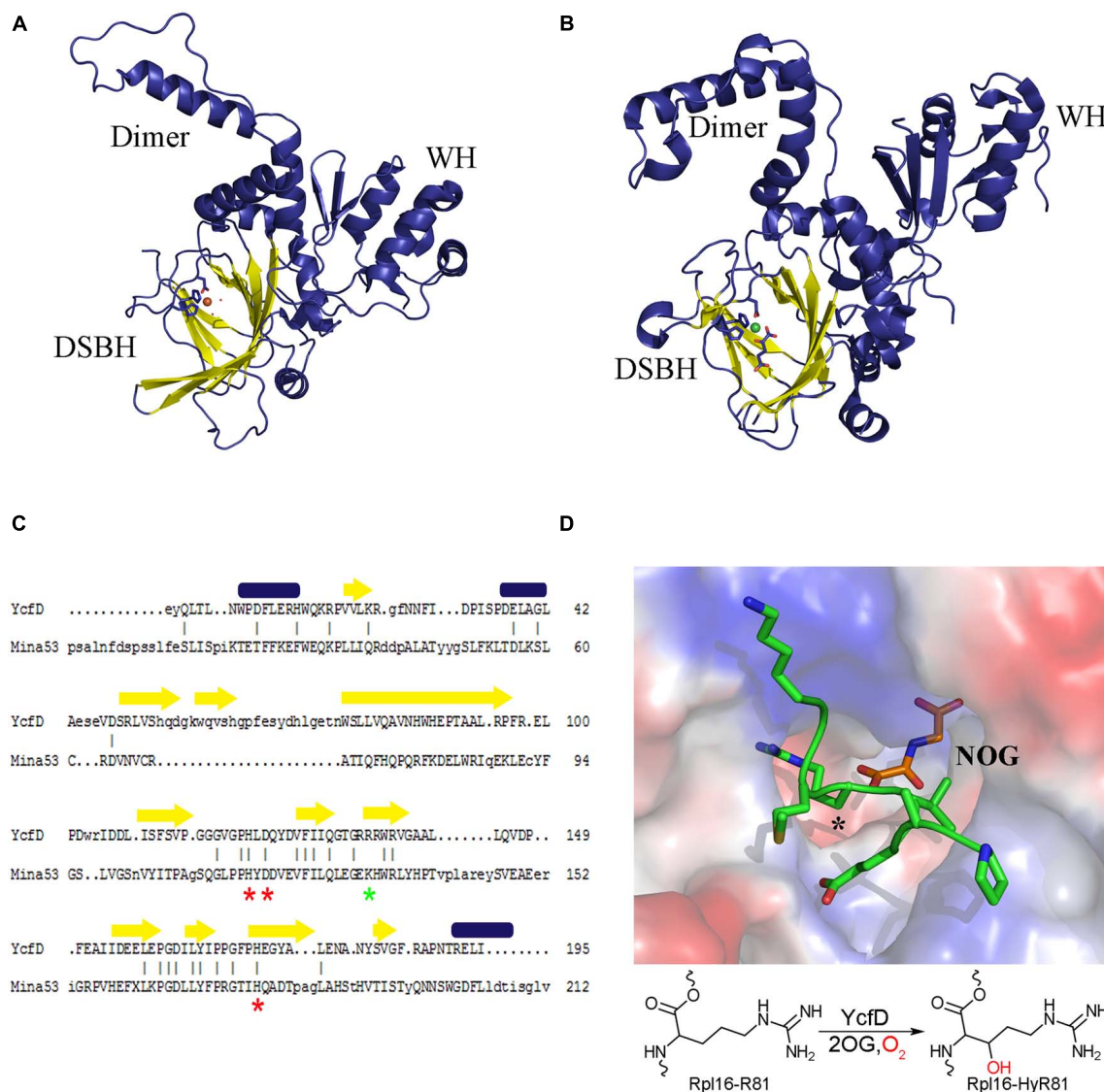


FIGURE 2 | Structure conservation of ROX enzymes. A structural comparison of (A) the bacterial ROX YcfD (PDB ID 4NUB) to (B) the eukaryotic ROX Mina53 (PDB ID 4BU2). The structures align with an overall RMSD of 2.6 Å. The characteristic DSBH is shown in yellow, and the dimerization domain (dimer) and the winged-helix domain (WH) are labeled. (C) Structure based sequence alignment of the DSBH from YcfD and Mina53. Conserved metal binding residues are marked with a red asterisk

and the 2OG binding residues are marked with a green asterisk. Alignment was done using Dalilite (Holm and Park, 2000). (D) Binding of YcfD to Rpl16 peptide. The surface of the *Rhodothermus marinus* YcfD (PDB ID 4CUG) active site is shown with an Rpl16 peptide (green) and the 2OG analog N-oxalylglycine bound (NOG; orange). The site of hydroxylation is marked with an asterisk (*). Below, a schematic hydroxylation of Rpl16-R81 by YcfD is shown.

2004; Zhang et al., 2005; Suzuki et al., 2007; Ge et al., 2012). Together, YcfD, Mina53, and NO66 are the founding members of a novel class of evolutionarily conserved ribosomal oxygenases (ROXs).

Structural studies of YcfD and other ROX enzymes showed that they are comprised of three domains: an N-terminal DSBH, followed by a dimerization domain and a C-terminal winged-helix domain (WH; Figures 2A,B; Chowdhury et al., 2014; van Staaldouin et al., 2014). The N-terminal DSBH displays the characteristic topology of a stereotypical 2OG oxygenase. Despite overall low sequence homology (15% homology to Mina53 and

NO66) YcfD is structurally very similar to the eukaryotic ROX enzymes (YcfD-Mina53 RMSD 2.6 Å). The DSBH is particularly well conserved with residues involved in metal and 2OG binding conserved (Figure 2C), while the dimerization and WHs show much lower conservation. The ROX active site is found in a pocket within the DSBH, and the substrate of YcfD, Rpl16 was shown to dock to the active site in a complementary manner (van Staaldouin et al., 2014). Co-crystallization of peptide substrates with the ROX enzymes provides more detailed insight into the interaction (Chowdhury et al., 2014). There are very minor changes observed when the Rpl16 peptide is bound by

YcfD; the overall structure remains largely unchanged with only a few residues in the active site shifting to accommodate the substrate. The arginine side chain to be hydroxylated sits deep in the active site with the β -carbon aligned with 2OG, in an ideal geometry for hydroxylation (**Figure 2D**). The surface of the area surrounding the active site of the YcfD is intimately involved with binding of the substrate with a number of clefts to allow docking of side chains to the surface of the enzyme. The dimerization domain is comprised of three α -helices which form intimate contacts with the dimerization domain of another molecule and have been shown to be important for catalytic activity (Chowdhury et al., 2014). The C-terminal WH distinguishes the ROX proteins from other 2OG oxygenases. Typically, WHs mediate protein–protein or protein–nucleic acid interactions (Teichmann et al., 2012); in this case, it is unlikely that the ROX proteins bind nucleic acids directly due to the overall negative charge of this domain (Chowdhury et al., 2014). Instead, it is likely that this essential domain plays a role in substrate binding, either binding substrate directly or interacting with another part of the ribosomal complex.

REGULATORY POTENTIAL OF ROX IN PROKARYOTES

The substrate of YcfD, Rpl16, is an essential late-assembly component of the 50S ribosomal subunit and is responsible for the architectural organization of the aminoacyl-tRNA binding site (Nierhaus, 1991). A loss of Rpl16 has been associated with defects in stages of both ribosomal assembly and function, including maturation of the 50S subunit (Jomaa et al., 2014), binding of the 30S subunit (Kazemie, 1975), association with aminoacyl-tRNA (Kazemie, 1976), peptidyl-tRNA hydrolysis activity (Tate et al., 1983), peptidyl transferase activity (Moore et al., 1975; Hampl et al., 1981), as well as antibiotic interactions (Nierhaus and Nierhaus, 1973; de Bethune and Nierhaus, 1978; Teraoka and Nierhaus, 1978). The structure of Rpl16 has been determined by NMR (PDB ID: 1WKI), revealing that the hydroxylation site is on an extended, flexible loop that becomes locked upon binding to the 23S rRNA, as observed in crystal structures of the bacterial ribosome (Harms et al., 2001; Nishimura et al., 2004; Dunkle et al., 2010). The site of YcfD hydroxylation, R81, is inserted between two 23S rRNA helices in the intact ribosome, indicating a role for the hydroxyl group in stabilizing the architecture of the aminoacyl-tRNA binding site through hydrogen bonding and, ultimately, in the spatial optimization of the Rpl16-rRNA complex. There is evidence that YcfD binds very specifically to Rpl16, and is capable of pulling down Rpl16 in the absence of other ribosomal proteins. In addition, Rpl16 plays a role as a late ribosomal assembly protein, which indicates a potential function for YcfD in sequestering Rpl16 prior to its addition to the maturing ribosome, thus ensuring proper assembly of the ribosome. The overall importance of Rpl16 in the competency of the bacterial ribosome, combined with the fact that it is the target of a number of antibiotics, indicate that hydroxylation of Rpl16 by YcfD may play a role in the regulation of protein translation and, consequently, in bacterial cell growth.

2-oxoglutarate oxygenases have been found to provide a link between metabolism and transcriptional regulation via evidence

that oxygenases involved in transcriptional regulation are inhibited by increased amounts of tricarboxylic acid cycle intermediates or 2-hydroxyglutarate in tumor cells (Ge et al., 2012; Mullen and DeBerardinis, 2012). A similar relationship between metabolism and translation through regulation of ROX activity may exist and investigation into the effects of metabolic molecules on ROX activity could lead to an understanding of this relationship. This connection between metabolism and translational regulation seems very intuitive, particularly for bacteria, as cell growth would need to decrease in response to limited nutrition and, conversely, under nutrient rich conditions the cells do not need to limit their growth. The activity of the ROX enzymes, like that of other 2OG oxygenases, was also found to be limited under hypoxic conditions (Ge et al., 2012). This loss of YcfD activity under anaerobic conditions suggests a regulatory role for the hydroxylase under hypoxic stress, resulting in reduced translation and subsequent loss of cell growth. As the connection between ROX enzyme activity and cell growth is better understood, there is opportunity for the development of new antibiotics which target YcfD, the YcfD-Rpl16 complex, or hydroxylated Rpl16.

CONCLUDING REMARKS

Post-translational hydroxylation, though well characterized in eukaryotes, remains understudied in prokaryotes. The discovery that YcfD is a bacterial ROX, responsible for the hydroxylation of an essential component of the bacterial ribosome, highlights the potential for post-translational hydroxylation as an important bacterial regulatory mechanism. The sensitivity of hydroxylases to alterations in metabolism and hypoxic conditions makes them ideal candidates for regulating bacterial cell response to changes in the environment. Investigation of other putative 2OG oxygenase could elucidate novel post-translational hydroxylation regulatory pathways in prokaryotes, as well as uncover novel therapeutic targets.

REFERENCES

- Chang, B., Chen, Y., Zhao, Y., and Bruick, R. K. (2007). JMJD6 is a histone arginine demethylase. *Science* 318, 444–447. doi: 10.1126/science.1145801
- Chowdhury, R., Sekirnik, R., Brissett, N. C., Krojer, T., Ho, C. H., Ng, S. S., et al. (2014). Ribosomal oxygenases are structurally conserved from prokaryotes to humans. *Nature* 510, 422–426. doi: 10.1038/nature13263
- Clifton, I. J., McDonough, M. A., Ehrismann, D., Kershaw, N. J., Granatino, N., and Schofield, C. J. (2006). Structural studies on 2-oxoglutarate oxygenases and related double-stranded beta-helix fold proteins. *J. Inorg. Biochem.* 100, 644–669. doi: 10.1016/j.jinorgbio.2006.01.024
- de Bethune, M. P., and Nierhaus, K. H. (1978). Characterisation of the binding of virginiamycin S to *Escherichia coli* ribosomes. *Eur. J. Biochem.* 86, 187–191. doi: 10.1111/j.1432-1033.1978.tb12298.x
- Dunkle, J. A., Xiong, L., Mankin, A. S., and Cate, J. H. (2010). Structures of the *Escherichia coli* ribosome with antibiotics bound near the peptidyl transferase center explain spectra of drug action. *Proc. Natl. Acad. Sci. U.S.A.* 107, 17152–17157. doi: 10.1073/pnas.1007988107
- Engel, J., and Bächinger, H. P. (2005). “Structure of the collagen triple helix,” in *Collagen*, eds J. Brinckmann, H. Notbohm, and P. K. Müller (Berlin Heidelberg: Springer), 7–33.
- Ge, W., Wolf, A., Feng, T., Ho, C. H., Sekirnik, R., Zayer, A., et al. (2012). Oxygenase-catalyzed ribosome hydroxylation occurs in prokaryotes and humans. *Nat. Chem. Biol.* 8, 960–962. doi: 10.1038/nchembio.1093
- Hampl, H., Schulze, H., and Nierhaus, K. H. (1981). Ribosomal components from *Escherichia coli* 50 S subunits involved in the reconstitution of peptidyltransferase activity. *J. Biol. Chem.* 256, 2284–2288.

- Harms, J., Schlunzen, F., Zarivach, R., Bashan, A., Gat, S., Agmon, I., et al. (2001). High resolution structure of the large ribosomal subunit from a mesophilic eubacterium. *Cell* 107, 679–688. doi: 10.1016/S0092-8674(01)00546-3
- Hausinger, R. P. (2004). FeII/alpha-ketoglutarate-dependent hydroxylases and related enzymes. *Crit. Rev. Biochem. Mol. Biol.* 39, 21–68. doi: 10.1080/10409230490440541
- Heim, A., Grimm, C., Muller, U., Haussler, S., Mackeen, M. M., Merl, J., et al. (2014). Jumoni domain containing protein 6 (Jmjd6) modulates splicing and specifically interacts with arginine-serine-rich (RS) domains of SR- and SR-like proteins. *Nucleic Acids Res.* 42, 7833–7850. doi: 10.1093/nar/gku488
- Hewitson, K. S., and Schofield, C. J. (2004). The HIF pathway as a therapeutic target. *Drug Discov. Today* 9, 704–711. doi: 10.1016/S1359-6446(04)03202-7
- Holm, L., and Park, J. (2000). DaliLite workbench for protein structure comparison. *Bioinformatics* 16, 566–567. doi: 10.1093/bioinformatics/16.6.566
- Holme, E. (1975). A kinetic study of thymine 7-hydroxylase from *Neurospora crassa*. *Biochemistry* 14, 4999–5003. doi: 10.1021/bi00693a033
- Huang, L. E., Arany, Z., Livingston, D. M., and Bunn, H. F. (1996). Activation of hypoxia-inducible transcription factor depends primarily upon redox-sensitive stabilization of its alpha subunit. *J. Biol. Chem.* 271, 32253–32259. doi: 10.1074/jbc.271.50.32253
- Hutton, J. J. Jr., Trappel, A. L., and Udenfriend, S. (1966). Requirements for alpha-ketoglutarate, ferrous ion and ascorbate by collagen proline hydroxylase. *Biochem. Biophys. Res. Commun.* 24, 179–184. doi: 10.1016/0006-291X(66)90716-9
- Ivan, M., Kondo, K., Yang, H., Kim, W., Valiano, J., Ohh, M., et al. (2001). HIF1alpha targeted for VHL-mediated destruction by proline hydroxylation: implications for O₂ sensing. *Science* 292, 464–468. doi: 10.1126/science.1059817
- Jaakkola, P., Mole, D. R., Tian, Y. M., Wilson, M. I., Gielbert, J., Gaskell, S. J., et al. (2001). Targeting of HIF-1alpha to the von Hippel-Lindau ubiquitylation complex by O₂-regulated prolyl hydroxylation. *Science* 292, 468–472. doi: 10.1126/science.1059796
- Jenkins, C. L., Bretscher, L. E., Guzei, I. A., and Raines, R. T. (2003). Effect of 3-hydroxyproline residues on collagen stability. *J. Am. Chem. Soc.* 125, 6422–6427. doi: 10.1021/ja034015j
- Jenkins, C. L., and Raines, R. T. (2002). Insights on the conformational stability of collagen. *Nat. Prod. Rep.* 19, 49–59. doi: 10.1039/a903001h
- Jomaa, A., Jain, N., Davis, J. H., Williamson, J. R., Britton, R. A., and Ortega, J. (2014). Functional domains of the 50S subunit mature late in the assembly process. *Nucleic Acids Res.* 42, 3419–3435. doi: 10.1093/nar/gkt1295
- Kazem, M. (1975). The importance of *Escherichia coli* ribosomal proteins L1, L11 and L16 for the association of ribosomal subunits and the formation of the 70S initiation complex. *Eur. J. Biochem.* 58, 501–510. doi: 10.1111/j.1432-1033.1975.tb02398.x
- Kazem, M. (1976). Binding of aminoacyl-tRNA to reconstituted subparticles of *Escherichia coli* large ribosomal subunits. *Eur. J. Biochem.* 67, 373–378. doi: 10.1111/j.1432-1033.1976.tb10701.x
- Lando, D., Peet, D. J., Gorman, J. J., Whelan, D. A., Whitelaw, M. L., and Bruick, R. K. (2002). FIH-1 is an asparaginyl hydroxylase enzyme that regulates the transcriptional activity of hypoxia-inducible factor. *Genes Dev.* 16, 1466–1471. doi: 10.1101/gad.991402
- Loenarz, C., and Schofield, C. J. (2011). Physiological and biochemical aspects of hydroxylations and demethylations catalyzed by human 2-oxoglutarate oxygenases. *Trends Biochem. Sci.* 36, 7–18. doi: 10.1016/j.tibs.2010.07.002
- Masson, N., Willam, C., Maxwell, P. H., Pugh, C. W., and Ratcliffe, P. J. (2001). Independent function of two destruction domains in hypoxia-inducible factor-1alpha chains activated by prolyl hydroxylation. *EMBO J.* 20, 5197–5206. doi: 10.1093/emboj/20.18.5197
- Moore, V. G., Atchison, R. E., Thomas, G., Moran, M., and Noller, H. F. (1975). Identification of a ribosomal protein essential for peptidyl transferase activity. *Proc. Natl. Acad. Sci. U.S.A.* 72, 844–848. doi: 10.1073/pnas.72.3.844
- Mullen, A. R., and DeBerardinis, R. J. (2012). Genetically-defined metabolic reprogramming in cancer. *Trends Endocrinol. Metab.* 23, 552–559. doi: 10.1016/j.tem.2012.06.009
- Myllyharju, J. (2003). Prolyl 4-hydroxylases, the key enzymes of collagen biosynthesis. *Matrix Biol.* 22, 15–24. doi: 10.1016/S0945-053X(03)00006-4
- Myllyharju, J., and Kivirikko, K. I. (2001). Collagens and collagen-related diseases. *Ann. Med.* 33, 7–21. doi: 10.3109/07853890109002055
- Myllyharju, J., and Kivirikko, K. I. (2004). Collagens, modifying enzymes and their mutations in humans, flies and worms. *Trends Genet.* 20, 33–43. doi: 10.1016/j.tig.2003.11.004
- Nierhaus, D., and Nierhaus, K. H. (1973). Identification of the chloramphenicol-binding protein in *Escherichia coli* ribosomes by partial reconstitution. *Proc. Natl. Acad. Sci. U.S.A.* 70, 2224–2228. doi: 10.1073/pnas.70.8.2224
- Nierhaus, K. H. (1991). The assembly of prokaryotic ribosomes. *Biochimie* 73, 739–755. doi: 10.1016/0300-9084(91)90054-5
- Nishimura, M., Yoshida, T., Shirouzu, M., Terada, T., Kuramitsu, S., Yokoyama, S., et al. (2004). Solution structure of ribosomal protein L16 from *Thermus thermophilus* HB8. *J. Mol. Biol.* 344, 1369–1383. doi: 10.1016/j.jmb.2004.10.011
- Palmer, B. F., and Clegg, D. J. (2014). Oxygen sensing and metabolic homeostasis. *Mol. Cell. Endocrinol.* 397, 51–58. doi: 10.1016/j.mce.2014.08.001
- Prockop, D. J., and Kivirikko, K. I. (1995). Collagens: molecular biology, diseases, and potentials for therapy. *Annu. Rev. Biochem.* 64, 403–434. doi: 10.1146/annurev.bi.64.070195.002155
- Roach, P. L., Clifton, I. J., Fulop, V., Harlos, K., Barton, G. J., Hajdu, J., et al. (1995). Crystal structure of isopenicillin N synthase is the first from a new structural family of enzymes. *Nature* 375, 700–704. doi: 10.1038/375700a0
- Stetten, M. R. (1949). Some aspects of the metabolism of hydroxyproline, studied with the aid of isotopic nitrogen. *J. Biol. Chem.* 181, 31–37.
- Suzuki, C., Takahashi, K., Hayama, S., Ishikawa, N., Kato, T., Ito, T., et al. (2007). Identification of Myc-associated protein with JmJC domain as a novel therapeutic target oncogene for lung cancer. *Mol. Cancer Ther.* 6, 542–551. doi: 10.1158/1535-7163.MCT-06-0659
- Tate, W. P., Schulze, H., and Nierhaus, K. H. (1983). The importance of the *Escherichia coli* ribosomal protein L16 for the reconstitution of the peptidyl-tRNA hydrolysis activity of peptide chain termination. *J. Biol. Chem.* 258, 12810–12815.
- Teichmann, M., Dumay-Odelot, H., and Fribourg, S. (2012). Structural and functional aspects of winged-helix domains at the core of transcription initiation complexes. *Transcription* 3, 2–7. doi: 10.4161/trns.3.1.18917
- Teraoka, H., and Nierhaus, K. H. (1978). Proteins from *Escherichia coli* ribosomes involved in the binding of erythromycin. *J. Mol. Biol.* 126, 185–193. doi: 10.1016/0022-2836(78)90358-3
- Teye, K., Tsuneoka, M., Arima, N., Koda, Y., Nakamura, Y., Ueta, Y., et al. (2004). Increased expression of a Myc target gene Mina53 in human colon cancer. *Am. J. Pathol.* 164, 205–216. doi: 10.1016/S0002-9440(10)63111-2
- Tsuneoka, M., Koda, Y., Soejima, M., Teye, K., and Kimura, H. (2002). A novel myc target gene, mina53, that is involved in cell proliferation. *J. Biol. Chem.* 277, 35450–35459. doi: 10.1074/jbc.M204458200
- Unoki, M., Masuda, A., Dohmae, N., Arita, K., Yoshimatsu, M., Iwai, Y., et al. (2013). Lysyl 5-hydroxylation, a novel histone modification, by Jumoni domain containing 6 (JMJD6). *J. Biol. Chem.* 288, 6053–6062. doi: 10.1074/jbc.M112.433284
- van Staaldin, L. M., Novakowski, S. K., and Jia, Z. (2014). Structure and functional analysis of YcfD, a novel 2-oxoglutarate/Fe²⁺-dependent oxygenase involved in translational regulation in *Escherichia coli*. *J. Mol. Biol.* 426, 1898–1910. doi: 10.1016/j.jmb.2014.02.008
- Vranka, J. A., Sakai, L. Y., and Bachinger, H. P. (2004). Prolyl 3-hydroxylase 1, enzyme characterization and identification of a novel family of enzymes. *J. Biol. Chem.* 279, 23615–23621. doi: 10.1074/jbc.M312807200
- Wang, F., He, L., Huangyang, P., Liang, J., Si, W., Yan, R., et al. (2014). JMJD6 promotes colon carcinogenesis through negative regulation of p53 by hydroxylation. *PLoS Biol.* 12:e1001819. doi: 10.1371/journal.pbio.1001819
- Wang, G. L., Jiang, B. H., Rue, E. A., and Semenza, G. L. (1995). Hypoxia-inducible factor 1 is a basic-helix-loop-helix-PAS heterodimer regulated by cellular O₂ tension. *Proc. Natl. Acad. Sci. U.S.A.* 92, 5510–5514. doi: 10.1073/pnas.92.12.5510
- Webby, C. J., Wolf, A., Gromak, N., Dreger, M., Kramer, H., Kessler, B., et al. (2009). Jmjd6 catalyzes lysyl-hydroxylation of U2AF65, a protein associated with RNA splicing. *Science* 325, 90–93. doi: 10.1126/science.1175865
- Weis, M. A., Hudson, D. M., Kim, L., Scott, M., Wu, J. J., and Eyre, D. R. (2010). Location of 3-hydroxyproline residues in collagen types I, II, III, and V/XI implies a role in fibril supramolecular assembly. *J. Biol. Chem.* 285, 2580–2590. doi: 10.1074/jbc.M109.068726

- Yamauchi, M., and Sricholpech, M. (2012). Lysine post-translational modifications of collagen. *Essays Biochem.* 52, 113–133. doi: 10.1042/bse0520113
- Yu, F., White, S. B., Zhao, Q., and Lee, F. S. (2001). HIF-1 α binding to VHL is regulated by stimulus-sensitive proline hydroxylation. *Proc. Natl. Acad. Sci. U.S.A.* 98, 9630–9635. doi: 10.1073/pnas.181341498
- Zhang, Y., Lu, Y., Yuan, B. Z., Castranova, V., Shi, X., Stauffer, J. L., et al. (2005). The Human mineral dust-induced gene, mdig, is a cell growth regulating gene associated with lung cancer. *Oncogene* 24, 4873–4882. doi: 10.1038/sj.onc.1208668

Conflict of Interest Statement: The authors declare that the research was conducted in the absence of any commercial or financial relationships that could be construed as a potential conflict of interest.

Received: 31 October 2014; accepted: 27 December 2014; published online: 15 January 2015.

Citation: van Staalduinen LM and Jia Z (2015) Post-translational hydroxylation by 2OG/Fe(II)-dependent oxygenases as a novel regulatory mechanism in bacteria. *Front. Microbiol.* 5:798. doi: 10.3389/fmicb.2014.00798

This article was submitted to *Microbial Physiology and Metabolism*, a section of the journal *Frontiers in Microbiology*.

Copyright © 2015 van Staalduinen and Jia. This is an open-access article distributed under the terms of the Creative Commons Attribution License (CC BY). The use, distribution or reproduction in other forums is permitted, provided the original author(s) or licensor are credited and that the original publication in this journal is cited, in accordance with accepted academic practice. No use, distribution or reproduction is permitted which does not comply with these terms.



Interaction between extracellular matrix molecules and microbial pathogens: evidence for the missing link in autoimmunity with rheumatoid arthritis as a disease model

Nidhi Sofat^{1*}, Robin Wait², Saralili D. Robertson¹, Deborah L. Baines¹ and Emma H. Baker¹

¹ Institute of Infection and Immunity, St George's, University of London, London, UK

² The Kennedy Institute of Rheumatology, Nuffield Department of Orthopaedics, Rheumatology and Musculoskeletal Sciences, University of Oxford, Oxford, UK

Edited by:

Ivan Mijakovic, Chalmers University of Technology, Sweden

Reviewed by:

J. Arturo García-Horsman, University of Helsinki, Finland

Wolfgang Eisenreich, Technische Universität München, Germany

*Correspondence:

Nidhi Sofat, Institute of Infection and Immunity, St George's, University of London, Cranmer Terrace, London SW17 0RE, UK
e-mail: nsifat@sgul.ac.uk

Rheumatoid arthritis (RA) is an autoimmune disease characterized by inflammation followed by tissue rebuilding or fibrosis. A failure by the body to regulate inflammation effectively is one of the hallmarks of RA. The interaction between the external environment and the human host plays an important role in the development of autoimmunity. In RA, the observation of anti-cyclic citrullinated peptide antibodies (ACPA) to autoantigens is well recognized. Citrullination is a post-translational modification mediated by peptidyl arginine deiminases, which exist in both mammalian and bacterial forms. Previous studies have shown how proteins expressed in the human extracellular matrix (ECM) acquire properties of damage-associated molecular patterns (DAMPs) in RA and include collagens, tenascin-C, and fibronectin (FN). ECM DAMPs can further potentiate tissue damage in RA. Recent work has shown that citrullination in RA occurs at mucosal sites, including the oral cavity and lung. Mucosal sites have been linked with bacterial infection, e.g., periodontal disease, where exogenous pathogens are implicated in the development of autoimmunity via an infectious trigger. Proteases produced at mucosal sites, both by bacteria and the human host, can induce the release of ECM DAMPs, thereby revealing neoepitopes which can be citrullinated and lead to an autoantibody response with further production of ACPA. In this perspectives article, the evidence for the interplay between the ECM and bacteria at human mucosal surfaces, which can become a focus for citrullination and the development of autoimmunity, is explored. Specific examples, with reference to collagen, fibrinogen, and FN, are discussed.

Keywords: rheumatoid arthritis, citrullination, lung, periodontal disease, extracellular matrix, infection, microbiome

INTRODUCTION

Rheumatoid arthritis (RA) is an immune-mediated inflammatory disease. It is often associated with chronic disability, early mortality, systemic complications, and places a high socioeconomic burden on society as a whole (McInnes and Schett, 2011). In the last few decades there have been improved treatments for RA, based on immune-modulation of inflammatory pathways. However, up to one-third of people with RA continue to experience high disease activity, despite treatment with strong immunomodulatory drugs such as tumour necrosis factor (TNF) inhibitors, methotrexate, and corticosteroids (Scott et al., 2010). An improved understanding of disease pathophysiology is therefore essential to develop new treatments to address this unmet need.

The development of RA results from a complex interplay between genotype, environment, and lifestyle factors such as smoking (Mahdi et al., 2009). An important clinical aspect in the diagnosis of RA includes the detection of anti-citrullinated peptide antibodies (ACPA) to auto-antigens. Citrullination, also known as deminination, is the conversion of the amino acid arginine in a protein into the amino acid citrulline. Enzymes called peptidylarginine deiminases (PADs) replace the primary ketamine group (=NH) by a ketone group (=O). Citrullination is involved in regulation of development during embryogenesis and in

deminination-regulated gene expression through histone modifications. Citrulline is not one of the standard 20 amino acids encoded by DNA in the genetic code; it is the result of a post-translational modification. The immune system often attacks citrullinated proteins, thereby leading to autoimmune phenomena in RA.

Twin studies have shown a concordance rate for RA of 15 to 30% among monozygotic twins and 5% among dizygotic twins (13). Genome-wide association analyses have identified immune regulatory factors that may underlie the disease; including PTPN22 among the single nucleotide polymorphisms (SNPs) identified (Wellcome Trust Case Control Consortium, 2007). An association with HLA-DRB1 has been established for RA patients who are positive for rheumatoid factor or ACPA (Gregersen et al., 1987). In keeping with the role of HLA-DRB1 in antigen presentation, a number of studies over the last two decades have shown that auto-reactive immune responses are mediated by T-cell repertoire selection, antigen presentation, or changes in peptide affinity (Panayi, 2006). The shared epitope (SE), carried by the vast majority of RA patients, is a 5-aa sequence motif in the third allelic hypervariable region of the HLA-DR β chain. Proposed explanations for the link between RA and the SE include molecular mimicry of the SE by microbial proteins, increased T cell senescence induced by SE-containing HLA molecules and a

potential pro-inflammatory signaling function that is unrelated to the role of the SE in antigen recognition (Weyand and Goronzy, 1990; De Almeida et al., 2010).

Gene–environment interactions are also important in RA development. Smoking and other environmental risks to the lung, such as silica exposure, increase the risk of RA in people with susceptibility HLA-DR4 alleles (Symmons et al., 1997; Klareskog et al., 2008). Smoking and HLA-DRB1 alleles synergistically increase the risk of developing the anti-citrullinated protein antibodies (ACPA) that are present in the majority of patients with RA (Li et al., 2007). It has therefore been proposed that environmental stress in the lung or other mucosal surfaces may promote post-translational modifications through activation of peptidyl arginine deiminase, type IV (PADIV), which can cause citrullination of mucosal proteins. Loss of tolerance to the neoepitopes generated by citrullination can be detected clinically in people with RA by the ACPA response (Vincent et al., 1999).

For many years, it has been recognized that infectious agents such as *cytomegalovirus*, *Escherichia coli*, *Epstein Barr virus*, *parvovirus*, and *proteus* species may play a role in the development of RA. Recently, the oral pathogen *Porphyromonas gingivalis* has been implicated in the pathogenesis of RA (Mikuls et al., 2014). Products of infectious agents, e.g., heat shock proteins and enzymes responsible for citrullination have been shown in several models to induce immune reactivity. For example, several citrullinated autoantigens can be identified in assays to test for ACPA, keratin, fibrinogen, fibronectin (FN), collagen, and vimentin (van der Woude et al., 2010). Many of the proteins described form part of the extracellular matrix (ECM) common to many structures in the joint, lung, skin, and mucosal tissue. Damage-associated molecular patterns (or DAMPSs) are molecules that can initiate and perpetuate the immune response in the non-infectious inflammatory response. Molecules including fibrinogen and FN, which are abundant in the arthritic joint, have been implicated described as DAMPs in RA pathophysiology and are susceptible to citrullination. It is also possible that cleavage of DAMPs by proteases during the arthritic process may lead to exposure of neoepitopes which are then susceptible to a heightened autoimmune response. Although unifying mechanisms for the link between infection and RA autoimmunity are not entirely established, the theory of molecular mimicry has been proposed (van Heemst et al., 2014). The formation of immune complexes during infection may trigger the induction of rheumatoid factor, which is a high affinity autoantibody against the Fc portion of immunoglobulin, often used in the diagnosis of RA (De Rycke et al., 2004). A link has been described between RA and periodontal disease (PD): *Porphyromonas gingivalis* produces bacterial peptidylarginine deiminase (PAD) which can promote citrullination of mammalian proteins (Wegner et al., 2010). Recently, the gastrointestinal microbiome has also been implicated in the development of autoimmunity (Scher et al., 2012).

ECM INTERACTIONS IN RA

In the sections below, we discuss the role of common ECM proteins found not only in the arthritic joint, but also highly expressed by mucosal surfaces including the lung, mouth, and gut. We

discuss how such ECM proteins may be cleaved and citrullinated at mucosal surfaces, thereby leading potentially to the breakdown of tolerance and the development of autoimmunity in RA.

COLLAGENS

Collagens comprise a superfamily of ECM proteins which provide a structural framework for many connective tissues. Collagens can be divided into several families or groups based on their exon structure, containing several homologous genes encoding polypeptides that have domains with similar sequences. All collagens have domains with a triple helical conformation (Bella et al., 1994) and are a major constituent of connective tissue. Collagen fibrils composed primarily of type II and XI collagen provide a structural framework to hyaline cartilage (Li et al., 2007), and type I/III and V collagens are a major constituent of skin, tendon, ligaments and bone, demonstrating how the major constituents of the joint require collagen for their structural integrity. Mutations in COL2A1 cause a spectrum of chondrodysplasias, including achondrogenesis II, hypochondrogenesis, spondyloepiphyseal dysplasia, and Kniest and Stickler syndromes (Mundlos and Olsen, 1997). Type II collagen can be injected peripherally to induce RA in murine arthritis in the collagen-induced arthritis (CIA)-model (Williams, 2004), which is one of the most commonly used murine models of inflammatory arthritis.

FIBRINOGENS

Fibrinogen is a soluble plasma protein. After cleavage by α -thrombin, it is converted to fibrin monomers (Blombäck, 1996). Fibrin monomers self-associate to form an insoluble homopolymeric structure, the fibrin clot. Fibrinogen can also bind to platelets, contributes to the formation of fibrin clots, as well as endothelial cells and leukocytes and plays a multifaceted role in the ECM response to injury. Fibrinogen expression is upregulated at mucosal surfaces during injury, thus participating in inflammatory responses. Congenital lack of fibrinogen results in a bleeding disorder, while increased plasma levels are associated with heightened arterial and venous thrombotic risk (Everse et al., 1998).

FIBRONECTIN

Fibronectin is an ECM glycoprotein present in tissues and body fluids that is involved in a range of processes, including cellular differentiation, adhesion, migration, wound healing, and neoplastic transformation (Hynes and Yamada, 1982). FN comprises the ECM in joint tissue, including the synovial membranes and cartilage. Expression of FN is upregulated in arthritic diseases including RA and osteoarthritis (Sofat et al., 2012). In addition, FN fragments have been detected in cartilage from people with RA and OA and are responsible for further cartilage matrix degradation (Sofat et al., 2012). Citrullination of FN has been found in RA synovial tissue (Chang et al., 2005) and antibodies to citrullinated FN have been detected in people with RA (Van Beers et al., 2012).

WHERE COULD CITRULLINATION TAKE PLACE? INSIGHTS FROM MUCOSAL SURFACES

Antibodies to citrullinated peptide antigens are associated with RA and predate disease onset in many cases (Ioan-Facsinay et al.,

2008). Since RA autoantibodies often pre-date the development of inflammation in the synovium, it is possible that primary citrullination occurs outside the synovium. It has been suggested that infectious agents release toxins such as lipopolysaccharide (LPS) at mucosal surfaces, triggering an inflammatory response with potential to cause citrullination of ECM. Citrullination may affect ECM proteins found both at mucosal surfaces such as lung, oral and gut mucosa, and in articulating joint tissue, including FN, fibrinogen, and collagen.

LUNG

Klareskog et al. (2008) suggested that the lung may be a site of citrullination, where co-factors such as smoking and exposure to LPS may result in altered immune status of the lung mucosa. The lung is susceptible to inflammatory responses triggered by infection and autoimmunity (Meyer, 2010). In addition to the increased prevalence of ACPA in smokers (Meyer, 2010) there is also increased ACPA prevalence in RA-related lung disease (Ruiz-Esquivel et al., 2012). Respiratory micro-organisms are also linked to the development of RA (Perry et al., 2014).

To explore the link between inflammation and modification of the ECM matrix in the lung, we investigated the effect of pulmonary LPS exposure on ECM expression in mice. Experiments were performed using 6–8 weeks old female BALB/c mice. Mice were anesthetized with isoflurane (in accordance with UK Home Office regulation), then 50 μ L of 0.125 mg/kg LPS from *E. coli* serotype 0127:B8 or saline control was administered intranasally. Mice were sacrificed after 24 h: the lungs were dissected out and fixed for 4 h in 4% paraformaldehyde and washed before embedding in paraffin wax. Our murine model showed an inflammatory response to LPS, with oedema, destruction of alveolar architecture, and a cellular infiltrate (**Figures 1A,B**). For histochemistry, lung tissue was sectioned into 4 μ m slices which were stained with haematoxylin and eosin or primary rabbit anti-FN antibody. The expression of FN, an ECM molecule which is expressed in the lung, was highly upregulated in LPS treated mice *vs.* saline controls ($n = 5$ in each group). FN protein was detected in the surrounding ECM of alveolar tissue, type II pneumocytes, and the cellular infiltrate demonstrated by immunostaining with primary anti-FN antibody followed by a secondary antibody conjugated with horseradish peroxidase by light microscopy (**Figure 1C**).

To determine whether the increased FN expression observed in the murine system was also relevant to human lung disease, we investigated the expression of FN in bronchoalveolar lavage fluid (BALF) from people with chronic severe asthma and/or COPD. BALF was probed for FN using SDS-PAGE and Western blotting (**Figure 1D**). We observed expression of full-length FN in all samples tested from human BALF with asthma and COPD. In addition, we observed increased expression of fragmented FN in all samples tested, suggesting cleavage of FN during asthma and COPD. A separate gel was run on SDS-PAGE, and samples of BALF from subjects with mild asthma were analyzed by liquid chromatography mass spectrometry (LC-MS) on 1-D gels by in-gel digestion (**Figure 1E**). Bands from SDS-PAGE were cut from the gel (**Figure 1E**) and subjected to mass spectrometry demonstrating a typical signature of protein expression from BALF samples,

including alpha-1 antitrypsin, complement, immunoglobulin, FN was also identified from samples mapping to the cell-binding region and the C-terminal heparin-binding region of FN. These FN regions identified in human BALF are the same regions as have previously been implicated in mediating chronic inflammation in arthritis (Sofat et al., 2012). Taken together, our findings show that acute inflammation in mouse lung induces increased FN expression and that expression and fragmentation of FN can also be demonstrated in human lung BALF extracts.

Other groups have described citrullination of FN in RA (Chang et al., 2005). Upregulation of FN expression at mucosal surfaces including the lung, as we have shown, may consequently contribute to mechanisms of RA pathogenesis such as citrullination. Our data showed increased FN expression in BALF samples and fragmented forms of FN, which may represent fragmentation by proteases. It is possible that FN and/or its fragments mediate chronic inflammation during lung injury and result in citrullination in RA driven by cofactors such as smoking and the SE.

PERIODONTAL SURFACES

The oral mucosa contains an abundance of bacterial organisms in health and disease. A strong link has been described between PD and RA, giving rise to investigation of the oral microbiome in RA. Recent work has suggested that environmental factors influencing autoimmunity include crosstalk between the human host and oral/intestinal microbiomes. Several lines of investigation have suggested a link between the oral microbes, PD and RA (Wegner et al., 2010; Mikuls et al., 2014). Recent studies have shown that people with RA have a high prevalence of PD. A genome sequencing approach using samples collected from the subgingival biofilm identified a number of organisms, including *Anaeroglobus geminatus*, *Porphyromonas gingivalis*, *Prevotella*, and *Leptotrichia* species in people with new-onset RA (Scher et al., 2012).

We investigated the ability of oral microbes to modify ECM proteins. *Porphyromonas gingivalis*, a known pathogen in PD (strain W83 from ATCC) was cultured for 24 h under full anaerobic conditions (3M Concept Plus anaerobic incubator). Bacterial supernatants were extracted and incubated with ECM substrates at 0.5 mg/ml at 37°C, with collection of digestion products from 0 to 180 min after digestion. ECM substrates chosen for these experiments were fibrinogen, FN and type I collagen, as these ECM proteins are found both in arthritic joints and in oral mucosa. The cleavage patterns of ECM substrates were evaluated by SDS-PAGE and Western blotting in the presence and absence of selective protease inhibitors.

We found that culture supernatants from *P. gingivalis* were effective at cleaving all the substrates tested. At 37°C the rate of cleavage was: fibrinogen 30 min for complete cleavage, FN was 180 min for complete cleavage and type I collagen was cleaved at a slower rate over 180 min (**Figure 2**). Intermediate digestion products for all three ECM proteins were demonstrated on SDS-PAGE (**Figure 2**). Our results show that cleavage pattern of ECM protein substrates was distinct for each of the substrates tested. The varying cleavage patterns are likely to have been influenced by the nature of the secreted proteases produced by *P. gingivalis*, and that the varying levels of protease expression produced by the microorganism had a differing effect on the digestion pattern and

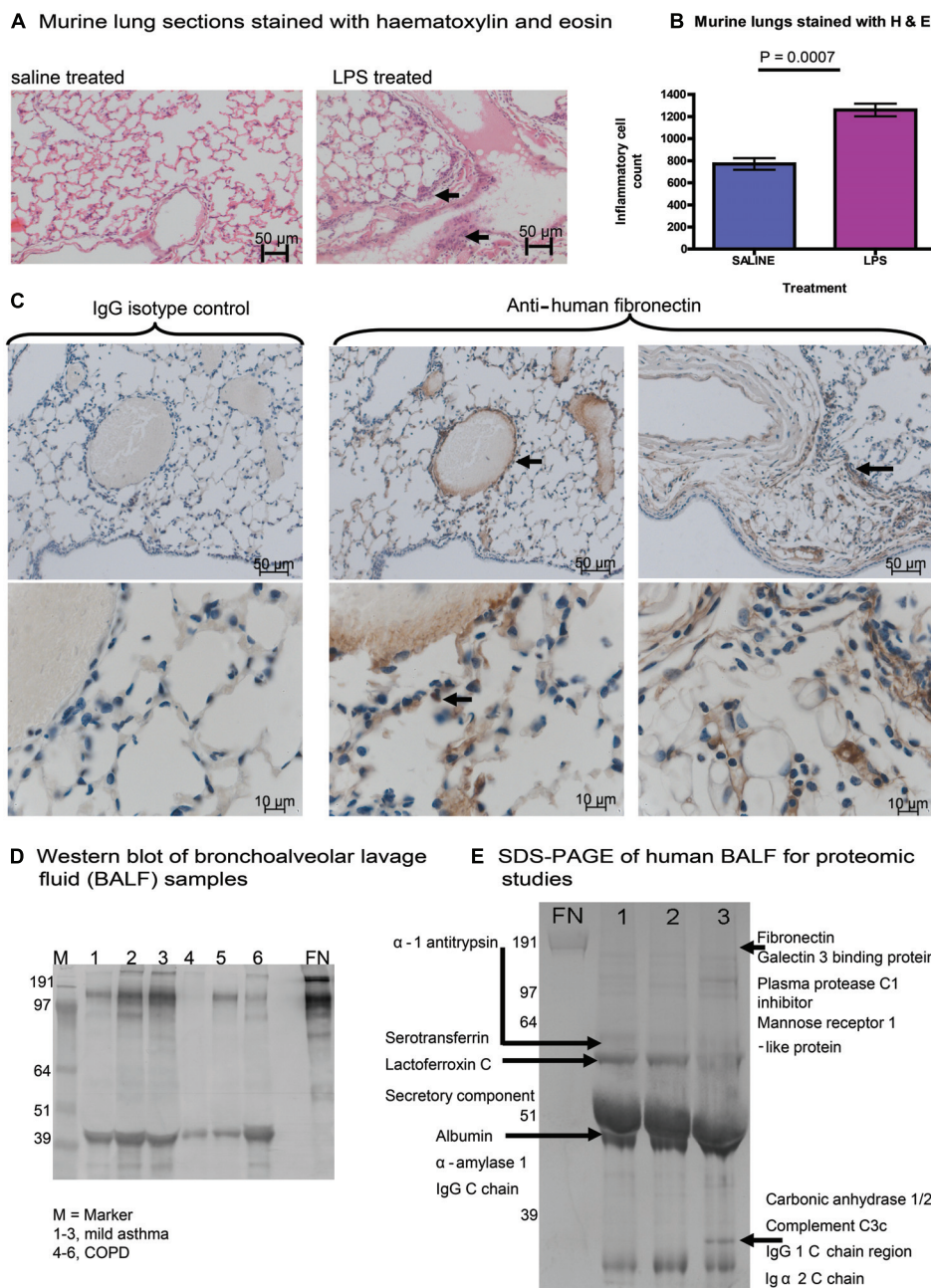
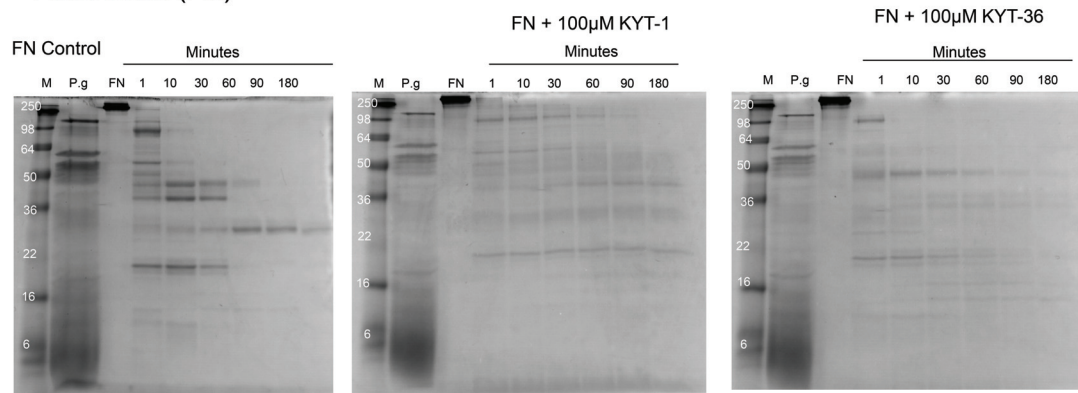


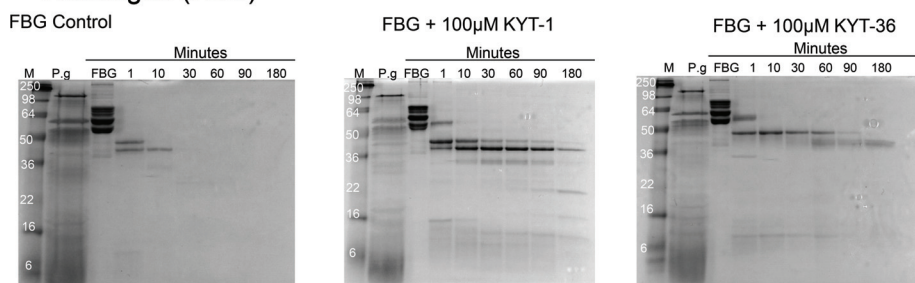
FIGURE 1 | Expression of fibronectin (FN) in murine and human lung tissue. (A) Experiments were performed using 6–8 weeks old female BALB/c mice. Mice were anesthetized with isoflurane, then 50 μ L of 0.125 mg/kg LPS from *Escherichia coli* serotype 0127:B8 or saline control was administered intranasally. Mice were sacrificed after 24 h: the lungs were dissected out and fixed for 4 h in 4% paraformaldehyde and washed before embedding in paraffin wax. Our murine model showed an inflammatory response to LPS, with oedema, destruction of alveolar architecture and a cellular infiltrate (arrows indicate areas of inflammatory infiltrate). (B) The cellular inflammatory infiltrate was quantified in five representative lung fields and was compared between mice treated with LPS or saline control. (C) We demonstrated the expression of FN, an ECM molecule in murine lung harvested after LPS treatment. Expression of FN (increased brown staining by horseradish peroxidase) was highly upregulated in LPS treated mice vs. saline controls ($n = 5$ in each group). FN protein was detected in the surrounding ECM of alveolar tissue, type II pneumocytes, and the cellular

infiltrate (arrows indicate perivascular staining of FN in lung ECM, alveolar tissue, and pneumocytes). For immunohistochemistry, lung tissue was sectioned into 4 μ m slices which were stained with haematoxylin and eosin or primary rabbit anti-FN antibody. FN antigen was detected using secondary antibodies conjugated to horseradish peroxidase and analyzed by light microscopy. (D) Expression of FN from bronchoalveolar lavage fluid (BALF) is shown in participant samples obtained with informed consent. Samples were obtained from people with mild asthma (1–3) or chronic obstructive pulmonary disease (COPD). SDS-PAGE was performed followed by immunoblotting. The Western blot was treated with a primary antibody to human FN (Sigma), with a secondary anti-rabbit antibody (Sigma) conjugated to alkaline phosphatase for development. (E) Bands from samples 1–3 of BALF from participants with mild asthma (D) were run separately on SDS-PAGE, bands of interest were cut out and then subjected to analysis using liquid chromatography mass spectrometry (LC-MS). Residues from proteins identified from BALF samples are shown.

A Fibronectin (FN)



B Fibrinogen (FBG)



C. Type I Collagen

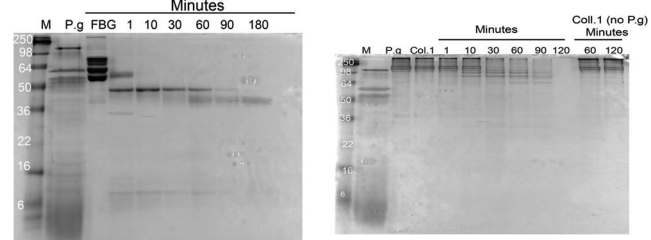


FIGURE 2 | Cleavage of ECM proteins FN, fibrinogen, and type I collagen by culture supernatants of *Porphyromonas gingivalis*.

Digestion patterns observed over a time course experiment from 0 up to 180 min was performed with culture supernatants from *P. gingivalis* incubated with FN, fibrinogen, and type I collagen, respectively. Digestion patterns for FN (A), fibrinogen (B), and type I collagen (C) are shown. For FN (A), almost full cleavage was observed after 180 min, an effect which was delayed in the presence of inhibitors KYT-1 and KYT-36. For fibrinogen (B), full cleavage was observed within 30 min. In contrast, with the gingipain inhibitors, cleavage was not observed in a rapid manner and

intermediate cleavage products remained after 180 min of digestion in the presence of KYT inhibitors. For type I collagen, slower cleavage was observed, but was more rapid than without co-culture with *P. gingivalis* supernatants, suggesting that all three ECM molecules tested are cleaved more rapidly in the presence of *P. gingivalis*. Culture supernatants of the anaerobe *P. gingivalis* (strain W83 from ATCC) were produced from 24 h cultures using full anaerobic conditions (3M Concept Plus anaerobic incubator). After culture, bacterial supernatants were extracted and incubated with the substrates at 0.5 mg/ml at 37°C, with collection of digestion products from 0 to 180 min.

kinetics of specific protein substrates. In the presence of gingipain inhibitors KYT-1 and KYT-36, cleavage of the substrates FN and fibrinogen was strongly inhibited, as demonstrated by the persistence of digestion products in the presence of both protease inhibitors. Due to the likely varying inhibition of selective proteases by specific inhibitors KYT-1 and KYT-36, we observed differing inhibition patterns. However, as observed by the lack of inhibition of complete cleavage of the substrates we tested, it is likely that other proteases are also important in cleaving the substrates tested. Based on our *in vitro* findings, it could be possible that ECM substrates such as fibrinogen, FN, and type I collagen could be cleaved by proteases in the oral mucosa, giving rise to neoepitopes which could then be available for citrullination. Taken together, our findings raise the possibility that modification of ECM proteins in the oral mucosa by bacterial products could drive production of autoantibodies against ECM proteins expressed both in the oral mucosa and in arthritic joints. Inhibition of cleavage of oral ECM proteins may have potential as a new therapeutic target in the management of RA.

CONCLUDING REMARKS

Our data and reports from other groups demonstrate that mucosal surfaces express ECM DAMPs and that selective proteases can cleave ECM substrates found in the lung and oral mucosa. Our previous work has shown that ECM FN is upregulated in arthritic cartilage (Sofat et al., 2012) and other groups have demonstrated citrullinated FN inhibits apoptosis and promotes production of pro-inflammatory cytokines in RA (Fan et al., 2012). Such findings suggest that ECM proteins shared in the oral mucosa, lung, and the arthritic joint may contribute to the development of autoimmunity in RA. Future work to identify the proteases involved in both cleavage and citrullination of autoantigens, which may then serve to act as DAMPs, both in human and microbial systems, will be crucial to our understanding of disease pathophysiology in RA. Inhibition of cleavage of such substrates may delay the production of ECM DAMPs that are targets for citrullination in RA. Therapeutic strategies aimed at inhibiting such cleavage of ECM substrates may be a novel therapeutic target in RA.

ACKNOWLEDGMENTS

We thank Prof. Clive Robinson for KYT inhibitors and useful discussions. We thank Dr. Monika Hermansson for useful discussions. We thank Dr. James Moffatt for assistance with murine experiments. We thank the Wellcome Trust for funding Saralili D. Robertson through a Value in People Award.

REFERENCES

- Bella, J., Eaton, M., Brodsky, B., and Berman, H. M. (1994). Crystal and molecular structure of a collagen-like peptide at 1.9 Å resolution. *Science* 266, 75–81. doi: 10.1126/science.7695699
- Blombäck, B. (1996). Fibrinogen and fibrin-proteins with complex roles in hemostasis and thrombosis. *Thromb. Res.* 83, 1–75. doi: 10.1016/0049-3848(96)00111-9
- Chang, X., Yamada, R., Suzuki, A., Kochi, Y., Sawada, T., and Yamamoto, K. (2005). Citrullination of fibronectin in rheumatoid arthritis synovial tissue. *Rheumatology (Oxford)* 44, 1374–1382. doi: 10.1093/rheumatology/kei023
- De Almeida, D. E., Ling, S., Pi, X., Hartmann-Scruggs, A. M., Pumpens, P., and Holoshitz, J. (2010). Immune dysregulation by the rheumatoid arthritis shared epitope. *J. Immunol.* 185, 1927–1934. doi: 10.4049/jimmunol.0904002
- De Rycke, L., Peene, I., Hoffman, I. E., Kruithof, E., Union, A., Meheus, L., et al. (2004). Rheumatoid factor and anticitrullinated protein antibodies in rheumatoid arthritis: diagnostic value, associations with radiological progression rate, and extra-articular manifestations. *Ann. Rheum. Dis.* 63, 1587–1593. doi: 10.1136/ard.2003.017574
- Everse, S. J., Spraggon, G., and Doolittle, R. F. (1998). A three-dimensional consideration of variant human fibrinogens. *Thromb. Haemost.* 80, 1–9.
- Fan, L., Wang, Q., Liu, R., Zong, M., Zhnag, H., Ding, Y., et al. (2012). Citrullinated fibronectin inhibits apoptosis and promotes the secretion of pro-inflammatory cytokines in fibroblast-like synoviocytes in rheumatoid arthritis. *Arthritis Res. Ther.* 14:R266. doi: 10.1186/ar4112
- Gregersen, P. K., Silver, J., and Winchester, R. J. (1987). The shared epitope hypothesis. An approach to understanding the molecular genetics of susceptibility to rheumatoid arthritis. *Arthritis Rheum.* 30, 1205–1213. doi: 10.1002/art.1780301102
- Hynes, R. O., and Yamada, K. M. (1982). Fibronectins: multifunctional modular glycoproteins. *J. Cell Biol.* 95(2 Pt 1), 369–377. doi: 10.1083/jcb.95.2.369
- Ioan-Facsinay, A., Willemze, A., Robinson, D. B., Peschken, C. A., Markland, J., van der Woude, D., et al. (2008). Marked differences in fine specificity and isotype usage of the anti-citrullinated protein antibody in health and disease. *Arthritis Rheum.* 58, 3000–3008. doi: 10.1002/art.23763
- Klareskog, L., Ronnelid, J., Lundberg, K., Padyukov, L., and Alfredsson, L. (2008). Immunity to citrullinated proteins in rheumatoid arthritis. *Annu. Rev. Immunol.* 26, 651–675. doi: 10.1146/annurev.immunol.26.021607.090244
- Li, Y., Xu, L., and Olsen, B. R. (2007). Lessons from genetic forms of osteoarthritis for the pathogenesis of the disease. *Osteoarthritis Cartilage* 15, 1101–1105. doi: 10.1016/j.joca.2007.04.013
- Mahdi, H., Fisher, B. A., Kallberg, H., Plant, D., Malmstrom, V., Ronnelid, J., et al. (2009). Specific interaction between genotype, smoking and autoimmunity to citrullinated alpha-enolase in the etiology of rheumatoid arthritis. *Nat. Genet.* 41, 1319–1324. doi: 10.1038/ng.480
- McInnes, I. B., and Schett, G. (2011). The pathogenesis of rheumatoid arthritis. *N. Engl. J. Med.* 365, 2205–2219. doi: 10.1056/NEJMra1004965
- Meyer, K. C. (2010). The role of immunity and inflammation in lung senescence and susceptibility to infection in the elderly. *Semin. Respir. Crit. Care Med.* 31, 561–574. doi: 10.1055/s-0030-1265897
- Mikuls, T. R., Payne, J. B., Yu, F., Thiele, G. M., Reynolds, R. J., Cannon, G. W., et al. (2014). Periodontitis and *Porphyromonas gingivalis* in patients with rheumatoid arthritis. *Arthritis Rheumatol.* 66, 1090–1100. doi: 10.1002/art.38348
- Mundlos, S., and Olsen, B. R. (1997). Heritable diseases of the skeleton. Part II. Molecular insights into skeletal development matrix components and their homeostasis. *FASEB J.* 11, 227–233.
- Panayi, G. S. (2006). Even though T-cell-directed trials have been of limited success, is there reason for optimism? *Nat. Clin. Pract. Rheumatol.* 2, 58–59. doi: 10.1038/ncprheum0094
- Perry, E., Kelly, C., Eggleton, P., De Soyza, A., and Hutchison, D. (2014). The lung in ACPA-positive rheumatoid arthritis: an initiating site of injury? *Rheumatology* 53, 1940–1950. doi: 10.1093/rheumatology/keu195
- Ruiz-Esqueda, V., Gomara, M. J., Peinado, V. I., Gómez Puerta, J. A., Barberá, J. A., Cañete Jde, D., et al. (2012). Anti-citrullinated peptide antibodies in the serum of heavy smokers without rheumatoid arthritis. A differential effect of chronic obstructive pulmonary disease? *Clin. Rheumatol.* 31, 1047–1050. doi: 10.1007/s10067-012-1971-y
- Scher, J. U., Ubeda, C., Equinda, M., Khanin, R., Buischi, Y., Viale, A., et al. (2012). Periodontal disease and the oral microbiota in new-onset rheumatoid arthritis. *Arthritis Rheum.* 64, 3083–3094. doi: 10.1002/art.34539
- Scott, D. L., Wolfe, F., and Huizinga, T. W. (2010). Rheumatoid arthritis. *Lancet* 376, 1094–1108. doi: 10.1016/S0140-6736(10)60826-4
- Sofat, N., Robertson, S. D., and Wait, R. (2012). Fibronectin III 13–14 domains induce joint damage via Toll-like receptor 4 activation and synergize with interleukin-1 and tumour necrosis factor. *J. Innate Immun.* 4, 69–79. doi: 10.1159/000329632
- Symmons, D. P., Bankhead, C. R., Harrison, B. J., Brennan, P., Barrett, E. M., Scott, D. G., et al. (1997). Blood transfusion, smoking, and obesity as risk factors for the development of rheumatoid arthritis: results from a primary care-based incident case-control study in Norfolk, England. *Arthritis Rheum.* 40, 1955–1961. doi: 10.1002/art.1780401106
- Van Beers, J. J., Willemze, A., Stammen-Vogelzangs, J., Drijfhout, J. W., Toes, R. E., and Pruijn, G. J. (2012). Anti-citrullinated fibronectin antibodies in rheumatoid arthritis are associated with human leukocyte antigen DRB1 shared epitope alleles. *Arthritis Res. Ther.* 14:R35. doi: 10.1186/ar3744
- van der Woude, D., Rantapää-Dahlqvist, S., Ioan-Facsinay, A., Onnekink, C., Schwarte, C. M., Verpoort, K. N., et al. (2010). Epitope spreading of the anti-citrullinated protein antibody response occurs before disease onset and is associated with the disease course of early arthritis. *Ann. Rheum. Dis.* 69, 1554–1561. doi: 10.1136/ard.2009.124537
- van Heemst, J., van der Woude, D., Huizinga, T. W., and Toes, R. E. (2014). HLA and rheumatoid arthritis: how do they connect? *Ann. Med.* 46, 304–310. doi: 10.3109/07853890.2014.907097
- Vincent, C., de Keyser, F., Masson-Bessière, C., Sebbag, M., Veys, E. M., and Serre, G. (1999). Anti-perinuclear factor compared with the so called “antikeratin” antibodies and antibodies to human epidermis filaggrin, in the diagnosis of arthritides. *Ann. Rheum. Dis.* 58, 42–48. doi: 10.1136/ard.58.1.42
- Wegner, N., Wait, R., Sroka, A., Eick, S., Nguyen, K. A., Lundberg, K., et al. (2010). Peptidylarginine deiminase from *Porphyromonas gingivalis* citrullinates human fibrinogen and alpha-enolase: implications for autoimmunity in rheumatoid arthritis. *Arthritis Rheum.* 62, 2662–2672. doi: 10.1002/art.27552
- Wellcome Trust Case Control Consortium. (2007). Genome-wide association study of 14,000 cases of seven common diseases and 3,000 shared controls. *Nature* 447, 661–678. doi: 10.1038/nature05911
- Weyand, C. M., and Goronzy, J. J. (1990). Disease-associated human histocompatibility leukocyte antigen determinants in patients with seropositive rheumatoid arthritis. Functional role in antigen-specific and allogeneic T cell recognition. *J. Clin. Invest.* 85, 1051–1057. doi: 10.1172/JCI114535
- Williams, R. O. (2004). Collagen-induced arthritis as a model for rheumatoid arthritis. *Methods Mol. Med.* 98, 207–216.

Conflict of Interest Statement: The authors declare that the research was conducted in the absence of any commercial or financial relationships that could be construed as a potential conflict of interest.

Received: 27 November 2014; accepted: 21 December 2014; published online: 14 January 2015.

Citation: Sofat N, Wait R, Robertson SD, Baines DL and Baker EH (2015) Interaction between extracellular matrix molecules and microbial pathogens: evidence for the missing link in autoimmunity with rheumatoid arthritis as a disease model. *Front. Microbiol.* 5:783. doi: 10.3389/fmicb.2014.00783

This article was submitted to *Microbial Physiology and Metabolism*, a section of the journal *Frontiers in Microbiology*.

Copyright © 2015 Sofat, Wait, Robertson, Baines and Baker. This is an open-access article distributed under the terms of the Creative Commons Attribution License (CC BY). The use, distribution or reproduction in other forums is permitted, provided the original author(s) or licensor are credited and that the original publication in this journal is cited, in accordance with accepted academic practice. No use, distribution or reproduction is permitted which does not comply with these terms.



Factors that mediate and prevent degradation of the inactive and unstable GudB protein in *Bacillus subtilis*

Lorena Stannek^{1†}, Katrin Gunka^{1†}, Rachel A. Care¹, Ulf Gerth² and Fabian M. Commichau^{1*}

¹ Department of General Microbiology, Georg-August-University Göttingen, Göttingen, Germany

² Institute of Microbiology, Ernst-Moritz-Arndt-University Greifswald, Greifswald, Germany

Edited by:

Ivan Mijakovic, Chalmers University of Technology, Sweden

Reviewed by:

Sven Halbedel, Robert Koch Institute, Germany

Oscar P. Kuipers, University of Groningen, Netherlands

*Correspondence:

Fabian M. Commichau, Department of General Microbiology, Georg-August-University Göttingen, Grisebachstraße 8, 37077 Göttingen, Germany
e-mail: fcommic1@gwdg.de

[†]These authors have contributed equally to this work.

The Gram-positive model bacterium *Bacillus subtilis* contains two glutamate dehydrogenase-encoding genes, *rocG* and *gudB*. While the *rocG* gene encodes the functional GDH, the *gudB* gene is cryptic (*gudB^{CR}*) in the laboratory strain 168 due to a perfect 18 bp-long direct repeat that renders the GudB enzyme inactive and unstable. Although constitutively expressed the GudB^{CR} protein can hardly be detected in *B. subtilis* as it is rapidly degraded within stationary growth phase. Its high instability qualifies GudB^{CR} as a model substrate for studying protein turnover in *B. subtilis*. Recently, we have developed a visual screen to monitor the GudB^{CR} stability in the cell using a GFP-GudB^{CR} fusion. Using fluorescent microscopy we found that the GFP protein is simultaneously degraded together with GudB^{CR}. This allows us to analyze the stability of GudB^{CR} in living cells. By combining the visual screen with a transposon mutagenesis approach we looked for mutants that show an increased fluorescence signal compared to the wild type indicating a stabilized GFP-GudB^{CR} fusion. We observed, that disruption of the arginine kinase encoding gene *mcsB* upon transposon insertion leads to increased amounts of the GFP-GudB^{CR} fusion in this mutant. Deletion of the cognate arginine phosphatase YwIE in contrast results in reduced levels of the GFP-GudB^{CR} fusion. Recently, it was shown that the kinase McsB is involved in phosphorylation of GudB^{CR} on arginine residues. Here we show that selected arginine-lysine point mutations of GudB^{CR} exhibit no influence on degradation. The activity of McsB and YwIE, however, are crucial for the activation and inhibition, respectively, of a proteolytic machinery that efficiently degrades the unstable GudB^{CR} protein in *B. subtilis*.

Keywords: proteolysis, arginine phosphorylation, protein modification, protein folding, glutamate dehydrogenase

INTRODUCTION

Posttranslational modifications of proteins allow bacteria to control several important cellular processes. Phosphorylation is such a posttranslational modification event that can severely affect the function of a protein, which is targeted by a specific kinase (Pawson and Scott, 2005; Jers et al., 2008; Kobir et al., 2011). In bacteria, phosphorylation of enzymes and of enzyme regulators is important for the re-direction of fluxes through central metabolic pathways (LaPorte and Koshland, 1983; Cozzzone and El-Mansi, 2005; Niebisch et al., 2006). Moreover, posttranslational modification of RNA- and DNA-binding transcription factors by phosphorylation may result in induction or repression of gene expression (Bird et al., 1993; Stülke et al., 1997; Jung et al., 2012; Mascher, 2014).

In the past years, several studies revealed that beside serine, threonine, histidine, and cysteine also amino acids like tyrosine and arginine are phosphorylated in bacteria (Meins et al., 1993; Hoch, 2000; Deutscher and Saier, 2005; Macek et al., 2007; Kobir et al., 2011). For instance, the activity of the UDP-glucose dehydrogenase in the Gram-positive model bacterium *Bacillus subtilis* is controlled by reversible phosphorylation of a tyrosine residue (Mijakovic et al., 2004). Phosphorylation of tyrosine residues has also been shown to be important for controlling the activity of DNA-binding proteins (Mijakovic et al.,

2006; Derouiche et al., 2013). Recently, phosphoproteomic studies revealed that phosphorylation of arginine residues is an emerging posttranslational modification, which is implicated in general stress response in *B. subtilis* (Elsholz et al., 2012; Schmidt et al., 2014; Trentini et al., 2014). The kinase responsible for arginine phosphorylation in *B. subtilis* was shown to be McsB (Fuhrmann et al., 2009). Under normal growth conditions McsB is bound and inhibited by the ClpC ATPase subunit of the ClpCP protease complex and/or the activator of McsB kinase activity, McsA. At the same time, the DNA-binding transcription factor CtsR represses the genes of the CtsR-regulon (Derré et al., 1999). In contrast, if the bacteria encounter heat stress, ClpC preferentially interacts with misfolded proteins and releases McsB, which finally targets CtsR for degradation (Kirstein et al., 2005). Inactivation of CtsR results in upregulation of genes that encode proteins of a central protein quality network. The proteins of this network include chaperones, proteases, and adaptor proteins that improve the recognition of substrates by proteases (Elsholz et al., 2010a; Battesti and Gottesmann, 2013). Recent findings indicate that the detachment of CtsR from the DNA provoked by heat seems to be mediated by an intrinsic protein domain that senses heat rather than by McsB-dependent phosphorylation of arginine residues (Elsholz et al., 2010b). By contrast, upon oxidative stress, McsA does not longer bind to and inhibit

McsB, which subsequently removes CtsR from the DNA (Elsholz et al., 2011). Thus, the way of how the DNA-binding activity of CtsR is controlled by oxidative stress and by heat is strikingly different.

In recent global phosphoproteomic studies using a *B. subtilis* *ywIE* mutant strain lacking the cognate phosphatase YwIE of the kinase McsB, several arginine phosphorylation sites were detected (Elsholz et al., 2012; Schmidt et al., 2014; Trentini et al., 2014). Two phosphorylatable arginine residues in the ClpC protein were shown to be important for McsB-dependent activation of the ATPase subunit of the ClpCP protease complex (Elsholz et al., 2012). In the same study it has been shown that the arginine kinase McsB and the cognate phosphatase YwIE may influence the expression of different global regulons. However, the impact of arginine phosphorylation on the physiology of *B. subtilis* is not yet fully understood. Analyses of the dynamic changes in the arginine phosphoproteome in response to heat and oxidative stress revealed that only a minor fraction of the phosphorylation sites were differentially modified (Schmidt et al., 2014).

We are interested in the regulation of glutamate metabolism in *B. subtilis*. In addition to *de novo* synthesis of the important amino group donor glutamate, the bacteria may use glutamate as a source of carbon and nitrogen (for a recent review see Gunka and Commichau, 2012). Utilization of glutamate requires expression of the *rocG* and *gudB* genes encoding the catabolically active glutamate dehydrogenases (GDHs) RocG and GudB, respectively (Belitsky and Sonenshein, 1998; Gunka et al., 2013). Some isolates of *B. subtilis* like the “wild” ancestor strain NCIB3610 indeed synthesize two active GDHs allowing the bacteria to use glutamate as the single source of carbon and nitrogen (Zeigler et al., 2008; unpublished results). In the domesticated *B. subtilis* strain 168 only the *rocG* gene encodes a functional GDH (Belitsky and Sonenshein, 1998; Zeigler et al., 2008). In this strain, the *gudB^{CR}* gene is cryptic (CR) due to a perfect 18 bp-long direct repeat (DR). This occurs in the part of the gene encoding the active center of the enzyme (Belitsky and Sonenshein, 1998). The GudB^{CR} is enzymatically inactive and also subject to rapid proteolytic degradation, especially when the bacteria starve for nutrients, which is the case when bacteria enter stationary phase (Gerth et al., 2008; Gunka et al., 2012, 2013). Although ClpP was shown to slightly affect GudB^{CR} stability (Gerth et al., 2008), other factors that are involved in the recognition and degradation of the protein are unknown. Interestingly, McsB was shown to phosphorylate the inactive GudB^{CR} protein on four arginine residues (Elsholz et al., 2012). It is tempting to speculate that this phosphorylation serves as a label that directs the inactive GudB^{CR} protein to the proteolytic machinery (see below).

In the present study, we apply a visual screen that is based on a GFP-GudB^{CR} fusion to monitor the GudB^{CR} stability *in vivo*. By applying microscopical and biochemical techniques, we found that GFP and GudB^{CR} are simultaneously degraded. Thus, the visual screen is suitable to analyze the cellular amount of GudB^{CR}. To identify novel factors that are involved in GudB^{CR} degradation, we combined the visual screen with a transposon mutagenesis approach. Afterward we looked for mutants that show an increased fluorescence, indicating increased amounts of the GFP-GudB^{CR}

fusion. Among the transposants we found one insertion in the *mcsB* gene encoding the arginine kinase McsB. Moreover, inactivation of the cognate phosphatase YwIE resulted in a decreased fluorescence of a strain synthesizing the GFP-GudB^{CR} fusion. The possible mechanisms of how the activity of the kinase McsB and the cognate phosphatase YwIE affect the amount of the GudB^{CR} protein are discussed.

MATERIALS AND METHODS

CHEMICALS, MEDIA, AND DNA MANIPULATION

The oligonucleotides were purchased from Sigma-Aldrich (Germany) and are listed in **Table 1**. *B. subtilis* chromosomal DNA was isolated using the DNeasy Blood & Tissue Kit (Qiagen, Germany). Plasmids were isolated from *Escherichia coli* using the Nucleospin Extract Kit (Macherey and Nagel, Germany). PCR products were purified using the PCR Purification Kit (Qiagen, Germany). Phusion DNA polymerase, restriction enzymes and T4 DNA ligase were purchased from Thermo Scientific (Germany) and used according to the manufacturer's instructions. Other chemicals and media were purchased from Sigma-Aldrich (Germany), Carl Roth (Karlsruhe, Germany) and Becton Dickinson (Heidelberg, Germany). Sequencing of DNA was performed by the SeqLab Sequence Laboratories (Göttingen, Germany).

BACTERIAL STRAINS, GROWTH CONDITIONS, AND CONSTRUCTION OF MUTANT STRAINS

B. subtilis strains (**Table 2**) were grown in LB and SP medium, respectively. LB and SP plates were prepared by the addition of 17 g agar/l (Roth, Germany) to LB and SP (8 g nutrient broth/l, 1 mM MgSO₄, 13 mM KCl, supplemented after sterilization with 2.5 μM ammonium ferric citrate, 500 μM CaCl₂, and 10 μM MnCl₂), respectively. When required, media were supplemented with antibiotics at the following concentrations: ampicillin (100 μg/ml), kanamycin (10 μg/ml), chloramphenicol (5 μg/ml), lincomycin/erythromycin (25/2 μg/ml), tetracycline (12.5 μg/ml), and spectinomycin (150 μg/ml). *B. subtilis* was transformed with plasmid and chromosomal DNA according to a previously described two-step protocol (Kunst and Rapoport, 1995).

CONSTRUCTION OF PLASMIDS

The plasmids for complementation of the *ywIE* and *mcsB* mutations in *B. subtilis* were constructed as follows. The *ywIE* and *mcsB* genes were amplified by PCR from chromosomal DNA using the oligonucleotide pairs LS92/LS93 and LS97/LS98, respectively (**Table 1**). The PCR products were digested with the enzymes *Bam*HI and *Pst*I and ligated to the plasmid pBQ200 that was cut with the same enzymes. The plasmids harboring the *ywIE* and *mcsB* genes and their native ribosome-binding sites were designated pBP183 and pBP186, respectively. Expression of the genes is driven by the constitutively active *P_{degQ}* promoter (Martin-Verstraete et al., 1994). The quadruple *gfp-gudB^{CR}* mutant (designated as *gfp-gudB^{CR}-mut*), encoding the GudB^{CR} protein in which the arginine residues 56, 83, 421, and 423 were replaced by lysine, was constructed by the Multiple-mutation reaction (MMR; Hames et al., 2005). The mutated *gudB^{CR}* allele was amplified with the oligonucleotide pair KG188/LS96 and the

Table 1 | Oligonucleotides used in this study.

Name	Sequence	Purpose
KG166	5'-GCGGGATACGTTTTACCC	direct repeat analysis
KG167	5'-CACCGCCATATGGAAGATC	direct repeat analysis
KG180	5'-TTTGTATAGTTCATCCATGCCATGTGTAATC	Construction of plasmid pBP187
KG181	5'-ACATGGCATGGATGAACATACAAA ATGGCAGCCGATCGAAACACCG	Construction of plasmid pBP187
KG184	5'-AAAGAATTCTCATTATATCCAGCCTCTAAAACGCG	Construction of plasmid pBP4
KG185	5'-TTTGGATCCCATTACAGCTTTCAGAAAGCTTACAGCGAATC	Construction of plasmid pBP4
KG188	5'-AAACAATTGCATTACAGCTTTCAGAAAGCTTACAGCGAATC	Construction of plasmid pBP184
KG190	5'-AAAGAATTCAAAGGAGGAAACAATCATGAGTAAAGG AGAAG AACTTTTCACT	Construction of plasmid pBP187
LS92	5'-AAAGGATCCAATAGAGAAAAATAAGGGGTGA CTGACATGGATATTA	Construction of plasmid pBP183
LS93	5'-TTTCTGCAGTTATCTACGGTCTTTTTTCAGCTGTTTTGCCAG	Construction of plasmid pBP183
LS94	5'-P-TAACGGTAAAAATACCTGTTAAGATGGACGAC GGTTACAGTAAAG	Construction of plasmid pBP184
LS95	5'-P-AACGAAAGGCGGGATAAAGTTTACCCGAACGTAACA	Construction of plasmid pBP184
LS96	5'-TTTGGATCCTTATATCCAGCCCTTAAACTTCGAAGCTT CAGCCATTTTG	Construction of plasmid pBP184
LS97	5'-AAAGGATCCGTACAGATAGTGAGGAGAACAGGAGTAA	Construction of plasmid pBP186
LS98	5'-TTTCTGCAGTCATATCGATTATCCTCCTGTCTTTTCCC	Construction of plasmid pBP186
pIC333_seq up	5'-AAGAGCGCCCAATACGCAACCGCC	Sequencing transposon plasmids
pIC333_seq down	5'-TTTGCATGCTTCAAAGCCTGTCTGGAATTGG	Sequencing transposon plasmids

Table 2 | *Bacillus subtilis* strains used in this study.

Name	Relevant genotype	Reference or source ^a
168	<i>trpC2</i>	Laboratory collection
BP25	<i>trpC2 Δ gudB::aphA3 amyE::(gfp-gudB^{CR} cat)</i>	pBP8 → GP1160
BP26	<i>trpC2 Δ gudB::aphA3 amyE::(gfp-gudB cat)</i>	pBP9 → GP1160
BP69	<i>trpC2 Δ gudB::aphA3 mcsB::Tn 10 spc amyE::(gfp-gudB^{CR} cat)</i>	pIC333 → BP25
BP74	<i>trpC2 Δ gudB::aphA3 ywIE::tet amyE::(gfp-gudB^{CR} cat)</i>	GP1459 → BP25
BP75	<i>trpC2 Δ gudB::aphA3 ywIE::tet amyE::(gfp-gudB cat)</i>	GP1459 → BP26
BP98	<i>trpC2 Δ gudB::aphA3 amyE::(gfp-gudB cat) clpC::spc</i>	<i>clpC::spc</i> → BP25
BP99	<i>trpC2 Δ gudB::aphA3 amyE::(gfp-gudB cat) clpP::tet</i>	<i>clpP::tet</i> → BP25
BP230	<i>trpC2 Δ gudB::aphA3 amyE::(gfp-gudB^{CR} R56K, R83K, R421K, R423K cat)</i>	pBP187 → GP1160
BP231	<i>trpC2 Δ gudB::aphA3 mcsB::Tn 10 spc amyE::(gfp-gudB^{CR} R56K, R83K, R421K, R423K cat)</i>	BP69 → BP230
BP311	<i>trpC2 Δ gudB::aphA3 mcsB::Tn 10 spc amyE::(gfp-gudB cat)</i>	pBP45 → BP26
GP1160	<i>trpC2 Δ gudB::aphA3</i>	Gunka et al. (2012)
GP1459	<i>trpC2 Δ ywIE::tet</i>	BDO01 → 168

^aArrows indicate construction by transformation.

mutagenic oligonucleotides LS94, LS95, and LS96 using plasmid pBP4 as a template. The MMR product was digested with the enzymes *MfeI* and *BamHI*, and ligated to the plasmid pAC5 that was cut with the enzymes *EcoRI* and *BamHI*. The resulting plasmid was designated as pBP184. This plasmid was used to amplify the promoterless quadruple *gudB^{CR}* mutant allele by PCR using the oligonucleotide pair KG181/LS96. The *gfp* gene

containing the ribosome-binding site of the *B. subtilis gapA* gene was amplified by PCR from plasmid pBP8 using the oligonucleotide pair KG180/KG190. The *gfp* and *gudB^{CR}* genes were fused by PCR using the external oligonucleotides KG190 and LS96, the PCR product was digested with *BamHI* and *EcoRI*, and ligated to the plasmid pBP7 that was cut with the same enzymes. The resulting plasmid pBP187 contains the native *gudB* promoter and

integrates in single copy into the *amyE* locus. Replacement of the arginine codons in the *gfp-gudB^{CR}* gene was confirmed by DNA sequencing. All cloning procedures were performed with the *E. coli* strain DH5α (Sambrook et al., 1989).

TRANSPOSON MUTAGENESIS

For transposon mutagenesis of the *B. subtilis* strain BP25, we used the mini-Tn10 delivery vector pIC333 (Steinmetz and Richter, 1994) as described previously (Chauvaux et al., 1998). The transposants were grown on SP agar plates for 48 h at 42°C and the intensity of the GFP signal was evaluated by stereo fluorescence microscopy. For the determination of the site of mini-Tn10 insertion, we made use of the fact that the integrated DNA fragment does not contain any *EcoRI* restriction sites. The chromosomal DNA of the mutants was digested with *EcoRI* and re-ligated. The ligation mixture was used to transform *E. coli* DH5α (Sambrook et al., 1989). For all mutants that were further analyzed, we obtained plasmids conferring spectinomycin resistance (Table 3). The insertion sites of the mini-Tn10 transposon were determined by DNA sequencing of the plasmids using the oligonucleotides pIC333_seq up and pIC333_seq down.

WESTERN BLOTTING

For Western blot analyses, proteins present in 20–50 µg of cell free crude extracts were separated by 12.5% SDS PAGE and transferred onto polyvinylidene difluoride membrane (BioRad, Germany) by semi-dry electroblotting. Anti-GFP (PromoKine, Germany; MBL, Japan), anti-YwIE, anti-McsB, and anti-GapA polyclonal antibodies were diluted 1:10.000, 1:1000, 1:5.000, and 1:30.000, respectively, and served as primary antibodies. The antibodies were visualized using anti-rabbit immunoglobulin alkaline phosphatase secondary antibodies (Promega, Germany) and the

CDP-Star detection system (Roche Diagnostics, Switzerland) as described previously (Commichau et al., 2007).

FLUORESCENCE MICROSCOPY

For fluorescence microscopy, cells were grown in SP medium to optical densities as indicated, and analyzed on agarose microscopy slides. Fluorescence images were obtained with an Axioskop 40 FL fluorescence microscope, equipped with digital camera Axio-Cam MRm and AxioVision Rel (version 4.8) software for image processing (Carl Zeiss, Göttingen, Germany) and Neofluar series objective at x 100 primary magnification. The applied filter set was eGFP HC-Filterset (band-pass [BP] 472/30, FT 495, and long-pass [LP] 520/35; AHF Analysentechnik, Tübingen, Germany) for GFP detection. Pictures of *B. subtilis* colonies were taken with a stereo fluorescence microscope Lumar.V12 (Zeiss, Jena, Germany) equipped with the ZEN lite 2011 (blue edition) software. The applied filter set was Lumar 38 for eGFP detection (Zeiss, Jena, Germany). Images were taken at room temperature and an exposure time of 1 s.

MONITORING GFP-GudB^{CR} LEVELS IN GROWING CULTURES

Cellular amounts of the GFP-GudB^{CR} fusion protein were determined by monitoring the fluorescence (excitation 489/9.0 nm, emission 509/9.0 nm) in a growing bacterial culture using the Synergy MX II multimode microplate reader (BioTek). For this purpose, 4 ml LB medium were inoculated with the precultures to an OD₆₀₀ of 0.1. The cultures, that had an approximate OD₆₀₀ of 1.0, were used to inoculate a 96 well plate (Corning, Sigma) containing 180 µl medium per well. To avoid evaporation, the outermost wells were filled with 200 µl sterile water. The plates were incubated for a maximum of 10 h at 37°C and fast shaking speed. OD₆₀₀ was measured every 10 min throughout the experiment. Background fluorescence of the parental strains was subtracted from the raw fluorescence of all *gfp* fusion strains at the same OD₆₀₀. The cellular amounts of the GFP-GudB^{CR} fusion protein correspond to the fluorescence divided by the OD₆₀₀ at each time point.

RESULTS

A STABLE SCREENING SYSTEM FOR IDENTIFYING FACTORS INVOLVED IN GudB^{CR} DEGRADATION

The fact that also the GFP-GudB^{CR} protein is degraded (Gunka et al., 2012, 2013) qualifies it as a substrate to uncover the proteolytic machinery. Before identifying factors that contribute to GudB^{CR} degradation, we constructed the *rocG* plus strain BP25 that is genetically stable (Gunka et al., 2012) and synthesizes the active GDH RocG as well as the inactive GFP-GudB^{CR} fusion. To test if the GFP-GudB^{CR} fusion protein is degraded in this strain, we compared the fluorescence signal of cells to those of strain BP26 harboring the active *gfp-gudB* fusion. As shown in Figure 1A, while the bacteria with the active GFP-GudB fusion were strongly fluorescent, the fluorescence signal of bacteria synthesizing the inactive GFP-GudB^{CR} protein was reduced. Thus, the inactive GFP-GudB^{CR} fusion is also degraded in the new strain background. We also tested whether the two strains can be distinguished from each other by monitoring the fluorescence emitted by colonies that were grown on rich

Table 3 | Plasmids used and constructed in this study.

Name	Purpose	Reference or source
pIC333	Transposon mutagenesis	Steinmetz and Richter (1994)
pAC5	Integration of DNA into the <i>amyE</i> locus	Martin-Verstraete et al. (1992)
pBQ200	Complementation studies	Martin-Verstraete et al. (1994)
pBP4	<i>PgudB^{CR} -gudB^{CR}</i> in pAC5	This work
pBP7	<i>PgudB^{CR}</i> in pAC5	Gunka et al. (2013)
pBP8	<i>gfp-gudB^{CR}</i> in pBP7	Gunka et al. (2013)
pBP45	Transposon plasmid <i>mcsB</i>	This work
pBP183	Expression of <i>ywIE</i>	This work
pBP184	Expression of <i>gudB^{CR}</i> (R56K R83K R421K R423K)	This work
pBP186	Expression of <i>mcsB</i>	This work
pBP187	Expression of <i>gfp-gudB^{CR}</i> (R56K R83K R421K R423K)	This work

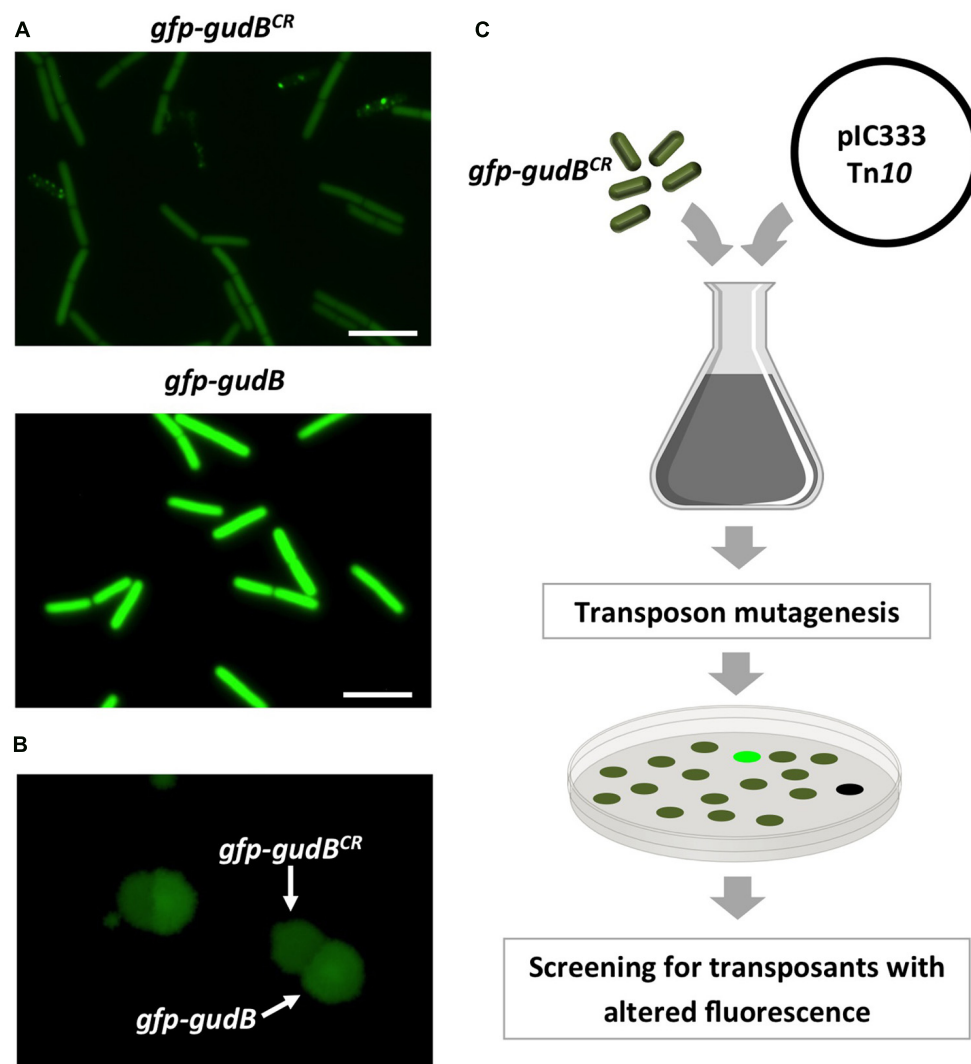


FIGURE 1 | Fluorescence of strains BP25 (*gfp-gudB^{CR}*) and BP26 (*gfp-gudB*) synthesizing the GFP-GudB^{CR} and GFP-GudB proteins, respectively, at the single cell (A) and at the colony level (B); transposon mutagenesis to identify factors involved in GFP-GudB^{CR} degradation (C).

For single cell analysis the bacteria were grown in SP medium. Exposure time, 5 s; scale bar, 5 μ m. To monitor fluorescence of colonies the strains were grown in SP medium, mixed and appropriate dilutions were propagated on SP plates, which were incubated for 24 h at 37°C. Exposure time, 1 s.

medium agar plates. For this purpose, the strains BP25 (*gfp-gudB^{CR}*) and BP26 (*gfp-gudB*) were grown in liquid medium, mixed in a 1:1 ratio and appropriate dilutions were propagated on SP plates to allow growth of individual colonies. By visual inspection of the plates using a stereo fluorescence microscope we found several colonies that were grown close to each other and showed different fluorescence signals (Figure 1B). We then re-streaked some of the colonies showing different fluorescence signals on agar plates to obtain individual colonies. Next, we performed colony PCRs and confirmed that the higher and lower fluorescence signals were due to the presence of the *gfp-gudB* and *gfp-gudB^{CR}* alleles, respectively. In conclusion, the visual screen seems to be suitable to look for mutants, lacking factors that enhance or decrease proteolytic degradation of GFP-GudB^{CR}.

IDENTIFICATION OF MscB CONTRIBUTING TO GudB^{CR} DEGRADATION

To identify factors that are involved in degradation or stabilization of GudB^{CR}, we performed a transposon mutagenesis with strain BP25 (*gfp-gudB^{CR}*) using the mini-Tn10 delivery vector pIC333 (Steinmetz and Richter, 1994). Afterward, we screened for mutants that show an altered fluorescence signal using a stereo fluorescence microscope (Figure 1C). Appropriate dilutions of the transposants were propagated on SP plates that were incubated for 48 h at 42°C. By visual inspection of about 8000 transposants we could identify one mutant that showed no fluorescence signal, whereas a second mutant showed an increase in fluorescence intensity. While the first mutant had obviously lost the ability to synthesize GFP because the transposon was inserted into the *gfp* gene, the mutant showing increased fluorescence had integrated the transposon at position 580 into the arginine kinase encoding

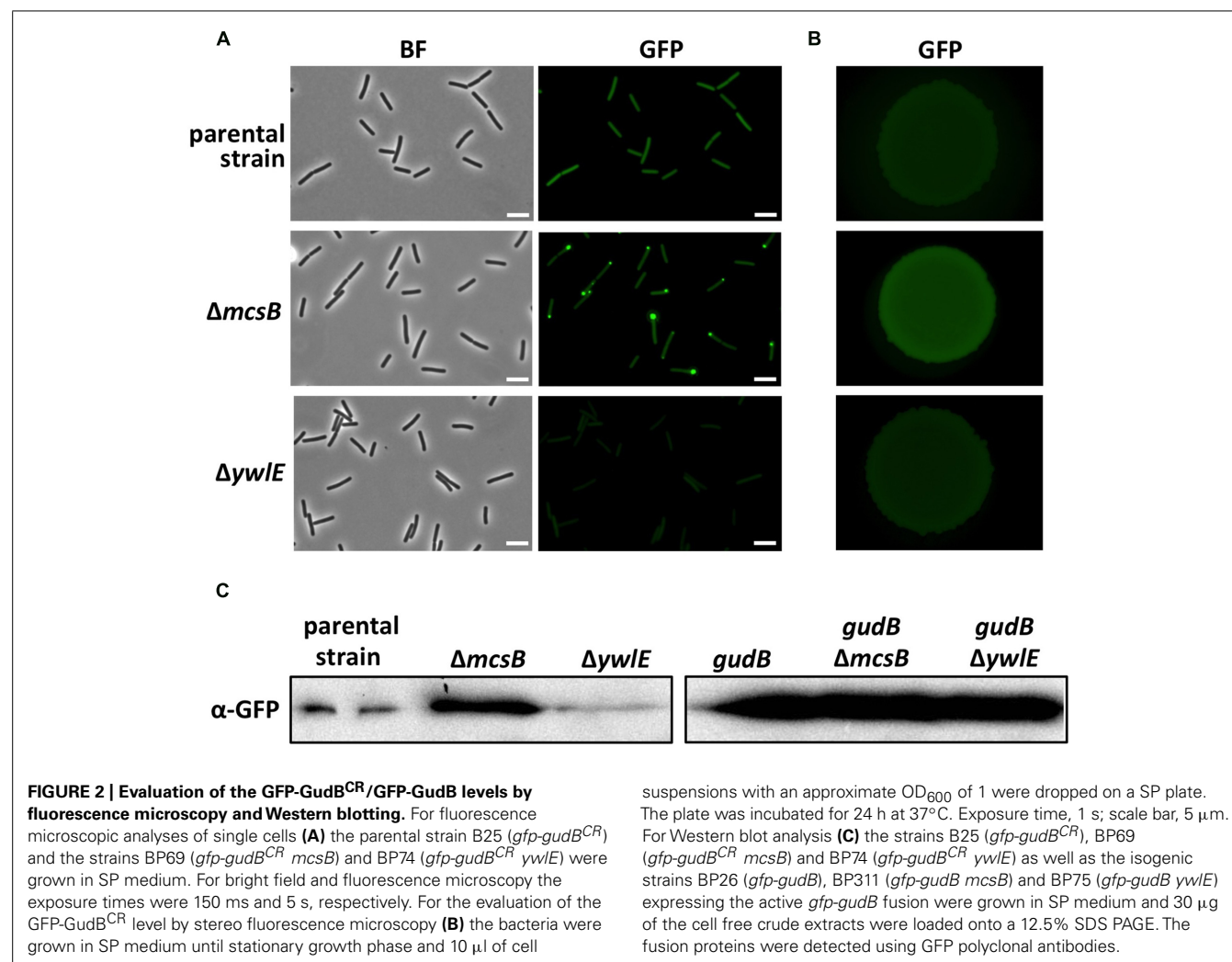
mcsB gene (Fuhrmann et al., 2009). This transposon mutant was designated as BP69. A re-evaluation of the fluorescence signal of single cells and of a colony of the *mcsB* transposon mutant revealed that the cellular amount of the GFP-GudB^{CR} fusion was increased when compared to that of the parent strain BP25 (Figures 2A,B). The lack of McsB also resulted in the formation of large aggregates of the GFP-GudB^{CR} fusion protein at the cell poles (Figure 2A), an observation that can be made when aggregation prone proteins are synthesized in bacteria (Rokney et al., 2009; Villar-Pique et al., 2012). In conclusion, using transposon mutagenesis in combination with a visual screen, we identified the arginine kinase McsB being a novel factor that contributes to GudB^{CR} degradation.

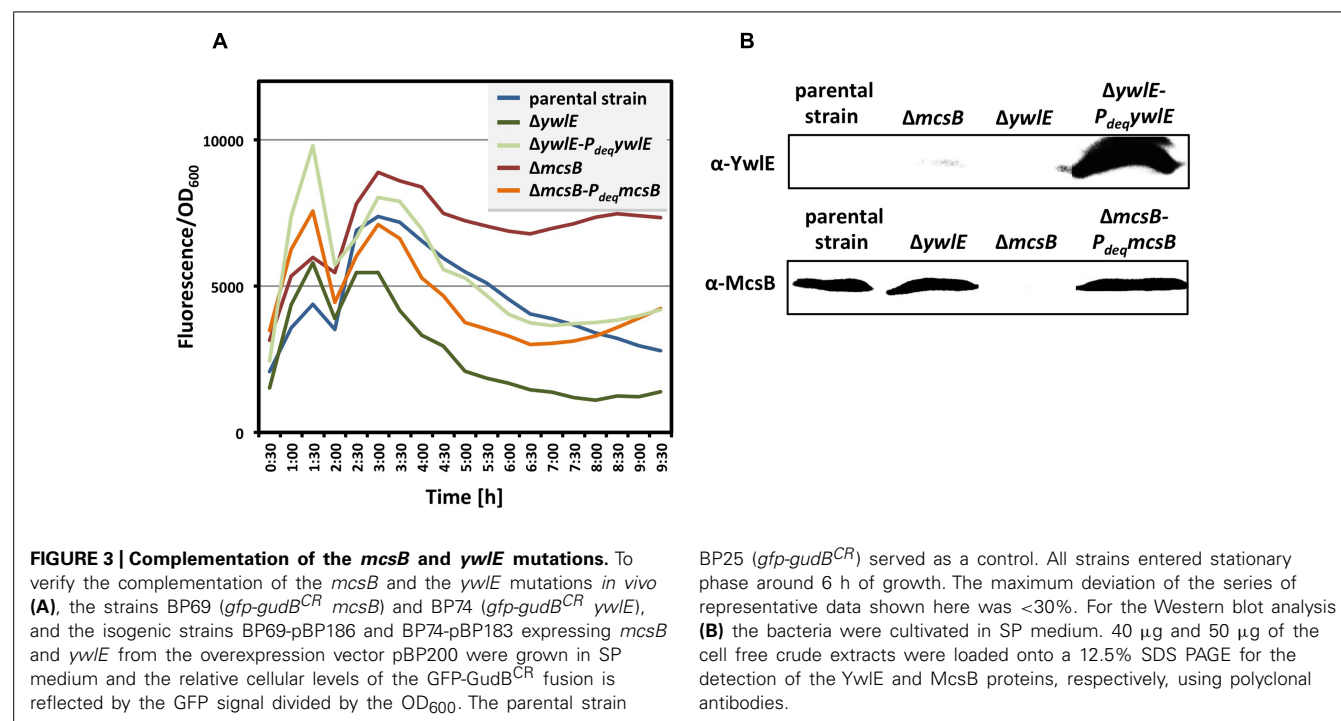
McsB AND YwlE ARE INVOLVED IN GudB^{CR} STABILITY

To underpin the role of arginine phosphorylation in the degradation of the GudB^{CR} protein, we inactivated the *ywlE* gene in the strain BP25 (*gfp-gudB^{CR}*). In case the arginine phosphatase YwlE counteracts the function of its cognate kinase McsB, we expected to observe that single cells as well as colonies of the *ywlE* mutant BP74 would show a reduced fluorescence. This was indeed the case

for single cells of the *ywlE* mutant strain in comparison to cells of the *mcsB* mutant and parent strains BP69 and BP25, respectively (Figure 2A). Although less pronounced, fluorescence of the *ywlE* mutant was also reduced at the level of single colonies (Figure 2B). However, a quantification of the fluorescence of the GFP-GudB^{CR} fusion protein monitored in growing cultures in the *ywlE* mutant strain clearly demonstrates that the phosphatase YwlE affects GudB^{CR} stability (see below, Figure 3A).

Next, we confirmed that the kinase McsB and the phosphatase YwlE affect the cellular levels of the GFP-GudB^{CR} fusion protein. For this purpose, we cultivated the parent strain BP25 as well as the *mcsB* and *ywlE* mutant strains BP69 and BP74, respectively, in SP medium until stationary phase (the OD₆₀₀ was around 3.0) and analyzed the amounts of the GFP-GudB^{CR} fusion protein by Western blotting using GFP-specific antibodies. As shown in Figure 2C, in strain BP69 lacking McsB the cellular amount of the GFP-GudB^{CR} fusion protein was strongly increased. By contrast, the inactivation of the *ywlE* gene resulted in a decrease of GFP-GudB^{CR} levels. In conclusion, the semi-quantitative Western Blot analyses are in perfect agreement with the fluorescence microscopical studies.





McsB AND YwIE DO NOT INFLUENCE THE CELLULAR LEVELS OF THE ACTIVE GudB PROTEIN

Subsequently, we wanted to answer the question of whether McsB and YwIE do also influence the cellular amounts of the enzymatically active GFP-GudB fusion protein lacking the duplication of three amino acids in the active center of the enzyme. For this purpose, we cultivated the parent strain BP26 (*gfp-gudB*) synthesizing the active GFP-GudB fusion and the isogenic *mcsB* and *ywIE* mutant strains BP311 and BP75 (Table 2), respectively, in SP medium until stationary phase (OD₆₀₀ of about 3.0). Afterward, we quantified the amount of the GFP-GudB protein by Western blotting using antibodies specific for GFP. As shown in Figure 2C, irrespective of the absence of either McsB or YwIE all strains synthesized similar amounts of the active GFP-GudB fusion protein. In conclusion, only the cellular amount of the inactive GFP-GudB^{CR} but not that of the active GFP-GudB fusion protein is significantly affected by McsB.

COMPLEMENTATION OF THE *mcsB* AND *ywIE* MUTATIONS

For complementation studies of the *mcsB* and *ywIE* mutant strains BP69 and BP74, respectively, we constructed the plasmids pBP186 (*mcsB*) and pBP183 (*ywIE*). Both plasmids are derivatives of the non-integrative overexpression plasmid pBQ200 and gene expression is driven by the constitutively active *P_{degQ}* promoter (Martin-Verstraete et al., 1994). The plasmids pBP186 and pBP183 were introduced into the corresponding mutant strains by transformation. Next, we compared the cellular amounts of the GFP-GudB^{CR} fusion protein in the *mcsB* and *ywIE* mutant strains BP69 and BP74, respectively, with those of the isogenic complementation strains by monitoring the fluorescence, which reflects the cellular amounts of the GFP-GudB^{CR} fusion protein during growth of the bacteria. The parent strain BP25 (*gfp-gudB^{CR}*)

served as a control. As shown in Figure 3A, the emitted fluorescence of all cultures was similar during exponentially growth. In the stationary phase the fluorescence signal was much higher in the *mcsB* mutant strain BP69 when compared to that of the parent strain BP25. By contrast, inactivation of the *ywIE* resulted in a strong decrease of the fluorescence signal. Overexpression of the *mcsB* and *ywIE* genes in the *mcsB* and *ywIE* mutant strains BP69 and BP74, respectively, restored the fluorescence signal in the stationary phase almost to the extent of the parent strain. Western blot experiments using antibodies specific for McsB and YwIE confirmed overexpression of the arginine kinase and the phosphatase from the complementation plasmids in the *mcsB* and *ywIE* mutant strains BP69 and BP74, respectively (Figure 3B). In conclusion, the cultivation experiments to detect the cellular levels of the GFP-GudB^{CR} fusion protein are in good agreement with the previous experiments showing that the lack of the McsB and YwIE results in elevated and reduced levels, respectively, of the inactive GDH. Moreover, together with the Western blot experiments the cultivation experiments also revealed that the *mcsB* and *ywIE* mutations can be complemented by expressing the *mcsB* and *ywIE* genes from plasmids.

McsB SEEMS TO ACT INDEPENDENTLY OF ClpC AND ClpP ON GudB^{CR} DEGRADATION

The *mcsB* gene lies immediately upstream of the *clpC* gene in the *ctsR mcsA mcsB clpC* operon. Since the *mcsB* mutation can be complemented, it can be ruled out that enhanced cellular levels of the GFP-GudB^{CR} fusion are a consequence of a polar effect of the transposon insertion into the *mcsB* gene leading to a reduced *clpC* expression and a lower proteolytic activity. However, the lower proteolytic activity in the *mcsB* mutant strain might be due to the missing of McsB-dependent activation of the ClpC-ClpP

protease complex. To exclude this possibility, we compared the cellular amounts of the GFP-GudB^{CR} fusion in the background of the *clpC* and *clpP* mutant strains BP98 and BP99, respectively, to that of the parent strain BP25 (*gfp-gudB^{CR}*). For this purpose, we grew the bacteria in SP medium and collected samples from exponential and stationary phases and performed Western blot analyses (Figure 4). The strain BP26 (*gfp-gudB*) as well as the *mcsB* and *ywlE* mutant strains BP69 and BP74, respectively, served as controls. As expected, in contrast to the inactive GFP-GudB^{CR} fusion protein the active GFP-GudB variant was more abundant during exponential and stationary phase. Moreover, as observed in the previous experiments, the GFP-GudB^{CR} levels were increased and decreased in the *mcsB* and *ywlE* mutants, respectively (see also Figure 2C). Finally, the GFP-GudB^{CR} levels in the *clpC* and *clpP* mutant strains BP98 and BP99, respectively, were similar to that of the parent strain BP25 (*gfp-gudB^{CR}*). Using GapA and GFP antibodies, we show that only the GFP-GudB^{CR} fusion but not GapA was degraded in stationary growth phase samples. Thus, McsB is involved in GudB^{CR} degradation in a rather ClpP and ClpC-independent manner.

REPLACEMENT OF PHOSPHORYLATION SITES DOES NOT AFFECT McsB-DEPENDENT GudB^{CR} DEGRADATION

In a recent phosphoproteome analysis it has been shown that the inactive GudB^{CR} protein is phosphorylated on the arginine residues at positions 56, 83, 421, and 423 (Elsholz et al., 2012). To evaluate whether phosphorylation of these sites is important for the degradation of the GFP-GudB^{CR} protein, we replaced the arginine by the structurally similar amino acid lysine and monitored the amount of the GudB^{CR} variant *in vivo*. For this purpose the parent strain BP25 (*gfp-gudB^{CR}*), the *mcsB* mutant strain BP69 (*mcsB*gfp-gudB^{CR}), the quadruple GFP-GudB^{CR} mutant strain BP230 (*gfp-gudB^{CR}-mut* (R56K R83K R421K R423K)), and the isogenic *mcsB* mutant strain BP231 (*mcsB*gfp-gudB^{CR}-mut (R56K R83K R421K R423K)) were cultivated in SP medium. Simultaneously, the cellular levels of the fusion proteins were determined by monitoring the fluorescence during bacterial growth. As shown in Figure 5, the fluorescence measurements revealed that the cellular levels of the fusion proteins in strains BP25 (*gfp-gudB^{CR}*) and BP230 (*gfp-gudB^{CR}-mut* (R56K R83K R421K R423K)) was much

lower in comparison to those of the isogenic *mcsB* mutant strains BP69 (*mcsB* gfp-gudB^{CR}), and BP231 (*mcsB* gfp-gudB^{CR}-mut (R56K R83K R421K R423K)). In conclusion, these observations suggest that phosphorylation of the arginine residues 56, 83, 421, and 423 sites is rather not important for the degradation of the inactive GudB^{CR} protein.

DISCUSSION

In the present study, we found that the inactivation of the *mcsB* arginine kinase gene resulted in stabilization of the inactive GDH GudB^{CR} during stationary growth phase of *B. subtilis*. Thus, beside its role in controlling the degradation of the DNA-binding transcription factor CtsR (Elsholz et al., 2010b) and delocalization of proteins involved in the development of transformability of *B. subtilis* (Hahn et al., 2009), McsB activity also mediates degradation of GudB^{CR}. Moreover, we found that the arginine phosphatase YwlE counteracts the function of McsB and prevents degradation of GudB^{CR}.

There are several possibilities how McsB and YwlE might stimulate and prevent GudB^{CR} degradation, respectively. As it has been reported previously for the proteolytic degradation of CtsR (Elsholz et al., 2012), McsB-dependent activation of the ATPase subunit ClpC of the ClpCP protease complex by phosphorylation of two specific arginine residues could also be crucial for GudB^{CR} degradation. However, according to our Western blot analysis ClpP and ClpC appear apparently not involved in GudB^{CR} degradation. Recent global phosphoproteomic studies have revealed that in the absence of YwlE several proteins, among them the GudB^{CR} protein are phosphorylated on arginine residues (Elsholz et al., 2012; Schmidt et al., 2014; Trentini et al., 2014). These studies prompted us to address the question of whether the phosphorylation of GudB^{CR} by McsB could serve as a label for proteolysis. However, although the cellular levels of the GudB^{CR} quadruple mutant, in which the arginine residues 56, 83, 421, and 423 were replaced by lysine residues, were slightly increased, the protein was still degraded in a McsB-dependent manner when the bacteria entered stationary phase (see Figure 5). Thus, the degradation of GudB^{CR} seems to be rather indirectly influenced by McsB. Finally, an unknown proteolytic machinery that remains to be identified might be responsible for the degradation of the misfolded and

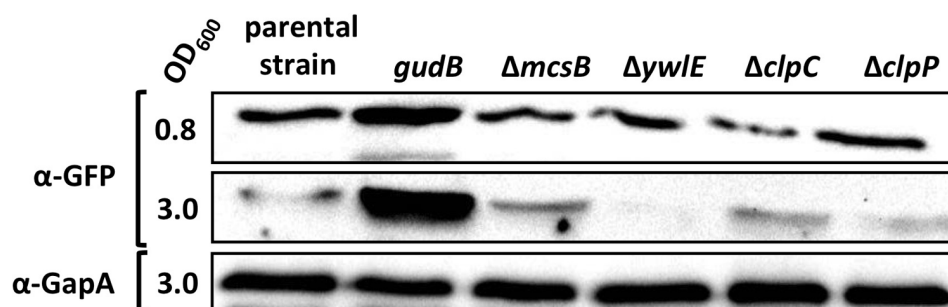


FIGURE 4 | McsB acts independently of ClpC and ClpP. For the Western blot analysis the parental strain BP25 (*gfp-gudB^{CR}*) and the strains BP26 (*gfp-gudB*), BP69 (*gfp-gudB^{CR} mcsB*), BP74 (*gfp-gudB^{CR} ywlE*), BP98 (*gfp-gudB^{CR} clpC*), and BP99 (*gfp-gudB^{CR} clpP*) were

cultivated in SP medium until the indicated optical densities (OD₆₀₀). 30 μg of the cell free crude extracts were loaded onto a 12.5% SDS PAGE for the detection of the GFP and GapA proteins using polyclonal antibodies.

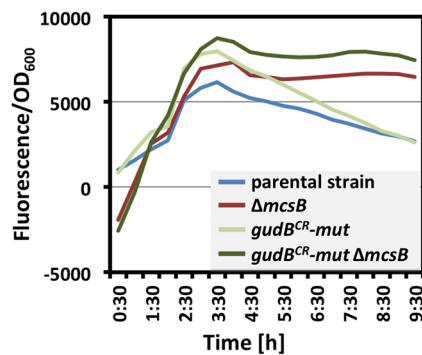


FIGURE 5 | Impact of McsB on the cellular levels of the GFP-GudB^{CR} and GFP-GudB^{CR}(R56K, R83K, R421K, R423K) proteins. The strains BP25 (*gfp-gudB^{CR}*), BP69 (*gfp-gudB^{CR} mcsB*), BP230 (*gfp-gudB^{CR}-mut*), and BP231 (*gfp-gudB^{CR}-mut mcsB*) were cultivated in SP medium and the relative cellular levels of the GFP-GudB^{CR} fusion is reflected by the GFP signal divided by the OD₆₀₀. The parental strain BP25 (*gfp-gudB^{CR}*) served as a control. All strains entered stationary phase around 6 h of growth. The maximum deviation of the series of representative data shown here was <30%.

inactive GDH GudB^{CR}. On one hand the activity of the proteolytic machinery might be controlled by McsB-dependent phosphorylation of an unknown adaptor protein that specifically recognizes GudB^{CR} and directs the protein to the protease for degradation. On the other hand McsB could be important for the activation of one of the AAA+ proteases or other unknown proteases that remain to be identified. One could also envision that McsB acts itself as the adaptor that mediates proteolysis of the GudB^{CR} protein. The interaction between McsB and GudB^{CR} could result in coincidental phosphorylation of the GDH. This could also be the case for the other arginine phosphorylations of the *B. subtilis* proteome (Elsholz et al., 2012).

As described above it is interesting to note that only the domesticated *B. subtilis* strains 160, 166, and 168, of which the latter one is used worldwide in basic research and in industry, harbor the *gudB^{CR}* gene that is enzymatically inactive and unstable (Zeigler et al., 2008). It has been suggested that the *gudB^{CR}* allele appeared as a consequence of X-ray mutagenesis and subsequent adaptation for rapid growth of the bacteria in minimal medium lacking the amino group donor glutamate (Burkholder and Giles, 1947). This hypothesis is supported by the observation that a strain that synthesizes in addition to RocG also the enzymatically active GDH GudB is rapidly outcompeted by the laboratory strain 168 (*rocG gudB^{CR}*) when exogenous glutamate is not available (Gunka et al., 2013; Stannek et al., 2014). Obviously, the presence of both, RocG and GudB is disadvantageous for the bacteria because the catabolic GDHs degrade the endogenously produced glutamate, which is needed in anabolism. Thus, under laboratory growth conditions a permanent selective pressure must act on the bacteria, which prevents the accumulation of mutants that have spontaneously mutated the cryptic *gudB^{CR}* gene and synthesize in addition to RocG the functional GDH GudB. Moreover, the selective pressure acting on the *B. subtilis* strain 168 might be an explanation for the observation that the cryptic *gudB^{CR}* gene is stably inherited since the bacterium has been domesticated. Recently, it has been shown

that bacteria rapidly lose genes and reduce their genome sizes when adapted to specialized environments. This might also be observed in the laboratory by experimental evolution of bacterial cell populations (Koskiniemi et al., 2012; Lee and Marx, 2012). Therefore, it is somewhat surprising that *B. subtilis* affords to waste energy by permanently synthesizing an inactive enzyme that is subject to rapid degradation. However, under certain growth conditions it must be advantageous for *B. subtilis* to harbor the cryptic *gudB^{CR}* gene that, when activated by spontaneous mutagenesis (Gunka et al., 2012), encodes a functional GDH. Indeed, a derivative of the *B. subtilis* 168 expressing *rocG* and *gudB* can use glutamate as a single source of carbon and nitrogen (Gunka et al., 2013). Thus, under very specific nutritional conditions bacteria that are endowed with high-level GDH activity have a strong selective growth advantage.

In the future it will be interesting to identify additional factors that are involved in the rapid degradation of the enzymatically inactive GDH GudB^{CR}. This goal might be achieved by monitoring the cellular amounts of the GFP-GudB^{CR} fusion protein in a mutant collection that have inactivated all non-essential genes by targeted gene deletion or by a next time saturated transposon mutagenesis. The identification of novel factors that are involved in GFP-GudB^{CR} proteolysis might be facilitated by monitoring growth and fluorescence over time because the fusion protein seems to be preferentially degraded in stationary phase. Moreover, it will be interesting to address the question whether arginine phosphorylation influences the physiological functions of other proteins in *B. subtilis*.

ACKNOWLEDGMENTS

This work was supported by the grant CO 1139/1-1 of the Deutsche Forschungsgemeinschaft (<http://www.dfg.de>), the Fonds der Chemischen Industrie (<http://www.vci.de/fonds>), the Göttingen Centre for Molecular Biology (GZMB), and the Max-Buchner-Forschungsförderung (<http://www.dechema.de/mbf.html>; MBFSt-Kennziffer 3381) to Fabian M. Commichau. Work of Katrin Gunka in the authors' lab was supported by the grant SFB860. Sabine Lentz is acknowledged for expert technical support. We are grateful to Miriam Dormeyer for critical reading of the manuscript and for helpful discussions.

REFERENCES

- Battesti, A., and Gottesmann, S. (2013). Roles of adaptor proteins in regulation of bacterial proteolysis. *Curr. Opin. Microbiol.* 16, 140–147. doi: 10.1016/j.mib.2013.01.002
- Belitsky, B. R., and Sonenshein, A. L. (1998). Role and regulation of *Bacillus subtilis* glutamate dehydrogenase genes. *J. Bacteriol.* 180, 6298–6305.
- Bird, T. H., Grimsley, J. K., Hoch, J. A., and Spiegelman, G. B. (1993). Phosphorylation of Spo0A activates its stimulation of in vitro transcription from the *Bacillus subtilis* spoIIIG operon. *Mol. Microbiol.* 9, 741–749. doi: 10.1111/j.1365-2958.1993.tb01734.x
- Burkholder, P. R., and Giles, N. H. (1947). Induced biochemical mutations in *Bacillus subtilis*. *Am. J. Bot.* 34, 345–348. doi: 10.2307/2437147
- Chauvaux, S., Paulsen, I. T., and Saier, M. H. Jr. (1998). CcpB, a novel transcription factor implicated in catabolite repression in *Bacillus subtilis*. *J. Bacteriol.* 180, 491–497.
- Commichau, F. M., Herzberg, C., Tripal, P., Valerius, O., and Stülke, J. (2007). A regulatory protein-protein interaction governs glutamate biosynthesis in *Bacillus subtilis*: the glutamate dehydrogenase RocG moonlights in

- controlling the transcription factor GltC. *Mol. Microbiol.* 65, 642–654. doi: 10.1111/j.1365-2958.2007.05816.x
- Cozzzone, A. J., and El-Mansi, M. (2005). Control of isocitrate dehydrogenase catalytic activity by protein phosphorylation in *E. coli*. *J. Mol. Microbiol. Biotechnol.* 9, 132–146. doi: 10.1159/000089642
- Derouiche, A., Bidnenko, V., Grenha, R., Pignonneau, N., Ventroux, M., Franz-Wachtel, M., et al. (2013). Interaction of bacterial fatty-acid-displaced regulators with DNA is interrupted by tyrosine phosphorylation in the helix-turn-helix domain. *Nucleic. Acids Res.* 41, 9371–9381. doi: 10.1093/nar/gkt709
- Derré, I., Rapoport, G., and Msadek, T. (1999). CtsR, a novel regulator of stress and heat shock response, controls clp and molecular chaperone gene expression in Gram-positive bacteria. *Mol. Microbiol.* 31, 117–131. doi: 10.1046/j.1365-2958.1999.01152.x
- Deutscher, J., and Saier, M. H. Jr. (2005). Ser/Thr/Tyr protein phosphorylation in bacteria – for long time neglected, now well established. *J. Mol. Microbiol. Biotechnol.* 9, 125–131. doi: 10.1159/000089641
- Elsholz, A. K., Gerth, U., and Hecker, M. (2010a). Regulation of CtsR activity in low GC, Gram+ bacteria. *Adv. Microb. Physiol.* 57, 119–144. doi: 10.1016/B978-0-12-381045-8.00003-5
- Elsholz, A. K. W., Michalik, S., Zühlke, D., Hecker, M., and Gerth, U. (2010b). CtsR, the Gram-positive master regulator of protein quality control, feels the heat. *EMBO J.* 29, 3621–3629. doi: 10.1038/emboj.2010.228
- Elsholz, A. K., Hempel, K., Pöther, D. C., Becher, D., Hecker, M., and Gerth, U. (2011). CtsR inactivation during thiol-specific stress in low GC, Gram+ bacteria. *Mol. Microbiol.* 79, 772–785. doi: 10.1111/j.1365-2958.2010.07489.x
- Elsholz, A. K., Turgay, K., Michalik, S., Hessling, B., Gronau, K., Oertel, D., et al. (2012). Global impact of protein arginine phosphorylation on the physiology of *Bacillus subtilis*. *Proc. Natl. Acad. Sci. U.S.A.* 109, 7451–7456. doi: 10.1073/pnas.1117483109
- Fuhrmann, J., Schmidt, A., Spiess, S., Lehner, A., Turgay, K., Mechtler, K., et al. (2009). McsB is a protein arginine kinase that phosphorylates and inhibits the heat-shock regulator CtsR. *Science* 324, 1323–1326. doi: 10.1126/science.1170088
- Gerth, U., Kock, H., Kusters, I., Michalik, S., Switzer, R. L., and Hecker, M. (2008). Clp-dependent proteolysis down-regulates central metabolic pathways in glucose-starved *Bacillus subtilis*. *J. Bacteriol.* 190, 321–331. doi: 10.1126/science.1170088
- Gunka, K., and Commichau, F. M. (2012). Control of glutamate homeostasis in *Bacillus subtilis*: a complex interplay between ammonium assimilation, glutamate biosynthesis and degradation. *Mol. Microbiol.* 85, 213–224. doi: 10.1111/j.1365-2958.2012.08105.x
- Gunka, K., Stanek, L., Care, R. A., and Commichau, F. M. (2013). Selection-driven accumulation of suppressor mutants in *Bacillus subtilis*: the apparent high mutation frequency of the cryptic gudB gene and the rapid clonal expansion of gudB(+) suppressors are due to growth under selection. *PLoS ONE* 8:e66120. doi: 10.1371/journal.pone.0066120
- Gunka, K., Tholen, S., Gerwig, J., Herzberg, C., Stülke, J., and Commichau, F. M. (2012). A high-frequency mutation in *Bacillus subtilis*: requirements for the decryptification of the gudB glutamate dehydrogenase gene. *J. Bacteriol.* 194, 1036–1044. doi: 10.1128/JB.06470-11
- Hahn, J., Kramer, N., Briley, K. Jr., and Dubnau, D. (2009). McsA and B mediate delocalization of competence proteins from cell poles of *Bacillus subtilis*. *Mol. Microbiol.* 72, 202–215. doi: 10.1111/j.1365-2958.2009.06636.x
- Hames, C., Halbedel, S., Schilling, O., and Stülke, J. (2005). Multiple-mutation reaction: a method for simultaneous introduction of multiple mutations into the glpK gene of *Mycoplasma pneumoniae*. *Appl. Environ. Microbiol.* 71, 4097–4100. doi: 10.1128/AEM.71.7.4097-4100.2005
- Hoch, J. A. (2000). Two-component and phosphorelay signal transduction. *Curr. Opin. Microbiol.* 3, 165–170. doi: 10.1016/S1369-5274(00)00070-9
- Jers, C., Soufi, B., Grangeasse, C., Deutscher, J., and Mijakovic, I. (2008). Phosphoproteomics in bacteria: towards a systemic understanding of bacterial phosphorylation networks. *Expert Rev. Proteomics* 5, 619–627. doi: 10.1586/14789450.5.4.619
- Jung, K., Fried, L., Behr, S., and Heermann, R. (2012). Histidine kinases and response regulators in networks. *Curr. Opin. Microbiol.* 15, 118–124. doi: 10.1016/j.mib.2011.11.009
- Kirstein, J., Zühlke, D., Gerth, U., Turgay, K., and Hecker, M. (2005). A tyrosine kinase and its activator control the activity of the CtsR heat shock repressor in *B. subtilis*. *EMBO J.* 24, 3435–3445. doi: 10.1038/sj.emboj.7600780
- Kobir, A., Shi, L., Boskovic, A., Grangeasse, C., Franjevic, D., and Mijakovic, I. (2011). Protein phosphorylation in bacterial signal transduction. *Biochim. Biophys. Acta* 1810, 989–994. doi: 10.1016/j.bbagen.2011.01.006
- Koskiniemi, S., Sun, S., Berg, O. G., and Andersson, D. I. (2012). Selection-driven gene loss in bacteria. *PLoS Genet.* 8:e1002787. doi: 10.1371/journal.pgen.1002787
- Kunst, F., and Rapoport, G. (1995). Salt stress is an environmental signal affecting degradative enzyme synthesis in *B. subtilis*. *J. Bacteriol.* 177, 2403–2407. doi: 10.1038/305286a0
- LaPorte, D. C., and Koshland, D. E. Jr. (1983). Phosphorylation of isocitrate dehydrogenase as a demonstration of enhanced sensitivity in covalent regulation. *Nature* 305, 286–290. doi: 10.1038/305286a0
- Lee, M. C., and Marx, C. J. (2012). Prepeated, selection-driven genome reduction of accessory genes in experimental populations. *PLoS Genet.* 8:e1002651. doi: 10.1371/journal.pgen.1002651
- Macek, B., Mijakovic, I., Olsen, J. V., Gnäd, F., Kumar, C., Jensen, P. R., et al. (2007). The serine/threonine/tyrosine phosphoproteome of the model bacterium *Bacillus subtilis*. *Mol. Cell. Proteomics* 6, 697–707. doi: 10.1074/mcp.M600464-MCP200
- Martin-Verstraete, I., Débarbouillé, M., Klier, A., and Rapoport, G. (1992). Mutagenesis of the *Bacillus subtilis* “-12, -24” promoter of the levanase operon and evidence for the existence of an upstream activating sequence. *J. Mol. Biol.* 226, 85–99. doi: 10.1016/0022-2836(92)90126-5
- Martin-Verstraete, I., Débarbouillé, M., Klier, A., and Rapoport, G. (1994). Interactions of wild-type and truncated LevR of *Bacillus subtilis* with the upstream activating sequence of the levanase operon. *J. Mol. Biol.* 241, 178–192. doi: 10.1006/jmbi.1994.1487
- Mascher, T. (2014). Bacterial (intramembrane-sensing) histidine kinases: signal transfer rather than stimulus perception. *Trends Microbiol.* 22, 559–565. doi: 10.1016/j.tim.2014.05.006
- Meins, M., Jenö, P., Müller, D., Richter, W. J., Rosenbusch, J. P., and Erni, B. (1993). Cysteine phosphorylation of the glucose transporter of *Escherichia coli*. *J. Biol. Chem.* 268, 11604–11609.
- Mijakovic, I., Petranovic, D., and Deutscher, J. (2004). How tyrosine phosphorylation affects the UDP-glucose dehydrogenase activity of *Bacillus subtilis* YwqF. *J. Mol. Microbiol. Biotechnol.* 8, 19–25. doi: 10.1159/000082077
- Mijakovic, I., Petranovic, D., Macek, B., Cepo, T., Mann, M., Davies, J., et al. (2006). Bacterial single-stranded DNA-binding proteins are phosphorylated on tyrosine. *Nucleic. Acids Res.* 34, 1588–1596. doi: 10.1093/nar/gkj514
- Niebis, A., Kabus, A., Schultz, C., Weil, B., and Bott, M. (2006). Corynebacterial protein kinase G controls 2-oxoglutarate dehydrogenase activity via the phosphorylation status of the OdhI protein. *J. Biol. Chem.* 281, 12300–12307. doi: 10.1074/jbc.M512515200
- Pawson, T., and Scott, J. D. (2005). Protein phosphorylation in signaling – 50 years and counting. *Trends Biochem. Sci.* 30, 286–290. doi: 10.1016/j.tibs.2005.04.013
- Rokney, A., Shagan, M., Kessel, M., Smith, Y., Rosenshine, I., and Oppenheim, A. B. (2009). *E. coli* transports aggregated proteins to the poles by a specific and energy-dependent process. *J. Mol. Biol.* 392, 589–601. doi: 10.1016/j.jmb.2009.07.009
- Sambrook, J., Fritsch, E. F., and Maniatis, T. (1989). *Molecular Cloning: A Laboratory Manual*. Cold Spring Harbor, NY: Cold Spring Harbor Laboratory.
- Schmidt, A., Trentini, D. B., Spiess, S., Fuhrmann, J., Ammerer, G., Mechtler, K., et al. (2014). Quantitative phosphoproteome reveals the role of protein arginine phosphorylation in the bacterial stress response. *Mol. Cell. Proteomics* 13, 1832–1839. doi: 10.1074/mcp.M113.032292
- Stannek, L., Egelkamp, R., Gunka, K., and Commichau, F. M. (2014). Monitoring intraspecies competition in a bacterial cell population by cocultivation of fluorescently labelled strains. *J. Vis. Exp.* 18:e51196. doi: 10.3791/51196
- Steinmetz, M., and Richter, R. (1994). Easy cloning of mini-Tn10 insertions from the *Bacillus subtilis* chromosome. *J. Bacteriol.* 176, 1761–1763.
- Stülke, J., Martin-Verstraete, I., Zagorec, M., Rose, M., Klier, A., and Rapoport, G. (1997). Induction of the *Bacillus subtilis* ptsGHI operon by glucose is controlled by a novel antiterminator, GlcT. *Mol. Microbiol.* 25, 65–78. doi: 10.1046/j.1365-2958.1997.4351797.x
- Trentini, D. B., Fuhrmann, J., Mechtler, K., and Clausen, T. (2014). Chasing phosphoarginine proteins: development of a selective enrichment method using a phosphatase trap. *Mol. Cell. Proteomics* 13, 1953–1964. doi: 10.1074/mcp.O113.035790
- Villar-Pique, A., de Groot, N. S., Sabaté, R., Acebrón, S. P., Celaya, G., Fernández-Busquets, X., et al. (2012). The effect of amyloidogenic peptides on bacterial aging

correlates with their intrinsic aggregation propensity. *J. Mol. Biol.* 421, 270–281. doi: 10.1016/j.jmb.2011.12.014

Zeigler, D. R., Prágai, Z., Rodriguez, S., Chevreux, B., Muffler, A., Albert, T., et al. (2008). The origins of 168, W23, and other *Bacillus subtilis* legacy strains. *J. Bacteriol.* 190, 6983–6995. doi: 10.1128/JB.00722-08

Conflict of Interest Statement: The authors declare that the research was conducted in the absence of any commercial or financial relationships that could be construed as a potential conflict of interest.

Received: 23 November 2014; accepted: 12 December 2014; published online: 07 January 2015.

Citation: Stannek L, Gunka K, Care RA, Gerth U and Commichau FM (2015) Factors that mediate and prevent degradation of the inactive and unstable GudB protein in *Bacillus subtilis*. *Front. Microbiol.* 5:758. doi: 10.3389/fmicb.2014.00758

This article was submitted to *Microbial Physiology and Metabolism*, a section of the journal *Frontiers in Microbiology*.

Copyright © 2015 Stannek, Gunka, Care, Gerth and Commichau. This is an open-access article distributed under the terms of the Creative Commons Attribution License (CC BY). The use, distribution or reproduction in other forums is permitted, provided the original author(s) or licensor are credited and that the original publication in this journal is cited, in accordance with accepted academic practice. No use, distribution or reproduction is permitted which does not comply with these terms.



Post-translational modification of P_{II} signal transduction proteins

Mike Merrick*

Department of Molecular Microbiology, John Innes Centre, Norwich, UK

Edited by:

Jörg Stülke, Georg-August-Universität Göttingen, Germany

Reviewed by:

Jörg Stülke, Georg-August-Universität Göttingen, Germany

Jan Gundlach,

Georg-August-Universität Göttingen, Germany

*Correspondence:

Mike Merrick, Department of Molecular Microbiology, John Innes Centre, Norwich Research Park, Norwich NR4 7UH, UK
e-mail: mike.merrick@jic.ac.uk

The P_{II} proteins constitute one of the most widely distributed families of signal transduction proteins in nature. They are pivotal players in the control of nitrogen metabolism in bacteria and archaea, and are also found in the plastids of plants. Quite remarkably P_{II} proteins control the activities of a diverse range of enzymes, transcription factors and membrane transport proteins, and in all known cases they achieve their regulatory effect by direct interaction with their target. P_{II} proteins in the Proteobacteria and the Actinobacteria are subject to post-translational modification by uridylylation or adenylylation respectively, whilst in some Cyanobacteria they can be modified by phosphorylation. In all these cases the protein's modification state is influenced by the cellular nitrogen status and is thought to regulate its activity. However, in many organisms there is no evidence for modification of P_{II} proteins and indeed the ability of these proteins to respond to the cellular nitrogen status is fundamentally independent of post-translational modification. In this review we explore the role of post-translational modification in P_{II} proteins in the light of recent studies.

Keywords: p_{II} protein, post-translational modification, uridylylation, adenylylation, phosphorylation

THE P_{II} PROTEIN FAMILY

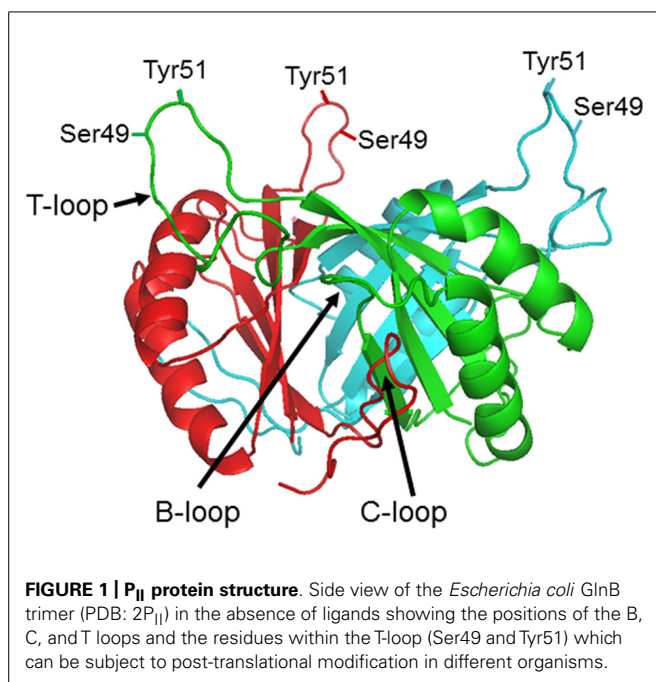
P_{II} proteins were first identified by B. M. Shapiro in the late 1960s when he was studying control of the activity of *Escherichia coli* glutamine synthetase (GS) by adenylylation/deadenylylation (Shapiro, 1969). Subsequent studies by Stadtman and co-workers characterized two proteins: P_I which was responsible for the adenylylation/deadenylylation of GS, and P_{II} which modulated these activities (Brown et al., 1971). Furthermore they observed that P_{II} itself existed in two forms, the interconversion of which appeared to involve the covalent attachment of a uridine derivative to P_{II}. In due course it was shown that P_{II} was encoded by *glnB*, that uridylylation occurred on residue Tyr51 in the T-loop of the protein, and that both uridylylation and deuridylylation were effected by the enzymatic activity of GlnD (Arcondéguy et al., 2001; Huergo et al., 2013).

Extensive genomic research has shown that P_{II} proteins are extremely widespread amongst bacteria, archaea, and plants (Sant'Anna et al., 2009). They are, however, not found in fungi or animals. Their presence in plants is considered to be a consequence of the cyanobacterial origin of the plastid and the protein, whilst encoded in the nucleus, is expressed in the chloroplast (Chellamuthu et al., 2013). Bacteria and archaea often encode multiple P_{II} proteins, e.g., proteobacteria typically encode two, designated GlnB and GlnK. However, cyanobacteria and plants usually encode just a single copy. All P_{II} proteins show a very high level of sequence conservation and protein crystallography studies of P_{II} proteins from bacteria, archaea, and plants indicates that their tertiary structure is also highly conserved (Figure 1). They are homotrimers with a core 12–13 kDa subunit. The trimer forms a compact cylindrical-shaped molecule from which three long exposed loops (the T-loops) protrude. Two smaller loops, the B- and C-loops, are located at the interface between adjacent subunits

of the trimer such that the T- and B-loops of one monomer and the C-loop of the adjacent monomer form an inter-subunit cleft that constitutes a ligand binding site. Although there is now extensive structural data on P_{II} proteins from a range of organisms no structures have been solved for uridylylated or phosphorylated forms (Huergo et al., 2013).

Whilst originally identified as regulating the activity of the GS adenylyltransferase in *E. coli*, P_{II} proteins are now known to control the activities of a very diverse range of enzymes, a large number of transcription factors and some membrane transport proteins. In all known cases they achieve their regulatory effect by direct interaction with their target and in the majority of cases studied to date that interaction involves the T-loops of the P_{II} protein.

The recognition that the T-loops are potentially very flexible and would be able to adopt a variety of structures together with the knowledge that uridylylation of the protein in proteobacteria occurs within the T-loop, suggested early on that post-translational modification could play a key role in facilitating the regulatory activity of P_{II} proteins. However, these proteins are able to bind both ATP/ADP and 2-oxoglutarate (2-OG) and biochemical and crystallographic studies indicate that these effectors alone can have major effects on T-loop structure and on the interaction of P_{II} proteins with many of their targets (Conroy et al., 2007; Jiang and Ninfa, 2007, 2009; Truan et al., 2010). ATP and ADP compete for binding to the same site in the inter-subunit cleft but 2-OG can only bind in the presence of Mg-ATP and ADP does not support 2-OG binding. The ability of P_{II} proteins to bind 2-OG allows them to respond to aspects of the cellular nitrogen and carbon status whilst it has been proposed that the competitive binding of ATP and ADP also makes P_{II} proteins potential sensors of the adenylylate energy charge.



The factors influencing effector binding and the physiological influences on their interactions with P_{II} are presently a matter of debate (Zeth et al., 2014). Changes of the effector pools *in vivo* under different physiological conditions have been studied in the case of the interaction of GlnK and AmtB in *E. coli* (Radchenko et al., 2010; Radchenko and Merrick, 2011). When the intracellular nitrogen status is high 2-OG levels in the cell are low and ADP is found bound to GlnK within the GlnK–AmtB complex (Conroy et al., 2007; Radchenko et al., 2013). The binding of ADP leads to concomitant change in the GlnK T-loop to form a structure in which the apex of the loop projects 28 Å above the core of the protein facilitating complex formation with AmtB (Conroy et al., 2007). Conversely when the intracellular nitrogen status is low, 2-OG levels in the cell are high (Radchenko et al., 2013). Under these conditions GlnK is expected to bind 2-OG and Mg-ATP, the T-loops are relatively unstructured and complex formation is not promoted (Truan et al., 2010, 2014).

The switch between the ATP and ADP bound forms of GlnK has been ascribed by Radchenko et al. (2013) to an ATPase activity of the protein that is only manifest in low 2-OG. Other authors have proposed that the nucleotide occupancy of the effector binding site is solely a reflection of the cellular ATP/ADP ratio (Jiang and Ninfa, 2007, 2009; Fokina et al., 2011; Zeth et al., 2014). Radchenko et al. (2013) propose that a drop in the intracellular 2-OG pool promotes hydrolysis of ATP to ADP leading to a rearrangement of residues in the binding pocket, most notably Gln39 and K58, and a concomitant change in the T-loop structure. Such a model is consistent with the observed GlnK–AmtB and P_{II}–PipX structures and the mode of action of the P_{II} proteins in both these cases (see later). However, it is not consistent with *in vitro* studies of P_{II}–N-acetylglutamate kinase (NAGK) complex formation which indicate that this interaction is promoted by ATP alone and is inhibited by 2-OG (Fokina et al., 2011; Zeth et al., 2014).

In summary, changes in T-loop structure in response to changes in cellular N status as reflected by the 2-OG pool, or possibly in response to changes in the cellular ATP/ADP ratio, are sufficient to explain the ability of P_{II} proteins to interact with their cognate targets. Consequently the role of post-translational modification of P_{II} proteins is a facet of P_{II} biology that needs to be re-evaluated and studied in much more detail.

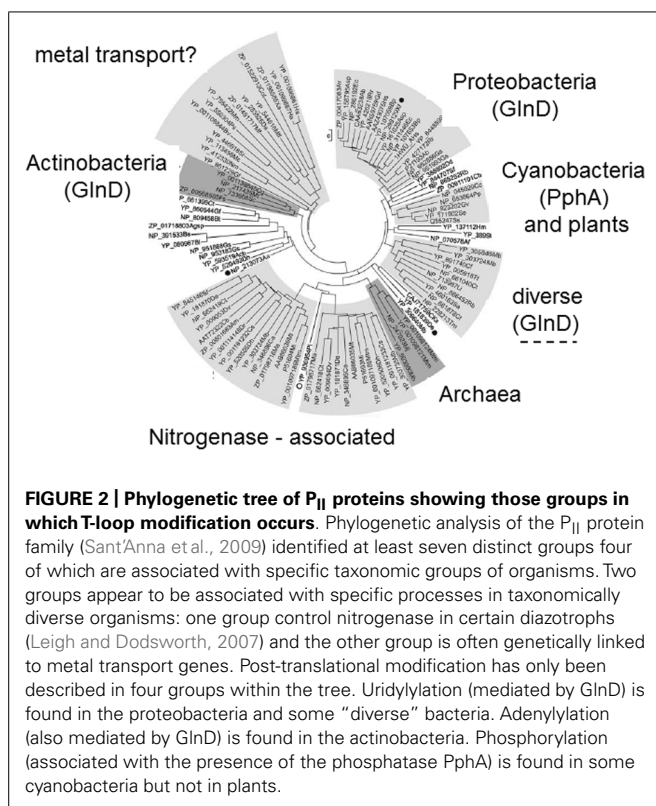
URIDYLYLATION AND ADENYLYLATION OF P_{II} PROTEINS

P_{II} uridylylation and deuridylylation are carried out by a single enzyme, encoded by *glnD*, that has been characterized from a number of proteobacteria. GlnD proteins have a molecular mass of about 100 kDa and contain a conserved nucleotidyltransferase superfamily motif. They have at least four domains of which the N-terminal domain encodes the uridylyltransferase (UTase) activity and the adjacent HD domain encodes the uridylyl-removing (UR) activity (Jiang et al., 1998; Zhang et al., 2010); hence, the two activities are not thought to share an active site. GlnD has a single glutamine-binding site and its activity is regulated by the intracellular glutamine level such that UTase activity predominates in low glutamine and UR activity is stimulated by high glutamine levels. P_{II} is the only known substrate for GlnD and the regulation of GlnD activity by glutamine means that in organisms where P_{II} is subject to uridylylation both the 2-OG and the glutamine pools influence P_{II} activity. The metabolic links between 2-OG and glutamine mean that usually the levels of these two effectors change in a reciprocal manner but there may be physiological conditions where the two are at least partially uncoupled.

The *glnD* gene is found ubiquitously in the proteobacteria and the actinobacteria, and sporadically in a few other diverse genera (Huergo et al., 2013). In the actinobacteria *glnD* is part of the *amtB*, *glnK*, *glnD* operon, whereas in the proteobacteria it is usually encoded elsewhere in the genome. Furthermore, studies of P_{II} modification in two actinobacteria, *Streptomyces coelicolor* and *Corynebacterium glutamicum*, found that in both these organisms the activity of GlnD is to adenylylate the single P_{II} protein, GlnK, rather than to uridylylate it (Hesketh et al., 2002; Strosser et al., 2004). The modification takes place on the equivalent Tyr51 residue of the T-loop and the exact basis for transfer of an adenylyl rather than an uridylyl group has not been determined. Hence, it is clear that within the P_{II} family post-translational modification by uridylylation/adenylylation is relatively restricted (Figure 2), and as with the P_{II} proteins (Sant'Anna et al., 2009) the distribution of *glnD* also suggests that horizontal gene transfer may have played a part in its present distribution.

PHOSPHORYLATION OF P_{II} PROTEINS

An alternative form of post-translational modification of P_{II} occurs in the cyanobacteria. In this case the T-loop is subject to phosphorylation on residue Ser49 and, as with uridylylation and adenylylation, the modification occurs in response to nitrogen limitation. T-loop phosphorylation has been observed in *Synechococcus elongatus* and in *Synechocystis* but despite conservation of residue Ser49 in the T-loop phosphorylation is not found in other cyanobacteria such as *Prochlorococcus* and *Anabaena* (Forchhammer et al., 2004). Furthermore, there is no evidence for post-translational modification of P_{II} in plants (Smith et al., 2004).



A completely novel modification, namely nitration of Tyr51, has been reported for *Anabaena* (Zhang et al., 2007).

The mechanism of P_{II} modification in cyanobacteria is also not fully understood. Dephosphorylation is driven by a specific phosphatase, PphA, the activity of which is inhibited by 2-OG in concert with Mg-ATP (Irmeler and Forchhammer, 2001; Ruppert et al., 2002). Hence, 2-OG plays a key role as an effector, both by binding to P_{II} in conditions of N-limitation and also by inhibiting the phosphatase and ensuring that P_{II} remains phosphorylated in this situation. However, despite considerable efforts, the kinase responsible for phosphorylation of P_{II} has yet to be identified and consequently the factors regulating its activity are also still unknown (Chellamuthu et al., 2013). Potentially the kinase could offer another signal transduction route into the system, for example if glutamine was to inhibit the kinase in an analogous mode to the inhibition by glutamine of GlnD UTase activity, but at present such hypotheses await discovery of the kinase.

THE ROLE OF P_{II} MODIFICATION

An assessment of the various taxonomic groups of P_{II} proteins identified by Sant'Anna et al. (2009) makes it clear that many members of the family are probably not subject to any form of post-translational modification (Figure 2). There are to date no reports of P_{II} modification in archaea, nor in the Firmicutes such as *Bacillus subtilis*. The novel group of P_{II} proteins that function specifically to regulate activity of the nitrogenase enzyme in a variety of bacteria have also not been found to be controlled by post-translational modification and, as discussed above, modification is scattered amongst groups such as the cyanobacteria. So it

would appear that P_{II} modification has arisen more than once in evolution and that many P_{II} proteins function effectively without such modification.

To assess the role of P_{II} modification in those organisms where it occurs it is necessary to examine model systems in which the interaction between a P_{II} protein and its target has been characterized in some detail, preferably both biochemically and structurally.

GlnK–AmtB

Regulation of the ammonium transporter AmtB by the P_{II} protein GlnK is widespread in both bacteria and archaea. The structural genes for these proteins are invariably linked in a single operon (*glnK amtB* or *amtB glnK*) and it has been suggested that this is the evolutionary origin of the P_{II} protein family (Thomas et al., 2000; Sant'Anna et al., 2009). The interaction of GlnK with AmtB has been studied in considerable detail both *in vivo* and *in vitro* and the structure of the complex from *E. coli* has been solved.

In N-limited conditions GlnK is fully uridylylated and free in the cytoplasm with Mg-ATP and 2-OG bound in the effector binding pocket as described earlier. An increase in the cellular N status leads to deuridylylation of GlnK and its sequestration to the inner membrane by AmtB (Radchenko et al., 2010). The crystal structure of the *E. coli* AmtB–GlnK complex shows that GlnK interacts with AmtB almost exclusively via the T-loop, the tip of which inserts deeply into the cytoplasmic pore exit of AmtB, thus blocking ammonia conduction into the cell (Conroy et al., 2007). The AmtB-bound GlnK has ADP bound in all three effector binding pockets. It is clear from the structure of the complex that uridylylation of GlnK will prevent complex formation and that deuridylylation is therefore a prerequisite for binding to GlnK. However, studies using a Tyr51Ala variant of GlnK that cannot be uridylylated have shown that this protein still responds to changes in cellular nitrogen status in a manner almost identical to the wild-type GlnK (Radchenko et al., 2014). As might be expected, when cells are subject to an ammonium shock the Tyr51Ala variant binds to AmtB slightly faster than the wild-type, presumably because the protein does not have to undergo deuridylylation prior to complex formation. Hence regulation of ammonia flux through AmtB by GlnK is not dependent on a functional T-loop modification and this is consistent with the fact that the GlnK–AmtB system is found in many organisms that do not exhibit post-translational modification of P_{II}.

P_{II}–PipX

This complex has been studied in the cyanobacterium *S. elongatus* where PipX is a co-activator of the transcription factor NtcA. P_{II} interacts with PipX to antagonize PipX–NtcA complex formation (Espinosa et al., 2006). In N-limited conditions de-phosphorylated P_{II} binds to PipX thereby freeing NtcA to activate transcription of genes required for growth in N-limitation. Complex formation between P_{II} and PipX is strongly reduced by ATP in concert with 2-OG, conditions that occur under N-sufficiency (Llacer et al., 2010). The complex has a 3:3 stoichiometry such that one trimer of P_{II} binds three molecules of PipX that are "caged" between the extended T-loops of the P_{II} trimer (Llacer et al., 2010; Zhao

et al., 2010). The T-loop conformation is similar to that seen in the GlnK–AmtB complex and consistent with this ADP has been shown to increase the affinity of P_{II} for PipX although no bound nucleotide was present in the structure of the complex. Residue Ser49 of the T-loop in P_{II} is positioned such that phosphorylation of Ser49 would not disrupt the complex and studies with a Ser49Glu variant that mimics phosphorylation confirm this (Llacer et al., 2010). Hence control of P_{II}–PipX association and dissociation appears to be independent of post-translational modification of P_{II}.

P_{II}–NAGK

N-acetylglutamate kinase is regulated by interaction with P_{II} in both cyanobacteria and plants (Burillo et al., 2004; Heinrich et al., 2004). NAGK is a key enzyme in arginine biosynthesis and arginine is used as a nitrogen store in these organisms. In conditions of N-sufficiency P_{II} binds to NAGK and enhances the enzyme's catalytic activity thereby increasing cellular arginine levels and allowing arginine to be used for nitrogen storage in the form of cyanophycin (Forchhammer, 2008).

Structures of the complex have been solved for both *S. elongatus* and *Arabidopsis thaliana* and both structures are very similar (Llacer et al., 2007; Mizuno et al., 2007). In each case a hexamer of NAGK is sandwiched between two P_{II} trimers and the T-loops constitute a major interface with NAGK. The *S. elongatus* complex had no bound nucleotide but the very similar *A. thaliana* complex had bound Mg-ATP. In *S. elongatus* ADP has been reported to inhibit P_{II}–NAGK complex formation (Maheswaran et al., 2004).

A Ser49Glu variant of P_{II} is unable to form a complex with NAGK (Heinrich et al., 2004) suggesting that phosphorylation inhibits the interaction and the structure of the complex clarifies how this occurs. Upon phosphorylation, one donor hydrogen bond formed with NAGK by the Ser49 OH group is lost. Furthermore, the bulkiness and negative charge of the phosphate triggers a steric and electrostatic clash with NAGK binding. However, it would appear that P_{II} phosphorylation is likely to occur after dissociation from NAGK and that, as with the other characterized P_{II} complexes, modification does not directly control complex formation and dissociation. It should also be noted that *A. thaliana* P_{II} is not subject to phosphorylation suggesting that, at least in this plant, NAGK regulation by P_{II} can function in the absence of post-translational modification.

GlnZ–DraG

In the diazotrophic proteobacterium *Azospirillum brasilense* the NifH subunit of nitrogenase is subject to post-translational modification by ADP-ribosylation and this modification is mediated by an ADP-ribosyltransferase (DraT) and an ADP-ribosylhydrolase (DraG; Huergo et al., 2012). The antagonistic activities of both DraT and DraG are regulated by P_{II} proteins; DraT by GlnB and DraG by GlnZ. In N-limited conditions both GlnB and GlnZ are uridylylated and do not interact with DraT and DraG. However, in N-sufficient conditions both P_{II} proteins undergo deuridylylation and then interact with their respective target proteins. The structures of DraT and of the GlnB–DraT complex have

yet to be solved so the role of T-loop modification in regulating DraT activity is not known. However, the structures of both DraG and of the GlnZ–DraG complex have been solved (Berthold et al., 2009; Li et al., 2009; Rajendran et al., 2011). The complex is unique amongst those P_{II} complexes for which structural information is presently available because the interface between the two proteins does not involve the T-loops. Hence GlnZ uridylylation will not apparently have a major influence on its interaction with DraG. Structural modeling indicates that DraG is inactivated when bound to GlnZ due to steric hindrance of the DraG active site (Rajendran et al., 2011).

CONCLUSION

Whilst post-translational modification has been recognized as a key feature of P_{II} protein biology since its recognition in *E. coli* in the early 1970s, subsequent studies have determined that it is not a universal feature of this large protein family. In the case of uridylylation mediated by GlnD in the proteobacteria (and probably the equivalent adenylation in archaea) this modification appears to serve to allow integration of sensing of the glutamine pool, through the regulation of GlnD activity by glutamine, with sensing of the 2-oxoglutarate pool by direct binding to P_{II}. In those cases where detailed biochemical and structural studies are available post-translational modification does not appear to be essential for regulation of complex formation, at least in the physiological conditions studied. However, it may influence the dynamics of the process.

The phosphorylation of P_{II} proteins seen in some cyanobacteria also has the potential to facilitate additional sensory input through regulation of the P_{II}-specific kinase but as the kinase has yet to be identified and characterized this concept remains hypothetical at present. Where cyanobacterial P_{II} systems involving phosphorylation have been characterized post-translational modification again does not appear to be essential for regulation of complex formation, and this is supported by the fact that P_{II} phosphorylation is not ubiquitous in the cyanobacteria (Forchhammer et al., 2004).

In summary, from the studies undertaken to date there appears to be no unifying role for post-translational modification of P_{II} proteins. Interaction of P_{II} proteins with their targets is predominantly controlled by effector binding (MgATP, ADP, and 2-OG) and consequent changes in T-loop conformation (Truan et al., 2010; Radchenko and Merrick, 2011; Radchenko et al., 2013). In a number of cases post-translational modification appears to have the potential to operate as a check-point by providing another signal transduction input that has to be accommodated before complex formation between P_{II} and at least some of its targets can proceed.

There is clearly a need for much more information both with respect to studies of many more P_{II} interactions and in a more varied range of physiological conditions. Both types of study may reveal further important roles for P_{II} modification. It is also the case that the majority of studies to date have been of steady state situations and there is a definite need for more studies of P_{II} behavior under conditions of physiological transition because these could well be the situations where the influence of P_{II} modifications are most apparent.

ACKNOWLEDGMENT

This work was funded by the Biotechnology and Biological Sciences Research Council Grant BB/E022308/1 to Mike Merrick.

REFERENCES

- Arcondéguy, T., Jack, R., and Merrick, M. (2001). PII signal transduction proteins: pivotal players in microbial nitrogen control. *Microbiol. Mol. Biol. Rev.* 65, 80–105. doi: 10.1128/MMBR.65.1.80-105.2001
- Berthold, C. L., Wang, H., Nordlund, S., and Høgbom, M. (2009). Mechanism of ADP-ribosylation removal revealed by the structure and ligand complexes of the dimanganese mono-ADP-ribosylhydrolase DraG. *Proc. Natl. Acad. Sci. U.S.A.* 106, 14247–14252. doi: 10.1073/pnas.0905906106
- Brown, M. S., Segal, A., and Stadtman, E. R. (1971). Modulation of glutamine synthetase adenylation and deadenylation is mediated by metabolic transformation of the PII regulatory protein. *Proc. Natl. Acad. Sci. U.S.A.* 68, 2949–2953. doi: 10.1073/pnas.68.12.2949
- Burillo, S., Luque, I., Fuentes, I., and Contreras, A. (2004). Interactions between the nitrogen signal transduction protein PII and N-acetyl glutamate kinase in organisms that perform oxygenic photosynthesis. *J. Bacteriol.* 186, 3346–3354. doi: 10.1128/JB.186.11.3346-3354.2004
- Chellamuthu, V. R., Alva, V., and Forchhammer, K. (2013). From cyanobacteria to plants: conservation of PII functions during plastid evolution. *Planta* 237, 451–462. doi: 10.1007/s00425-012-1801-0
- Conroy, M. J., Durand, A., Lupo, D., Li, X. D., Bullough, P. A., Winkler, F. K., et al. (2007). The crystal structure of the *Escherichia coli* AmtB-GlnK complex reveals how GlnK regulates the ammonia channel. *Proc. Natl. Acad. Sci. U.S.A.* 104, 1213–1218. doi: 10.1073/pnas.0610348104
- Espinosa, J., Forchhammer, K., Burillo, S., and Contreras, A. (2006). Interaction network in cyanobacterial nitrogen regulation: pipX, a protein that interacts in a 2-oxoglutarate dependent manner with PII and NtcA. *Mol. Microbiol.* 61, 457–469. doi: 10.1111/j.1365-2958.2006.05231.x
- Fokina, O., Herrmann, C., and Forchhammer, K. (2011). Signal-transduction protein PII from *Synechococcus elongatus* PCC 7942 senses low adenylate energy charge in vitro. *Biochem. J.* 440, 147–156. doi: 10.1042/BJ20110536
- Forchhammer, K. (2008). PII signal transducers: novel functional and structural insights. *Trends Microbiol.* 16, 65–72. doi: 10.1016/j.tim.2007.11.004
- Forchhammer, K., Irmeler, A., Kloft, N., and Ruppert, U. (2004). P signalling in unicellular cyanobacteria: analysis of redox-signals and energy charge. *Physiol. Plant.* 120, 51–56. doi: 10.1111/j.0031-9317.2004.0218.x
- Heinrich, A., Maheswaran, M., Ruppert, U., and Forchhammer, K. (2004). The *Synechococcus elongatus* P signal transduction protein controls arginine synthesis by complex formation with N-acetyl-L-glutamate kinase. *Mol. Microbiol.* 52, 1303–1314. doi: 10.1111/j.1365-2958.2004.04058.x
- Hesketh, A., Fink, D., Gust, B., Rexer, H. U., Scheel, B., Chater, K., et al. (2002). The GlnD and GlnK homologues of *Streptomyces coelicolor* A3(2) are functionally dissimilar to their nitrogen regulatory system counterparts from enteric bacteria. *Mol. Microbiol.* 46, 319–330. doi: 10.1046/j.1365-2958.2002.03149.x
- Huergo, L. F., Chandra, G., and Merrick, M. (2013). PII signal transduction proteins: nitrogen regulation and beyond. *FEMS Microbiol. Rev.* 37, 251–283. doi: 10.1111/j.1574-6976.2012.00351.x
- Huergo, L. F., Pedrosa, F. O., Muller-Santos, M., Chubatsu, L. S., Monteiro, R. A., Merrick, M., et al. (2012). PII signal transduction proteins: pivotal players in post-translational control of nitrogenase activity. *Microbiology* 158, 176–190. doi: 10.1099/mic.0.049783-0
- Irmeler, A., and Forchhammer, K. (2001). A PP2C-type phosphatase dephosphorylates the PII signaling protein in the cyanobacterium *Synechocystis* PCC 6803. *Proc. Natl. Acad. Sci. U.S.A.* 98, 12978–12983. doi: 10.1073/pnas.231254998
- Jiang, P., and Ninfa, A. J. (2007). *Escherichia coli* PII signal transduction protein controlling nitrogen assimilation acts as a sensor of adenylate energy charge in vitro. *Biochemistry* 46, 12979–12996. doi: 10.1021/bi701062t
- Jiang, P., and Ninfa, A. J. (2009). Sensation and signaling of alpha-ketoglutarate and adenylate energy charge by the *Escherichia coli* PII signal transduction protein require cooperation of the three ligand-binding sites within the PII trimer. *Biochemistry* 48, 11522–11531. doi: 10.1021/bi9011594
- Jiang, P., Peliska, J. A., and Ninfa, A. J. (1998). Enzymological characterization of the signal-transducing uridylyltransferase/uridylyl-removing enzyme (EC 2.7.7.59) of *Escherichia coli* and its interaction with the PII protein. *Biochemistry* 37, 12782–12794. doi: 10.1021/bi980667m
- Leigh, J. A., and Dodsworth, J. A. (2007). Nitrogen regulation in bacteria and archaea. *Annu. Rev. Microbiol.* 61, 349–377. doi: 10.1146/annurev.micro.61.080706.093409
- Li, X. D., Huergo, L. F., Gasperina, A., Pedrosa, F. O., Merrick, M., and Winkler, F. K. (2009). Crystal structure of dinitrogenase reductase activating glycohydrolase (DRAG) reveals conservation in the ADP-ribosylhydrolase fold and specific features in the ADP-ribose-binding pocket. *J. Mol. Biol.* 390, 737–746. doi: 10.1016/j.jmb.2009.05.031
- Llaser, J. L., Contreras, A., Forchhammer, K., Marco-Marin, C., Gil-Ortiz, F., Maldonado, R., et al. (2007). The crystal structure of the complex of PII and acetylglutamate kinase reveals how PII controls the storage of nitrogen as arginine. *Proc. Natl. Acad. Sci. U.S.A.* 104, 17644–17649. doi: 10.1073/pnas.0705987104
- Llaser, J. L., Espinosa, J., Castells, M. A., Contreras, A., Forchhammer, K., and Rubio, V. (2010). Structural basis for the regulation of NtcA-dependent transcription by proteins PipX and PII. *Proc. Natl. Acad. Sci. U.S.A.* 107, 15397–15402. doi: 10.1073/pnas.1007015107
- Maheswaran, M., Urbanke, C., and Forchhammer, K. (2004). Complex formation and catalytic activation by the PII signaling protein of N-acetyl-L-glutamate kinase from *Synechococcus elongatus* strain PCC 7942. *J. Biol. Chem.* 279, 55202–55210. doi: 10.1074/jbc.M410971200
- Mizuno, Y., Moorhead, G. B., and Ng, K. K. (2007). Structural basis for the regulation of N-acetylglutamate kinase by PII in *Arabidopsis thaliana*. *J. Biol. Chem.* 282, 35733–35740. doi: 10.1074/jbc.M707127200
- Radchenko, M., and Merrick, M. (2011). The role of effector molecules in signal transduction by PII proteins. *Biochem. Soc. Trans.* 39, 189–194. doi: 10.1042/BST0390189
- Radchenko, M. V., Thornton, J., and Merrick, M. (2010). Control of AmtB-GlnK complex formation by intracellular levels of ATP, ADP and 2-oxoglutarate. *J. Biol. Chem.* 285, 31037–31045. doi: 10.1074/jbc.M110.153908
- Radchenko, M. V., Thornton, J., and Merrick, M. (2013). P(II) signal transduction proteins are ATPases whose activity is regulated by 2-oxoglutarate. *Proc. Natl. Acad. Sci. U.S.A.* 110, 12948–12953. doi: 10.1073/pnas.1304386110
- Radchenko, M. V., Thornton, J., and Merrick, M. (2014). Association and dissociation of the GlnK–AmtB complex in response to cellular nitrogen status can occur in the absence of GlnK post-translational modification. *Front. Microbiol.* 5:731. doi: 10.3389/fmicb.2014.00731
- Rajendran, C., Gerhardt, E. C., Bjelic, S., Gasperina, A., Scarduelli, M., Pedrosa, F. O., et al. (2011). Crystal structure of the GlnZ–DraG complex reveals a different form of PII–target interaction. *Proc. Natl. Acad. Sci. U.S.A.* 108, 18972–18976. doi: 10.1073/pnas.1108038108
- Ruppert, U., Irmeler, A., Kloft, N., and Forchhammer, K. (2002). The novel protein phosphatase PphA from *Synechocystis* PCC 6803 controls dephosphorylation of the signalling protein PII. *Mol. Microbiol.* 44, 855–864. doi: 10.1046/j.1365-2958.2002.02927.x
- Sant’Anna, F. H., Trentini, D. B., de Souto, W. S., Cecagno, R., da Silva, S. C., and Schrank, I. S. (2009). The PII superfamily revised: a novel group and evolutionary insights. *J. Mol. Evol.* 68, 322–336. doi: 10.1007/s00239-009-9209-6
- Shapiro, B. M. (1969). The glutamine synthetase deadenylation enzyme system from *Escherichia coli*. Resolution into two components, specific nucleotide stimulation, and cofactor requirements. *Biochemistry* 8, 659–670. doi: 10.1021/bi00830a030
- Smith, C. S., Morrice, N. A., and Moorhead, G. B. (2004). Lack of evidence for phosphorylation of *Arabidopsis thaliana* PII: implications for plastid carbon and nitrogen signaling. *Biochim. Biophys. Acta* 1699, 145–154. doi: 10.1016/j.bbapap.2004.02.009
- Strosser, J., Ludke, A., Schaffer, S., Kramer, R., and Burkovski, A. (2004). Regulation of GlnK activity: modification, membrane sequestration and proteolysis as regulatory principles in the network of nitrogen control in *Corynebacterium glutamicum*. *Mol. Microbiol.* 54, 132–147. doi: 10.1111/j.1365-2958.2004.04247.x
- Thomas, G., Coutts, G., and Merrick, M. (2000). The glnKamtB operon: a conserved gene pair in prokaryotes. *Trends Genet.* 16, 11–14. doi: 10.1016/S0168-9525(99)01887-9
- Truan, D., Bjelic, S., Li, X. D., and Winkler, F. K. (2014). Structure and thermodynamics of effector molecule binding to the nitrogen signal transduction PII protein GlnZ from *Azospirillum brasilense*. *J. Mol. Biol.* 426, 2783–2799. doi: 10.1016/j.jmb.2014.05.008
- Truan, D., Huergo, L. F., Chubatsu, L. S., Merrick, M., Li, X. D., and Winkler, F. K. (2010). A new PII protein structure identifies the

- 2-oxoglutarate binding site. *J. Mol. Biol.* 400, 531–539. doi: 10.1016/j.jmb.2010.05.036
- Zeth, K., Fokina, O., and Forchhammer, K. (2014). Structural basis and target-specific modulation of ADP sensing by the *Synechococcus elongatus* PII signaling protein. *J. Biol. Chem.* 289, 8960–8972. doi: 10.1074/jbc.M113.536557
- Zhang, Y., Pohlmann, E. L., Serate, J., Conrad, M. C., and Roberts, G. P. (2010). Mutagenesis and functional characterization of the four domains of GlnD, a bifunctional nitrogen sensor protein. *J. Bacteriol.* 192, 2711–2721. doi: 10.1128/JB.01674-09
- Zhang, Y., Pu, H., Wang, Q., Cheng, S., Zhao, W., Zhang, Y., et al. (2007). PII is important in regulation of nitrogen metabolism but not required for heterocyst formation in the cyanobacterium *Anabaena* sp. PCC 7120. *J. Biol. Chem.* 282, 33641–33648. doi: 10.1074/jbc.M706500200
- Zhao, M. X., Jiang, Y. L., Xu, B. Y., Chen, Y., Zhang, C. C., and Zhou, C. Z. (2010). Crystal structure of the cyanobacterial signal transduction protein PII in complex with PipX. *J. Mol. Biol.* 402, 552–559. doi: 10.1016/j.jmb.2010.08.006
- Conflict of Interest Statement:** The author declares that the research was conducted in the absence of any commercial or financial relationships that could be construed as a potential conflict of interest.
- Received: 28 October 2014; accepted: 15 December 2014; published online: 06 January 2015.
- Citation: Merrick M (2015) Post-translational modification of P_{II} signal transduction proteins. *Front. Microbiol.* 5:763. doi: 10.3389/fmicb.2014.00763
- This article was submitted to *Microbial Physiology and Metabolism*, a section of the journal *Frontiers in Microbiology*.
- Copyright © 2015 Merrick. This is an open-access article distributed under the terms of the Creative Commons Attribution License (CC BY). The use, distribution or reproduction in other forums is permitted, provided the original author(s) or licensor are credited and that the original publication in this journal is cited, in accordance with accepted academic practice. No use, distribution or reproduction is permitted which does not comply with these terms.



Association and dissociation of the GlnK–AmtB complex in response to cellular nitrogen status can occur in the absence of GlnK post-translational modification

Martha V. Radchenko[†], Jeremy Thornton and Mike Merrick*

Department of Molecular Microbiology, John Innes Centre, Norwich, UK

Edited by:

Jörg Stülke, Georg-August-Universität Göttingen, Germany

Reviewed by:

Wolfgang Buckel, Philipps-Universität Marburg, Germany
Sven Halbedel, Robert Koch Institute, Germany

*Correspondence:

Mike Merrick, Department of Molecular Microbiology, John Innes Centre, Norwich Research Park, NR4 7UH Norwich, UK
e-mail: mike.merrick@jic.ac.uk

[†]Present address:

Martha V. Radchenko, Department of Biochemistry and Molecular Biology, Rosalind Franklin University of Medicine and Science, North Chicago, IL, USA

P_{II} proteins are pivotal players in the control of nitrogen metabolism in bacteria and archaea, and are also found in the plastids of plants. P_{II} proteins control the activities of a diverse range of enzymes, transcription factors and membrane transport proteins, and their regulatory effect is achieved by direct interaction with their target. Many, but by no means all, P_{II} proteins are subject to post-translational modification of a residue within the T-loop of the protein. The protein's modification state is influenced by the cellular nitrogen status and in the past this has been considered to regulate P_{II} activity by controlling interaction with target proteins. However, the fundamental ability of P_{II} proteins to respond to the cellular nitrogen status has been shown to be dependent on binding of key effector molecules, ATP, ADP, and 2-oxoglutarate which brings into question the precise role of post-translational modification. In this study we have used the *Escherichia coli* P_{II} protein GlnK to examine the influence of post-translational modification (uridylylation) on the interaction between GlnK and its cognate target the ammonia channel protein AmtB. We have compared the interaction with AmtB of wild-type GlnK and a variant protein, GlnKTyr51Ala, that cannot be uridylylated. This analysis was carried out both *in vivo* and *in vitro* and showed that association and dissociation of the GlnK–AmtB complex is not dependent on the uridylylation state of GlnK. However, our *in vivo* studies show that post-translational modification of GlnK does influence the dynamics of its interaction with AmtB.

Keywords: P_{II} protein, GlnK, post-translational modification, uridylylation, ammonium transport, AmtB

INTRODUCTION

Proteins of the P_{II} signal transduction superfamily play a major role in coordinating the regulation of nitrogen metabolic processes, and have recently also been implicated in regulation of at least one facet of carbon metabolism (Huergo et al., 2013; Rodrigues et al., 2014). They mediate their effects by protein–protein interaction and their targets include key metabolic and regulatory enzymes, transcription factors, and nutrient transporters. The P_{II} proteins are the most widely distributed signalling proteins in nature, with ubiquitous members among prokaryotes, and representatives among nitrogen-fixing Archaea and in the chloroplasts of eukaryotic phototrophs (Sant'Anna et al., 2009; Huergo et al., 2013). They are highly conserved homotrimeric proteins consisting of 12–13 kDa subunits that form a cylindrical body with three protruding T-loops have been shown to be capable of adopting a variety of conformations (Conroy et al., 2007; Truan et al., 2010; Huergo et al., 2013). In the majority of cases where the structure of a P_{II} protein bound to one of its targets has been determined the T-loops play a key role in that interaction.

The universally conserved mechanism by which P_{II} activity is regulated involves binding of the effector molecules 2-oxoglutarate (2-OG) and Mg-ATP or ADP in the lateral clefts formed between the monomers (Radchenko et al., 2010; Radchenko and Merrick,

2011). When the intracellular nitrogen status is low, and 2-OG levels are high, P_{II} proteins bind 2-OG and Mg-ATP in the lateral clefts and in this condition the T-loops are relatively unstructured. However when the intracellular nitrogen status rises 2-OG levels fall and 2-OG dissociates from the effector binding site. Studies of *E. coli* GlnK indicate that in the absence of 2-OG the bound ATP is subject to P_{II}-mediated hydrolysis to ADP (Radchenko et al., 2013). This in turn leads to a rearrangement of particular residues in the GlnK binding pocket, most notably Gln39 and Lys58, and a concomitant change in the T-loop to form a more defined structure such that the apex of the loop projects very markedly above the protein's surface (Conroy et al., 2007; Truan et al., 2010). Hence the switch from the MgATP, 2-OG form of P_{II} in N-limited conditions to the ADP-bound form in N-sufficient conditions is reflected in a concomitant change in T-loop structure which could potentially be sufficient to regulate the ability of P_{II} proteins to interact with their cognate targets.

Nevertheless, in addition to this conserved mode of regulation, some P_{II} proteins have another regulatory mechanism that involves post-translational modification of the T-loop. The *E. coli* P_{II} proteins, GlnB and GlnK, are subject to uridylylation of the conserved tyrosine residue (Tyr51) in the T-loop by a uridylyltransferase/uridylyl-removing enzyme (UTase/UR or GlnD; Jiang et al., 1998; Atkinson and Ninfa, 1999). In N-limiting

conditions UTase activity is predominant and GlnB, and GlnK are uridylylated, whereas in N-sufficient conditions the intracellular glutamine concentration rises, glutamine binds to GlnD and the UR activity deuridylylates the P_{II} proteins. Uridylylation of P_{II} proteins is widespread in the Proteobacteria (Jiang et al., 1998) and a very similar GlnD-mediated adenylylation of P_{II} proteins occurs in some Actinobacteria (Hesketh et al., 2002; Strosser et al., 2004). Furthermore, in some Cyanobacteria P_{II} proteins are subject to phosphorylation of the T-loop (Forchhammer et al., 2004). It is, however, notable that in many organisms P_{II} is not subject to any form of post-translational modification (Huergo et al., 2013) which raises the question of the biological role of this modification in those organisms where it occurs. We have chosen to investigate this in a model P_{II} interaction, namely that of *E. coli* GlnK with the integral membrane ammonia transporter protein AmtB.

The primary function of *E. coli* GlnK is to regulate the activity of AmtB which is a homotrimer with an ammonia conduction channel through each subunit (Thomas et al., 2000; Coutts et al., 2002; Zheng et al., 2004). In *E. coli* an increase in the cellular N status promotes binding of GlnK to AmtB and the crystal structure of the complex shows that GlnK has a molecule of ADP bound to each monomer. GlnK interacts with AmtB almost exclusively via the T-loops the tips of which insert deeply into the cytoplasmic pore exits of AmtB such that residue Arg47 blocks ammonia conduction into the cell (Conroy et al., 2007). Initial studies of GlnK–AmtB interaction noted that complex formation in response to an ammonium shock occurred synchronously with deuridylylation of GlnK (Coutts et al., 2002) suggesting that association/dissociation of the complex was regulated by the post-translational state of GlnK.

The GlnK–AmtB interaction is highly conserved in bacteria and Archaea as reflected by conserved linkage between the structural genes (Thomas et al., 2000). Indeed it has been proposed that regulation of AmtB is the ancestral function of GlnK (Sant'Anna et al., 2009). However the *glnK amtB* operon is found in many organisms where there is no evidence of post-translational modification of P_{II} and it was noted by Coutts et al. (2002) that this suggested that regulation of the complex in those organisms would require an alternative mechanism. In this study we describe experiments to examine this topic and show that association/dissociation of the GlnK–AmtB complex can indeed respond to the cellular N status in the absence of post-translational modification of GlnK.

MATERIALS AND METHODS

STRAINS, PLASMIDS, AND GROWTH MEDIA

The strains and plasmids used are listed in Table 1. Plasmid pAD2 and its derivatives were expressed in GT1000 and used for His₆AmtB–GlnK (wild-type or variants) complex purification. Plasmid pJT25 or its derivatives in *E. coli* BL21(DE3)pLysS were used for overexpression of GlnK (wild type or variants). Derivatives of pAD2, plasmids pADR47A, and pADY51A, and derivatives of pJT25, plasmids pJTR47A, and pJTY51A, were generated using the QuickChange Lightning Site-directed Mutagenesis Kit (Agilent Technologies). *E. coli* strains were routinely grown in Luria Bertani medium, and for nitrogen-limited growth M9Gln medium (Javelle

Table 1 | Strains and plasmids.

	Relevant genotype/phenotype	Reference
<i>Escherichia coli</i> strain		
GT1000	<i>rbs lacZ::IS1 gyrA hutC_K ΔglnKamtB</i>	Coutts et al. (2002)
BL21(DE3)pLysS	F [−] ompT gal dcm lon hsdS _B (r _B [−] m _B [−]) λ(DE3) pLysS(cm ^R)	Studier et al. (1990)
Plasmid		
pAD2	<i>glnK His6amtB</i>	Durand and Merrick (2006)
pADR47A	<i>glnK_R47A His6amtB</i>	This work
pADY51A	<i>glnK_Y51A His6amtB</i>	This work
pJT25	<i>glnK</i>	Radchenko et al. (2010)
pJTR47A	<i>glnK_R47A</i>	This work
pJTY51A	<i>glnK_Y51A</i>	This work

et al., 2005) was used. Ampicillin (100 μg ml^{−1}), chloramphenicol (30 μg ml^{−1}) were included as appropriate.

PURIFICATION OF His6-AmtB AND GlnK PROTEINS

GlnK–AmtB complexes and Histidine-tagged AmtB (His6–AmtB) were obtained by purifying the AmtB–GlnK complex as described previously (Durand and Merrick, 2006; Radchenko et al., 2010). GlnK wild-type and variants were purified from whole cell extracts of BL21(DE3)pLysS carrying pJT25, pJTR47A, or pJTY51A that were heated to 80°C for 4 min and centrifuged at 30,000 g for 30 min to remove debris (Moure et al., 2012). Supernatants were processed by affinity chromatography on a Heparin column (GE Healthcare), using a step gradient of 5, 10, 20, 40, and 100% elution buffer (protein eluted at 20% step). Equilibration buffer was 50 mM Tris, 0.1 M KCl, pH 7.5, and elution buffer was 50 mM Tris, 1.0 M KCl, pH 7.5.

ANALYSIS OF GlnK–AmtB INTERACTION IN VITRO

The ability of the variant GlnK proteins to interact with AmtB was assessed by *in vitro* binding assays as described previously (Radchenko et al., 2010). For assessment of association His6–AmtB (400 μg) was immobilized on a HIS-Select spin column previously equilibrated with buffer A [50 mM Tris-HCl (pH 8.0), 100 mM NaCl, 10% (v/v) glycerol, 0.05% (w/v) *n*-dodecyl-*N,N*-dimethylamine-*N*-oxide (LDAO)] containing 5 mM imidazole. The flow through was collected, and unbound proteins were removed by two washes with the same buffer. Three additional washes were carried out in buffer A containing 5 mM imidazole, 300 μg GlnK protein and various combinations of effectors. The effector concentrations used were reflective of those measured *in vivo* under conditions of N-limitation and N-sufficiency (Radchenko et al., 2010). As a control, buffer A containing 5 mM imidazole, 300 μg GlnK protein and 0.6 M NaCl was used. The molar ratio of AmtB to GlnK was approximately 1:3. A single

column was used for each condition tested. Elution of His₆AmtB or His₆AmtB–GlnK complex was performed by the addition of buffer A containing 500 mM imidazole. The eluted fractions were analyzed on 15% SDS-PAGE. For assessment of dissociation, complexes of AmtB with bound GlnK (wild-type or variants) were applied to a HIS-Select spin column in the presence of different combinations of effectors and washed and eluted fractions were analyzed by SDS-PAGE.

IN VIVO DETECTION OF GlnK MEMBRANE SEQUESTRATION FOLLOWING AMMONIUM SHOCK

Escherichia coli cultures of GT1000 carrying plasmids pAD2, pADR47A, and pADY51A were grown in M9Gln medium at 30°C and subjected to ammonium shock by the addition of NH₄Cl to a final concentration of 200 μM. Samples were taken prior to ammonium addition and then at 0.5, 1, 2, 3, 5, 10, and 15 mins after addition. Whole cell protein extracts, membrane and cytoplasmic protein fractions were prepared as described previously (Coutts et al., 2002). Membrane fractions were subjected to two high-salt washes (600 mM NaCl) prior to analysis. Protein quantification of the fractions was determined with Coomassie PlusTM protein assay reagent (Thermo Scientific) using an albumin standard (Thermo Scientific).

To determine the cellular location of GlnK membrane protein fractions were separated by 12.5% SDS-PAGE (5–10 μg/lane), analyzed by Western blotting and detected as described elsewhere (Radchenko et al., 2010). The uridylylation state of GlnK was also assessed for each sample by separation of the different GlnK states (UMP₀–UMP₃) using native PAGE followed by Western blotting. All experiments were replicated three times.

RESULTS

In order to investigate the influence of GlnK uridylylation on the interaction between GlnK and AmtB we constructed two T-loop variants for comparison with the wild-type. Residue Tyr51 was changed to Ala thereby generating a variant that would not be subject to uridylylation. As a control residue Arg 47 was also changed to Ala, generating a variant that would still be subject to modification but lacked the charged residue at the tip of the T-loop in the GlnK–AmtB complex. The variants were analyzed in two assays. Firstly the purified GlnK proteins were analyzed *in vitro* for their ability to interact with AmtB in response to the effector molecules ATP, 2-OG, and ADP. Secondly the ability of GlnK wild-type and the variants to be sequestered to the membrane by AmtB was analyzed *in vivo* during a transition from N-limited to N-sufficient conditions.

ASSOCIATION AND DISSOCIATION OF GlnK–AmtB COMPLEXES IN VITRO

The ability of the variant GlnK proteins to interact with AmtB was assessed by *in vitro* binding assays as described previously (Radchenko et al., 2010). For assessment of association His₆AmtB was bound to a HIS-Select spin column and the ability of GlnK wild-type and variants to bind to AmtB in the presence of a variety of effector concentrations was studied. For assessment of dissociation complexes of AmtB with bound GlnK (wild-type or variants) were bound to a HIS-Select spin column

and the dissociation of GlnK in the presence of a variety of effector concentrations was studied. The effectors concentrations used were reflective of those measured *in vivo* under conditions of N-limitation and N-sufficiency (Radchenko et al., 2010).

In all conditions tested the GlnK variants, Arg47Ala, and Tyr51Ala, behaved in the same way as wild-type GlnK. In N-limited conditions *in vivo* the intracellular 2-OG pool is around 1.5 mM and this falls rapidly following ammonium shock to 0.3 mM (Radchenko et al., 2010). GlnK behavior *in vitro* reflects this, in that association with AmtB requires a low 2-OG level (Figure 1). Following ammonium shock intracellular ADP levels rise transiently to around 0.75 mM (Radchenko et al., 2010) and this level of ADP promotes complex formation (Figure 1). Dissociation of the complex *in vitro* (Figure 2) only occurred in a combination of low ADP (0.35 mM) and high ATP (4.5 mM) and 2-OG (1.5 mM) and these are conditions comparable to those found *in vivo* when cells that are subject to N-limitation (Radchenko et al., 2010).

GlnK–AmtB COMPLEX FORMATION IN VITRO

Cells were grown in N-limitation and then subject to an ammonium shock by addition of NH₄Cl to the culture medium. Aliquots of the culture were taken prior to ammonium addition and then periodically over a period of 15 mins following the ammonium shock. The interaction of GlnK with AmtB was monitored by detection of GlnK association with the membrane fraction and the uridylylation state of GlnK was monitored by native PAGE as described previously (Radchenko et al., 2010).

As reported previously (Radchenko et al., 2010), sequestration of wild-type GlnK to the membrane was maximal 2 mins after ammonium shock and corresponded exactly with the time

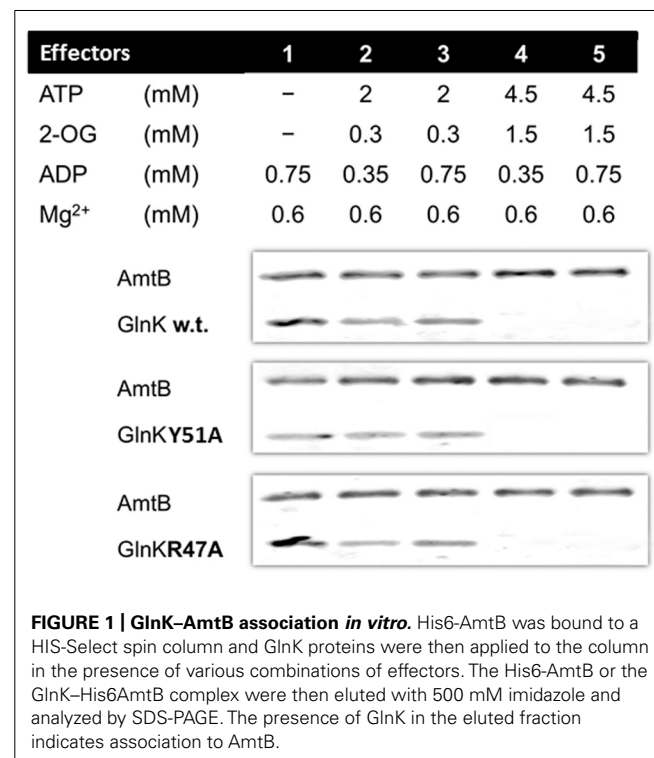


FIGURE 1 | GlnK–AmtB association *in vitro*. His₆AmtB was bound to a HIS-Select spin column and GlnK proteins were then applied to the column in the presence of various combinations of effectors. The His₆AmtB or the GlnK–His₆AmtB complex were then eluted with 500 mM imidazole and analyzed by SDS-PAGE. The presence of GlnK in the eluted fraction indicates association to AmtB.

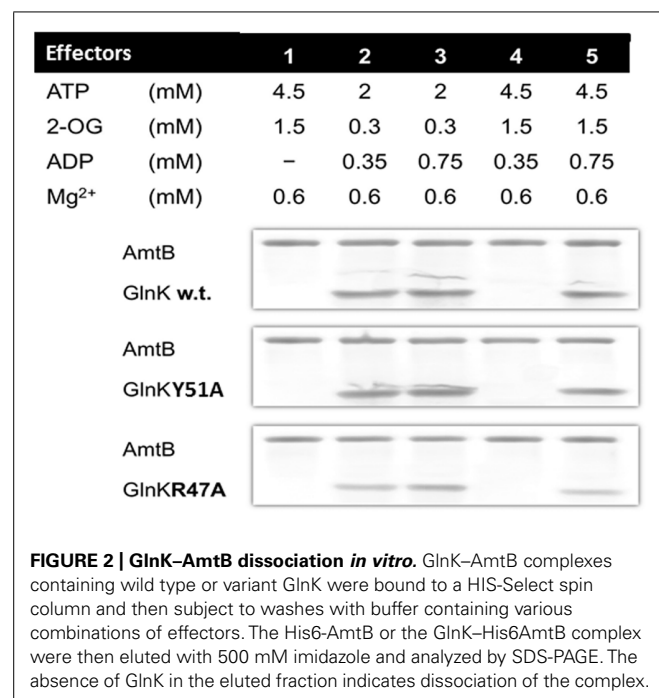


FIGURE 2 | GlnK–AmtB dissociation *in vitro*. GlnK–AmtB complexes containing wild type or variant GlnK were bound to a HIS-Select spin column and then subject to washes with buffer containing various combinations of effectors. The His6-AmtB or the GlnK–His6AmtB complex were then eluted with 500 mM imidazole and analyzed by SDS-PAGE. The absence of GlnK in the eluted fraction indicates dissociation of the complex.

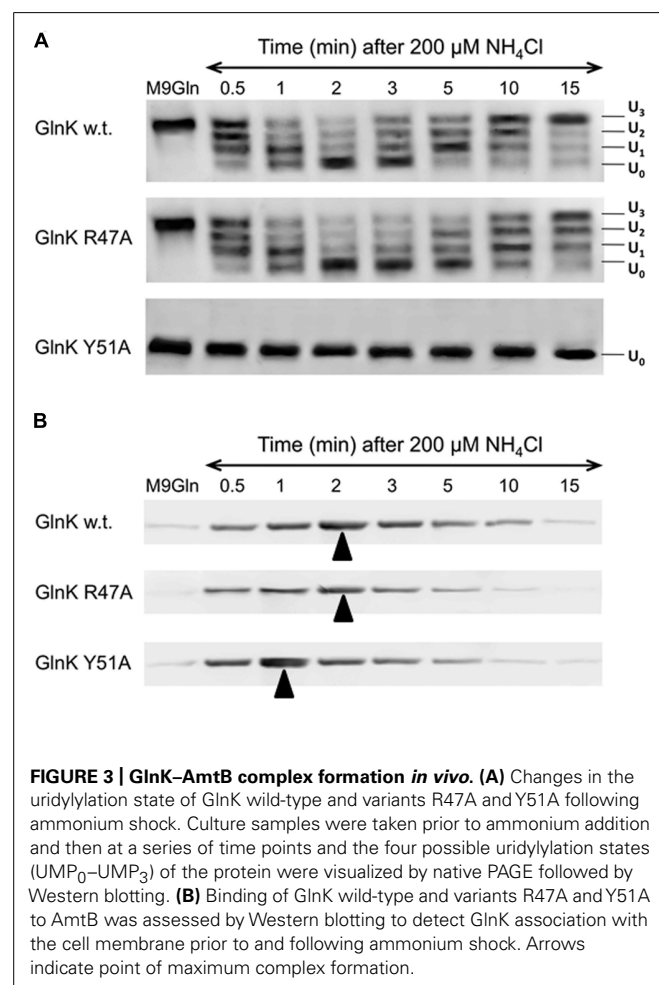


FIGURE 3 | GlnK–AmtB complex formation *in vivo*. (A) Changes in the uridylylation state of GlnK wild-type and variants R47A and Y51A following ammonium shock. Culture samples were taken prior to ammonium addition and then at a series of time points and the four possible uridylylation states (UMP₀–UMP₃) of the protein were visualized by native PAGE followed by Western blotting. (B) Binding of GlnK wild-type and variants R47A and Y51A to AmtB was assessed by Western blotting to detect GlnK association with the cell membrane prior to and following ammonium shock. Arrows indicate point of maximum complex formation.

taken for the protein to become fully deuridylylated (**Figure 3**). As the added ammonium was metabolised the cells returned to N-limitation and 15 mins after ammonium addition GlnK was again dissociated from the membrane and fully uridylylated (**Figure 3**). The GlnK Arg47Ala variant showed an identical membrane sequestration profile to the wild-type. It was also deuridylylated at an identical rate to wild-type but took very slightly longer to be reuridylylated (**Figure 3**). As expected, the Tyr51Ala variant was fully deuridylylated regardless of the N-status of the cells. Nevertheless it still responded to ammonium shock by becoming rapidly sequestered to the membrane. However, in this case the sequestration rate was significantly more rapid than observed with wild-type GlnK or the Arg47Ala variant such that sequestration to the membrane was maximal only 1 min after ammonium shock (**Figure 3**). These experiments were repeated three times with essentially identical results on each occasion.

DISCUSSION

We have employed a combination of *in vitro* and *in vivo* studies to investigate the role of GlnK uridylylation with respect to the interaction of GlnK with its primary target, the ammonium transport protein AmtB. Prior to the recognition of the role that the effector molecules ATP, ADP, and 2-OG play in influencing the conformation of the T-loop in P_{II} proteins it seemed possible that post-translational modification of the T-loop could be the primary factor controlling the interaction of P_{II} proteins with their targets (Coutts et al., 2002). In such a model, uridylylation of the GlnK T-loop in N-limiting conditions would prevent interaction with AmtB and deuridylylation in response to an elevated cellular N-status would leave the T-loops free to effect complex formation. However, in contradiction of such a model many organisms that encode a *glnK amtB* operon and are predicted to regulate AmtB function by GlnK–AmtB interaction do not have mechanisms for post-translational modification of GlnK.

We have studied two GlnK T-loop variants; one (Tyr51Ala) that is unable to uridylylate GlnK and one (Arg47Ala) that is able to be uridylylated but that lacks the charged residue at the tip of the T-loop which interacts with the pore of AmtB. Both variants behaved *in vitro* in an identical manner to wild-type GlnK in that they showed association with AmtB in the presence of physiological concentrations of ADP (0.35–0.75 mM) excepting in those effector conditions seen in *E. coli* cells subject to N-limitation (4.5 mM ATP, 1.5 mM 2-OG, and 0.35 mM ADP). Hence *in vitro* the Tyr51Ala variant of GlnK was able to associate to and dissociate from AmtB independently of any post-translational modification.

When assessed *in vivo*, for both changes in uridylylation state and dynamics of interaction with AmtB in response to an ammonium shock, the Arg47Ala variant of GlnK behaved essentially as the wild-type. As expected the Tyr51Ala variant was not uridylylated under any of the conditions tested but was fully competent to associate with and dissociate from AmtB in response to the ammonium shock. This confirms that post-translational modification is not essential to regulate the interaction of GlnK with AmtB. Our *in vitro* studies indicate that binding of the effectors, MgATP/ADP, and 2-OG, in response to the metabolic state of the cell is sufficient to control the interaction of GlnK with AmtB

through the effect on the conformation of the T-loop. Indeed it seems likely that in many, if not most, cases this could be the primary factor controlling association/dissociation of the P_{II}-target complex.

However uridylylation of GlnK did influence the dynamics of GlnK–AmtB association, such that in the absence of the need to deuridylylate the protein GlnK was able to associate more rapidly with its target when the cellular N-status increased. Deuridylylation of GlnK is triggered by a rise in the intracellular glutamine pool and binding of glutamine to GlnD leading to enhancement of its uridyl-removing (UR) activity. Hence it would appear that the deuridylylation of GlnK prior to complex formation with AmtB acts as a check-point that integrates glutamine availability into the signal transduction network. In the proteobacteria and the actinobacteria *glnD* is widespread (Huergo et al., 2013) presumably reflecting a selective advantage of this enhanced signal transduction network. However, in organisms where post-translational modification of P_{II} is apparently absent it seems that regulation of AmtB activity is controlled by the cellular 2-OG pool as the sole measure of N-status. Studies of the P_{II}–PipX interaction in *Synechococcus elongatus* have similarly shown that, although P_{II} is subject to phosphorylation of the T-loop, association/dissociation of the P_{II}–PipX complex appears to be independent of P_{II} modification (Llacer et al., 2010). Indeed to date there is little evidence of P_{II} target interactions where post-translational modification of the T-loops plays an essential role (Merrick, 2015). There is therefore clearly a need for much more information on the function of post-translational modification of P_{II}, both with respect to studies of many more P_{II} interactions with different targets and in a wide range of physiological conditions.

ACKNOWLEDGMENT

This work was funded by the Biotechnology and Biological Sciences Research Council Grant BB/E022308/1 to Mike Merrick.

REFERENCES

- Atkinson, M., and Ninfa, A. J. (1999). Characterization of the GlnK protein of *Escherichia coli*. *Mol. Microbiol.* 32, 301–313. doi: 10.1046/j.1365-2958.1999.01349.x
- Conroy, M. J., Durand, A., Lupo, D., Li, X. D., Bullough, P. A., Winkler, F. K., et al. (2007). The crystal structure of the *Escherichia coli* AmtB–GlnK complex reveals how GlnK regulates the ammonia channel. *Proc. Natl. Acad. Sci. U.S.A.* 104, 1213–1218. doi: 10.1073/pnas.0610348104
- Coutts, G., Thomas, G., Blakey, D., and Merrick, M. (2002). Membrane sequestration of the signal transduction protein GlnK by the ammonium transporter AmtB. *EMBO J.* 21, 536–545. doi: 10.1093/emboj/21.4.536
- Durand, A., and Merrick, M. (2006). In vitro analysis of the *Escherichia coli* AmtB–GlnK complex reveals a stoichiometric interaction and sensitivity to ATP and 2-oxoglutarate. *J. Biol. Chem.* 281, 29558–29567. doi: 10.1074/jbc.M602477200
- Forchhammer, K., Irmeler, A., Kloft, N., and Ruppert, U. (2004). P signalling in unicellular cyanobacteria: analysis of redox-signals and energy charge. *Physiol. Plant.* 120, 51–56. doi: 10.1111/j.0031-9317.2004.0218.x
- Hesketh, A., Fink, D., Gust, B., Rexer, H. U., Scheel, B., Chater, K., et al. (2002). The GlnD and GlnK homologues of *Streptomyces coelicolor* A3(2) are functionally dissimilar to their nitrogen regulatory system counterparts from enteric bacteria. *Mol. Microbiol.* 46, 319–330. doi: 10.1046/j.1365-2958.2002.03149.x
- Huergo, L. F., Chandra, G., and Merrick, M. (2013). PII signal transduction proteins: nitrogen regulation and beyond. *FEMS Microbiol. Rev.* 37, 251–283. doi: 10.1111/j.1574-6976.2012.00351.x
- Javelle, A., Thomas, G., Marini, A. M., Kramer, R., and Merrick, M. (2005). In vivo functional characterisation of the *E. coli* ammonium channel AmtB: evidence for metabolic coupling of AmtB to glutamine synthetase. *Biochem. J.* 390, 215–222. doi: 10.1042/BJ20042094
- Jiang, P., Peliska, J. A., and Ninfa, A. J. (1998). Enzymological characterization of the signal-transducing uridylyltransferase/uridylyl-removing enzyme (EC 2.7.7.59) of *Escherichia coli* and its interaction with the PII protein. *Biochemistry* 37, 12782–12794. doi: 10.1021/bi980667m
- Llacer, J. L., Espinosa, J., Castells, M. A., Contreras, A., Forchhammer, K., and Rubio, V. (2010). Structural basis for the regulation of NtcA-dependent transcription by proteins PipX and PII. *Proc. Natl. Acad. Sci. U.S.A.* 107, 15397–15402. doi: 10.1073/pnas.1007015107
- Merrick, M. (2015). Post-translational modification of PII signal transduction proteins. *Front. Microbiol.* 5:763. doi: 10.3389/fmicb.2014.00763
- Moure, V. R., Razzera, G., Araujo, L. M., Oliveira, M. A., Gerhardt, E. C., Muller-Santos, M., et al. (2012). Heat stability of Proteobacterial PII protein facilitate purification using a single chromatography step. *Protein Expr. Purif.* 81, 83–88. doi: 10.1016/j.pep.2011.09.008
- Radchenko, M., and Merrick, M. (2011). The role of effector molecules in signal transduction by PII proteins. *Biochem. Soc. Trans.* 39, 189–194. doi: 10.1042/BST0390189
- Radchenko, M. V., Thornton, J., and Merrick, M. (2010). Control of AmtB–GlnK complex formation by intracellular levels of ATP, ADP and 2-oxoglutarate. *J. Biol. Chem.* 285, 31037–31045. doi: 10.1074/jbc.M110.153908
- Radchenko, M. V., Thornton, J., and Merrick, M. (2013). P(II) signal transduction proteins are ATPases whose activity is regulated by 2-oxoglutarate. *Proc. Natl. Acad. Sci. U.S.A.* 110, 12948–12953. doi: 10.1073/pnas.1304386110
- Rodrigues, T. E., Gerhardt, E. C., Oliveira, M. A., Chubatsu, L. S., Pedrosa, F. O., Souza, E. M., et al. (2014). Search for novel targets of the PII signal transduction protein in *Bacteria* identifies the BCCP component of acetyl-CoA carboxylase as a PII binding partner. *Mol. Microbiol.* 91, 751–761. doi: 10.1111/mmi.12493
- Sant’Anna, F. H., Trentini, D. B., de Souto, W. S., Cecagno, R., da Silva, S. C., and Schrank, I. S. (2009). The PII superfamily revised: a novel group and evolutionary insights. *J. Mol. Evol.* 68, 322–336. doi: 10.1007/s00239-009-9209-6
- Strosser, J., Ludke, A., Schaffer, S., Kramer, R., and Burkovski, A. (2004). Regulation of GlnK activity: modification, membrane sequestration and proteolysis as regulatory principles in the network of nitrogen control in *Corynebacterium glutamicum*. *Mol. Microbiol.* 54, 132–147. doi: 10.1111/j.1365-2958.2004.04247.x
- Studier, F. W., Rosenberg, A. H., Dunn, J. J., and Dubendorff, J. W. (1990). Use of T7 RNA polymerase to direct expression of cloned genes. *Methods Enzymol.* 185, 60–89. doi: 10.1016/0076-6879(90)85008-C
- Thomas, G., Coutts, G., and Merrick, M. (2000). The *glnKamtB* operon: a conserved gene pair in prokaryotes. *Trends Genet.* 16, 11–14. doi: 10.1016/S0168-9525(99)01887-9
- Truan, D., Huergo, L. F., Chubatsu, L. S., Merrick, M., Li, X. D., and Winkler, F. K. (2010). A new PII protein structure identifies the 2-oxoglutarate binding site. *J. Mol. Biol.* 400, 531–539. doi: 10.1016/j.jmb.2010.05.036
- Zheng, L., Kostrewa, D., Bernèche, S., Winkler, F. K., and Li, X.-D. (2004). The mechanism of ammonia transport based on the crystal structure of AmtB of *E. coli*. *Proc. Natl. Acad. Sci. U.S.A.* 101, 17090–17095. doi: 10.1073/pnas.0406475101

Conflict of Interest Statement: The authors declare that the research was conducted in the absence of any commercial or financial relationships that could be construed as a potential conflict of interest.

Received: 28 October 2014; accepted: 04 December 2014; published online: 23 December 2014.

Citation: Radchenko MV, Thornton J and Merrick M (2014) Association and dissociation of the GlnK–AmtB complex in response to cellular nitrogen status can occur in the absence of GlnK post-translational modification. *Front. Microbiol.* 5:731. doi: 10.3389/fmicb.2014.00731

This article was submitted to *Microbial Physiology and Metabolism*, a section of the journal *Frontiers in Microbiology*.

Copyright © 2014 Radchenko, Thornton and Merrick. This is an open-access article distributed under the terms of the Creative Commons Attribution License (CC BY). The use, distribution or reproduction in other forums is permitted, provided the original author(s) or licensor are credited and that the original publication in this journal is cited, in accordance with accepted academic practice. No use, distribution or reproduction is permitted which does not comply with these terms.



Complexity of bacterial phosphorylation interaction network

Imrich Barák *

Department of Microbial Genetics, Institute of Molecular Biology, Slovak Academy of Sciences, Bratislava, Slovakia

*Correspondence: imrich.barak@savba.sk

Edited by:

Christophe Grangeasse, Centre National de la Recherche Scientifique, France

Reviewed by:

Christophe Grangeasse, Centre National de la Recherche Scientifique, France

Sylvie Nessler, University Paris-Sud, France

Keywords: *Bacillus subtilis*, protein phosphorylation, bacterial cell division, sporulation, BY-kinase

A commentary on

Protein-tyrosine phosphorylation interaction network in *Bacillus subtilis* reveals new substrates, kinase activators and kinase cross-talk

by Shi, L., Pignonneau, N., Ventroux, M., Derouiche, A., Bidnenko, V., Mijakovic, I. et al. (2014) *Front. Microbiol.* 5:538, doi: 10.3389/fmicb.2014.00538

Protein phosphorylation is a vital mechanism in the regulation of all processes in eukaryotic and prokaryotic cells. It is one of the most important of those post-translational modifications which allow proteins to reversibly change their enzymatic activity, cellular localization, oligomeric state, half-life and interaction partners.

Protein phosphorylation is mainly used by bacteria to adapt to changes in their environment (where the conditions can alter rapidly), but it is also used for intercellular communication (reviewed in Kobir et al., 2011). An important part of the bacterial phosphorylation network is made up of two component systems, which are found only in bacteria and certain plants. The first component of these systems is a sensory kinase which autophosphorylates one of its histidine residues as a result of the recognition of a particular signal. This kinase then phosphorylates the second component, a response regulator, on an aspartate. Phosphorylated forms of the response regulator often bind specific DNA sequences at promoter regions, thereby regulating gene expression and thus triggering a

cellular response. These systems are characterized by a high recognition fidelity between a given sensory kinase and its response regulator, with minimal cross-talk with other two-component systems. There does seem to be a wide range of additional regulators, however, which are able to interfere with the phosphotransfer reactions and thus join a given two-component system to other signaling pathways.

In bacteria, proteins can be phosphorylated on serine, threonine and tyrosine residues. Serine and threonine phosphorylation is mostly carried out by the Hanks family of serine/threonine kinases. Kinases from a different family, the protein-tyrosine kinases (BY-kinases) are normally used for tyrosine phosphorylation (reviewed in Chao et al., 2014). These BY-kinases do not have either sequence or structural homology with eukaryotic tyrosine kinases and they phosphorylate tyrosine residues using an ATP/GTP-binding Walker motif. BY-kinases take part in many different cellular processes, including DNA replication, sporulation, antibiotic resistance, heat shock response, biofilm formation and virulence.

In a recent paper in *Frontiers in Microbiology*, Shi et al. (2014a) described the protein-tyrosine phosphorylation network in *Bacillus subtilis*. Their wide interactome study identified many potential new substrates of kinases and phosphatases. Three findings in particular stand out: (i) their results clearly show that cross-talk does take place between the BY-kinase and the Hanks type Ser/Thr

kinase interaction networks; (ii) new kinase substrates were found, including those involved in DNA replication, transcription regulation and cell division; and (iii) tyrosine kinases can be bound by several cytosolic or transmembrane modulators. One of the most interesting of these is MinD, a binding partner of kinase PtkA. They found that MinD modulates the kinase activity of PtkA *in vitro* and that MinD attracts PtkA to the cell poles. MinD is an ATPase which binds to the membrane as a dimer in its ATP-bound state through an amphipathic helix. It attracts the cell division inhibitor MinC to the membrane and it also interacts with MinJ, which, in turn, interacts with DivIVA. DivIVA localizes to the negative curvature of the forming septum and persists at the cell poles together with the MinCDJ complex during vegetative growth. This mechanism appears to block asymmetric septation during vegetative growth. This blocking mechanism must be overridden before the first morphologically distinct stage of sporulation, the formation of a thin asymmetric septum, can occur.

It has been established that DivIVA has at least two different roles during sporulation. One role is to bind the DNA-binding RacA protein, thereby allowing proper chromosomal segregation to occur in the small part of the cell (the so-called forespore) after asymmetric cell division (Ben Yehuda et al., 2003). A second role, only recently described, is to localize the SpoIIE phosphatase to the site of asymmetric septation (Eswaramoorthy et al., 2014). On the other hand, there are no

known roles for the MinD, MinC and MinJ proteins during sporulation (Barak, 2013). Although depleting any or all of these proteins has only a minimal effect on sporulation frequency (Cha and Stewart, 1997), it is still not possible to exclude the possibility that the Min system has at least a partial role in sporulation because a sporulation-like septum appears, in some *minD* mutant cells, to be misplaced from its normal polar site (Barak et al., 1998). In addition, quite different experiments have shown that MinCD-dependent repression of SpoIIIE assembly in the forespore is crucial for the proper segregation of the chromosome to the forespore after asymmetric septum formation (Sharp and Pogliano, 2002).

The study by Shi et al. (2014a) provides a large amount of additional data about interactions between and phosphorylation of the proteins involved in vegetative and asymmetric cell division and chromosome segregation during sporulation. In brief, they found new potential protein–protein interactions, new substrates and new modulators for kinases involved in the above mentioned processes. Interestingly, they showed that MinD is a modulator of the PtkA kinase activity and also serves as a determinant for its localization. Secondly they showed that DivIVA is a PtkA substrate and they found new putative interaction partners for SpoIIIE. What would be the reason for such a wide interconnection

between so many different phosphorylation networks? Perhaps the main reason is to finely tune different cellular processes and link them together (Shi et al., 2014b). In any case, all of this data gives a completely new twist to our former, more simplistic view of these processes; they show that they are in truth much more complex. Nevertheless, it is clear that many of their findings must still be shown to be biologically relevant, which will require additional work.

REFERENCES

- Barak, I. (2013). Open questions about the function and evolution of bacterial Min systems. *Front. Microbiol.* 4:378. doi: 10.3389/fmicb.2013.00378
- Barak, I., Prepiak, P., and Schmeisser, F. (1998). MinCD proteins control the septation process during sporulation of *Bacillus subtilis*. *J. Bacteriol.* 180, 5327–5333.
- Ben Yehuda, S., Rudner, D. Z., and Losick, R. (2003). RacA, a bacterial protein that anchors chromosomes to the cell poles. *Science* 299, 532–536. doi: 10.1126/science.1079914
- Cha, J.-H., and Stewart, G. C. (1997). The *divIVA* minicell locus of *Bacillus subtilis*. *J. Bacteriol.* 179, 1671–1683.
- Chao, J. D., Wong, D., and Av-Gay, Y. (2014). Microbial protein-tyrosine kinases. *J. Biol. Chem.* 289, 9463–9472. doi: 10.1074/jbc.R113.520015
- Eswaramoorthy, P., Winter, P. W., Wawrzusin, P., York, A. G., Shroff, H., and Ramamurthi, K. S. (2014). Asymmetric division and differential gene expression during a bacterial developmental program requires DivIVA. *PLoS Genet.* 10:e1004526. doi: 10.1371/journal.pgen.1004526
- Kobir, A., Shi, L., Boskovic, A., Grangeasse, C., Franjevic, D., and Mijakovic, I. (2011). Protein phosphorylation in bacterial signal transduction. *Biochim. Biophys. Acta* 1810, 989–994. doi: 10.1016/j.bbagen.2011.01.006
- Sharp, M. D., and Pogliano, K. (2002). MinCD-dependent regulation of the polarity of SpoIIIE assembly and DNA transfer. *EMBO J.* 21, 6267–6274. doi: 10.1093/emboj/cdf597
- Shi, L., Pignonneau, N., Ravikumar, V., Dobrinic, P., Macek, B., Franjevic, D., et al. (2014b). Cross-phosphorylation of bacterial serine/threonine and tyrosine protein kinases on key regulatory residues. *Front. Microbiol.* 5:495. doi: 10.3389/fmicb.2014.00495
- Shi, L., Pignonneau, N., Ventroux, M., Derouiche, A., Bidnenko, V., Mijakovic, I., et al. (2014a). Protein-tyrosine phosphorylation interaction network in *Bacillus subtilis* reveals new substrates, kinase activators and kinase cross-talk. *Front. Microbiol.* 5:538. doi: 10.3389/fmicb.2014.00538

Conflict of Interest Statement: The author declares that the research was conducted in the absence of any commercial or financial relationships that could be construed as a potential conflict of interest.

Received: 13 November 2014; accepted: 02 December 2014; published online: 17 December 2014.

Citation: Barák I (2014) Complexity of bacterial phosphorylation interaction network. *Front. Microbiol.* 5:725. doi: 10.3389/fmicb.2014.00725

This article was submitted to *Microbial Physiology and Metabolism*, a section of the journal *Frontiers in Microbiology*.

Copyright © 2014 Barák. This is an open-access article distributed under the terms of the Creative Commons Attribution License (CC BY). The use, distribution or reproduction in other forums is permitted, provided the original author(s) or licensor are credited and that the original publication in this journal is cited, in accordance with accepted academic practice. No use, distribution or reproduction is permitted which does not comply with these terms.



Far from being well understood: multiple protein phosphorylation events control cell differentiation in *Bacillus subtilis* at different levels

Jan Gerwig and Jörg Stülke *

Department of General Microbiology, Institute for Microbiology and Genetics, University of Göttingen, Göttingen, Germany

*Correspondence: jstuelke@gwdg.de

Edited by:

Ivan Mijakovic, Chalmers University of Technology, Sweden

Reviewed by:

Carsten Jers, Technical University of Denmark, Denmark

Colin Harwood, Newcastle University, UK

Keywords: biofilm formation, cross-talk, tyrosine phosphorylation, EpsB, PtkA

CELL DIFFERENTIATION IN *BACILLUS SUBTILIS*

In their endless struggle to survive in harsh and rapidly changing environments, many bacteria depend on their ability to live together as multicellular communities, also known as biofilms. In these communities cells are embedded within a self-produced slimy matrix that is mainly composed out of extracellular polysaccharides and proteins (Hall-Stoodley et al., 2004). This matrix enables the cells to cover a solid surface or to float as a community and can protect them from harmful environmental substances, such as antibiotics or competitors. In addition, biofilm or matrix production can also function as a virulence factor, as described for the genetic disorder cystic fibrosis that goes along with colonization by a *Pseudomonas aeruginosa* biofilm (Costerton et al., 1999). The Gram-positive soil bacterium *Bacillus subtilis* can choose between a variety of lifestyles such as sporulation, motility as an explorative lifestyle, biofilm formation, and the acquisition of genetic competence for the uptake of foreign DNA (López and Kolter, 2010).

In the *B. subtilis* biofilm communities, different groups of cells fulfill distinct functions, which are important for the well-being of the whole community of clonal identical bacteria. Some bacteria produce extracellular polysaccharides and proteins and thereby provide the matrix for the community. Other cells secrete exoproteases for degradation of protein as an alternative energy source

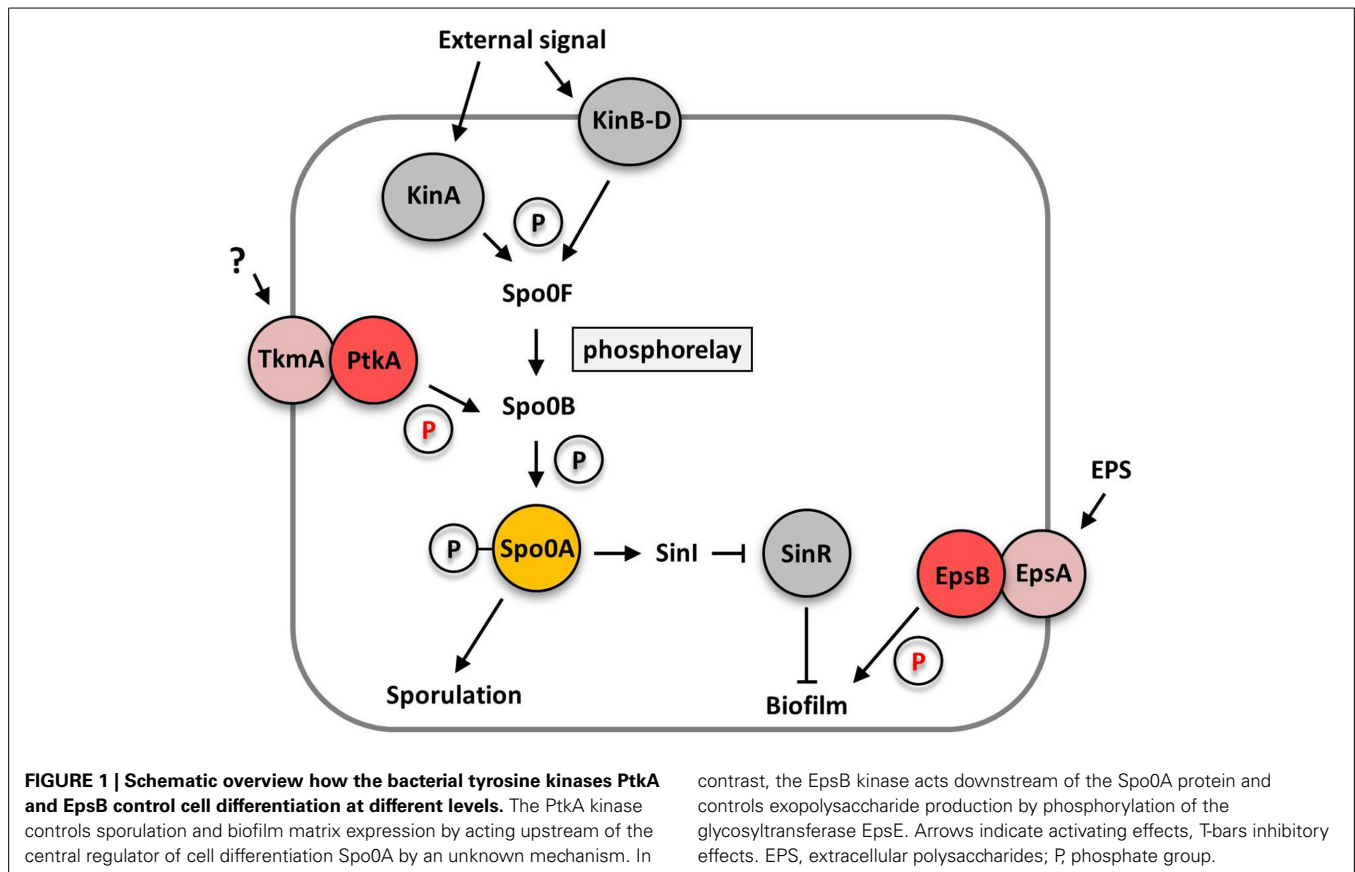
(Marlow et al., 2014). Furthermore, cells within the biofilm can differentiate into spores when the community gets older and nutrients are limiting (López and Kolter, 2010). However, not all cells within a biofilm differentiate into spores upon nutrient limitation. Some members of a biofilm community can regain motility. This allows them to leave the biofilm and explore the environment for new sources of nutrients. From an evolutionary point of view the presence of different cell forms provides versatility and enables the bacterium to adapt rapidly to different environmental conditions. But how are these complex communities and the observed cell differentiation processes regulated?

NOVEL REGULATORY TYROSINE PHOSPHORYLATION ADDS EVEN MORE COMPLEXITY TO THE REGULATORY NETWORK FOR CELL DIFFERENTIATION

Recent studies in *B. subtilis* suggest that tyrosine phosphorylation plays an important role in the regulation of biofilm formation and cell differentiation, in addition to the known mechanisms of transcriptional regulation and protein-protein interactions (for review see Vlamakis et al., 2013; Mielich-Süss and Lopez, 2014; Mhatre et al., 2014). In Gram-positive bacteria, tyrosine kinases consist of a transmembrane modulator protein and a cytosolic kinase protein (Grangeasse et al., 2012). *B. subtilis* encodes two protein tyrosine kinase/modulator couples, PtkA/ TkmA, and

EpsB/ EpsA. Interestingly, the simultaneous deletion of either both kinase or modulator genes totally abolished extracellular polysaccharide production causing a biofilm defect. The single mutants did not phenocopy the kinase or modulator double mutant and were still able to produce exopolysaccharides. However, colony structure and pellicle formation was affected in the single mutants (Gerwig et al., 2014) suggesting that both kinase systems contribute in a distinct way to biofilm formation. The loss of the EpsB kinase reduced wrinkle formation and the production of extracellular polysaccharides, but did not destroy the rough colony surface, which is indicative of the formation of fruiting bodies for sporulation (Elsholz et al., 2014; Gerwig et al., 2014). Thus, EpsB does not seem to affect sporulation. In contrast, loss of the EpsB homolog PtkA did not affect extracellular polysaccharide production but instead drastically reduced sporulation in biofilm cells thus leading to a loss of the rough appearance of the outer region of the colonies (Kiley and Stanley-Wall, 2010; Gerwig et al., 2014). These observations indicate that the protein tyrosine kinases EpsB and PtkA influence cell differentiation of *B. subtilis* at different levels: EpsB acts downstream of the central regulator of cell differentiation, Spo0A, whereas PtkA is likely to act upstream of Spo0A (see Figure 1).

In principle, the stochastic phosphorylation state of the Spo0A protein determines to which promoters the protein binds and consequently if cells



differentiate into a spore or become a matrix producer. High levels of phosphorylated Spo0A induce spore development, whereas medium levels lead to matrix production (Fujita and Losick, 2005; Fujita et al., 2005). Of course, Spo0A phosphorylation is highly regulated: it receives its phosphoryl groups via a complex phosphorelay system consisting of several sensor kinases and the Spo0F and Spo0B phosphotransferases. The phosphorelay is activated in response to multiple triggers such as the potassium concentration, plant polysaccharides and oxygen availability that are sensed by the Kin family sensor kinases (López et al., 2009; Beauregard et al., 2013; Kolodkin-Gal et al., 2013, see **Figure 1**). This highly complex regulatory network controlling the phosphorylation state of the central regulator of cell differentiation Spo0A allows the integration of many different signals into the phosphorelay. Furthermore, the phosphorelay provides multiple potential targets for post-translational control by the PtkA tyrosine kinase.

HOW DO THE TYROSINE KINASES PtkA AND EpsB INFLUENCE CELL DIFFERENTIATION?

In order to influence sporulation efficiency as shown by Kiley and Stanley-Wall (2010), PtkA most likely has to affect the phosphorelay that governs the phosphorylation state of the Spo0A protein. Since PtkA is a tyrosine kinase it seems likely that this influence involves post-translational tyrosine phosphorylation rather than acting e.g., on transcriptional level. Unfortunately, the most difficult question has not yet been solved: what is the phosphorylation target of the PtkA kinase and how can we identify it?

In order to explain altered biofilm formation and the sporulation defect of the *ptkA* mutant, Kiley and Stanley-Wall (2010) conducted an intensive search for possible phosphorylation targets but failed to identify one. Deletion of the long-known PtkA targets (the UDP-Glucose dehydrogenases Ugd and TuaD) did not exert an effect on biofilm formation. Moreover, several other targets proposed by large-scale phosphoproteomics and

other studies (Macek et al., 2007; Jers et al., 2010) were not of relevance. Therefore, it remains unclear how PtkA affects biofilm formation and sporulation. Unfortunately, a recent phosphoproteome study did not reveal obvious targets related to the phosphorelay (Ravikumar et al., 2014), except the regulator of transition phase genes AbrB was found to be phosphorylated on a tyrosine residue. However, the physiological relevance of this phosphorylation is unclear, and serine phosphorylation of AbrB was observed in another study (Kobir et al., 2014). Clearly, more work is required to dissect the potential control of AbrB activity by phosphorylation.

A more obvious problem for the identification of tyrosine phosphorylated proteins with the potential to control biofilm formation and sporulation is that most published data relates to cells harvested from exponentially growing cultures rather than from biofilms. Moreover, the studies were performed with strains derived from a domesticated strain that does not produce robust biofilms. Thus, it is reasonable to assume that not all of the

proteins that might be relevant for biofilm formation and sporulation are expressed under these conditions. Furthermore, regulatory phosphorylation is a rapid method for adapting cellular processes to environmental changes. Thus, it seems safe to assume that not all phosphorylations are present permanently. Interestingly, all currently identified tyrosine phosphorylation reactions with functional relevance have been found by attempts other than large-scale phosphoproteomics analyses. Examples include the regulator of unsaturated fatty acid synthesis FatR (Derouiche et al., 2013), single stranded DNA-binding proteins (Mijakovic et al., 2006) and the glycosyltransferase EpsE, a target of the tyrosine kinase EpsB (Elsholz et al., 2014). With the exception of UDP-glucose dehydrogenase Ugd (by Macek et al., 2007), none of these proteins were identified in the latest large-scale phosphoproteome experiments (Macek et al., 2007; Ravikumar et al., 2014). In conclusion, identification of the PtkA phosphorylation target and explanation of the sporulation defect of the mutant remains elusive but it is tempting to speculate that the highly complex network for the control of Spo0A is affected by the PtkA kinase. Since cross-phosphorylation of kinases is an established concept in eukaryotes and hints supporting this idea in prokaryotes are emerging (Baer et al., 2014; Shi et al., 2014) phosphorylation of phosphorelay proteins is a highly attractive hypothesis.

The second level of regulatory tyrosine phosphorylation is provided by the EpsB kinase that phosphorylates the glycosyltransferase EpsE (Elsholz et al., 2014). The kinase and the phosphorylation target are both encoded in the *eps* operon for exopolysaccharide production. Hence, the regulation of the two corresponding genes is similar. The *eps* operon is only strongly expressed if the SinR anti-activator protein is inhibited by either of its antagonists SinI and SlrR under biofilm forming conditions (Kearns et al., 2005; Newman et al., 2013; Winkelman et al., 2013). This observation implies that EpsB-mediated phosphorylation might not have a global effect and that the phosphorylated target is among the proteins expressed under biofilm forming conditions that are also subject to repression by SinR. Indeed, deletion of the *epsB* gene only affects

exopolysaccharide production but leaves sporulation unaffected (Gerwig et al., 2014). Strikingly, deletion of the gene for the EpsE glycosyltransferase leads to a complete loss of exopolysaccharide production and complex colony formation, whereas deletion of the gene for the EpsB kinase has a milder effect (Guttenplan et al., 2010). Therefore, it is tempting to speculate that PtkA can partially take over the function of EpsB. However, this has not been demonstrated experimentally.

FUNCTIONAL CROSS-TALK BETWEEN TYROSINE KINASE/ MODULATOR COUPLES

Straight signal transduction is an important issue for many conserved multi-component signal transduction system families and has been extensively studied for two-component regulatory systems and phosphotransferase system-controlled RNA-binding antitermination proteins. These systems have evolved to avoid non-cognate interactions either by restricting the interactions with non-cognate proteins partners, ligands, and target molecules. Moreover, differential gene expression of the non-cognate components has been observed to prevent non-productive cross-talk (Schilling et al., 2006; Szurmant and Hoch, 2010; Hübner et al., 2011; Podgornaia and Laub, 2013).

However, this might be different for regulatory tyrosine phosphorylation, as suggested for the interplay between EpsB and PtkA. In yeast (Shi et al., 2014) and bacterial two-hybrid studies the TkmA modulator and the EpsB kinase interact with each other, whereas the EpsA modulator and the PtkA kinase do not interact. Additionally, a genetic analysis of a potential cross-talk in the laboratory strain 168 revealed that simultaneous loss of PtkA and EpsA does not affect stable pellicle formation, whereas simultaneous deletion of the genes for EpsB and TkmA inhibited stable pellicle formation. These observations further support a functional connection between the two systems. However, confirmation of this result was not obtained in the background of the NCIB3610 wild type strain. Although the functional relevance of the TkmA/EpsB cross-talk remains unclear, similar observations come from *Staphylococcus aureus* that also contains two similar tyrosine

kinase/ modulator couples. In this case, the Cap5A1 modulator protein of one couple and the Cap5B2 protein tyrosine kinase of the other couple show functional cross-talk suggesting that interplay between different tyrosine/ modulator couples might not be limited to *B. subtilis* (Soulat et al., 2007).

OUTLOOK

The detection of a regulatory interplay between protein tyrosine phosphorylation and classical sensing via the phosphorelay in the control of cell differentiation in *B. subtilis* is one of the most exciting results of recent studies. This is underlined by the observation of extensive links between the different signal transduction systems that involve post-translational modifications (van Noort et al., 2012; Shi et al., 2014). One main task for future work is the identification of phosphorylation targets of the tyrosine kinase PtkA in order to get a better understanding of its implication in biofilm formation and sporulation. To demonstrate that PtkA affects cell differentiation upstream of the central regulator Spo0A, the phosphorylation state of Spo0A has to be analyzed in a *ptkA* deletion mutant. Furthermore, large-scale phosphoproteomics under biofilm-promoting conditions could help to identify potential tyrosine phosphorylated targets. Additional tasks are the identification of substances that can be sensed by the PtkA modulator protein TkmA and to further dissect the potential cross-talk between the two known tyrosine kinase/ modulator couples EpsB/ EpsA and PtkA/ TkmA in *B. subtilis*.

ACKNOWLEDGMENTS

We thank Katrin Bäsell, Sabryna Junker, and Dörte Becher for helpful discussions. Work in the authors' lab is supported by the Deutsche Forschungsgemeinschaft through SFB860.

REFERENCES

- Baer, C. E., Iavarone, A. T., Alber, T., and Sassetti, C. M. (2014). Biochemical and spatial coincidence in the provisional Ser/Thr protein kinase interaction network of *Mycobacterium tuberculosis*. *J. Biol. Chem.* 289, 20422–20433. doi: 10.1074/jbc.M114.559054
- Beauregard, P. B., Chai, Y., Vlamakis, H., Losick, R., and Kolter, R. (2013). *Bacillus subtilis* biofilm induction by plant polysaccharides. *Proc. Natl. Acad. Sci. U.S.A.* 110, E1621–E1630. doi: 10.1073/pnas.1218984110

- Costerton, J. W., Stewart, P. S., and Greenberg, E. P. (1999). Bacterial biofilms: a common cause of persistent infections. *Science* 284, 1318–1322. doi: 10.1126/science.284.5418.1318
- Derouiche, A., Bidnenko, V., Grenha, R., Pignonneau, N., Ventroux, M., Franz-Wachtel, M., et al. (2013). Interaction of bacterial fatty-acid-displaced regulators with DNA is interrupted by tyrosine phosphorylation in the helix-turn-helix domain. *Nucleic Acids Res.* 41, 9371–9381. doi: 10.1093/nar/gkt709
- Elsholz, A. K. W., Wacker, S. A., and Losick, R. (2014). Self-regulation of exopolysaccharide production in *Bacillus subtilis* by a tyrosine kinase. *Genes Dev.* 28, 1710–1720. doi: 10.1101/gad.246397.114
- Fujita, M., González-Pastor, J. E., and Losick, R. (2005). High- and low-threshold genes in the Spo0A regulon of *Bacillus subtilis*. *J. Bacteriol.* 187, 1357–1368. doi: 10.1128/JB.187.4.1357-1368.2005
- Fujita, M., and Losick, R. (2005). Evidence that entry into sporulation in *Bacillus subtilis* is governed by a gradual increase in the level and activity of the master regulator Spo0A. *Genes Dev.* 19, 2236–2244. doi: 10.1101/gad.1335705
- Gerwig, J., Kiley, T. B., Gunka, K., Stanley-Wall, N., and Stülke, J. (2014). The protein tyrosine kinases EpsB and PtkA differentially affect biofilm formation in *Bacillus subtilis*. *Microbiology* 160, 682–691. doi: 10.1099/mic.0.074971-0
- Grangeasse, C., Nessler, S., and Mijakovic, I. (2012). Bacterial tyrosine kinases: evolution, biological function and structural insights. *Philos. Trans. R. Soc. Lond. B. Biol. Sci.* 367, 2640–2655. doi: 10.1098/rstb.2011.0424
- Guttenplan, S. B., Blair, K. M., and Kearns, D. B. (2010). The EpsE flagellar clutch is bifunctional and synergizes with EPS biosynthesis to promote *Bacillus subtilis* biofilm formation. *PLoS Genet.* 6:e1001243. doi: 10.1371/journal.pgen.1001243
- Hall-Stoodley, L., Costerton, J. W., and Stoodley, P. (2004). Bacterial biofilms: from the natural environment to infectious diseases. *Nat. Rev. Microbiol.* 2, 95–108. doi: 10.1038/nrmicro821
- Hübner, S., Declerck, N., Diethmaier, C., Le Coq, D., Aymerich, S., and Stülke, J. (2011). Prevention of cross-talk in conserved regulatory systems: Identification of specificity determinants in RNA-binding antitermination proteins of the BglG family. *Nucleic Acids Res.* 39, 4360–4372. doi: 10.1093/nar/gkr021
- Jers, C., Pedersen, M. M., Paspaliari, D. K., Schütz, W., Johnsson, C., Soufi, B., et al. (2010). *Bacillus subtilis* BY-kinase PtkA controls enzyme activity and localization of its protein substrates. *Mol. Microbiol.* 77, 287–299. doi: 10.1111/j.1365-2958.2010.07227.x
- Kearns, D. B., Chu, F., Branda, S. S., Kolter, R., and Losick, R. (2005). A master regulator for biofilm formation by *Bacillus subtilis*. *Mol. Microbiol.* 55, 739–749. doi: 10.1111/j.1365-2958.2004.04440.x
- Kiley, T. B., and Stanley-Wall, N. R. (2010). Post-translational control of *Bacillus subtilis* biofilm formation mediated by tyrosine phosphorylation. *Mol. Microbiol.* 78, 947–963. doi: 10.1111/j.1365-2958.2010.07382.x
- Kobir, A., Poncet, S., Bidnenko, V., Delumeau, O., Jers, C., Zouhir, S., et al. (2014). Phosphorylation of *Bacillus subtilis* gene regulator AbrB modulates its DNA-binding properties. *Mol. Microbiol.* 92, 1129–1141. doi: 10.1111/mmi.12617
- Kolodkin-Gal, I., Elsholz, A. K. W., Muth, C., Girguis, P. R., Kolter, R., and Losick, R. (2013). Respiration control of multicellularity in *Bacillus subtilis* by a complex of the cytochrome chain with a membrane-embedded histidine kinase. *Genes Dev.* 27, 887–899. doi: 10.1101/gad.215244.113
- López, D., Fischbach, M. A., Chu, F., Losick, R., and Kolter, R. (2009). Structurally diverse natural products that cause potassium leakage trigger multicellularity in *Bacillus subtilis*. *Proc. Natl. Acad. Sci. U.S.A.* 106, 280–285. doi: 10.1073/pnas.0810940106
- López, D., and Kolter, R. (2010). Extracellular signals that define distinct and coexisting cell fates in *Bacillus subtilis*. *FEMS Microbiol. Rev.* 34, 134–149. doi: 10.1111/j.1574-6976.2009.00199.x
- Macek, B., Mijakovic, I., Olsen, J. V., Gnad, F., Kumar, C., Jensen, P. R., et al. (2007). The serine/threonine/tyrosine phosphoproteome of the model bacterium *Bacillus subtilis*. *Mol. Cell. Proteomics* 6, 697–707. doi: 10.1074/mcp.M600464-MCP200
- Marlow, V. L., Cianfanelli, F. R., Porter, M., Cairns, L. S., Dale, J. K., and Stanley-Wall, N. R. (2014). The prevalence and origin of exoprotease-producing cells in the *Bacillus subtilis* biofilm. *Microbiology* 160, 56–66. doi: 10.1099/mic.0.072389-0
- Mhatre, E., Monterrosa, R. G., and Kovács, A. T. (2014). From environmental signals to regulators: modulation of biofilm development in Gram-positive bacteria. *J. Basic Microbiol.* 54, 616–632. doi: 10.1002/jobm.201400175
- Mielich-Süss, B., and Lopez, D. (2014). Molecular mechanisms involved in *Bacillus subtilis* biofilm formation. *Environ. Microbiol.* doi: 10.1111/1462-2920.12527. [Epub ahead of print].
- Mijakovic, I., Petranovic, D., Macek, B., Cepo, T., Mann, M., Davies, J., et al. (2006). Bacterial single-stranded DNA-binding proteins are phosphorylated on tyrosine. *Nucleic Acids Res.* 34, 1588–1596. doi: 10.1093/nar/gkj514
- Newman, J. A., Rodrigues, C., and Lewis, R. J. (2013). Molecular basis of the activity of SinR protein, the master regulator of biofilm formation in *Bacillus subtilis*. *J. Biol. Chem.* 288, 10766–10778. doi: 10.1074/jbc.M113.455592
- Podgoraia, A. I., and Laub, M. T. (2013). Determinants of specificity in two-component signal transduction. *Curr. Opin. Microbiol.* 16, 156–162. doi: 10.1016/j.mib.2013.01.004
- Ravikumar, V., Shi, L., Krug, K., Derouiche, A., Jers, C., Cousin, C., et al. (2014). Quantitative phosphoproteome analysis of *Bacillus subtilis* reveals novel substrates of the kinase PrkC and phosphatase PrpC. *Mol. Cell. Proteomics* 13, 1965–1978. doi: 10.1074/mcp.M113.035949
- Schilling, O., Herzberg, C., Hertrich, T., Vörsmann, H., Jessen, D., Hübner, S., et al. (2006). Keeping signals straight in transcription regulation: specificity determinants for the interaction of a family of conserved bacterial RNA-protein couples. *Nucleic Acids Res.* 34, 6102–6115. doi: 10.1093/nar/gkl733
- Shi, L., Pigeonneau, N., Ravikumar, V., Dobrinic, P., Macek, B., Franjevic, D., et al. (2014). Cross-phosphorylation of bacterial serine/threonine and tyrosine protein kinases on key regulatory residues. *Front. Microbiol.* 5:495. doi: 10.3389/fmicb.2014.00495
- Soulat, D., Grangeasse, C., Vaganay, E., Cozzzone, A. J., and Duclos, B. (2007). UDP-acetyl-mannosamine dehydrogenase is an endogenous protein substrate of *Staphylococcus aureus* protein-tyrosine kinase activity. *J. Mol. Microbiol. Biotechnol.* 13, 45–54. doi: 10.1159/000103596
- Szurmant, H., and Hoch, J. A. (2010). Interaction fidelity in two-component signaling. *Curr. Opin. Microbiol.* 13, 190–197. doi: 10.1016/j.mib.2010.01.007
- van Noort, V., Seebacher, J., Bader, S., Mohammed, S., Vonkova, I., Betts, M. J., et al. (2012). Cross-talk between phosphorylation and lysine acetylation in a genome-reduced bacterium. *Mol. Syst. Biol.* 8, 571. doi: 10.1038/msb.2012.4
- Vlamakis, H., Chai, Y., Beauregard, P., Losick, R., and Kolter, R. (2013). Sticking together: building a biofilm the *Bacillus subtilis* way. *Nat. Rev. Microbiol.* 11, 157–168. doi: 10.1038/nrmicro2960
- Winkelman, J. T., Bree, A. C., Bate, A. R., Eichenberger, P., Gourse, R. L., and Kearns, D. B. (2013). RemA is a DNA-binding protein that activates biofilm matrix gene expression in *Bacillus subtilis*. *Mol. Microbiol.* 88, 984–997. doi: 10.1111/mmi.12235

Conflict of Interest Statement: The authors declare that the research was conducted in the absence of any commercial or financial relationships that could be construed as a potential conflict of interest.

Received: 29 October 2014; accepted: 27 November 2014; published online: 10 December 2014.

Citation: Gerwig J and Stülke J (2014) Far from being well understood: multiple protein phosphorylation events control cell differentiation in *Bacillus subtilis* at different levels. *Front. Microbiol.* 5:704. doi: 10.3389/fmicb.2014.00704

This article was submitted to *Microbial Physiology and Metabolism*, a section of the journal *Frontiers in Microbiology*.

Copyright © 2014 Gerwig and Stülke. This is an open-access article distributed under the terms of the Creative Commons Attribution License (CC BY). The use, distribution or reproduction in other forums is permitted, provided the original author(s) or licensor are credited and that the original publication in this journal is cited, in accordance with accepted academic practice. No use, distribution or reproduction is permitted which does not comply with these terms.



Protein-tyrosine phosphorylation interaction network in *Bacillus subtilis* reveals new substrates, kinase activators and kinase cross-talk

Lei Shi^{1,2†}, Nathalie Pigeonneau^{1†}, Magali Ventroux¹, Abderahmane Derouiche^{1,2}, Vladimir Bidnenko², Ivan Mijakovic^{1,2} and Marie-Françoise Noirot-Gros^{1*}

¹ Institut National de la Recherche Agronomique, UMR1319 Micalis, Jouy-en-Josas, France

² Systems and Synthetic Biology, Department of Chemical and Biological Engineering, Chalmers University of Technology, Gothenburg, Sweden

Edited by:

Christophe Grangeasse, Centre National de la Recherche Scientifique, France

Reviewed by:

Bettina Siebers, University of Duisburg-Essen, Germany
Imrich Barak, Slovak Academy of Sciences, Slovakia

*Correspondence:

Marie-Françoise Noirot-Gros, Institut National de la Recherche Agronomique, UMR1319 Micalis, Domaine de Vilvert, 78350 Jouy-en-Josas, France
e-mail: marie-francoise.gros@jouy.inra.fr

[†] These authors have contributed equally to this work.

Signal transduction in eukaryotes is generally transmitted through phosphorylation cascades that involve a complex interplay of transmembrane receptors, protein kinases, phosphatases and their targets. Our previous work indicated that bacterial protein-tyrosine kinases and phosphatases may exhibit similar properties, since they act on many different substrates. To capture the complexity of this phosphorylation-based network, we performed a comprehensive interactome study focused on the protein-tyrosine kinases and phosphatases in the model bacterium *Bacillus subtilis*. The resulting network identified many potential new substrates of kinases and phosphatases, some of which were experimentally validated. Our study highlighted the role of tyrosine and serine/threonine kinases and phosphatases in DNA metabolism, transcriptional control and cell division. This interaction network reveals significant crosstalk among different classes of kinases. We found that tyrosine kinases can bind to several modulators, transmembrane or cytosolic, consistent with a branching of signaling pathways. Most particularly, we found that the division site regulator MinD can form a complex with the tyrosine kinase PtkA and modulate its activity *in vitro*. *In vivo*, it acts as a scaffold protein which anchors the kinase at the cell pole. This network highlighted a role of tyrosine phosphorylation in the spatial regulation of the Z-ring during cytokinesis.

Keywords: protein phosphorylation, protein-protein network, bacterial protein kinase, bacterial cell division, bacterial signaling

INTRODUCTION

In eukarya, protein phosphorylation on serine/threonine and tyrosine residues is catalyzed by the Hanks-type family of protein kinases (Hanks et al., 1988). In bacteria, Hanks-type kinases catalyze phosphorylation of proteins only on serine and threonine residues (Pereira et al., 2011), and a distinct family of kinases, termed bacterial tyrosine kinases (BY-kinases), phosphorylate proteins on tyrosine (Grangeasse et al., 2007). BY-kinases have been initially described as autophosphorylating enzymes involved in exopolysaccharide synthesis and export (Whitfield, 2006). More recently, it became apparent that they phosphorylate many protein substrates and regulate their activity (Shi et al., 2010). Arguably the best characterized bacterial system with respect to physiological substrates of BY-kinases is the Firmicute model organism *Bacillus subtilis* (Mijakovic et al., 2005b). *B. subtilis* possesses a well characterized BY-kinase PtkA (Mijakovic et al., 2003) and a putative BY-kinase PtkB (EpsB). In order to phosphorylate its substrates, PtkA requires a transmembrane activator TkmA (Mijakovic et al., 2003), which is encoded by the same operon as the kinase. PtkB-encoding operon also codes for a transmembrane activator termed TkmB (Mijakovic et al., 2005b). While structurally the TkmB/PtkB pair constitutes a

bona fide BY-kinase, its activity toward substrates has never been experimentally demonstrated. Recent study suggested that TkmB interaction with PtkB could modulate its function in biofilm formation in *B. subtilis* (Gerwig et al., 2014). Homologs of TkmA and TkmB exist also in proteobacteria, but there they are “fused” with the BY-kinases in a single polypeptide chain, encoded by a single gene (Jadeau et al., 2012). The rationale behind these different architectures has puzzled researchers for years. One hypothesis suggests that dissociation of BY-kinases from transmembrane activators in Firmicutes may enable these kinases to interact with alternative (possibly cytosolic) modulator proteins (Shi et al., 2010).

B. subtilis PtkA is known to phosphorylate a broad spectrum of substrates, including UDP-glucose dehydrogenases (Mijakovic et al., 2003), single-stranded DNA-binding proteins (Mijakovic et al., 2006), transcription factors (Derouiche et al., 2013) and other enzymes (Jers et al., 2010). Cells devoid of PtkA exhibit a pleiotropic phenotype with defects in cell cycle (Petranovic et al., 2007) and biofilm formation (Kiley and Stanley-Wall, 2010). In addition to regulating the enzyme activity of certain substrates, PtkA also seems to affect sub-cellular localization of others (Jers et al., 2010). Bacterial Hanks-type serine/threonine

(Ser/Thr) kinases are equally promiscuous toward their substrates (Pereira et al., 2011). This is exemplified by the Hanks-type kinase PrkC from *B. subtilis*, which phosphorylates the essential translation factor EF-G (Gaidenko et al., 2002) and the enzymes involved in carbohydrate metabolism: the transaldolase YwjH, the glutamine synthetase GlnA, the isocitrate dehydrogenase Icd and the acetolactate-decarboxylase AlsD (Pietack et al., 2010). While recent phosphoproteomic studies in *B. subtilis* have revealed about a dozen proteins phosphorylated on tyrosine, and many more on serine and threonine (Macek et al., 2007; Soufi et al., 2010), identification of kinases responsible for these phosphorylation events *in vivo* remains a major challenge. The full complement of protein kinases in *B. subtilis* includes BY-kinases PtkA and PtkB (Mijakovic et al., 2003), the serine/threonine kinases of the Hanks type PrkC, PrkD, and YabT (Madec et al., 2002; Bidnenko et al., 2013), the unique serine/threonine kinase HprK/P (Galinier et al., 1998), the two-component-like serine/threonine kinases RsbT, RsbW, and SpoIIAB (Garsin et al., 1998; Pane-Farre et al., 2005), and 37 standard two component system kinases (Fabret et al., 1999; Kobayashi et al., 2001). The complement of corresponding phosphatases is much smaller, including the phosphotyrosine-protein phosphatases PtpZ (YwqE), YfkJ, and YwIE (Mijakovic et al., 2005a; Musumeci et al., 2005), and phosphoserine/threonine-protein phosphatases PrpC and SpoIIE (Duncan et al., 1995; Obuchowski et al., 2000). In addition, an arginine phosphorylation system has been described recently in *B. subtilis*, involving the kinase McsB and the phosphatase YwIE (Elsholz et al., 2012).

To address these crucial questions on the physiological relationships of the kinases, their substrates and alternative kinase modulators, we set out to construct a high confidence protein-protein interaction network centered on known BY-kinases, activators and phosphatases in *B. subtilis*. Our yeast two-hybrid interactome approach identified numerous candidates of high biological relevance for interactions with protein kinases and cognate phosphatases. In addition, it detected clustering of shared substrates at the interface between kinase and phosphatase nodes. It confirmed several known kinase-substrate relationships, and revealed a number of new ones, notably substrates involved in DNA replication, transcriptional regulation and cell division. Most importantly, we identified the division site selection factor MinD as an anchoring protein which modulates PtkA activity. Our approach also pointed to the existence of cross-talk between the BY-kinase and the Hanks-type Ser/Thr kinase interaction networks, revealing that the two are tightly interconnected. This suggests that bacterial protein kinases (BY- and Ser/Thr Hanks-type) could be regulated by complex signaling cascades, similar to the ones found so far only in eukarya. This study constitutes the most comprehensive view of a bacterial signaling network based on protein phosphorylation to date.

MATERIAL AND METHODS

CONSTRUCTION OF VECTORS FOR PROTEIN EXPRESSION

All PCR amplifications were performed using *B. subtilis* 168 genomic DNA as template and primers as listed in Table S4. To construct the knock-out *minD* mutant, a PCR-amplified internal fragment of the *minD* gene was inserted into pMUTIN2 (Vagner

et al., 1998). To obtain the CFP-N terminally fused proteins, *minD* and *ptkA* gene coding sequences were first inserted into a pSG1911 plasmid derivative (Feucht and Lewis, 2001) prior to insertion at the *amyE* platform locus. For protein expression and purification, PCR fragments were inserted into plasmid pQE-30 Xa (Qiagen) to get the 6xHis-tag fusion proteins. Strep-tagged versions of proteins were obtained from a pQE-30 vector with His6-tag replaced by the strep-tag (Jers et al., 2010). For yeast two hybrid the PCR-amplified gene coding sequences (listed in Table S4-A) were cloned into the bait vector pGBDU-C1, in frame with the binding domain of Gal4 (James et al., 1996), and transformed in PJ69-4A yeast haploid strain (James et al., 1996).

STRAIN CONSTRUCTIONS

Strains used in this study as well as primers employed for constructions are precised in Table S4-A,B. The *zapA::Spc^R* disruption mutation was transferred into Δ *ptkA* background by transformation of the competent Δ *ptkA* cells with chromosomal DNA from LH165 (L. Hamoen; Kawai and Ogasawara, 2006) to spectinomycin resistance. The *minD* gene was inactivated using the vector pMUTIN2 (Vagner et al., 1998). *MinD* inactivation mutation was then transferred into the Δ *ptkA* background by transformation with pMUTIN::*minD* to erythromycin resistance.

YEAST TWO HYBRID SCREENINGS OF A *B. SUBTILIS* GENOMIC LIBRARY

The bait vectors were used to screen the pGAD-expressed *B. subtilis* genomic library in yeast using a previously described mating strategy (Noirot-Gros et al., 2002; Marchadier et al., 2011). Colonies were then tested for their ability to grow on SC -LUH and -LUA plates (lacking leucine, uracil, histidine or adenine). The prey candidates were identified by PCR amplification and sequencing of the DNA inserts from the pGAD plasmids. The potential false-positive interactions were eliminated experimentally using a specificity assays as previously described (Noirot-Gros et al., 2002). About $3\text{--}5 \times 10^7$ yeast haploid cells expressing the BD-bait protein were mated against 3×10^8 haploid cells of complementary mating type, expressing the *B. subtilis* genomic library of AD-fusion prey protein fragments (Noirot-Gros et al., 2002). Mating efficiencies (15–30%) allowed to test up to 10^8 possible interactions in one screen. For each screen, the mixture of mated cells was plated on rich medium and incubated for 4–5 h at 30°C, then collected, washed and spread on selective SC-LUH (synthetic complete medium lacking leucine, uracil, and histidine) plates supplemented with 0.5 mM 3-aminotriazole. After 7–10 days at 30°C, the His⁺ colonies were transferred on SC-LUA (synthetic complete medium lacking leucine, uracil, and adenine) plates for 3 days at 30°C. All the His⁺ Ade⁺ colonies were subjected to PCR amplification targeting AD prey-inserts were sequenced and compared with the *B. subtilis* genome.

INTERACTION SPECIFICITY ASSAY OF IDENTIFIED BAIT-PREYS PROTEIN PAIRS

False-positive interactions were experimentally removed by a specificity assay. Main sources of false positives in yeast two hybrid are (i) auto-activation of the reporter genes independently to the ability of the targeted protein to bind to a protein partner,

(ii) proteins with stickiness properties and (iii) modification of the basal reporter gene expression in the yeast diploid cell. This last category mostly gives non reproducible growth phenotypes. False positive were eliminated experimentally by rescuing the protein-encoding prey plasmids from the His⁺ Ade⁺ colonies and reintroducing in PJ69–4 α strain in order to perform binary interaction test assays. The rescue of the prey plasmid from diploid cells was carried out using a “gap-repair” cloning procedure as described elsewhere (Weir and Keeney, 2014). Using oligonucleotides priming upstream and downstream of the DNA insert, the prey gene fusion flanked by 150 pb homologous to the vector was amplified by PCR and co-transformed with pGAD linearized vector (digested with appropriated restriction sites within the MCS), in fresh yeast haploid cells. The yeast cell expressing the recombination-based reassembled prey plasmid were then mated against compatible haploid cells carrying (i) an empty pGBDU vector expressing and infused Gal4-BD domain, (ii) a vector expressing the targeted BD-bait protein and (iii) expressing more than three unrelated BD-protein fusions. An interaction is qualified as specific when reproduced twice with the original bait protein, without exhibiting auto-activation nor any unspecific stickiness phenotypes. As already observed (Noirot-Gros et al., 2002) 100% of the prey candidates identified as overlapping fragments of a given gene (class C1, Table S1) were found to be specific while only 20% of the prey proteins found as an unique fragment (class C2, Table S1) have passed the specificity test. In total, a given protein pair qualified as “specific” would have trigger interacting phenotypes up to three time (once during the genomic screen and at least twice during the matricial specificity test assay). The resulting network of specific bait-prey interactions is thus strongly enriched in complex with biological relevance. The protein interactions from this publication have been submitted to the IMEx consortium through IntAct (<http://www.imexconsortium.org>) (Orchard et al., 2014) and assigned the identifier IM-22270.

PPI NETWORK CONSTRUCTION

In the network the specific protein pairs were represented as nodes connected with edges using the open source software tool Cytoscape 3.0. The network was built from data on connected bait and preys as listed in Table S2.

PROTEINS EXPRESSION AND PURIFICATION

E. coli K12 NM522 and M15 (expressing chaperonin GroEL/GroES) were used for vector construction and protein purification, respectively. Cells were routinely grown in LB medium supplemented with appropriated antibiotics. Protein synthesis and purifications were carried out as described previously (Mijakovic et al., 2003). Induction of expression was initiated at OD₆₀₀ = 0.6 by the addition of IPTG (1 mM). Cells were harvested 3 h later and sonicated. From crude extracts, the 6xHis- or Strep-tagged proteins were purified using Ni-NTA (Qiagen), or Strep-Tactin affinity chromatography (Novagen), prior to desalting by PD-10 columns (GE Healthcare). Protein purity was estimated by scanning densitometry of coomassie stained SDS-Page gels (Table S5).

FAR-WESTERN BLOTTING

Proteins were separated by 12% SDS-PAGE and transferred onto nitrocellulose membranes. Proteins were then renatured (Wu et al., 2007) and incubated with MinD labeled with Strep-Tactin (conjugated to horse radish peroxidase, IBA) (Machida and Mayer, 2009) in TBS-T buffer (50 mM Tris, pH 7.5, 150 mM NaCl, 0.05% Tween 20) containing 1% BSA. For labeling, 50 μ l of 0.1 μ g/ μ l Strep-tagged MinD was incubated with 5 μ g Strep-Tactin on ice for 1 h. Signal was detected by AEC staining Kit (Sigma).

IN VITRO PHOSPHORYLATION ASSAYS

Proteins were incubated at 37°C in a reacting buffer (50 mM TrisHCl pH 7.5, 100 mM NaCl, 5 mM MgCl₂, 5% glycerol) containing 50 μ M ATP and 20 μ Ci/mmol [γ -³²P]-ATP, for 1 h, prior to migration on an 8–12% SDS-polyacrylamide gel. The radioactive signal was captured by a FUJI phosphorimager (Mijakovic et al., 2003). *In vitro* phosphorylation of RecA by PtkA was performed by mixing PtkA (2.5 μ M) and RecA (5 μ M) in the absence or presence of TkmA (2.5 μ M). Phosphorylation and dephosphorylation of RecA by YabT and SpoIIE, was performed by incubating RecA (1 μ M) with YabT (0.5 μ M). Then SpoIIE (5 μ M) was added to the reaction. Phosphorylation and dephosphorylation of RacA by YabT and SpoIIE was performed by mixing RacA (0.8 μ M) with YabT (0.15 μ M) at 37°C for 1 h. Centricon was used to remove ATP from the sample, prior to addition of SpoIIE (2 μ M) and DnaK (0.8 μ M). Phosphorylation of DnaC by PrkD was performed by mixing 1 μ M of DnaC/I stable co-purified complex with 0.1 μ M PrkD. Only DnaC (50.6 kD vs. 30.1 kD for DnaI) was found to be phosphorylated by PrkD. MinD potential kinase activity was assayed by mixing equimolar concentrations of TkmA, PtkA K59M, and MinD (2 μ M). *In vitro* phosphorylation of DivIVA was assayed by mixing equimolar concentrations of PtkA and TkmA (2 μ M) with DivIVA (3.5 μ M). MinD-mediated activation of PtkA was tested by incubating PtkA (2 μ M) with 0.5, 1.0, 2.0, 4.0, and 8.0 μ M of MinD. All the *in vitro* phosphorylation assays were reproduced at least three time.

FLUORESCENT MICROSCOPY

Strains were grown in liquid LB medium containing appropriated antibiotic overnight at 37°C prior to 1/1000 dilution in LB. Cell were then grown up to OD₆₀₀ 0.3. Samples were mounted on 1.2% agarose pads for examination of living cells by epifluorescent microscopy. The plasma membrane of *B. subtilis* cells were labeled using the vital stain FM 4–64 and nucleoids were stained with DAPI. CFP/GFP fluorescence was observed using appropriated dichroic filter sets.

RESULTS

A PROTEIN-PROTEIN INTERACTION NETWORK CENTERED ON BY-Kinases

A network of high biological significance was constructed using a yeast two-hybrid interactome walking approach, comprising a strategy for systematic elimination of false positives (Noirot-Gros et al., 2002; Marchadier et al., 2011). We first performed genome-wide yeast two-hybrid screens of a *B. subtilis* library to identify the proteins that physically associated with the BY-kinases

PtkA and PtkB, their cognate modulators TkmA and TkmB, and the three identified phosphotyrosine-protein phosphatases PtpZ (Mijakovic et al., 2005a), YwIE and YfkJ (Musumeci et al., 2005). To increase the likelihood of identifying potential kinase substrates, we also used PtkA mutant derivatives as baits, carrying point mutations either within the catalytic pocket (D81A or K59M) or within the C-terminal cluster with autophosphorylation sites (Y225F, Y227F, and Y228F) (Mijakovic et al., 2003).

In addition to the expected interactions between the BY-kinases and their respective modulators PtkA-TkmA and PtkB-TkmB, we observed a cross-connection between PtkB and TkmA as well as between TkmA and TkmB (Figure S1). The phosphotyrosine-protein phosphatase PtpZ appeared to interact with TkmA, whereas YwIE and YfkJ, the two low molecular weight phosphotyrosine-protein phosphatases (LMPTPs), lay separately from the BY-kinase and modulators (Figure S1). These findings are in agreement with previous studies indicating that PtpZ is the phosphatase dedicated to dephosphorylating substrates of PtkA/TkmA (Mijakovic et al., 2003, 2005a, 2006). *B. subtilis* LMPTPs presumably have a different role in stress resistance (Musumeci et al., 2005). Furthermore, we noticed that PtpZ shares common interactants with PtkB, suggesting that PtpZ might also act on putative substrates of PtkB (Figure S1). Common prey proteins were also found between the phosphatases YwIE and YfkJ, indicating they may have redundant activities. The BY-kinase PtkA also interacted with Sala and MinD, two MRP-like/MinD-family ATPases that bear structural resemblance with BY-kinases (Mijakovic et al., 2005b). Additionally, MinD was found to interact with PtkB and PtpZ. Last but not least, this first round of screens also revealed an interaction between the Ser/Thr kinase of the Hanks-type, YabT, and TkmA, the activator of the BY-kinase PtkA.

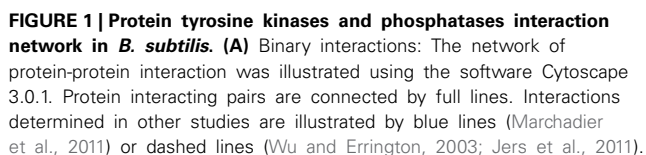
We then performed a second round of genomic screenings using MinD, Sala, and YabT as baits (Figure S1). In addition, we completed this set with the YabT-cognate phosphoserine-protein phosphatase SpoIIE. Interestingly, Sala and MinD were found to connect with Hanks-type Ser/Thr kinases. Indeed, save for its known interaction with the cell division regulator MinC, MinD also made contact with YabT while Sala interacted with PrkD. Both YabT and SpoIIE were highly connected, thus emerging like hubs in this network. Particularly, YabT made contact with TkmA and PtkB, suggesting the possibility of interference between the serine/threonine and the tyrosine phosphorylation networks. This assumption was strengthened by two outcomes from our third and last rounds of screenings. We observed that YvcJ, a P-loop containing GTPase with identified kinase activity (Pompeo et al., 2011), interacted with TkmB. Furthermore, we identified several connections between the stressosome controlling Ser/Thr protein kinase RsbT (Kang et al., 1998) and kinase and phosphatase proteins from both the Tyr (PtkA, PtpZ) and Ser/Thr (PrkD) phosphorylation pathways (Figure S1).

After addition of connecting edges from the *B. subtilis* interactome (Marchadier et al., 2011), the resulting interaction map of proteins involved in phosphorylation pathways comprises 137 specific interactions linking 82 proteins (Figure 1A, Tables S1, S2). This network is of high confidence and contains many

proteins with already documented phosphosites. These positive controls include recently characterized phosphoproteins RecA, phosphorylated by YabT (Bidnenko et al., 2013), and FatR, phosphorylated by PtkA (Derouiche et al., 2013). SrfAA and YqbO, which were detected in a previous phosphoproteome study (Macek et al., 2007), also appear in the network connected with YabT and SpoIIE, respectively. DegS, which was previously characterized as a substrate for both YabT and PrkD, was added to the network (Jers et al., 2011). About 44% of proteins were detected as overlapping fragments, delineating discrete minimal interacting domains (Table S2). These high-confidence interactions provide an important validation of our approach. A significant fraction (20%) of the prey proteins were found to interact with both a kinase and a cognate phosphatase (Table 1), suggesting they could be regulated by reversible phosphorylation. These proteins have been grouped into functional categories (Figure 1B, Table S3). Two thirds of them belong to four main functional classes: post translational modifications, transport of metabolites (ions or peptides), transcription and DNA metabolism.

NEW SUBSTRATES OF BY-KINASES INVOLVED IN TRANSCRIPTIONAL CONTROL AND DNA METABOLISM

In the first set of screens, the network revealed the interaction of PtkA-activator TkmA with a transcription regulator FatR. In a separate study we reported that FatR is phosphorylated by PtkA in the presence of TkmA, at residue Y45 located in the DNA binding domain (Derouiche et al., 2013). The consequence of FatR phosphorylation is its dissociation from its DNA operator sequence with derepression of the *fatR-cyp102A3* operon. The MRP-like gene regulator Sala which was found to interact with PtkA was also proved to be a substrate for phosphorylation (Derouiche A. and Mijakovic I. unpublished result). In this case PtkA-dependent phosphorylation stimulated DNA-binding of Sala, which in turn repressed the transition state regulator *scoC* (Derouiche A. and Mijakovic I. unpublished result). Furthermore, we found that TkmA interacted with the N-terminal domain of the general DNA recombinase RecA (Figure 2A). Supporting this observation, we show here that RecA can be phosphorylated by PtkA in the presence of TkmA *in vitro* (Figure 2B). To date, no direct substrates of the putative BY-kinase PtkB have been identified in *B. subtilis*, since solubility issues precluded *in vitro* studies with PtkB (Mijakovic et al., 2003). Our network revealed several interaction partners of PtkB involved in various processes involving the DNA metabolism (Figures 2D, 3C). These include the RNA polymerase β -subunit RpoB, the DNA helicase PcrA, the DNA polymerase PolA, the ATP-dependent DNA helicase/nuclease AddB and the DNA mismatch repair protein MutL. In fact, with the exception of AddB, these proteins also interact with the phosphotyrosine-protein phosphatase PtpZ, highlighting that they indeed could be targeted for modifications through phosphorylation/dephosphorylation on tyrosine residues. RpoB was previously identified as phosphorylated on tyrosine (Ge et al., 2011) and serine (Sun et al., 2010) residues in *Helicobacter pylori* and *Streptococcus pneumoniae*, respectively. Both RpoB and the UvrD-like helicase PcrA were also reported to be phosphorylated on tyrosine in *Klebsiella pneumoniae* (Lin et al., 2009). In our



Reciprocal interactions have been omitted for more clarity (see Table S1). Members of the tyrosine phosphorylation pathway in *B. subtilis* are indicated as red nodes. Phosphoproteins characterized in the literature are labeled in red. **(B)** Pie chart diagram illustrating the functional classification of interacting proteins according to the biological processes as shown in Table S4.

Table 1 | Proteins contacted by a kinase and a cognate phosphatase in the *B. subtilis* PPI network.

Proteins	Function	Kinase	Phosphatase
MutL	DNA mismatch repair factor	PtkB	PtpZ
PolA	DNA polymerase I	PtkB	PtpZ
RpoB	RNA polymerase β subunit	PtkB	PtpZ
MinD	ATPase activator of MinC	PtkA/PtkB	PtpZ
RsbT	Ser/Thr Kinase	PtkA	PtpZ
YabT	Ser/Thr Kinase	PtkB	PtpZ
RecA	SOS repair factor/DNA processing	YabT	SpoIIE
RacA	chromosome-anchoring protein	YabT	SpoIIE
DegS	PTS sensory kinase	YabT	SpoIIE
SbcE	DSB repair	YabT	SpoIIE
SwrC	transporter/ swarming	YabT	SpoIIE
YqfF	phosphodiesterase	YabT	SpoIIE
YkcC	putative glycosyltransferase	YabT	SpoIIE
YqbD	putative DNA welding protein/skin element	YabT	SpoIIE
YqbO	putative lytic transglycosylase/skin element	YabT	SpoIIE
FruA	phosphotransferase system (PTS) fructose-specific	YabT	SpoIIE
CisA	site-specific DNA recombinase	YabT	SpoIIE
XhlA	cell lysis/PBSX	YabT	SpoIIE
YhgE	putative methyl accepting protein	YabT	SpoIIE
NatB	Na ⁺ exporter	YabT	SpoIIE

network, PtkB was also found to interact not only with its cognate modulator TkmB but also with TkmA, the cognate modulator of PtkA, suggesting a cross-talk between the two tyrosine kinase systems. In conclusion, our PPI network revealed a number of new substrates of PtkA which we have experimentally validated. In addition it pointed to potential substrates of PtkB.

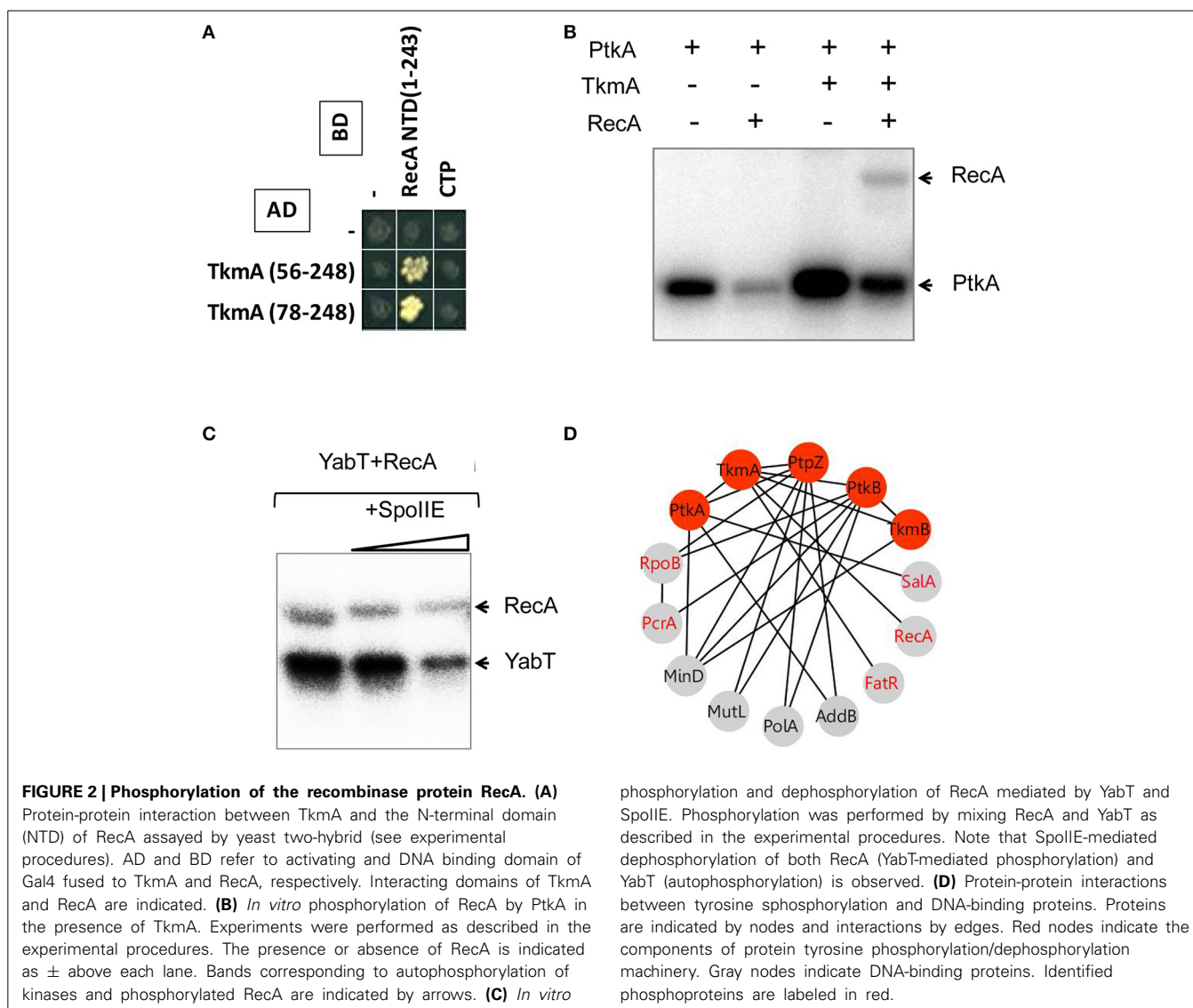
NEW SUBSTRATES OF THE HANKS-TYPE Ser/Thr Kinases AND PHOSPHATASES

The interaction of the activator TkmA and the Ser/Thr-kinase YabT established in the first round of screens suggested that the tyrosine and serine/threonine phosphorylation pathways could be connected. This connection was further substantiated in the second round, via the Ser/Thr kinase PrkD, the GTPase YvcJ, the RNA polymerase β -subunit RpoB, the recombinase RecA, and the transcriptional factors YesS, and YdeL which were found to connect with both BY-kinase and Ser/Thr-kinase nodes. We explored the Ser/Thr-kinase nodes with the same approach to examine whether PPI network allows identification of new substrates. YabT and its cognate phosphatase SpoIIE are encoded by the same operon and are strongly up-regulated during sporulation. SpoIIE is known to modulate the phosphorylation state of the anti-anti sigma F factor SpoIIAA (Arigoni et al., 1996). YabT is an unusual Hanks-type kinase possessing a transmembrane helix, but no extracellular signal-binding domain. In a recent study we showed that YabT localizes at the septum during spore formation and is activated by binding ssDNA (Bidnenko et al., 2013). Activated YabT phosphorylates the recombinase RecA at the onset

of sporulation and regulates its role in maintaining chromosome integrity. Interaction profiles of YabT and SpoIIE revealed numerous protein partners. Indeed, YabT appears as a hub protein that connects 32 proteins, about half of which (including RecA) also interact with SpoIIE (Figure 3A, Table 2). We speculated that proteins interacting with both a kinase and a phosphatase are very likely to undergo phosphorylation. Supporting this hypothesis, we found that RecA, a known substrate of YabT, can be dephosphorylated by SpoIIE (Figure 2C). The DNA-binding developmental protein RacA was also investigated (Figure 4). During sporulation RacA anchors the segregating chromosome at the cell pole in a DivIVA-dependent manner (Ben-Yehuda et al., 2003). Examination of the condition-dependent transcription profiles of *racA* and *spoIIE* shows they are members of the same synexpression group mainly up-regulated during sporulation, indicating that they are involved the same biological process (Figure 4C, Nicolas et al., 2012). The phosphorylation and dephosphorylation of RacA by YabT and SpoIIE, respectively, were confirmed *in vitro* (Figure 4B). This observation highlights a potential role of the kinase YabT in the regulation of RacA activity, and further validates our assumption that interaction partners of a kinase and a phosphatase are presumably substrates for both enzymes.

Classification of all proteins of the YabT hub revealed that 69% of partners are transmembrane proteins, with a high proportion of metabolite- and ion-transporters. Among cytosolic interacting proteins, 67% exhibited HTH motifs suggesting DNA binding properties (Figure 3B). Of note, this parallels the properties of YabT itself, a transmembrane kinase activated by DNA binding (Bidnenko et al., 2013). In addition to RecA and RacA, YabT/SpoIIE were found to interact with SbcE, a structural maintenance of chromosome (SMC)-like protein involved in DNA double-strand break repair (Krishnamurthy et al., 2010) and CisA, a site-specific DNA recombinase necessary for reconstitution of the sigma factor K during sporulation (Kunkel et al., 1990) (Figure 3C). Given the ability of YabT to be stimulated by ssDNA, our identification of potential substrates with DNA-binding properties and/or proteins involved in DNA metabolism substantiates its observed involvement in maintenance of DNA integrity (Bidnenko et al., 2013).

Further, our PPI network revealed a direct interaction between the YabT paralogue PrkD and the replicative DNA helicase DnaC (Figure 5, Tables S1, S2). Interaction of the kinase with DnaC in yeast two-hybrid requires the DnaC C-terminal domain comprising the helicase function. We confirmed the ability of PrkD to phosphorylate DnaC *in vitro* (Figure 5B), suggesting that PrkD could be involved in regulating DnaC activity. DnaC loading onto a melted single strand DNA fork is assisted by DnaB and DnaI (56). Analysis of condition-dependent transcriptome of *B. subtilis* shows that *prkD* (old name *ybdM*) and *dnaB* exhibit a high pairwise correlation throughout ~100 different physiological conditions (Nicolas et al., 2012; Figure 5C), further strengthening the notion that PrkD could participate to the regulation of chromosomal replication. In conclusion, our PPI network revealed that both YabT and PrkD interact with, and phosphorylate, proteins with crucial roles in DNA metabolism.

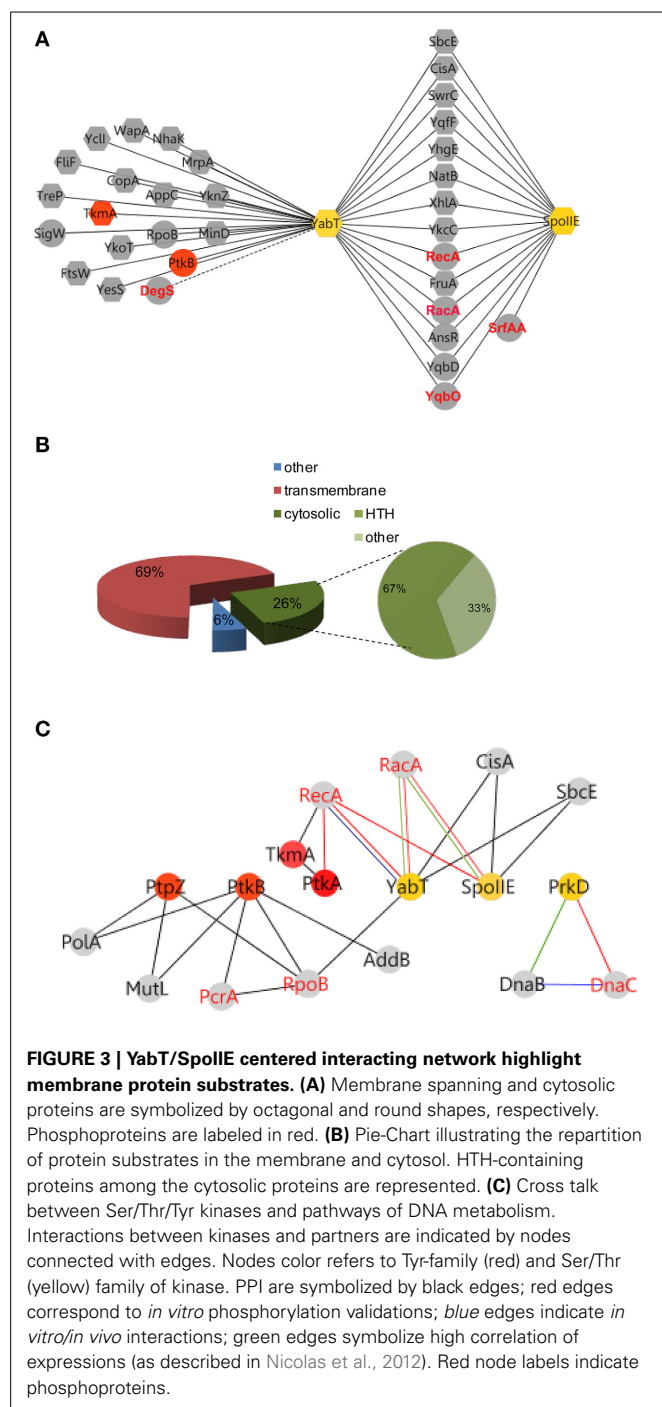


MinD, A NEW MODULATOR OF THE BY-Kinase PtkA

The MinD ATPase, required for the correct positioning of the division site, was identified as interacting partner of the two BY-kinases, PtkA and PtkB, as well as the phosphotyrosine-protein phosphatase PtpZ (Figure 6A). This pointed to MinD as a potential target for tyrosine phosphorylation. However, we found that MinD was not phosphorylated by PtkA *in vitro* (data not shown). We first validated the interaction between MinD and PtkA by far Western blotting (Figure 6B). In this assay we detected the expected MinD-MinC complex and confirmed the physical interaction between MinD and PtkA, but not TkMA, in agreement with the two-hybrid. MinD is an ATPase from the P-loop NTPase superfamily previously reported to be a close structural homolog of BY-kinases, but lacking the C-terminal tyrosine cluster necessary for kinase autophosphorylation (Mijakovic et al., 2005b). We therefore explored potential kinase activity of MinD *in vitro* (Figure 6C). MinD was found unable to autophosphorylate or to phosphorylate a PtkA derivative carrying a substituted catalytic

residue (K59M), corroborating that MinD does not act as a kinase. During cytokinesis, MinD is known to functionally interact with the cell division initiator protein DivIVA in the presence of the bridging protein MinJ, by preventing the formation of a septum near the cell pole (Levin et al., 1992; Lee and Price, 1993; Marston et al., 1998). Interestingly, we found that DivIVA could undergo phosphorylation by PtkA in the presence of TkMA (Figure 6D).

We then tested the ability of MinD to promote the activation of PtkA in the absence of TkMA *in vitro* (Figure 6E). Incubation of PtkA with increasing amounts of MinD activated its autophosphorylation, indicating that MinD is able to act as modulator of PtkA activity similar to TkMA (Figure 6Ea). However, incubation of PtkA with TkMA or MinD revealed that MinD-mediated PtkA activation was much less efficient compared to TkMA (Figure 6Eb). Finally, we showed that in the presence of excess of MinD, the activation of PtkA in the presence of TkMA was inhibited, indicating that MinD was able to compete



with TkmA for binding to PtkA (Figure 6Ec). We investigated the functional elements of PtkA required for interaction with MinD and TkmA by looking for their ability to interact with several PtkA mutant derivatives in yeast two-hybrid (Figure 6F). The mutants included substitutions of key active site residues (catalytic K59M and Mg-coordinating D81A) and the tyrosine autophosphorylation sites (Y225, Y227, and Y228 changed into F). Mutations within the C-terminal tyrosine cluster did not affect the PtkA interaction with either TkmA or MinD. Interestingly,

Table 2 | Proteins contacted by more than one kinase in the *B. subtilis* PPI network.

Proteins	Function	Phosphorylation pathways	
		Y- kinases	S/T-kinases
MutL	DNA mismatch repair factor	PtkB	YrzF
RpoB	RNA polymerase β subunit	PtkB	YabT
SalA	transcriptional regulator (MarR family)	PtkA	PrkD
MinD	ATPase activator of MinC	PtkA/PtkB	YabT
DegS	Two component histidine kinase		PrkD/YabT
RsbT	Ser/Thr kinase	PtkA	PrkD
YesS	transcriptional regulator (AraC/XylS family)	TkmA	YabT
RecA	SOS repair factor/DNA processing	TkmA/PtkA	YabT/SpolIE
TkmA	tyrosine kinase PtkA modulator	TkmB/PtkA	YabT
PtkB	tyrosine kinase	TkmA/TkmB	YabT

the substitution of either active site residues specifically impaired PtkA interaction with MinD but not with TkmA. This result points to different modes of binding of TkmA and MinD to PtkA.

PtkA PLAYS A ROLE IN CELL DIVISION

Transcription profiles of *minD*, *divIVA*, *ptkA*, and *tkmA* exhibit a high degree of correlation throughout all physiological conditions, suggesting they function in the same biological process (Figure 7A). A close examination of *ptkA* single mutant revealed a mild cell division defect with a noticeable proportion of cells containing double septa (7%), compare to the wild type cells (<1%) (Figures 8A,B). We investigated for PtkA-associated phenotypes in cells deficient in the division factor *zapA*. *B. subtilis zapA* mutant exhibits no remarkable division phenotype (Gueiros-Filho and Losick, 2002). However, a *zapA* null mutation was described to exacerbate cytokinesis block-induced phenotypes when combined with other actors of cell division (Gueiros-Filho and Losick, 2002; Dempwolff et al., 2012; Surdova et al., 2013). In rich media, *zapA ptkA* double mutant exhibited a higher proportion of cell with double septa (12%) as well as cells containing asymmetric septa (3%), sometimes leading to anucleated cells (Figures 8A,B). These observations suggest a role of PtkA in the regulation of cytokinesis.

To further understand the role of MinD in PtkA activity, we examined their subcellular localization. MinD is known to exhibit a very specific localization pattern at the cell poles as well as at mid cell. When fused to CFP, PtkA was found to localize as a single focus, preferentially at the old cell poles of elongating cells (Figure 7B). The absence of MinD typically leads to the formation of anucleated minicells, resulting from the mislocalisation of septum at the cell poles (Burmann et al., 2011). Here we found that the inactivation of *minD* also abolished the polar localization of PtkA foci, indicating it is MinD-dependant. This result provides *in vivo* validation of the MinD/PtkA interaction and hints at a role of MinD in holding PtkA at the cell pole during cytokinesis.

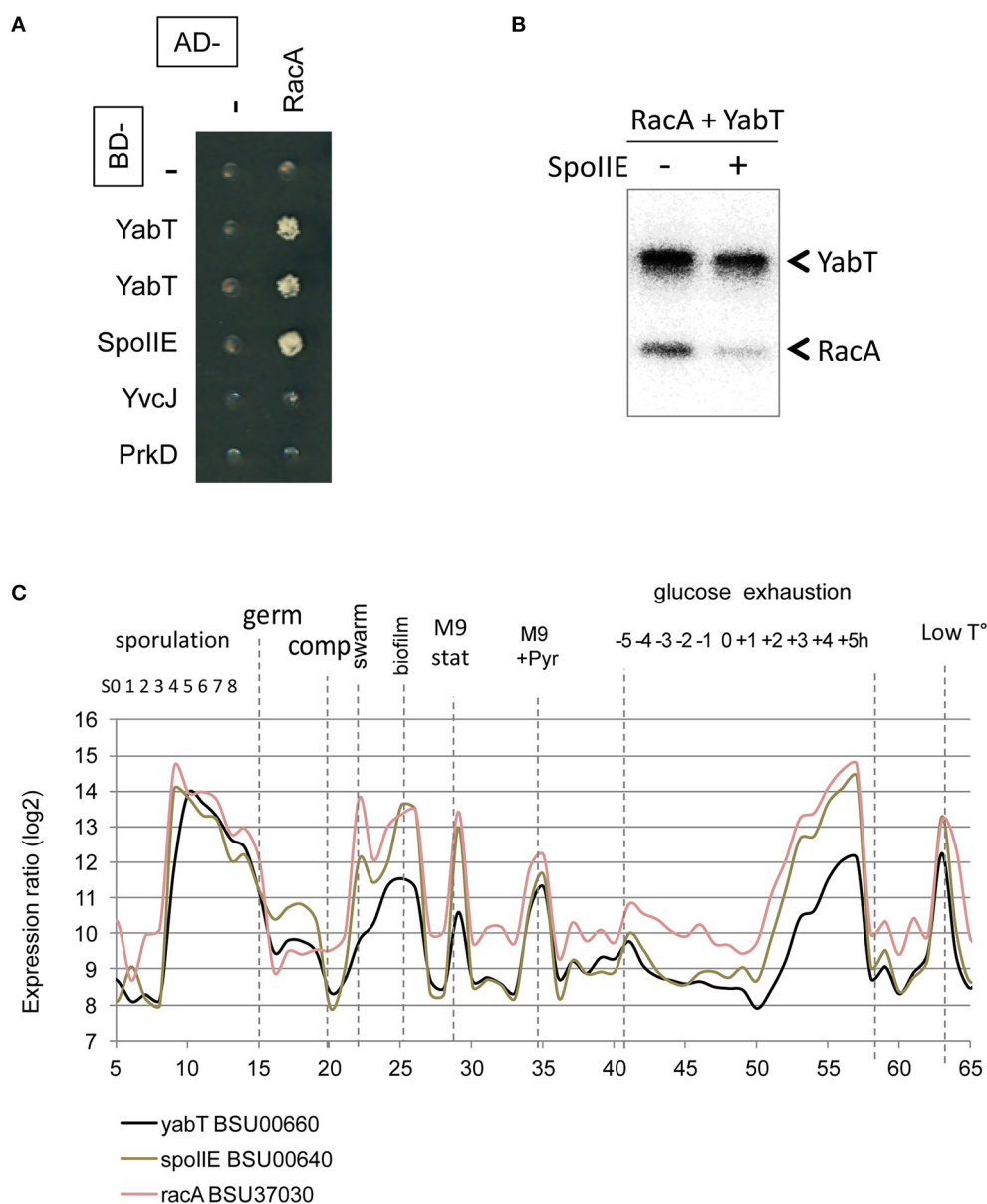


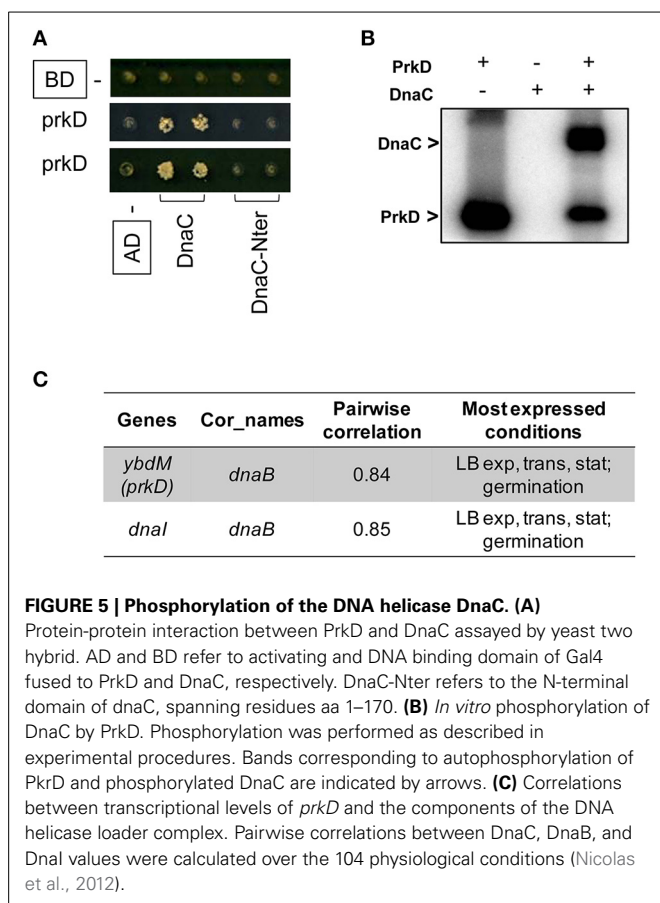
FIGURE 4 | Reversible Ser/Thr phosphorylation of RacA. (A) RacA interaction with YabT and SpoIIIE by yeast 2HB. Gal4 BD- (line) and AD-fusions (column) expressed in yeast haploid cells of complementary mating type were mated and assayed for expression of interaction phenotype as described in the experimental procedures. Diploids co-expressing an AD-RacA fusion (aa

81-194/194) and BD-YabT or BD-SpoIIIE are able to grow onto -LUH selective media. **(B)** *In vitro* phosphorylation/dephosphorylation of RacA by YabT, and SpoIIIE. Phosphorylation was performed as described in the experimental procedures. **(C)** Condition-dependent transcriptomes of *yabT* (black), *spoIIIE* (gray) and *racA* (light red), as obtained in Nicolas et al. (2012).

DISCUSSION

A hallmark of BY-kinases from Gram-positive bacteria is that the cytosolic kinase and its transmembrane activator are individual proteins encoded by separate adjacent genes. This differs from their Gram-negative counterparts where the two activities are encoded by the same gene. A functional consequence of this particular architectural feature could be that it enables the kinases from Gram-positive bacteria to interact with alternative activators, which may provide different substrate specificities. We presented here a protein-protein interaction landscape of the

tyrosine phosphorylation network of *B. subtilis*. Combined with a systematic and experimental elimination of false positives, our approach has proved effective for identifying numerous substrates of BY-kinases and phosphatases, as well as new proteins that modulate their activity. This PPI network not only provided a kinase context for already identified phosphoproteins, but also identified new protein partners for kinases, including other kinases and phosphatases. This network can be considered of high biological relevance, with numerous proteins being contacted by both a kinase and cognate phosphatase, strongly suggesting they are true



substrates or they belong to the same regulatory assembly. Our examination of kinase/substrates and kinase/modulators from the tyrosine but also the serine/threonine phosphorylation pathways corroborated these assumptions. This study highlights the role of protein phosphorylation in the regulation of various aspects of the *B. subtilis* cell cycle as DNA replication, transcription, cell division and sporulation.

Common signaling mechanisms often involve multisite protein phosphorylation to regulate the various activities of a protein whether carried out by the same kinase or by the sequential action of several kinases. In *B. subtilis*, the best characterized example is the two-component histidine kinase DegS, which was shown to be phosphorylated by the two Ser/Thr kinases PrkD and YabT *in vitro* (Jers et al., 2011). PrkD-dependent phosphorylation was specific to serine 76 located in the signal sensing domain and led to increased efficiency of phosphotransfer to DegU. *In vivo*, DegS phosphorylation at serine 76 was shown to affect various aspects of cellular behavior such as competence, swarming and motility. Our *B. subtilis* interaction network also revealed that other proteins can be phosphorylated by more than one kinase (Table S3-B). A notable example is the multifunctional DNA recombinase protein RecA recently found regulated by phosphorylation on a serine (Lusetti and Cox, 2002; Butala et al., 2009; Bidnenko et al., 2013). Here, our data suggest that tyrosine phosphorylation could also play a role in the regulation of RecA activity. RecA binding to TkmA involves its N-terminal moiety,

which is required for the formation of a presynaptic nucleoprotein filament (Lee and Wang, 2009). Whether this activity could be modulated by tyrosine phosphorylation in the cell remains to be determined. Dual phosphorylation involving modification on tyrosine, serine or threonine could also be proposed for the transcriptional regulators SalA and YesS as well as for the RNA polymerase subunit RpoB, which was found to interact with more than one component of the Ser/Thr and Tyr phosphorylation pathways. Together, these observations suggest the existence of dynamic regulations of protein activities in *B. subtilis* cells, where multiple and sequential phosphorylation events could mediate integration of several input signals to better adjust the cellular response to environmental changes, similar to what is described in eukarya.

Remarkably, our network reveals important crosstalk among different classes of kinases. Interactions were observed between components of the Tyrosine and Ser/Thr phosphorylation pathways, as well as among Ser/Thr-kinases. These connections strongly suggest that kinases might phosphorylate each other, generating signaling cascades similar to what was observed in eukarya. This hypothesis has been explored in a separate study, in which the ability of all soluble *B. subtilis* BY- and Ser/Thr kinases to phosphorylate each other *in vitro* was explored. This assay revealed many trans-phosphorylations at functionally critical residues indicative of kinase regulation by phosphorylation (Shi et al., 2014). A similar study carried out recently in *M. tuberculosis* also provided strong evidence for a hierarchical and spatially organized crosstalk among Ser/Thr kinases in this bacteria (Baer et al., 2014). These results support the existence of kinase cross-phosphorylation to form complex eukaryotic-like signaling networks in bacteria. Furthermore, promiscuous binding of BY- kinases PtkA and PtkB with different modulators was observed throughout the network suggesting a functional interplay. Whether PtkB performs *in vivo* as a kinase remains to be determined. An alternative hypothesis could be that PtkB acts as a pseudokinase to mediate interaction with protein substrates for subsequent tyrosine modification by PtkA. Our data also hints at a potential a role of modulators in recruiting some substrates. In agreement with this notion is the finding that the transcriptional regulator FatR, which interacts with TkmA, is regulated by PtkA (Derouiche et al., 2013). On the whole, our PPI network highlights elaborate mechanisms for phosphorylation of tyrosine in the signal transduction pathways that regulate various aspects of DNA metabolism.

A remarkable feature of this PPI network is the central position of the cell division regulator protein MinD which appears as a hub protein densely connected with many members of the tyrosine phosphorylation pathways. MinD shares sequence and structural homology with BY-kinases, but lacks crucial tyrosine residues involved in phosphoryltransfer activity (Mijakovic et al., 2005b). As such, MinD could be considered as a pseudokinase with a non enzymatic-like function. Our results indicate a role of MinD in the activation of PtkA *in vitro*, as well as in its *in vivo* localization as a focus at the cell poles. It has been previously reported that PtkA co-localizes with its transmembrane adapter TkmA at the cell membrane in exponentially growing cells (Jers et al., 2010). However, in the previous study *ptkA*

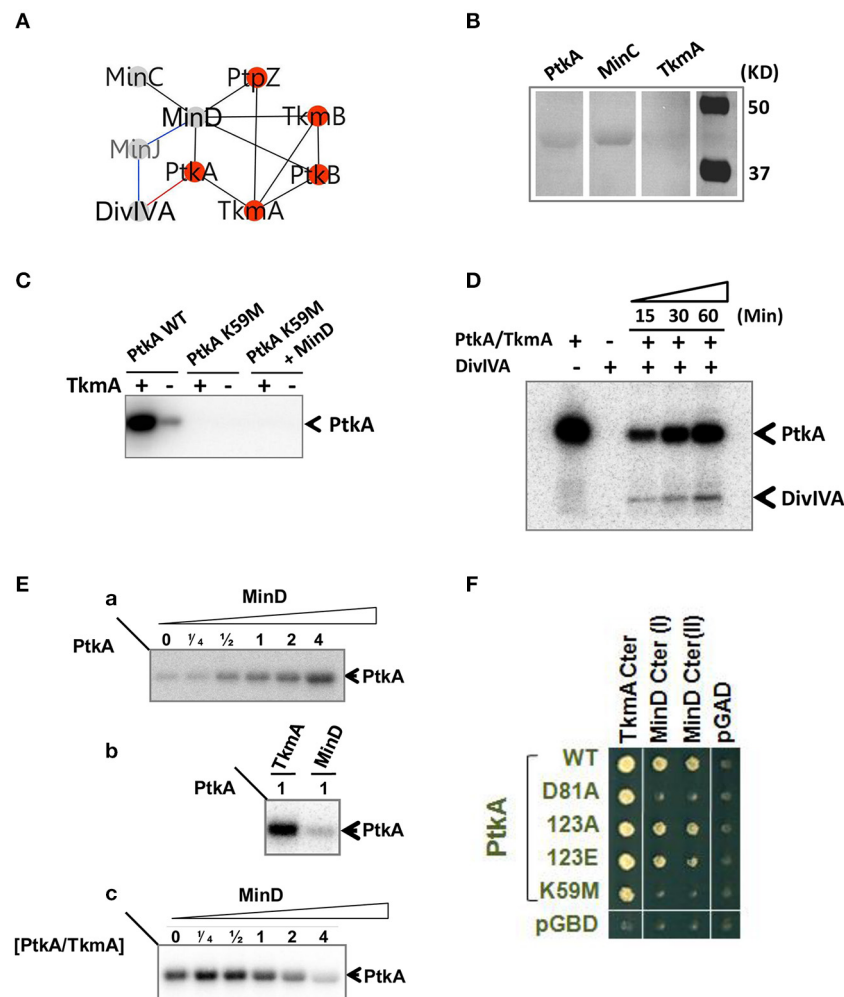


FIGURE 6 | Functional analysis of MinD/PtkA interaction. (A)

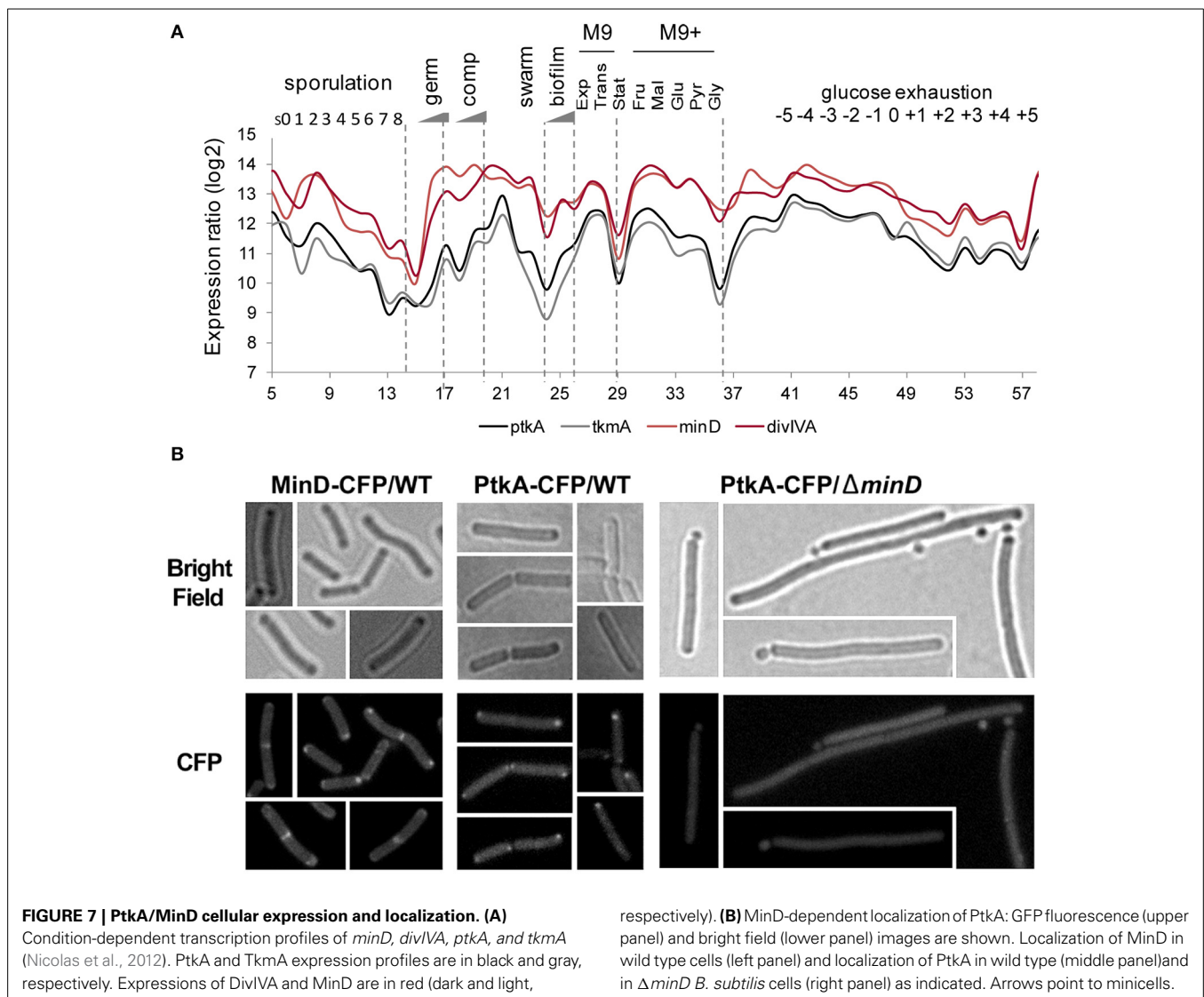
MinD-centered interaction networks. Interactions are illustrated by edges connecting nodes (proteins). Interactions were identified by yeast 2HB (black), genetic (blue) and *in vitro* (red). **(B)** Interaction between PtkA and MinD detected by far-western blotting. PtkA, MinC, and TkmaA were separated by SDS-PAGE and transferred onto nitrocellulose membrane. Interaction was determined by strep tagged MinD which was revealed by Strep-Tactin. MinC acts as a positive control and TkmaA acts as a negative control. **(C)** MinD is not acting as a kinase. All proteins were mixed in equimolar concentration. The presence or absence of TkmaA is indicated as \pm above each lane. Bands corresponding to phosphorylated PtkA are indicated by arrows. **(D)** *In vitro* phosphorylation of DivIVA by PtkA in the presence of TkmaA. The presence or absence of proteins is indicated as \pm above each lane. Time dependence of the reaction was followed and the incubation times (15, 30, or 60 mins) are given above the lanes. Bands corresponding to autophosphorylated PtkA and phosphorylated DivIVA are

indicated by arrows. **(E)** MinD acts as an activator of PtkA.

Autoradiography of SDS-polyacrylamide gels showing the influence of MinD on autophosphorylation of PtkA. **(a)** PtkA was incubated with increasing concentrations of MinD. The ratio of MinD to PtkA was indicated above each lane. **(b)** MinD activates PtkA less efficiently than TkmaA. PtkA was incubated with equivalent concentration of TkmaA or MinD. **(c)** MinD can compete with TkmaA for PtkA activation. PtkA were incubated in the presence of increasing amount of MinD. The ratio of MinD to TkmaA/PtkA was indicated above each lane. Bands corresponding to autophosphorylated PtkA are indicated by arrows. **(F)** Yeast two-hybrid interaction between MinD and PtkA. C-terminal domain of TkmaA (aa187–248) and C-terminal domains of MinD (I: aa135–268; II: aa89–268) were fused to the activating domain of Gal4 (AD, labeled in black). PtkA wt and mutant derivatives (as indicated) are fused with the binding domain of Gal4 (BD, labeled in green). PGAD and pGBDU are control empty plasmids expressing the Gal4-AD and BD domains.

and *tkmA* genes were simultaneously overexpressed which may account for this discrepancy. In our present study the localization was detected with wild type expression levels from the *ptkA* natural promoter, without overexpression of *tkmA*. Based on these results, we propose that MinD could act as a platform protein that would tether PtkA at a specific cellular area. Additionally MinD would also act as an activator of PtkA for signal transmission to DivIVA. The biological significance of

DivIVA phosphorylation by PtkA during cytokinesis in *B. subtilis* remains to be investigated, but our data clearly points to a role of PtkA in the regulation of cytokinesis. This is in agreement with the cell cycle phenotype of the *ptkA* mutant which was reported previously (Petranovic et al., 2007). A parallel can be drawn between the MinD/PtkA interplay and the A parallel can be drawn with scaffold-directed assembly of signaling components in eukarya. Eukaryotic scaffold proteins are often described



as catalytically inactive kinases that can bring together multiple components of signaling cascades, regulating and promoting their interactions at particular localizations in the cell. An example of this process is the Ste5 protein scaffold in the mitogen-activated protein kinase (MAPK) pathway, which directs mating signaling by promoting an activation cascade mediated by three insulated protein kinases MAPKKK Ste11, MAPKK ste7 and MAPK Fus3 (Good et al., 2009). Here, MinD was found connected with other kinases besides PtkA (PktB, YabT) and a phosphatase (PtpZ) thus bringing various components of tyrosine, but also serine/threonine phosphorylation pathways in close proximity. A hypothesis worth exploring would be whether MinD could orchestrate the intracellular location of several kinases and phosphatases, similar to eukaryal anchoring proteins (Pawson and Scott, 1997).

In several bacteria, the phosphorylation of DivIVA was shown to be a key step in the regulation of cytokinesis. So far, this regulation is known to be mediated by Ser/Thr Hank-type kinases. In *Streptomyces coelicolor*, the polarization machinery

is regulated by AfsK, a Ser/Thr protein kinase which localizes at hyphal tips and phosphorylates DivIVA on its C-terminus (Hempel et al., 2012; Saalbach et al., 2013). In *S. pneumoniae*, StkP localizes at the division site and specifically phosphorylates DivIVA on threonine 201 (Fleurie et al., 2012). In *Mycoplasma pneumoniae*, phosphorylation of the DivIVA homolog Wag31 by S/T kinases PknA/PknB affects cell shape control (Kang et al., 2005). Our results indicate that in *B. subtilis*, this regulation may involve the phosphorylation of DivIVA on a tyrosine residue.

In conclusion, this study shows that bacterial regulatory network based on protein phosphorylation is considerably more complex and inter-connected than previously believed. The BY-kinase sub-network is inextricably connected to the Ser/Thr-kinase sub-network. Together with the separate study (Shi et al., 2014) providing evidence that kinases can cross-phosphorylate each other, our data highlighted that BY-kinases are activated by alternative modulators, and that substrates are phosphorylated by different kinases, leading to a better integration of a multitude

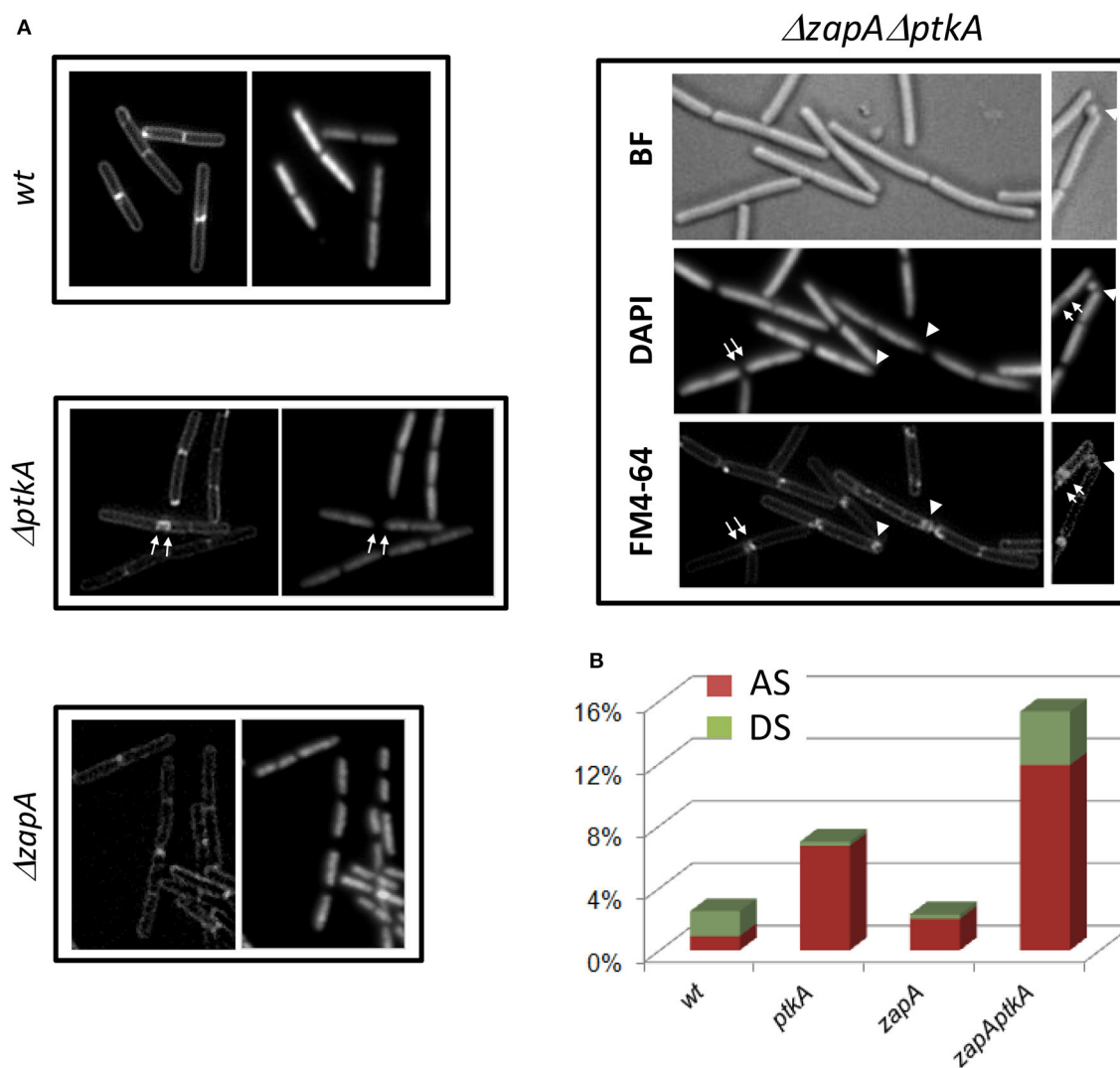


FIGURE 8 | PtkA is involved in regulation of correct septal positioning. (A) $\Delta ptkA$ cells in wild type or $zapA$ deficient background were observed by fluorescent microscopy. Cells were visualized by membrane staining (FM4-64, or left panel), nucleoid staining (Dapi, or right panel), or bright field

(BF). Septum defects are indicated by white arrows (double septum) and white triangles (asymmetric septum or anucleated cell). **(B)** Defaults in septal formation in each strain are estimated as % over a total number of cells >500. AS: asymmetric septum, red; DS: double septum, green.

of signals. Significant additional efforts will be required to decipher the functioning of this complex and dynamic regulatory network.

ACKNOWLEDGMENTS

We thank Stephen McGovern for providing purified DnaC protein. This work was supported by the Agence Nationale de la Recherche (2010-BLAN-1303-01 to Ivan Mijakovic and Marie-Françoise Noirot-Gros) and the Federation pour la Recherche Medicale (SPF20111223359 to Ivan Mijakovic and Lei Shi). The costs of publication of this article were defrayed in part by the payment of page charges. The article must therefore be hereby marked “advertisement” in accordance with 18 U.S.C. Section 1734 solely to indicate this fact. Protein-protein interaction data reported in this paper has been submitted to the

IMEx consortium through IntAct (<http://www.imexconsortium.org>) and assigned the identifier IM-22270.

SUPPLEMENTARY MATERIAL

The Supplementary Material for this article can be found online at: <http://www.frontiersin.org/journal/10.3389/fmicb.2014.00538/abstract>

REFERENCES

- Arigoni, F., Duncan, L., Alper, S., Losick, R., and Stragier, P. (1996). SpoIIE governs the phosphorylation state of a protein regulating transcription factor sigma F during sporulation in *Bacillus subtilis*. *Proc. Natl. Acad. Sci. U.S.A.* 93, 3238–3242. doi: 10.1073/pnas.93.8.3238
- Baer, C. E., Iavarone, A. T., Alber, T., and Sasseti, C. M. (2014). Biochemical and spatial coincidence in the provisional Ser/Thr protein kinase interaction network of mycobacterium tuberculosis. *J. Biol. Chem.* 289, 20422–20433. doi: 10.1074/jbc.M114.559054

- Ben-Yehuda, S., Rudner, D. Z., and Losick, R. (2003). RacA, a bacterial protein that anchors chromosomes to the cell poles. *Science* 299, 532–536. doi: 10.1126/science.1079914
- Bidnenko, V., Shi, L., Kobir, A., Ventroux, M., Pigeonneau, N., Henry, C., et al. (2013). *Bacillus subtilis* serine/threonine protein kinase YabT is involved in spore development via phosphorylation of a bacterial recombinase. *Mol. Microbiol.* 88, 921–935. doi: 10.1111/mmi.12233
- Burmans, F., Ebert, N., Van Baarle, S., and Bramkamp, M. (2011). A bacterial dynamin-like protein mediating nucleotide-independent membrane fusion. *Mol. Microbiol.* 79, 1294–1304. doi: 10.1111/j.1365-2958.2011.07523.x
- Butala, M., Zgur-Bertok, D., and Busby, S. J. (2009). The bacterial LexA transcriptional repressor. *Cell Mol. Life Sci.* 66, 82–93. doi: 10.1007/s00018-008-8378-6
- Dempwolff, F., Wischhusen, H. M., Specht, M., and Graumann, P. L. (2012). The deletion of bacterial dynamin and flotillin genes results in pleiotrophic effects on cell division, cell growth and in cell shape maintenance. *BMC Microbiol.* 12:298. doi: 10.1186/1471-2180-12-298
- Derouiche, A., Bidnenko, V., Grenha, R., Pignonneau, N., Ventroux, M., Franz-Wachtel, M., et al. (2013). Interaction of bacterial fatty-acid-displaced regulators with DNA is interrupted by tyrosine phosphorylation in the helix-turn-helix domain. *Nucleic Acids Res.* 41, 9371–9381. doi: 10.1093/nar/gkt709
- Duncan, L., Alper, S., Arigoni, F., Losick, R., and Stragier, P. (1995). Activation of cell-specific transcription by a serine phosphatase at the site of asymmetric division. *Science* 270, 641–644. doi: 10.1126/science.270.5236.641
- Elsholz, A. K., Turgay, K., Michalik, S., Hessling, B., Gronau, K., Oertel, D., et al. (2012). Global impact of protein arginine phosphorylation on the physiology of *Bacillus subtilis*. *Proc. Natl. Acad. Sci. U.S.A.* 109, 7451–7456. doi: 10.1073/pnas.1117483109
- Fabret, C., Feher, V. A., and Hoch, J. A. (1999). Two-component signal transduction in *Bacillus subtilis*: how one organism sees its world. *J. Bacteriol.* 181, 1975–1983.
- Feucht, A., and Lewis, P. J. (2001). Improved plasmid vectors for the production of multiple fluorescent protein fusions in *Bacillus subtilis*. *Gene* 264, 289–297. doi: 10.1016/S0378-1119(01)00338-9
- Fleurie, A., Cluzel, C., Guiral, S., Freton, C., Galisson, F., Zanella-Cleon, I., et al. (2012). Mutational dissection of the S/T-kinase StkP reveals crucial roles in cell division of *Streptococcus pneumoniae*. *Mol. Microbiol.* 83, 746–758. doi: 10.1111/j.1365-2958.2011.07962.x
- Gaidenko, T. A., Kim, T. J., and Price, C. W. (2002). The PrpC serine-threonine phosphatase and PrkC kinase have opposing physiological roles in stationary-phase *Bacillus subtilis* cells. *J. Bacteriol.* 184, 6109–6114. doi: 10.1128/JB.184.22.6109-6114.2002
- Galinier, A., Kravanja, M., Engelmann, R., Hengstenberg, W., Kilhoffer, M. C., Deutscher, J., et al. (1998). New protein kinase and protein phosphatase families mediate signal transduction in bacterial catabolite repression. *Proc. Natl. Acad. Sci. U.S.A.* 95, 1823–1828. doi: 10.1073/pnas.95.4.1823
- Garsin, D. A., Duncan, L., Paskowitz, D. M., and Losick, R. (1998). The kinase activity of the antisigma factor SpoIIB is required for activation as well as inhibition of transcription factor sigmaF during sporulation in *Bacillus subtilis*. *J. Mol. Biol.* 284, 569–578. doi: 10.1006/jmbi.1998.2202
- Ge, R., Sun, X., Xiao, C., Yin, X., Shan, W., Chen, Z., et al. (2011). Phosphoproteome analysis of the pathogenic bacterium *Helicobacter pylori* reveals over-representation of tyrosine phosphorylation and multiply phosphorylated proteins. *Proteomics* 11, 1449–1461. doi: 10.1002/pmic.201000649
- Gerwig, J., Kiley, T. B., Gunka, K., Stanley-Wall, N., and Stulke, J. (2014). The protein tyrosine kinases EpsB and PtkA differentially affect biofilm formation in *Bacillus subtilis*. *Microbiology* 160, 682–691. doi: 10.1099/mic.0.074971-0
- Good, M., Tang, G., Singleton, J., Remenyi, A., and Lim, W. A. (2009). The Ste5 scaffold directs mating signaling by catalytically unlocking the Fus3 MAP kinase for activation. *Cell* 136, 1085–1097. doi: 10.1016/j.cell.2009.01.049
- Grangeasse, C., Cozzone, A. J., Deutscher, J., and Mijakovic, I. (2007). Tyrosine phosphorylation: an emerging regulatory device of bacterial physiology. *Trends Biochem. Sci.* 32, 86–94. doi: 10.1016/j.tibs.2006.12.004
- Gueiros-Filho, F. J., and Losick, R. (2002). A widely conserved bacterial cell division protein that promotes assembly of the tubulin-like protein FtsZ. *Genes Dev.* 16, 2544–2556. doi: 10.1101/gad.1014102
- Hanks, S. K., Quinn, A. M., and Hunter, T. (1988). The protein kinase family: conserved features and deduced phylogeny of the catalytic domains. *Science* 241, 42–52. doi: 10.1126/science.3291115
- Hempel, A. M., Cantlay, S., Molle, V., Wang, S. B., Naldrett, M. J., Parker, J. L., et al. (2012). The Ser/Thr protein kinase AfsK regulates polar growth and hyphal branching in the filamentous bacteria *Streptomyces*. *Proc. Natl. Acad. Sci. U.S.A.* 109, E2371–E2379. doi: 10.1073/pnas.1207409109
- Jadeau, F., Grangeasse, C., Shi, L., Mijakovic, I., Deleage, G., and Combet, C. (2012). BYKdb: The Bacterial protein Tyrosine Kinase database. *Nucleic Acids Res.* 40, D321–D324. doi: 10.1093/nar/gkr915
- James, P., Halladay, J., and Craig, E. A. (1996). Genomic libraries and a host strain designed for highly efficient two-hybrid selection in yeast. *Genetics* 144, 1425–1436.
- Jers, C., Kobir, A., Sondergaard, E. O., Jensen, P. R., and Mijakovic, I. (2011). *Bacillus subtilis* two-component system sensory kinase DegS is regulated by serine phosphorylation in its input domain. *PLoS ONE* 6:e14653. doi: 10.1371/journal.pone.0014653
- Jers, C., Pedersen, M. M., Paspaliari, D. K., Schutz, W., Johnsson, C., Soufi, B., et al. (2010). *Bacillus subtilis* BY-kinase PtkA controls enzyme activity and localization of its protein substrates. *Mol. Microbiol.* 77, 287–299. doi: 10.1111/j.1365-2958.2010.07227.x
- Kang, C. M., Abbott, D. W., Park, S. T., Dascher, C. C., Cantley, L. C., and Husson, R. N. (2005). The Mycobacterium tuberculosis serine/threonine kinases PknA and PknB: substrate identification and regulation of cell shape. *Genes Dev.* 19, 1692–1704. doi: 10.1101/gad.1311105
- Kang, C. M., Vijay, K., and Price, C. W. (1998). Serine kinase activity of a *Bacillus subtilis* switch protein is required to transduce environmental stress signals but not to activate its target PP2C phosphatase. *Mol. Microbiol.* 30, 189–196. doi: 10.1046/j.1365-2958.1998.01052.x
- Kawai, Y., and Ogasawara, N. (2006). *Bacillus subtilis* EzrA and FtsL synergistically regulate FtsZ ring dynamics during cell division. *Microbiology* 152, 1129–1141. doi: 10.1099/mic.0.28497-0
- Kiley, T. B., and Stanley-Wall, N. R. (2010). Post-translational control of *Bacillus subtilis* biofilm formation mediated by tyrosine phosphorylation. *Mol. Microbiol.* 78, 947–963. doi: 10.1111/j.1365-2958.2010.07382.x
- Kobayashi, K., Ogura, M., Yamaguchi, H., Yoshida, K., Ogasawara, N., Tanaka, T., et al. (2001). Comprehensive DNA microarray analysis of *Bacillus subtilis* two-component regulatory systems. *J. Bacteriol.* 183, 7365–7370. doi: 10.1128/JB.183.24.7365-7370.2001
- Krishnamurthy, M., Tadesse, S., Rothmaier, K., and Graumann, P. L. (2010). A novel SMC-like protein, SbcE (YhaN), is involved in DNA double-strand break repair and competence in *Bacillus subtilis*. *Nucleic Acids Res.* 38, 455–466. doi: 10.1093/nar/gkp909
- Kunkel, B., Losick, R., and Stragier, P. (1990). The *Bacillus subtilis* gene for the development transcription factor sigma K is generated by excision of a dispensable DNA element containing a sporulation recombinase gene. *Genes Dev.* 4, 525–535. doi: 10.1101/gad.4.4.525
- Lee, C. D., and Wang, T. F. (2009). The N-terminal domain of Escherichia coli RecA have multiple functions in promoting homologous recombination. *J. Biomed. Sci.* 16:37. doi: 10.1186/1423-0127-16-37
- Lee, S., and Price, C. W. (1993). The minCD locus of *Bacillus subtilis* lacks the minE determinant that provides topological specificity to cell division. *Mol. Microbiol.* 7, 601–610. doi: 10.1111/j.1365-2958.1993.tb01151.x
- Levin, P. A., Margolis, P. S., Setlow, P., Losick, R., and Sun, D. (1992). Identification of *Bacillus subtilis* genes for septum placement and shape determination. *J. Bacteriol.* 174, 6717–6728.
- Lin, M. H., Hsu, T. L., Lin, S. Y., Pan, Y. J., Jan, J. T., Wang, J. T., et al. (2009). Phosphoproteomics of *Klebsiella pneumoniae* NTUH-K2044 reveals a tight link between tyrosine phosphorylation and virulence. *Mol. Cell. Proteomics* 8, 2613–2623. doi: 10.1074/mcp.M900276-MCP200
- Lusetti, S. L., and Cox, M. M. (2002). The bacterial RecA protein and the recombinational DNA repair of stalled replication forks. *Annu. Rev. Biochem.* 71, 71–100. doi: 10.1146/annurev.biochem.71.083101.133940
- Macek, B., Mijakovic, I., Olsen, J. V., Gnad, F., Kumar, C., Jensen, P. R., et al. (2007). The serine/threonine/tyrosine phosphoproteome of the model bacterium *Bacillus subtilis*. *Mol. Cell. Proteomics* 6, 697–707. doi: 10.1074/mcp.M600464-MCP200
- Machida, K., and Mayer, B. J. (2009). Detection of protein-protein interactions by far-western blotting. *Methods Mol. Biol.* 536, 313–329. doi: 10.1007/978-1-59745-542-8_34
- Madec, E., Laszkiewicz, A., Iwanicki, A., Obuchowski, M., and Seror, S. (2002). Characterization of a membrane-linked Ser/Thr protein kinase in *Bacillus subtilis*, implicated in developmental processes. *Mol. Microbiol.* 46, 571–586. doi: 10.1046/j.1365-2958.2002.03178.x

- Marchadier, E., Carballido-Lopez, R., Brinster, S., Fabret, C., Mervelet, P., Bessieres, P., et al. (2011). An expanded protein-protein interaction network in *Bacillus subtilis* reveals a group of hubs: exploration by an integrative approach. *Proteomics* 11, 2981–2991. doi: 10.1002/pmic.201000791
- Marston, A. L., Thomaides, H. B., Edwards, D. H., Sharpe, M. E., and Errington, J. (1998). Polar localization of the MinD protein of *Bacillus subtilis* and its role in selection of the mid-cell division site. *Genes Dev.* 12, 3419–3430. doi: 10.1101/gad.12.21.3419
- Mijakovic, I., Musumeci, L., Tautz, L., Petranovic, D., Edwards, R. A., Jensen, P. R., et al. (2005a). *In vitro* characterization of the *Bacillus subtilis* protein tyrosine phosphatase YwqE. *J. Bacteriol.* 187, 3384–3390. doi: 10.1128/JB.187.10.3384-3390.2005
- Mijakovic, I., Petranovic, D., Bottini, N., Deutscher, J., and Ruhdal Jensen, P. (2005b). Protein-tyrosine phosphorylation in *Bacillus subtilis*. *J. Mol. Microbiol. Biotechnol.* 9, 189–197. doi: 10.1159/000089647
- Mijakovic, I., Petranovic, D., Macek, B., Cepo, T., Mann, M., Davies, J., et al. (2006). Bacterial single-stranded DNA-binding proteins are phosphorylated on tyrosine. *Nucleic Acids Res.* 34, 1588–1596. doi: 10.1093/nar/gkj514
- Mijakovic, I., Poncet, S., Boel, G., Maze, A., Gillet, S., Jamet, E., et al. (2003). Transmembrane modulator-dependent bacterial tyrosine kinase activates UDP-glucose dehydrogenases. *EMBO J.* 22, 4709–4718. doi: 10.1093/emboj/cdg458
- Musumeci, L., Bongiorno, C., Tautz, L., Edwards, R. A., Osterman, A., Perego, M., et al. (2005). Low-molecular-weight protein tyrosine phosphatases of *Bacillus subtilis*. *J. Bacteriol.* 187, 4945–4956. doi: 10.1128/JB.187.14.4945-4956.2005
- Nicolas, P., Mader, U., Dervyn, E., Rochat, T., Leduc, A., Pigeonneau, N., et al. (2012). Condition-dependent transcriptome reveals high-level regulatory architecture in *Bacillus subtilis*. *Science* 335, 1103–1106. doi: 10.1126/science.1206848
- Noirot-Gros, M. F., Dervyn, E., Wu, L. J., Mervelet, P., Errington, J., Ehrlich, S. D., et al. (2002). An expanded view of bacterial DNA replication. *Proc. Natl. Acad. Sci. U.S.A.* 99, 8342–8347. doi: 10.1073/pnas.122040799
- Obuchowski, M., Madec, E., Delattre, D., Boel, G., Iwanicki, A., Foulger, D., et al. (2000). Characterization of PrpC from *Bacillus subtilis*, a member of the PPM phosphatase family. *J. Bacteriol.* 182, 5634–5638. doi: 10.1128/JB.182.19.5634-5638.2000
- Orchard, S., Ammari, M., Aranda, B., Breuza, L., Briganti, L., Broackes-Carter, F., et al. (2014). The MIntAct project—IntAct as a common curation platform for 11 molecular interaction databases. *Nucleic Acids Res.* 42, D358–D363. doi: 10.1093/nar/gkt1115
- Pane-Farre, J., Lewis, R. J., and Stulke, J. (2005). The RsbRST stress module in bacteria: a signalling system that may interact with different output modules. *J. Mol. Microbiol. Biotechnol.* 9, 65–76. doi: 10.1159/000088837
- Pawson, T., and Scott, J. D. (1997). Signaling through scaffold, anchoring, and adaptor proteins. *Science* 278, 2075–2080. doi: 10.1126/science.278.5346.2075
- Pereira, S. F., Goss, L., and Dworkin, J. (2011). Eukaryote-like serine/threonine kinases and phosphatases in bacteria. *Microbiol. Mol. Biol. Rev.* 75, 192–212. doi: 10.1128/MMBR.00042-10
- Petranovic, D., Michelsen, O., Zahradka, K., Silva, C., Petranovic, M., Jensen, P. R., et al. (2007). *Bacillus subtilis* strain deficient for the protein-tyrosine kinase PtkA exhibits impaired DNA replication. *Mol. Microbiol.* 63, 1797–1805. doi: 10.1111/j.1365-2958.2007.05625.x
- Pietack, N., Becher, D., Schmidl, S. R., Saier, M. H., Hecker, M., Commichau, F. M., et al. (2010). *In vitro* phosphorylation of key metabolic enzymes from *Bacillus subtilis*: PrkC phosphorylates enzymes from different branches of basic metabolism. *J. Mol. Microbiol. Biotechnol.* 18, 129–140. doi: 10.1159/000308512
- Pompeo, F., Luciano, J., Brochier-Armanet, C., and Galinier, A. (2011). The GTPase function of YvcJ and its subcellular relocalization are dependent on growth conditions in *Bacillus subtilis*. *J. Mol. Microbiol. Biotechnol.* 20, 156–167. doi: 10.1159/000329298
- Saalbach, G., Hempel, A. M., Vigouroux, M., Flardh, K., Buttner, M. J., and Naldrett, M. J. (2013). Determination of phosphorylation sites in the DivIVA cytoskeletal protein of *Streptomyces coelicolor* by targeted LC-MS/MS. *J. Proteome Res.* 12, 4187–4192. doi: 10.1021/pr400524d
- Shi, L., Kobir, A., Jers, C., and Mijakovic, I. (2010). Bacterial Protein-Tyrosine Kinases. *Curr. Proteomics* 7, 188–194. doi: 10.2174/157016410792928198
- Shi, L., Pigeonneau, N., Ravikumar, V., Dobrinic, P., Macek, B., Franjevic, D., et al. (2014). Cross-phosphorylation of bacterial serine/threonine and tyrosine protein kinases on key regulatory residues. *Front. Microbiol.* 5:495. doi: 10.3389/fmicb.2014.00495
- Soufi, B., Kumar, C., Gnäd, F., Mann, M., Mijakovic, I., and Macek, B. (2010). Stable isotope labeling by amino acids in cell culture (SILAC) applied to quantitative proteomics of *Bacillus subtilis*. *J. Proteome Res.* 9, 3638–3646. doi: 10.1021/pr100150w
- Sun, X., Ge, F., Xiao, C. L., Yin, X. F., Ge, R., Zhang, L. H., et al. (2010). Phosphoproteomic analysis reveals the multiple roles of phosphorylation in pathogenic bacterium *Streptococcus pneumoniae*. *J. Proteome Res.* 9, 275–282. doi: 10.1021/pr900612v
- Surdova, K., Gamba, P., Claessen, D., Siersma, T., Jonker, M. J., Errington, J., et al. (2013). The conserved DNA-binding protein WhiA is involved in cell division in *Bacillus subtilis*. *J. Bacteriol.* 195, 5450–5460. doi: 10.1128/JB.00507-13
- Vagner, V., Dervyn, E., and Ehrlich, S. D. (1998). A vector for systematic gene inactivation in *Bacillus subtilis*. *Microbiology* 144 (Pt 11), 3097–3104. doi: 10.1099/00221287-144-11-3097
- Weir, M., and Keeney, J. B. (2014). PCR mutagenesis and gap repair in yeast. *Methods Mol. Biol.* 1205, 29–35. doi: 10.1007/978-1-4939-1363-3_3
- Whitfield, C. (2006). Biosynthesis and assembly of capsular polysaccharides in *Escherichia coli*. *Annu. Rev. Biochem.* 75, 39–68. doi: 10.1146/annurev.biochem.75.103004.142545
- Wu, L. J., and Errington, J. (2003). RacA and the Soj-Spo0J system combine to effect polar chromosome segregation in sporulating *Bacillus subtilis*. *Mol. Microbiol.* 49, 1463–1475. doi: 10.1046/j.1365-2958.2003.03643.x
- Wu, Y., Li, Q., and Chen, X. Z. (2007). Detecting protein-protein interactions by Far western blotting. *Nat. Protoc.* 2, 3278–3284. doi: 10.1038/nprot.2007.459

Conflict of Interest Statement: The Associate Editor, Christophe Grangeasse, declares that, despite having collaborated with authors Ivan Mijakovic and Lei Shi, the review process was handled objectively and no conflict of interest exists. The authors declare that the research was conducted in the absence of any commercial or financial relationships that could be construed as a potential conflict of interest.

Received: 19 August 2014; accepted: 26 September 2014; published online: 22 October 2014.

Citation: Shi L, Pigeonneau N, Ventroux M, Derouiche A, Bidnenko V, Mijakovic I and Noirot-Gros M-F (2014) Protein-tyrosine phosphorylation interaction network in *Bacillus subtilis* reveals new substrates, kinase activators and kinase cross-talk. *Front. Microbiol.* 5:538. doi: 10.3389/fmicb.2014.00538

This article was submitted to *Microbial Physiology and Metabolism*, a section of the journal *Frontiers in Microbiology*.

Copyright © 2014 Shi, Pigeonneau, Ventroux, Derouiche, Bidnenko, Mijakovic and Noirot-Gros. This is an open-access article distributed under the terms of the Creative Commons Attribution License (CC BY). The use, distribution or reproduction in other forums is permitted, provided the original author(s) or licensor are credited and that the original publication in this journal is cited, in accordance with accepted academic practice. No use, distribution or reproduction is permitted which does not comply with these terms.



Cross-phosphorylation of bacterial serine/threonine and tyrosine protein kinases on key regulatory residues

Lei Shi¹, Nathalie Pigeonneau², Vaishnavi Ravikumar³, Paula Dobrinic⁴, Boris Macek³, Damjan Franjevic⁴, Marie-Francoise Noirot-Gros² and Ivan Mijakovic^{1*}

¹ SysBio, Department of Chemical and Biological Engineering, Chalmers University of Technology, Göteborg, Sweden

² UMR1319 Micalis, Institut National de Recherche Agronomique, Jouy-en-Josas, France

³ Proteome Center Tübingen, Interfaculty Institute for Cell Biology, University of Tübingen, Tübingen, Germany

⁴ Division of Biology, Faculty of Science, Zagreb University, Zagreb, Croatia

Edited by:

Christophe Grangeasse, Centre National de la Recherche Scientifique, France

Reviewed by:

Didier Soulat, Universitätsklinikum Erlangen, Germany

Carsten Jers, Technical University of Denmark, Denmark

*Correspondence:

Ivan Mijakovic, Systems and Synthetic Biology, Chalmers University of Technology, Kemivägen 10, Göteborg, SE-41296, Sweden
e-mail: ivan.mijakovic@chalmers.se

Bacteria possess protein serine/threonine and tyrosine kinases which resemble eukaryal kinases in their capacity to phosphorylate multiple substrates. We hypothesized that the analogy might extend further, and bacterial kinases may also undergo mutual phosphorylation and activation, which is currently considered as a hallmark of eukaryal kinase networks. In order to test this hypothesis, we explored the capacity of all members of four different classes of serine/threonine and tyrosine kinases present in the firmicute model organism *Bacillus subtilis* to phosphorylate each other *in vitro* and interact with each other *in vivo*. The interactomics data suggested a high degree of connectivity among all types of kinases, while phosphorylation assays revealed equally wide-spread cross-phosphorylation events. Our findings suggest that the Hanks-type kinases PrkC, PrkD, and YabT exhibit the highest capacity to phosphorylate other *B. subtilis* kinases, while the BY-kinase PtkA and the two-component-like kinases RsbW and SpoIIAB show the highest propensity to be phosphorylated by other kinases. Analysis of phosphorylated residues on several selected recipient kinases suggests that most cross-phosphorylation events concern key regulatory residues. Therefore, cross-phosphorylation events are very likely to influence the capacity of recipient kinases to phosphorylate substrates downstream in the signal transduction cascade. We therefore conclude that bacterial serine/threonine and tyrosine kinases probably engage in a network-type behavior previously described only in eukaryal cells.

Keywords: protein phosphorylation, bacterial protein kinase, protein kinase cross-talk, phosphorylation cascade, kinase activation

INTRODUCTION

In eukarya, protein kinases are known to participate in regulatory networks involved in cell cycle control, signal transduction, and other complex regulatory phenomena (Colinge et al., 2014). Most of the characterized eukaryal kinases exhibit two key functional features: each protein kinase phosphorylates a number of different protein substrates, and kinases phosphorylate and activate each other, thus participating in elaborate phosphorylation cascades (Marshall, 1994). Bacteria, whose cellular makeup is considered to be simplified and optimized for rapid bursts of growth, were usually thought not to possess such complicated kinase networks. The main sensing and signal transduction devices in bacteria are the so-called two-component systems, based on histidine/aspartate kinases (Goulian, 2010). The two component systems are very rapid signal transmission devices, linking environmental stimuli to gene expression. However, they operate mostly as linear signaling pathways, with essentially no cross-talk among different two-component systems (Podgornaia and Laub, 2013). Even in extended bacterial signaling systems, involving sequential phosphorylation of several two-component-like kinases, the flow of information remains

linear (Burbulys et al., 1991). In addition to two-component systems, bacteria also possess serine/threonine (Pereira et al., 2011) and tyrosine protein kinases (Shi et al., 2014). While most bacterial serine/threonine kinases share the origin with their orthologs in eukarya, the bacterial tyrosine kinases do not (Shi et al., 2014). Nevertheless, they all exhibit some properties similar to their eukaryal counterparts. The capacity of bacterial serine/threonine and tyrosine kinases to phosphorylate multiple substrates has been clearly established. Examples of well-characterized bacterial kinases with multiple substrates include a number of Hanks-type serine/threonine kinases from *Mycobacterium tuberculosis* (Grundner et al., 2005; Molle and Kremer, 2010; Baer et al., 2014) and *Bacillus subtilis* (Absalon et al., 2009; Pietack et al., 2010; Ravikumar et al., 2014), as well as the tyrosine kinase PtkA from *B. subtilis* (Petranovic et al., 2009; Jers et al., 2010; Derouiche et al., 2013). By contrast, the capacity of bacterial protein kinases to phosphorylate each other is far less documented. Cross-phosphorylation among some Hanks-type serine/threonine kinases has recently been reported in *M. tuberculosis* (Baer et al., 2014). There is also evidence that Hanks-type serine/threonine kinases from *B. subtilis* can

phosphorylate and activate a two-component histidine/aspartate kinase DegS (Jers et al., 2011). We have previously hypothesized that bacterial serine/threonine and tyrosine kinases, given their functional similarity to eukaryal kinases, might also constitute signal integration hubs by phosphorylating each other (Cousin et al., 2013). In order to test this hypothesis, we have elected to use *B. subtilis* as the system of study, due to the fact that this model organism possesses four distinct well characterized classes of bacterial serine/threonine and tyrosine kinases. These include two tyrosine kinases: PtkA (Jers et al., 2010) and PtkB (EpsB) (Gerwig et al., 2014); three Hanks-type serine/threonine kinases: PrkC (Madec et al., 2002), PrkD (Kobir et al., 2014), and YabT (Bidnenko et al., 2013); the twin-function kinase/phosphorylase HprK/P involved in carbon catabolite regulation (Hanson et al., 2002); and the three two-component-like serine/threonine kinases: RsbT (Kang et al., 1998), RsbW (Yang et al., 1996), and SpoIIAB (Min et al., 1993). While all of these kinases have been characterized to varying degrees with respect to their physiological role and substrate phosphorylation, their capacity to phosphorylate each other has not been tested previously. Using *in vitro* phosphorylation assays with purified proteins, we demonstrated an extensive network of cross-phosphorylation events involving all four classes of kinases. This cross-talk was also supported by interactomics data. In select cases, we have determined the residues phosphorylated on the “recipient” kinases by various “donor” kinases. The identity of these residues clearly suggests functional importance of cross-phosphorylation events, influencing the activity of the “recipient” kinases.

MATERIALS AND METHODS

PROTEIN SYNTHESIS AND PURIFICATION

The following kinase and substrate genes were PCR-amplified using the *B. subtilis* 168 genomic DNA as template and the primers listed in **Table 1**: *rsbT*, *hprK*, *rsbW*, *ptkA*, *prkD*, *yabT*, *prkC*, *spoIIAB*, *rsbV*, *spoIIAA*, and *rsbS*. Site-directed mutagenic PCR (mutagenic primers listed in **Table 1**) was performed as described previously (Mijakovic et al., 2003), in order to inactivate the catalytic sites of kinases by replacing the catalytic residues: *rsbT* N49A, *hprK* K159M, *rsbW* N53A, *ptkA* K59D, *prkD* K54D, *yabT* K55D, *prkC* K40D, and *spoIIAB* N50A. PCR products were inserted in the plasmid pQE-30 (Qiagen) to produce the 6xHis-tagged fusions of proteins. Strep-tagged versions of proteins were obtained using a pQE-30 vector with His6-tag replaced by a strep-tag (Jers et al., 2010). *Escherichia coli* K12 NM522 and M15 (expressing chaperonins GroEL/GroES) were used for vector construction and protein synthesis, respectively. Cells were routinely grown in LB medium supplemented with appropriate antibiotics when necessary (ampicillin 100 µg/ml and kanamycin 25 µg/ml). Protein synthesis and purification were carried out as described previously (Mijakovic et al., 2003). Briefly, induction was performed at OD₆₀₀ = 0.6 by adding 1 mM IPTG. Cells were harvested 3 h later and disrupted by sonication. The 6xHis- or Strep-tagged proteins were purified from crude extracts using Ni-NTA (Qiagen), or Strep Tactin affinity chromatography (Novagen), respectively. For the insoluble proteins, PrkD K54D and YabT K55D, the inclusion bodies were

Table 1 | List of PCR primers used in this study.

Name	Sequence
<i>rsbT fwd</i>	cgcggtccatgaacgaccaatcctgtgtaag
<i>rsbT rev</i>	aaaactgcagctaccgaagccatttgatggcttg
<i>hprK fwd</i>	cgcggtccatggcaaggttcgcacaaaag
<i>hprK rev</i>	aaaactgcagctattctctgttcaccgcttc
<i>rsbW fwd</i>	cgcggtccatgaagaataatgctgattac
<i>rsbW rev</i>	aaaactgcagttagtagtttcgtagttttga
<i>ptkA fwd</i>	cgcggtccatggcgcttagaaaaaacaga
<i>ptkA rev</i>	aaaactgcagttattttgcatgaaattgtcc
<i>prkD fwd</i>	cgggatccatggcattaaaactctaaaaaactgc
<i>prkD rev</i>	aaaactgcagttatgtgaccgattgaatggcccg
<i>yabT fwd</i>	cgcagatctatgatgaacgacgcttgacgagt
<i>yabT rev</i>	ggactgcagtcacccaccgacttagccggtttct
<i>prkC fwd</i>	gaagatctatgtaatcggaagcggtacagcgggcg
<i>prkC rev</i>	aaaactgcagttacaaaaccacggcactttttttgccc
<i>spoIIAB fwd</i>	cgcggtccatgaaaaatgaatgcaccttg
<i>spoIIAB rev</i>	aaaactgcagttatattacaaagcgctttgct
<i>rsbV fwd</i>	cgcggtccatgaataataatgttgatgtg
<i>rsbV rev</i>	aaaactgcagtcattgcactccacctct
<i>spoAA fwd</i>	cgcggtccatgagccttgaattgacatg
<i>spoAA rev</i>	aaaactgcagtcattgatgccaccccca
<i>rsbS fwd</i>	cgcggtccatgagacatccgaaaatcccg
<i>rsbS rev</i>	aaaactgcagctattcccccaattcccgtt
<i>rsbT N49A fwd</i>	ttagccagggtctatttattatgcccgaagggcagattg
<i>rsbT N49A rev</i>	tataataatagccctggctaatctgaatagccgttgtaattc
<i>hprK K159M fwd</i>	cgcgctcggaatgagcgaacacgcgtagagctgtgaaaagag
<i>hprK K159M rev</i>	ctgtttcgtcattccgacgcgcgttttctgtgatcagcagc
<i>rsbW N53A fwd</i>	gctgtcacagctgcgggttcagcagccttacaagaagataaa
<i>rsbW N53A rev</i>	gctgaaccgcagctgtgcacgcctcactgactgcgattttc
<i>ptkA K59D fwd</i>	ggggaaggagattcaacaacgcgcgcgaacctggctgtc
<i>ptkA K59D rev</i>	cgttgttgaatccttcccccgacaagccgattgaat
<i>prkD K54D fwd</i>	ttagtcttagatcagcttcggcgacaaaagccaaaag
<i>prkD K54D rev</i>	gccgaagctgatctaagacataaggtgtttgagctagg
<i>YabT K55D fwd</i>	tgttgcttagatgtgagtgatgacagcctgtctattac
<i>YabT K55D rev</i>	catcactcacatcgaagcaacatgctccatctgatgtt
<i>prkC K40D fwd</i>	agtcgcaattgatatactcggtttgactatgcaaatg
<i>prkC K40D rev</i>	caaacccgagcaggtatcaattgcgacttcacggtcagaatg
<i>spoIIAB N50A fwd</i>	gctgtcacggctgcgattatccatggatgaagagaactgtg
<i>spoIIAB N50A rev</i>	gataatcgacgcgtgacagcctctgacacgactgtttgat

dissolved in the buffer containing 6 M guanidine hydrochloride, 50 mM Tris pH 7.5, 100 mM NaCl, 5 mM MgCl₂, and 5% glycerol. The purification was performed as mentioned before but in the buffer with additional 6 M guanidine hydrochloride. To refold the proteins, the concentration of guanidine hydrochloride was lowered to 0.2 M. Purified proteins were desalted on PD-10 columns (GE Healthcare), and stored at −80°C in 10% glycerol.

IN VITRO KINASE CROSS-PHOSPHORYLATION PHOSPHORYLATION ASSAY

Phosphorylation reactions were incubated in a buffer containing: 50 mM Tris pH 7.5, 100 mM NaCl, 5 mM MgCl₂, 5% glycerol,

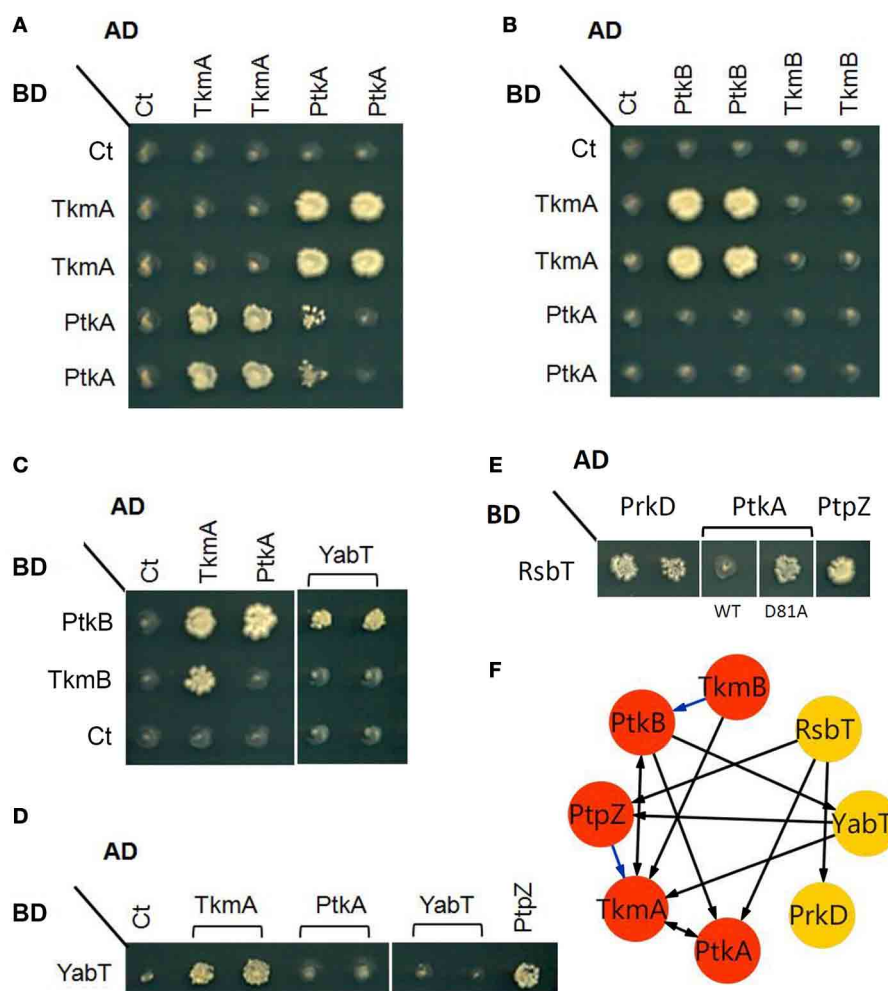


FIGURE 1 | Protein-protein interactions between some components of the tyrosine and serine/threonine signal transduction pathway.

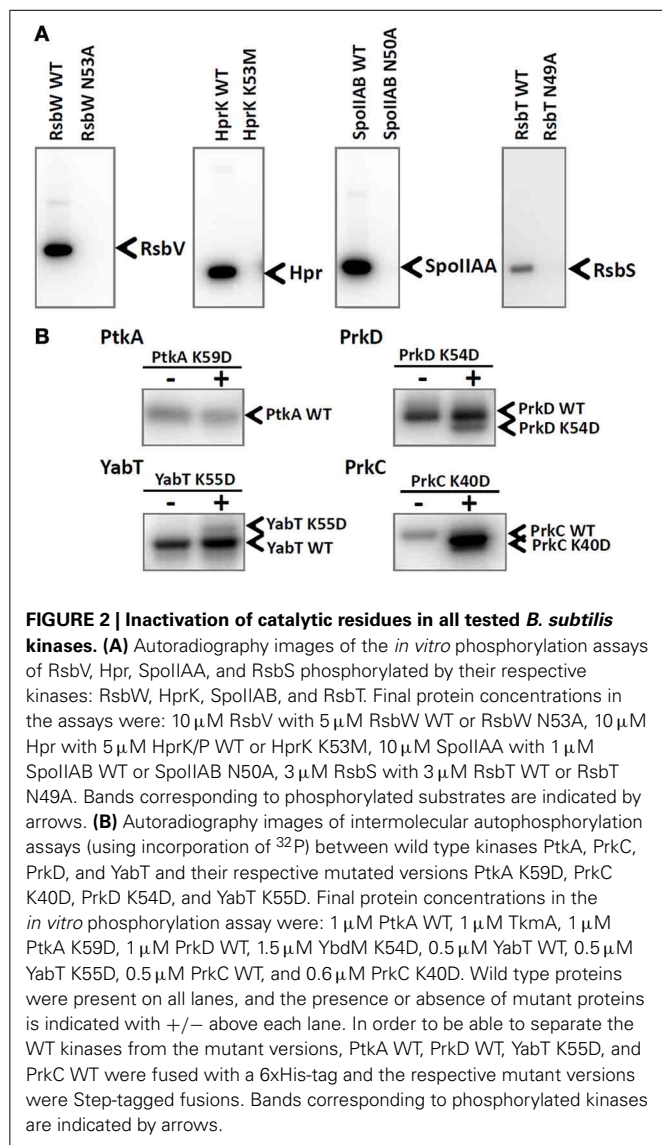
Interaction phenotypes were monitored by the ability of the yeast cells co-expressing a given bait (Gal4 BD-fusion) and prey (Gal4 AD-fusion) pair of proteins to grow on selective media, as described in the experimental procedures. **(A)** Reciprocal interactions between PtkA and its cognate modulator TkmA (fused to either AD or BD). **(B)** Interactions among components of the two BY-kinase systems: PtkA/TkmA (fused to BD) and PtkB/TkmB (fused to AD). **(C–E)** Examples of interactions between

different families of kinases: **(C)** In addition of TkmA (here as positive control), PtkB (fused to BD) interacts with PtkA and YabT (fused to AD). **(D)** YabT (fused to BD) interacts with TkmA and PtpZ (fused to AD). **(E)** RsbT (fused to BD) interacts PrkD, PtpZ and catalytically inactive PtkA (D81A) (fused with AD). **(F)** A graphical representation of the interactions revealed by yeast two-hybrid. Proteins (nodes) are linked by edges (arrows) directed from bait to prey. Blue edges indicate additional interactions found after yeast two-hybrid screenings of the *B. subtilis* genomic library (Shi et al., unpublished results).

50 μ M ATP, and 20 μ Ci/mmol [γ - 32 P]-ATP. Each phosphorylation reaction contained one wild type active kinase and one catalytically deficient kinase. The assay was assembled using the following final protein concentrations: 3 μ M RsbT WT, 3 μ M HprK WT, 5 μ M RsbW WT, 5 μ M PtkA WT with 5 μ M TkmA, 2 μ M PrkD WT, 1 μ M YabT WT, 1 μ M PrkC WT, 5 μ M SpoIIAB WT, 9 μ M RsbT N49A, 4 μ M HprK K159M, 9 μ M RsbW N53A, 3 μ M PtkA K59D, 3 μ M PrkD K54D, 2 μ M YabT K55D, 3 μ M PrkC K40D, 9 μ M SpoIIAB N50A. Phosphorylation reactions were incubated for 1 h at 37°C, stopped by boiling at 100°C, and samples were separated on an 8–12% SDS-polyacrylamide gel. Autoradiography signals were revealed using the FUJI phosphorimager.

IN VITRO PHOSPHORYLATION OF HPr

Proteins (2 μ M PrkD, 2 μ M HprK/P, 6 μ M HPr) were incubated in a buffer containing 50 mM Tris pH 7.5, 100 mM NaCl, 5 mM MgCl₂, 5% glycerol, and 1 mM ATP to perform the phosphorylation reactions. The reactions were incubated for 1 h at 37°C, stopped by boiling at 100°C, and samples were separated on an 8–12% SDS-polyacrylamide gel. Signals from phosphorylated protein have been revealed by Pro-Q® Diamond phosphoprotein stain (Life Technologies). After two fixation steps in a solution containing 50% methanol and 10% acetic acid (30 min each), the gel was stained by the Pro-Q® Diamond phosphoprotein stain for 90 min. The gel was de-stained by three 30-min washes in a solution containing 20% acetonitrile and 50 mM sodium acetate,



pH 4.0. The gel was washed twice with ultrapure water for 5 min, before scanning.

IDENTIFICATION OF PHOSPHORYLATED RESIDUES BY MASS SPECTROMETRY

In vitro phosphorylation reactions of PrkD K54D, YabT K55D, PtkA K59D, SpoIIAB N50A, and HprK K159M phosphorylated by PrkC, PtkA, PrkC, PrkD, and PrkD, respectively, were performed as described above, with the only difference of using only non-radioactive ATP. Denaturation of the samples was performed by buffer exchange to 6 M urea and 2 M thiourea in 10 mM Tris-HCl pH 8.0. Mass spectrometry analysis of phosphorylation sites was performed essentially as described previously (Derouiche et al., 2013). Briefly, in-solution digestion with trypsin was followed by phosphopeptide enrichment. Phosphopeptide analysis was performed on a Proxeon Easy-LC system (Proxeon Biosystems) coupled to an LTQ-Orbitrap-XL (Thermo Fisher Scientific) equipped with a nanoelectrospray ion source (Proxeon

Biosystems). The five most intense precursor ions were fragmented by activation of neutral loss ions at -98 , -49 , and -32.6 relative to the precursor ion (multistage activation). Acquired MS spectra were processed with MaxQuant software package (version 1.2.2.9). False discovery rates at peptide, phosphorylation site, and protein group level were set to 1%. Within the modified peptide, phosphorylation events detected with localization probability of at least 0.75 were considered as assigned to a specific residue.

YEAST TWO-HYBRID ASSAYS

Kinase-kinase binary interactions between various kinases and phosphatases were assessed essentially as described previously (Noirot-Gros et al., 2002). The genes encoding the BY-kinases (PtkA, PtkA) Hanks-type serine/threonine-kinases (PrkC, PrkD, YabT), two-component-like serine-kinases (SpoIIAB, RsbT, and RsbW), BY-kinase modulators (TkmA, TkmB), and the phosphotyrosine—and phosphoserine/threonine protein phosphatases (PtpZ, SpoIIE) were inserted in the pGBDU and pGAD yeast two-hybrid vectors to generate in-frame fusions with the DNA-binding domain (BD) and the activating domain (AD), respectively, of Gal4 (James et al., 1996). The pGBD and pGAD constructs were used to transform yeast (a) and (α) strains, respectively. Binary matrix of interactions was made by mixing haploid cells of complementary mating types, harboring various BD-kinase and AD-kinase fusions, in a 96 wells format. Interaction phenotypes were assessed by the ability of the diploid forms to grow on selective media depleted for histidine. Positive interactants were identified by DNA sequencing.

SEQUENCE ALIGNMENTS AND 3D-STRUCTURE MODELING

Sequence alignments were performed using MAFFT (Katoh and Toh, 2008). Structural models of PrkD (residues 17–253), YabT (residues 25 to 268), PtkA (residues 10 to 226), and HprK (residues 6 to 299) were obtained using the SWISS-MODEL (Bordoli et al., 2009). The residues 227 and 228 of PtkA were added to the structure manually to cover the autophosphorylation site Y228. Both PrkD and YabT were modeled based on PknB from *M. tuberculosis* (1mruB) (Young et al., 2003) as template. PtkA was modeled based on CapB from *Staphylococcus aureus* (2vedB) (Oliveras-Illana et al., 2008), and HprK/P was modeled based on HprK/P from *Staphylococcus xylosus* (Márquez et al., 2002) (1ko7A). SpoIIAB structure has been experimentally resolved (1thnC) (Masuda et al., 2004).

RESULTS AND DISCUSSION

CROSS-PHOSPHORYLATION OF BACILLUS SUBTILIS SERINE/THREONINE AND TYROSINE KINASES

In this study we set out to explore the possibility of cross-phosphorylation among eight *B. subtilis* protein kinases: PrkC, PrkD, YabT, PtkA, HprK/P, RsbT, RsbW, and SpoIIAB. The second BY-kinase PtkB (EpsB) (Gerwig et al., 2014) was left out from *in vitro* studies due to known solubility issues (Mijakovic et al., 2003). First we explored the capacity of the kinases to physically interact with each other, by performing two-hybrid screens using individual kinases as baits (Figure 1). An interaction detected

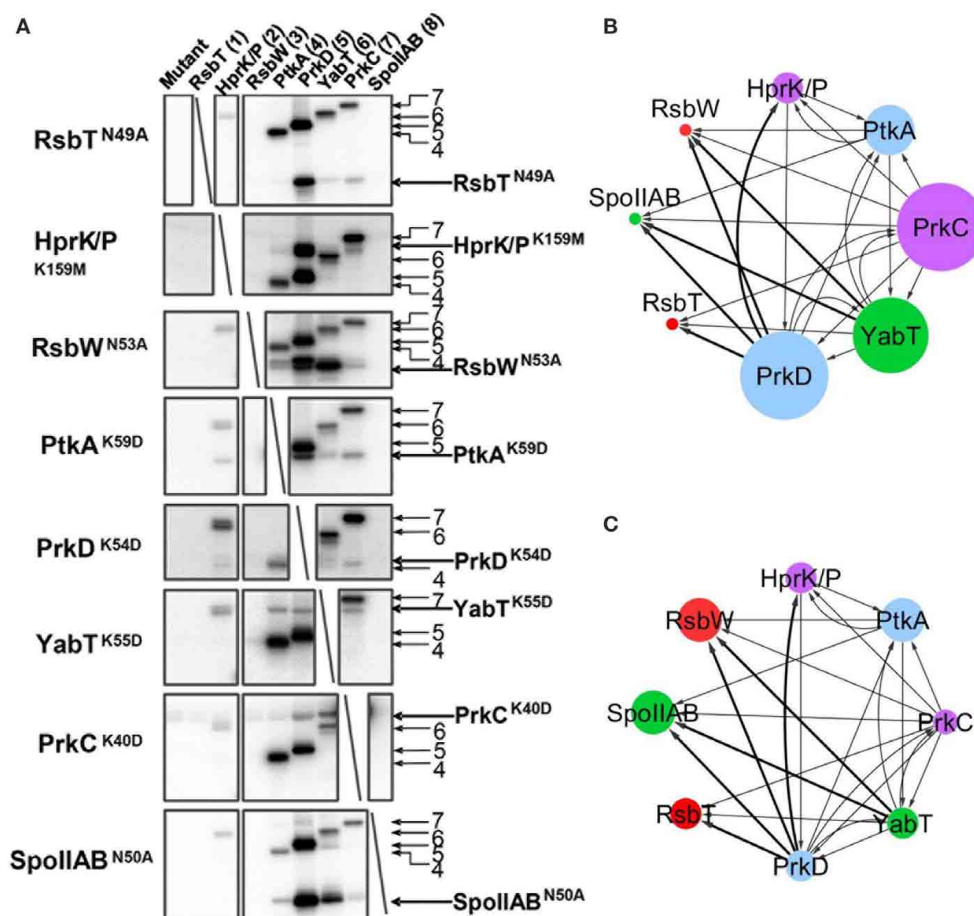


FIGURE 3 | *In vitro* phosphorylation assay showing cross-phosphorylation among kinases. Catalytically deficient protein kinase mutants carrying a substitution of the catalytic residue (indicated in each row) have been assayed pair-wise for phosphorylation by 8 different wild type kinases (indicated in columns and numbered) in the presence of ^{32}P - γ -ATP. Signals from phosphorylated kinases have been revealed by autoradiography. First lane of each gel is the inactivated kinase substrate alone as a negative control. Bands corresponding to autophosphorylation of wild type kinases (numbered) and phosphorylation of mutated kinase substrates are indicated by arrows.

(B,C) Graphical overview of the results shown in (A). Panel (B) presents the outgoing degree of connectivity (number of phosphorylation reactions catalyzed by the kinase), and panel (C) shows the incoming degree of connectivity (number of phosphorylation reactions undergone by the kinase). The size of the nodes refers to the degree of connectivity of each kinase. Color of nodes refers to the physiological condition for up-regulation of kinase expression based on Nicolas et al. (2012): sporulation (green), germination (purple), oxidative stress (red), biofilm formation and swarming (blue). Connecting line width illustrates relative phosphorylation efficiency.

between two proteins in both directions, i.e., irrespective of which one of them is used as a bait or prey, is termed reciprocal. An interaction is termed non-reciprocal when it has been detected with only one bait-prey configuration, but not the other. In our assay, we detected a reciprocal interaction between the BY-kinase PtkA and its cognate modulator TkmA, first described by Mijakovic et al. (2003) (Figure 1A). Next, we detected a reciprocal interaction between TkmA and the second BY-kinase PtkB (Figures 1B,C). There were also two non-reciprocal interactions: that of PtkA and PtkB and TkmA and TkMB (Figure 1C). The BY-kinases PtkA and PtkB were connected to the Hanks-type serine/threonine kinase YabT either via a direct interaction (PtkB, Figure 1C) or via an interaction with the PtkA modulator TkmA (Figure 1D). YabT also interacted with the phosphotyrosine-protein phosphatase PtpZ,

known to dephosphorylate PtkA substrates (Mijakovic et al., 2005). The two-component-like kinase RsbT interacted directly with the BY-kinase PtkA and its cognate phosphatase PtpZ (Figure 1E). Interestingly, the RsbT did not interact with the wild-type PtkA, but interacted with the catalytically inactive mutant D81A. A direct interaction was also observed between RsbT and the Hanks-type kinase PrkD (Figure 1E). Hanks-type kinases YabT and PrkD also interacted directly with the sensory histidine kinase DegS which they are known to phosphorylate (Jers et al., 2011) (data not shown). Another link between tyrosine phosphorylation systems and the two-component systems was established through a binary interaction involving the phosphotyrosine-protein phosphatase YwIE (Musumeci et al., 2005) and the two-component response regulator YxdJ (Joseph et al., 2004) (data not shown). These findings suggest that

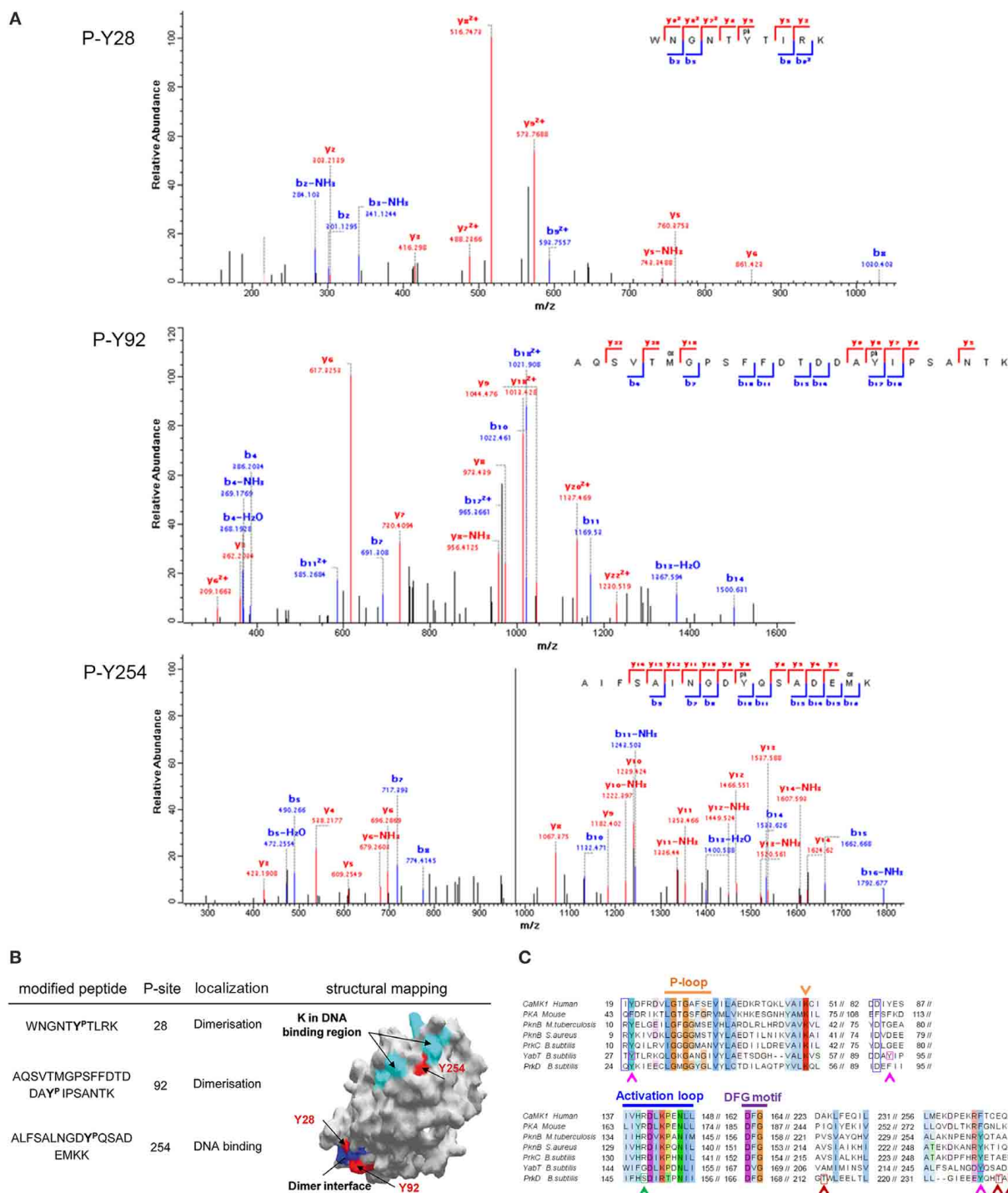
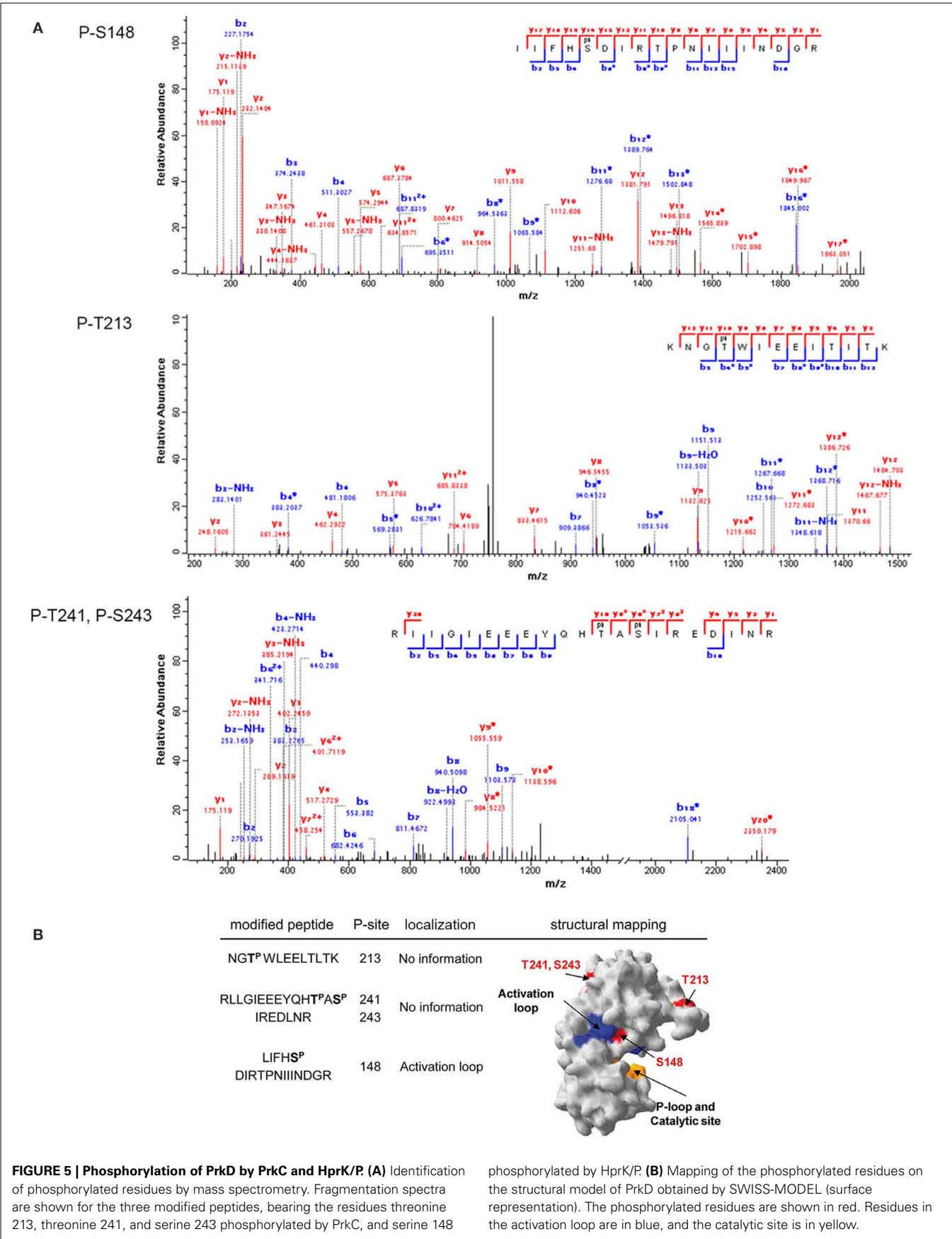
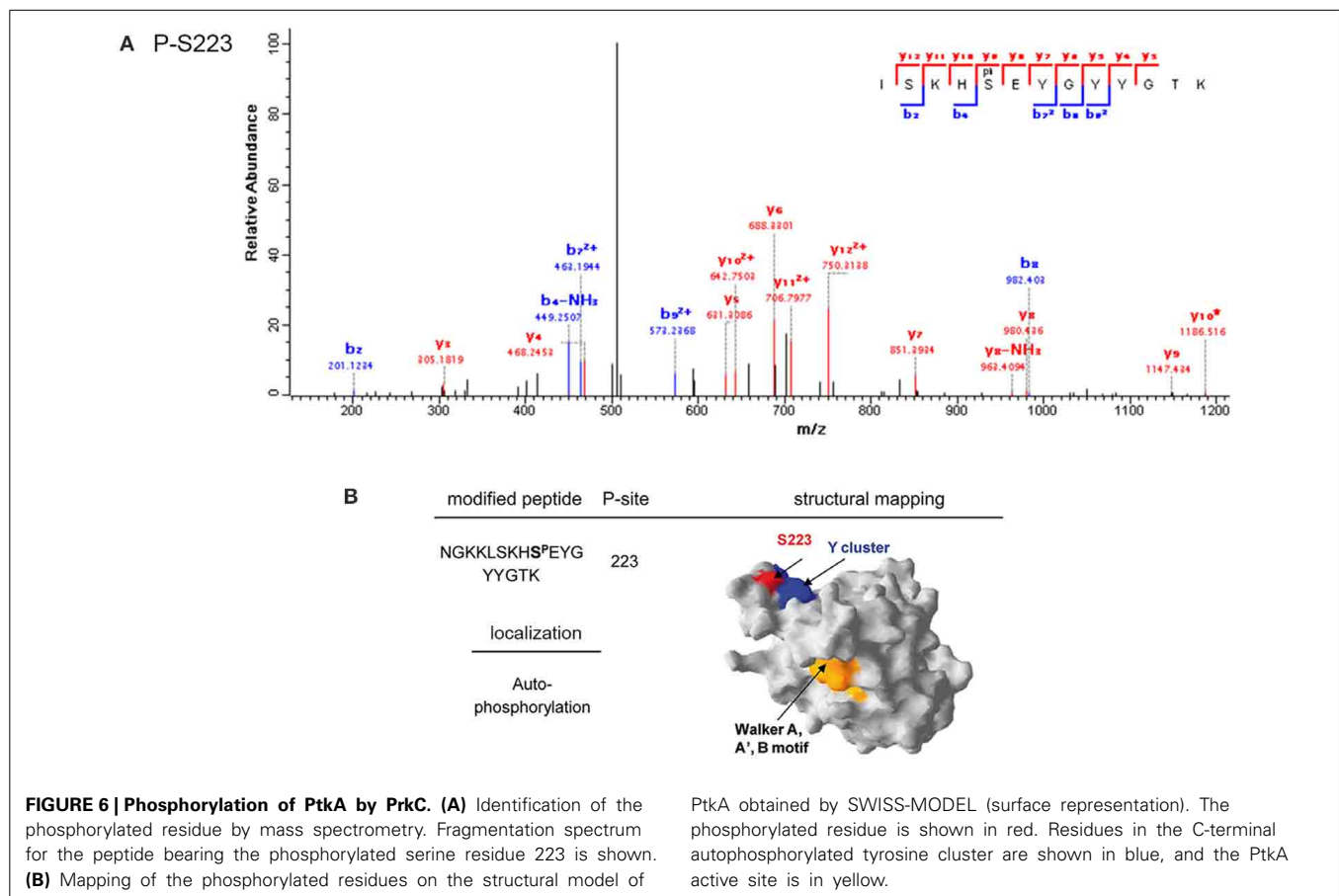


FIGURE 4 | Phosphorylation of YabT by PtkA. (A) Identification of phosphorylated residues by mass spectrometry. Fragmentation spectra for the three modified peptides, bearing the phosphorylated tyrosine residues 28, 92, and 254, are shown. **(B)** Mapping of the phosphorylated residues on the structural model of YabT obtained by SWISS-MODEL (surface representation). The phosphorylated residues are shown in red, residues in blue are associated with the region involved in the formation of dimers in YabT and in PknB (Rakette et al., 2012) and the residues in cyan represent the DNA binding region of YabT (Bidnenko et al., 2013). **(C)** Alignment of *B. subtilis* YabT, PrkC, and PrkD sequences with Hanks-type kinase homologs:

the kinase domains of calcium/calmodulin-dependent protein kinase (CaMK1, human), protein kinase A (PKA, mouse), PknB from *M. tuberculosis* and *Staphylococcus aureus*. The P-loop, catalytic site (K), catalytic loop and the DFG motif are indicated (Young et al., 2003). The residues R9 and D75 in PknB of *S. aureus* which are involved in dimer formation (Rakette et al., 2012) are indicated with blue boxes. For YabT, the residues Y28, Y92 and Y254, which are phosphorylated by PtkA, are indicated with pink boxes and arrows. For PrkD, the residues T213, T241, and S243, which is phosphorylated by PrkC, are indicated with red boxes and arrows, and the S148, which is phosphorylated by HprK/P, is indicated with a green box and arrow.





physical interactions exist among three different classes of kinases: Hanks-type kinases, BY-kinases, and two-component systems-like kinases. The bi-functional kinase/phosphorylase HprK/P did not appear to interact with other kinases in the two-hybrid assay (data not shown). A weak growth phenotype, featuring a possible PtkA self-interaction was also observed in only one of the two tested AD-PtkA fusions (**Figure 1A**). This could be explained by differential levels of expression of the AD-PtkA fusions in the two different haploid yeast strains.

Next, we explored the capacity of purified protein kinases to phosphorylate each other. We first purified mutant versions of each kinase with inactivated catalytic residues. Since several of the studied kinases, HprK/P, RsbT, RsbW, and SpoIIB, do not autophosphorylate, we tested their catalytically inactive mutant versions (HprK/P K53M, RsbT N49A, RsbW N53A, SpoIIA N50A) on their respective substrates: Hpr, RsbS, RsbV, and SpoIIAA (**Figure 2A**). All mutant kinases were unable to phosphorylate the substrates, indicating that the catalytic site inactivation has been completed successfully. Next, we examined the capacity for intermolecular autophosphorylation for the autophosphorylating kinases PtkA, PrkC, PrkD, and YabT (**Figure 2B**). In case of PrkC, PrkD and YabT, intermolecular autophosphorylation was indeed detected. The mutant versions PrkC K40D, PrkD K54D, and YabT K55D were all phosphorylated by their respective wild type counterparts, which is

consistent with the known mode of activation of Hanks-type kinases through a binary interaction (Barthe et al., 2010). This signal of phosphorylation on PrkC K40D was particularly strong, suggesting that this kinase is very efficient in intermolecular autophosphorylation. Since PrkC is the only Hanks-type kinase in *B. subtilis* that possesses an extracellular ligand-binding domain, it seems plausible that its mode of activation follows the canonical trans-phosphorylation triggered by ligand-induced dimerization at the membrane. By contrast, YabT is known to be activated by binding DNA at the asymmetric septum during spore development (Bidnenko et al., 2013) and for the soluble PrkD, the activation mechanism is not known. For the BY-kinase PtkA we could not detect trans-autophosphorylation, which is in agreement with our previous findings (Mijakovic et al., 2003). For the remaining kinases, HprK/P, RsbT, RsbW and SpoIIB, intermolecular autophosphorylation was not observed, as expected (data not shown).

The catalytically deficient kinases were then subjected to cross-phosphorylation by the entire set of wild type kinases, in an eight by eight matrix experiment (**Figure 3A**). The reactions were assembled based on the assumption that kinases are present in roughly equimolar concentrations in the *B. subtilis* cell (Nicolas et al., 2012). Small variations in the final kinase concentrations in the assay are a result of optimization to simultaneously visualize signals of kinases migrating close

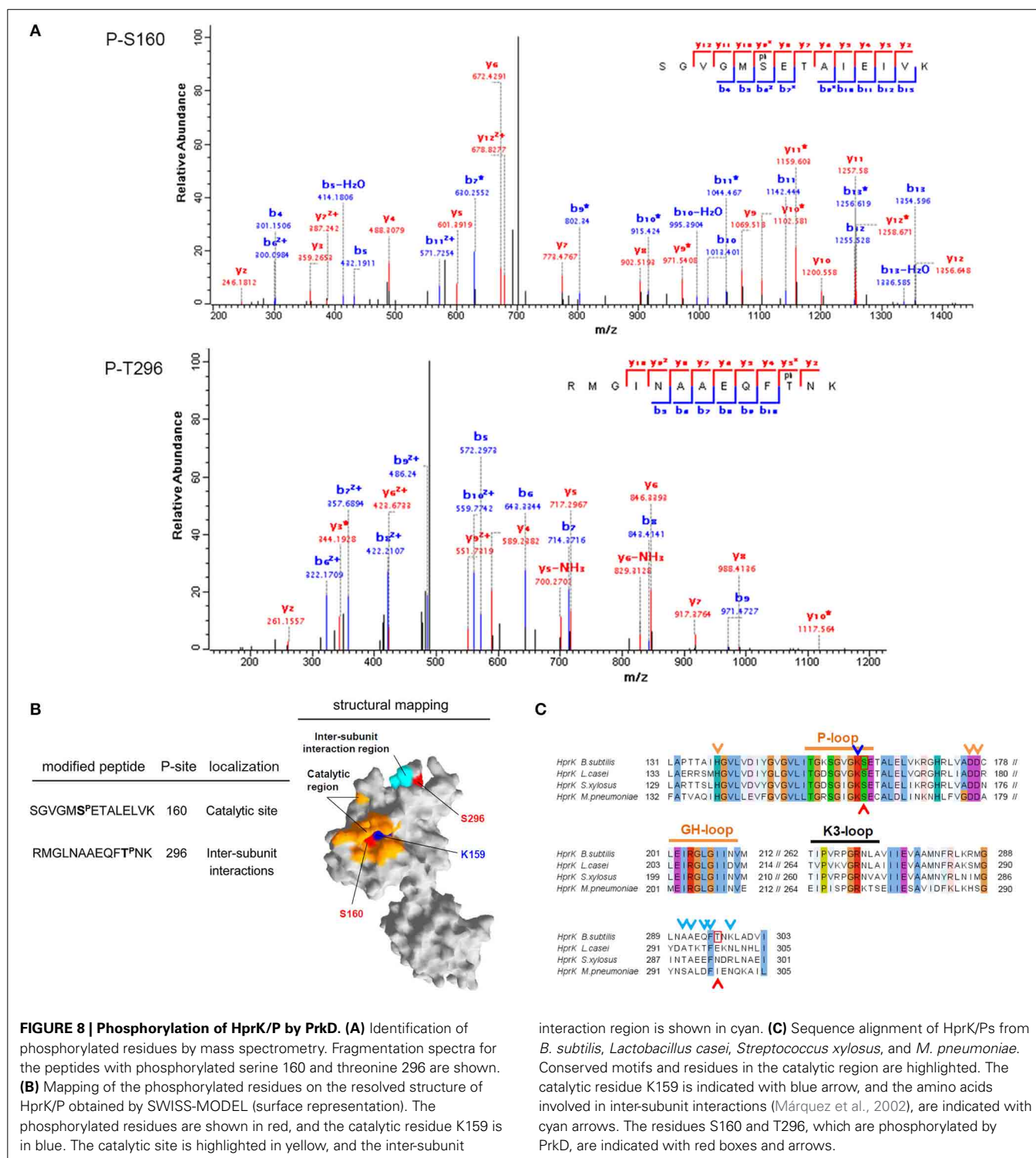


FIGURE 8 | Phosphorylation of HprK/P by PrkD. (A) Identification of phosphorylated residues by mass spectrometry. Fragmentation spectra for the peptides with phosphorylated serine 160 and threonine 296 are shown. **(B)** Mapping of the phosphorylated residues on the resolved structure of HprK/P obtained by SWISS-MODEL (surface representation). The phosphorylated residues are shown in red, and the catalytic residue K159 is in blue. The catalytic site is highlighted in yellow, and the inter-subunit

interaction region is shown in cyan. **(C)** Sequence alignment of HprK/Ps from *B. subtilis*, *Lactobacillus casei*, *Streptococcus xyloosus*, and *M. pneumoniae*. Conserved motifs and residues in the catalytic region are highlighted. The catalytic residue K159 is indicated with blue arrow, and the amino acids involved in inter-subunit interactions (Márquez et al., 2002), are indicated with cyan arrows. The residues S160 and T296, which are phosphorylated by PrkD, are indicated with red boxes and arrows.

to affect the YabT interaction with DNA, while phosphorylation at Y28 and Y92 might affect dimerization of the kinase. These findings clearly suggest that PtkA-dependent phosphorylation of YabT could modulate the activity of the recipient kinase. Sequence alignment of YabT with other Hanks-type serine/threonine kinases shows that the residues Y28 and Y254 in YabT are highly

conserved (Figure 4C), suggesting that the regulatory mechanism involving their phosphorylation could be widely conserved.

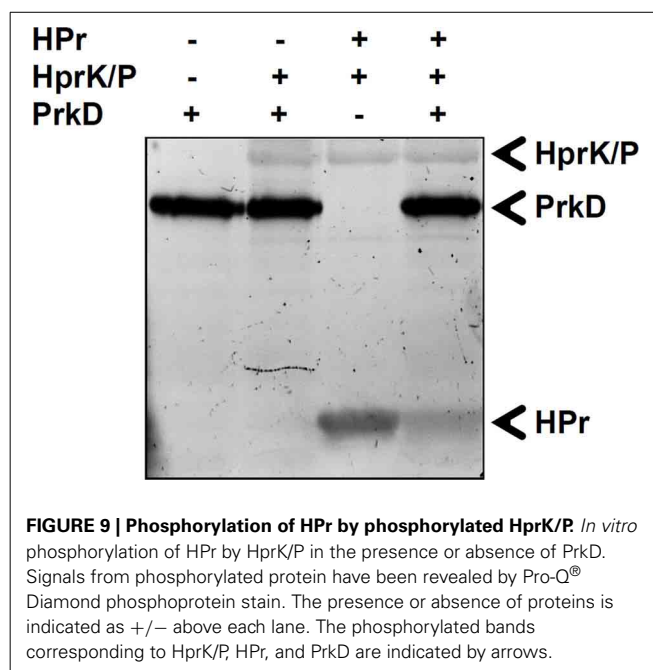
PrkD is a cytosolic Hanks-type serine/threonine kinase with no transmembrane helix. For its transmembrane paralogs, PrkC and YabT, the activation mechanism by respective binding of muopeptides (Shah et al., 2008) and DNA (Bidnenko et al., 2013)

has been clearly established. By contrast, the activation mechanism of PrkD is not known. We have detected that PrkD can be phosphorylated by PrkC and HprK/P. Phosphorylation of PrkD by PrkC occurred on residues T213, T241, and S243 (Figure 5A), which are in the catalytic domain, but distant from the active site (Figure 5B). Any putative regulatory potential of these phosphorylation events can not be deduced directly. However, HprK/P phosphorylated PrkD on the residue S148 (Figure 5A) in the activation loop, with a very probable consequence of stimulating the PrkD kinase activity (Figure 5B). The residue serine 148 is not conserved in Hanks-type kinases (Figure 4C). The structure of PrkD, lacking the transmembrane helix, is also unusual for bacterial Hanks-type kinases. This configuration with another kinase phosphorylating the activation loop of PrkD (usually accomplished by intermolecular autophosphorylation leading to activation of canonical Hanks-type kinases) could represent an idiosyncratic mechanism to activate this cytosolic kinase.

The BY-kinase PtkA was phosphorylated by PrkC at S223 (Figure 6A). This residue is positioned in the immediate vicinity of the C-terminal tyrosine cluster, containing PtkA autophosphorylation sites (Y225, Y227, and Y228) (Figure 6B). BY-kinase autophosphorylation on these tyrosines is known to trigger the dissociation of the activator-bound octameric ring (Oliveras-Illana et al., 2008). Interestingly, we have previously observed that PtkA autophosphorylation at Y228 is strongly enhanced *in vivo* in the $\Delta prkC$ strain (Ravikumar et al., 2014). This suggests that PrkC-dependent phosphorylation of PtkA at S223 could inhibit its autophosphorylation, and thus regulate its oligomerization state and interaction with the activator TkmA (Mijakovic et al., 2003).

The two-component system-like serine/threonine kinase SpoIIAB was phosphorylated by PrkD at S13 (Figure 7A). This residue is located on the interface interacting with the anti-anti-sigma factor SpoIIAA (Figure 7B), close to the residues R20, T49, and E104, which are known to be essential for this interaction (Masuda et al., 2004). SpoIIAA is also an inhibitor of the SpoIIAB kinase activity, and must dissociate from the complex in order for the kinase to be active. Phosphorylation of SpoIIAB by PrkD at S13 might be an alternative route to destabilize the SpoIIAA/SpoIIAB complex, and its phosphorylation is therefore likely to have a regulatory role.

Finally, the bifunctional HprK/P was phosphorylated by PrkD at residues S160 and S296 (Figure 8A). S296 is situated in the region necessary for subunit interactions in the HprK/P hexamer (Márquez et al., 2002) (Figure 8B), but it is not conserved (Figure 8C). By contrast, the phosphorylated S160 is situated adjacent to the catalytic residue K159 and is highly conserved (Figures 8B,C). We speculated that its phosphorylation is very likely to affect the catalytic activity of HprK/P, which depends on the positively charged catalytic lysine. In order to test this assumption, we phosphorylated HprK/P with PrkD *in vitro*, and then compared the capacity of phosphorylated vs. non-phosphorylated HprK/P to phosphorylate its substrate HPr (Figure 9). The presence of PrkD in the phosphorylation assay significantly diminished the capacity of HprK/P to phosphorylate HPr. The Pro-Q® Diamond-stained signal from phosphorylated HprK/P comprises the pre-existing artificial autophosphorylation



of this kinase in its 6xHis tag (Josef Deutscher, personal communication), and therefore additional phosphorylation by PrkD is not readily discernable. While this finding supports the notion that HprK/P activity is regulated by PrkD-dependent phosphorylation, its physiological relevance remains to be determined *in vivo*.

CONCLUSIONS AND PERSPECTIVES

Our global interactomics screen of the regulatory network based on serine/threonine/tyrosine phosphorylation in *B. subtilis* (Shi et al., unpublished results) revealed a high degree of connectivity among different classes of kinases, kinase activators, substrates, and phosphatases. Here we have explored whether the connectivity at the protein-protein interaction level may point to a functional interaction, i.e., cross-phosphorylation among the four classes of *B. subtilis* serine/threonine and tyrosine protein kinases. Our data suggest an even higher degree of connectivity than the interactomics studies, with all tested kinases engaging in cross phosphorylation, either as donors or recipients. Moreover, the identity of residues phosphorylated on recipient kinases in most cases supports the notion that phosphorylation of one kinase by another has a functional/regulatory consequence. The phosphorylated residues are situated in, or immediately adjacent to, protein-protein or protein-DNA interaction surfaces, activating loops or the kinase active sites. It is therefore likely that bacteria also possess kinase cascades similar to those described in eukarya (Marshall, 1994). Given the existing evidence on involvement of these kinases in complex phenomena such as bacterial cell cycle control and control of spore and biofilm development, this finding is not entirely unexpected. The kinase phosphorylation sites that we report here were not detected in the previous phosphoproteomics studies performed on *B. subtilis* (Macek et al., 2007; Ravikumar et al., 2014), which is not surprising due to

the non-exhaustive nature of published bacterial phosphoproteomes. Nevertheless, the final verdict on the importance of kinase cross-phosphorylation and the putative kinase cascades in bacteria will have to come from *in vivo* studies.

ACKNOWLEDGMENT

This work was supported by grants from the Agence Nationale de la Recherche (2010-BLAN-1303-01 to IM and MFNG), the Federation pour la Recherche Medicale (to Ivan Mijakovic and Lei Shi), and the Chalmers University of Technology (to Ivan Mijakovic). We are grateful to Josef Deutscher for providing the *B. subtilis* HPr protein for *in vitro* kinase assays.

REFERENCES

- Absalon, C., Obuchowski, M., Madec, E., Delattre, D., Holland, I. B., and Séror, S. J. (2009). CpgA, EF-Tu and the stressosome protein YezB are substrates of the Ser/Thr kinase/phosphatase couple, PrkC/PrpC, in *Bacillus subtilis*. *Microbiology* 155, 932–943. doi: 10.1099/mic.0.022475-0
- Baer, C. E., Iavarone, A. T., Alber, T., and Sassetti, C. M. (2014). Biochemical and spatial coincidence in the provisional Ser/Thr protein kinase interaction network of *Mycobacterium tuberculosis*. *J. Biol. Chem.* 289, 20422–20433. doi: 10.1074/jbc.M114.559054
- Barthe, P., Mukamolova, G. V., Roumestand, C., and Cohen-Gonsaud, M. (2010). The structure of PknB extracellular PASTA domain from *Mycobacterium tuberculosis* suggests a ligand-dependent kinase activation. *Structure* 18, 606–615. doi: 10.1016/j.str.2010.02.013
- Bidnenko, V., Shi, L., Kobir, A., Ventroux, M., Pigeonneau, N., Henry, C., et al. (2013). *Bacillus subtilis* serine/threonine protein kinase YabT is involved in spore development via phosphorylation of a bacterial recombinase. *Mol. Microbiol.* 88, 921–935. doi: 10.1111/mmi.12233
- Bordoli, L., Kiefer, F., Arnold, K., Benkert, P., Battey, J., and Schwede, T. (2009). Protein structure homology modeling using SWISS-MODEL workspace. *Nat. Protoc.* 4, 1–13. doi: 10.1038/nprot.2008.197
- Burbulys, D., Trach, K. A., and Hoch, J. A. (1991). Initiation of sporulation in *B. subtilis* is controlled by a multicomponent phosphorelay. *Cell* 64, 545–552. doi: 10.1016/0092-8674(91)90238-T
- Campbell, E. A., Masuda, S., Sun, J. L., Muzzin, O., Olson, C. A., Wang, S., et al. (2002). Crystal structure of the *Bacillus stearothermophilus* anti-sigma factor SpoIIAB with the sporulation sigma factor sigmaF. *Cell* 108, 795–807. doi: 10.1016/S0092-8674(02)00662-1
- Colinge, J., César-Razquin, A., Huber, K., Breitwieser, F. P., Májek, P., and Superti-Furga, G. (2014). Building and exploring an integrated human kinase network: global organization and medical entry points. *J. Proteomics* 107, 113–127. doi: 10.1016/j.jpro.2014.03.028
- Cousin, C., Derouiche, A., Shi, L., Pagot, Y., Poncet, S., and Mijakovic, I. (2013). Protein-serine/threonine/tyrosine kinases in bacterial signaling and regulation. *FEMS Microbiol. Lett.* 346, 11–19. doi: 10.1111/1574-6968.12189
- Derouiche, A., Bidnenko, V., Grenha, R., Pigeonneau, N., Ventroux, M., Franz-Wachtel, M., et al. (2013). Interaction of bacterial fatty-acid-displaced regulators with DNA is interrupted by tyrosine phosphorylation in the helix-turn-helix domain. *Nucleic Acids Res.* 41, 9371–9381. doi: 10.1093/nar/gkt709
- Gerwig, J., Kiley, T. B., Gunka, K., Stanley-Wall, N., and Stülke, J. (2014). The protein tyrosine kinases EpsB and PtkA differentially affect biofilm formation in *Bacillus subtilis*. *Microbiology* 160, 682–691. doi: 10.1099/mic.0.074971-0
- Goulian, M. (2010). Two-component signaling circuit structure and properties. *Curr. Opin. Microbiol.* 13, 184–189. doi: 10.1016/j.mib.2010.01.009
- Grundner, C., Gay, L. M., and Alber, T. (2005). *Mycobacterium tuberculosis* serine/threonine kinases PknB, PknD, PknE, and PknF phosphorylate multiple FHA domains. *Protein Sci.* 14, 1918–1921. doi: 10.1110/ps.051413405
- Hanson, K. G., Steinhauer, K., Reizer, J., Hillen, W., and Stülke, J. (2002). HPr kinase/phosphatase of *Bacillus subtilis*: expression of the gene and effects of mutations on enzyme activity, growth and carbon catabolite repression. *Microbiology* 148, 1805–1811. Available online at: <http://mic.sgmjournals.org/content/148/6/1805.long>
- James, P., Halladay, J., and Craig, E. A. (1996). Genomic libraries and a host strain designed for highly efficient two-hybrid selection in yeast. *Genetics* 144, 1425–1436.
- Jers, C., Kobir, A., Søndergaard, E. O., Jensen, P. R., and Mijakovic, I. (2011). *Bacillus subtilis* two-component system sensory kinase DegS is regulated by serine phosphorylation in its input domain. *PLoS ONE* 6:e14653. doi: 10.1371/journal.pone.0014653
- Jers, C., Pedersen, M. M., Paspaliari, D. K., Schütz, W., Johnsson, C., Soufi, B., et al. (2010). *Bacillus subtilis* BY-kinase PtkA controls enzyme activity and localization of its protein substrates. *Mol. Microbiol.* 77, 287–299. doi: 10.1111/j.1365-2958.2010.07227.x
- Joseph, P., Guiseppi, A., Sorokin, A., and Denizot, F. (2004). Characterization of the *Bacillus subtilis* YxdJ response regulator as the inducer of expression for the cognate ABC transporter YxdLM. *Microbiology* 150, 2609–2617. doi: 10.1099/mic.0.27155-0
- Kang, C. M., Vijay, K., and Price, C. W. (1998). Serine kinase activity of a *Bacillus subtilis* switch protein is required to transduce environmental stress signals but not to activate its target PP2C phosphatase. *Mol. Microbiol.* 30, 189–196. doi: 10.1046/j.1365-2958.1998.01052.x
- Katoh, K., and Toh, H. (2008). Recent developments in the MAFFT multiple sequence alignment program. *Brief Bioinform.* 9, 286–298. doi: 10.1093/bib/bbn013
- Kobir, A., Poncet, S., Bidnenko, V., Delumeau, O., Jers, C., Zouhir, S., et al. (2014). Phosphorylation of *Bacillus subtilis* gene regulator AbrB modulates its DNA-binding properties. *Mol. Microbiol.* 92, 1129–1141. doi: 10.1111/mmi.12617
- Macek, B., Mijakovic, I., Olsen, J. V., Gnad, F., Kumar, C., Jensen, P. R., et al. (2007). The serine/threonine/tyrosine phosphoproteome of the model bacterium *Bacillus subtilis*. *Mol. Cell. Proteom.* 6, 697–707. doi: 10.1074/mcp.M600464-MCP200
- Madec, E., Laszkiewicz, A., Iwanicki, A., Obuchowski, M., and Séror, S. (2002). Characterization of a membrane-linked Ser/Thr protein kinase in *Bacillus subtilis*, implicated in developmental processes. *Mol. Microbiol.* 46, 571–586. doi: 10.1046/j.1365-2958.2002.03178.x
- Márquez, J. A., Hasenbein, S., Koch, B., Fieulaine, S., Nessler, S., Russell, R. B., et al. (2002). Structure of the full-length HPr kinase/phosphatase from *Staphylococcus xylosum* at 1.95 Å resolution: mimicking the product/substrate of the phospho transfer reactions. *Proc. Natl. Acad. Sci. U.S.A.* 99, 3458–3463. doi: 10.1073/pnas.052461499
- Marshall, C. J. (1994). MAP kinase kinase kinase, MAP kinase kinase and MAP kinase. *Curr. Opin. Genet. Dev.* 4, 82–89. doi: 10.1016/0959-437X(94)90095-7
- Masuda, S., Murakami, K. S., Wang, S., Anders Olson, C., Donigian, J., Leon, F., et al. (2004). Crystal structures of the ADP and ATP bound forms of the *Bacillus* anti-sigma factor SpoIIAB in complex with the anti-anti-sigma SpoIIAA. *J. Mol. Biol.* 340, 941–956. doi: 10.1016/j.jmb.2004.05.040
- Mijakovic, I., Musumeci, L., Tautz, L., Petranovic, D., Edwards, R. A., Jensen, P. R., et al. (2005). *In vitro* characterization of the *Bacillus subtilis* protein tyrosine phosphatase YwqE. *J. Bacteriol.* 187, 3384–3390. doi: 10.1128/JB.187.10.3384-3390.2005
- Mijakovic, I., Poncet, S., Boël, G., Mazé, A., Gillet, S., Jamet, E., et al. (2003). Transmembrane modulator-dependent bacterial tyrosine kinase activates UDP-glucose dehydrogenases. *EMBO J.* 22, 4709–4718. doi: 10.1093/emboj/cdg458
- Min, K. T., Hilditch, C. M., Diederich, B., Errington, J., and Yudkin, M. D. (1993). Sigma F, the first compartment-specific transcription factor of *B. subtilis*, is regulated by an anti-sigma factor that is also a protein kinase. *Cell* 74, 735–742. doi: 10.1016/0092-8674(93)90520-Z
- Molle, V., and Kremer, L. (2010). Division and cell envelope regulation by Ser/Thr phosphorylation: *Mycobacterium* shows the way. *Mol. Microbiol.* 75, 1064–1077. doi: 10.1111/j.1365-2958.2009.07041.x
- Musumeci, L., Bongiorno, C., Tautz, L., Edwards, R. A., Osterman, A., Perego, M., et al. (2005). Low-molecular-weight protein tyrosine phosphatases of *Bacillus subtilis*. *J. Bacteriol.* 187, 4945–4956. doi: 10.1128/JB.187.14.4945-4956.2005
- Nicolas, P., Mäder, U., Dervyn, E., Rochat, T., Leduc, A., Pigeonneau, N., et al. (2012). Condition-dependent transcriptome reveals high-level regulatory architecture in *Bacillus subtilis*. *Science* 335, 1103–1106. doi: 10.1126/science.1206848
- Noirot-Gros, M. F., Dervyn, E., Wu, L. J., Mervelet, P., Errington, J., Ehrlich, S. D., et al. (2002). An expanded view of bacterial DNA replication. *Proc. Natl. Acad. Sci. U.S.A.* 99, 8342–8347. doi: 10.1073/pnas.122040799

- Olivares-Illana, V., Meyer, P., Bechet, E., Gueguen-Chaignon, V., Soulat, D., Lazereg-Riquier, S., et al. (2008). Structural basis for the regulation mechanism of the tyrosine kinase CapB from *Staphylococcus aureus*. *PLoS Biol.* 6:e143. doi: 10.1371/journal.pbio.0060143
- Pereira, S. F., Goss, L., and Dworkin, J. (2011). Eukaryote-like serine/threonine kinases and phosphatases in bacteria. *Microbiol. Mol. Biol. Rev.* 75, 192–212. doi: 10.1128/MMBR.00042-10
- Petranovic, D., Grangeasse, C., Macek, B., Abdillatef, M., Gueguen-Chaignon, V., Nessler, S., et al. (2009). Activation of *Bacillus subtilis* Ugd by the BY-kinase PtkA proceeds via phosphorylation of its residue tyrosine 70. *J. Mol. Microbiol. Biotechnol.* 17, 83–89. doi: 10.1159/000206635
- Pietack, N., Becher, D., Schmidl, S. R., Saier, M. H., Hecker, M., Commichau, F. M., et al. (2010). *In vitro* phosphorylation of key metabolic enzymes from *Bacillus subtilis*: PrkC phosphorylates enzymes from different branches of basic metabolism. *J. Mol. Microbiol. Biotechnol.* 18, 129–140. doi: 10.1159/000308512
- Podgornaia, A. I., and Laub, M. T. (2013). Determinants of specificity in two-component signal transduction. *Curr. Opin. Microbiol.* 16, 156–162. doi: 10.1016/j.mib.2013.01.004
- Rakette, S., Donat, S., Ohlsen, K., and Stehle, T. (2012). Structural analysis of *Staphylococcus aureus* serine/threonine kinase PknB. *PLoS ONE* 7:e39136. doi: 10.1371/journal.pone.0039136
- Ravikumar, V., Shi, L., Krug, K., Derouiche, A., Jers, C., Cousin, C., et al. (2014). Quantitative phosphoproteome analysis of *Bacillus subtilis* reveals novel substrates of the kinase PrkC and phosphatase PrpC. *Mol. Cell. Proteom.* 13, 1965–1978. doi: 10.1074/mcp.M113.035949
- Shah, I. M., Laaberki, M. H., Popham, D. L., and Dworkin, J. (2008). A eukaryotic-like Ser/Thr kinase signals bacteria to exit dormancy in response to peptidoglycan fragments. *Cell* 135, 486–496. doi: 10.1016/j.cell.2008.08.039
- Shi, L., Ji, B., Kolar-Znika, L., Boskovic, A., Jadeau, F., Combet, C., et al. (2014). Evolution of bacterial protein-tyrosine kinases and their relaxed specificity toward substrates. *Genome Biol. Evol.* 6, 800–817. doi: 10.1093/gbe/evu056
- Yang, X., Kang, C. M., Brody, M. S., and Price, C. W. (1996). Opposing pairs of serine protein kinases and phosphatases transmit signals of environmental stress to activate a bacterial transcription factor. *Genes Dev.* 10, 2265–2275. doi: 10.1101/gad.10.18.2265
- Young, T. A., Delagoutte, B., Endrizzi, J. A., Falick, A. M., and Alber, T. (2003). Structure of *Mycobacterium tuberculosis* PknB supports a universal activation mechanism for Ser/Thr protein kinases. *Nat. Struct. Biol.* 10, 168–174. doi: 10.1038/nsb897

Conflict of Interest Statement: The authors declare that the research was conducted in the absence of any commercial or financial relationships that could be construed as a potential conflict of interest.

Received: 23 July 2014; accepted: 03 September 2014; published online: 17 September 2014.

Citation: Shi L, Pigeonneau N, Ravikumar V, Dobrinic P, Macek B, Franjevic D, Noirot-Gros M-F and Mijakovic I (2014) Cross-phosphorylation of bacterial serine/threonine and tyrosine protein kinases on key regulatory residues. *Front. Microbiol.* 5:495. doi: 10.3389/fmicb.2014.00495

This article was submitted to *Microbial Physiology and Metabolism*, a section of the journal *Frontiers in Microbiology*.

Copyright © 2014 Shi, Pigeonneau, Ravikumar, Dobrinic, Macek, Franjevic, Noirot-Gros and Mijakovic. This is an open-access article distributed under the terms of the Creative Commons Attribution License (CC BY). The use, distribution or reproduction in other forums is permitted, provided the original author(s) or licensor are credited and that the original publication in this journal is cited, in accordance with accepted academic practice. No use, distribution or reproduction is permitted which does not comply with these terms.



Production of a recombinant vaccine candidate against *Burkholderia pseudomallei* exploiting the bacterial *N*-glycosylation machinery

Fatima Garcia-Quintanilla^{1†}, Jeremy A. Iwashkiw^{1†}, Nancy L. Price¹, Chad Stratilo² and Mario F. Feldman^{1*}

¹ Department of Biological Sciences, University of Alberta, Edmonton, AB, Canada

² Defence Research and Development Canada – Suffield Research Centre, Medicine Hat, AB, Canada

Edited by:

Ivan Mijakovic, Chalmers University of Technology, Sweden

Reviewed by:

Brendan Wren, University of London, UK

Lei Shi, Chalmers University of Technology, Sweden

*Correspondence:

Mario F. Feldman, Department of Biological Sciences, University of Alberta, CCIS 6-063, 116 Street, 85 Avenue, Edmonton, AB T6G 2R3, Canada
e-mail: mfeldman@ualberta.ca

[†] Fatima Garcia-Quintanilla and Jeremy A. Iwashkiw have equally contributed to this work.

Vaccines developing immune responses toward surface carbohydrates conjugated to proteins are effective in preventing infection and death by bacterial pathogens. Traditional production of these vaccines utilizes complex synthetic chemistry to acquire and conjugate the glycan to a protein. However, glycoproteins produced by bacterial protein glycosylation systems are significantly easier to produce, and could possibly be used as vaccine candidates. In this work, we functionally expressed the *Burkholderia pseudomallei* O polysaccharide (OPS II), the *Campylobacter jejuni* oligosaccharyltransferase (OTase), and a suitable glycoprotein (AcrA) in a designer *E. coli* strain with a higher efficiency for production of glycoconjugates. We were able to produce and purify the OPS II-AcrA glycoconjugate, and MS analysis confirmed correct glycan was produced and attached. We observed the attachment of the *O*-acetylated deoxyhexose directly to the acceptor protein, which expands the range of substrates utilized by the OTase PglB. Injection of the glycoprotein into mice generated an IgG immune response against *B. pseudomallei*, and this response was partially protective against an intranasal challenge. Our experiments show that bacterial engineered glycoconjugates can be utilized as vaccine candidates against *B. pseudomallei*. Additionally, our new *E. coli* strain SDB1 is more efficient in glycoprotein production, and could have additional applications in the future.

Keywords: glycobiology, vaccines, protein glycosylation, microbiology and biotechnology, molecular biology, mass spectrometry

INTRODUCTION

Burkholderia pseudomallei, a Gram-negative saprophyte, is the causative agent for melioidosis and is endemic in Southeast Asia and Northern Australia (Cheng and Currie, 2005). It is highly resistant to harsh environmental pressures, and it is classified as a potential class B bioterrorism weapon due to its high infectivity when aerosolized (Silva and Dow, 2013). Several virulence factors have been identified, including multiple Type III and VI secretion systems, toxins, capsular polysaccharide, and lipopolysaccharide (LPS; Nandi and Tan, 2013). Two different LPS structures named O-polysaccharide (OPS) I and II are present in *B. pseudomallei*, and OPS II was shown to be required for serum resistance and virulence (Knirel et al., 1992; Perry et al., 1995; DeShazer et al., 1998). *B. pseudomallei* has an intrinsically high resistance to several different classes of antibiotics, which increases the potential danger of this organism. Due to the increasing prevalence of new resistance genes, and the increasing number of cases, new alternatives to treat and prevent melioidosis are required.

Immunization is one of the best available tools against infection, and it is significantly more cost effective than treatment after disease has occurred. Three main classes of vaccines are commercially produced. Live attenuated bacteria that have been shown to be highly effective as vaccine candidates however, drawbacks such as safety, reactogenicity, stability, and manufacturing remain

problematic (Galen and Curtiss, 2013). Whole-cell-killed bacterial vaccines are easy to commercially manufacture, but have problems with stability, long-term protection, and present biosafety risks in the case of class III pathogens. Purified surface carbohydrates have been utilized as a vaccine candidate, but typically only produce short-term protection and are not effective in children or mature individuals (Lockhart, 2003). Traditional conjugate vaccines, where bacterial surface polysaccharides are chemically conjugated to a carrier protein, have been demonstrated to be highly effective. The best example is the *Haemophilus influenzae* type b conjugate vaccine, which has nearly eliminated infections in vast parts of the world (Pollard et al., 2009). However, manufacturing these conjugate vaccines requires complex synthetic chemistry for the attachment of the glycan to protein carriers. Additionally, the polysaccharides are either obtained from the target pathogen, which constitutes a major health hazard, or by laborious, chemical synthesis. Often, bacterial polysaccharides are too complex to be synthesized efficiently, making this process economically prohibitive. Finally, chemical attachment of the sugar to the carrier protein can result in large and heterogeneous conjugates, modifying the native structure, and thus decreasing the protective nature of the vaccine. Both live attenuated and killed bacterial vaccines have been tested against *B. pseudomallei*, but provide little to no protection against disease

and mortality in murine virulence models (Peacock et al., 2012). Additionally, since *B. pseudomallei* requires class III biosafety facilities, manufacturing glycoconjugates containing glycans from its native host is challenging and possibly hazardous. Recently, it has been demonstrated a protein chemically conjugated with the *B. pseudomallei* OPS and CPS was able to increase survival against *B. pseudomallei* infection (Scott et al., 2014). Additionally, protection has been demonstrated using *B. thailandensis* E555 as a live vaccine due to homology of CPS structures (Scott et al., 2013).

A novel method of synthesizing conjugate vaccines is through the exploitation of the protein glycosylation machineries of bacteria (Iwashkiw et al., 2012; Cuccui et al., 2013; Wetter et al., 2013). The cornerstone of bacterial glycosylation is the oligosaccharyltransferase (OTase) enzymes, which covalently attach glycan structures to either asparagine (N-linked) or serine/threonine (O-linked) residues (Nothhaft and Szymanski, 2010). OTases have high substrate promiscuity, and thus can transfer a wide range of glycan structures to acceptor proteins, in a process called OTase-dependent glycosylation. The best characterized N-glycosylation system in bacteria is from *Campylobacter jejuni* (Nothhaft et al., 2010). Briefly, a unique initiating glycosyltransferase attaches a nucleotide-activated monosaccharide-1P to the lipid carrier undecaprenyl phosphate (Und-P) in the cytoplasmic face of the inner membrane. Subsequently, a series of other glycosyltransferases attach additional monosaccharides to first residue, and when completed, the lipid-linked oligosaccharide (LLO) is translocated to the periplasmic face of the inner membrane by a flippase. Finally, PglB (N-OTase) covalently attaches the glycan to asparagine residues with the sequon D/E-X-N-Y-S/T (X,Y ≠P; Kowarik et al., 2006). Earlier studies demonstrated PglB has relaxed glycan specificity, allowing the transfer of a vast array of glycans, including O antigens, to acceptor proteins (Feldman et al., 2005). It was later shown that O-OTases share this feature (Faridmoayer et al., 2008). Thus, bacterial glycosylation systems can be exploited to synthesize novel glycoconjugates for vaccination and diagnostic purposes as previously demonstrated (Ihssen et al., 2010; Iwashkiw et al., 2012; Cuccui et al., 2013; Wetter et al., 2013; Wacker et al., 2014). Glycoconjugates produced by this method are significantly less expensive, less challenging to produce, and produce less hazardous waste than conventional chemical methods.

In this work, we demonstrate that the biosynthesis of the *B. pseudomallei* OPS II can be reconstituted in *Escherichia coli* (*E. coli*). Successful generation of the conjugate required the expression of the corresponding *B. pseudomallei* OPS II genes in an *E. coli* strain lacking both the *waaL* ligase and *wecA* initiating glycosyltransferase (SDB1). This glycoconjugate, when injected into mice, was able to develop a directed IgG immune response toward *B. pseudomallei*, and provide partial protection against infection in a murine model of melioidosis.

MATERIALS AND METHODS

BACTERIAL STRAINS, PLASMIDS, AND GROWTH CONDITIONS

Escherichia coli strains were grown on LB broth at 37°C. Trimethoprim (100 µg/ml), spectinomycin (80 µg/ml), and ampicillin

(100 µg/ml) were added to the media for plasmid selection as needed. The strains and plasmids used are listed in Table 1.

WESTERN BLOTTING

Glycan expression and glycosylation were analyzed by SDS-PAGE on 10% gels. The gels were electroblotted onto a nitrocellulose membrane via semi-dry membrane transfer and analyzed with antibodies α-His (Santa Cruz Biotechnology) and α-BPs OPSII glycan kindly provided by Dr. Joanne Prior (1:1,000). Membranes were visualized using the Odyssey Infrared Imaging System (Li-Cor Biosciences, USA).

CLONING AND EXPRESSION OF *Burkholderia pseudomallei* TYPE II OPS

To obtain the plasmid expressing the type II O-antigen polysaccharide of *Burkholderia pseudomallei* under an arabinose promoter we used the pCC1FOS-BPF16β_E10 vector kindly provided by Professor R. Titball (University of Exeter), which contains the LPS cluster of *B. pseudomallei* K96243, coordinates 3191324–3229257. The pCC1FOS-BPF16β_E10 vector was digested with *NheI*, *KpnI*, and *PciI* to get an 8673 bp fragment, corresponding to genes between *rmlD* and *wbiC*, and with *SnaBI* and *KpnI* to get a 9367 bp fragment that includes the genes between *wbiC* and *wbiI*. These two fragments containing the 15 genes required for *B. pseudomallei* type II OPS expression were inserted into pBAD24 digested with *NheI* and *SmaI*. Arabinose-dependent expression of the type II O-antigen was confirmed by Western blot.

CONSTRUCTION OF SDB1 *waaL* AND *wecA* DEFICIENT STRAIN

Construction of SDB1 strain was done using the P1 transduction protocol adapted from Thomason et al. (2007). The P1 bacteriophage was first grown on the strain (BW25113 *rfe::kan*) from the Keio collection library (Baba et al., 2006). This strain has a kanamycin-resistant cassette on the *wecA* gene as a donor. The resulting phage lysate was used to infect the recipient strain CLM24 ($\Delta waaL$). Recombinant strains were confirmed by PCR using the oligonucleotides *rfe* for comp (5'-GCAATGACCAAGACCAATGACG-3') and *rfe* rev comp (5'-GCTGCTGCGAGTAATATCCC-3'). The kanamycin cassette was removed using the FLP recombinase expressed from pFLP2.

PRODUCTION AND PURIFICATION OF GLYCOSYLATED AcrA

SDB1 strain transformed with *C. jejuni* PglB (pMAF10), AcrA (pIH18), and BPs type II O-antigen (pEQ3) was grown overnight at 37°C. Culture was reinoculated 1/33 into fresh LB media using a culture/flask ratio 1:10. After 2 h at 37°C with shaking at 200 rpm, the cultures were induced with 0.1 mM isopropyl 1-thio-β-D-galactopyranoside (IPTG; Sigma) and 0.2% (w/v) L-(+)-arabinose (MP Biomedicals). To increase the glycosylation yield in SDB1, we also added MnCl₂ (4 mM). Five hours after induction at 37°C, arabinose was added again to ensure PglB expression. Cells were harvested by centrifugation after an overnight induction period and the periplasmic extract containing the glycoproteins was extracted using a lysozyme treatment as described previously (Iwashkiw et al., 2012). For purification, the periplasmic fraction was equilibrated with 1/9 vol 10× loading buffer (0.1 M imidazole, 3 M NaCl, 0.2 M Tris-HCl, pH 8.0) and subjected to a Ni²⁺-affinity chromatography as described (Iwashkiw

Table 1 | List of strains and plasmids utilized.

Strain	Genotype or description	Reference
EPI300	F-mcrA Δ (mrr-hsdRMS-mcrBC) Φ 80dlac Δ M15 Δ lacX74 recA1 endA1 araD139 Δ (ara, leu)7697 galU galK λ -rpsL (Str ^R) nupG trfA dhfr	Epicentre
Top 10	F-mcrA Δ (mrr-hsdRMS-mcrBC) ϕ 80lac Δ M15 Δ lacX74 nupG recA1 araD139 Δ (ara-leu)7697 galE15 galK16 rpsL(Str ^R) endA1 λ ⁻	Invitrogen
CLM24	W3110, Δ waaL ligase	Feldman et al. (2005)
CLM37	W3110, Δ wecA	Linton et al. (2005)
BW25113 rfe::kan	F- Δ (araD-araB)567 Δ lacZ4787(::rrnB-3) LAM-rph-1 Δ (rhaD-rhaB)568 hsdR514	Baba et al. (2006)
SDB1	W3110, Δ waaL ligase, Δ wecA GalNAc transferase	This study
Plasmids		
pBAD24	Cloning and expression vector, Arabinose inducible, Amp ^R	Guzman et al. (1995)
pEXT21	Cloning and expression vector, IPTG inducible, Sp ^R	Dykxhoorn et al. (1996)
pMLBAD	Cloning and expression vector, Arabinose inducible, Tp ^R	Lefebvre and Valvano (2002)
pEQ3	<i>B. pseudomallei</i> type II OPS, Ap ^R	This study
pIH18	Soluble periplasmic <i>C. jejuni</i> acrA _{6xHis} cloned into pEXT21, Sp ^R	Hug et al. (2010)
pMAF10	<i>C. jejuni</i> pglB cloned into pMLBAD, Tp ^R	Feldman et al. (2005)
pFLP2	Source of Flp recombinase, Ap ^R	Hoang et al. (1998)
pCA24N-waaL	<i>E. coli</i> waaL cloned into pCA24N from ASKA library; Cm ^R	Kitagawa et al. (2005)
pCA21	<i>E. coli</i> wecA cloned into pEXT21, Sp ^R	Alaimo et al. (2006)
pJHCV32	HindIII cosmid clone in pVK102, 07+ Tcr	Valvano and Croisa (1989)
pCC1FOS-BPF16 β _E10	LPS cluster of <i>B. pseudomallei</i> K96243, coordinates 3191324-3229257	Titball Lab (unpublished)

et al., 2012). Purified protein was quantified by Bradford assay (BioRad).

SUGAR QUANTIFICATION OF GLYCOPROTEINS

The protocol was adapted from Dubois et al. (1956). In a small glass tube was mixed 10 μ l of sample, 90 μ l of ddH₂O, and 100 μ l of freshly made 5% phenol in ddH₂O. Then 1 ml of concentrated H₂SO₄ was briskly added into the mixture and immediately vortex for several seconds. An orange color with intensity proportional to concentration began to develop and reached a maximum about 2 h at 30°C. The samples were read against glucose standards at OD₅₀₀.

VACCINATION

BALB/c mice ($n = 5$ per group, 6-week-old female) were immunized with three doses of purified recombinant bioconjugate vaccine, carrier protein, or gamma-irradiated killed whole cells (3×10^4 *Burkholderia pseudomallei* K96234), via the intraperitoneal route (i.p.) over 6 weeks. The doses were administered with Imject Alum Adjuvant (Thermo Scientific), not used with whole killed cells or when noted. Sera samples were collected for antibody analysis, prior to immunization 2 weeks after vaccination and boost. The antibody titre of total IgG was analyzed by ELISA. Briefly, wells of microtiter plates were coated (18 h, 4°C) with gamma-irradiated whole *Burkholderia pseudomallei* cells at a 1/100 dilution in 100 μ l of coating buffer (0.05 M Na₂CO₃, 0.05 M NaHCO₃, pH 9.6) and were then blocked with 2% (w/v) BSA in PBS for 2 h at 37°C. Sera samples at a 1/200 dilution in 100 μ l

of antibody dilution buffer [2% (w/v) BSA, 0.1% (v/v) Tween 20] were incubated for 1 h at 37°C. HRP-conjugated goat anti-mouse IgG at a 1/8000 in antibody dilution buffer was added for 1 h at 37°C and then the reaction was visualized by the addition of 100 μ l chromogenic substrate (ultra-TMB) for 5 min. The reaction was stopped with 100 μ l H₃PO₄ and absorbance at 405 nm was measured using ELISA plate reader. Plates were washed five times with washing buffer [0.1% (v/v) Tween 20] after each step.

INTRANASAL CHALLENGE MODEL

The murine melioidosis infection model used was carried out under ABSL-3 containment practices. Briefly, female BALB/c mice were challenged via the i.n. route (50 μ l) with approximately 2×10^3 CFU (approximately 10–12 LD₅₀) of *B. pseudomallei* K96243. Mice were weighed prior to inoculation and monitored for 21 days post-infection. Mice were anesthetized, held vertically, and 50 ml of the inoculum was released into the nares for inhalation. Following challenge, the inoculum was back titrated on agar plates to confirm delivered dose. Using this model, control mice died or were euthanized according to predetermined humane end points 3–6 days post-challenge.

STATISTICS

Survival curves were generated by use of Kaplan–Meier estimators. The survival distributions of each treatment group vs. control protein carrier group were compared by unpaired *T* test or Mann–Whitney test using GraphPad Prism version 6.0.

ETHICS STATEMENT

This study was carried out in accordance with the Canadian animal care guidelines. The protocols were approved by the Animal Care and Use Committees of Defence Research and Development Canada. Mice were anesthetized by intraperitoneal injection of a sodium pentobarbital solution.

RESULTS

CLONING AND EXPRESSION OF THE *B. pseudomallei* K96243 O ANTIGEN POLYSACCHARIDE II (OPS II) LOCUS IN *E. coli*

Previous work identified a region consisting of 21 potential open reading frames, and further investigation identified a cluster of 15 genes required for the biosynthesis of *B. pseudomallei* K96243 OPS II (Figure 1A; DeShazer et al., 1998). A previous study demonstrated by NMR analysis that the structure of OPS II is a polymer of a disaccharide repeating structure composed of -3-)- β -D-glucopyranose-(1-3)- α -L-6-deoxy-talopyranose-(1-, with variable O-methyl and O-acetyl modifications (Figure 1B; Perry et al., 1995). In order to recombinantly express the *B. pseudomallei* OPS II in *E. coli*, the 15 essential genes were subcloned (genes *rmlB* to *wbiI*) from the plasmid pCC1FOS-BPF16 β _E10 by restriction digest into the arabinose inducible expression vector pBAD24, generating pEQ3 (Figure 1A). Expression of the *B. pseudomallei* OPS II in *E. coli* CLM37 was visualized by Western blot as a typical ladder of immunoreactive bands, confirming the production of the carbohydrate structure (Figure 1C).

GENERATION OF AN *E. coli* STRAIN OPTIMIZED FOR OPS II PRODUCTION AND PROTEIN GLYCOSYLATION

We attempted to generate a N-linked glycoprotein with the OPS II by exploiting the *C. jejuni* N-glycosylation system as previously described (Ihssen et al., 2010; Iwashkiw et al., 2012; Cuccui et al., 2013; Wetter et al., 2013). In earlier work, N-glycosylated AcrA was synthesized in *E. coli* by co-expression of *C. jejuni* PglB and AcrA with an appropriate carbohydrate structure. We therefore expressed PglB (pMAF10), AcrA (pIH18), and the *B. pseudomallei*

OPS II antigen (pEQ3) in both a traditional expression (EPI300) and *wecA*- (CLM37) strains and tested for glycosylation by Western blot. We were unable to detect any evidence of glycosylation of purified AcrA (data not shown).

One issue with exploiting O antigens using protein glycosylation may be the precursor can also be used by the WaaL ligase in *E. coli*, thus siphoning off the substrate, and decreasing the glycosylation efficiency (Figure 2). Additionally, *E. coli* strains express the initiating glycosyl transferase (*wecA*), which transfers a GlcNAc onto the undecaprenyl-diphosphate (Und-PP) carrier. This would interfere with the synthesis of the glycan of interest onto the same lipid if the first sugar in the structure is not a GlcNAc, as in the case of the OPS II. We hypothesized that deletion of WaaL and WecA would result in an increased efficiency of protein glycosylation (Figure 2C).

We therefore constructed the *E. coli* *wecA*⁻ *waaL*⁻ mutant strain SDB1. Using the KEIO strain collection (Baba et al., 2006), the *wecA* mutation was transduced into CLM24, an *E. coli* *waaL* mutant (Feldman et al., 2005), creating SDB1. To functionally confirm the double mutation, we analyzed the LPS produced by SDB1 transformed with plasmid pJHCV32 (Figure 3). The plasmid pJHCV32 drives the constitutive expression of the *E. coli* O7 antigen, but relies on the chromosomal copy of the glycosyltransferase WecA (Valvano and Crosa, 1989). Expression *in trans* of either WecA or WaaL individually in this background did not result in the production of a smooth LPS containing the O7 antigen (lanes 1–8). However, when both genes were co-expressed in SDB1, we observed the characteristic polymerization of O antigen previously observed for the *E. coli* O7 LPS (lanes 9 and 10), confirming the creation of the double mutation.

IN VIVO SYNTHESIS AND PURIFICATION OF AN N-LINKED GLYCOCONJUGATE WITH THE *Burkholderia* OPSII GLYCAN

To create an N-linked glycoconjugate, we transformed the *E. coli* strain SDB1 with the pEQ3 (OPS II), pMAF10 (PglB), and pIH18 (AcrA). Cultures of the transformed strain were grown

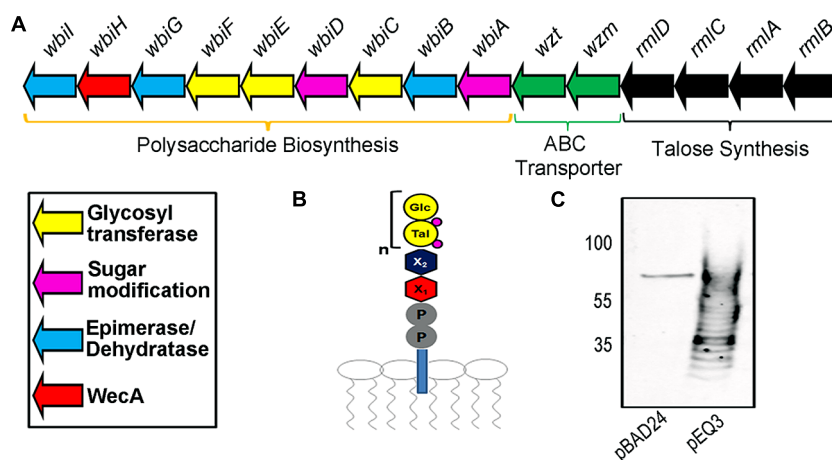
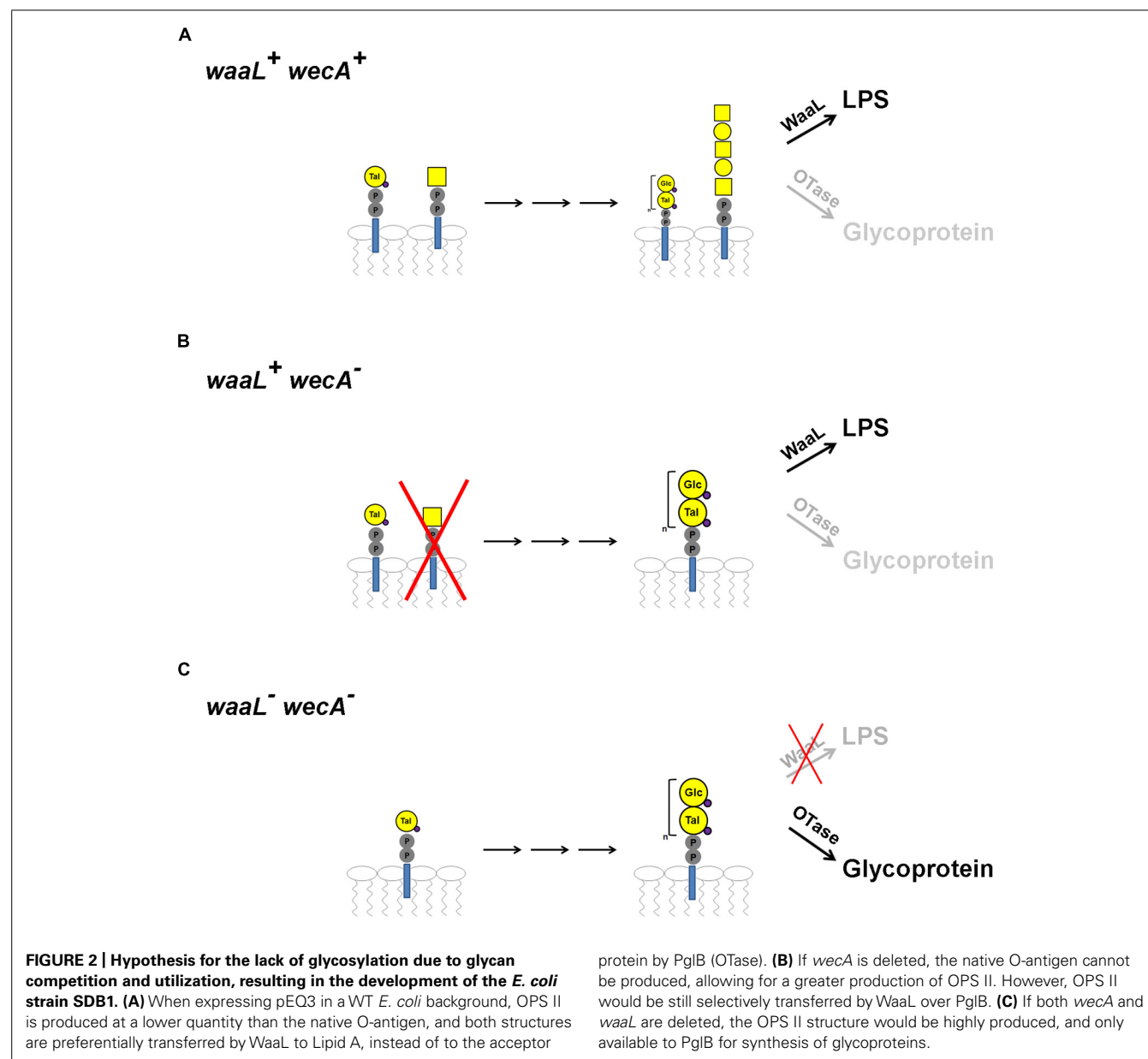


FIGURE 1 | Description of *Burkholderia pseudomallei* O-polysaccharide II (OPSII) cluster. (A) Representation of the required 15 genes for the synthesis of OPS II and predicted functions. **(B)** Expected glycan intermediate structure

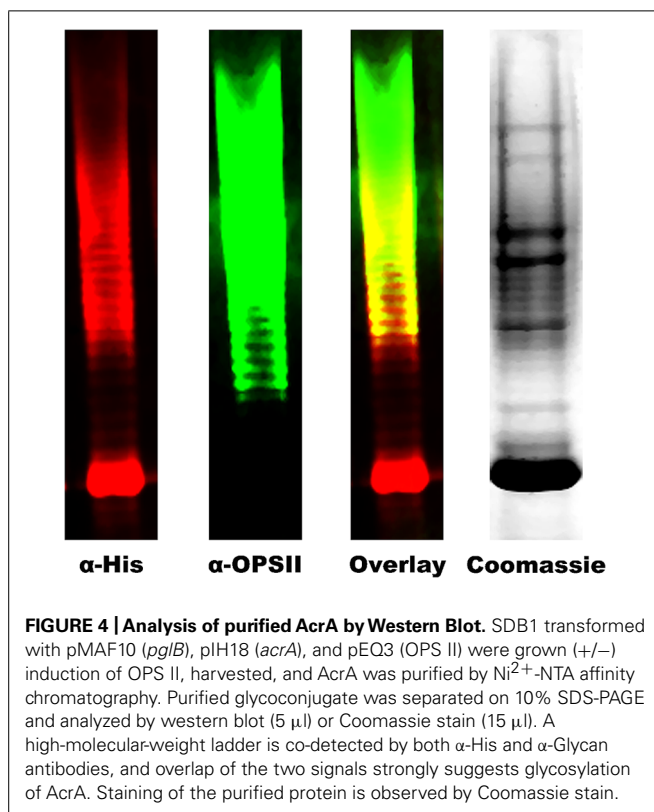
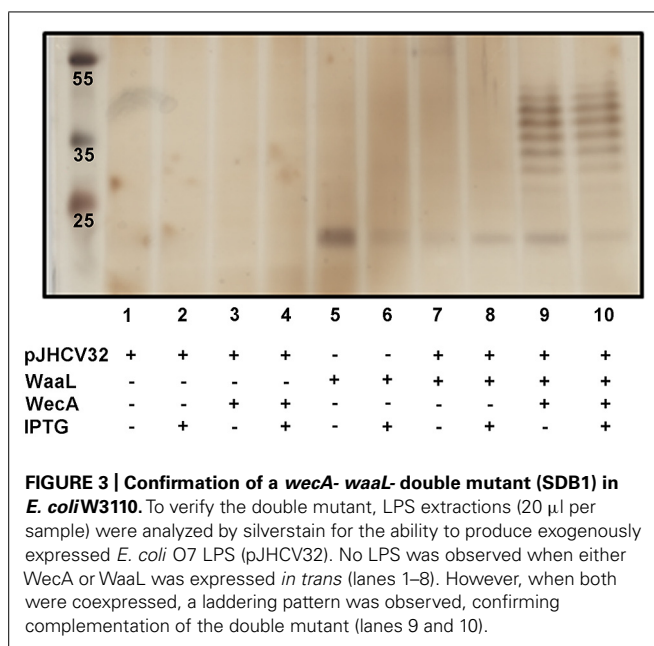
attached to Undecaprenyl pyrophosphate. **(C)** Western blot of 10 μ l of whole-cell extracts utilizing an anti-Glycan antibody reveals expression of OPS II (subcloned in pEQ3) in *E. coli* produces a polymer in whole-cell extracts.



and induced as required, and AcrA was purified from periplasmic extracts by Ni^{2+} affinity chromatography. To determine if AcrA was glycosylated, we analyzed the purified protein by either Western blot with antibodies specific to either AcrA or OPS II, or Coomassie stain, and when visualized together, we observed an overlap of the signal, suggesting glycosylation of AcrA with the OPSII glycan (Figure 4).

To confirm AcrA was glycosylated with the *B. pseudomallei* OPS II carbohydrate, we employed mass spectrometry (MS) techniques. The purified glycoprotein was tryptically digested in-solution, and the resulting peptides were examined by LC-ESI-Q-TOF MS and MS/MS. Manual analysis of the MS data (MassLynx; Waters Corporation) revealed a peak with an m/z 1152.06³⁺, and further inspection of this peak by MS/MS revealed a glycopeptide that corresponded to the previously identified second

glycosylation site of AcrA (AVFDNNSTLLPGAFATITSEGFQK; m/z 2754.1) with the addition of an m/z 700.2 modification (Figure 5). *De novo* peak annotation identified the modification to be a tetramer of 188–162–188–162. The mass of 188 Da is consistent with an *O*-acetyl deoxyhexose residue, and the 162 Da is consistent with a hexose residue. We were also able to identify in the low-molecular region both an individual *O*-acetyl deoxyhexose (189.0 Da), and a subunit of the dimer with a mass of 351.1 Da. Our MS characterization of the *B. pseudomallei* OPS II glycan is consistent with the previously published data identifying it to be a polymer of dimers of *O*-acetylated deoxytalose and glucose (Perry et al., 1995). These data combined with the immunoreactivity of our glycoconjugate to the *B. pseudomallei* OPS II antibody confirm that we were able to synthesize and glycosylate AcrA with the correct glycan structure in *E. coli* SDB1.



MICE INJECTED WITH PURIFIED *N*-LINKED BIOGLYCOCONJUGATE DEVELOPED A PARTIALLY PROTECTIVE IgG IMMUNE RESPONSE TOWARD *B. pseudomallei* WHOLE CELLS

To evaluate the potential use of the glycoprotein as conjugate vaccine, the purified AcrA containing OPS II was injected intraperitoneally into mice to measure the immune response compared to whole-cell-killed *B. pseudomallei*. Groups of five

mice were injected with PBS, unglycosylated AcrA as control, glycoconjugate in different quantities, or whole-cell-killed cells. The IgG immune response was tested by ELISA against whole-cell extracts of *B. pseudomallei* (Figure 6). All test groups were compared to the PBS control, and showed no initial immune response toward *B. pseudomallei* in the pre-injection sera. The AcrA-injected group had a slight increase in IgG response, but did not increase after additional boosts. A significant increase in IgG response was observed in each of the glycosylated test groups after the primary vaccination, with varying degrees of improvement in immune response after a second and third boost. The best immune response was observed in the mice injected with whole-cell lysates of *B. pseudomallei* had a significantly stronger immune response as compared to the glycoconjugate sera, but this was expected as whole cells were used as antigen for the ELISA.

We next tested the immunized mice for a preliminary evaluation of the efficacy of the glycoconjugate. We employed an intranasal murine melioidosis model against *B. pseudomallei* infection with a dose of $12 \times \text{LD}_{50}$ (Figure 7). Mice vaccinated with only protein carrier died or were euthanized according to pre-determined humane end points after 6 days. For the PBS-injected control group, 80% of the mice died or were euthanized after 6 days, and one mouse survived until day 13 of the challenge. All of the mice vaccinated with the glycoconjugate showed a significant increase in survival time as compared to the control protein carrier group. However, contrary to the ELISA results that showed the best IgG immune response in mice vaccinated with 2 μ g of glycosylated AcrA, 40% of the mice survived until day 12, with the remaining being sacrificed on day 14. Mice injected with 1 μ g of glycoprotein without any adjuvant saw survival until day 18, while one mouse vaccinated with 1 μ g survived until day 22. The difference in mean time to death was not statistically significant between the groups receiving the various glycoprotein preparations. In comparing our glycoconjugate to whole-cell-killed bacteria as vaccine candidates, we observed highly similar survival of the mice, with all mice succumbing to infection by day 18 of the challenge. Overall, these results demonstrate that the *N*-glycoconjugate containing the *B. pseudomallei* OPS II is capable of providing partial immune protection against a $12 \times \text{LD}_{50}$ dose, and it is comparable to whole-cell-killed bacteria in protection against infection.

DISCUSSION

Due to a combination of factors including the increasing number of reported cases of *B. pseudomallei* infections, the risk posed by the bacterium as a potential biological warfare agent, and an absence of an effective vaccine, we explored the possibility that by exploiting the *N*-linked glycosylation system of *C. jejuni*, we could produce a glycoconjugate vaccine containing the OPS II of *B. pseudomallei*. This strategy was only demonstrated in a few cases (Iwashkiw et al., 2012; Cuccui et al., 2013; Wetter et al., 2013). Since *B. pseudomallei* is a biosafety class III agent we were unable to directly exploit the native OPS II by expressing the *N*-glycosylation system in the host as previously shown (Iwashkiw et al., 2012). Instead, we utilized previous knowledge of the genetic loci responsible for the biosynthesis of OPS II (DeShazer et al., 1998), and subcloned the key 15 genes into an *E. coli* expression vector. We observed high levels of expression of the OPS II in *E. coli* strains

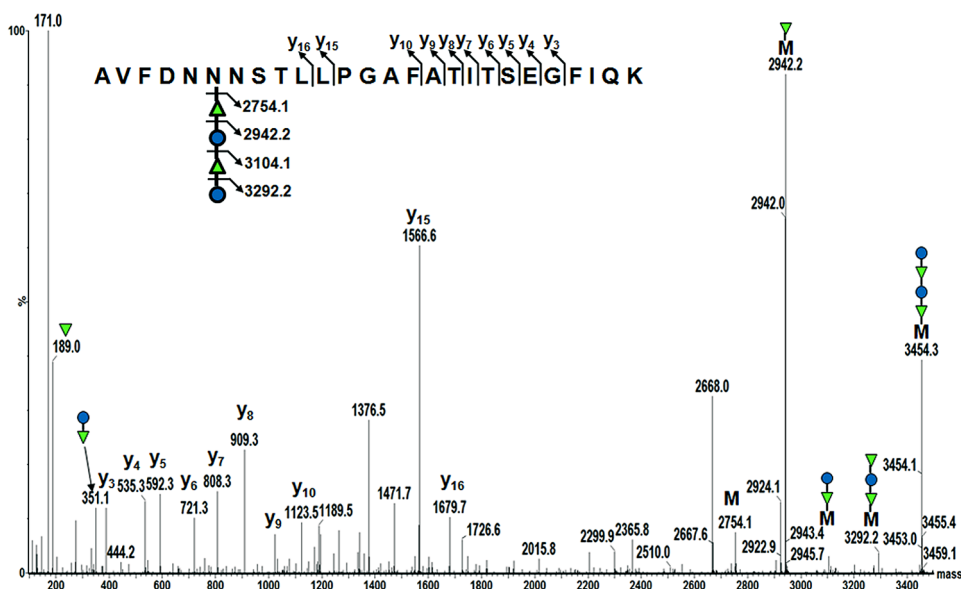


FIGURE 5 | Mass spectrometry identification of the *B. pseudomallei* OPS II glycan attached to AcrA. MS analysis of tryptically digested glycosylated AcrA revealed a peak of m/z 1152.06³⁺. MS/MS of this peak showed a previously characterized glycosylation site of AcrA (AVFDNNSTLLPGAFATITSEGFQK; 2754.1 Da) with a modification of

700.2 Da. Analysis of the modification revealed a tetrameric glycan, with a structure of 188–162–188–162. This structure is consistent with the previously determined structure of *B. pseudomallei* OPS II being a polymer of dimers of *O*-acetylated deoxytalose (188 Da) and glucose (162 Da).

by Western blot, and attempted to create the glycoconjugate in a basic expression and *wecA*-*E. coli* strains as previously described (Ihsen et al., 2010; Cuccui et al., 2013; Wetter et al., 2013). We did not observe any evidence of glycosylation, and hypothesized that the OPS II was being utilized exclusively to modify the LPS. Therefore, we engineered an *E. coli* strain (SDB1) lacking both the *waaL* ligase, and *wecA*. Construction of the SDB1 strain was confirmed by expressing either or both *WecA* and *WaaL* with a plasmid encoding the *E. coli* O7 LPS cluster that lacks *WecA* homolog. Analysis of LPS extractions by silverstain showed that the O7 antigen structure was only transferred to lipid A in the presence of both enzymes. Our engineered strain in theory should be able to produce the OPS II-AcrA glycoconjugate with high efficiency due to no other competition for either the undecaprenyl-phosphate lipid carrier by *WecA* or the OPS II-Und-PP substrate from *WaaL*.

We showed that SDB1 produced the desired glycoconjugate when OPS II (pEQ3), PglB (pMAF10), and AcrA (pIH18) were co-expressed. The generation of the conjugate was shown via Western blot and MS. Interestingly, glycosylation of AcrA required the addition of $MnCl_2$ to the media. Although Mn^{2+} is required for PglB activity and was observed in the active site of the crystal structure (Lizak et al., 2011), we did not have to add Mn^{2+} to obtain glycosylated proteins in previous experiments. The direct relationship between its addition and glycosylation efficiency is unclear. The MS examination of the purified glycoconjugate revealed the presence of a tetrameric glycan moiety corresponding to two repeats of *O*-acetylated deoxyhexose and hexose, in agreement with previously published characterization of the structure (Perry et al., 1995). Interestingly, previous work has shown that the *C. jejuni* OTase PglB can only transfer glycans with a reducing monomer

with an *N*-acetyl group, whereas the *B. pseudomallei* OPS II structure has been shown to possess an *O*-acetyl modification. This finding expands our knowledge on the substrate specificity of PglB. We did not observe any larger glycan structures that were detected by Western blot, but this could be due to limitations of our MS instruments. Most of the Wzy-independent glycans require an adapter composed of two monosaccharides linking the lipid carrier to the polymeric structure (Whitfield, 2006; Greenfield and Whitfield, 2012). The finding that the *O*-acetylated deoxytalose appears to be directly linked to the protein indicates that a linker glycan (proposed in Figure 1A as X1 and X2) is not present in the OPS II structure. Our experiments demonstrate that in the genetically engineered strain SDB1, we were able to produce a glycoconjugate with the *B. pseudomallei* OPS II carbohydrate.

We carried out preliminary experiments to determine if our glycoconjugate could be utilized as a vaccine against *B. pseudomallei*. We injected different quantities of the glycoconjugate into mice. We observed virtually no response toward *B. pseudomallei* for the mice injected with the protein carrier alone, whereas a significantly stronger response from the mice injected with all groups of the glycoconjugate. Interestingly, an intermediate response was observed in the 1 μ g glycoconjugate groups, regardless of the addition of an adjuvant. We then challenged the vaccinated mice with *B. pseudomallei* K96243, and after 6 days post challenge, none of the carrier control injected mice survived, whereas survival was observed each of the glycoconjugate groups, with the longest survival in the 1 μ g group, irrespective of the addition of an adjuvant. Why lower levels of antibody production resulted in better protection remains unknown, although these differences in protection were not statistically significant between groups receiving

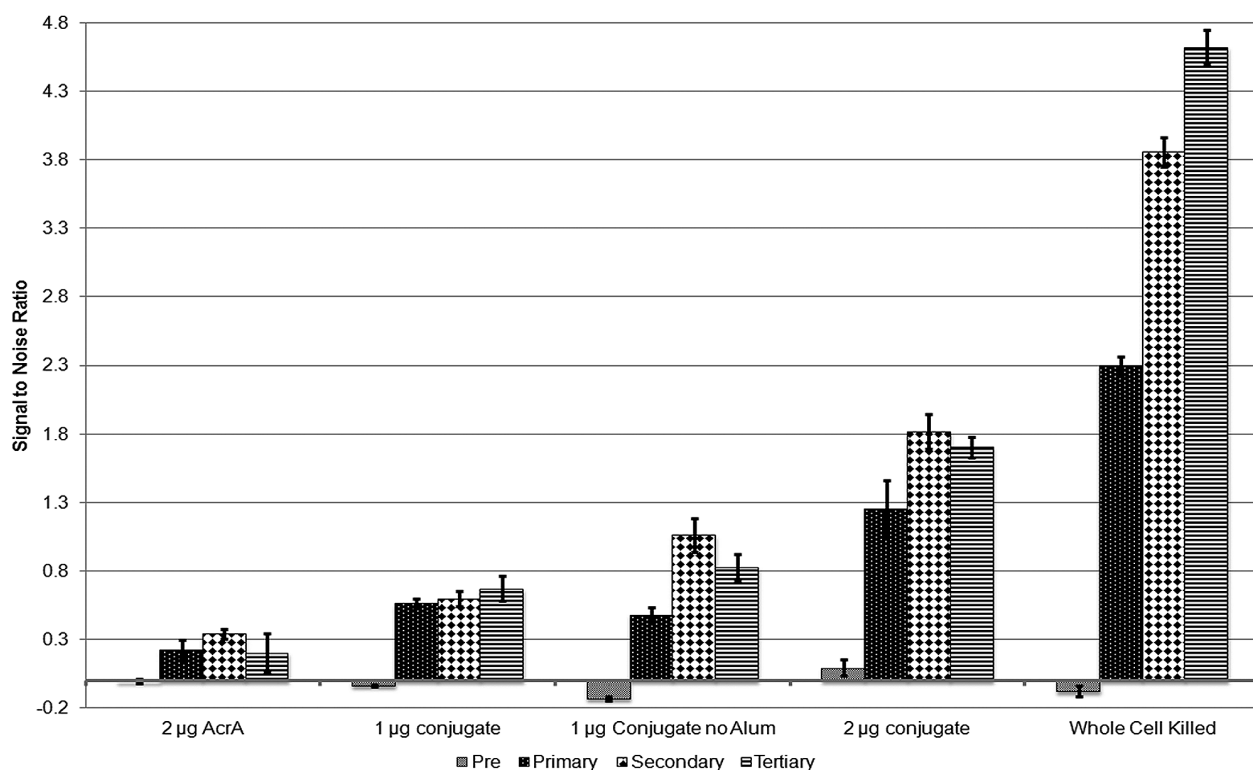


FIGURE 6 | ELISA of the IgG immune response of immunized mice toward whole-cell extracts of *B. pseudomallei*. All data were normalized to the PBS-injected control mice, and no response was observed in all groups prior to immunization. A low level of response

was observed at a consistent level for the unglycosylated AcrA control, whereas all test groups injected with glycosylated AcrA had a significant IgG response. The results are the median of five mice in each test group.

the glycoprotein. It is possible that the carrier protein, AcrA, due to its high immunogenic nature, acts as an adjuvant itself. This could also possibly explain why both of the 1 µg groups while having a lower detected IgG immune response compared to the 2 µg group have a longer survival period. Our results are consistent with these previous studies with the non-protected mice succumbing to infection after ~1 week (Nelson et al., 2004; Su et al., 2010; Nieves et al., 2011). Interestingly, our initial studies with the glycoconjugate gave similar protection levels to whole-cell-killed *B. pseudomallei*. Further optimization of our vaccine candidate is currently undergoing. This includes testing different amounts of conjugate, and replacing the acceptor protein from AcrA of *C. jejuni* to a *B. pseudomallei* protein, which may enhance the immunogenicity of the conjugate.

Several other studies have been published attempting to develop a vaccine against *B. pseudomallei* (reviewed in Silva and Dow, 2013). Many of these vaccine candidates have dealt with either attenuated strains, whole-cell-killed bacteria, or purified proteins directly from *B. pseudomallei*, which requires class III biosafety facilities, and would lead to higher significant problems for commercialization of the product. Other groups attempted to recombinantly express and purify *B. pseudomallei* proteins in *E. coli*, with limited success. However, our work has demonstrated that the OPS II carbohydrate of *B. pseudomallei* can be functionally expressed in *E. coli*, and be utilized by PglB to

create a glycoconjugate that is partially protective against infection. Glycoengineered therapeutics are simple to produce, cost effective, and have been demonstrated to provide long-term protection against several pathogens. Additionally, previous work has used a similar glycoconjugate with the *Y. enterocolitica* O9 O-antigen as a diagnostic tool (Iwashkiw et al., 2012). Conjugation of the glycoconjugate to magnetic nanobeads has shown significant promise in detection of disease in cattle and human sera samples (Ciocchini et al., 2013, 2014). A similar system may have future potential for diagnosing individuals infected with *B. pseudomallei*.

In summary, we have demonstrated that the OPS II glycan of *B. pseudomallei* can be functionally expressed in *E. coli*. Additionally, this glycan was transferred to the carrier protein AcrA by the OTase PglB, both from *C. jejuni*, to generate a glycoconjugate. We also described a novel *E. coli* strain SDB1 which lacks *wecA* and *waaL*, resulting in a higher efficiency of glycosylation as compared to previously used strains. Mice injected with this glycoprotein were able to develop a long-term IgG immune response, and showed significantly longer survival when challenged with *B. pseudomallei* as compared to the naive controls. This new biologically engineered strain may be used for the future creation of commercial bioglycoconjugate therapeutics, and glycoconjugate may have future potential for diagnostic applications or vaccination against *B. pseudomallei* infections.

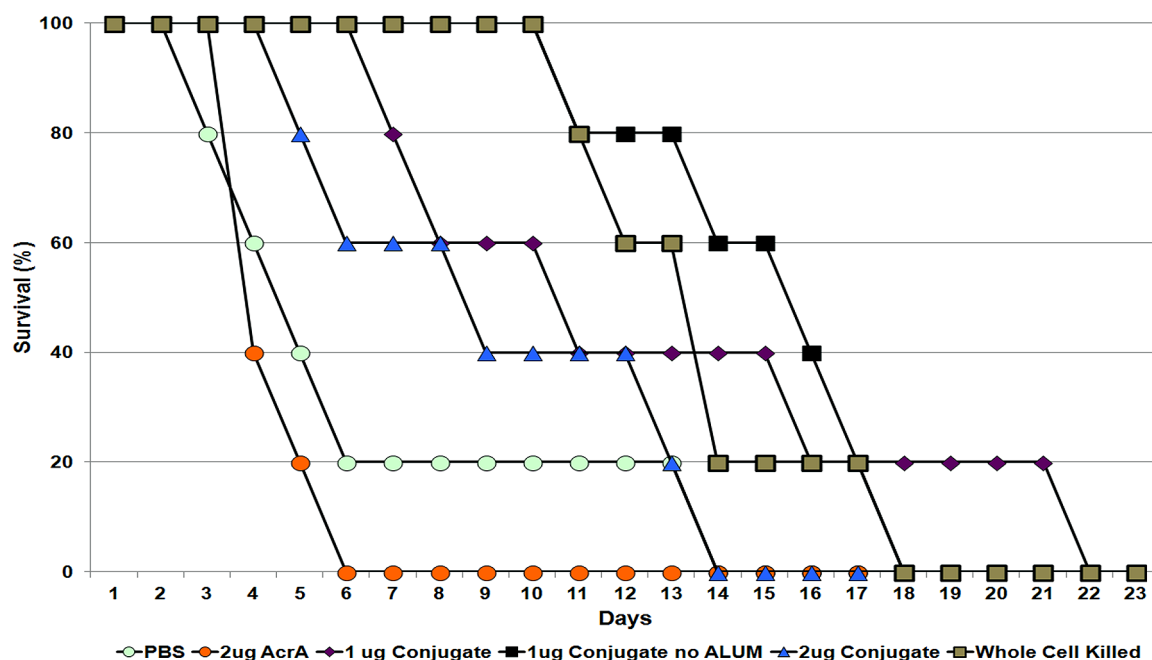


FIGURE 7 | Murine survival of different test groups to a 12× LD₅₀ i.n. challenge of *B. pseudomallei*. Mice vaccinated with either PBS or unglycosylated AcrA controls had a significantly lower survival period as

compared to the mice injected with OPS II glycosylated AcrA. Interestingly, mice vaccinated with 1 μg glycoconjugate (+/– adjuvant) had a higher survivorship percentage as compared to the 2 μg vaccinated group.

ACKNOWLEDGMENTS

This work was supported by grants from the Natural Sciences and Engineering Research Council (NSERC) to Mario F. Feldman and by DRDC ARP funds. Mario F. Feldman is an Alberta Heritage Foundation for Medical Research (AHFMR) Scholar and a Canadian Institutes of Health Research (CIHR) new investigator. Jeremy A. Iwashkiw is an Alberta Innovates Health Solutions (AIHS) scholar. The authors acknowledge the technical assistance of Scott Jager and Melissa Crichton.

REFERENCES

- Alaimo, C., Catrein, I., Morf, L., Marolda, C. L., Callewaert, N., Valvano, M. A., et al. (2006). Two distinct but interchangeable mechanisms for flipping of lipid-linked oligosaccharides. *EMBO J.* 25, 967–976. doi: 10.1038/sj.emboj.7601024
- Baba, T., Ara, T., Hasegawa, M., Takai, Y., Okumura, Y., Baba, M., et al. (2006). Construction of *Escherichia coli* K-12 in-frame, single-gene knockout mutants: the Keio collection. *Mol. Syst. Biol.* 2, 1–11. doi: 10.1038/msb4100050
- Cheng, A. C., and Currie, B. J. (2005). Melioidosis: epidemiology, pathophysiology, and management. *Clin. Microbiol. Rev.* 18, 383–416. doi: 10.1128/CMR.18.2.383-416.2005
- Ciocchini, A. E., Rey Serantes, D. A., Melli, L. J., Iwashkiw, J. A., Deodato, B., Wallach, J., et al. (2013). Development and validation of a novel diagnostic test for human brucellosis using a glyco-engineered antigen coupled to magnetic beads. *PLoS Negl. Trop. Dis.* 7:e2048. doi: 10.1371/journal.pntd.0002048
- Ciocchini, A. E., Serantes, D. A., Melli, L. J., Guidolin, L. S., Iwashkiw, J. A., Elena, S., et al. (2014). A bacterial engineered glycoprotein as a novel antigen for diagnosis of bovine brucellosis. *Vet. Microbiol.* doi: 10.1016/j.vetmic.2014.04.014 [Epub ahead of print].
- Cuccui, J., Thomas, R. M., Moule, M. G., D'Elia, R. V., Laws, T. R., Mills, D. C., et al. (2013). Exploitation of bacterial N-linked glycosylation to develop a novel recombinant glycoconjugate vaccine against *Francisella tularensis*. *Open Biol.* 3, 130002. doi: 10.1098/rsob.130002
- DeShazer, D., Brett, P. J., and Woods, D. E. (1998). The type II O-antigenic polysaccharide moiety of *Burkholderia pseudomallei* lipopolysaccharide is required for serum resistance and virulence. *Mol. Microbiol.* 30, 1081–1100. doi: 10.1046/j.1365-2958.1998.01139.x
- Dubois, M., Gilles, K. A., Hamilton, J. K., Rebers, P. A., and Smith, F. (1956). Colorimetric method for the determination of sugars and related substances. *Anal. Chem.* 28, 350–356. doi: 10.1021/ac60111a017
- Dykxhoorn, D. M., St Pierre, R., and Linn, T. (1996). A set of compatible tac promoter expression vectors. *Gene* 177, 133–136. doi: 10.1016/0378-1119(96)00289-2
- Faridmoayer, A., Fentabil, M. A., Haurat, M. F., Yi, W., Woodward, R., Wang, P. G., et al. (2008). Extreme substrate promiscuity of the *Neisseria* oligosaccharyl transferase involved in protein O-glycosylation. *J. Biol. Chem.* 283, 34596–34604. doi: 10.1074/jbc.M807113200
- Feldman, M. F., Wacker, M., Hernandez, M., Hitchen, P. G., Marolda, C. L., Kowarik, M., et al. (2005). Engineering N-linked protein glycosylation with diverse O antigen lipopolysaccharide structures in *Escherichia coli*. *Proc. Natl. Acad. Sci. U.S.A.* 102, 3016–3021. doi: 10.1073/pnas.0500044102
- Galen, J. E., and Curtiss, R. III. (2013). The delicate balance in genetically engineering live vaccines. *Vaccine* doi: 10.1016/j.vaccine.2013.12.026 [Epub ahead of print].
- Greenfield, L. K., and Whitfield, C. (2012). Synthesis of lipopolysaccharide O-antigens by ABC transporter-dependent pathways. *Carbohydr. Res.* 356, 12–24. doi: 10.1016/j.carres.2012.02.027
- Guzman, L. M., Belin, D., Carson, M. J., and Beckwith, J. (1995). Tight regulation, modulation, and high-level expression by vectors containing the arabinose PBAD promoter. *J. Bacteriol.* 177, 4121–4130.
- Hoang, T. T., Karkhoff-Schweizer, R. R., Kutchma, A. J., and Schweizer, H. P. (1998). A broad-host-range Flp-FRT recombination system for site-specific excision of chromosomally-located DNA sequences: application for isolation of unmarked *Pseudomonas aeruginosa* mutants. *Gene* 212, 77–86. doi: 10.1016/S0378-1119(98)00130-9
- Hug, I., Couturier, M. R., Rooker, M. M., Taylor, D. E., Stein, M., and Feldman, M. F. (2010). *Helicobacter pylori* lipopolysaccharide is synthesized via a novel pathway with an evolutionary connection to protein N-glycosylation. *PLoS Pathog.* 6:e1000819. doi: 10.1371/journal.ppat.1000819

- Ihssen, J., Kowarik, M., Diletto, S., Tanner, C., Wacker, M., and Thony-Meyer, L. (2010). Production of glycoprotein vaccines in *Escherichia coli*. *Microb. Cell Fact.* 9, 61. doi: 10.1186/1475-2859-9-61
- Iwashkiw, J. A., Fentabil, M. A., Faridmoayer, A., Mills, D. C., Peppler, M., Czibener, C., et al. (2012). Exploiting the *Campylobacter jejuni* protein glycosylation system for glycoengineering vaccines and diagnostic tools directed against brucellosis. *Microb. Cell Fact.* 11, 13. doi: 10.1186/1475-2859-11-13
- Kitagawa, M., Ara, T., Arifuzzaman, M., Ioka-Nakamichi, T., Inamoto, E., Toyonaga, H., et al. (2005). Complete set of ORF clones of *Escherichia coli* ASKA library (a complete set of *E. coli* K-12 ORF archive): unique resources for biological research. *DNA Res.* 12, 291–299. doi: 10.1093/dnares/dsi012
- Knirel, Y. A., Paramonov, N. A., Shashkov, A. S., Kochetkov, N. K., Yarullin, R. G., Farber, S. M., et al. (1992). Structure of the polysaccharide chains of *Pseudomonas pseudomallei* lipopolysaccharides. *Carbohydr. Res.* 233, 185–193. doi: 10.1016/S0008-6215(00)90930-3
- Kowarik, M., Young, N. M., Numao, S., Schulz, B. L., Hug, I., Callewaert, N., et al. (2006). Definition of the bacterial N-glycosylation site consensus sequence. *EMBO J.* 25, 1957–1966. doi: 10.1038/sj.emboj.7601087
- Lefebvre, M. D., and Valvano, M. A. (2002). Construction and evaluation of plasmid vectors optimized for constitutive and regulated gene expression in *Burkholderia cepacia* complex isolates. *Appl. Environ. Microbiol.* 68, 5956–5964. doi: 10.1128/AEM.68.12.5956-5964.2002
- Linton, D., Dorrell, N., Hitchen, P. G., Amber, S., Karlyshev, A. V., Morris, H. R., et al. (2005). Functional analysis of the *Campylobacter jejuni* N-linked protein glycosylation pathway. *Mol. Microbiol.* 55, 1695–1703. doi: 10.1111/j.1365-2958.2005.04519.x
- Lizak, C., Gerber, S., Numao, S., Aebi, M., and Locher, K. P. (2011). X-ray structure of a bacterial oligosaccharyltransferase. *Nature* 474, 350–355. doi: 10.1038/nature10151
- Lockhart, S. (2003). Conjugate vaccines. *Expert Rev. Vaccines* 2, 633–648. doi: 10.1586/14760584.2.5.633
- Nandi, T., and Tan, P. (2013). Less is more: *Burkholderia pseudomallei* and chronic melioidosis. *MBio* 4, e00709–00713. doi: 10.1128/mBio.00709-713
- Nelson, M., Prior, J. L., Lever, M. S., Jones, H. E., Atkins, T. P., and Titball, R. W. (2004). Evaluation of lipopolysaccharide and capsular polysaccharide as subunit vaccines against experimental melioidosis. *J. Med. Microbiol.* 53, 1177–1182. doi: 10.1099/jmm.0.45766-0
- Nieves, W., Asakrah, S., Qazi, O., Brown, K. A., Kurtz, J., Aucoin, D. P., et al. (2011). A naturally derived outer-membrane vesicle vaccine protects against lethal pulmonary *Burkholderia pseudomallei* infection. *Vaccine* 29, 8381–8389. doi: 10.1016/j.vaccine.2011.08.058
- Nothaft, H., Liu, X., McNally, D. J., and Szymanski, C. M. (2010). N-linked protein glycosylation in a bacterial system. *Methods Mol. Biol.* 600, 227–243. doi: 10.1007/978-1-60761-454-8_16
- Nothaft, H., and Szymanski, C. M. (2010). Protein glycosylation in bacteria: sweeter than ever. *Nat. Rev. Microbiol.* 8, 765–778. doi: 10.1038/nrmicro2383
- Peacock, S. J., Limmathurotsakul, D., Lubell, Y., Koh, G. C., White, L. J., Day, N. P., et al. (2012). Melioidosis vaccines: a systematic review and appraisal of the potential to exploit biodefense vaccines for public health purposes. *PLoS Negl. Trop. Dis.* 6:e1488. doi: 10.1371/journal.pntd.0001488
- Perry, M. B., Maclean, L. L., Schollaardt, T., Bryan, L. E., and Ho, M. (1995). Structural characterization of the lipopolysaccharide O antigens of *Burkholderia pseudomallei*. *Infect. Immun.* 63, 3348–3352.
- Pollard, A. J., Perrett, K. P., and Beverley, P. C. (2009). Maintaining protection against invasive bacteria with protein-polysaccharide conjugate vaccines. *Nat. Rev. Immunol.* 9, 213–220. doi: 10.1038/nri2494
- Scott, A. E., Burtnick, M. N., Stokes, M. G., Whelan, A. O., Williamson, E. D., Atkins, T. P., et al. (2014). *Burkholderia pseudomallei* capsular polysaccharide conjugates provide protection against acute melioidosis. *Infect. Immun.* 82, 3206–3213. doi: 10.1128/IAI.01847-14
- Scott, A. E., Laws, T. R., D'Elia, R. V., Stokes, M. G., Nandi, T., Williamson, E. D., et al. (2013). Protection against experimental melioidosis following immunization with live *Burkholderia thailandensis* expressing a manno-heptose capsule. *Clin. Vaccine Immunol.* 20, 1041–1047. doi: 10.1128/CI.00113-13
- Silva, E. B., and Dow, S. W. (2013). Development of *Burkholderia mallei* and pseudo-mallei vaccines. *Front. Cell Infect. Microbiol.* 3:10. doi: 10.3389/fcimb.2013.00010
- Su, Y. C., Wan, K. L., Mohamed, R., and Nathan, S. (2010). Immunization with the recombinant *Burkholderia pseudomallei* outer membrane protein Omp85 induces protective immunity in mice. *Vaccine* 28, 5005–5011. doi: 10.1016/j.vaccine.2010.05.022
- Thomason, L. C., Costantino, N., and Court, D. L. (2007). *E. coli* genome manipulation by P1 transduction. *Curr. Protoc. Mol. Biol.* Chap. 1, Unit 1.17. doi: 10.1002/0471142727.mb0117s79
- Valvano, M. A., and Crosa, J. H. (1989). Molecular cloning and expression in *Escherichia coli* K-12 of chromosomal genes determining the O7 lipopolysaccharide antigen of a human invasive strain of *E. coli* O7:K1. *Infect. Immun.* 57, 937–943.
- Wacker, M., Wang, L., Kowarik, M., Dowd, M., Lipowsky, G., Faridmoayer, A., et al. (2014). Prevention of *Staphylococcus aureus* infections by glycoprotein vaccines synthesized in *Escherichia coli*. *J. Infect. Dis.* 209, 1551–1561. doi: 10.1093/infdis/jit800
- Wetter, M., Kowarik, M., Steffen, M., Carranza, P., Corradin, G., and Wacker, M. (2013). Engineering, conjugation, and immunogenicity assessment of *Escherichia coli* O121 O antigen for its potential use as a typhoid vaccine component. *Glycoconj. J.* 30, 511–522. doi: 10.1007/s10719-012-9451-9
- Whitfield, C. (2006). Biosynthesis and assembly of capsular polysaccharides in *Escherichia coli*. *Annu. Rev. Biochem.* 75, 39–68. doi: 10.1146/annurev.biochem.75.103004.142545

Conflict of Interest Statement: The authors declare that the research was conducted in the absence of any commercial or financial relationships that could be construed as a potential conflict of interest.

Received: 03 June 2014; paper pending published: 29 June 2014; accepted: 08 July 2014; published online: 29 July 2014.

Citation: Garcia-Quintanilla F, Iwashkiw JA, Price NL, Stratilo C and Feldman MF (2014) Production of a recombinant vaccine candidate against *Burkholderia pseudomallei* exploiting the bacterial N-glycosylation machinery. *Front. Microbiol.* 5:381. doi: 10.3389/fmicb.2014.00381

This article was submitted to *Microbial Physiology and Metabolism*, a section of the journal *Frontiers in Microbiology*.

Copyright © 2014 Garcia-Quintanilla, Iwashkiw, Price, Stratilo and Feldman. This is an open-access article distributed under the terms of the Creative Commons Attribution License (CC BY). The use, distribution or reproduction in other forums is permitted, provided the original author(s) or licensor are credited and that the original publication in this journal is cited, in accordance with accepted academic practice. No use, distribution or reproduction is permitted which does not comply with these terms.

ADVANTAGES OF PUBLISHING IN FRONTIERS



FAST PUBLICATION

Average 90 days
from submission
to publication



COLLABORATIVE PEER-REVIEW

Designed to be rigorous –
yet also collaborative, fair and
constructive



RESEARCH NETWORK

Our network
increases readership
for your article



OPEN ACCESS

Articles are free to read,
for greatest visibility



TRANSPARENT

Editors and reviewers
acknowledged by name
on published articles



GLOBAL SPREAD

Six million monthly
page views worldwide



COPYRIGHT TO AUTHORS

No limit to
article distribution
and re-use



IMPACT METRICS

Advanced metrics
track your
article's impact



SUPPORT

By our Swiss-based
editorial team